THE UNIVERSITY *of* EDINBURGH

THE ROLE OF MEPE IN CHONDROCYTE MATRIX MINERALISATION

Katherine Staines

This thesis is presented for the degree of Doctor of Philosophy at The University of Edinburgh

2012

Declaration

I declare that this thesis has been composed entirely by the candidate, Katherine Staines. This work has not previously been submitted for a Doctor of Philosophy, a degree or any professional qualification. I have done all the work, unless acknowledged otherwise. All sources of information have been acknowledged.

Katherine Staines

Acknowledgements

I would firstly like to thank my supervisors Colin Farquharson, and Vicky MacRae. I have received outstanding supervision, support and advice throughout the course of my PhD and I am certain that my subsequent career in science will be shaped by their guidance.

Thanks must also be paid to everyone in the Bone Biology group who have helped me when in need of support and advice throughout my years at the Roslin Institute. In particular I would like to give thanks to Neil Mackenzie, Matt Prideaux and Phillip Newton for their assistance with the collaborative experiments we have conducted. I would also like to acknowledge the collaborators I have been fortunate to work with during this project: Claire Clarkin, Graham Williams, Adele Boskey, Lynda Bonewald, Steve Mitchell and Peter Rowe. I would also like to give gratitude to the BBSRC for funding this project, as well as the European Calcified Tissue Society for providing the funding for a laboratory exchange visit and Eli-Lilly for the antibodies used in this project.

I would also like to pay special thanks to my wonderful friends, especially those I have made here in Edinburgh. I am very fortunate to have you in my life and cannot thank you enough. Finally I would not be here without my family. I would like to thank my parents and my brother for their continuous and unconditional love, support and encouragement.

Abstract

Matrix Extracellular Phosphoglycoprotein (MEPE) is a member of a family of proteins called small integrin-binding ligand, N-linked glycoproteins (SIBLINGs) which play key roles in biomineralisation. Altered MEPE expression is associated with several phosphate and bone-mineral metabolic disorders such as oncogenic osteomalacia and hypophosphatemic rickets. Despite this, it remains undetermined what impact MEPE has on the growth plate; the cartilage anlagen from which endochondral ossification, the process responsible for linear bone growth, occurs.

The work of this thesis has characterised the ATDC5 cell line and the metatarsal organ culture as useful *in vitro* models of endochondral ossification. These will prove vital in the pursuit of underpinning the molecular mechanisms involved in endochondral bone growth. These models form the basis of the further studies in this thesis examining the role of MEPE within this highly orchestrated process.

Before such role can be defined, this thesis details the spatial and temporal localisation patterns of MEPE in 10-day- and 4-week-old murine growth plates. More specifically, MEPE protein and mRNA were preferentially expressed by the hypertrophic chondrocytes as shown by immunohistochemistry and in situ hybridisation respectively. Microdissection of the murine growth plate confirmed this. Localisation of the cleavage product of MEPE, a 2.2kDa acidic serine- and aspirate-rich motif (ASARM) peptide, followed a similar pattern of expression.

The localisation of MEPE to sites of mineralisation serves to strengthen its potential role in chondrocyte matrix mineralisation. This thesis identified this role in both mineralising ATDC5 cells and the metatarsal organ culture. The ASARM peptide was found to be the functional component of MEPE and this function was dependent upon its post-translational phosphorylation. Phosphorylated (p)ASARM peptides significantly inhibited chondrocyte matrix mineralisation without altering

the proliferation or differentiation of the chondrocyte cells, or their ability to produce an extracellular matrix. mRNA analysis by qPCR indicted a feedback system by which the pASARM peptide functions to allow the release of further ASARM peptides. Moreover, the pASARM peptide inhibited mRNA expression of markers of vascular angiogenesis highlighting a novel mechanism by which they may inhibit chondrocyte matrix mineralisation.

This thesis also determines the regulatory cross-talk between the chondrocytes of the murine growth plate, with the most abundant bone cell type, the osteocyte. This cross-talk inhibits chondrocyte matrix mineralisation and is attributed to sclerostin, an osteocyte-specific secretory protein. Furthermore, it is shown that sclerostin acts through the MEPE-ASARM axis to regulate chondrocyte matrix mineralisation and thus endochondral ossification.

The work described herein has characterised and validated *in vitro* models of growth plate chondrocyte matrix mineralisation and has used these to identify the role of MEPE within chondrocyte matrix mineralisation.

Publications

Original peer reviewed papers

Newton P*., **Staines K.A*.,** Spevak L., Boskey A., MacRae V.E., Canfield A., Farquharson C. 2012 Development and characterization of a rapidly mineralizing chondrocyte ATDC5 culture model. *International Journal of Molecular Medicine* 30(5):1187-93 ***Joint first authorship**

Staines K.A., Mackenzie N.C.W., Clarkin C.E., Zelenchuk L., Rowe P.S., MacRae V.E., Farquharson C. 2012 MEPE is a novel regulator of growth-plate cartilage mineralization. *Bone* 51(3):418-430

Reviews

Staines K.A., MacRae V.E., Farquharson C. 2012 The role of the SIBLING family of proteins in skeletal mineralization and remodeling. *Journal of Endocrinology* 214(3):241-55

Staines K.A., MacRae V.E., Farquharson C. 2012 Cartilage development and degeneration: a Wnt Wnt situation. *Cell Biochemistry & Function* doi: 10.1002/cbf.2852

Commentaries

Farquharson C. and **Staines K.A.** 2011 The skeleton: no bones about it. *Journal of Endocrinology* 211(2):107-108

Published Abstracts

Staines K.A., Mackenzie N.C.W., Prideaux M., Clarkin C.E., Zelenchuk L., Bonewald L., Rowe P.S., MacRae V.E., Farquharson C. 2012 The MEPE-ASARM axis regulates chondrocyte matrix mineralisation. *Osteoporosis International:23 (Suppl 5) O9*

Staines K.A., Mackenzie N.C.W., Prideaux M., Clarkin C.E., Zelenchuk L., Bonewald L., Rowe P.S., MacRae V.E., Farquharson C. 2012 Regulation of endochondral ossification by the MEPE-ASARM axis. *Bone:* 50 (Suppl 1); S97

Staines K.A., MacRae V., Farquharson C. 2011 MEPE-ASARM Peptides: Novel Regulators of growth-plate mineralisation. *Journal of Bone and Mineral Research*: 26 (Suppl 1)

Staines K.A., MacRae V., Farquharson C. 2011 Mepe regulates growth-plate mineralisation through its cleavage to the ASARM peptide. *Frontiers in Endocrinology; Conference Abstract:* (OC24)

Staines K.A., MacRae V., Farquharson C. 2011 Is Mepe a novel regulator of growth-plate mineralisation? *Endocrine Abstracts*: 25;OC4.2

Staines K.A., MacRae V., Farquharson C. 2010 Patterns of *Mepe, Dmp1, Phex and Fgf23* expression in growth-plate chondrocytes. *Bone:* 47 (S1); S150

Staines K.A., MacRae V., Farquharson C. 2009 The expression of FGF23 signalling cascade components in growth-plate chondrocytes. *Calcified Tissue International:* 85 (2); 168

Abbreviations

βGP	Beta-glycerophosphate
μCT	Micro computed tomography
ADHR	Autosomal-dominant hypophosphatemic rickets
ALP	Alkaline phosphatase
ANOVA	Analysis of variance
ARHR	Autosomal-recessive hypophosphatemic rickets
ASARM	Acidic serine- and aspirate- rich motif
ATP	Adenosine triphosphate
BMP	Bone morphogenetic protein
BSA	Bovine serum albumin
BSP	Bone sialoprotein
BV	Bone volume
Ca^{2+}	Calcium
cDNA	Complimentary DNA
CM4	IDG-SW3 conditioned media day 4
CM21	IDG-SW3 conditioned media day 21
CO_2	Carbon dioxide
DAB	Diaminobenzidine
DAPI	4',6-diamidino-2-phenylindole
DEPC	Diethylpyrocarbonate
dH_2O	Distilled water
DKK1	Dickkopf 1
DMEM	Dulbecco's modified eagle medium
DMP1	Dentin matrix protein 1
DMSO	Dimethyl sulfoxide
DNA	Deoxyribonucleic acid
dNTP	Deoxyribonucleotide triphosphate
DSPP	Dentin sialophosphoprotein
DTT	Dithiothreitol
ECL	Electrochemiluminescence
ECM	Extracellular matrix
EDTA	Ethylenediaminetetraacetic acid
ERK	Extracellular signal-regulated kinases
FGF	Fibroblast growth factor
FGFR	Fibroblast growth factor receptor
Frz	Frizzled
FT-IR	Fourier transform infrared spectroscopy
GAG	Glycosaminoglycans
GFP	Green fluorescent protein
GH	Growth hormone
GHR	Growth hormone receptor
H&E	Haemotoxylin and eosin

HRP	Horseradish peroxidase
HZ	Hypertrophic zone
IFN-γ	Interferon gamma
IGF-1	Insulin like growth factor – 1
IGF-1R	Insulin like growth factor – 1 receptor
IgG	Immunoglobulin G
Ihh	Indian hedgehog
LB	Lysogeny broth
LDS	Lithium dodecyl sulphate
LRP	Low-density lipoprotein receptors
MAR	Mineral apposition rate
MB	Metaphyseal bone
M-CSF	Macrophage colony-stimulating factor
MEPE	Matrix extracellular phosphoglycoprotein
miRNA	Micro ribonucleic acid
MMP	Matrix metalloproteinase
mRNA	Messenger RNA
MV	Matrix vesicle
MZ	Mineralisation zone
NBF	Neutral buffered formalin
N-cadherin	Neural cadherin
N-CAM	Neural cell adhesion molecule
NCP	Non-collagenous protein
NFW	Nuclease free water
npASARM	Non-phosphorylated ASARM
OCT	Optimal cutting temperature
OPN	Osteopontin
pASARM	Phosphorylated ASARM
PBS	Phosphate buffered solution
PCR	Polymerase chain reaction
PFA	Paraformaldehyde
PHEX	Phosphate regulating gene with homologies to endopeptidases on the X chromosome
P_i	Inorganic phosphate
PO_4	Phosphate
PP_i	Inorganic pyrophosphate
PTHrP	Parathyroid hormone-related protein
PTM	Post translational modification
PVA	Polyvinyl acetate
PZ	Proliferative zone
qPCR	Quantitative PCR
RANKL	Receptor for activation of nuclear factor kappa B ligand
RIPA	Radio-immunoprecipitation assay
RNA	Ribonucleic acid
RNase	Ribonuclease

RUNX2	Runt-related transcription factor 2
SCPP	Secretory calcium-binding phosphoprotein
SDS	Sodium dodecyl sulphate
SEM	Standard error of the mean
sFRP	Secreted frizzled related protein
Shh	Sonic hedgehog
shRNA	Short hairpin ribonucleic acid
SIBLING	Small integrin-binding ligand N-linked glycoprotein
TAE	Tris-actetic acid- ethylenediaminetetraacetic acid
TBS	Tris-buffered saline
TBS/T	Tris-buffered saline/Tween-20
TEM	Transmission electron microscopy
TGF-β	Transforming growth factor – beta
TL	Total length
TNF	Tumour necrosis factor
TRAP	Tartrate-resistant acid phosphatase
TV	Tissue volume
UV	Ultraviolet
VEGF	Vascular endothelial growth factor
VSV-G	Vesicular stomatitis Indiana virus – G protein
XLH	X-linked hypophosphatemic rickets

Table of Contents

Chapter 1: Background

Chapter 2: Materials and methods

Chapter 6: Osteocyte regulation of endochondral ossification: a MEPE dependent mechanism?

List of Figures

List of Tables

Chapter 1

Introduction

Preface

The skeleton is a highly intricate and complex organ that has a range of functions spanning from locomotion to ion homeostasis. Its growth and development, by a process termed endochondral ossification, is integral to effective functioning with disruption giving rise to a multitude of growth abnormalities. This thesis will investigate the process of endochondral ossification, in particular, the hypothesis that matrix extracellular phosphoglycoprotein (MEPE) is a novel regulator of chondrocyte matrix mineralisation. It is vital that we better understand the mechanisms involved in these processes to aid the development of therapeutics for bone growth disorders such as hypophosphatemic rickets. It should be noted that many sections of this introduction are based on the published reviews by Staines *et al.,* on the effects of the small integrin-binding ligand N-linked glycoprotein (SIBLING) family of proteins on skeletal mineralisation and the role of the Wnt signalling pathway on cartilage development and degeneration (Staines *et al.* 2012a; Staines *et al.* 2012b).

1.1 The structure and function of bone

Bone is often thought of as dead and inert, however it has been known for centuries that bone is in fact a highly dynamic tissue composed of numerous cell types that interact to successfully perform its many functions; to act as a supportive framework, to protect the vital organs and to provide a source of calcium and phosphorus. It has recently come to light that bone also acts as an endocrine organ (Lee *et al.* 2007; Lee & Karsenty 2008).

The structure of bone is adapted to its function. It consists of an organic and an inorganic component which combine to allow the skeleton to be strong and stiff to withstand loading, and yet light for movement and flexible to prevent fracture. Two types of bone structure exist; cortical (compact) and cancellous (trabecular) bone (Fig. 1.1). Cortical bone constitutes 80% of the total skeletal mass and

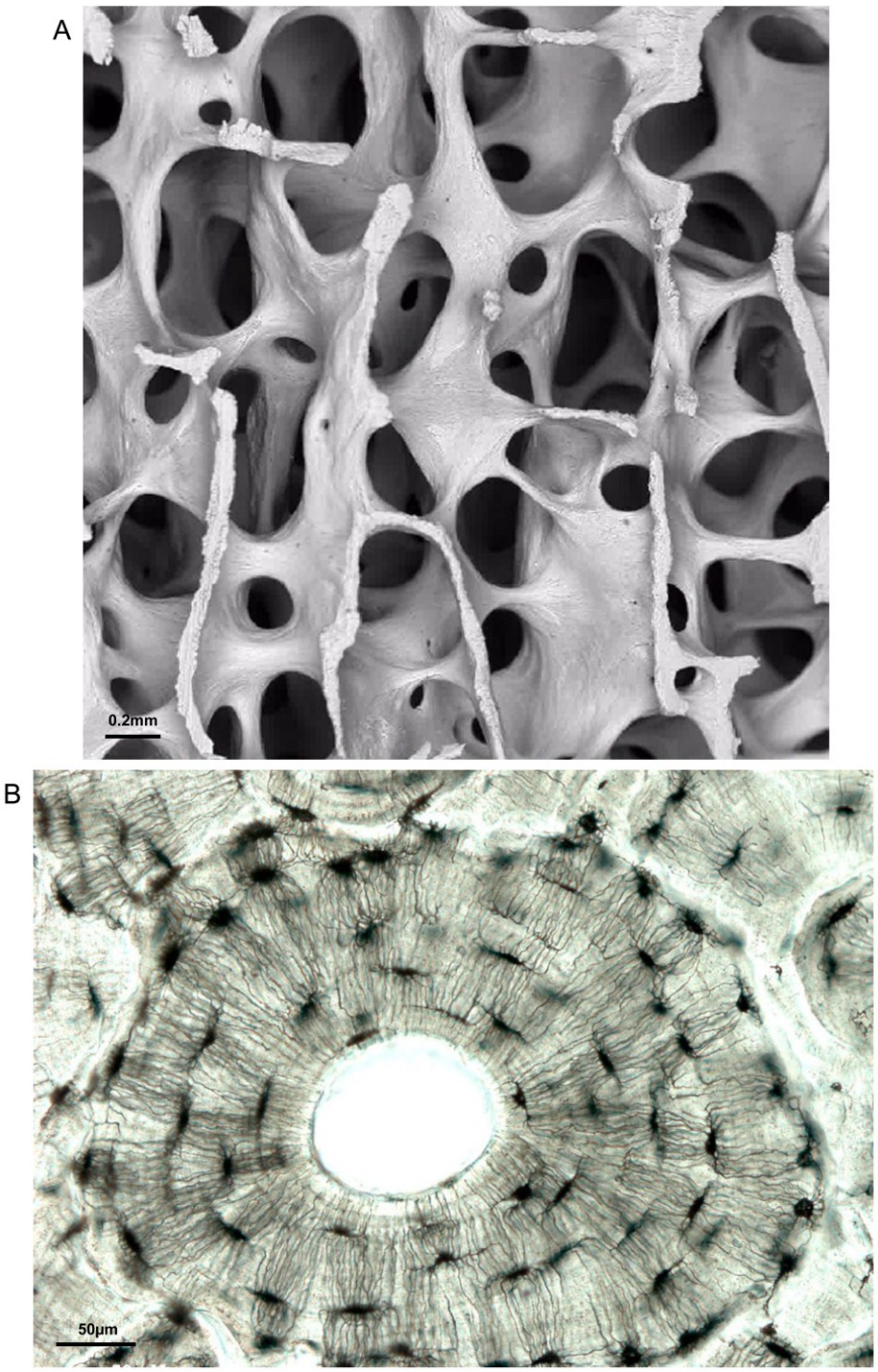

Figure 1.1 The structure of bone

Bone consists of both cancellous and cortical bone **(A)** Low power scanning electron microscopy shows normal cancellous bone architecture. Clearly visible are the strong struts of trabecular bone organised so as to withstand compressive forces **(B)** The structure of cortical bone found in the shaft of the bone. Centrally is the Haversian canal in which nerves and blood vessels reside. Surrounding this are concentric layers of bone matrix and osteocytes. Images provided from the Bone Research Society, by kind permission of (A) Alan Boyde (B) Tim Arnett.

anatomically, is primarily present in the shaft of the bone (the diaphysis) (Sambrook *et al.* 1993). Intrinsically, cortical bone is arranged into concentric lamaellae in Haversian systems, with a central canal in which blood vessels and nerves reside. This compact arrangement is advantageous as cortical bone is placed under acute mechanical demands and thus it is required to have a high resistance to tensile forces.

Cancellous bone represents approximately 20% of the total bone mass and is thin struts of lamellar bone without Haversian systems. It has a higher turnover rate than cortical bone. It is a site for abundant haemopoietic tissue and fat, reducing the weight of the bone. The major function of cancellous bone is to withstand the forces experienced during weight bearing and thus it is less dense and more elastic than cortical bone (Sommerfeldt & Rubin 2001).

1.2 Embryonic bone formation

The skeleton forms through two distinct mechanisms both of which are reliant upon a complex assimilation of biochemical and morphological events. Intramembranous ossification is the direct transformation of mesenchymal cells into osteoblasts and is important in the development of the flat bones such as the skull and the clavicle. Endochondral ossification is attributed to the formation and longitudinal growth of the long bones during both pre- and post-natal life and involves the replacement of a hyaline cartilage template by bone (Kronenberg 2003).

1.2.1 Endochondral ossification

Endochondral ossification is initiated by the condensation of cells within the limb bud during embryogenesis (Fig. 1.2). Initially, committed, undifferentiated mesenchymal precursor cells which arise from the somatopleure of the lateral plate mesoderm, are recruited to the future sites of skeletal development where they produce an extracellular matrix (ECM) which is rich in hyaluronan, fibronectin and type I collagen (Dessau *et al.* 1980; Sandell 1994). Concomitant with cellular condensation is an increase in hyaluronidase activity, the expression of adhesion

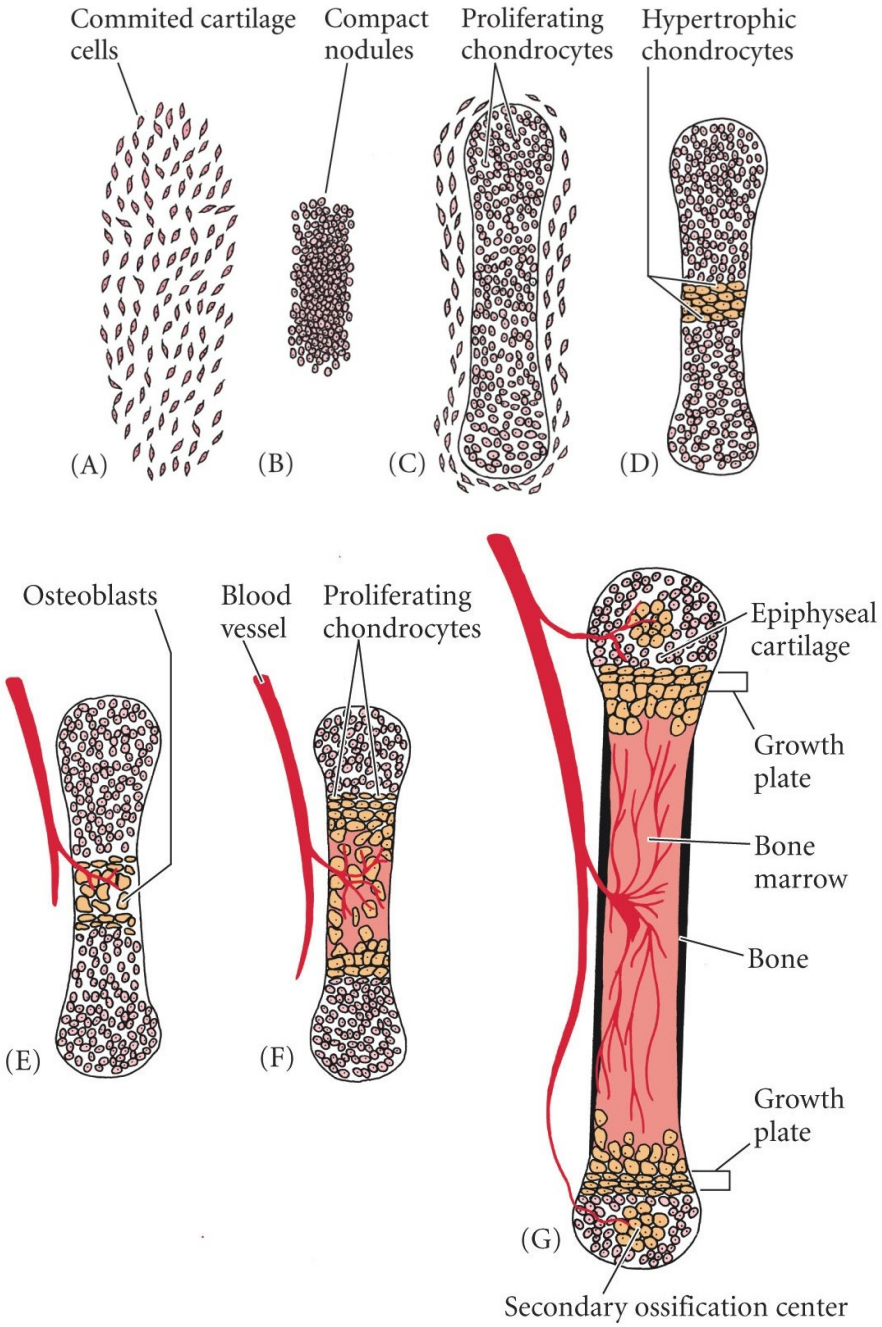

Figure 1.2 Endochondral Ossification

The process of endochondral ossification. **(A)** Mesenchymal stem cells condense and aggregate to form the cartilage anlagen **(B). (C)** Pre-chondrocytes differentiate into chondrocytes which secrete an extra cellular matrix. **(D)** These chondrocytes become hypertrophic and mineralise their surrounding matrix. **(E) T**he vascular invasion of the cartilage analgen allows the infiltration of osteoblasts and osteoclasts, and the formation of the primary ossification centre. **(F)** Bone formation expands towards the epiphysis. **(G)** Bone formation in the epiphysis allows the development of the mature growth plates and the secondary ossification centre. The epiphyseal growth plates function until the point in which the two ossification centres fuse and growth ceases (Gilbert, 2006).

molecules such as neural cadherin (N-cadherin) and neural cell adhesion molecule (N-CAM), and the expression of the nuclear transcription factor Sox9. Despite not being expressed in early mesenchymal condensations, Sox5 and Sox6 are co-expressed with Sox9 during chondrocyte differentiation (Lefebvre *et al.* 1998). This facilitates further condensation through increasing cell-cell and cell-ECM interactions (Dessau *et al.* 1980; DeLise & Tuan 2002).

Finally, the mesenchymal cells undergo differentiation to the chondrogenic lineage. The Wnt signalling pathway is one of many regulators of chondrogenic differentiation, namely by influencing the crucial cell adhesion interactions (Staines *et al.* 2012a). Concomitant with chondrogenesis is the expression of chondrocyte-specific molecules such as collagen type II and aggrecan, the principal cartilage proteoglycan (Hall & Miyake 2000; Goldring *et al.* 2006). This forms the cartilage model which expands through chondrocyte proliferation. The chondrocytes then undergo hypertrophy and ossification of the cartilage anlagen occurs. Blood vessels, bone marrow, osteoclasts (the cartilage- and bone-resorbing cells, section 1.4.2) andosteoblast precursors (section 1.4.1) invade the bone to form the primary ossification centre. This primary centre expands and secondary ossification centres subsequently form at each end of the cartilage model, leaving a developmental cartilaginous region between the two, the growth plate. The growth plate is responsible for postnatal linear bone growth and is a fundamental aspect of this thesis. Currently there are various clonal cell line models used for the *in vitro* analysis of chondrogenic differentiation and matrix mineralisation including CFK-2 (Bernier & Goltzman 1993), RCJ3.1C5 (Grigoriadis *et al.* 1996), HCS-2/8 (Takigawa *et al.* 1989), and ATDC5 cells (Atsumi *et al.* 1990).

1.2.2 The growth plate

The epiphyseal growth plate is a highly specialised cartilaginous structure located between the head and the shaft of the bone. The growth plate consists of chondrocytes arranged in columns that parallel the axis of the bone surrounded by

their ECM (Ballock & O'Keefe 2003; Mackie *et al.* 2008). This matrix consists of collagens, proteoglycans and numerous other non-collagenous proteins (NCP) (Gentili & Cancedda 2009; Heinegard 2009). The chondrocytes of the growth plate sit in distinct cellular zones of maturation, separated by longitudinal and transverse septa (Fig. 1.3). The cells proceed through the different stages of differentiation whilst maintaining their spatially fixed locations (Fig. 1.4) (Hunziker *et al.* 1987). Interference with the maturational progression of growth plate chondrocytes leads to abnormal cartilage formation and abnormalities in bone formation and rates of bone formation e.g. rickets and dwarfism.

1.2.2.1 The resting zone

The first zone, often known as the resting or germinal zone, consists of the resting chondrocytes and undifferentiated progenitors. These cells are located at the top of the growth plate, nearest the epiphysis. Unlike the rest of the growth plate, the cells of the resting zone are distributed sporadically and are surrounded by large volumes of ECM (Ballock & O'Keefe 2003; Melrose *et al.* 2008). With low proliferation rates and low proteoglycan and collagen type II production, the resting chondrocytes are rich in lipids and cytoplasmic vacuoles, thought to be stored as a nutrient source for subsequent zones (Hunziker *et al.* 1987; Mackie *et al.* 2008).

1.2.2.2 The proliferative zone

From the resting zone, the chondrocytes progress to a proliferative phenotype in which they adopt a flattened, oblate shape and arrange themselves spatially into longitudinal columns (Fig. 1.3) (Hunziker *et al.* 1987). Here the chondrocytes undergo high mitotic activity as is determined by numerous factors including endocrine regulation, circadian rhythm and age (section 1.3) (Farnum *et al.* 2002). Following the cessation of proliferation, these cells undergo a period of high secretory activity as they produce a collagen type II and proteoglycan rich matrix. They then progress through the differentiation pathway and exit the cell cycle. At this point, the pre-hypertrophic, maturing chondrocytes have minimal deoxyribonucleic acid (DNA) synthesis (Hunziker *et al.* 1987).

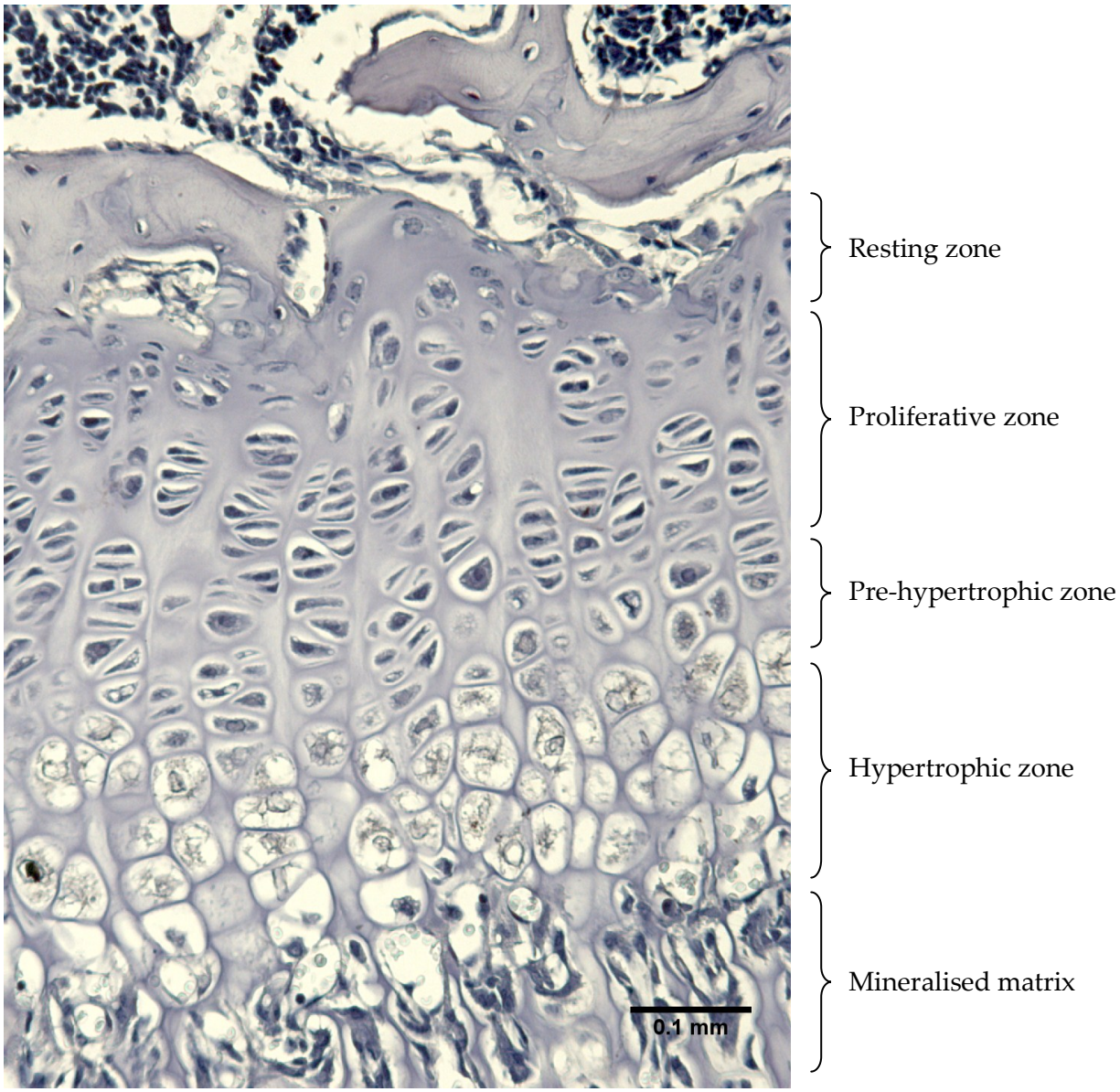

Figure 1.3 The epiphyseal growth plate

The morphology of a 3-week-old mouse tibia growth plate. Labelled are the various zones of the growth plate; the resting, proliferating, pre-hypertrophic and hypertrophic chondrocytes. Also labelled is the mineralised matrix. Bar = 0.1mm.

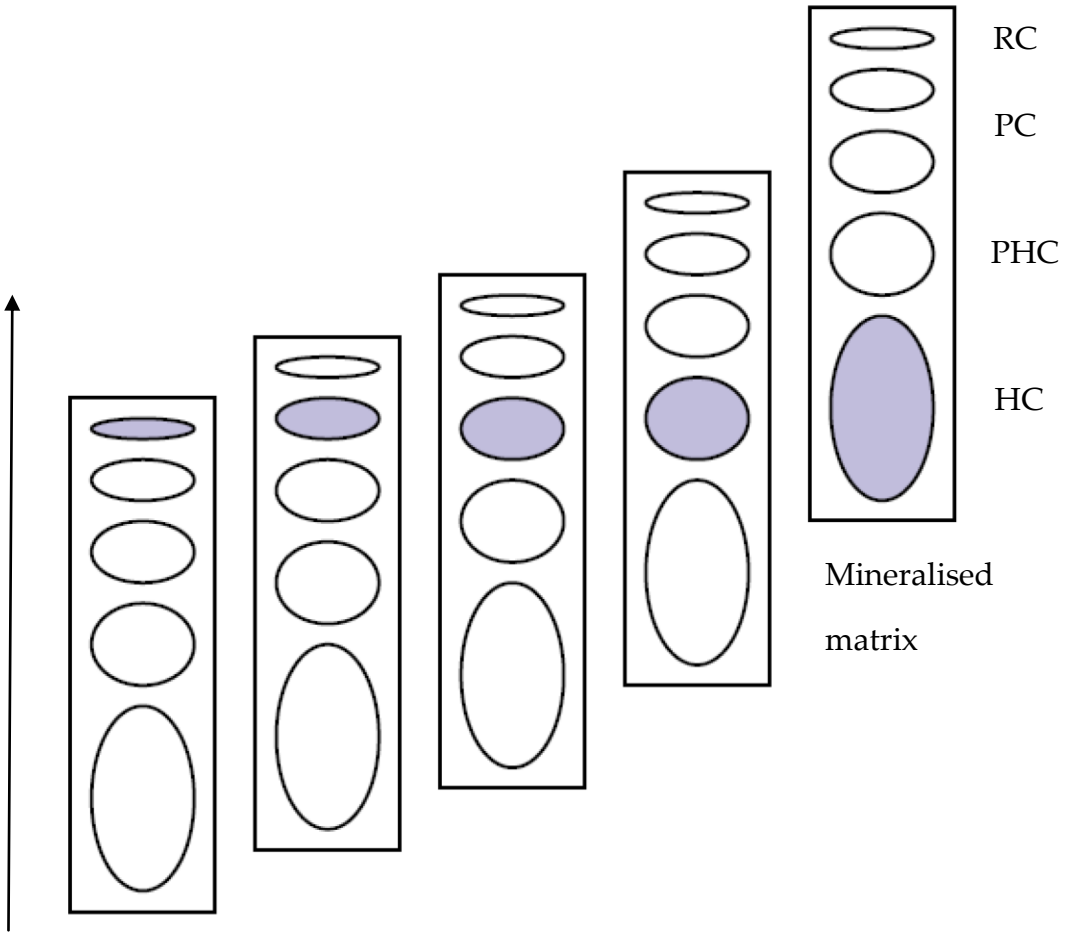

Figure 1.4 Representation of growth plate chondrocyte enlargement and longitudinal bone growth

As longitudinal bone growth occurs, the index cell (shaded) remains in a constant position while the growth plate undergoes its developmental changes. Labelled are the resting chondrocytes (RC), proliferative chondrocytes (PC), prehypertrophic chondrocytes (PHC) and hypertrophic chondrocytes (HC). The mineralised matrix beneath the growth plate is also labeled, as is the direction of longitudinal bone growth. Adapted from (Hochberg 2002).

1.2.2.3 The hypertrophic zone

In the hypertrophic zone, chondrocytes undergo major phenotypic changes. These cells have an increase in cellular volume of approximately 10 times larger than that of the proliferative chondrocytes, and a height increase of approximately five fold between the proliferative and hypertrophic zones (Fig. 1.3 & 1.5) (Buckwalter *et al.* 1986; Hunziker *et al.* 1987; Farnum *et al.* 2002).

Initially, the enlargement of the hypertrophic chondrocyte was described as hypertrophy associated with an increase in cell organelle volumes such as mitochondria, the endoplasmic reticulum and Golgi membranes. There is a two-five fold increase in the mean surface area of these organelles (Hunziker *et al.* 1987). However this is only attributable to 15% of the cell volume increase with the remaining 85% arising from cytoplasm and nucleoplasm expansion (Buckwalter *et al.* 1986; Hunziker *et al.* 1987; DeLise *et al.* 2000). This cell swelling involves the net movement of water into the chondrocyte and is governed solely by an osmotic gradient (Bush *et al.* 2008). Despite this, the precise mechanisms which drive this expansion remain largely undefined although some evidence is emerging regarding the regulatory role of membrane transporters (Bush *et al.* 2010; Lewis *et al.* 2011). The voluminous increase in chondrocyte size is associated with an increase in organelles and is responsible for approximately 80% of bone lengthening (Buckwalter *et al.* 1986).

The rate of bone growth varies widely between different species. In the domestic fowl, the proximal tibia grows at 0.86mm/day whilst in the rat and rabbit this is 0.22 and 0.39mm/day respectively. The growth rates of these two species reflect the slow rate in mammals as a whole. Indeed in humans, this has been estimated at 0.04mm/day (Scanes 2003). This rate is controlled by numerous factors including, the number of proliferating and hypertrophic cells, the rate of cell proliferation, chondrocyte ECM synthesis, the rate of hypertrophic cell voluminous increase and

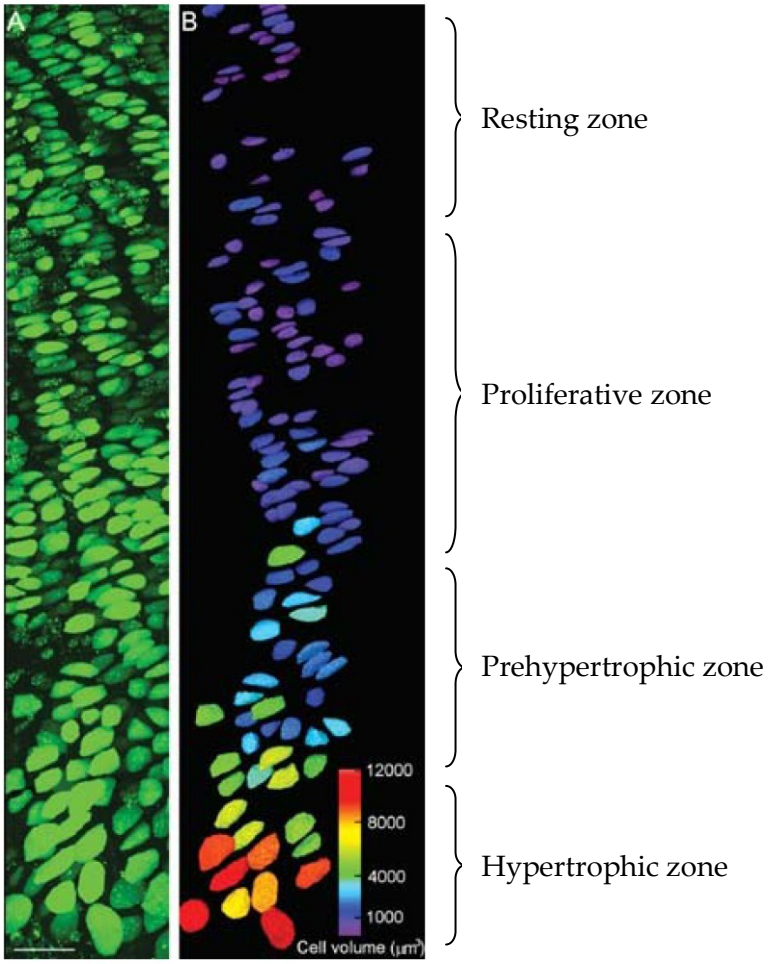

Figure 1.5 Increases in chondrogenic volume from proliferative to hypertrophic growth plate zones

Images of the rat growth plate **(A)** calcein-labelled chondrocytes **(B)** selected chondrocytes colour coded as to volume analysis. Labelled are the different zones of the growth plate. Adapted from (Bush *et al.* 2008).

the final volume attained by these cells (Buckwalter *et al.* 1986; Hunziker *et al.* 1994; Wilsman *et al.* 1996).

Associated with this differentiation is the increased expression of collagen type X, chondrocalcin, osteonectin and osteopontin, as well as the increased membrane activity of alkaline phosphatase (ALP) (Sommer *et al.* 1996; Shen 2005). It is also associated with the decreased expression of collagen type II, and other early chondrocyte marker genes, indicative of the final maturation phase.

During this terminal differentiation, the hypertrophic chondrocytes mineralise their surrounding matrix, localised to the longitudinal septa of the growth plate (Castagnola *et al.* 1988). This biphasic process facilitates the deposition of hydroxyapatite and is integral to this thesis; as such it is described in detail in section 1.6.

1.2.2.4 Vascular invasion of the ECM

Mineralisation of the ECM not only facilitates the deposition of hydroxyapatite, but also enables vascular invasion; a significant phase in endochondral ossification and the development of the skeleton. Hypertrophic chondrocytes express factors such as vascular endothelial growth factor (VEGF) (Gerber *et al.* 1999; Horner *et al.* 1999; Zelzer *et al.* 2002). VEGF has chemo-attractive properties which induce the migration of osteoclasts to resorb the cartilaginous mineralised matrix (Engsig *et al.* 2000). Furthermore, it facilitates the penetration of blood vessels into the cartilaginous mineralised matrix through which osteoblasts migrate to replace this degraded cartilage with a bone matrix (Mackie *et al.* 2011).

1.2.2.5 The fate of the terminally differentiated chondrocytes

The fate of the terminally differentiated chondrocyte at the chondro-osseous junction is still a matter of debate. However it is well accepted that it does require to be removed so as to maintain the steady-state thickness of the growth plate (Fig. 1.3 & 1.4).

There has been significant evidence to suggest that the chondrocytes die by apoptosis and this appears the most accepted mechanism (Magne *et al.* 2003; Shapiro *et al.* 2005). Indeed the activation of caspases and the decreased expression of the apoptotic factor Bcl-2 in hypertrophic chondrocytes certainly suggest this (Amling *et al.* 1997; Adams & Shapiro 2002). However, the distinct lack of typical apoptotic morphological changes in the terminal hypertrophic chondrocytes has challenged this theory (Emons *et al.* 2009; Carames *et al.* 2010). It would be expected that the condensation of cellular chromatin and the fragmentation of the cell nucleus would be visible, associated with the eventual break down of the cell into several vesicles which are then phagocytosed. Instead, the presence of autophagic vacuoles and the expression of autophagy-regulating genes by growth plate chondrocytes suggest these cells undergo processes more similar to autophagy than apoptosis (Roach & Clarke 2000; Shapiro *et al.* 2005). Furthermore, the transdifferentiation of chondrocytes has also been proposed (Cancedda *et al.* 1995; Roach 1997). This involves the division of the terminal hypertrophic chondrocyte to produce one daughter cell which undergoes apoptosis and one which trans-differentiates into an osteoblast phenotype. However this theory has yet to be fully ratified.

1.2.2.6 Closure of the growth plate

Longitudinal bone growth occurs at the growth plate until it closes once sexual maturity has been reached. At this point, the primary and secondary ossification centres meet and fusion occurs. The chondrocytes of the growth plate reach a state of senescence as they exhaust their proliferative potential, and longitudinal bone growth is ceased. In humans, gonadal steroids like oestrogen and androgen mediate these effects as is described in section 1.3.1 (Nilsson *et al.* 2005; Mackie *et al.* 2011). It is interesting to note that in mice and rats, whilst growth will eventually slow, the growth plate never closes.

1.3 Regulation of endochondral bone growth

This growth is tightly regulated by an array of autocrine/paracrine and endocrine factors to ensure effective longitudinal bone growth (Fig. 1.6). Genetic mutations in

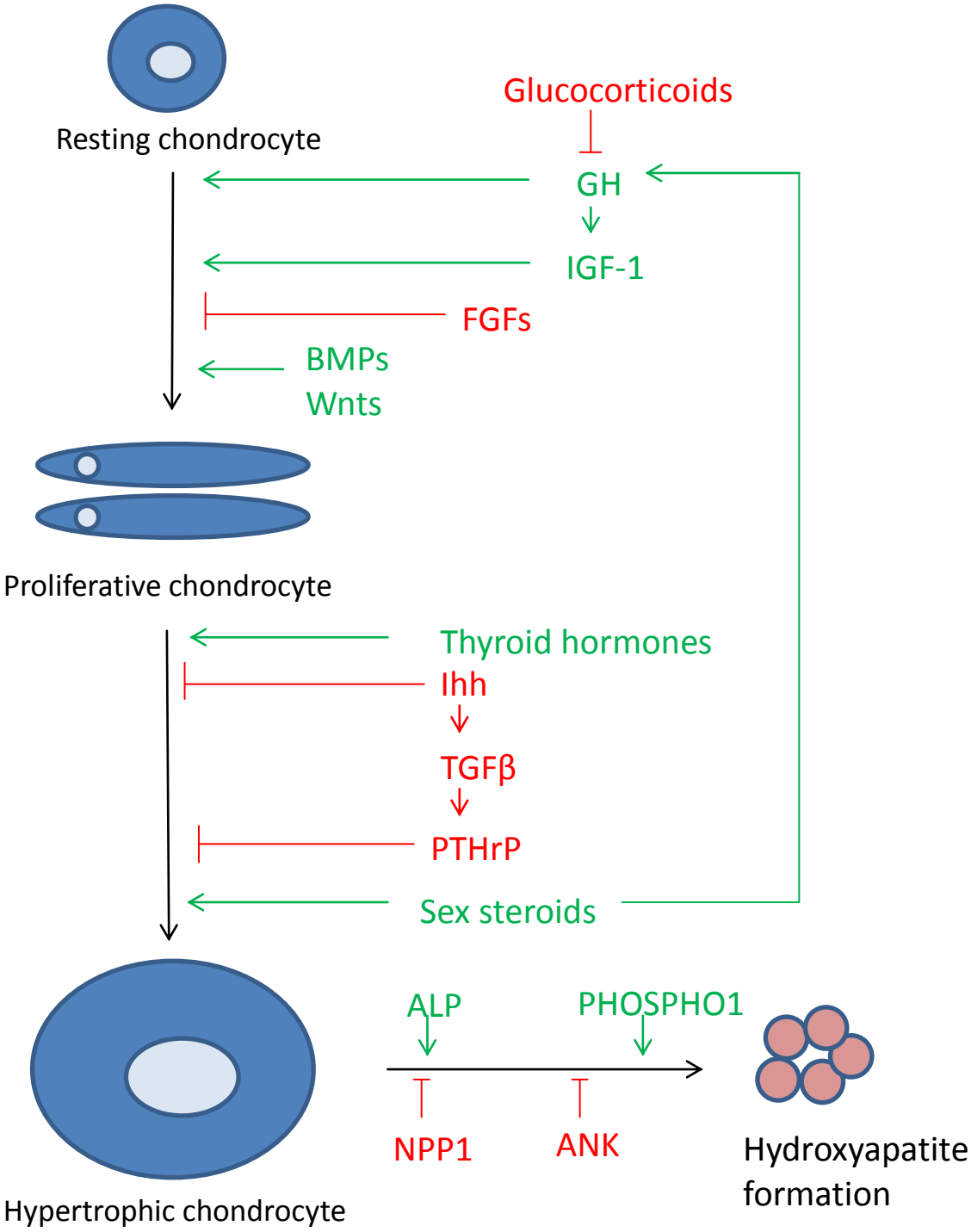

Figure 1.6 Factors regulating endochondral ossification

The various systemic, local secreted and transcription factors regulating endochondral ossification at the growth plate. Stimulation/activation is indicated by a green arrow, whereas inhibition is depicted by a red line.

the regulatory molecules detailed below result in abnormal chondrocyte phenotypes and skeletal dysplasias (Krakow & Rimoin 2010).

1.3.1 Endocrine factors

The most significant endocrine factor to affect endochondral bone growth is growth hormone (GH). Produced in the anterior pituitary gland, GH acts directly through interactions with growth plate chondrocyte GH receptors (GHR) and/or indirectly through enhanced levels of systemically derived liver Insulin-like growth factor I (IGF-I) (Salmon, Jr. & Daughaday 1957; Isaksson *et al.* 1982; Nilsson *et al.* 1986; Melmed 1999; Pass *et al.* 2009). It is likely that these two systems function in a highly coordinated manner to regulate growth plate function and linear bone growth. This is highlighted by the skeletal abnormalities observed with the dysregulation of the GH/IGF-1 axis; excess growth is observed in children with elevated GH levels whilst a deficiency of GH leads to impaired growth. Furthermore, studies with Snell (dw/dw) and Ames (df/df) hypopituitary dwarf mice and also mice with global inactivation of GHR, GHRHR, IGF-1, and IGF-1 receptor (IGF-1R) all result in reduced body weight and growth retardation (Sinha *et al.* 1975; Li *et al.* 1990; Sornson *et al.* 1996; Sims *et al.* 2000; Yakar *et al.* 2009; Ahmed & Farquharson 2010). Moreover, the chondrocyte specific deletion of IGF-1R leads to chondrocyte hypoproliferation and increased apoptosis (Wang *et al.* 2011).

Oestrogen signalling via the oestrogen receptor-α is crucial for normal skeletal maturation. Rising levels of oestrogen are associated with increased bone formation at the epiphyseal growth plate and this leads to the eventual replacement of the growth plate by mineralised bone and as such, the closure of the growth plate and the cessation of bone growth. Prior to this, oestrogen stimulates the final hypertrophy stage such that bone formation, and thus longitudinal growth, is rapidly increased accounting for the pubertal surge noted in both boys and girls (Nilsson *et al.* 2005). Patients with oestrogen deficiency or defective oestrogen receptors display failed growth plate closure and as such, have increased adult

height. Conversely, premature oestrogen production results in the early closure of the growth plate and a short stature (Smith et al. 1994; Morishima et al. 1995; Nilsson et al. 2005). As well as its direct effects through oestrogen receptors α and β, oestrogen is also thought to stimulate GH/IGF-1 signalling (Juul 2001; Borjesson et al. 2010; Borjesson et al. 2012). Androgen is another sex steroid involved in growth plate regulation directly through stimulating proliferation and hypertrophic differentiation of chondrocytes, and indirectly through its conversion to oestrogen by the enzyme aromatase (Oz *et al.* 2001; Nilsson *et al.* 2005).

Glucocorticoids, such as dexamethasone, are released by the adrenal cortex during stress. They act to reduce inflammation and as immunosuppressants, and as such they have wide clinical use. However their prolonged use results in an inhibition of chondrocyte proliferation and increased apoptosis, and as a result of this, growth retardation (Owen *et al.* 2009; Lui & Baron 2011). The mechanism of action of glucocorticoids is through the inhibition of GHR and IGF-1 expression, and therefore the subsequent inhibition of IGF-1 mediated chondrocyte proliferation (MacRae *et al.* 2007; Lui & Baron 2011).

Thyroid hormones are also important mediators of the growth plate, as is demonstrated by patients with hypothyroidism in which the reduced growth observed is attributed to narrower growth plates (Stevens *et al.* 2000; O'Shea *et al.* 2003). This can be explained by the thyroid hormones, triiodothyronine and thyroxine which stimulate chondrocyte hypertrophy and increase the expression of collagen type X and ALP, potentially though the Wnt signalling pathway (Ballock & Reddi 1994; Shao *et al.* 2006; Wang *et al.* 2007; Wang *et al.* 2010b).

Vitamin D has an important role in bone development which is highlighted by its deficiency that results in rickets: a disorder in which the growth plate enlarges and defective mineralisation occurs (Dean *et al.* 2001). Vitamin D can be obtained from sunlight irradiation of the skin, or from dietary sources. It has to undergo two

successive hydroxylations in the liver and kidney to become its active form: 1,25dihydroxyvitamin D_3 ($1,25(OH)_2D_3$). This involves the enzymes 25-hydroxylase of the liver and 1α-hydroxylase of the kidney, both of which are activated by GH and IGF-I. Vitamin D inhibits the proliferation of the growth plate chondrocytes and aids the synthesis of collagens and proteoglycans (Nilsson *et al.* 2005).

1.3.2 Autocrine and paracrine factors

In addition to endocrine factors, there are numerous locally acting autocrine and paracrine molecules which act to regulate endochondral bone growth (Fig. 1.6). Local IGF-1 production and a second IGF, IGF-2, which is also expressed by growth plate chondrocytes play critical roles in normal embryonic growth (DeChiara *et al.* 1991; van der Eerden *et al.* 2003; Parker *et al.* 2007; Ahmed & Farquharson 2010).

A key regulatory pathway of chondrocyte hypertrophy is the feedback loop involving parathyroid hormone related peptide (PTHrP), indian hedgehog (Ihh) and transforming growth factor (TGF) -β. Cells undergoing hypertrophy secrete Ihh which acts upon the proliferating chondrocytes to continue their proliferation and to resist their hypertrophy. Ihh also stimulates TGF-β production which in turn upregulates PTHrP. This acts on the pre-hypertrophic chondrocytes to prevent their further differentiation and thus the production of Ihh (Vortkamp *et al.* 1996; St-Jacques *et al.* 1999; Minina *et al.* 2002). One such mechanism of action of PTHrP is through the phosphorylation of the transcription factor Sox9 (Huang *et al.* 2001). Alternatively, PTHrP inhibits chondrocyte expression of RUNX2. This transcription factor, the activity of which is under regulation of oxygen tension, stimulates the differentiation of proliferating chondrocytes to a hypertrophic phenotype (Guo *et al.* 2006; Hirao *et al.* 2007).

Bone morphogenetic proteins (BMP) regulate endochondral ossification in numerous ways, including through regulation of the Ihh/PTHrP axis. There are various members of this family, constituting the TGF-β superfamily and acting to

initiate chondrogenesis, maintain chondrocyte proliferation as well as induce collagen type X expression by hypertrophic chondrocytes (Minina *et al.* 2001; Yoon *et al.* 2006). Whilst BMPs can induce Ihh expression, Ihh can in turn induce the expression of various BMPs offering a feedback mechanism by which these two signalling pathways work in parallel in both a dependent and an independent manner (Minina *et al.* 2001; Grimsrud *et al.* 2001).

Fibroblast growth factors (FGF) and their receptors (FGFR) constitute a large family of growth factors, many of which are expressed throughout endochondral ossification (Lazarus *et al.* 2007). In particular FGFR3 plays an important role as its expression by proliferating and pre-hypertrophic chondrocytes negatively regulates chondrocyte proliferation and differentiation. Moreover, the mutation of this gene in humans results in dwarfism (Shiang *et al.* 1994).

1.4 Bone remodelling and modelling

Throughout life, bone is continuously remodelled; a process that involves bone resorption by the osteoclast co-ordinated with bone formation by the osteoblast. Tight regulation of this process by autocrine, paracrine and endocrine factors, as described in section 1.3, maintains an equilibrium such that disorders of bone mass, such as osteoporosis or osteopetrosis, do not occur (Manolagas 2000). Bone remodelling of the cancellous bone is responsible for the annual replacement of approximately 10% of the adult human skeleton (Frost 1990), is important in fracture healing and repair. It involves a motile collection of cells, known as the basic multicellular unit. This consists of osteoclasts and osteoblasts working in synergy at the area requiring remodelling, as well as blood vessels, nerves and connective tissue (Manolagas 2000). Remodelling of bone is under tight local control, thought to be primarily regulated by the osteocyte (Hill 1998; Henriksen *et al.* 2009). All 3 bone cell types function in unity to regulate effective bone turnover.

1.4.1 Osteoblasts

Osteoblasts, like chondrocytes, adipocytes and stromal cells, are derived from multipotent mesenchymal stem cells originating in the bone marrow (Manolagas 2000). The primary function of the osteoblast is to synthesise bone matrix, termed the osteoid, consisting namely of collagen (94%) in addition to proteoglycans and other NCPs. For this reason, osteoblasts are located on the bone surface and they have abundant mitochondria, Golgi apparatus, ribosomes and endoplasmic reticulum (Dudley & Spiro 1961). It is the subsequent mineralisation of this matrix that results in the mineralised bone.

The differentiation of osteoblasts is dependent upon the coordinated expression and activation of a number of transcription factors such as RUNX2, osterix, Ihh, sonic (Shh) hedgehog, TGFβ and the BMPs (Yamaguchi *et al.* 2000; Ducy 2000). The Wnt signalling pathway is another enticing pathway implicated in bone development, in particular in osteoblastogenesis. Activation of the Wnt signalling pathway by the binding of Wnt ligands to the frizzled receptor (Frz) and low-density lipoprotein-related protein (LRP) 5/6 complex promotes osteoblast differentiation and therefore increases bone formation (Krishnan *et al.* 2006a). Several inhibitors of the Wnt signalling pathway have been identified in bone including secret frizzled-related protein 1 (sFRP-1), the Dickkopf (DKK1) family of proteins, and sclerostin (Kawano & Kypta 2003; Bodine *et al.* 2004; Semenov *et al.* 2005). Following matrix deposition and mineralisation, the osteoblast either remains on the surface of the bone as inactive lining cells; undergo apoptosis; or as they become entombed by the matrix which they secrete, they differentiate into osteocytes (Dallas & Bonewald 2010).

1.4.2 Osteoclasts

Osteoclasts are responsible for the resorption of mineralised bone. They originate from a haemopoietic lineage and their differentiation is stimulated by factors such as macrophage colony-stimulating factor (M-CSF), osteoprotegerin, and receptor for activation of nuclear factor kappa B ligand (RANKL). Despite their opposing roles,

compelling evidence now exists to support a pivotal role for osteoblasts in the regulation of osteoclast differentiation. Indeed osteoblasts progenitor cells express RANKL on their membrane surface, and the RUNX2 knockout mouse model is characterised by a deficiency of osteoblasts and interestingly, osteoclasts as well (Komori *et al.* 1997; Manolagas 2000).

Osteoclast precursors are polarised to specific sites and upon maturation, the formation of a ruffled border allows the large, multinucleated osteoclast to attach to the bone surface. The demineralisation and degradation of the bone ECM occurs at this site through the release of protons and enzymes, such as tartrate-resistant acid phosphatase (TRAP) and members of the cathepsin and matrix metalloproteinase (MMP) families, respectively (Sommerfeldt & Rubin 2001; Mellis *et al.* 2011). The tight regulation of osteoclast function is critical as excessive bone resorption, as is observed with age, can lead to a reduction in the overall amount of bone and osteoporosis.

1.4.3 Osteocytes

Osteocytes are the most abundant bone cell, accounting for approximately 90% of all cells and are the terminally differentiated form of the osteoblast cell lineage (Bonewald 2007). However, research into their function and development has been hindered somewhat by their location deep within the mineralised bone ECM. The osteocyte has a characteristic stellate morphology consisting of a cell body with many long dendritic processes which connect the osteocyte to other osteocytes, osteoblasts and osteoclasts (Bonewald 2002). These cellular projections reside in thin channels termed canaliculi and form an intense network through which biochemical, electrical and mechanical signals can be transferred.

An early postulated function of the osteocyte is as a mechanosensory cell due to its location within the bone ECM, and to its unique morphology. It has long been known that the skeleton is able to respond to the external forces placed upon it

during every day loading and during exercise. More recently it has been shown that osteocytes are integral to this as are able to translate mechanical strain into biochemical signals (Rubin & Lanyon 1984; Skerry *et al.* 1989; Burger & Klein-Nulend 1999; Bonewald & Johnson 2008). This can bring about a change in the bone micro-structure as bone formation occurs independent of bone resorption, known as bone modelling (Frost 1990).

Additionally, proteins highly expressed by osteocytes have been shown to be involved in mineral metabolism. These include phosphate-regulating gene with homologies to endopeptidases on the X chromosome (PHEX), FGF23, and the SIBLING family members MEPE and dentin matrix protein 1 (DMP1), all of which are known to co-operatively control calcium and phosphate regulation, as is discussed in section 1.7.3 (Quarles 2003; Feng *et al.* 2006; Liu *et al.* 2007b). Accumulating evidence has suggested a role for the osteocyte in bone remodelling. The secretion of SCL, an osteocyte specific protein, has identified a mechanism by which osteocytes can regulate osteoblast activity. Furthermore, osteocytes can recruit osteoclasts to sites of remodelling and can, through Wnt signalling, regulate osteoclast activity (Bonewald 2010; Kramer *et al.* 2010).

1.5 Matrix mineralisation

Hypertrophic chondrocytes and osteoblasts mineralise their surrounding ECM facilitating the deposition of hydroxyapatite. The hydroxyapatite formed in bone and teeth is a highly substituted analogue of the geological mineral hydroxyapatite ($Ca_{10}(PO_4)_6(OH)_2$), and its formation at least in cartilage is widely accepted to involve membrane-limited matrix vesicles (MV). These are approximately 200nm in diameter and have a trilaminar membrane. They bud off from the hypertrophic chondrocyte plasma membrane, and their positioning is limited to areas of mineralisation which are the longitudinal septae of the growth plate (Fig. 1.7).

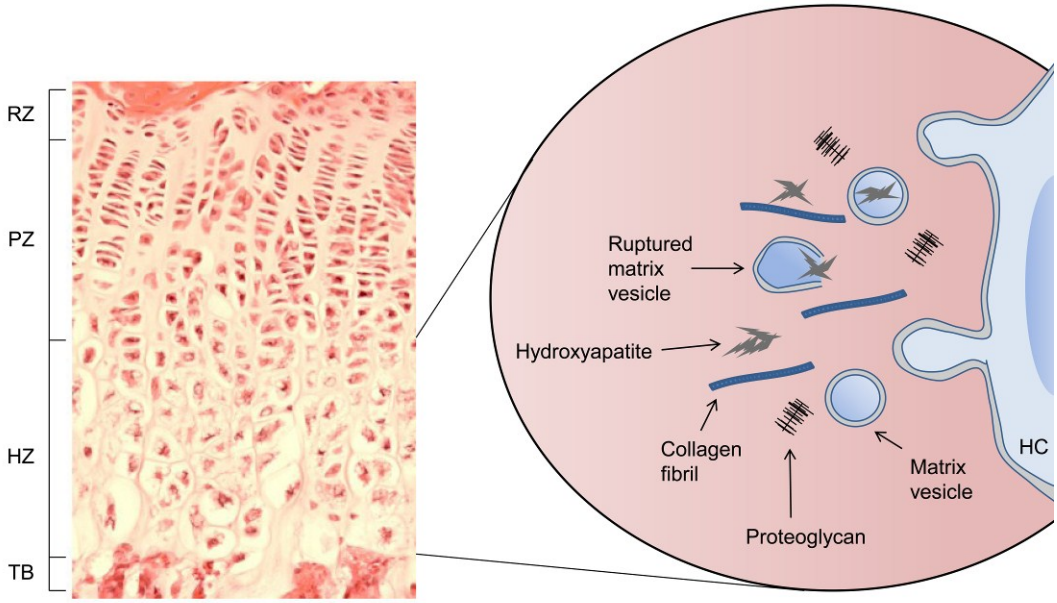

Figure 1.7 Mineralisation of the extracellular matrix within matrix vesicles

Mineralisation of the growth plate extracellular matrix occurs within the membrane limiting matrix vesicles. These form from the plasma membrane of the hypertrophic chondrocyte. Calcium and phosphate precipitate within the matrix vesicles to form hydroxyapatite. This then penetrates the membrane to align itself along the collagen fibrils of the proteoglycan rich ECM (RZ: resting zone, PZ: proliferative zone, HZ: hypertrophic zone, TB: trabecular bone, HC: hypertrophic chondrocyte).

Mineralisation is a biphasic process initiated by the accumulation of calcium ions (Ca^{2+}) and inorganic phosphate (P_i) within the MVs (Anderson 2003). When sufficient concentrations of both exist, calcium phosphate begins to precipitate which is firstly non crystalline, but then through a series of intermediates forms hydroxyapatite crystals (Fig. 1.7, 1.8A & 1.9A). This initial phase of mineralisation is followed by the penetration of the MV trilaminar membrane by the hydroxyapatite crystals such that they are exposed to the extracellular fluid, thus permitting their further growth and development (Figs. 1.8B & 1.9B & C). Mineral crystals form in alignment with the collagen fibrils of the ECM (Figs. 1.10A & B) (Anderson 1995; Wu *et al.* 2002; Anderson 2003; Golub 2011).

1.6 Regulation of mineralisation

Mineralisation is dependent upon levels of Ca^{2+} and P_i that are permissive for effective hydroxyapatite formation, and on the presence of mineralisation inhibitors such as inorganic pyrophosphate (PP_i). The ratio of P_i to PP_i controls the deposition of bone mineral and this is regulated by ALP, ecto-nucleotide pyrophosphatase/phosphodiesterase-1 (NPP1) and the ankylosis protein (ANK). More recently, a novel phosphatase PHOSPHO1 has been identified. Moreover, the role of key NCPs, namely the SIBLING family of proteins, has been identified as critical in the regulation of matrix mineralisation.

1.6.1 ALP

ALP is located on the outer membrane of osteoblasts and chondrocytes, and their MVs (Fig. 1.11) (Ali *et al.* 1970; Anderson 1995). Classically, ALP was thought to be responsible for hydrolysing the mineralisation inhibitor PP_i but evidence has shown it also has ATPase activity and generates P_i required for hydroxyapatite formation, thus achieving a ratio of P_i/PP_i permissive for hydroxyapatite crystal formation and growth (Moss *et al.* 1967; Majeska & Wuthier 1975; Hessle *et al.* 2002; Anderson 2003). PP_i, in addition to altering mineral accretion, also inhibits the enzymatic activity of ALP offering a feedback loop by which mineralisation is mediated (Addison *et al.* 2007). Deactivating mutations of the ALP gene lead to

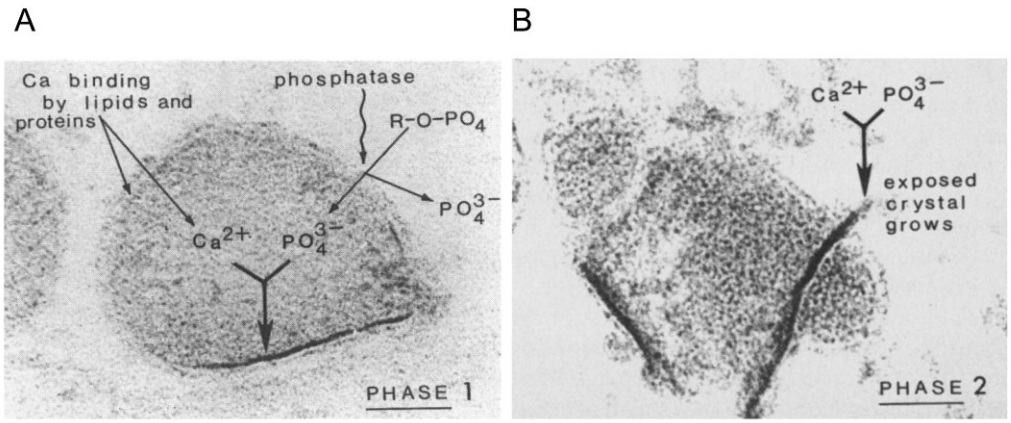

Figure 1.8 Electron micrographs of mineral formation

(A) Within the matrix vesicle, approximately 200nm in diameter, Ca^{2+} and P_i accumulate and form hydroxyapatite crystals. **(B)** These crystals grow in size and penetrate the matrix vesicle membrane allowing their further growth and development outwith the matrix vesicle (Anderson 1995).

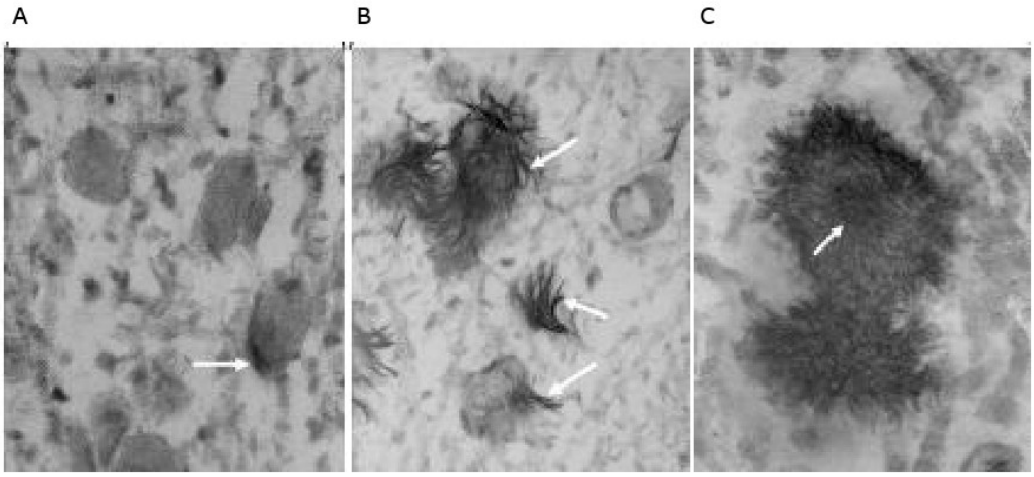

Figure 1.9 Initiation and propagation of hydroxyapatite

(A) Initiation of hydroxyapatite formation within the ~ 200nm diameter membrane limiting matrix vesicle **(B, C)** Propagation of hydroxyapatite as it extrudes the matrix vesicle membrane, as indicated by the arrows (Millan 2006).

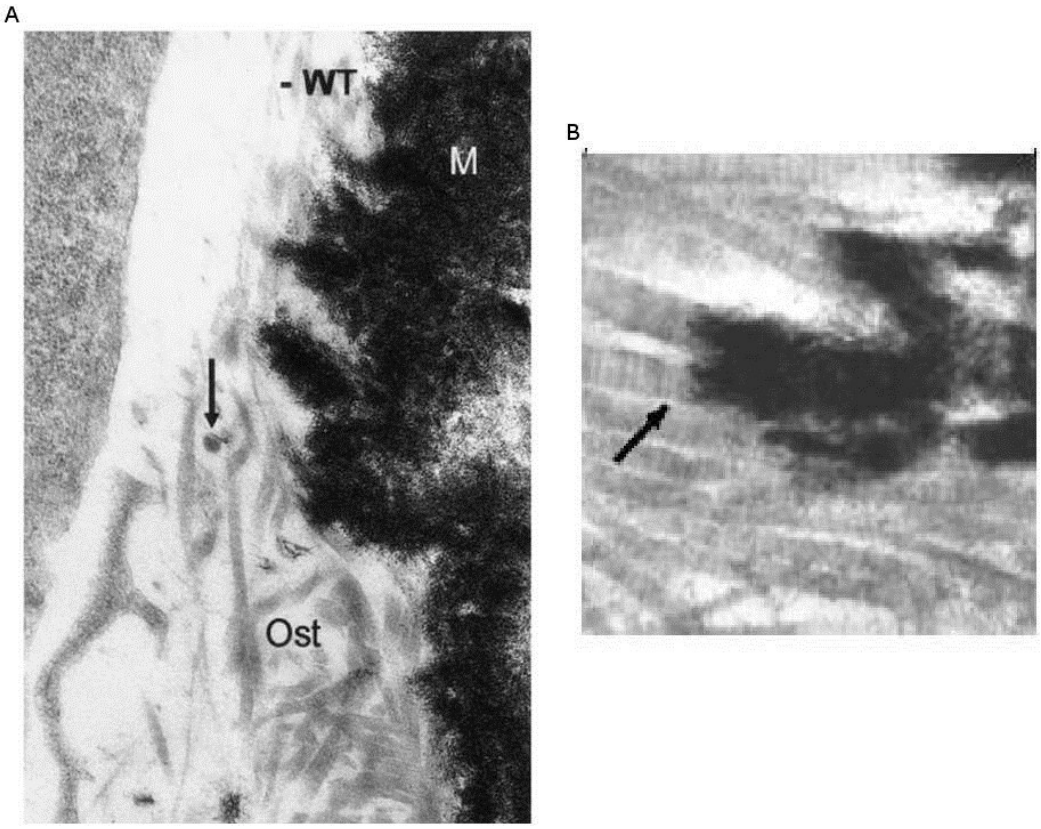

Figure 1.10 Mineral formation in alignment with collagen fibrils

(A) Analysis of mineralised (M) osteoid (Ost) in wild-type (WT) mice (Anderson *et al.* 2004) **(B)** Mineral formed within the ECM is in alignment with collagen fibrils of the ECM (Millan 2006).

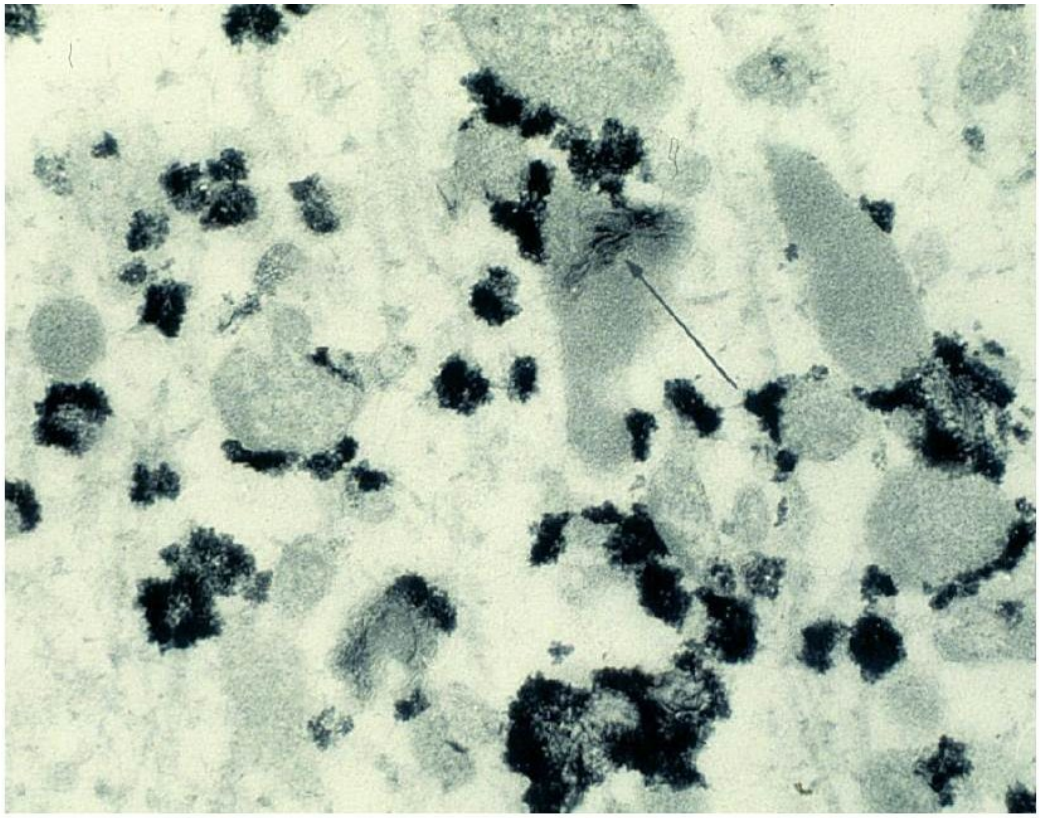

Figure 1.11 Ultrastructural localisation of alkaline phosphatase activity

Black reaction product denotes areas of alkaline phosphatase activity on the outer membrane of hypertrophic growth plate chondrocyte matrix vesicles. Arrow indicates mineral formation within the matrix vesicles. These are approximately 200nm in diameter, in comparison to the hypertrophic chondrocytes which are approximately 30μm in diameter (Anderson 1995).

increased levels of PP_i and skeletal hypomineralisation and rickets, as has been shown in the knockout mouse (Hessle *et al.* 2002; Anderson *et al.* 2004). This hypomineralised pathology of mice deficient in ALP function (*Akp2*$^{-/-}$) phenocopies the human condition hypophosphatasia, an inborn error of metabolism resulting in rickets and osteomalacia (Whyte 1994).

1.6.2 ANK/NPP1/ATP

Like ALP, NPP1 is expressed on the surface of osteoblasts and chondrocytes as well as MVs derived from these cell types. Contradictory to the ALP null mouse, NPP1 knockout mice show hypermineralisation defects and spontaneous aortic calcification (Johnson *et al.* 2005; Mackenzie *et al.* 2012).

It is known that whilst NPP1 ectoplasmically generates extracellular PP_i from extracellular nucleotides such as adenosine triphosphate (ATP), ANK mediates the channelling of that produced intracellularly to the ECM (Hakim *et al.* 1984; Terkeltaub *et al.* 1994; Ho *et al.* 2000; Nurnberg *et al.* 2001). These extracellular nucleotides have a dual inhibitory effect on bone mineralisation through P2 receptor-mediated signalling. In chondrocytes, receptors P2X2, $P2Y_1$, and $P2Y_2$ are known to be expressed, and these have been shown to inhibit matrix mineralisation and concomitant with this, inhibit ALP expression and activity (Hatori *et al.* 1995; Orriss *et al.* 2007; Burnstock *et al.* 2010; Gartland *et al.* 2012).

1.6.3 PHOSPHO1

Since its discovery and characterisation, PHOSPHO1 has been proposed to play a crucial role in the accumulation of P_i through a high phosphohydrolase activity towards phosphoethanolamine and phosphocholine (Houston *et al.* 2002; Roberts *et al.* 2004). Unlike the other regulators of mineralisation described above, PHOSPHO1 is located and is active within the osteoblast- and chondrocyte-derived MVs (Stewart et al. 2006). The PHOSPHO1 null mouse, consistent with a role in the primary stage of matrix mineralisation, displays spontaneous fractures, bowed long bones, osteomalacia, and scoliosis in early life (Huesa *et al.* 2011). Although mice

deficient for both ALP and PHOSPHO1 are embryonic lethal they are completely devoid of a mineralised skeleton at late gestation (E16.5) (Yadav et al. 2011). These data are strongly supportive of independent, non-redundant mechanisms of action of both phosphatases in the mineralisation process (Yadav *et al.* 2011). Whilst PHOSPHO1 null mice have lower ALP activity and higher PP_i levels, normalisation of PP_i levels by overexpressing ALP did not correct the hypomineralised phenotype and resultant bone fractures (Yadav *et al.* 2011). The biochemical pathways by which PHOSPHO1, NPP1 and ALP act together to regulate P_i/PP_i levels and the complete subsequent mineralisation process remains unclear.

1.6.4 SIBLING family of proteins

In addition to the action of phosphatases, recent progress in biomineralisation research has also identified roles for key NCPs in the regulation of hydroxyapatite crystal initiation and propagation, namely the small integrin binding ligand N-linked glycoprotein (SIBLING) family of proteins. This family consists of osteopontin (OPN), bone sialoprotein (BSP), dentin sialophosphoprotein (DSPP), DMP1 and MEPE.

It is likely that the SIBLING protein family arose from the secretory calcium-binding phosphoprotein (SCPP) family by gene duplication, due to their apparent common evolutionary heritage (Kawasaki & Weiss 2006; Kawasaki *et al.* 2007; Kawasaki 2011; Rowe 2012a). It is therefore somewhat surprising that the SIBLING proteins have little intrinsic sequence homology and yet they share the following characteristics: (i) all are located to a 375kb region on the human chromosome 4q21, and 5q in mouse (ii) they display similar exon structures (iii) display an Arg-Gly-Asp (RGD) motif that mediates cell attachment/signalling (iv) are principally expressed in bone and dentin, and are secreted into the ECM during osteoid formation and subsequent mineralisation (Rowe *et al.* 2000; Fisher *et al.* 2001; Fisher & Fedarko 2003; Rowe 2004; Qin *et al.* 2004; Huq *et al.* 2005; Bellahcene *et al.* 2008; Rowe 2012a). More recently, work by Peter Rowe and colleagues, primarily focused upon MEPE, has

identified a new functional domain termed the ASARM peptide (acidic serine- and aspirate-rich motif) which is highly conserved across species and is a common SIBLING motif (Rowe *et al.* 2000; Rowe *et al.* 2004). This peptide is proving critical in the functional activity of the SIBLING proteins, as are the varying SIBLING post translational modifications such as phosphorylation and glycosylation (Rowe 2004; Boskey *et al.* 2009a; David *et al.* 2010).

This functional activity, as well as the expression patterns, of OPN, BSP, DSPP and DMP1 are summarised in Table 1. This thesis focuses upon the role that MEPE plays in chondrocyte matrix mineralisation and as such, the current literature surrounding MEPE function will next be detailed.

1.7 MEPE

1.7.1 Discovery and localisation

MEPE was first isolated in 2000 from a patient with tumour induced osteomalacia and was further described as an approximately 58kDa bone-specific protein termed osteoblast/osteocyte factor 45 (Rowe *et al.* 2000; Petersen *et al.* 2000). Mouse *Mepe* was subsequently isolated, highlighting a 56% overall homology with the human sequence, and *Mepe* was subsequently mapped to the 4q21 chromosome along with the other SIBLING proteins (MacDougall *et al.* 1998; Argiro *et al.* 2001; Fisher & Fedarko 2003).

In the mouse skeleton, *Mepe* is detected as early as 2-days postpartum and it is localised to the osteocytes as well as by osteoblasts in the skeleton (Nampei *et al.* 2004). It is also expressed by odontoblasts and in the proximal tubule of the kidney (Ogbureke & Fisher 2004).

1.7.2 Function in biomineralisation

The expression of MEPE increases throughout life and this fuelled the first evidence for a direct role of MEPE in bone mineralisation. An increased messenger

Cellular expression pattern	Mouse bone phenotype		Clinical condition of gene mutation	Cleavage product & post translational modification	Role of cleavage products in mineralisation	References
	Knockout	Overexpression				
DMP1						
Osteoblasts, osteoclasts, osteocytes, hypertrophic chondrocytes & dentin	Lower mineral content, defective cartilage formation resembling dwarfism with chondrodysplasia. Hypophosphatemia and increased FGF23	Narrow growth plate with accelerated mineralisation & increased bone turnover	Autosomal recessive hypophosphatemic rickets	Full length, unphosphorylated DMP1	Promotion	Toyosawa *et al.*, 2001 Fen *et al.*, 2002 Feng *et al.*, 2003 Qin *et al.*, 2003 Tartaix *et al.*, 2004 Ye *et al.*, 2005 Feng *et al.*, 2006 Marin *et al.*, 2008
				Full length, phosphorylated DMP1	Inhibition	
				N-terminal fragment	Promotion	
				C-terminal	Promotion	
				ASARM peptide	Inhibition	
OPN						
Osteoblasts, osteoclasts, osteocytes & hypertrophic chondrocytes	Increased mineral content & size. Increased osteoclast production	Bone phenotype not defined	Unknown	> ASARM peptide - 3 serine phosphorylation	Inhibition	Dodds et al., 1995 Sodek *et al.*, 1995 Boskey et al., 2002 Landis *et al.*, 2003 Addison *et al.*, 2007 Boskey *et al.*, 2012
				> N-terminal	Promotion	
				> C-terminal fragment	Promotion	
				> Central fragment	Inhibition	
BSP						
Osteoblasts, osteoclasts, osteocytes, chondrocytes & dentin	Short hypomineralised bones with high trabecular bone mass & low bone turnover	Mild dwarfism, decreased BMD, & decreased trabecular bone volume	Unknown	Unknown	Promoter	Chen *et al.*, 1992 Gordon *et al.*, 2007 Malaval *et al.*, 2008 Valverde *et al.*, 2008
DSPP						
Dentin, bone & cementum	Defect in dentin mineralisation. Bones display accelerated mineralisation & changes in structural properties	DSP - acclerated mineralisation in teeth yet DPP - deletrious effects on enamel	Dentinogenesis imperfecta type II/III & dentine dysplasia	DPP, phosphorylated	Promoter	Sreenath *et al.*, 2003 Kim *et al.*, 2005 Yamakoshi *et al.*, 2005 Verdelis *et al.*, 2008 Prasad *et al.*, 2010
				DPP, unphosphorylated	No effect	
				DSP	Promoter	
				DGP	Unknown	

Table 1. The functional role of OPN, BSP, DSPP and DMP1 in biomineralisation

The functional role of OPN, BSP, DSPP and DMP1 in biomineralisation as is dependent upon their cleavage and post translational modification. Detailed is: (i) the cellular expression pattern (ii) the phenotype of the knockout mouse (iii) the phenotype of transgenic mice (iv) clinical conditions associated with mutation in this gene (v) cleavage products and post translational modification (vi) known role of each cleavage product in ECM mineralisation (vii) list of relevant references (Staines *et al.* 2012b).

ribonucleic acid (mRNA) expression level of *Mepe* is observed during osteoblast matrix mineralisation (Petersen *et al.* 2000; Argiro *et al.* 2001). This expression is under the control of several known regulators including FGF2, BMP2 and most recently, Wnt3a (Siggelkow *et al.* 2004; Lu *et al.* 2004; Zhang *et al.* 2004; Cho *et al.* 2011)The development of a MEPE null mouse further fuelled the proposed role for MEPE in ECM mineralisation. This mouse model had increased bone mass, with associated increased numbers and thickness of trabeculae. The mineral apposition rate (MAR) was dramatically increased as was the activity of MEPE null osteoblasts in culture (Gowen *et al.* 2003). Conversely, the overexpression of MEPE in mice, under the control of the *Col1a1* promotor, leads to a growth and mineralisation defect, due to a decrease in bone remodelling. The MEPE transgenic mice displayed wider epiphyseal growth plates, and expanded primary spongiosa and a significant decrease in the MAR (David *et al.* 2009).

Like the other SIBLING proteins described in Table 1, it appears that the activity of MEPE is dependent upon its state of cleavage and its phosphorylation. Recent work has identified the 2.2kDa ASARM peptide of MEPE as the functional component of MEPE. This ASARM peptide is highly conserved across the SIBLING proteins and in MEPE, is located immediately downstream of a cathepsin B cleavage site (Fig. 1.12) (Rowe *et al.* 2000).

The ASARM peptide of MEPE inhibits matrix mineralisation by osteoblasts by directly binding to hydroxyapatite crystals (Martin *et al.* 2008; Addison *et al.* 2008). Integral to this inhibitory effect is the post translational phosphorylation of the ASARM peptide at three serine residues. In osteoblasts it appears that without this phosphorylation, the ASARM peptide has no effect on mineralisation (Martin *et al.* 2008; Addison *et al.* 2008). Recently it has been reported that a truncated form of MEPE which has the ASARM peptide removed, can promote bone mineralisation in culture and in mice (Sprowson *et al.* 2008). Furthermore, a mid-terminal fragment of MEPE (termed ‘AC100’ or dentonin) has been shown to enhance cell binding,

through the stimulation of focal adhesion kinase and extracellular signal-regulated kinases (ERK) (Fig. 1.12) (Hayashibara *et al.* 2004). Taken together, these results highlight the importance of post-translational processing in determining the functional role of MEPE.

MEPE was first identified as a substrate for PHEX following analysis of its cleavage sites. Since then, the interaction between MEPE and PHEX has been well documented in the literature. PHEX plays a central role in the protection of MEPE from proteolytic cleavage by cathepsin B; it can bind to MEPE and prevent the release of the ASARM peptide (Guo *et al.* 2002). The *Hyp* mouse, a spontaneous *Phex* knockout model, has an increased expression of cathepsin D, an upstream activator of cathepsin B (Rowe *et al.* 2006). This therefore suggests that PHEX can alter the activation of cathepsin B, and therefore the cleavage of MEPE to the ASARM peptide. Furthermore, PHEX can bind to free ASARM peptides therefore neutralising their activity by sequestration and hydrolysis (Liu *et al.* 2007a; Addison *et al.* 2008; Martin *et al.* 2008). Recently it has been disclosed that sclerostin, a potent inhibitor of the canonical Wnt signalling pathway and bone formation, may also act through the MEPE-PHEX axis, highlighting its significance in biomineralisation (Atkins *et al.* 2011).

MEPE transgenic mice display a decrease in ALP enzyme activity in both the growth plate and the primary spongiosa (David *et al.* 2009). *In vivo*, the addition of the phosphorylated ASARM peptide also reduced the number of ALP-positive cells in an osteoblast cell culture model (Martin *et al.* 2008). However, this remains controversial as normal ALP activity has been reported in osteoblasts treated with phosphorylated ASARM (pASARM) peptide (Addison *et al.* 2008). In the MEPE overexpressing mouse vascularisation is increased, as is VEGF expression, highlighting a role for MEPE in angiogenesis, an important stage in endochondral ossification (David *et al.* 2009). Consonant with angiogenesis is the infiltration of osteoclasts for bone resorption. Interestingly, in mice administered with

recombinant MEPE or mice transgenic for MEPE both have a significant decrease in the numbers and activity of osteoclasts (Hayashibara *et al.* 2007; David *et al.* 2009).

1.7.3 The PHEX-MEPE-ASARM hypothesis and its function in mineral metabolism

Accumulating evidence has implicated the ASARM peptide and its interactions with PHEX, and FGF23 in bone renal P_i homeostasis and mineralisation (Fig. 1.13). This hypothesis can be used to explain numerous disorders of mineralisation including tumour induced osteomalacia, autosomal-dominant hypophosphatemic rickets (ADHR), and X-linked hypophosphatemic rickets (XLH).

XLH is the most common form of inherited rickets, characterised by defective bone and tooth mineralisation, growth retardation, and defective renal re-absorption of P_i (Carpenter *et al.* 2011). Mutations in PHEX have been associated with XLH in humans, and have led to the development of the *Hyp* mouse (Holm *et al.* 1997). Hypophosphatemia alone is insufficient to explain the bone defect seen in the *Hyp* mouse as correction of the hypophosphatemia failed to correct the mineralisation defect observed (Ecarot *et al.* 1992; Rowe *et al.* 2006). Furthermore, when osteoblast cells from the *Hyp* mouse are grown in culture, they have a defective ECM production and thus reduced mineralisation (Xiao *et al.* 1998). This therefore suggests that PHEX has multiple substrates which are involved in regulating mineralisation directly and this has allowed the creation of the ASARM hypothesis (Rowe 2004; David *et al.* 2010; Rowe 2012a). The ASARM hypothesis is based upon the concept of a minhibin, an unknown secreted factor which is a substrate for PHEX and therefore would accumulate in the *Hyp* mouse and in patients with XLH.

MEPE was first identified as a potential substrate for PHEX and this is strengthened by the observed increased levels of MEPE-ASARM peptides in the *Hyp* mouse and in patients with XLH (Bresler *et al.* 2004). However *in vitro* studies have failed to demonstrate PHEX-dependent hydrolysis of MEPE and instead it appears that it is

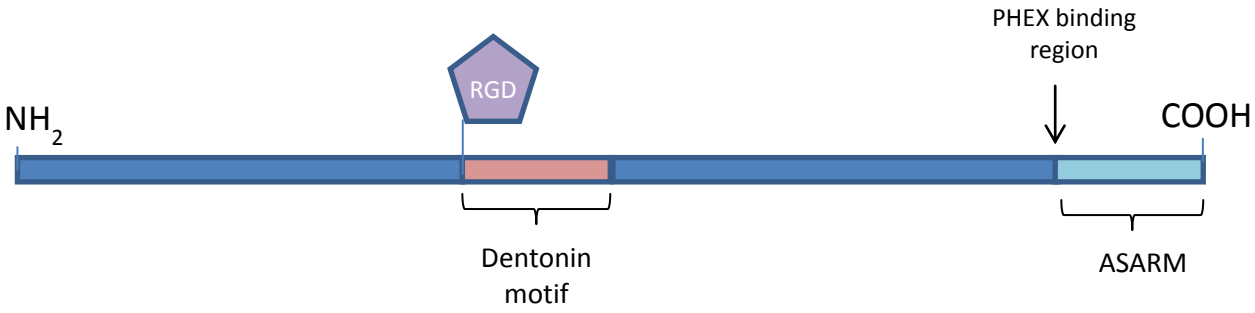

Figure 1.12 The secondary structure of MEPE

The predicted secondary structure of MEPE. Detailed are the RDG and dentonin binding motifs. Also labelled is the C-terminal ASARM peptide which inhibits matrix mineralisation, and the binding region for PHEX which prevents the cathepsin B mediated cleavage of the ASARM peptide.

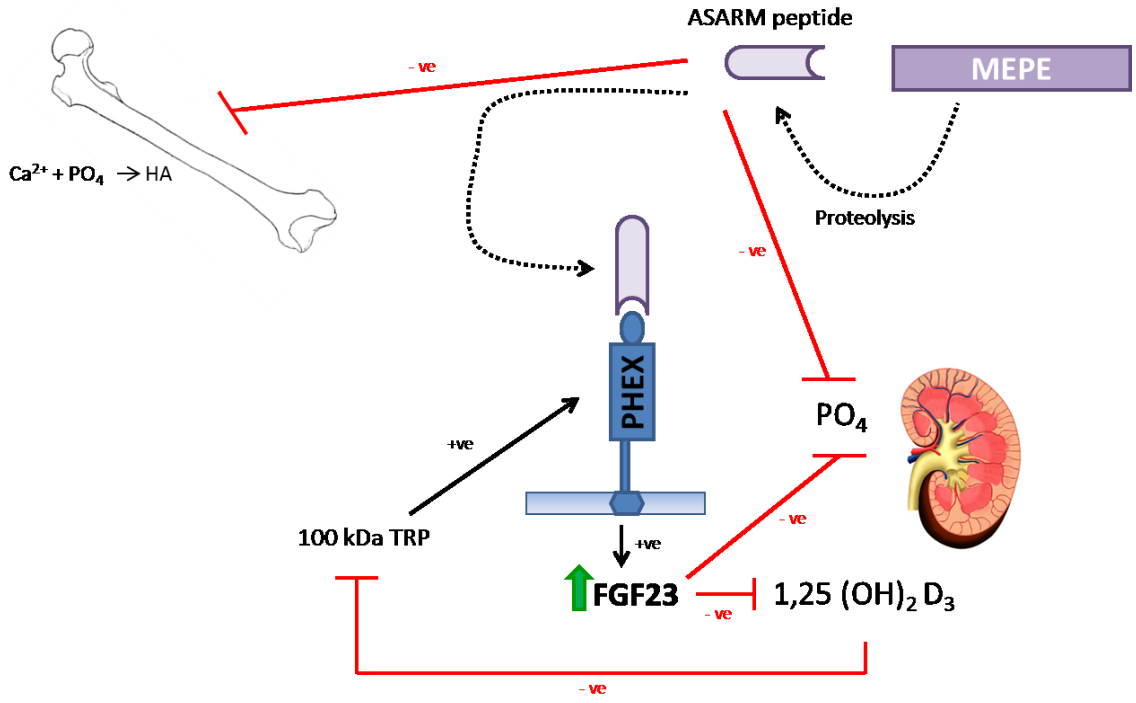

Figure 1.13 ASARM function in biomineralisation and mineral metabolism

MEPE is cleaved by cathepsin B to ASARM peptide. This peptide has dual roles in biomineralisation and phosphate homeostasis which is dependent upon its phosphorylation. The ASARM peptide inhibits hydroxyapatite formation in bones. It also regulates FGF23 expression through its interaction with PHEX. In turn this inhibits renal phosphate regulation. Adapted from (Rowe 2004; Rowe 2012a).

the ASARM peptide which PHEX digests (Guo *et al.* 2002; Addison *et al.* 2008; Martin *et al.* 2008; Boukpessi *et al.* 2010; Addison *et al.* 2010).

It also appears that PHEX regulates FGF23 expression as increased FGF23 expression is observed in the *Hyp* mouse and patients with XLH (Liu *et al.* 2006). Accordingly, FGF23 knockout reversed the hypophosphatemia observed in *Hyp* mice (Sitara *et al.* 2004). Although initial studies appeared to confirm FGF23 as a substrate for PHEX, this has not been shown since (Bowe *et al.* 2001). Interestingly, a similar increase in FGF23 expression is observed in models of loss of DMP1, along with associated autosomal-recessive hypophosphatemic rickets (ARHR) (Feng *et al.* 2006; Lorenz-Depiereux *et al.* 2006). This has led to the suggestion that a PHEX-DMP1 interaction is responsible for orchestrating mineralisation through decreasing FGF23 expression. Furthermore, current paradigm suggests that ASARM peptides can competitively displace this PHEX-DMP1 complex and this would therefore increase FGF23 activity as is seen in the *Hyp* mouse and in patients with XLH (David *et al.* 2010; Martin *et al.* 2011; Rowe 2012a).

Additionally, the accumulation of ASARM peptides can directly inhibit Na^+ - dependent P_i uptake in the kidney, as has been shown both *in vivo* and *in vitro* thus exacerbating the upregulation of FGF23 expression, the downregulation of $1,25(OH)_2D_3$ and the hypophosphatemia observed in XLH, ARHR and ADHR (Rowe *et al.* 2004; Marks *et al.* 2008; Dobbie *et al.* 2008; David *et al.* 2010; Shirley *et al.* 2010). The decrease in $1,25(OH)_2D_3$ provides a feedback loop for increased PHEX expression through the increased expression of a 100kDa transcription factor, a requirement for this PHEX expression (Fig. 1.13) (Ecarot & Desbarats 1999).

This regulatory loop of ASARM, PHEX and FGF23 expression and function highlights the multiple and complex functions of the SIBLING ASARM peptides in both P_i homeostasis and matrix mineralisation in disease and health. It is therefore

vital that we endeavour to fully establish the interactions within this hypothesis to allow future therapeutic developments.

1.8 Aims and strategy

Despite an emerging role for MEPE in biomineralisation, its impact on chondrocyte ECM mineralisation is largely undefined. Therefore, the aim of this project was to test the hypothesis that MEPE and its ASARM peptide are essential for the control of growth plate cartilage mineralisation and endochondral bone growth. For this, I have completed the following aims:

1. Establish suitable and reproducible *in vitro* models of endochondral ossification

2. Define the localisation of MEPE and its ASARM peptide in the murine growth plate

3. Determine the functional role of MEPE in chondrocyte matrix mineralisation

4. Examine the potential regulation of chondrocyte matrix mineralisation by osteocytes through MEPE expression

These aims have been achieved through the use of *in vitro* models which will firstly be characterised (Chapter 3) by their mineralisation capability and their expression of chondrocyte specific genes. These models include the ATDC5 cell line (a mouse embryonal carcinoma-derived cell line), primary murine costochondral chondrocytes and an embryonic metatarsal organ culture system. This chapter determined the suitability of each specific model for further studies into chondrocyte ECM mineralisation.

Before attempting to unravel the regulatory mechanisms that MEPE may have in mammalian chondrocyte ECM mineralisation, it is first necessary to understand its spatial expression pattern within the growth plate (Chapter 4). Therefore the protein and gene expression of MEPE, and its ASARM peptide were defined in the murine growth plate. Furthermore, their expression in the *in vitro* models described in Chapter 3 was examined.

The localisation of MEPE to sites of mineralisation would serve to cement its pivotal role in the regulation of growth plate matrix mineralisation. This role was examined in ATDC5 cell and metatarsal organ culture models, with the function of both the full length MEPE and its ASARM peptide being investigated (Chapter 5).

It has been suggested that SCL, a known inhibitor of bone formation, may act through the MEPE-ASARM axis (Atkins *et al.* 2011). Therefore, the role of SCL in chondrocyte ECM mineralisation was examined as this has yet to be established within the literature (Chapter 6). This role was examined with regards to MEPE and its ASARM peptide in metatarsal organ cultures, utilising the IDG-SW3 cell line, a recently characterised osteocyte-like cell line which is known to express high quantities of SCL as the cells differentiate into their osteocyte phenotype (Woo *et al.* 2011). This chapter also provided an insight into any potential osteocyte-chondrocyte crosstalk.

In conclusion, these studies have defined suitable and reproducible models of endochondral ossification that have been exploited to examine the functional role of MEPE in chondrocyte ECM mineralisation, as has yet to be established. Furthermore, these studies have tested the hypothesis that SCL inhibits growth plate mineralisation through a MEPE-ASARM dependent mechanism. This will enable a more complete picture of the role of MEPE in biomineralisation and will therefore allow investigation into its potential therapeutic application to disorders of mineralisation.

Chapter 2

Materials and Methods

2.1 Reagents and solutions

All chemicals were purchased from Sigma-Aldrich (Dorset, UK), and tissue culture media and buffers were purchased from Invitrogen (Paisley, UK) unless otherwise stated. All medium and buffer recipes are shown in Appendix I.

2.2 Cell Culture

2.2.1 ATDC5 cells

Chondrogenic ATDC5 cells (RIKEN cell bank) (Shukunami *et al.* 1997) were cultured in maintenance media (Appendix I) at 37°C with 5% carbon dioxide (CO_2) and maintained at sub-confluence. Dulbecco's modified eagle medium (DMEM)/F12 containing phenol red, a pH indicator, was used. For passaging, cells were rinsed in serum-free DMEM/F12 and detached from the culture flasks by addition of trypsin-ethylenediaminetetraacetic acid (EDTA) at 37°C. Differentiation media (Appendix I) containing serum to inactivate the trypsin was then added to the flasks, and cells were collected by centrifugation at 1000g for 5 minutes. Cells were resuspended in differentiation media, counted using a haemocytometer and then plated in multi-well plates at a density of 6 x $10^3/cm^2$ for experimentation. 10mM β-glycerophosphate (βGP) and 50μg/ml ascorbic acid were added once the cells had reached confluency. Cells were incubated in a humidified atmosphere (37°C, 5% CO_2) for up to 41 days with medium changed every second or third day.

2.2.2 Freezing/Thawing ATDC5 cells

To maintain stocks of ATDC5 cells, cells were trypsinised and counted as described in 2.2.1. The cells were centrifuged at 1000g for 5 minutes and resuspended in 50/50 maintenance media and freezing mix (Appendix I) to give a cell concentration of 3 x 10^6 cells/ml. The cells within a cryovial (Corning, Surrey, UK) were then wrapped in cotton wool within a polystyrene box and kept at -80°C for 4-7 days and then to -150°C for longer term storage. Cells were thawed at 37°C and added drop wise to 5ml of pre-warmed maintenance media. The cell suspension was then mixed and spun at 1000g for 5 minutes to remove the dimethyl sulfoxide (DMSO), which acts

as a cryoprotectant to prevent cell death during the freezing process. The cell pellet was resuspended in maintenance media and transferred to a T175 tissue culture flask.

2.2.3 Isolating primary chondrocytes

Sternal primary chondrocytes were isolated from 1- to 3-day old wild-type C57/BL6 mice as previously described (MacRae *et al.* 2009). The rib cage and sternum were dissected and the organs, spine and excess tissue removed. Ribcages were washed in sterile phosphate buffered solution (PBS; 1X) and incubated at 37°C in 2mg/ml protease in PBS for 30 minutes with agitation. After washing in PBS, the ribcages were incubated at 37°C for 15 minutes in sterile collagenase type 2 (Worthington Biochemical Corporation, USA) at 3mg/ml in DMEM. Muscle and soft tissue were then removed from the ribs and sternum by gentle pipetting. The cartilage rods were then finally digested by incubation at 37°C in sterile collagenase type 2 (3mg/ml in DMEM) for 3 to 4 hours with regular agitation. Cells were filtered through a 45μm sieve, pelleted by centrifugation and re-suspended in DMEM before being counted using a haemocytometer. Approximately 1 x 10^6 cells were isolated per mouse pup, of which approximately 70% were viable. Cells were plated in a 12-well plate at a density of $10^5/cm^2$ in primary chondrocyte media (Appendix I). For mineralisation studies, once cells had reached confluency, mineralisation was induced by supplementation with 10mM βGP and 50μg/ml ascorbic acid. Cells were incubated in a humidified atmosphere (37°C, 5% CO_2) for up to 28 days with medium changed every second or third day.

2.2.4 IDG-SW3 cells

The IDG-SW3 cell line, isolated from 3-month-old *Immortomouse*$^{+/-}$*/Dmp1-green fluorescent protein (GFP)*$^{+/-}$ mice which carry an interferon gamma (IFN-γ) inducible promoter enabling immortalisation of cells, was a generous gift from Professor Lynda Bonewald (University of Missouri-Kansas City, Missouri, USA) and was cultured as detailed previously (Woo *et al.* 2011). Cells were expanded in permissive conditions, at 33°C in IDG-SW3 cell media (Appendix I) containing 50U/ml IFN-γ,

on rat tail type I collagen coated plastic ware. For mineralisation experiments, cells were seeded at 8 x 10^4 cells/cm^2 in osteogenic conditions (37°C with 50μg/ml ascorbic acid and 4mM βGP) in the absence of IFN-γ.

2.3 Procedures for ATDC5 mineral assessment

2.3.1 Fourier transform infrared spectroscopy (FT-IR)

ATDC5 cells were cultured for 41 days as described in section 2.2.1. The cell monolayers were fixed in 95% methanol and embedded in LR white resin. Samples were analysed in the laboratory of Professor Adele Boskey (Hospital for Special Surgery, New York) using a Thermo-Nicolet 4700 spectrometer (Waltham, MA, USA). The spectra were corrected for background and the areas under the phosphate (900-1200 cm^{-1}) and amide I (1585-1720 cm^{-1}) peaks were determined. The mineral to matrix (Min/AM1) ratio was calculated as the ratio of the two areas.

2.3.2 Transmission electron microscopy (TEM)

ATDC5 cells were seeded onto nitrocellulose discs (Nunc, Roskilde, Denmark) in 24-well plates and cultured in differentiation medium for 15 days, as detailed in section 2.2.1. The media were then removed from the cultures and cells were fixed in 2.5% glutaraldehyde in 0.1M sodium cacodylate buffer at 37°C for 1 hour. The cells were then stored in the glutaraldehyde/cacodylate solution at 4°C until required for processing. During processing, the cell monolayers were washed 3 times in 0.1M sodium cacodylate, post-fixed in 1% osmium tetroxide, then washed 3 times in distilled H_2O (dH_2O) and dehydrated through graded alcohols (35%, 70%, 95% and 100%). The monolayers were then processed to Epon in a vacuum oven at 60°C, with 3 changes and a final 24 hour incubation. Monolayers were viewed using a Phillips CMIRO TEM (FEI Vic Ltd, Cambridge, UK) and images taken on Gatan Orius ICD camera (Gratan, Oxford, UK). Sample processing was performed by Steve Mitchell at The University of Edinburgh.

2.4 Histological procedures of cell cultures

2.4.1 Alizarin red stain

Calcium deposition in cell cultures was assessed by alizarin red staining. Cells were fixed in 4% paraformaldehyde (PFA) for 5 minutes following rinsing with PBS. 2% alizarin red stain pH4.2 was used to stain cell layers for 5 minutes at room temperature. Staining was quantified by the addition of 200µl 10 % cetylpyridinium chloride for 10 minutes. The optical density of the resultant solution was analysed using a spectrophotometer (Thermo Scientific, Northumberland, UK) at a wavelength of 570nm. 10 % cetylpyridinium chloride was used as a blank. Reactions were completed in triplicate at each cell culture time point.

2.4.2 Alcian blue stain

Glycosaminoglycan (GAG) presence was assessed in cell cultures by alcian blue staining. Cell layers were fixed in 95% methanol for 20 minutes following rinsing with PBS. Alcian blue stain (Thermo Scientific, Roskilde, Denmark) was added for 18 hours at room temperature. Quantification of staining was completed following the addition of 180µl 6M guanidine hydrochloride and analysed at 630nm on a spectrophotometer. Guanidine hydrochloride was used as a blank. Reactions were completed in triplicate at each cell culture time point.

2.4.3 Sirius red stain

The production of collagen was assessed in cell cultures by sirius red staining. Following rinsing in PBS, cells were fixed in 4% PFA for 5 minutes. 'Sircol' dye reagent (Sirius red and picric acid, Biocolor, County Antrim, UK) was added for 1 hour at room temperature. Unbound dye was removed with 0.001M HCl and the fixed stain was leeched from the matrix in 0.1M NaOH. The absorbance of the resultant solution was read on a spectrophotometer at a wavelength of 570nm. 0.1M NaOH was used as a blank. Reactions were completed in triplicate at each cell culture time point.

2.5 *Ex vivo* studies

2.5.1 Animal welfare

Animals were maintained under conventional housing conditions with a 12 hour light/dark cycle. All animal experiments were approved by The Roslin Institute's Animal Users Committee and the animals were maintained in accordance with Home Office guidelines for the care and use of laboratory animals.

2.5.2 Isolation and culture of embryonic murine metatarsals

The middle three metatarsals of E17 and E15 mice were isolated under a dissecting microscope. Throughout the dissection the bones were kept under preparation medium (Appendix I). Metatarsals were cultured in 24-well plates containing one bone in 300µl metatarsal media (Appendix I) for up to 12 days. For the E17 metatarsal bones, the medium was changed every second or third day and for the E15 metatarsal bones, the medium was not changed throughout the culture period (Haaijman *et al.* 1999). The total length of the bone through the centre of the mineralising zone was determined using image analysis software (DS Camera Control Unit DS-L1; Nikon) every second or third day. The length of the central mineralisation zone was also measured. Bones were incubated in a humidified atmosphere (37^{o}C, 5% CO_2).

2.5.3 Co-culture of embryonic murine metatarsals and IDG-SW3 cells

For co-culture experiments, 12 Well Thincert, 0.4µm pore diameter, transparent co-culture plates were used (Grenier Bio-one Inc, Stonehouse, UK). IDG-SW3 cells were plated and maintained for up to 21 days as described in section 2.2.4. At this point, E15 metatarsal bones were dissected as detailed in section 2.5.2, and were placed upon the insert which was suspended above the IDG-SW3 cells to allow diffusion of the two cell mediums. Metatarsal bones were cultured for up to 10 days in a humidified atmosphere. The total length of the bone through the centre of the mineralising zone, as well as the length of the central mineralisation zone, was

determined using image analysis software (DS Camera Control Unit DS-L1; Nikon) every second or third day.

2.6 *In vivo* studies

2.6.1 Paraffin embedded tissue

Proximal tibiae from 3-4 week old wild-type male and female C57/BL6 mice were dissected and excess tissue was removed immediately after culling of mice by cervical dislocation. Tibias dissected were fixed in either 10% neutral buffered formalin (NBF; for *in situ* hybridisation) or in 70% ethanol (for immunohistochemistry) for 24 hours. Bones were decalcified in 10% EDTA (pH 7.4) with agitation at 4°C for approximately 3 weeks, with regular EDTA changes. Tissue was then dehydrated through a series of alcohol steps at room temperature as follows: two washes in PBS; two 1 hour incubations in 70% ethanol; two 1 hour incubations in 80% ethanol; two 1 hour incubations in 95% ethanol; 1 hour incubation in 100% ethanol; overnight incubation in 100% ethanol. The tissue specimens were transferred into a wax embedding cassette and rolled in xylene for 2 hours. The cassettes were then transferred to pre-melted wax at 60°C for 2 hours. This allowed wax infiltration of the tissues before they were embedded into plastic moulds. Using a microtome (Ernst Leitz AG, Germany; blades used were MX35 Premier+ Microtome Blades, Thermo Scientific, Cheshire, UK), wax blocks were trimmed to expose the sample surface. The paraffin embedded samples were then cooled and tissues were sectioned at a 5μm thickness. Sections were transferred to a 40°C water bath for 1 minute before being transferred to a poly-l-lysine coated microscope slide (VWR International Ltd, Lutterworth, UK). Slides were stored at room temperature until required.

2.6.2 Frozen tissue

For microdissection of the murine growth plate, tissue was frozen so RNA could be efficiently extracted. Bone tissue samples were coated in 5% polyvinyl acetate (PVA) and then snap frozen in a cooled hexane bath for 30 seconds after which they were

stored at -80°C until use. Frozen sections were cut using a cryostat (OTF500/HS-001, Brights, Huntingdon, UK) with the knife blade angle set to 25°. Firstly, frozen tissue was embedded in optimal cutting temperature (OCT) embedding medium (Brights) and attached to a metal chuck. Following trimming of excess OCT, 30µm sections were cut at -30°C, and then stored at -80°C.

2.6.3 Haematoxylin and eosin and von kossa staining

Paraffin embedded metatarsal sections which had been processed as section 2.6.1 were stained for von kossa followed by haematoxylin and eosin (H&E) such that growth plate zone widths could be measured. Slides were de-waxed in xylene and rehydrated through a series of alcohols to dH_2O. They were then incubated with 5% silver nitrate (BDH, Poole, Dorset; in dH_2O) for 30 minutes under a strong light, washed in dH_2O and fixed in 2.5% sodium thiosulphate. The slides were then counterstained with H&E using Leica Autostainer and mounted in DePeX (VWR, Lutterworth, UK). The zone widths were measured at x4 magnification using a Nikon eclipse TE300 microscope with a digital camera attached, using Image Tool (Image Tool Version 3.00).

2.7 *In situ* hybridisation

2.7.1 MEPE plasmid

A murine *Mepe* IMAGE clone (ID: 8733911) was purchased as a glycerol stock (Source BioScience UK Ltd, Nottingham, UK). The *Mepe* IMAGE clone glycerol stock was streaked onto lysogeny broth (LB) media (Appendix I) ampicillin plates (100µg/ml) with a sterilised wire loop, and incubated at 37°C overnight with constant agitation for glycerol stocks and minipreps.

2.7.2 Preparation of glycerol stocks

Single colonies were picked from the streaked agar plates described in section 2.7.1. These were incubated in 5ml LB media containing 100µg/ml ampicillin at 37°C overnight with constant agitation. 10µl of the overnight culture was added to 4ml

LB media and incubated for approximately 7 hours at 37°C, again with constant agitation. This was then mixed with 2ml 50% glycerol and aliquoted for storage at -80°C until further use.

2.7.3 Minipreparation of plasmid DNA

The remaining bacterial culture was used for plasmid DNA production utilising the Qiagen miniprep spin kit (Appendix I) (West Sussex, UK) according to the manufacturer's instructions. Briefly the culture was spun at 17,900g for 10 minutes and re-suspended in 250µl buffer P1. The cells were then lysed by addition of 250µl buffer P2, and incubated at room temperature for 5 minutes. The genomic DNA and proteins were precipitated from the lysate by addition of 350µl buffer N3 and centrifuged at 17,900g for 15 minutes to clear the lysate. The supernatant was centrifuged through a Qiagen column containing a silica membrane to selectively adsorb plasmid DNA in the high salt buffer. The membrane was the washed with buffer PE and plasmid DNA eluted by centrifugation at 17,900g with 30µl buffer EB. DNA obtained was used for sequencing (The Sequencing Service, Dundee).

2.7.4 EndoFree maxipreparation of plasmid DNA

The Qiagen Endofree Maxiprep kit was used to isolate endotoxin-free plasmid DNA from bacterial cultures according to the manufacturer's instructions (Appendix I). Briefly, 250ml of LB (with 100µg/ml ampicillin) was inoculated with a 100µl aliquot of the liquid culture described in section 2.4.3 and grown overnight at 37°C with constant agitation. The bacterial cells were harvested by centrifugation at 6000g for 60 minutes at 4°C. The supernatant was removed and bacterial pellet re-suspended in 10ml buffer P1, the cells were then lysed by addition of 10 ml buffer P2, mixed thoroughly by inverting and incubated at room temperature for 5 minutes. The genomic DNA, proteins, cell debris, and sodium dodecyl sulphate (SDS) were precipitated by addition of 10 ml chilled buffer P3, which was mixed by inverting 4–6 times. The lysate was poured into the barrel of the QIAfilter cartridge and incubated at room temperature for 10 minutes. The lysate was then passed into a sterile tube and 2.5 ml buffer ER was added to remove endotoxin and incubated on

ice for 30 minutes. The filtered lysate was then applied to a QIAGEN-tip equilibrated with buffer QBT and allowed to enter the resin by gravity flow. The QIAGEN-tip was washed with 2 x 30 ml buffer QC. The DNA was eluted by addition of 15 ml buffer QN and precipitated through the addition of 0.7 volumes of room temperature isopropanol. This was mixed and centrifuged at 15000g for 90 minutes at 4°C to pellet the plasmid DNA. The supernatant was decanted and pellet washed with 5 ml of endotoxin-free 70% ethanol and centrifuged at 15000g for a further 30 minutes. The supernatant was decanted and the pellet left to air dry for 10 minutes. The DNA pellet was then re-dissolved in 100µl endotoxin-free buffer TE and stored at -80°C.

2.7.5 Restriction digest

Digestion of DNA using restriction enzymes (*Nco1*, Roche, Burgess Hill, West Sussex) was carried out for linearisation. A typical 10µl digest contained 1µg DNA, 1µl of *Nco1*, 1µl of the appropriate 10X reaction buffer and was made up with dH_20. Digests were left overnight at 37°C and then subjected to agarose gel electrophoresis. A 1% agarose gel was prepared using 1x Tris-actetic acid-EDTA (TAE) buffer (Appendix I). The agarose/TAE solution was supplemented with 0.1µl/ml SYBR-Safe, and poured into a mould (with a comb to form the wells) to set. The gel was submerged in TAE buffer and DNA samples were mixed with loading buffer (Bioline, London, UK) and loaded onto the gel. An electrical current of 120V was applied across the gel until the DNA fragments were separated according to their size. Fragments were visualised under ultraviolet (UV) light for linearisation.

2.7.6 Probe synthesis

Anti-sense and sense digoxigenin-labeled cRNA probes were synthesised using T3 and T7 RNA polymerases respectively (Roche). A typical 20µl reaction contained 1µg DNA, 2µl 10x NTP labelling mix, 2µl 10x transcription buffer, 1µl ribonuclease (RNase) inhibitor, 2µl Polymerase (T7 or T3) and then was made up with dH_2O. The reaction was left for 2 hours at 37°C. 2µl DNase I was added for 15 minutes

incubation at 37°C, before 2µl 0.2M EDTA was added. Both probes were stored at -80°C until further use.

2.7.7 *In situ* hybridisation technique

Hybridisations were completed following an optimised *in situ* hybridisation protocol from Imperial College London as previously detailed, using diethylpyrocarbonate (DEPC) treated equipment and reagents to diminish RNase contamination (Stevens *et al.* 2000). Paraffin embedded sections (as detailed in section 2.6.1) were de-waxed in xylene and rehydrated through a series of graded alcohols to dH_2O. The mRNA of these deparaffinized sections was exposed by digestion with 20µg/ml proteinase K in TE buffer for 15 minutes. Sections were acetylated in 0.1M triethanolamine and 0.3 M acetic anhydride for 10 minutes before washing, dehydrating, and drying. Hybridization solution (1X Denhardt's solution, 50% deionized formamide, 20% dextran sulfate, and 2µg probe) was heated to 80°C for 90 seconds, added to sections, and incubated overnight at 50°C. Sections were washed in 50% formamide in 0.15M NaCl, 5mM NaH_2PO_4, 5mM Tris/HCl, and 2.5mM EDTA (pH 6.8) at 50°C for 30 minutes followed by washing in TNE buffer at room temperature every 10 minutes for 1 hour at constant agitation. 3% bovine serum albumin (BSA) in 100mM Tris/Cl and 150mM NaCl (pH 7.5), was added to sections for 1 hour. ALP-conjugated antidigoxygenin Fab fragments (Roche) were diluted 1:500 in blocking solution and added for 1 hour at room temperature. Slides were washed in PBS and developed in nitroblue tetrazolium chlorine/5-bromo-4-chloro-3-indolyl-phosphate-4-toluidine to detect ALP. The sections were rinsed in tap water and counterstained with haematoxylin using Leica Autostainer XL. Finally, sections were dehydrated through graded alcohols, cleared with xylene and mounted in DePeX

2.8 Microdissection of the murine growth plate

Frozen sections as detailed in section 2.6.2 were briefly thawed and then passaged through the following solutions at room temperature, for 1 minute each: 70% ethanol, 100% methanol for fixing, 95% ethanol for washing, staining in eosin (0.2%

eosin, 0.5% acetic acid, 75% ethanol). Stained slides were then washed in 70% ethanol, dehydrated in 100% ethanol, and finally placed in xylene. Throughout the microdissection technique, sections were kept under a xylene droplet. Using an inverted microscope, razor blades and hypodermic needles, growth plate sections were separated into zones of proliferating chondrocytes, hypertrophic chondrocytes and metaphyseal bone based upon the histology of the growth plate as previously described (Nilsson *et al.* 2007). For each zone, tissue dissected from both proximal tibial growth plates of three animals (14–22 sections) was pooled in 2.88µl β-mercaptoethanol and 400µl Solution C (0.322g guanidine thiocyanate, 0.377ml nuclease free water (NFW), 0.023ml 0.75M sodium citrate).

RNA isolation was performed as previously described (Heinrichs *et al.* 1994). Samples were diluted in 300µl of buffered proteinase K solution (Appendix I). Following a 20 minute digestion at room temperature, RNA was extracted by centrifugation in the presence of 150µl of buffer saturated phenol and 150µl chloroform: Isoamyl alcohol. 40µl of 3M sodium acetate (pH5.2) added to the aqueous phase, along with an equal volume of isopropanol (approximately 440µl). The RNA was precipitated at -20°C overnight and collected by centrifugation at 13,900g for 30 minutes. The resulting pellet was washed in 75% ethanol, dried and re-suspended in 20µl DEPC-treated water. 20µl of 8M lithium chloride was added for a second RNA precipitation step at -20°C for 3 hours and collected by centrifugation at 17,900g for 30 minutes. The supernatant was discarded leaving the final pellet which was washed with 75% ethanol, allowed to dry and stored in 10µl DEPC-treated water at -80°C until required.

2.9 Immunohistochemistry

For immunohistochemical analysis, paraffin embedded sections (as detailed in section 2.6.1) were de-waxed in xylene and rehydrated through a series of graded alcohols to dH_2O. Antibodies were purchased and concentrations used as to Appendix III. For the cathepsin B antibody, sections were incubated at 37°C for 30

minutes in 0.1% trypsin for demasking. For the MEPE-ASARM antibodies, sections were incubated for 1 hour at 37°C in citric acid buffer for demasking. Endogenous peroxidise activity was blocked by treatment with 0.03% H_2O_2 in methanol for 30 minutes at room temperature.

From this point onwards, the Vectastain ABC kit (Vector Laboratories, Peterborough, UK) was used according to the manufacturer's instructions. Sections were given 3 x 5 minute washes in PBS and blocked in blocking buffer (1:50 dilution of the appropriate normal serum in PBS) for 30 minutes at room temperature. The sections were then incubated in primary antibody, which was diluted to an appropriate concentration in blocking buffer (Appendix III), at 4°C overnight. Unbound primary antibody was removed by 3 x 5 minute washes in PBS and the sections were then incubated in the appropriate secondary antibody (Appendix III) at room temperature for 30 minutes. After 3 x 5 minute washes in PBS, sections were incubated with ABC reagent (avidin and horseradish peroxidise (HRP)) for 30 minutes at room temperature before further 3 x 5 minutes washes in PBS. Staining was then developed in diaminobenzidine (DAB) solution (0.06% DAB in 0.1% H_2O_2 in PBS) for 5 minutes. The sections were rinsed in tap water and counterstained with haematoxylin using Leica Autostainer XL. Finally, sections were dehydrated through graded alcohols, cleared with xylene and mounted in DePeX.

2.10 ATDC5 transfections

2.10.1 ATDC5 blasticidin kill curve

It is routinely recommended to perform a kill curve for each species, strain, and medium used to determine the appropriate concentration of blasticidin to use for selecting resistant cells (Gong *et al.* 2005). Therefore ATDC5 cells were seeded at 1.5 x 10^5 cells/cm^2 in a 12 well plate and supplemented with varying concentrations of blasticidin ranging from 5-35μg/ml. Cell death was observed upon the detachment of the cells from the culture plastic and an approximation of the total number of dead cells as a percentage of the viable cells was calculated (Fig. 2.1).

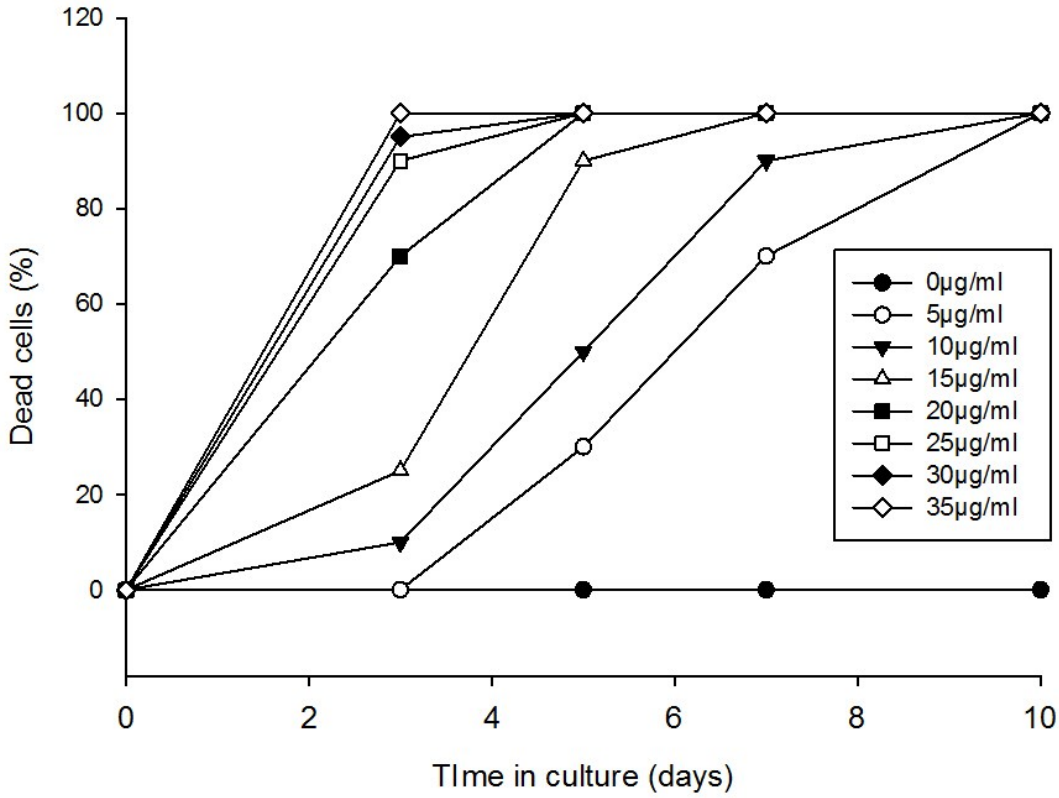

Figure 2.1 ATDC5 blasticidin kill curve

Percentage of ATDC5 cells killed upon addition of varying concentrations of blasticidin over a 10-day culture period.

2.10.2 MEPE overexpressing and knockdown vectors

pLZ2-Ub.MEPE overexpressing and pLZ2-Ub.Empty vectors were a kind gift from Dr Neil Mackenzie (The University of Edinburgh). MEPE shRNA vectors were purchased as glycerol stocks from Sigma (Appendix IV).

2.10.3 Transfection of ATDC5 cells

For ATDC5 transfection, FuGENE HD (Roche) was used. ATDC5 cells were maintained in differentiation medium as previously described (section 2.2.1) and seeded in $10cm^2$ culture dishes at a density of 1.5×10^6 cells/$10cm^2$. The cells were transfected when 60-70% confluent. The transfection mix was prepared in Opti-Mem media containing MEPE-overexpressing and shRNA knockdown constructs at a ratio of 7:2 FuGENE HD to DNA. This was pre-incubated at room temperature for 15 minutes and the transfection reagent:DNA complex added to ATDC5 cells in a drop-wise manner. The cells were incubated in a humidified atmosphere (37^oC, 5% CO_2) for 48 hours, after which the medium was changed to maintenance media containing 20μg/ml blasticidin as determined by the ATDC5 blasticidin kill curve (Fig. 2.1) (section 2.10.1).

2.10.4 Growing single colonies of transfected cells

Blasticidin resistant individual colonies, originating from single cells, were picked using cloning cylinders, expanded in differentiation medium containing blasticidin to maintain selection pressure, frozen and maintained at -150^oC until further use. Three MEPE-overexpressing and three empty-vector clones were picked for analysis.

2.11 Viral transduction of metatarsals

2.11.1 Cell culture

For tissue culture, all liquid waste was aspirated into 1% Virkon solution. Any plastic-ware that was in contact with lentivirus particles was incubated in 1% Virkon solution for at least 24 hours. All cells were maintained at 37^oC with 5% CO_2

For lentiviral techniques, two cell types were used; Human embryonic kidney fibroblasts (293T, a kind gift form Dr. Simon Lillico, The University of Edinburgh), and D17 (canine osteosarcoma, ATCC, Teddington, UK).

2.11.2 Transfections

For each virus, 4 x T175 flasks were seeded at $0.9x10^6$ HEK293T cells in 6mls media (Appendix I). Cells were incubated for 24 hours and transfected at 70-80% confluency. The transfection media was prepared in 4ml Optim-Mem media containing 56μg of the lentiviral packaging plasmid psPAX2, 28μg of the viral envelope coding plasmid vesicular stomatitis Indiana virus – G protein (VSV-G), and 42μg of the packaging plasmid for MEPE, or the empty-vector control. To this, 476μl Fugene HD was carefully added according to the manufacturer's instructions, and incubated at room temperature for 15 minutes. The transfection mix was then carefully added to the HEK293T cells prior to overnight incubation at 37°C, 5% CO_2.

2.11.3 Viral harvest

The supernatant containing viral particles released from the packaging cells was removed from each of the flasks at 24 and 48 hours post transfection. The supernatant was centrifuged at 2000g for 5 minutes to remove any large cell debris. The 24 hour harvest was stored at 4°C overnight until the 48 hour harvest was removed, after which the harvests were combined and then filtered through a 0.45μm filter unit (Nalgene, USA) prior to concentration.

2.11.4 Concentration of virus

The viral harvest was centrifuged at 7000g at 4°C in a Sorval RC6 centrifuge overnight. The pellet was then resuspended in 10mls TSSM for 30 minutes at 4°C with careful agitation, and after 30 minutes the pellet was broken up by careful pipetting, ensuring no bubbles are introduced as these are thought to damage the envelope proteins of the virus. The viral harvest was then transferred to a Beckman ultra-centrifuge tube, topped up to 13ml with PBS to ensure the tube was full prior to centrifugation at 20,000g for 2 hours at 4°C in a Beckman XL-70 ultra-centrifuge.

The virus was re-suspended by incubation for 1 hour in 200µl TSSM buffer at 4°C with gentle agitation. The resultant suspension was centrifuged at 100g for 5 minutes to remove cellular debris and the concentrated virus was aliquoted and stored at -80°C.

2.11.5 D17 cell blasticidin kill curve

As in section 2.10.1, to determine the optimum concentration of blasticidin required to kill all non-transfected cells, D17 cells (derived from canine osteosarcoma) were seeded at 1.5 x 10^5 cells/cm^2 in a 12 well plate and supplemented with concentrations of blasticidin ranging from 5-35µg/ml. Cell death was observed upon the detachment of the cells from the culture plastic and an approximation of the total number of dead cells as a percentage of the viable cells was calculated (Fig. 2.2).

2.11.6 Titration

6 x 10-fold dilutions of the concentrated virus were made in D17 cell medium supplemented with 8µg/ml Polybrene, starting with a 1/1000 dilution. 500µl of each virus were added to D17 cells in duplicate and incubated for 4-6 hours before a further 500µl medium was added. The cells were incubated for 8 days, in the presences of 20µg/ml blasticidin (Fig. 2.2) with a full medium change after 48 hours. Colonies were then counted and the number multiplied by the dilution factor and doubled to give a value for effective transducing units in D17 cells per ml of virus (TU_{1080}/ml).

2.11.7 Transduction of E15 metatarsals

To examine the transduction efficiency and for proof of concept, GFP virus particles (a kind gift from Dr. Neil Mackenzie, The University of Edinburgh) were added to E15 metatarsals on day 0 of culture with 0.6µl Polybrene at a concentration of 2 x 10^6 virus particles/metatarsal bone. Due to production limitations, MEPE-overexpressing and empty-vector viruses were added to metatarsal bones at a concentration of 6 x 10^4 virus particles/metatarsal bone with

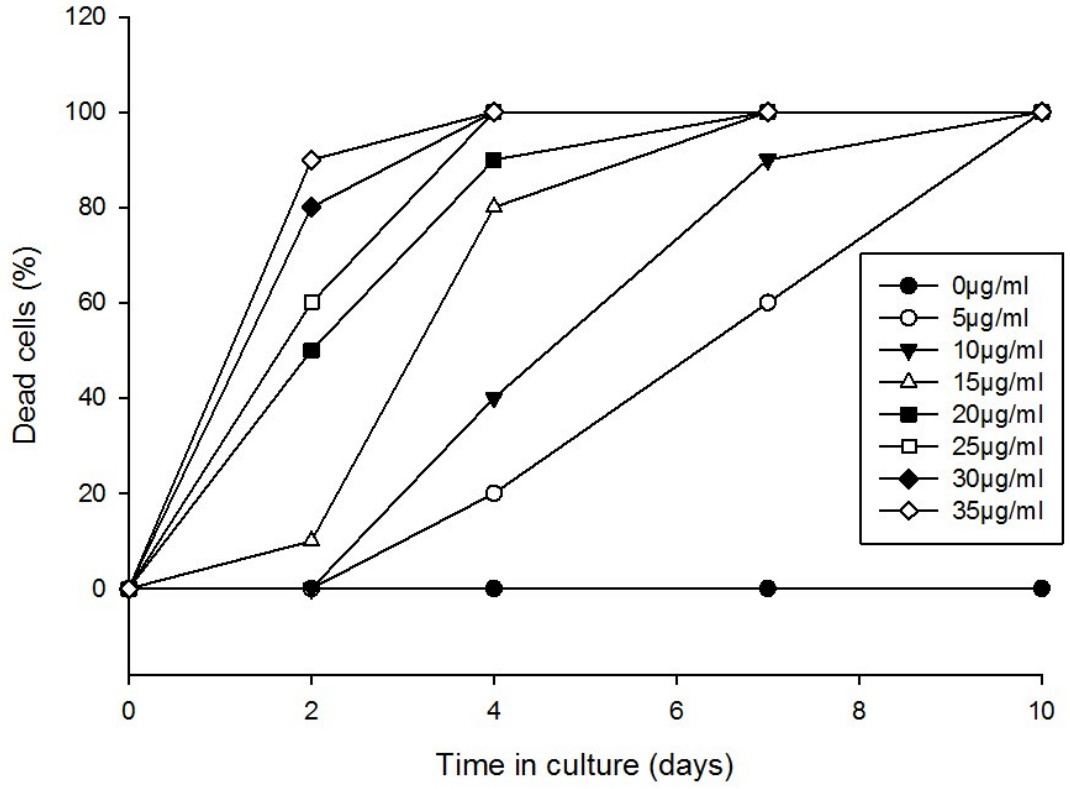

Figure. 2.2 D17 blasticidin kill curve

Percentage of D17 cells killed upon addition of varying concentrations of blasticidin over a 10-day culture period.

0.6µl Polybrene on day 0 of culture. Bones were left in a humidified atmosphere for up to 12 days.

2.11.8 Morphometric analysis of lentiviral murine metatarsals

Metatarsals transducted with GFP lentivirus particles were visualised using a Nikon EC1 inverted confocal microscope. MEPE-overexpressing and empty-vector metatarsals were morphometrically analysed as described in section 2.5.2.

2.12 RNA methods

2.12.1 Isolation of total RNA from cells

Cells (ATDC5 and primary chondrocytes) were scraped from individual wells in 500µl PBS, pelleted and stored at -80°C. RNA was extracted using a Qiagen RNeasy Kit, according to the manufacturer's instructions. The concentration and quality (the ratio of wavelengths 260nm/280nm) of RNA was measured using a nanodrop spectrophometer (Thermo Scientific, UK). Samples were diluted to the same concentration (that of the lowest sample) in NFW.

2.12.2 Isolation of total RNA from metatarsals

For metatarsal organ cultures, 4 bones from each control or experimental group were pooled in 100µl Trizol reagent at days 5 and 7 of culture, and RNA extracted according to the manufacturer's instructions. Briefly, metatarsals were homogenised using a small hand-held homogeniser and frozen at -80°C until use. 20µl chloroform was added to samples and inverted to mix. This was incubated for 3 minutes at room temperature before being centrifuged at 12,000g for 15 minutes at 4°C. The aqueous phase was removed and 50µl isopropanol was added, mixed and incubated at room temperature for 10 minutes. Samples were centrifuged for 10 minutes at 4°C at 12,000g. The supernatant was discarded and the pellet was washed with 100µl 75% ethanol, centrifuged at 7500g for 5 minutes at 4°C and air-dried in a sterile hood for 10 minutes. The RNA pellet was then dissolved in 20µl RNase-free H_2O, and then stored at -80°C until further use.

2.12.3 Reverse transcription

Complementary DNA (cDNA) was prepared from total RNA using the enzyme reverse transcriptase II. 10µl diluted RNA was incubated with 2µl random hexamers (random primers diluted 1:60; Invitrogen) at 70°C for 10 minutes in a Hybaid polymerase chain reaction (PCR) Express Thermal cycler (Thermo Scientific). The sample was then rapidly cooled on ice. A master mix of 2µl 10X PCR Reaction buffer, 2µl $MgCl_2$ (25mM), 2µl dithiothreitol (DTT) (0.1M), 1µl deoxyribonucleotide triphosphate (dNTP) mix (10mM) and 1µl Superscript II RNase H enzyme was prepared and 8µl was added to each sample. The samples were run on the following programme in the Hybaid PCR machine: 25°C for 10 minutes; 42ºC for 50 minutes; 70°C for 15 minutes and held at 4°C. The neat cDNA samples were stored at -20°C.

2.12.4 PCR

cDNA was diluted to 25ng/µl in NFW. Primers were obtained as to Appendix II. A master mix of primer pairs (1µl), Comp A (11.4µl), Comp B (0.6µl) was prepared and 13µl of this was added to 4µl of cDNA template. Samples were run for 40 cycles. A 1.5% agarose gel was prepared containing 2.5µl SYBRsafe DNA gel stain. 4µl 5x loading buffer (Bioline, London, UK) was added to each sample and samples were loaded onto the gel at a volume of 12µl before the gel was run at 150V for 45 minutes. PCR products were visualised under UV light using a Gel Logic 200 Imaging System and software (Kodak). After completion, DNA bands were cut out of the gel and DNA purified using a Qiaquick Gel Extraction Kit (Qiagen). DNA was sent off for sequencing to The Sequencing Service, University of Dundee.

2.12.5 Quantitative polymerase chain reaction (qPCR)

qPCR reactions were conducted in a 96 well plate (Thermo Scientific) and cycled in a Stratagene Mx3000P PCR cycler (Agilent Technologies, Santa Clara, USA). Primers were purchased as Appendix II. Reactions using primers purchased from Primer Design (Southampton, UK) contained 50ng (5µl) cDNA template, 200nM forward and reverse primer, 10µl 2x FastStart Universal SYBR Green Master Mix (Roche)

and was made up to a volume of 20µl with H_2O. The qPCR reaction was cycled using the following protocol: 1 cycle of 95°C for 10 minutes followed by 50 cycles of 95°C for 15 seconds and 60°C for 60 seconds. Reactions using primers purchased from MWG Eurofins (London, UK) contained 50ng (5µl) cDNA template, 0.5µl forward primer (10pmol/µl), 0.5µl reverse primer (10pmol/µl), 6.5µl NFW, and 12.5µl FastStart Universal SYBR Green Master Mix (ROX) (Roche). The qPCR reaction was cycled using the following protocol: 1 cycle of 2 minutes at 50°C, and then 2 minutes at 95°C, followed by 40 cycles of 95°C for 15 seconds, 60°C for 30 seconds, 95°C for 1 minute, 60°C for 30 seconds, 95°C for 15 seconds and finally 25°C for 30 seconds. A reaction of H_2O in place of cDNA was also amplified as a negative control.

2.12.6 Optimisation of qPCR primers

To test primer efficiency, serial dilutions of cDNA (known to express the gene of interest) were used to create a standard graph line. Primers were considered acceptable if the amplification efficiency was within the range of 90-110%, with an R^2 value between 0.90 and 1.00, and an amplification curve with sigmoid curves at regular intervals along the dilution series. Primer specificity was demonstrated by the generation of a single peak in the dissociation curve.

2.12.7 Quantification of gene expression

Each sample was tested in triplicate and compared to a housekeeping gene using MxPro software (Cheshire, UK). The relative expression of the analysed genes was calculated using the $\Delta\Delta C_T$ method (Livak and Schmittgen 2001) whereby an arbitrary amplification threshold is set and relative expression levels of the samples are determined by comparison of the number of amplification cycles required to cross this threshold (C_T).

2.13 Protein Methods

2.13.1 Protein extraction

Cell monolayers (ATDC5 and primary chondrocytes) were rinsed in ice-cold PBS and scraped in an appropriate volume of radio-immunoprecipitation assay (RIPA) buffer (Appendix I) containing 0.15 x volume of Complete mini protease inhibitor cocktail (Roche). Samples were vortexed and stored at -20^{o}C until further use.

2.13.2 Quantification of protein

Once thawed, samples were vortexed aggressively and pelleted. The supernatant was removed and its protein content was determined using Bio-Rad DC Protein Assay reagents (Bio-Rad Laboratories, Hertfordshire, UK). Standards were made using lyophilised bovine plasma gamma globulin protein, 2mg/ml (Bio-Rad Laboratories) in RIPA buffer. Into each well of a 96-well plates, 5µl sample/standard, 25µl Reagent A' (containing 20µl Reagent S per ml Reagent A) and 200µl Reagent B was added. Protein levels were then measured using a Multiskan Ascent plate reader at 690nm. The protein concentration in each sample was calculated from the standard curve.

2.13.3 Western blot

Appropriate volumes of 4x lithium dodecyl sulfate (LDS) sample buffer and reducing agent DTT were added to the protein samples as was calculated from the DC assay (section 2.13.2). The same quantity of protein was added for each sample, depending on the lowest yield achieved. The concentration used was in 10-30ug protein range. Samples were denatured at 70°C for 10 minutes. The denatured protein samples and a pre-stained molecular weight marker (All Blue, Bio-Rad, Hemel Hempstead, UK) were then loaded onto a pre-cast 10% Bis-Tris gel (Invitrogen). The gel was run in 1xMOPS running buffer at 200V for 40 minutes to separate the proteins using an XCell surelock western blot module. Protein transfer onto a Hybond-Electrochemiluminescence (ECL) Nitrocellulose membrane (GE

Healthcare, Buckinghamshire, UK) was conducted on ice in a transfer module at 30V for 2 hours.

Following transfer, the nitrocellulose was washed in TBS/T (Tris-buffered saline/Tween-20) and blocked overnight at 4°C in 5% dried skimmed milk/3% BSA/0.1% normal serum of the species which the secondary antibody is raised in. Primary antibody was prepared as detailed in Appendix III in 5% BSA TBS/T. The nitrocellulose was incubated with primary antibody at 4°C overnight. The nitrocellulose was rinsed with TBS/T before probing with the relevant secondary antibody (Appendix III). Nitrocellulose membranes were incubated with secondary antibody for 1.5 hours at room temperature and washed in TBS/T. Bound antibody was detected by chemiluminescence with Amersham ECL Western blotting detection reagents A and B (GE Healthcare) at a 1:1 ratio. Chemiluminescence was detected with Amersham ECL Hyperfilm (GE Healthcare), which was developed using a Medical Film Processor (SRX-101A; Konica Minolta, Banbury, UK).

2.13.4 Stripping nitrocellulose

Nitrocellulose membranes were stripped of antibody by incubating in 20ml Restore Western Blot Stripping buffer (Thermo Scientific) at 37°C for 30 minutes. Antibody detection by chemiluminescence was repeated to ensure bound antibody had been removed. In the event of significant antibody remaining, this was repeated.

2.14 Cell proliferation and differentiation assays

2.14.1 [^{3}H]-thymidine incorporation assay

On day 7 of culture, 3µCi/ml [^{3}H]-thymidine (Amersham Biosciences, Little Chalfont, UK) was added to each metatarsal for the last 6 hours of culture (Mushtaq *et al.* 2004). After washing in PBS (3x15min), the unbound thymidine was extracted using 5% trichloroacetic acid (2x30min). Metatarsals were then washed in PBS before being solubilised (NCS-II tissue solubiliser, 0.5N, Amersham) at 60°C for 1

hour. The DNA incorporating [^{3}H]-thymidine was determined using a scintillation counter (Wallac 1410; Pharmacia Biotech, Uppsala, Sweden).

2.14.2 ALP activity

At the end of the culture period, ALP activity within the ATDC5 cells and the metatarsal bones was determined. The ATDC5 cell layer was lysed in 0.9% NaCl and 0.2% Triton X-100 and centrifuged at 12,000g for 15 min at 4^{o}C. The supernatant was assayed for protein content and ALP activity (Farquharson *et al.* 1995). Each metatarsal was permeabilised in 100µl of 10mmol/litre glycine (pH 10.5) containing 0.1mmol/litre $MgCl_2$, 0.01mmol/litre $ZnCl_2$, and 0.1% Triton X-100 by freeze-thawing three times (Mushtaq *et al.* 2004). Each extract was assayed for ALP activity by measuring the rate of cleavage of 10mM *p*-nitrophenyl phosphate. Total ALP activity was expressed as nanomoles *p*-nitrophenyl phosphate hydrolysed per minute per metatarsal bone.

2.15 Statistical analysis

Data were checked to be normally distributed using a Kolmogorov-Smirnov normality test using Sigma Plot (Sigma Plot 11; Germany). Data were analysed by one-way analysis of variance (ANOVA) for which suitable post-tests for multiple comparisons were conducted, or the Student's t-test. If data were not normally distributed, a suitable non-parametric test was performed. All data are expressed as the mean ± standard error of the mean (SEM). Statistical analysis was performed using Sigma Plot and $P<0.05$ was considered to be significant.

Chapter 3

Establishing a suitable *in vitro* model of chondrocyte matrix mineralisation

3.1 Introduction

The growth plate and its primary cell type, the chondrocyte, are integral to endochondral ossification and thus the linear growth of the long bones (Kronenberg 2003). In humans, non-invasive methods have to be adopted to study bone development thus limiting investigation into the mechanisms and interactions involved. However, the development of *in vitro* methods such as cell lines, primary chondrocytes, and the metatarsal organ culture model, has opened a new chapter in chondrocyte biology.

To investigate chondrogenic differentiation and matrix mineralisation, various clonal cell model systems have been employed including CFK-2 (Bernier & Goltzman 1993), RCJ3.1C5 (Grigoriadis *et al.* 1996), HCS-2/8 (Takigawa *et al.* 1989), and ATDC5 cells (Atsumi *et al.* 1990). First isolated from the differentiating teratocarcinoma stem cell line AT805, the ATDC5 cell is proving popular in chondrocyte *in vitro* research - to date, there are almost 300 studies in which this cell line has been utilised (Atsumi *et al.* 1990). ATDC5 cells differentiate specifically to a chondrocyte phenotype when in the presence of insulin, as evidenced by the expression of *Col2a1, Col10a1* and aggrecan, typical markers for chondrogenesis (Atsumi *et al.* 1990). In culture, ATDC5 cells proliferate and grow to a point at which the spontaneous cessation of growth occurs. Then, an assimilation of hypertrophic cell appearance, *Col10a1* mRNA expression and increased ALP enzyme activity indicates the potential for ATDC5 cells to mineralise their surrounding ECM (Shukunami *et al.* 1996). The ATDC5 cartilage nodules formed stain positive for alizarin red, therefore indicating effective ECM mineralisation, after 5 weeks in culture. Electron microscopy and electron probe microanalysis confirmed that the mineral was initially formed in the MVs, and then deposited along the axis of the collagen fibril orientation, as is observed during *in vivo* endochondral ossification. Furthermore, the mineral formed by these ATDC5 cells is similar to apatitic mineral, as shown by FT-IR analysis (Shukunami *et al.* 1997).

However, the method developed by Shukunami *et al.*, not only comprises of an impractical culture time period, but also requires a change of culture conditions. Both the cell culture medium and the CO_2 concentration have to be altered after 21 days of culture to facilitate mineralisation. For this reason, various studies have attempted to simplify the culture method whilst maintaining the chondrogenic differentiation and formation of physiological mineral. One such study found that as well as changing the culture conditions at day 21 of culture, the addition of 4mM P_i to the cells at this time point initiated mineralisation within 8 hours, and strongly increased it after 24 hours. After 7 days of culture in the presence of P_i, the mineral formed by these cells was deemed physiological by TEM and FT-IR assessment. Despite this, the sudden and seemingly spontaneous onset of mineralisation in this culture system questions its physiological relevance as a model of *in vivo* endochondral ossification (Magne *et al.* 2003). Another study has detailed that the addition of ascorbic acid shortened the proliferation phase of the ATDC5 cells from 21 days to 7 days (Altaf *et al.* 2006). Whilst the temporal expressions of markers of chondrogenic differentiation were examined, the mineralisation capability of the ATDC5 cells under these culture conditions was not. Therefore, the development of an ATDC5 culture model which produces both consistent chondrogenesis and ECM mineralisation in a more physiological and practical time period would be of great benefit in aiding chondrocyte research.

It is however well recognised that transformed cell lines may not represent the primary cells from which they were developed. For this reason, primary chondrocytes isolated from different anatomical regions have been widely used as a more physiologically relevant model to study chondrogenesis. However, it is widely known that the de-differentiation of primary chondrocyte cells in monolayer culture is a common occurrence, and a major problem. Once cultured, primary chondrocytes adopt a flattened and elongated morphology that resembles that of a fibroblast as opposed to the more spheroidal morphology expected of a chondrocyte (Abbott & Holtzer 1966). This de-differentiation is associated with an upregulation

of various genes not associated with chondrogenesis, most notably *Col1a1* (Lefebvre *et al.* 1994; Hering *et al.* 1994). It has been suggested that this phenomenon is in part related to the seeding density of the cells, as well as the medium in which the cells are cultured in (Hering *et al.* 1994; Ronziere *et al.* 1997). Despite these limitations, methods which allow for the differentiation and subsequent ECM mineralisation by the primary chondrocyte cells have previously been detailed (Garimella *et al.* 2004; Gartland *et al.* 2005; Rodriguez *et al.* 2005). A full characterisation of the cellular differentiation and mineral formed has not however been conducted thus, whether primary chondrocytes are a reliable model for chondrocyte matrix mineralisation is yet to be elucidated.

The use of bone organ cultures in bone research was pioneered more than 50 years ago by Dame Honor Fell, and since then various types of bones have been used; neonatal calvaria, foetal long bones and metatarsal bones (Fell & Mellanby 1952). Embryonic metatarsal bones provide a physiological model for studying endochondral ossification and bone growth as the growth rate of the bones mimics that seen *in vivo*. Moreover, it allows for the separation of systemic and local factors therefore permitting the specific analysis of the local effects on the growth plate. Uniquely, the metatarsal organ culture allows the examination of chondrocytes in different phases of chondrogenesis and maintains cell-cell and cell-matrix interactions, therefore providing conditions closer to the *in vivo* situation than cells in culture (Scheven & Hamilton 1991; Coxam *et al.* 1996). Foetal murine metatarsal bones isolated at different ages, and therefore at different developmental stages, have been utilised as models of longitudinal bone growth. However, like primary chondrocyte cultures, the assessment of their mineralisation capability has yet to be fully characterised.

It is imperative that a model of endochondral ossification is reproducible, reliable, and retains both the expected stages of chondrogenic differentiation as well as the formation of physiological mineral. Although various models exist, their full

characterisation is required to aid future chondrocyte research and ultimately to develop novel therapeutic methods.

3.2 Hypothesis

The onset of mineralisation in the ATDC5 cell line can be reduced by the addition of ascorbic acid and βGP. The differentiation of ATDC5 cells and of primary chondrocytes is characterised by the expression of chondrogenic markers, and the mineral formed resembles that of true physiological hydroxyapatite. As such, the ATDC5 cell line and primary chondrocytes can be used as suitable models for endochondral ossification. Furthermore, the isolation and culture of foetal metatarsal bones at different developmental stages provides a suitable model of chondrocyte matrix mineralisation.

3.3 Aims

I Establish the temporal ECM formation and associated expression patterns of chondrocyte differentiation markers of the ATDC5 cell line and of the primary chondrocyte cell model

II Determine the suitability of the ATDC5 cell line as a model for mineralisation through analysis of the mineral formed

III Examine the use of embryonic metatarsal organ cultures as a model for both bone growth and mineralisation at different developmental stages

3.4 Materials and Methods

3.4.1 ATDC5 and primary cell culture

ATDC5 cells were seeded at 6 x 10^4 cells/cm^2 in differentiation media and when confluent, were supplemented with 10mM βGP and 50μg/ml ascorbic acid, as described in section 2.2.1. For levamisole experiments, ATDC5 cells were cultured in varying concentrations of levamisole (0-1000μM) for up to 15 days. Primary

costochondral chondrocytes were isolated from 1-3 day old mice and cultured as described in section 2.2.3. Confluent primary cultures were maintained for up to 28 days in primary chondrocyte media supplemented with 10mM βGP and 50μg/ml ascorbic acid.

3.4.2 ECM formation

As outlined in section 2.4.2, to assess the formation of the ECM, ATDC5 cells and primary chondrocytes were stained with alcian blue having been fixed in 95% methanol. Staining was quantified by spectrophotometry.

3.4.3 Mineralisation

The ECM mineralisation of ATDC5 cells and primary chondrocytes was assessed by alizarin red staining. Cell monolayers were fixed at defined time points in 4% PFA and staining was quantified by spectrophotometry as detailed in section 2.4.1.

3.4.4 Analysis of ATDC5 mineral deposition

ATDC5 cells were maintained in culture for 41 days in differentiation media, as described in section 2.2.1. Cells were then fixed in 95% methanol and embedded in LR white resin (see section 2.3.1). Mineral was analysed by FT-IR in the laboratory of Professor Adele Boskey (Hospital for Special Surgery, New York).

3.4.5 Ultrastructural imaging of ATDC5 mineral deposition

ATDC5 cells were seeded on nitrocellulose discs and cultured in mineralising conditions for 16 days. Cell monolayers were processed for TEM as detailed in section 2.3.2 by Steve Mitchell (University of Edinburgh). Samples were visualised using a Phillips CMIRO TEM and images taken on a Gatan Orius ICD camera.

3.4.6 qPCR analysis of chondrocyte differentiation and ECM mineralisation genes

At defined time points, RNA samples were extracted from ATDC5 cells and primary chondrocytes using a Qiagen RNeasy kit according to the manufacturer's instructions. cDNA was prepared (section 2.12.3) and was used at 10ng/μl for qPCR analysis, as detailed in section 2.12.5. Results were normalised to the *18S*

housekeeping gene and the relative gene expression level was calculated using the ΔΔCt method (Livak & Schmittgen 2001).

3.4.7 Metatarsal organ culture

The middle three metatarsals of E17 and E15 mice were isolated under a dissecting microscope, as described in section 2.5.2. Metatarsals were cultured in metatarsal media for up to 10 days. The total length of the bone through the centre of the mineralising zone was determined using image analysis software (DS Camera Control Unit DS-L1; Nikon) every second or third day. The length of the central mineralisation zone was also measured.

3.4.8 Lactate dehydrogenase activity

Lactate dehydrogenase (LDH) activity was determined in the culture medium of 15-day-old 0mM and 10mM βGP treated ATDC5 cells using a kit from Roche Diagnostics (Lewes, East Sussex, UK). LDH activity was related to the total LDH activity of the cultures.

3.5 Results

3.5.1 Chondrogenic differentiation of ATDC5 cells

ATDC5 cell monolayers reached confluence after six days of culture and adopted a more spheroidal morphology (Fig. 3.1A). At this point, ATDC5 cells were cultured with the addition of βGP, a commonly used organic phosphate source (Coe *et al.* 1992), and ascorbic acid which is required for collagen processing and secretion into the ECM and has previously been shown to reduce the onset of mineralisation (Altaf *et al.* 2006). This initiated cell condensation and the formation of cell aggregates, which produce a vast ECM (Fig 3.1B). In the centre of these condensations, the cells become hypertrophic and increase in size which is the main drive for longitudinal bone growth, as discussed in section 1.2.2.3. The cells mineralise their surrounding extracellular matrix as visualised at day 15 of culture (Fig. 3.1C). From this point onwards, mineral formation radiates throughout the culture monolayer (Fig. 3.1D).

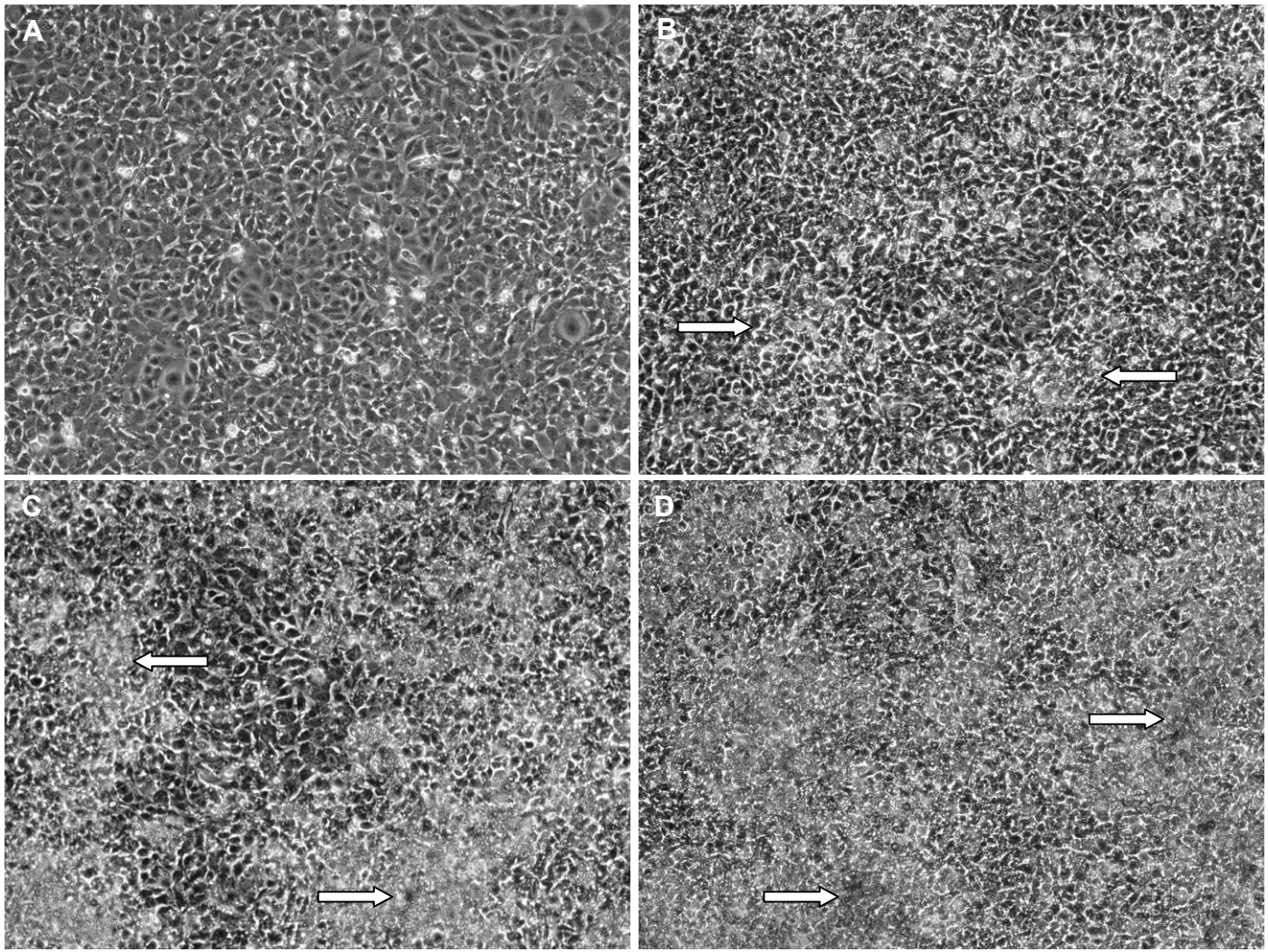

Figure 3.1 Phase contrast images of ATDC5 cell cultures

Phase contrast images of ATDC5 cells cultured for up to 20 days in the presence of ascorbic acid and βGP (**A)** Day 6. Cells reach confluency by day 6 of culture and have a spheroidal morphology (**B)** Day 10. By this point, cells begin to condense and form aggregates whilst producing large volumes of ECM (arrows) (**C)** Day 15. Opaque regions form in the ECM which indicate mineral formation (arrows) (**D)** Day 20. Cell aggregations conjoin and mineralisation increases (arrows). Scale bars are 1mm.

The formation of an ECM is a vital component of chondrogenic differentiation. ATDC5 monolayers began to form their ECM at day 8 of culture, as visualised by alcian blue staining for glycosaminoglycans (Fig. 3.2A). This was increased throughout the time course (Fig. 3.2B), significantly so between days 13 and 10 ($P<0.01$), days 15 and 13 ($P<0.01$), and days 17 and 15 ($P<0.001$). In comparison to day 8, alcian blue staining was significantly increased from day 13 onwards ($P<0.001$). This provided indication that the ATDC5 cells underwent the expected stages of differentiation observed in endochondral ossification. Furthermore mRNA expression levels of *Col2a1*, the major component of the cartilage ECM, were significantly increased at day 10 of culture in comparison to day 8 of culture ($P<0.05$, Fig. 3.2C). Concomitant with this, the mRNA expression of *Col10a1* increased at days 13 and 17 of culture, as is in concordance with its specific expression by the hypertrophic chondrocytes (in comparison to day 8 of culture, $P<0.001$, Fig. 3.2D).

3.5.2 Mineralisation of ATDC5 cell matrix

The deposition of mineral by ATDC5 cells was determined by alizarin red staining and quantified by spectrophotometry. For maximal mineralisation at day 15 of culture, ATDC5 cells require culturing in the presence of both insulin and βGP, as indicated by the significantly reduced alizarin red staining when ATDC5 cells were cultured without these components ($P<0.001$, in comparison to ATDC5 cells cultured in the presence of both insulin and βGP, Fig. 3.3C). ATDC5 cells were therefore cultured in media containing insulin, with the addition of βGP over a 20-day culture period. Alizarin red positive mineral formation was observed initially at day 13 of culture. At day 15, mineral formation was significantly increased in comparison to day 13 of culture ($P<0.001$), and from this point onwards, mineral formation was significantly increased in comparison to day 8 of culture ($P<0.001$, (Figs. 3.3A & B). The levels of *Alpl* mRNA expression, for the membrane bound enzyme ALP, were examined throughout the culture period. *Alpl* mRNA increased up to day 15 of culture ($P<0.001$ compared to day 8, Fig. 3.3D) after which it decreased at day 17 ($P<0.01$ compared to day 15), and remained so at day 20 of

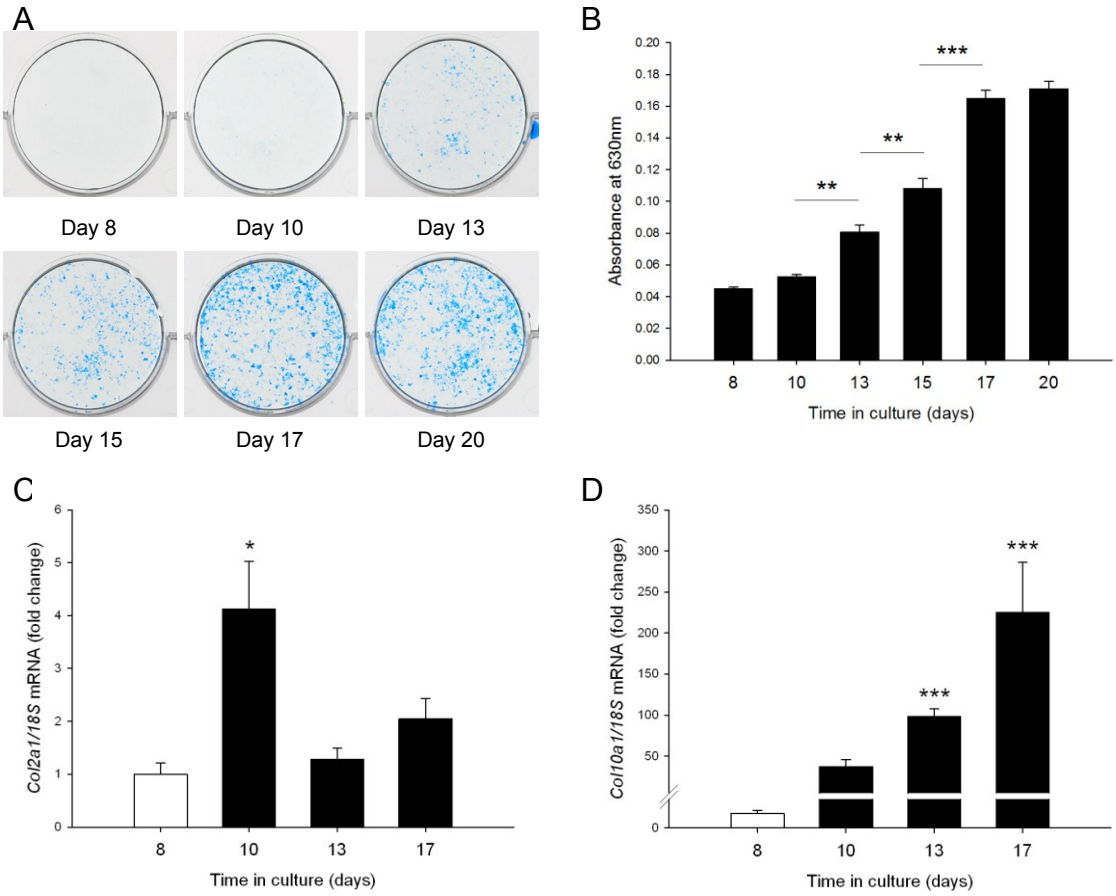

Figure 3.2 The chondrogenic differentiation of ATDC5 cells

(A) Alcian blue staining of ATDC5 cells cultured in the presence of ascorbic acid and βGP for up to 20 days (**B)** Quantification of alcian blue staining by spectrophotometry. From day 13 onwards, staining was significantly increased in comparison to day 8 (P<0.001). Significance between consecutive time points is indicated on graph (**C)** *Col2a1* mRNA expression in ATDC5 cells as determined by qPCR in comparison to day 8 (**D)** *Col10a1* mRNA expression in ATDC5 cells as determined by qPCR in comparison to day 8. Data are represented as mean ± S.E.M (n=3 replicates) *P<0.05, **P<0.01, ***P<0.001.

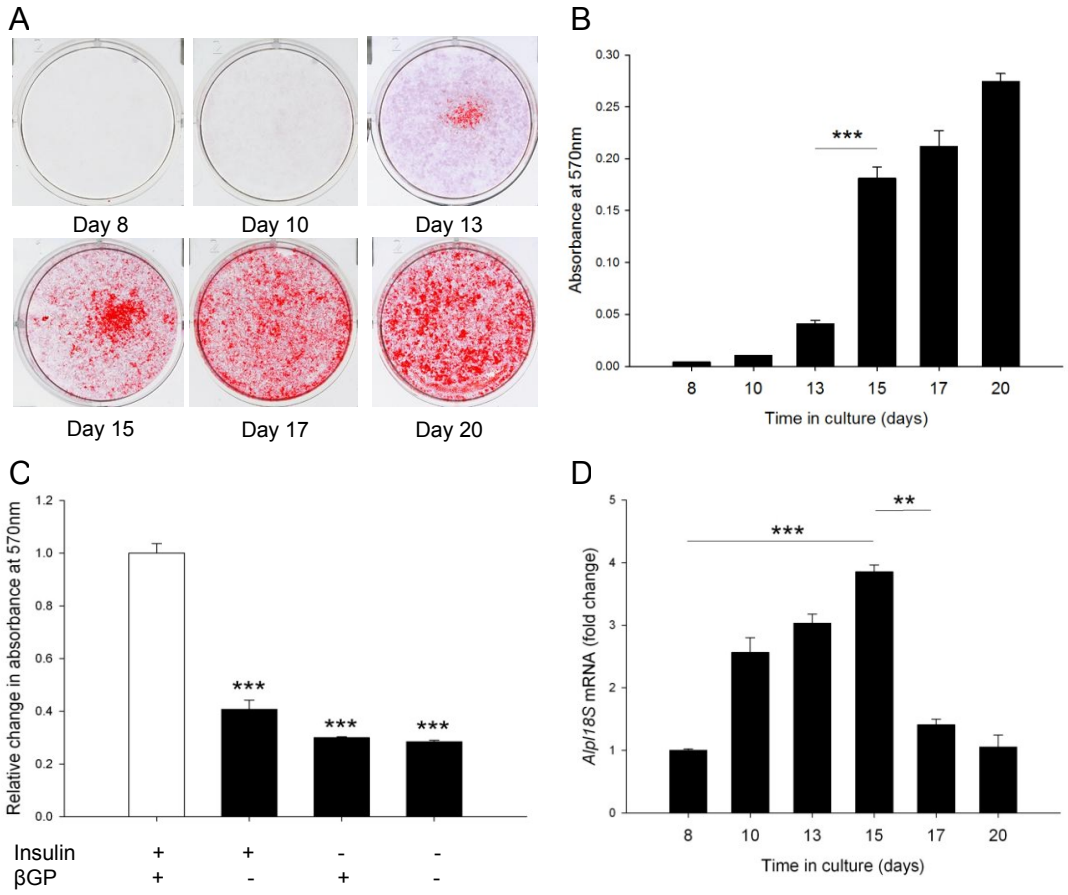

Figure 3.3 Mineralisation of ATDC5 cell cultures

(A) Alizarin red staining of ATDC5 cells cultured in the presence of ascorbic acid and βGP for up to 20 days (**B)** Quantification of alizarin red staining by spectrophotometry. From day 15 onwards, staining was significantly increased in comparison to day 8 ($P<0.001$). Significance between consecutive time points is indicated on graph (**C)** Effects of culturing without insulin and/or βGP on ATDC5 cell ECM mineralisation in comparison to cells cultured in the presence of both insulin and βGP (**D)** *Alpl* mRNA expression in ATDC5 cells by qPCR. Data are represented as mean ± S.E.M (n=3 replicates) **P<0.01, ***P<0.001.

culture (Fig. 3.3D). The use of βGP in cell culture is rather controversial, with studies detailing the formation of dystrophic mineral that does not resemble true physiologic hydroxyapatite (Khouja *et al.* 1990). Levamisole, a well-established inhibitor of ALP, was therefore added to ATDC5 cultures. Levamisole inhibited ATDC5 ECM mineralisation at concentrations in excess of 300μM at day 15 of culture ($P<0.001$) (Figs. 3.4A & B) with no apparent alterations in the ATDC5 cells morphology. This therefore indicates that the enzyme ALP is required and the mineral formed is not simply a precipitation of calcium and P_i and therefore dystrophic.

Furthermore, FT-IR and TEM were adopted as two well recognised methods to determine whether the mineral formed in culture is similar to that which forms in nature (Boskey & Roy 2008). The mineral formed was assessed at the ultrastructural level by TEM. Mineral deposition was observed which appeared to be aligned along the axis of the collagen fibrils, as is seen in endochondral ossification (Fig. 3.5A-C). The spectrum formed by analysis of the ATDC5 cell cultures was similar to that formed by E14 embryonic bone, with similarities in the regions of interest to the 4-week-old post-natal bone (Fig. 3.5D). The parameters of ATDC5 cell ECM mineralisation shown here were also comparable to that seen in embryonic bone (Table 3.1) (Anderson *et al.* 2004; Boskey *et al.* 2009b).

3.5.3 Characterisation of the primary chondrocyte model

To examine whether primary chondrocytes can be used as a reliable model for chondrocyte matrix mineralisation, cells were isolated from 1-3 day old mice and cultured at a density of 10^5 cells/cm^2, in the presence of ascorbic acid and βGP. After 9 days in culture, primary chondrocytes appeared confluent and had begun to form aggregations. Cells were producing large volumes of ECM as indicated by alcian blue staining for glycosaminoglycans (Figs. 3.6A-D). By day 14, cells had begun to mineralise their surrounding ECM as shown in the phase contrast images (Fig. 3.7B). This was confirmed by quantification of alizarin red staining (compared to

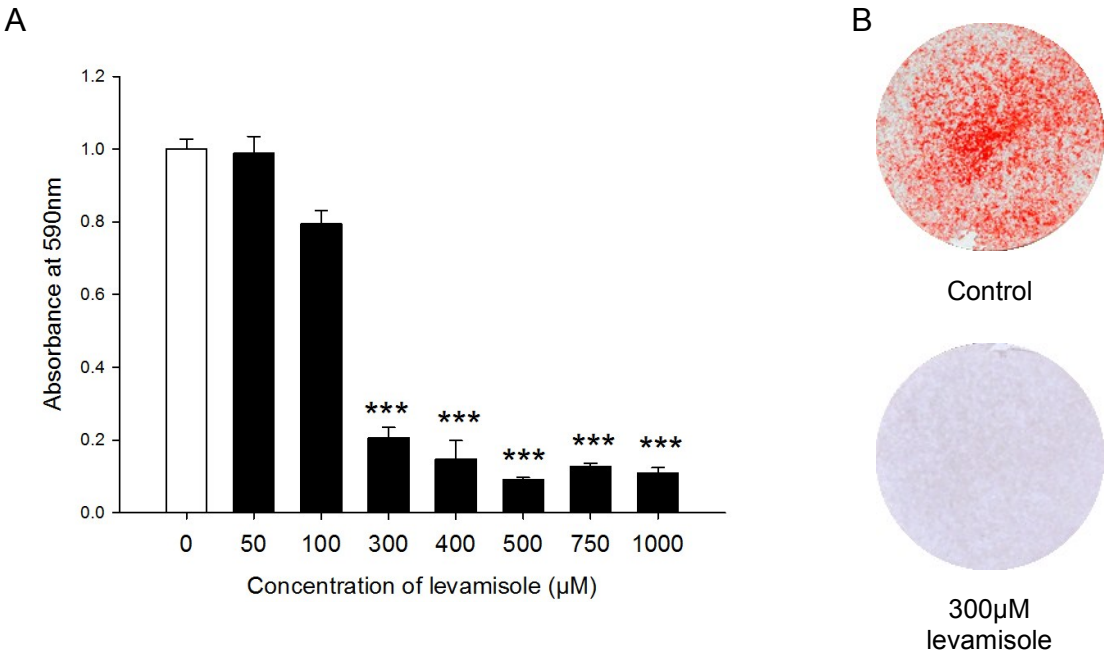

Figure 3.4 Levamisole inhibits mineralisation of ATDC5 cultures

Levamisole, an inhibitor of ALP enzyme activity, was added to ATDC5 cell cultures from when they reached confluency **(A)** Levamisole dose dependently inhibited ATDC5 ECM mineralisation as indicated by quantification of alizarin red staining **(B)** Alizarin red stained images of control cells and cells treated with 300μM levamisole at day 15 of culture. Data are represented as mean ± SEM (n=3 replicates) in comparison to 0μM levamisole ***P<0.001.

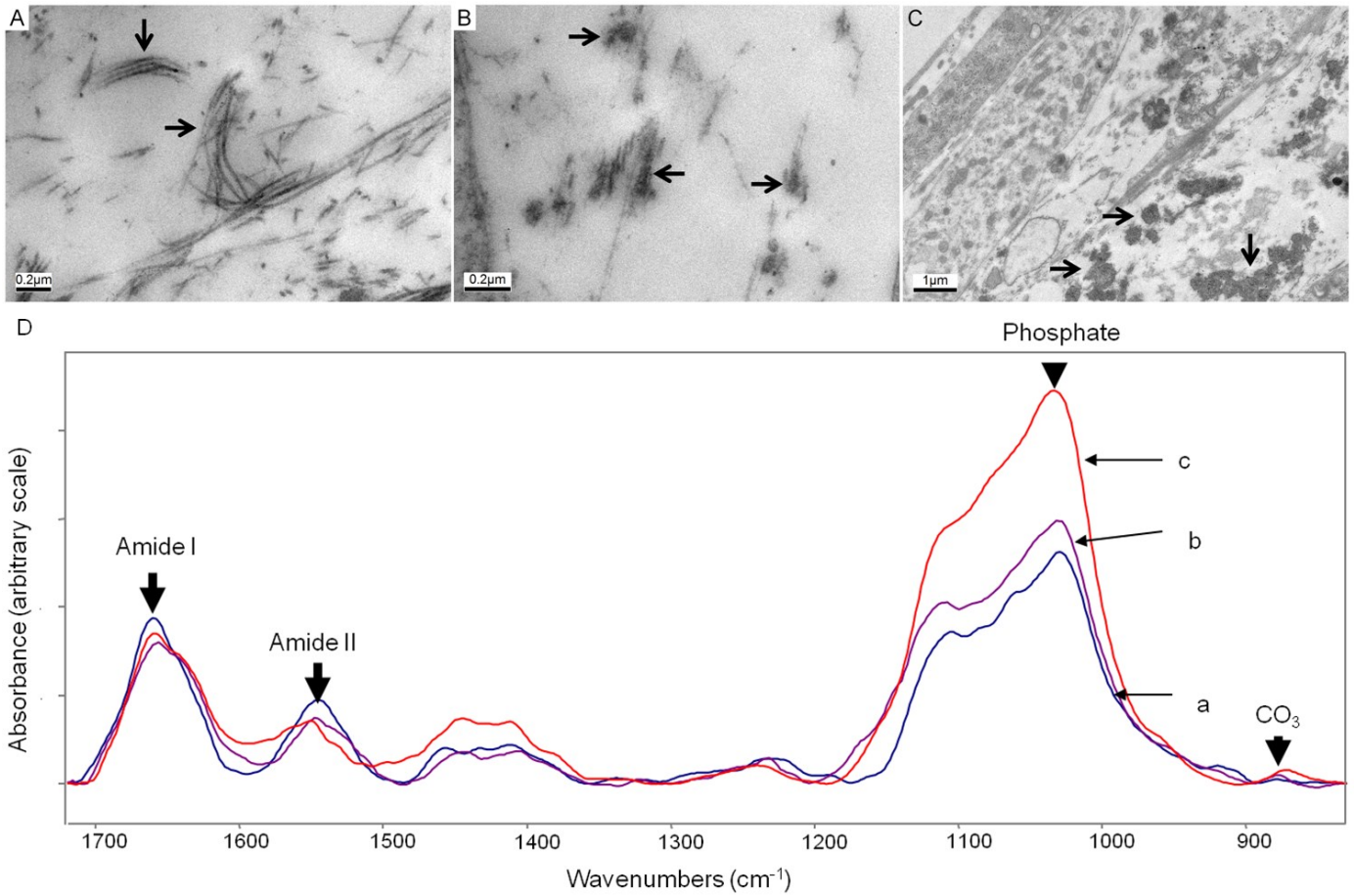

Figure 3.5 Analysis of ATDC5 cell mineral deposition

Transmission electron microscopy images of ATDC5 cultures at day 16 of culture **(A)** Collagen fibres are present in the ECM (arrows) **(B)** Mineral deposition can be seen along collagen fibres; arrows indicate an electron-dense material, likely to be mineralisation spreading along the collagen fibres within the ECM **(C)** Mineral deposition within the ECM (arrows) **(D)** FT-IR analysis of **(a)** ATDC5 monolayer at 41 days of culture; **(b)** mineralised embryonic mouse bone at E14; **(c)** cortical bone from the tibia of four-month old mouse. Absorbance of the phosphate peaks (900-1200 cm^{-1}), which represents mineralisation, and the amide-I peak (1585-1725 cm^{-1}), which indicates protein, were used to estimate the mineral-to-matrix ratio of the mineralised ECM. Absorbance values for each plot are arbitrary and not to scale.

Sample	Mineral-to-matrix	Carbonate-to-mineral	Crystallinity
A	3.000 ± 0.917	0.008 ± 0.005	1.128 ± 0.009
B	2.200 ± 2.500	0.005 ± 0.002	1.072 ± 0.062
C	6.500 ± 0.900	0.006 ± 0.001	1.130 ± 0.030

Table 3.1 Mineralisation parameters from FT-IR analysis

Using peak areas from FT-IR spectra, the mineral-to-matrix ratio (900-1200 cm^{-1} / 1585-1725 cm^{-1}), carbonate-to-mineral ratio (850-950 cm^{-1} / 900-1200 cm^{-1}) and crystallinity (1030 cm^{-1} / 1020 cm^{-1}) were calculated for mineralised regions of (**A)** ATDC5 monolayer grown to 41 days of culture, (**B)** mineralised E14 mouse bone, (**C)** cortical bone from the tibia of four-month old mouse.

day 7, P<0.001) (Figs. 3.7C & D). This alizarin red staining for mineral significantly increased at day 21 of culture and remained so at day 28 (compared to day 8, P<0.001) (Fig. 3.7E).

Although primary chondrocytes are commonly used their de-differentiation in monolayer culture is well documented (Abbott & Holtzer 1966; Hering *et al.* 1994; Lefebvre *et al.* 1994). Therefore, to fully establish the chondrogenic differentiation of the primary chondrocytes used in this model, *Col10a1*, *Col2a1* and *Col1a1* mRNA expression was assessed by qPCR throughout the culture period. Rather surprisingly, the mRNA expression of *Col2a1* decreased throughout the culture period (compared to day 7, P<0.05) (Fig. 3.8A), as did that of *Col10a1* (compared to day 7, P<0.05) (Fig. 3.8B). Rather, it would be expected that the mRNA expression of these genes would increase during the culture period. Therefore, this is not indicative of normal chondrogenic differentiation as is observed in the ATDC5 cultures (Fig. 3.5) and suggests that the primary chondrocytes had indeed de-differentiated. This was further confirmed by the mRNA expression pattern of *Col1a1* which would be expected to be negligible in these cultures. However mRNA expression increased at day 14 of culture (in comparison to day 7, P<0.01) before decreasing at days 21 and 28 of culture (at day 28, in comparison to day 14, P<0.001) (Fig. 3.9).

3.5.4 Embryonic metatarsal organ culture

When isolated, E17 metatarsal bones display a central core of mineralised cartilage juxtaposed by a translucent area on both sides representing the hypertrophic chondrocytes (Fig. 3.10B). These metatarsal bones increased in total length (up to 80% compared to day 0, P<0.001) (Figs. 3.10B, C & E) after 10 days in culture in the presence of βGP. Concomitant to this, the length of the mineralisation zone also increased (up to 590%, compared to day 0, P<0.01) (Figs. 3.10B, C & D). When isolated at an earlier time point (E15), metatarsal bones consist of early proliferating cartilage and there is no evidence of a mineralised core (Fig. 3.11B). After 6 days in

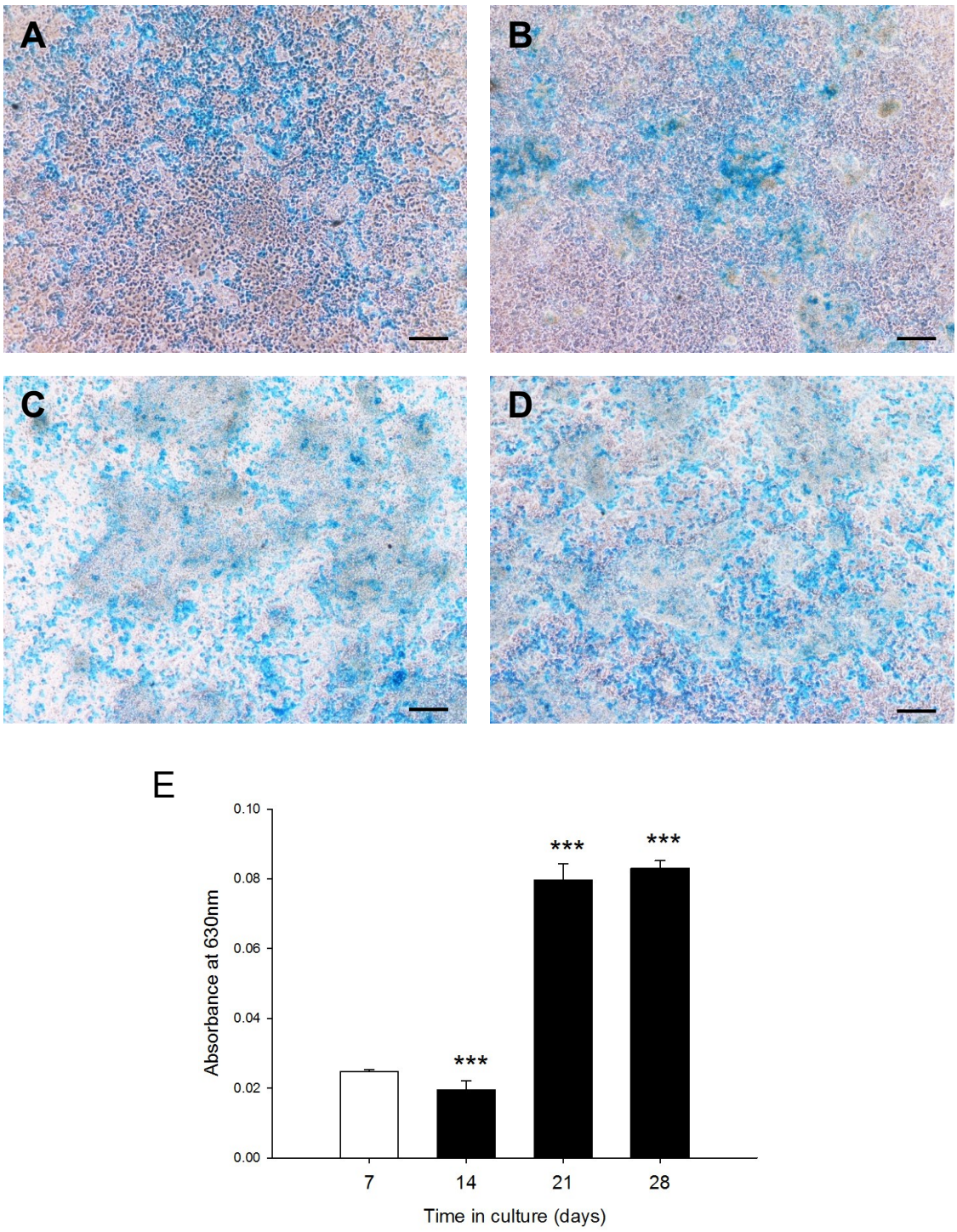

Figure 3.6 De-differentiation of primary chondrocyte cell cultures

Phase contrast images of alcian blue stained primary chondrocytes at **(A)** day 7 **(B)** day 14 **(C)** day 21 and **(D)** day 28 of culture. Alcian blue staining increased throughout the culture period as quantified by spectrophotometry **(E)**. Data are represented as mean ± SEM (n=3 replicates) in comparison to day 7 of culture ***P<0.001. Scale bar 0.1mm.

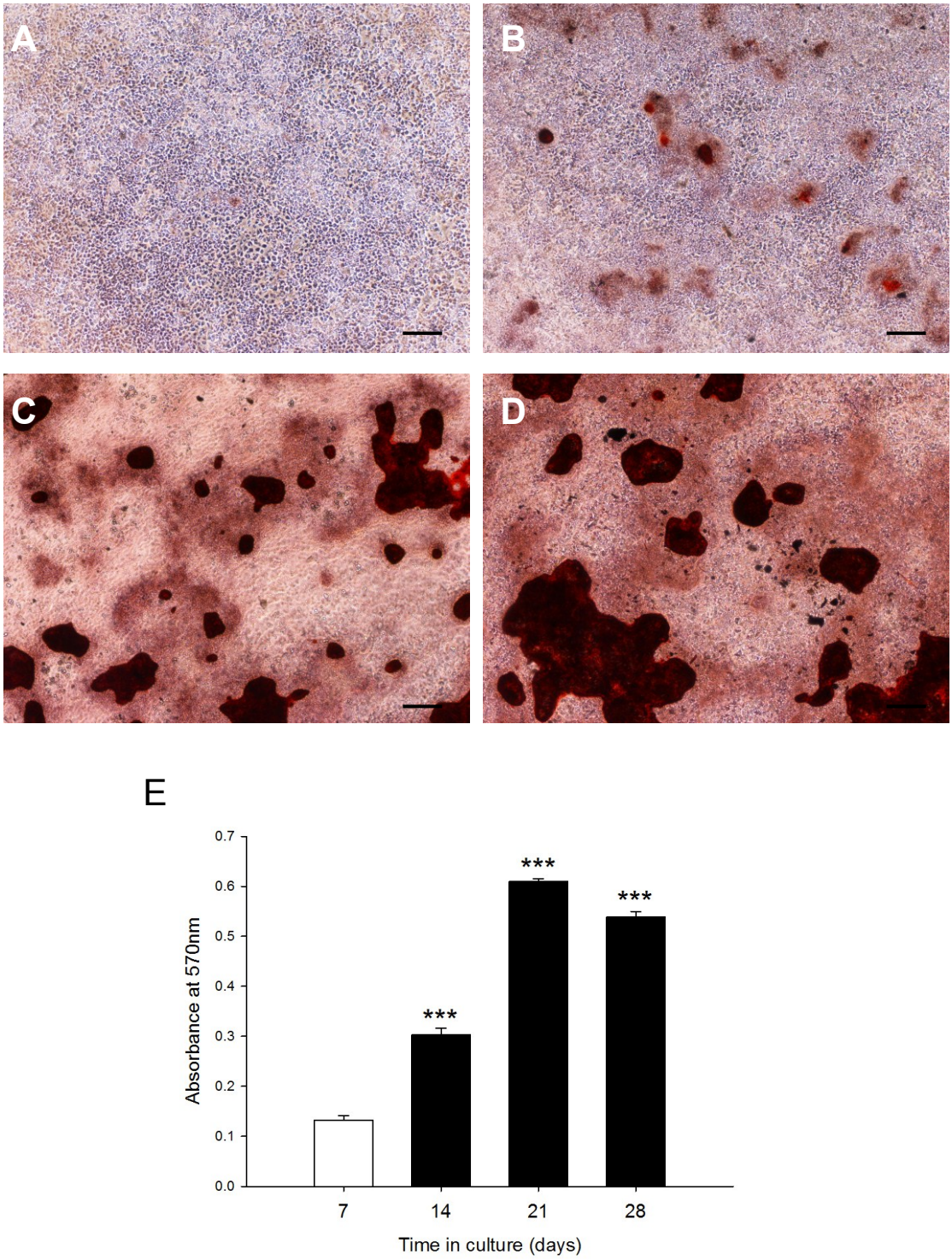

Figure 3.7 Mineralisation of primary chondrocyte cell cultures

Phase contrast images of alizarin red stained primary chondrocytes at **(A)** day 7 **(B)** day 14 **(C)** day 21 and **(D)** day 28 of culture. Alizarin red staining increased throughout the culture period as quantified by spectrophotometry **(E)**. Data are represented as mean ± SEM (n=3 replicates) in comparison to day 7 of culture ***P<0.001. Scale bar 0.1mm.

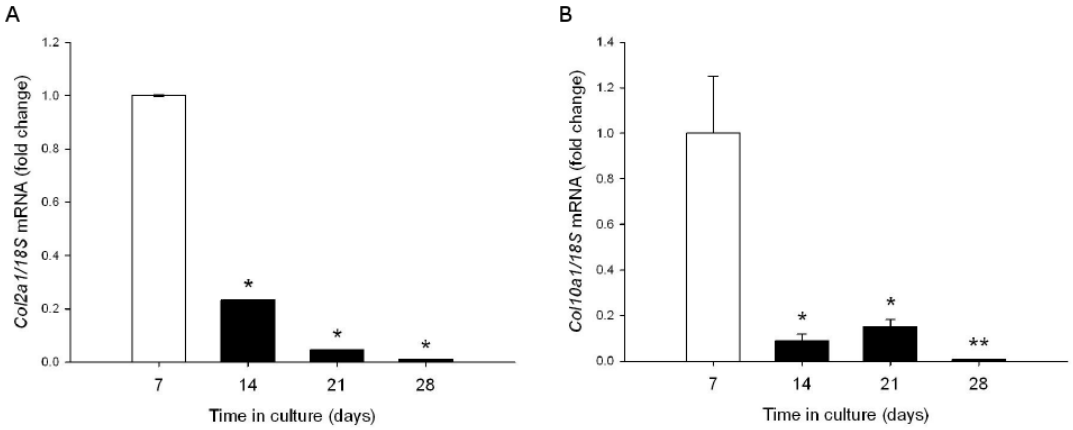

Figure 3.8 Decreased expression of *Col2a1* and *Col10a1* mRNA in primary chondrocyte cultures

The temporal expression pattern of the chondrogenic marker genes **(A)** *Col2a1* **(B)** *Col10a1.* Data are represented as mean ± SEM (n=3 replicates) in comparison to day 7 of culture *P<0.05, **P<0.01.

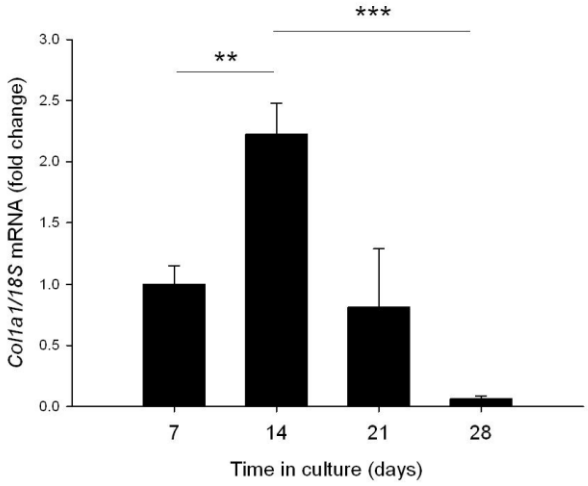

Figure 3.9 Temporal expression of *Col1a1* mRNA expression

The mRNA expression pattern of *Col1a1* in primary chondrocytes over a 28 day culture period. Data are represented as mean ± SEM (n=3 replicates) **P<0.01, ***P<0.001.

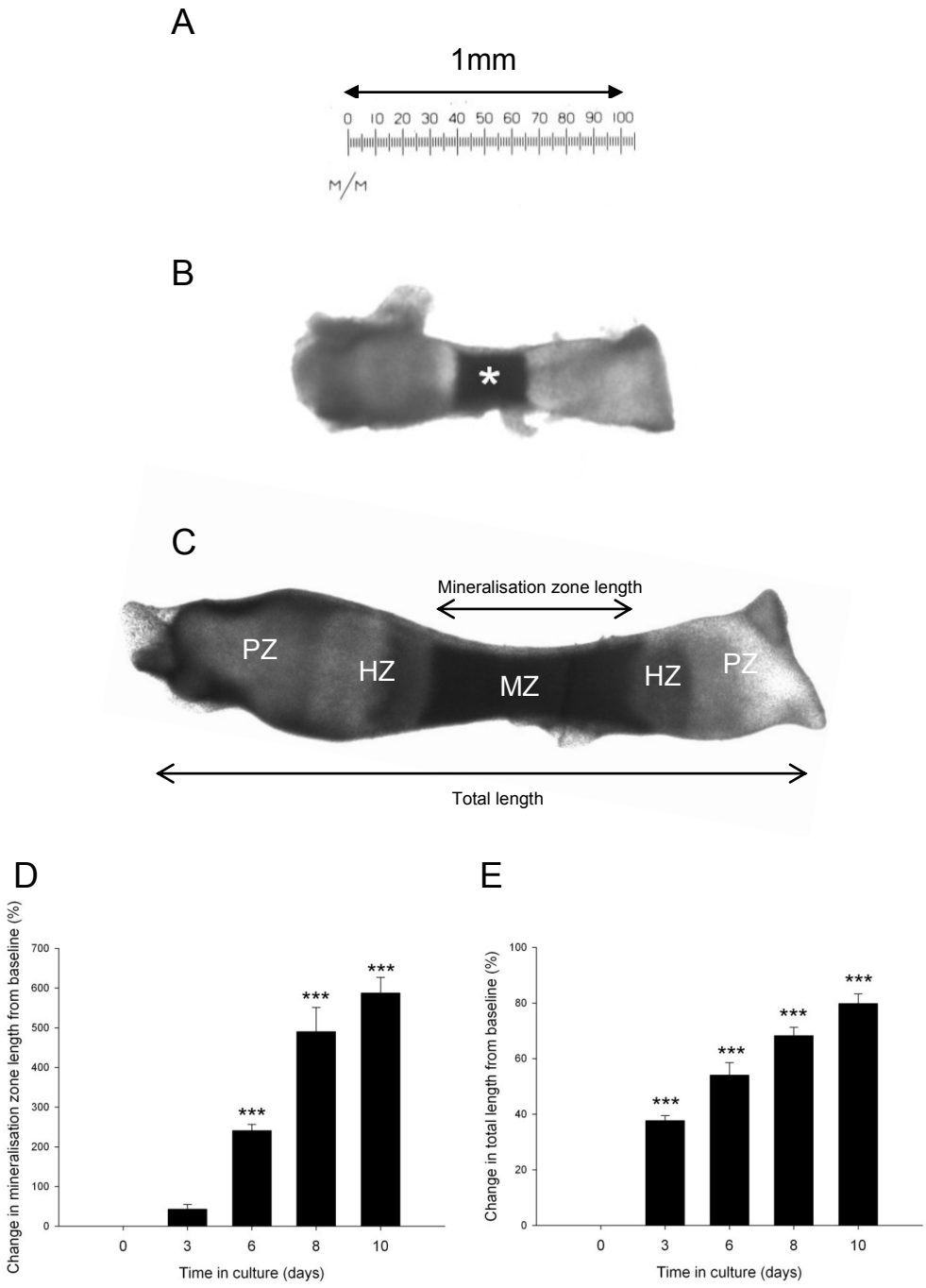

Figure 3.10 Growth trajectory and mineralisation capability of E17 metatarsal bones

Measurements of digital images of E17 mouse metatarsal bones in culture with clearly delineated mineralising zones **(A)** Calibrated ruler used for metatarsal length measurements **(B)** E17 metatarsal bone on day of harvest, termed day 0 of culture. Clearly shown are the locations of the proliferating (PZ), hypertrophic (HZ) and mineralising (MZ) zones, as well as the total length measurement **(C)** E17 metatarsal bone after 10 days in culture **(D)** Percentage change in the length of the MZ from baseline, taken on the day 0 **(E)** Percentage change in the total metatarsal length from baseline over the 10 day culture period. Data are represented as mean ± SEM of six bones in comparison to day 0 measurements, ***P<0.001.

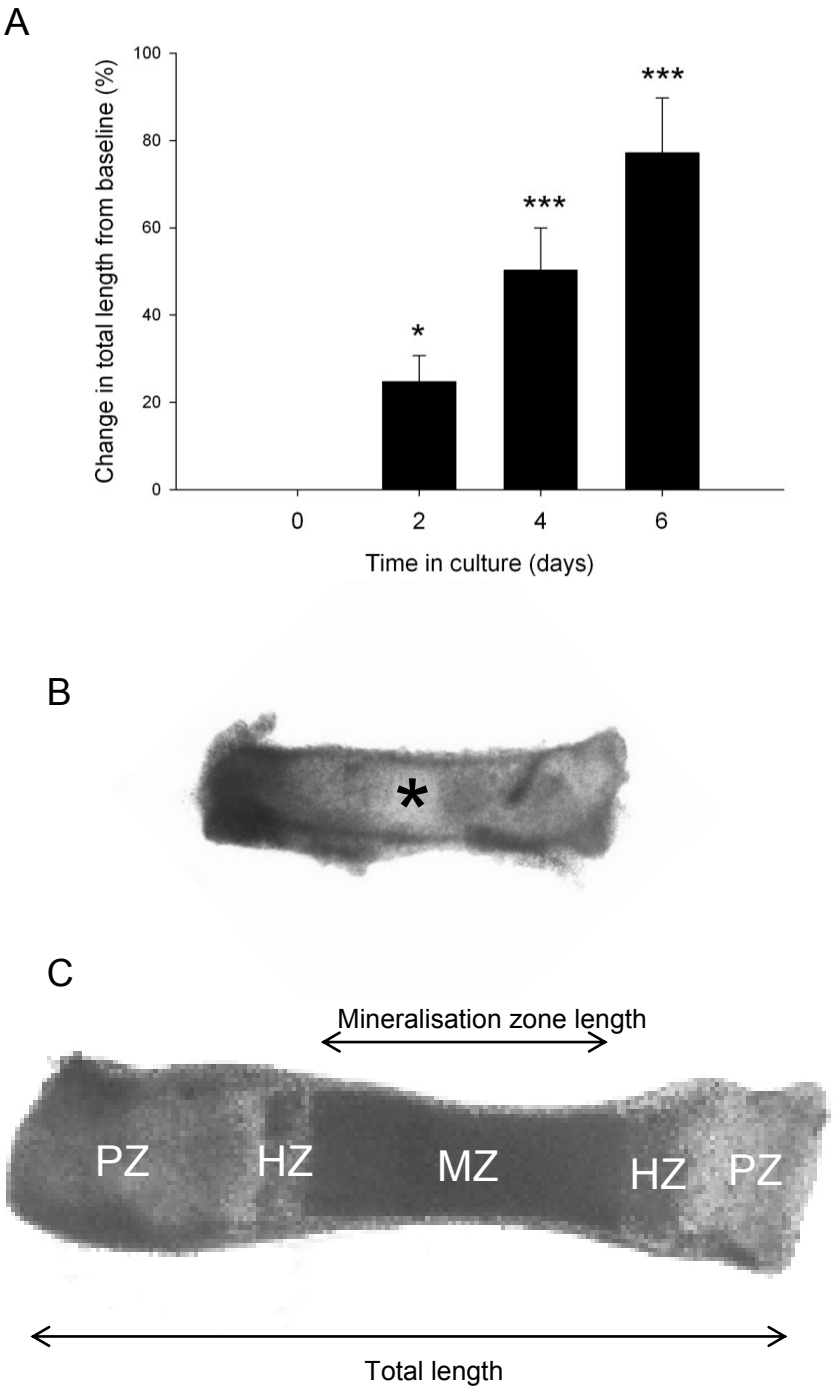

Figure 3.11 Growth trajectory and mineralisation capability of E15 metatarsal bones

Measurements of digital images of E15 mouse metatarsal bones in culture **(A)** Percentage change in the total metatarsal length from baseline over the 6 day culture period **(B)** E15 metatarsal bone on day of harvest, termed day 0 of culture. The bones consist of proliferating cartilage and no evidence of a mineralised core (asterisk) **(C)** E15 metatarsal bone after 6 days of culture. The total length of the bone is increased and the central core of mineralised cartilage has formed (MZ). The hypertrophic zone (HZ) and proliferative zone (PZ) of chondrocytes are labelled as are the measurements taken. Data are represented as mean ± SEM of six bones in comparison to day 0 measurements, *P<0.05, ***P<0.001.

culture, these bones grew in total length (up to 65%, compared to day 0, $P<0.001$) (Fig. 3.11A) and the chondrocytes in the centre of the bone became hypertrophic, as visualised by microscopy and histology, and mineralised their surrounding matrix (Fig. 3.11C). Both E17 and E15 metatarsal isolated at an earlier time point (E15), metatarsal bones consist of early proliferating organ cultures are therefore physiological models of endochondral ossification.

3.6 Discussion

Attempts to unravel the underlying mechanisms of endochondral ossification have been limited by current models. The data presented in this chapter identifies two mineralisation models as practical and useful tools for studying physiological chondrocyte ECM mineralisation that are highly reproducible.

Immortalised cell lines provide a homogenous population of cells which can theoretically allow reproducible and reliable results. The ATDC5 cell line has been used extensively within chondrocyte research. However, for mineralisation studies it is currently limited by a complex culture method and an extensive culture time period. The method proposed by Shukunami *et al.*, involved reducing the CO_2 concentration. The pH of cell culture medium is entirely dependent upon the fine balance between dissolved carbon dioxide and bicarbonate ions. Therefore any alterations in the atmospheric CO_2 levels will undoubtedly change the pH of the culture medium which is known to have significant effects on cell matrix mineralisation (Arnett 2003; Brandao-Burch *et al.* 2005; Orriss *et al.* 2007; Arnett 2010). Exposing the ATDC5 cultures to a lower CO_2 concentration will increase the pH of the culture medium and therefore will favour mineralisation conditions. The method proposed in this thesis removes this conflicting factor as it uses a constant CO_2 concentration.

Furthermore, the method proposed by Shukunami and colleagues involved changing the culture medium after 21 days of culture to one which contained

ascorbate. The use of ascorbic acid in skeletal cell culture systems is common as it is an essential cofactor for prolyl lysyl hydroxylase, an enzyme which is key to collagen production (Schwarz *et al.* 1981). It has also been found that ascorbate stimulates GAG production, increases the mRNA expression of chondrogenic differentiation markers in bovine articular cartilage, and in chick chondrocytes it increases ALP activity and *Col10a1* mRNA expression (Leboy *et al.* 1989; Kao *et al.* 1990; Hering *et al.* 1994; Farquharson *et al.* 1995). A deficiency of ascorbic acid in humans results in scurvy, and at the growth plate there is decreased chondrocyte proliferation with an associated impairment of ECM synthesis (Kipp *et al.* 1996). ATDC5 cells have previously been cultured with ascorbic acid and this was shown to reduce the proliferation phase of the cells and promote their differentiation (Altaf *et al.* 2006; Temu *et al.* 2010). Here cells were cultured in the presence of 50μg/ml ascorbic acid from when they reached confluency and in concurrence with previous studies, this promoted their ECM formation. The increased mRNA expression of the chondrogenic marker *Col2a1* correlated with the onset of alcian blue stained cartilaginous nodules and the increased mRNA expression of *Col10a1* with the differentiation of the cells to a hypertrophic phenotype (Fig. 3.2).

In addition to ascorbic acid, an exogenous phosphate source is routinely added to cell cultures to induce and stimulate mineralisation of the ECM. Here, ATDC5 cells showed significant mineral formation from day 15 of culture (Fig. 5.4). This is consistent with a previous study in which ATDC5 cells were cultured for mineralisation assessment (Idelevich *et al.* 2011). The use of an exogenous phosphate source to induce mineralisation has been a matter of concern with studies questioning whether the mineral formed is physiological, or whether it is simply an indication of calcium and P_i presence within the cultures and thus dystrophic mineral as has previously been found (Gronowicz *et al.* 1989; Rohde & Mayer 2007).

In bone biology, βGP is a preferential exogenous organic phosphate source as it is a substrate for ALP and therefore the cells indirectly dictate when the P_i increase

occurs through their differentiation to a hypertrophic phenotype. This is advantageous as mineralisation occurs in a more temporal manner as opposed to the seemingly spontaneous mineral formation described in the study by Magne et al., 2003. It is therefore necessary that the membrane-bound enzyme ALP is present for chondrocyte ECM mineralisation and in the method of ATDC5 cell culture developed here, the mRNA expression levels of ALP increase concomitantly with the onset of mineralisation. This is consistent with previous studies in which the activity of ALP has been investigated in ATDC5 cells (Shukunami *et al.* 1997). Furthermore, the addition of levamisole, a potent inhibitor of ALP to ATDC5 cultures inhibited their mineralisation, as did cells cultured in the presence of βGP but not insulin (Figs. 3.3 & 3.4) (Borgers 1973; Van 1976). This therefore suggests that mineral formation is dependent upon both chondrogenic differentiation and the subsequent presence of ALP. Additionally, the inhibition of mineralisation when cells were cultured without insulin further emphasises that the mineral formed here is not dystrophic.

Routinely used as indicators of mineralisation, alizarin red stain reacts with calcium and other cations whilst von kossa stain visualises phosphate and carbonate anions (Puchtler *et al.* 1969). However, neither stain is sufficient when determining mineral formation as the presence of calcium and/or phosphate does not indicate hydroxyapatite formation *per se* (Bonewald et al. 2003). For this reason, various methods exist to examine whether the mineral formed in culture is of a similar size and structure to physiologic hydroxyapatite crystals, and whether these crystals form in alignment with the collagen fibrils of the ECM, as is seen in endochondral ossification (Boskey & Roy 2008). Here, FT-IR and TEM were adopted and confirmed that the addition of 10mM βGP to ATDC5 cells produced mineral that could be comparable to physiological hydroxyapatite (Fig. 3.5). In concordance with other studies, TEM showed mineral deposits to be associated with banded collagen fibrils (Shukunami *et al.* 1997; Magne *et al.* 2003). Examination of the amide and phosphate (PO_4) peaks determined by FT-IR analysis by Shukunami *et al.*, suggests a

lesser mineral-to-matrix ratio than the cultures here. This mineral-to-matrix ratio has been investigated in various studies of chondrocyte mineralisation and ranges from 1.9 to 5.48 in 10-week-old mice (Wu *et al.* 1989; Boskey *et al.* 1996; Paschalis *et al.* 1996; Anderson *et al.* 2004). Despite the distinct variation, the value obtained here (3.0) was within the range observed in other studies. Furthermore, the crystallinity of this mineral was similar to that seen in previous studies of 10-day-old mouse growth plates (Anderson *et al.* 2004), and 10-week-old mice (Boskey *et al.* 2009b).

Primary chondrocytes cultured for up to 28 days appeared to form mineralised regions associated with the development of an ECM as indicated by histochemical analysis. However the de-differentiation of these cells is a common occurrence. Here, attempts were made to limit the de-differentiation of primary chondrocyte cells such that they could be used as a model for chondrocyte matrix mineralisation by increasing the plating density of the cells, and by culturing the cells in the presence of ascorbic acid and βGP. Other methods which could have been examined to limit the de-differentiation include the micromass culture system however previous attempts of this by others within the group were unsuccessful (data not shown). Despite attempts to limit de-differentiation, primary cell cultures still exhibited a decreased expression of *Col2a1* and *Col10a1* mRNA expressions and an increase in *Col1a1* mRNA expression as has been previously reported (Fig. 3.6 & 3.7) (Lefebvre *et al.* 1994; Hering *et al.* 1994). These patterns of expression are consistent with the de-differentiation of the cells into a fibroblastic phenotype. It has been shown in chick chondrocyte cultures that an increased mRNA expression of *Col1a1* in these cultures is not necessarily translated into protein (Focht & Adams 1984; Bennett *et al.* 1989). A steady-state expression of *Col1a1* mRNA may suggest a lack of de-differentiation however that is not the case here (Gartland *et al.* 2005; Goldring 2005). However, here the significant increase in *Col1a1* mRNA expression at day 14 of culture, concomitant with the significant decreases in *Col2a1* and *Col10a1* mRNA expression suggests that the primary chondrocyte cells do not undergo normal

differentiation as seen *in vivo* and thus cannot be considered as a suitable model of endochondral ossification.

3-dimensional culture systems have been previously suggested as solutions to the de-differentiation seen when culturing primary cells. Classically, alginate gels have been used as a supporting matrix for entrapping articular chondrocyte cells providing a more physiological model through increased cell-cell interactions. The use of alginate gels allows the chondrocyte cells to maintain their normal phenotype, as is lost when cultured in monolayer. Similarly, growth plate derived chondrocytes can be used in this manner to investigate differentiation processes (Albrecht *et al.* 2009). However, the use of alginate gels as a model for mineralisation has yet to be established and the practicalities surrounding this method are equivocal.

The metatarsal organ culture provides conditions closer to the *in vivo* situation compared to cell cultures as the chondrocytes within the bones exist in the three principal stages of chondrogenesis whilst retaining direct interactions with each other. Nevertheless, careful consideration is required when extrapolating the results seen due to the artificial environment in which they are cultured. Commonly, a postnatal metatarsal organ culture is used to delineate the mechanisms surrounding postnatal bone growth as it is understood that postnatal bone growth and foetal bone growth are regulated differently (Andrade *et al.* 2011). However, foetal metatarsals have a greater capacity for studying chondrogenesis and mineralisation as they are at an earlier stage of development. Here foetal metatarsal bones were aseptically dissected at E15 and at E17 and cultured for up to 10 days. Developmentally, the skeletal system first appears around day 10.5 post coitum in mice. By E15, most precartilage structures have been replaced by cartilage and despite a considerable degree of periosteal ossification occurring in the long bones, the metatarsal bones exist as a precartilage model. By E17, this ossification has started to occur (Kaufman, 1992). This mineralisation is apparent in the bones

dissected here. Like *in vivo*, these E17 bones have an increase in their longitudinal growth as well as increased mineralisation when cultured (Fig. 3.9). Similarly, E15 bones display an increased longitudinal growth and the central mineralisation zone develops after approximately 2 days in culture, as is consistent with the *in vivo* development described (Fig. 3.10). The metatarsal organ culture systems described here therefore share many important characteristics with chondrocyte *in vivo* differentiation and mineralisation.

In conclusion, ATDC5 cells cultured using the method defined here show evidence of chondrogenic differentiation and subsequent mineralisation of their ECM that resembles that seen in endochondral ossification. The method allows for a more practical time period without the seemingly spontaneous onset of mineralisation as described upon the addition of P_i as a phosphate source (Magne *et al.* 2003). Furthermore, the foetal metatarsal organ culture model can provide the examination of chondrocytes in different phases of chondrogenesis as well as of their mineralisation capability. These features therefore allow these models to be considered as practical and suitable *in vitro* models of chondrocyte matrix mineralisation

Chapter 4

The expression and localisation of MEPE in the murine growth plate

4.1 Introduction

The epiphyseal growth plates are the cartilage anlagen, developed from mesenchymal precursors, through which linear bone growth occurs by endochondral ossification. The growth plate consists of chondrocytes arranged in columns that parallel the axis of the bone surrounded by their ECM (Ballock & O'Keefe 2003; Mackie *et al.* 2008; Mackie *et al.* 2011). The chondrocytes sit in distinct cellular zones of maturation as are clearly visible, and proceed through various stages of differentiation whilst maintaining their spatially fixed locations (Fig. 1.4) (Hunziker *et al.* 1987). It is the terminally differentiated hypertrophic chondrocyte that mineralises its surrounding ECM, localised to the longitudinal septa of the growth plate (Castagnola *et al.* 1988). Mineralisation is a highly regulated biphasic process. MVs are widely believed to be the initial sites for hydroxyapatite formation by providing an environment permissive for calcium and P_i ion precipitation. This initial phase of mineralisation is followed by the penetration of the MV trilaminar membrane by the hydroxyapatite crystals such that they are exposed to the extracellular fluid, thus permitting their further growth and development in alignment with the collagen fibrils of the ECM (Anderson 1995; Anderson 2003; Golub 2011). This cartilagenous ECM is rich in collagens, proteoglycans and numerous other NCPs (Gentili & Cancedda 2009; Heinegard 2009; Mackie *et al.* 2011).

The SIBLING family of proteins are one such family of NCPs and include OPN, BSP, DMP1, DSPP and MEPE. The SIBLING family of proteins share some structural and functional characteristics; all are located to a 375kb region on the human chromosome 4q21, and 5q in mouse, and have similar exon structures. Additionally, all SIBLING proteins undergo similar post translational modifications (PTM) such as phosphorylation and glycosylation, the extent of which is crucial in determining their function (Boskey *et al.* 2009a). It has long been known that the SIBLING proteins have an Arg-Gly-Asp (RGD) sequence which facilitates cell attachment and cell signalling by binding to cell surface integrins (Fisher *et al.* 2001). More recently,

work primarily focused upon MEPE has identified a new functional domain termed the ASARM peptide which is highly conserved across species (Rowe *et al.* 2000; Rowe *et al.* 2004). This peptide is proving critical in the functional activity of the SIBLING proteins. Similarly, the SIBLING proteins are principally expressed in bone and dentin, and are secreted into the ECM during osteoid formation and subsequent mineralisation (Fisher & Fedarko 2003; Huq *et al.* 2005; Staines *et al.* 2012b).

MEPE was first identified in 2000 from patients with tumour induced osteomalacia, and quickly after rat and mouse MEPE were cloned (Petersen *et al.* 2000; Rowe *et al.* 2000; Argiro *et al.* 2001). In concordance with the other SIBLING proteins, MEPE was soon established to be expressed in bone and dentin, as well as the renal proximal convoluted tubule highlighting its role in phosphate homeostasis (Fisher & Fedarko 2003; Ogbureke & Fisher 2005). Analysis of *Mepe* mRNA in the rat bone compartments indicated its presence in tibial shaft, the metaphysis and the growth plate (Petersen *et al.* 2000). More specifically, in bone MEPE is primarily expressed by osteocytes and osteoblasts, whilst in dentin it is expressed by odontoblasts (MacDougall *et al.* 1998; Nampei *et al.* 2004). Analysis of the developing mouse skeleton indicates *Mepe* mRNA to be detected as early as 2-days postpartum (Lu *et al.* 2004).

The expression of *Mepe* mRNA is increased during osteoblast matrix mineralisation suggesting a function for MEPE in bone mineralisation (Petersen *et al.* 2000; Argiro *et al.* 2001). This has been further fuelled by analysis of the MEPE null mouse in which the ablation of MEPE leads to an increased bone mass due to increased numbers and activity of osteoblasts (Gowen *et al.* 2003). Recent work has identified the 2.2kDa ASARM peptide of MEPE as the central provider for the mineralisation activity of MEPE. Located immediately downstream of a cathepsin B cleavage site, this ASARM peptide inhibits osteoblast ECM mineralisation (Rowe *et al.* 2000;

Martin *et al.* 2008; Addison *et al.* 2008). However, the functional role of MEPE in chondrocyte matrix mineralisation has yet to be established.

Before attempting to unravel the regulatory mechanisms that MEPE may have in mammalian chondrocyte matrix mineralisation, it is first necessary to understand its spatial expression pattern within the growth plate. Despite some evidence for MEPE expression in the growth plate, this has yet to be fully established (Petersen *et al.* 2000). The localisation of MEPE to sites of mineralisation would serve to strengthen its potential role within growth plate matrix mineralisation.

4.2 Hypothesis

MEPE is expressed by murine growth plate chondrocytes and ATDC5 cells with its localisation within the growth plate consistent with a role in ECM mineralisation.

4.3 Aims

I To determine the gene and protein localisation pattern of MEPE and its ASARM peptide within the murine growth plate *in vivo* by *in situ* hybridisation and immunohistochemistry, respectively

II To quantify *Mepe* mRNA expression within the murine growth plate

III To determine the gene and protein expression of MEPE within mineralising ATDC5 cells, murine metatarsal organ cultures and primary chondrocyte cells

4.4 Materials and Methods

4.4.1 ATDC5 cells

As outlined in section 2.2.1, ATDC5 cells were cultured at a density of 6 x 10^4 cells/cm^2 in a humidified atmosphere (37°C, 5% CO_2) for up to 20 days. When

confluent, cells were supplemented with 10mM βGP and 50μg/ml ascorbic acid with the medium being changed every 2-3 days.

4.4.2 RNA analysis of ATDC5 cells

RNA was isolated from ATDC5 cells at specific time points using a Qiagen RNeasy kit according to the manufacturer's instructions and cDNA was prepared (section 2.12.3). For PCR analysis, cDNA was used at 25ng/μl and amplified as described in section 2.12.4. PCR products were analysed on a 1.5% agarose gel and visualised under UV light using a Gel Logic 200 Imaging System and software (Kodak). For qPCR analysis, cDNA was used at 10ng/μl, as detailed in section 2.12.5. Results were normalised to the *18S* housekeeping gene and the relative gene expression level was calculated using the ΔΔCt method (Livak & Schmittgen 2001). Primers used are detailed in Appendix II.

4.4.3 Protein extraction from ATDC5 cells and western blotting

At defined time points, protein was extracted from ATDC5 cells in RIPA buffer as detailed in section 2.13.1. Protein samples were quantified (section 2.13.2) and appropriate quantities were used for western blot analysis (section 2.13.3). MEPE protein expression was determined using a sheep anti-mouse anti-MEPE antibody at a dilution of 1:200 and a HRP-labelled donkey anti-sheep secondary antibody (1:5000). Antibody labelling was visualized using the ECL detection kit. Equality of protein loading was confirmed by also probing the membrane with mouse monoclonal HRP-labelled anti-β actin antibody (1:50000).

4.4.4 Primary chondrocytes

Primary chondrocytes were extracted from the rib cages of 1-3 day old mice as detailed in section 2.2.3. Cells were cultured for 2 days at 37°C in primary cell culture media before RNA was extracted and reverse transcribed (sections 2.12.1 and 2.12.3). For PCR analysis, cDNA was used at 25ng/μl and amplified as described in section 2.12.4. PCR products were analysed on a 1.5% agarose gel and

visualised under UV light using a Gel Logic 200 Imaging System and software (Kodak). Primers used are detailed in Appendix II.

4.4.5 Murine metatarsals

Murine metatarsals were isolated at E15 as described in section 2.4.2. Metatarsals were cultured under the calcifying conditions described in section 2.4.2 for 7 days. After this, RNA was extracted and reverse transcribed for PCR analysis (sections 2.12.2, 2.12.3, and 2.12.4). PCR products were analysed on a 1.5% agarose gel and visualised under UV light using a Gel Logic 200 Imaging System and software (Kodak). Primers used are detailed in Appendix II.

4.4.6 Immunohistochemical staining of the murine growth plate *in vivo*

4-week old and 10-day old C57BL/6 mice were sacrificed by cervical dislocation and the tibiae were dissected and fixed in 70% ethanol for 24 hours. The tibiae were decalcified in 10% EDTA and processed into wax as described in section 2.6.1. Immunohistochemical staining of 5μm-thick tibiae sections was performed using antibodies for MEPE-ASARM (1:200), MEPE-mid terminal (1:200), and cathepsin B (1:50) and the Vectastain ABC kit, as outlined in section 2.9 and Appendix III. Immunohistochemical labelling was visualised using DAB chromagen. Appropriate immunoglobulin G (IgG) concentrations were used instead of the primary antibodies as negative controls.

4.4.7 *In situ* hybridisation of MEPE in the murine growth plate

For *in situ* hybridisation, 3-week old and 10-day old C57BL/6 mice were sacrificed by cervical dislocation. Tibiae were dissected, fixed in 10% NBF for 24 hours, and processed to wax following decalcification in 10% EDTA, as described in section 2.6.1. MEPE sense and antisense digoxigenin-labelled cRNA probes were synthesised as detailed in sections 2.7.1-2.7.6. *In situ* hybridisation was performed following an optimised protocol from Imperial College London as detailed in section 2.7.7.

4.4.8 Microdissection of the murine growth plate

3-week old C57BL/6 mice were sacrificed by cervical dislocation and the proximal part of the tibiae was coated in 5% PVA and then immersed in a cooled hexane bath for 30 seconds. Sections were prepared as described in section 2.6.2. Microdissection of the murine growth plate was performed under a xylene droplet using an inverted microscope. Growth plate sections were separated into the proliferating zone (PZ), hypertrophic zone (HZ) and metaphyseal bone (MB). For each zone, tissue dissected from both proximal tibias of three animals (14–22 sections) was pooled. RNA isolation was performed as described in section 2.8. cDNA was prepared (section 2.12.3) and was used at 10ng/μl for qPCR analysis, as detailed in section 2.12.5. Results were normalised to the *18S* housekeeping gene and the relative gene expression level was calculated using the ΔΔCt method (Livak & Schmittgen 2001). The accuracy and validity of the microdissection technique was assessed by quantification of *Col10a1* mRNA expression.

4.5 Results

4.5.1 Temporal expression of MEPE in ATDC5 cells

To determine whether MEPE is expressed by growth plate chondrocytes, MEPE expression was first examined in ATDC5 cells. Cells were cultured under calcifying conditions for up to 20 days and RNA extracted at days 8, 15 and 20 of culture. PCR analysis indicated *Mepe* mRNA (129bp) to be expressed throughout the ATDC5 cell culture period as was normalised to *18S* mRNA (488bp) (Fig. 4.1A). This was further confirmed by western blotting at days 8, 15 and 20 of ATDC5 culture for MEPE protein expression (Fig. 4.1B). The C-terminal fragment of MEPE (~37kDa) is known to contain the ASARM peptide (Rowe *et al.* 2000). This fragment appeared to be slightly increased at day 15 of culture in comparison to day 8 of culture (Fig. 4.1B).

This therefore warranted the analysis of the temporal expression of *Mepe* mRNA in ATDC5 cells over a mineralisation time course. The time course selected represented the ATDC5 cells at times points before (days 8 & 10), at the onset of

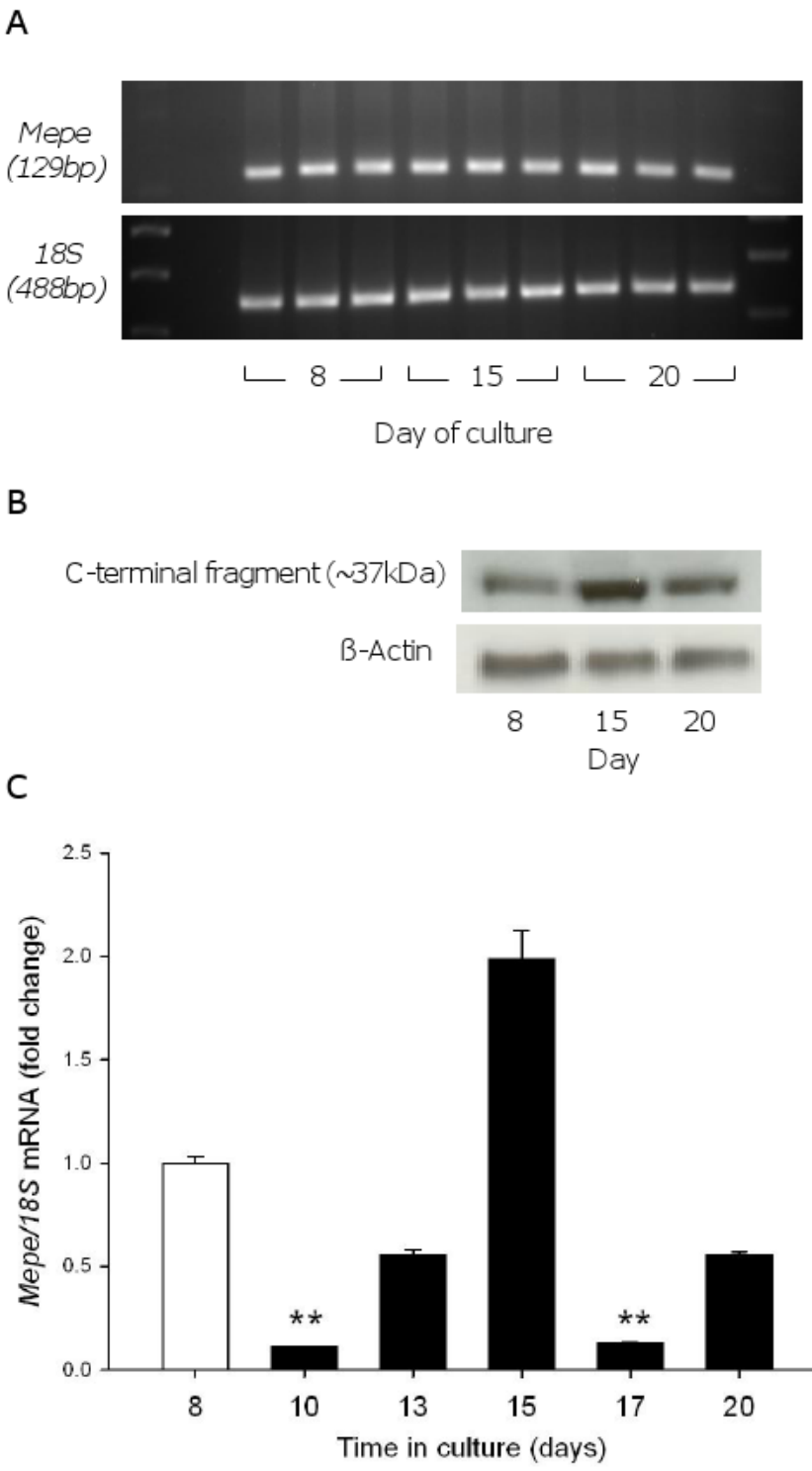

Figure 4.1 The expression of MEPE in ATDC5 cells

To examine the expression of MEPE by growth plate chondrocytes, ATDC5 cells were cultured for up to 20 days under calcifying conditions. (A) PCR analysis indicated MEPE presence at days 8, 15 and 20 of culture. *18S* mRNA expression was used as a control (B) Western blotting further confirmed MEPE expression in ATDC5 cells. β-actin was used as a loading control (C) The temporal expression of *Mepe* mRNA was examined in ATDC5 cells by qPCR in comparison to day 8. Results were normalised to the *18S* housekeeping gene. Data are represented as mean ± S.E.M (n=3 replicates) **P<0.01.

(days 13 & 15) and after (days 17 & 20) matrix mineralisation, as defined in Chapter 3. RNA was extracted at defined time points and analysed by qPCR. In comparison to day 8 of culture, *Mepe* mRNA expression was significantly decreased at day 10 of culture ($P<0.01$) and at day 17 of culture ($P<0.01$) (Fig. 4.1C). At days 13, 15 and 20 of culture, there were no significant changes in *Mepe* mRNA expression (Fig. 4.1C). These temporal changes in MEPE protein and mRNA expression *in vitro* warrant investigation into its expression patterns *in vivo*.

4.5.2 *Mepe* mRNA expression in primary chondrocytes and in E15 murine metatarsal bones

To establish whether the expression of MEPE in ATDC5 cells mimics that seen in a more physiological model, primary chondrocytes were isolated and cultured for 3 days before RNA was extracted. This allowed analysis of primary cells without the de-differentiation observed in a mineralisation model as described in Chapter 3. *Mepe* mRNA was expressed in primary chondrocytes as indicated by PCR analysis (Fig. 4.2). This was also the case with mineralised E15 metatarsals (Fig. 4.2) thus confirming the expression of MEPE in growth plate chondrocytes.

4.5.3 *Mepe* mRNA expression in the murine growth plate

For examination of the spatial localisation of *Mepe* mRNA in the murine growth plate, *in situ* hybridisation was adopted in 10-day old murine tibiae. *Mepe* mRNA was expressed abundantly by both growth plate chondrocytes and by osteoblasts within the metaphysis. Observed was a particularly high expression in the HZ of chondrocytes (Fig. 4.3A). This led to the analysis of 3-week old tibiae to assess whether a similar spatial localisation is observed at this developmental age in which the growth plate has fully formed between the primary and secondary ossification centres. Indeed *Mepe* mRNA was similarly expressed abundantly by growth plate chondrocytes and by osteoblasts within the metaphysis (Fig. 4.4A). In the growth plate, high levels of *Mepe* mRNA were observed, especially in the hypertrophic chondrocytes (Figs. 4.4B & C). Representative images of the sense probe analysis are shown (Figs. 4.3C and 4.4D & E). This spatial expression pattern was further

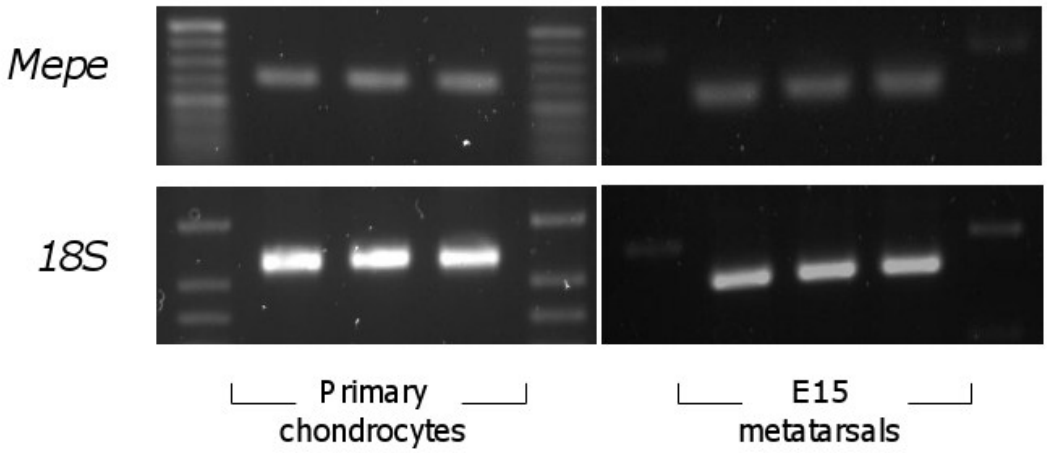

Figure 4.2 The expression of *Mepe* mRNA in mouse primary chondrocyte cells and E15 metatarsals

Mepe mRNA was present in both primary chondrocyte cells cultured for 3 days and in E15 metatarsals cultured for 7 days, as indicated by PCR analysis. *18S* mRNA expression was used as a control. Each lane represents individual primary cell cultures of groups of 4 pooled metatarsal bones.

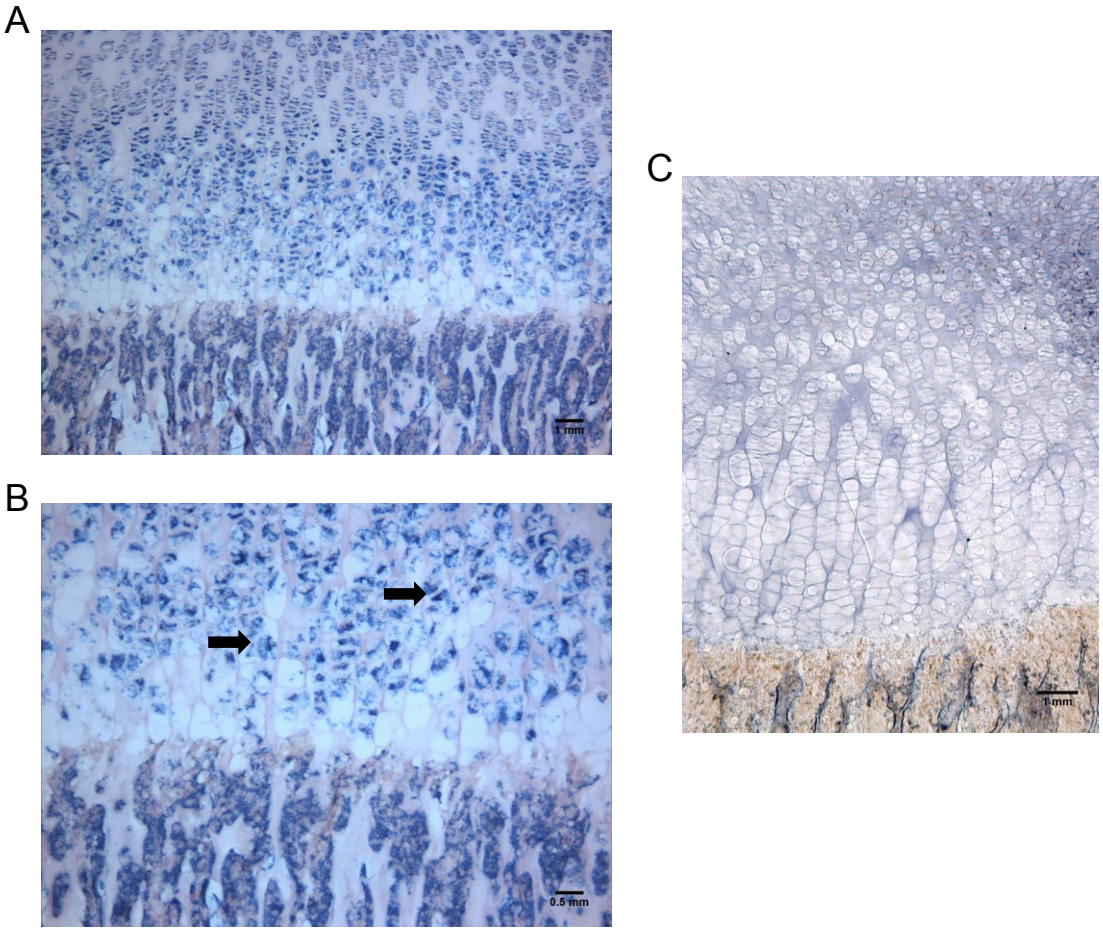

Figure 4.3 *In situ* hybridisation of *Mepe* mRNA expression in the 10 day old murine growth plate

In situ hybridisation of *Mepe* mRNA in 10 day old mouse tibia **(A)** *Mepe* was found to be abundantly expressed by growth plate chondrocytes and osteoblasts of the metaphysis **(B)** Expression was high in the HZ of the growth plate, as indicated by the arrows **(C)** Analysis of the *Mepe* sense probe indicated no specific binding to *Mepe* mRNA. Positive *Mepe* mRNA is indicated by blue stain. Scale bar 1mm (A & C), 0.5mm (B).

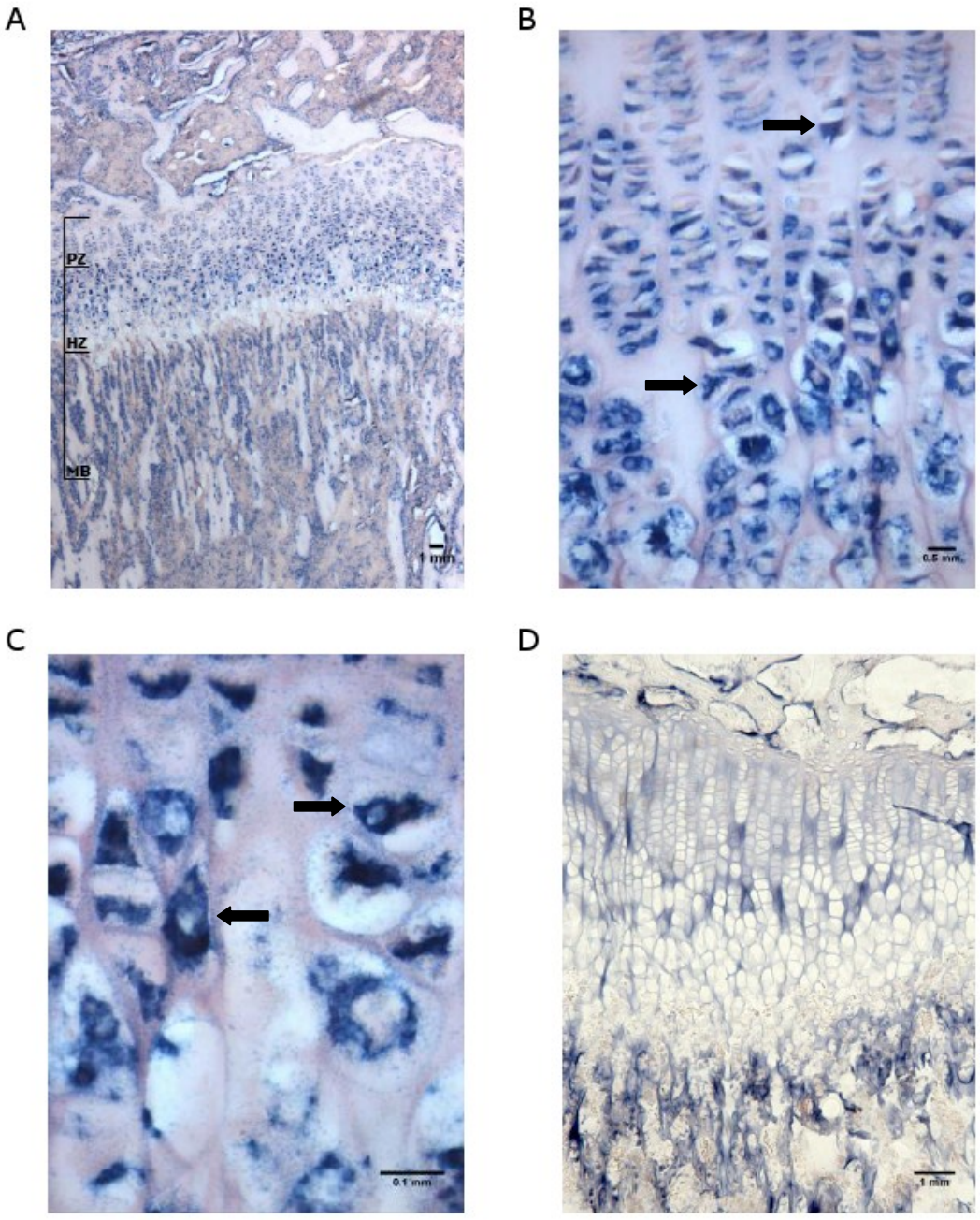

Figure 4.4 *In situ* hybridisation of *Mepe* mRNA expression in the 3 week old old murine growth plate

In situ hybridisation of *Mepe* mRNA in 3-week-old mouse tibia **(A)** *Mepe* was found to be abundantly expressed by growth plate chondrocytes and osteoblasts of the metaphysis **(B)** Expression was present in both the PZ and the HZ of the growth plate, as indicated by the arrows **(C)** There was an apparent increase in expression in the HZ of chondrocytes **(D)** Analysis of the *Mepe* sense probe indicated no specific binding to *Mepe* mRNA. Positive *Mepe* mRNA indicated by blue stain.

examined and quantified by microdissection of 3-week old growth plates. To validate the microdissection technique, qPCR of C*ol10a1* mRNA expression was conducted to ensure that the HZ could be considered as an enriched pool of hypertrophic chondrocytes (Fig. 4.5A). There was approximately a ten-fold increase in C*ol10a1* mRNA expression in the HZ in comparison to the PZ ($P<0.01$). This increase in C*ol10a1* mRNA expression is in concordance with previous studies done using a similar technique (Hutchison *et al.* 2007). *Mepe* mRNA had a significantly higher expression ($P<0.05$) in the HZ in comparison to the PZ of the growth plate (Fig. 4.5B) therefore confirming the *in situ* hybridisation data.

4.5.4 Immunohistochemical staining of the murine growth plate

To assess whether the spatial expression of MEPE protein mimicked that of its mRNA expression pattern, immunolocalisation of MEPE was conducted in 14-day old and 4-week old murine growth plates. Indeed this verified the *in situ* hybridisation and microdissection data as demonstrated by its preferential localisation to the HZ of chondrocytes (Figs. 4.6A - D).

The immunolocalisation of the MEPE-ASARM peptide was also examined in the two ages of growth plates. This too was localised to the hypertrophic chondrocytes (Figs. 4.7A - D). This ASARM peptide is cleaved from MEPE by the protease cathepsin B thus the immunolocalisation of cathepsin B was examined in the 14-day old and 4-week old murine growth plates to determine if its localisation was associated with regions of MEPE-ASARM expression (Figs. 4.8A - D). Cathepsin B was expressed at the chondro-osseous junction as is in concordance with previous studies (Lee *et al.* 1995; Gartland *et al.* 2009). Representative images of the appropriate negative controls are shown (Figs. 4.6, 4.7 & 4.8 E & F). Together these data indicate that MEPE-ASARM peptide is preferentially expressed by hypertrophic chondrocytes of the growth plate and this localisation is consistent with a role for this peptide in regulating cartilage mineralisation.

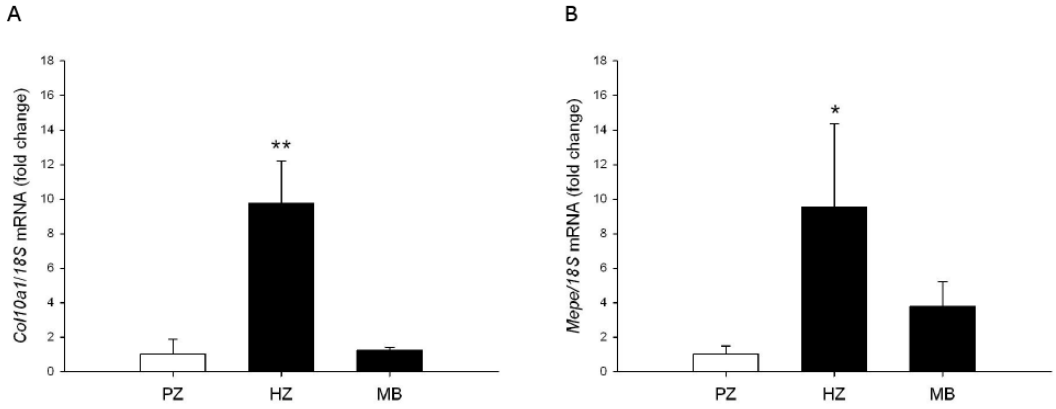

Figure 4.5 Microdissection of the murine growth plate

Microdissection of the growth plate was adopted to assess *Mepe* mRNA expression. **(A)** The accuracy of the microdissection technique was determined by the relative change in C*ol10a1* mRNA expression throughout the zones of the growth plate (PZ, HZ) and the MB **(B)** This was then used to examine the relative change in *Mepe* mRNA expression in these zones Values generated by qPCR and normalised to *18S* housekeeping gene. Data are represented as mean ± S.E.M, in comparison to the PZ, *P<0.05 **P<0.01.

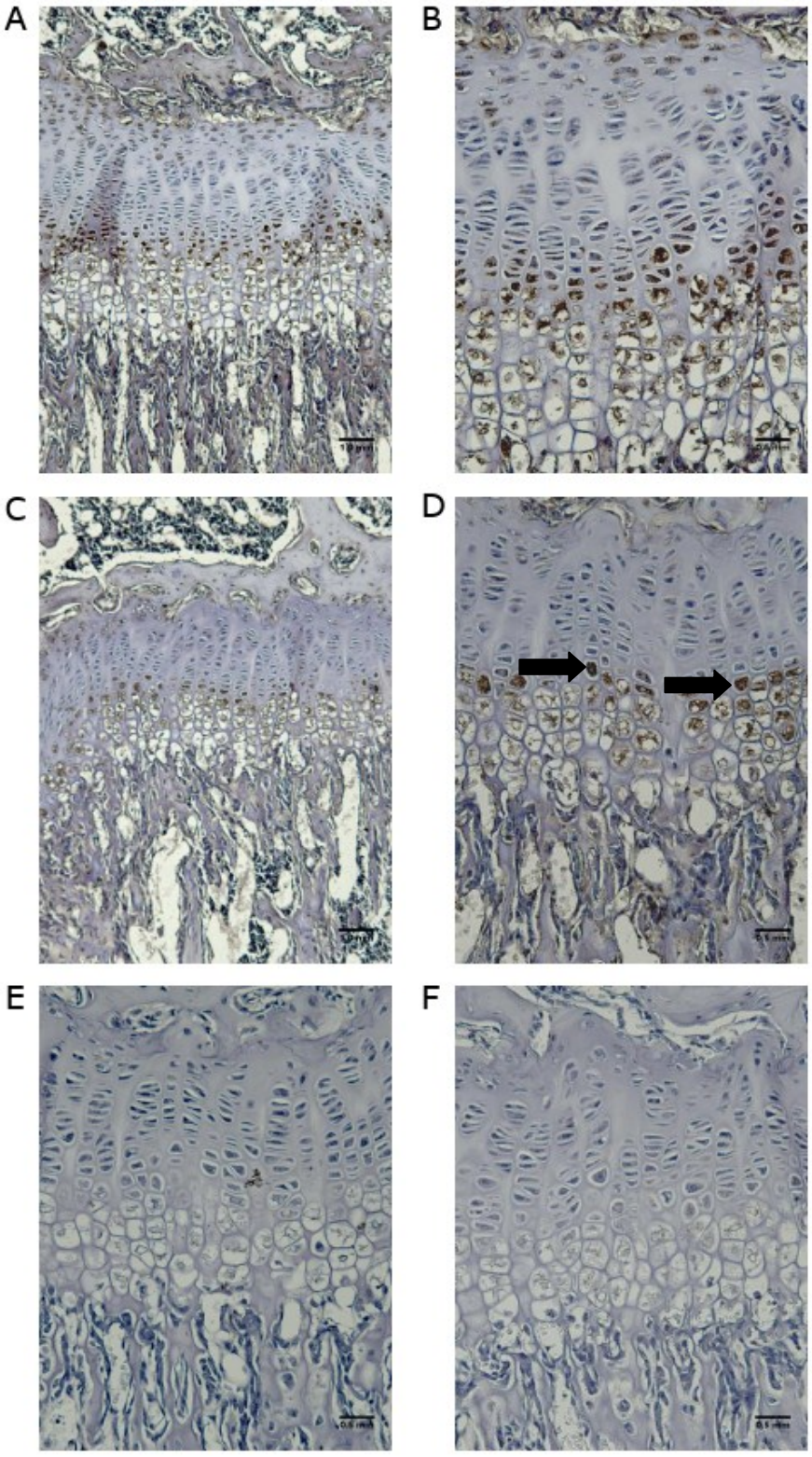

Figure 4.6 Immunolocalisation of MEPE in the murine growth plate

Immunohistochemistry shows MEPE to be expressed in **(A)** the tibia of 14-day old mice **(B)** Its expression in the growth plate is limited to the hypertrophic zone of chondrocytes as indicated by the arrows **(C & D)** A similar localisation is observed in 4-week old growth plates. Representative images of appropriate negative control are shown **(E)** 14-day old growth plate **(F)** 4-week old growth plate. Positive MEPE protein is indicated by brown stain.

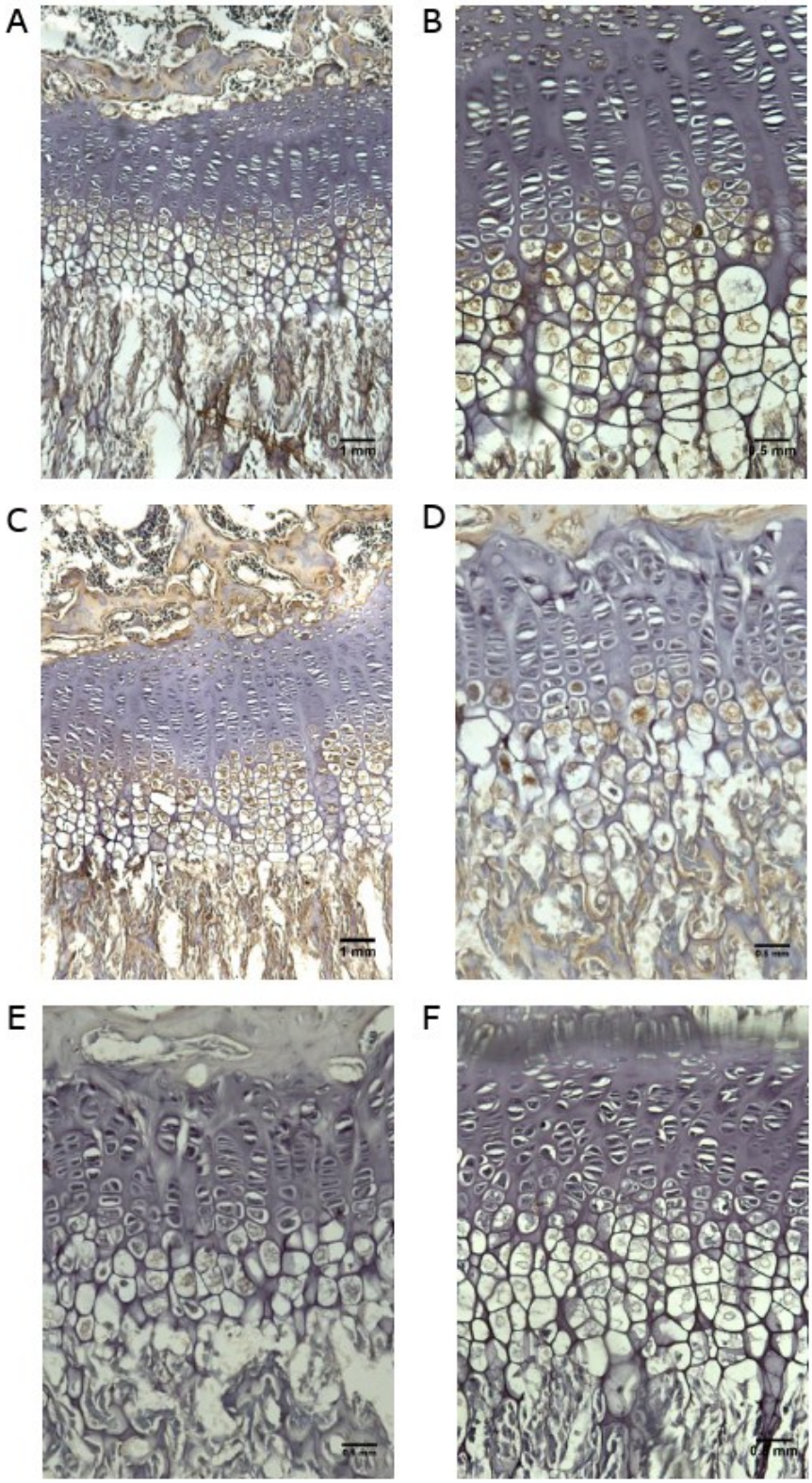

Figure 4.7 Immunolocalisation of MEPE-ASARM in the murine growth plate

Immunohistochemistry shows the ASARM peptide to be expressed in **(A)** the tibia of 14-day old mice **(B)** Its expression in the growth plate is limited to the hypertrophic chondrocytes as indicated by the arrows **(C & D)** A similar localisation is observed in 4-week old growth plates. Representative images of appropriate negative control are shown **(E)** 14-day old growth plate **(F)** 4-week old growth plate. Positive MEPE stain is indicated by brown stain.

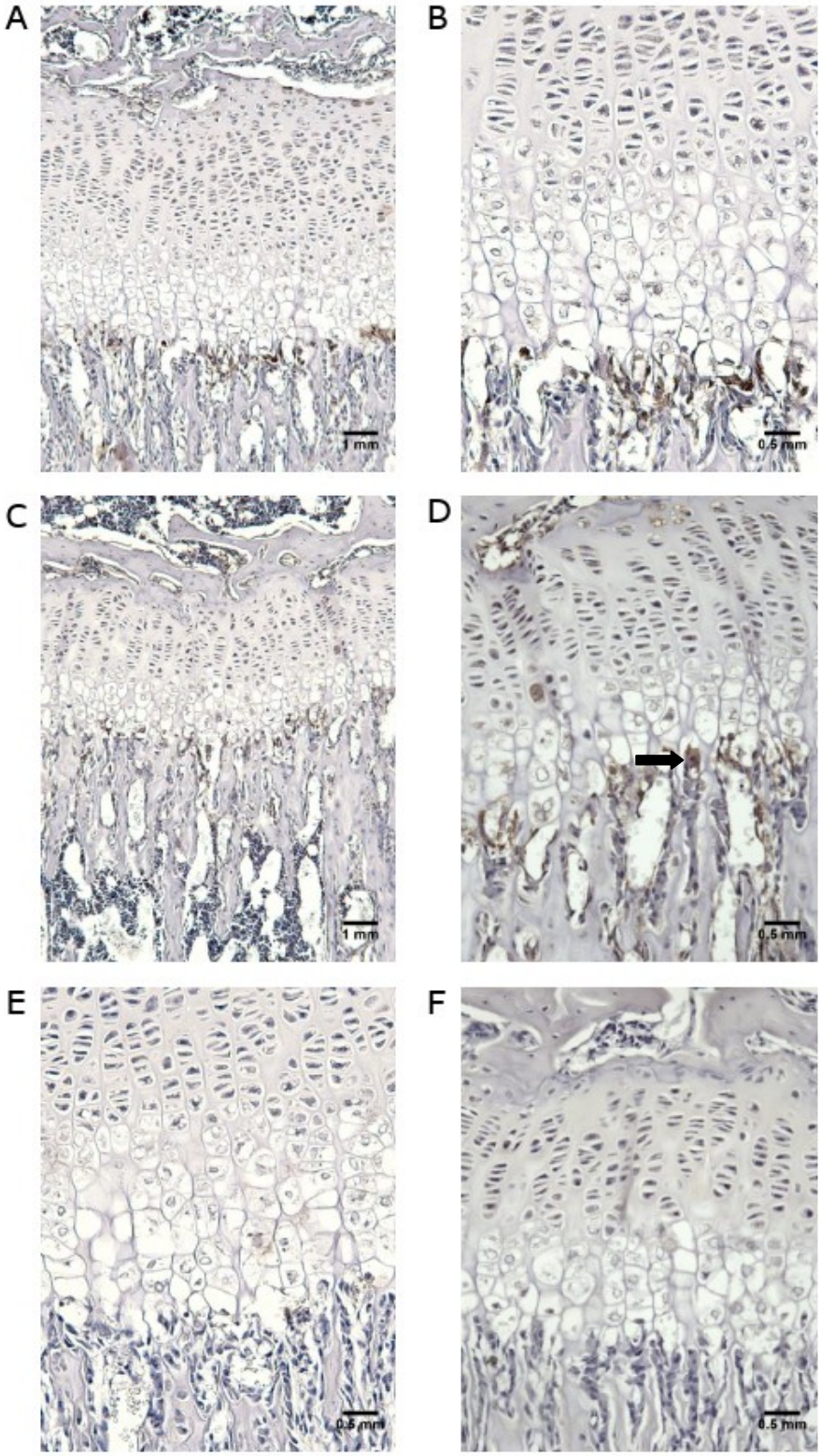

Figure 4.8 Immunolocalisation of cathepsin B in the murine growth plate

Immunohistochemistry shows cathepsin B to be expressed in **(A)** the tibia of 14-day old mice **(B)** Its expression in the growth plate is limited to the chondro-osseous junction as indicated by the arrows **(C & D)** A similar localisation is observed in 4-week old growth plates. Representative images of appropriate negative control are shown **(E)** 14-day old growth plate **(F)** 4-week old growth plate. Positive MEPE protein is indicated by brown stain.

4.6 Discussion

MEPE is a member of the SIBLING family of proteins and has previously been shown to be expressed by mature osteoblasts, osteocytes, odontoblasts and the proximal convoluted tubules of the kidney (Gowen *et al.* 2003; Ogbureke & Fisher 2004; Rowe *et al.* 2006; Boukpessi *et al.* 2010). Moreover, there has been some indication of MEPE expression in the rat growth plate (Petersen *et al.* 2000). Here, the expression and spatial localisation of MEPE within the murine growth plate and its primary cell type, the chondrocyte, was determined (Fig. 4.1). ATDC5 cells, primary chondrocyte cell cultures, and embryonic metatarsal bones all expressed *Mepe* mRNA. The mineralisation capability of ATDC5 cells has previously been defined in Chapter 3. This was then utilised to examine the expression of *Mepe* mRNA over a 20-day culture period. In ATDC5 cells *Mepe* mRNA had a differential expression pattern, possibly suggesting MEPE to have a role in the chondrocyte matrix mineralisation process. However, in comparison to osteoblast cultures in which the mRNA expression of *Mepe* was temporally increased in line with mineralisation of the cell's ECM, here a decrease was observed (Petersen *et al.* 2000).

Furthermore, the ATDC5 data is seemingly contradictory to the immunohistochemistry and *in situ* hybridisation data here in which *Mepe* mRNA and protein were observed in the growth plate respectively (Figs. 4.3-5 & 4.6-8). In particular, a higher expression of MEPE was observed in the hypertrophic zone of chondrocytes, as was confirmed by microdissection of the growth plate (Fig. 4.5). It is these hypertrophic cells that mineralise their surrounding ECM and thus the localisation of MEPE to this zone strengthens its hypothesised role in chondrocyte matrix mineralisation. The reasons behind the discrepancy between ATDC5 cell line and growth plate expression are unclear however the differences between *in vitro* and *in vivo* culture systems could provide some explanation.

The *in situ* hybridisation and microdissection data are in concordance with a microarray study in which *Mepe* mRNA was found to be upregulated in

hypertrophic cartilage (Horvat-Gordon *et al.* 2010). Since the commencement of these studies, the expression of MEPE within the growth plate has since been examined in the MEPE overexpressing mouse in comparison to its wild-type counterpart by immunohistochemistry (David *et al.* 2009). MEPE was found to be expressed in wild-type growth plates, in particular in the hypertrophic zone of chondrocytes, as is in concordance with the results shown here. Similarly, the MEPE-overexpressing mouse displayed expression of MEPE in the hypertrophic chondrocytes, at a greater level than that in its wild-type counterparts. This was associated with wider epiphyseal growth plates, expanded primary spongiosa and shorter bones in the MEPE-overexpressing mouse.

The authors of this study, David *et al*, also investigated the localisation of the MEPE-ASARM peptide in the MEPE-overexpressing and wild-type mice. The ASARM peptide was first identified by Peter Rowe and colleagues as the functional domain of MEPE, located immediately downstream of a cathepsin B cleavage site, within the C-terminal fragment of MEPE (Rowe *et al.* 2000). In concordance with the localisation of MEPE, its ASARM peptide was expressed in the hypertrophic zone of chondrocytes in wild-type mice. Similarly, here the ASARM peptide was shown to be localised to the hypertrophic chondrocytes in both 14-day old and 4-week old murine growth plates by immunohistochemistry. Moreover, the differential regulation of the protein expression of this ASARM peptide, as determined by western blotting, indicates its presumed role in chondrocyte matrix mineralisation.

This presumed role of MEPE in chondrocyte ECM mineralisation is further indicated by the widened growth plates observed in the MEPE-overexpressing mouse. However it is worth noting that this growth plate disruption may be a consequence of other activities within the growth plate outwith mineralisation, for example altered proliferation, differentiation or vascular invasion. Analysis of the *Hyp* mouse, a spontaneous *Phex* knockout model also provides evidence for a presumed role for MEPE in mineralisation. The *Hyp* mouse is the mouse model of

the hypophosphatemic disorder XLH. It is well documented that the ASARM peptide is upregulated in these mice (Bresler *et al.* 2004). Like in the MEPE-overexpressing mouse, studies of this *Hyp* mouse show severe morphological widening of the growth plate with widened epiphysis. This disruption was partially corrected by the administration of cathepsin inhibitors, including the specific cathepsin B inhibitor CA074 (Rowe *et al.* 2006). Cathepsin B is known to cleave MEPE, releasing its functional ASARM peptide. The localisation of cathepsin B at the chondro-osseous junction here is in concordance with previous studies detailing the cathepsin B rich septoclast (Fig. 4.8) (Lee *et al.* 1995; Gartland *et al.* 2009). These cells, thought to be of macrophage or osteoclast origin, are postulated to play a key role in the degradation of unmineralised cartilage (Lee *et al.* 1995). It is likely that the cathepsin B provided at the chondro-osseous junction cleaves MEPE at its distal COOH-region to the ASARM peptide.

PHEX, a cell membrane associated glycoprotein, plays a central role in the protection of MEPE from proteolytic cleavage by cathepsin B. It acts by binding to MEPE and preventing the release of the ASARM peptide (Guo *et al.* 2002). The *Hyp* mouse has an increased expression of cathepsin D, an upstream activator of cathepsin B (Rowe *et al.* 2006). This therefore suggests that PHEX can alter the activation of cathepsin B, and therefore the cleavage of MEPE to the ASARM peptide. Similar to the expression of MEPE, PHEX protein expression is observed in the hypertrophic chondrocytes, as well as the proliferative zone, of wild-type mouse growth plates (Miao *et al.* 2004). This suggests a regulatory mechanism for MEPE expression in the murine growth plate and further indicates a role for MEPE in chondrocyte matrix mineralisation.

In conclusion, in this study MEPE has been shown to be expressed by growth plate chondrocytes with a spatial localisation to the hypertrophic zone of the growth plate. The ASARM peptide, the functional component of MEPE, is also localised to the hypertrophic chondrocytes. This spatial expression data is consistent with data

which was published during the completion of these studies. As it is the hypertrophic chondrocytes that mineralise their ECM, this therefore suggests a role for MEPE and its ASARM peptide in chondrocyte ECM mineralisation.

Chapter 5

The functional involvement of MEPE in chondrocyte matrix mineralisation

5.1 Introduction

Chondrocyte matrix mineralisation is a biphasic process which is under tight enzymatic, protein and membrane control so as to ensure levels of Ca^{2+} and P_i are permissive for effective hydroxyapatite formation (Anderson 1995). Molecules such as ALP, NPP1, ANK and PHOSPHO1, have been identified as imperative in regulating matrix mineralisation (Meyer 1984; Anderson 1995). However, the identification of a key group of NCPs, the SIBLING family of proteins, has allowed new insights into the mechanisms surrounding the formation of hydroxyapatite. One such SIBLING protein is MEPE, a 58kDa protein first isolated from a patient with tumour induced osteomalacia (Rowe *et al.* 2000).

Although little is known about MEPE function in chondrocytes, it has been investigated in other cell types including bone cells. The first evidence for a direct role of MEPE in bone mineralisation came from the increased mRNA expression levels of *Mepe* seen during osteoblast matrix mineralisation (Petersen *et al.* 2000; Argiro *et al.* 2001). This role has been further fuelled by analysis of the MEPE null mouse in which the ablation of MEPE in mice leads to an increased bone mass due to increased numbers and activity of osteoblasts (Gowen *et al.* 2003). Furthermore, using the Col1a1 promoter, the specific overexpression of MEPE in osteoblasts of mice, leads to defective mineralisation. Associated with this defect are increased levels of an acidic 2.2kDa peptide, the ASARM peptide (David *et al.* 2009).

In vitro studies have identified that the observed inhibitory effect of MEPE on osteoblast and odontoblast matrix mineralisation is dependent upon its cleavage to this ASARM peptide (Rowe *et al.* 2004; Martin *et al.* 2008; Wang *et al.* 2010a). This cleavage-dependent activity of MEPE is seemingly characteristic of the SIBLING family of proteins (Boskey *et al.* 2009a; Staines *et al.* 2012b). In MEPE, the ASARM peptide is located immediately downstream of a cathepsin B cleavage site, and it is responsible for the mineralisation defect observed in XLH, the most common form of inherited rickets (Rowe *et al.* 2000; Rowe *et al.* 2004; Martin *et al.* 2008). This defect

can be reversed by administration of cathepsin inhibitors CAO74 or pepstatin (Rowe *et al.* 2006). PHEX plays a central role in the protection of MEPE from proteolytic cleavage by cathepsin B; it can bind to MEPE and prevent the release of the ASARM peptide (Guo *et al.* 2002). The *Hyp* mouse, a spontaneous *Phex* knockout model, has an increased expression of cathepsin D, an upstream activator of cathepsin B (Rowe *et al.* 2006). Therefore PHEX may also assist in decreasing the activation of cathepsin B.

Previous studies have shown that the post translational modification of the MEPE-ASARM peptide is key to its functional role. MEPE has a number of potential casein kinase II phosphorylation motifs, and it is here that the ASARM motif is phosphorylated at 3 serine residues (Rowe *et al.* 2000). When released as this phosphorylated peptide, it can inhibit mineralisation in murine calvarial osteoblasts and in bone marrow stromal cells by the direct binding of the MEPE-ASARM peptide to hydroxyapatite crystals. Without phosphorylation, the ASARM peptide has no effect on osteoblast matrix mineralisation (Martin *et al.* 2008; Addison *et al.* 2008). The role of MEPE in osteoblast matrix mineralisation is established however its functional role in growth plate chondrocyte matrix mineralisation and endochondral ossification has yet to be elucidated.

5.2 Hypothesis

MEPE has a direct functional role in chondrocyte matrix mineralisation which is dependent upon the release of its pASARM peptide

5.3 Aims

I. Examine the overexpression and knockdown of MEPE on ATDC5 cell matrix and embryonic metatarsal mineralisation

II. Analyse the effects of the ASARM peptide on ATDC5 matrix mineralisation

III. Exploit the embryonic metatarsal culture to investigate the effects of the ASARM peptide on chondrocyte matrix mineralisation

5.4 Materials and Methods

5.4.1 ATDC5 and embryonic metatarsal organ culture

ATDC5 cells were seeded at 6 x 10^3 cells/cm^2 in differentiation media and when confluent, were supplemented with 10mM βGP and 50μg/ml ascorbic acid, as described in section 2.2.1. Cells were cultured for up to 15 days at 37°C, 5% CO_2. Metatarsals were isolated from E17 and E15 embryonic mice and cultured as described in section 2.5.2 for up to 10 days. The total length of the bone through the centre of the mineralising zone was determined using image analysis software every second or third day. The length of the central mineralisation zone was also measured. All results are expressed as a percentage change from harvesting length which was regarded as baseline.

5.4.2 Establishment of stable MEPE-overexpressing ATDC5 cells

pLZ2-Ub.MEPE and pLZ2-Ub.Empty vectors were a kind gift from Dr Neil Mackenzie (The University of Edinburgh) (Appendix IV). ATDC5 cells were maintained in differentiation medium as described in section 5.4.1 and seeded at 150,000 cells/cm^2. Cells were transfected with pLZ2-Ub.MEPE and pLZ2-Ub.EMPTY constructs at a ratio of 7:2 FuGENE HD to DNA, according to the manufacturer's instructions (section 2.10.3). Blasticidin resistant colonies were picked using cloning cylinders, expanded, frozen and maintained at -150°C until further use as described in section 2.10.4. Three MEPE-overexpressing and three empty-vector clones were picked for analysis.

5.4.3 Overexpression of MEPE in murine E15 metatarsals

For proof of concept, GFP virus particles (Dr. Neil Mackenzie, The University of Edinburgh) were added to E15 metatarsal cultures for 7 days, as detailed in section 2.11.7. GFP is a protein that exhibits green fluorescence when exposed to UV light,

therefore making it a useful tool as a reporter for expression. Metatarsal bones were incubated with 4',6-diamidino-2-phenylindole (DAPI) stain for 5 minutes. A Nikon EC1 inverted confocal microscope was used for GFP and DAPI visualisation. MEPE-overexpressing and empty-vector viruses were produced as described in sections 2.11.1 - 2.11.6. Viruses were added to E15 metatarsal bones at a concentration of 6 x 10^4 virus particles/metatarsal bone with 0.6µl Polybrene on day 0 of culture. Bones were left in a humidified atmosphere for 12 days. The total length of the bone through the centre of the mineralising zone was determined using image analysis software every second or third day. The length of the central mineralisation zone was also measured (section 2.5.2).

5.4.4 shRNA knockdown of MEPE in ATDC5 cells

MEPE short hairpin ribonucleic acid (shRNA) glycerol stocks were obtained from Sigma (Appendix IV) and plasmid DNA was obtained through maxi preparation as described in section 2.7.4. ATDC5 cells were maintained in differentiation medium as described in section 5.4.1 and seeded at 150,000 cells/cm^2. Cells were transfected with 2 different shRNA MEPE plasmids and a negative shRNA plasmid as a control (a kind gift from Dr. Neil Mackenzie). FuGENE HD was used at a ratio of 7:2, according to the manufacturer's instructions (section 2.10.3). Cells were left for 24, 48 and 72 hours before RNA and protein were extracted for analysis as described in sections 2.12 and 2.13

5.4.5 MEPE-ASARM peptide

MEPE ASARM peptide were synthesised (Peptide Synthetics, Bishops Waltham, UK) as pASARM with the sequence RDDSSESSDSG(Sp)S(Sp)SSE(Sp)SDGD, and also non-phosphorylated ASARM (npASARM) with the sequence RDDSSESSDSGSSSESDGD (Sp: serine phosphorylation). pASARM and npASARM peptides were added to cultures at concentrations of 10, 20 and 50µM, with controls treated with a DMSO carrier (0.1%). In further studies, peptides were added at a final concentration of 20µM with experiments being performed at least 3 times.

5.4.6 Histological staining of cell cultures

ATDC5 cell cultures were stained for calcium deposition (alizarin red), collagen production (Sirius red), and glycosaminoglycan presence (alcian blue) as described in section 2.4. The optical densities of the resultant stains were analysed using a spectrophotometer (Thermo Scientific, Northumberland, UK) along with an appropriate blank control. Reactions were completed in triplicate at each time point.

5.4.7 RNA analysis of ATDC5 cells and metatarsals

RNA was extracted from ATDC5 cell cultures using an RNeasy mini kit according to the manufacturer's instructions (section 2.12.1). For metatarsal organ cultures, 4 bones from each control or experimental group were pooled in 100µl Trizol reagant at either day 5 or 7 of culture, and RNA was extracted according to the manufacturer's instructions (section 2.12.2). For each sample, total RNA content was assessed by absorbance at 260nm and purity by A260/A280 ratios, and then reverse-transcribed as described in section 2.12.3. qPCR was performed using the SYBR green detection method on a Stratagene Mx3000P real-time qPCR system as detailed in section 2.12.5. Primers were purchased from PrimerDesign Ltd, or designed in house and synthesised by MWG Eurofins (Appendix II). Reactions were run in triplicate and routinely normalised against *18S*. Sequences are detailed in Supplemental Table S1. qPCR analysis of angiogenesis markers was performed in collaboration with Dr. Claire Clarkin, University of Southampton, and normalised to *β-actin* mRNA transcript levels.

5.4.8 3D-microtomography of metatarsals

Metatarsal bones were fixed in 70% ethanol and stained with eosin dye (for visualisation) at day 7 of culture. 3D-microtomography of metatarsals was performed in collaboration with Ms. Lesya Zelenchuk and Prof. Peter Rowe, The University of Kansas Medical Center, Kansas City USA. Briefly, metatarsal bones were embedded in paraffin blocks and then were scanned with a high-resolution micro computed tomography (µCT) (µCT40; Scanco Medical, Southeastern, PA) as previously described (Rowe *et al.* 2006; David *et al.* 2009). Data were acquired at 55

KeV with 6μm^3. Three-dimensional reconstructions for bone samples were generated with the following parameters: Gauss Sigma = 4.0; Support = 2, Lower Threshold= 90 and Upper Threshold =1000. Tissue mineral density was derived from the linear attenuation coefficient of threshold bone through precalibration of the apparatus for the acquisition voltage chosen. The bone volume (BV) / tissue volume (TV) was measured using sections encompassing the entire metatarsal on a set of 85 sections that was geometrically aligned for each sample.

5.4.9 Metatarsal [^{3}H]-thymidine proliferation assay

As described in section 2.14.1, metatarsal bones were incubated with 3 μCi/ml [^{3}H]-thymidine for the last 6 hours of their 7-day culture. Metatarsals were solubilised at 60^{o}C for an hour and then the DNA incorporating [^{3}H]-thymidine determined using a scintillation counter.

5.4.10 ALP enzyme activity

ALP activity was determined in metatarsal bones at day 7 of culture using an assay for ALP according to the manufacturer's instructions. The method is detailed in section 2.14.2. Total ALP activity was expressed as nanomoles *p*-nitrophenyl phosphate hydrolysed per minute per bone.

5.5 Results

5.5.1 Overexpression of MEPE in ATDC5 cells

To examine the functional role of MEPE in chondrocyte matrix mineralisation, MEPE overexpressing ATDC5 cells were generated for culture in mineralising conditions as characterised in Chapter 3. The efficiency of this overexpression was assessed by qPCR and western blotting. *Mepe* mRNA was increased in all three MEPE overexpressing clones by > 43 fold (average = 61 fold in comparison to average of empty vector clones, Fig. 5.1A $P<0.001$). Intriguingly, assessment of MEPE protein expression by western blotting failed to detect any significant change in MEPE protein level between empty and MEPE-overexpressing clones (Fig. 5.1B).

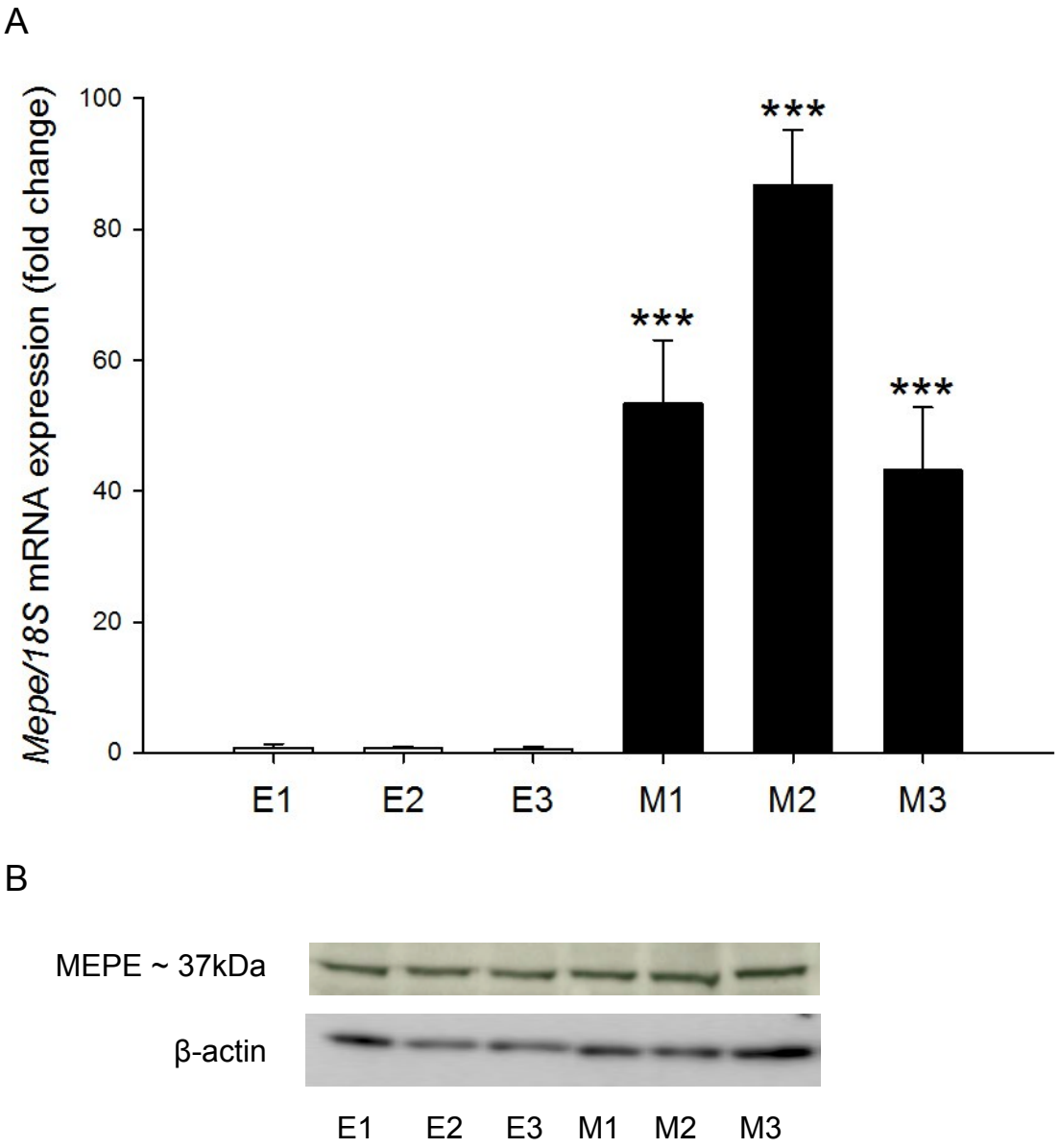

Figure 5.1 The overexpression of *Mepe* mRNA in ATDC5 cells

Chondrogenic ATDC5 cells were transfected with MEPE-overexpressing and empty vector constructs. Three clones for each were examined for *Mepe* mRNA and protein expression. **(A)** *Mepe* mRNA was significantly increased in all three clones in comparison to empty-vector controls as determined by qPCR **(B)** Western blot analysis revealed no apparent changes in MEPE protein level between empty and MEPE-overexpressing clones. Results are normalised to the *18S* housekeeping gene. Data are represented as mean ± SEM (n=3 replicates) ***P<0.001.

5.5.2 Inhibition of ATDC5 cell matrix mineralisation by overexpression of MEPE

When cultured under mineralising conditions for up to 15 days (Chapter 3), individual MEPE-overexpressing clones showed an inhibition of mineralisation as visualised by alizarin red staining and quantified by spectrophotometry at days 8, 12 and 15 of culture (Fig. 5.2A & C). Average quantification of alizarin red staining showed significant decreases in mineralisation of MEPE-overexpressing clones at the aforementioned time points (in comparison to empty vector clones, Fig. 5.2B, $P<0.01$). The mRNA expression of *Col2a1*, *Col10a1* and *Alpl* were examined by qPCR as markers of endochondral ossification and these were unchanged between MEPE-overexpressing and empty-vector controls at day 15 of culture (Fig. 5.3 A – C). Further chondrocyte marker genes of differentiation and mineralisation (*Ank*, *Enpp1*, *Atf3*, *PthIh*, *Ihh* and *Mmp13*) were examined for mRNA expression and again no differences were found between the MEPE-overexpressing and the empty-vector controls (Fig. 5.4). Interestingly, *Phex* mRNA levels were significantly decreased in MEPE-overexpressing clones in comparison to empty-vector controls at day 15 of culture (Fig. 5.3D, $P<0.05$).

5.5.3 Overexpression of MEPE in E15 metatarsals

Following the successful overexpression of MEPE in ATDC5 cells (section 5.5.1), this was attempted in the E15 metatarsal organ culture model defined in Chapter 3. To establish proof of concept, E15 metatarsal bones were transfected with GFP virus particles and visualised for GFP uptake following 7 days in culture. This was achieved successfully (Fig. 5.5A - C) and as such, MEPE lenti-virus constructs were made for transfection of E15 metatarsal bones. However, due to time and procedure constraints, the MEPE overexpressing lenti-virus and its empty-virus control were added to the metatarsals at a lesser concentration than that optimised with GFP virus particles (2×10^6 virus particles/metatarsal bone, section 2.11.7). No differences in the mineralisation capability or in the longitudinal growth of the bones were observed (Fig. 5.6A & B).

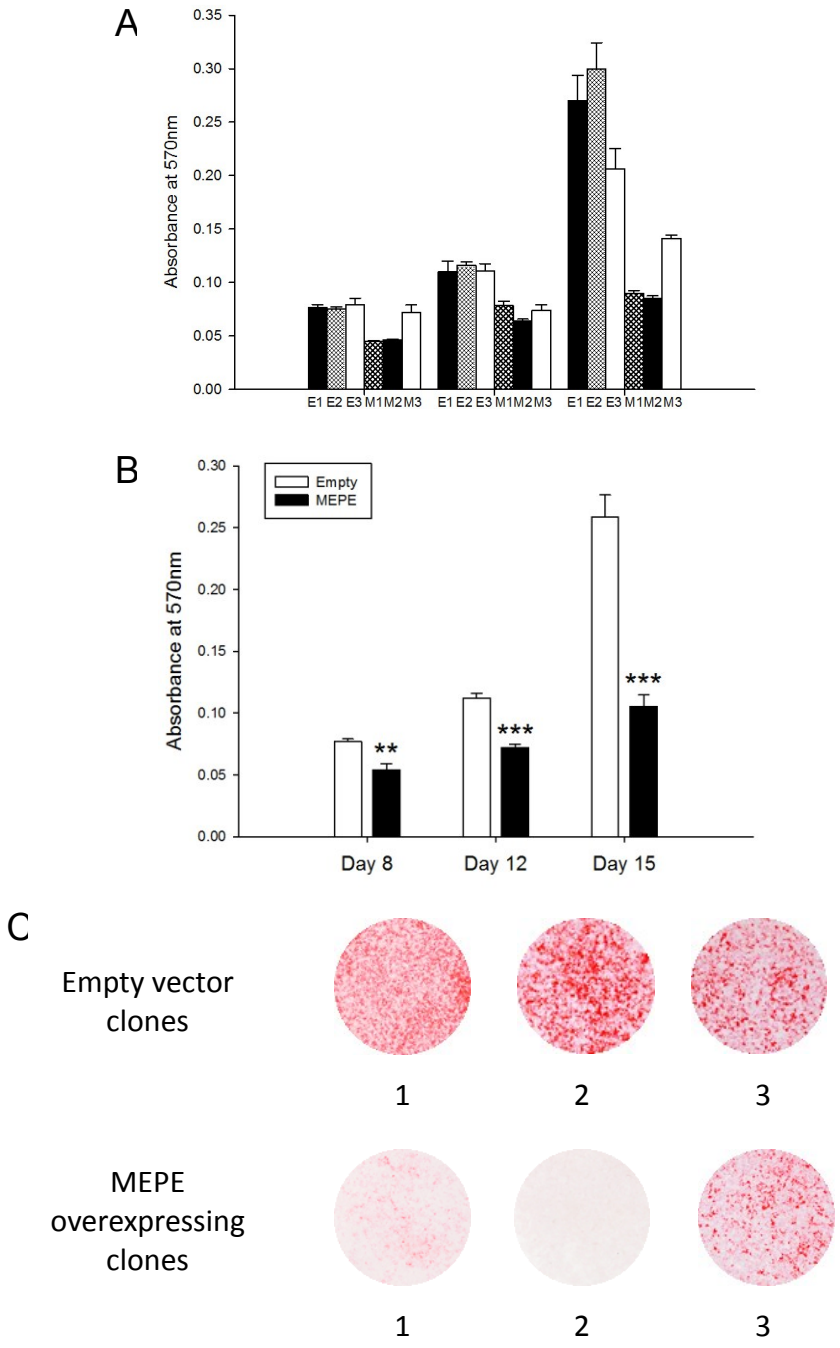

Figure 5.2 The overexpression of *Mepe* mRNA inhibits ATDC5 culture mineralisation

Chondrogenic ATDC5 cells were transfected with *Mepe* mRNA-overexpressing and empty-vector constructs and cultured for up to 15 days in mineralising conditions. Three individual clones for each were examined for mineralisation by alizarin red staining. **(A)** Quantification of staining indicated decreased mineralisation in all individual MEPE-overexpressing clones (M1, M2 and M3) in comparison to all individual empty-vector clones (E1,E2 and E3) at days 8, 12 and 15 of culture **(B)** Average absorbance of all MEPE and all empty-vector clones indicated an average significant inhibition of matrix mineralisation in MEPE-overexpressing cells in comparison to empty-vector controls **(C)** Single representative images of alizarin red staining in all six clones at day 15 of culture. Data are represented as mean ± SEM (n=3 separate cultures) in comparison to empty-vector controls **P<0.01, ***P<0.001.

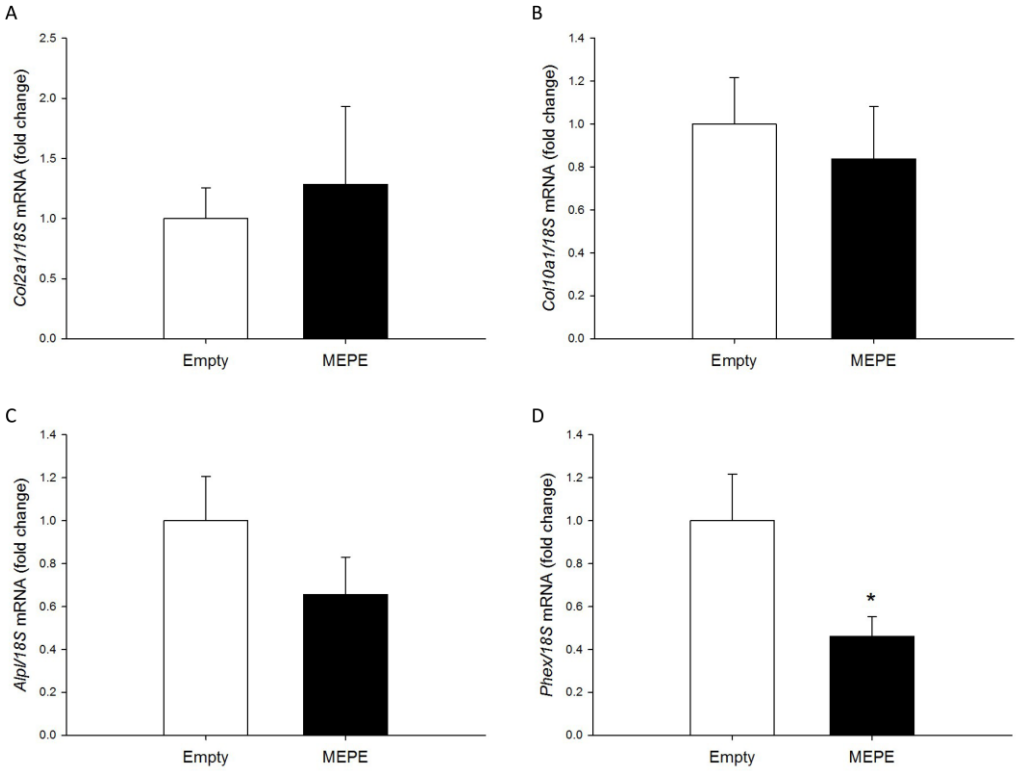

Figure 5.3 Gene expression in MEPE-overexpressing ATDC5 cells

MEPE-overexpressing ATDC5 cells showed no differences in the mRNA expression of **(A)** *Col2a1* **(B)** *Col10a1* **(C)** *Alpl*. However *Phex* mRNA expression was significantly decreased in comparison to empty-vector controls **(D)**. Data are represented as mean of 3 clones ± SEM *P<0.05.

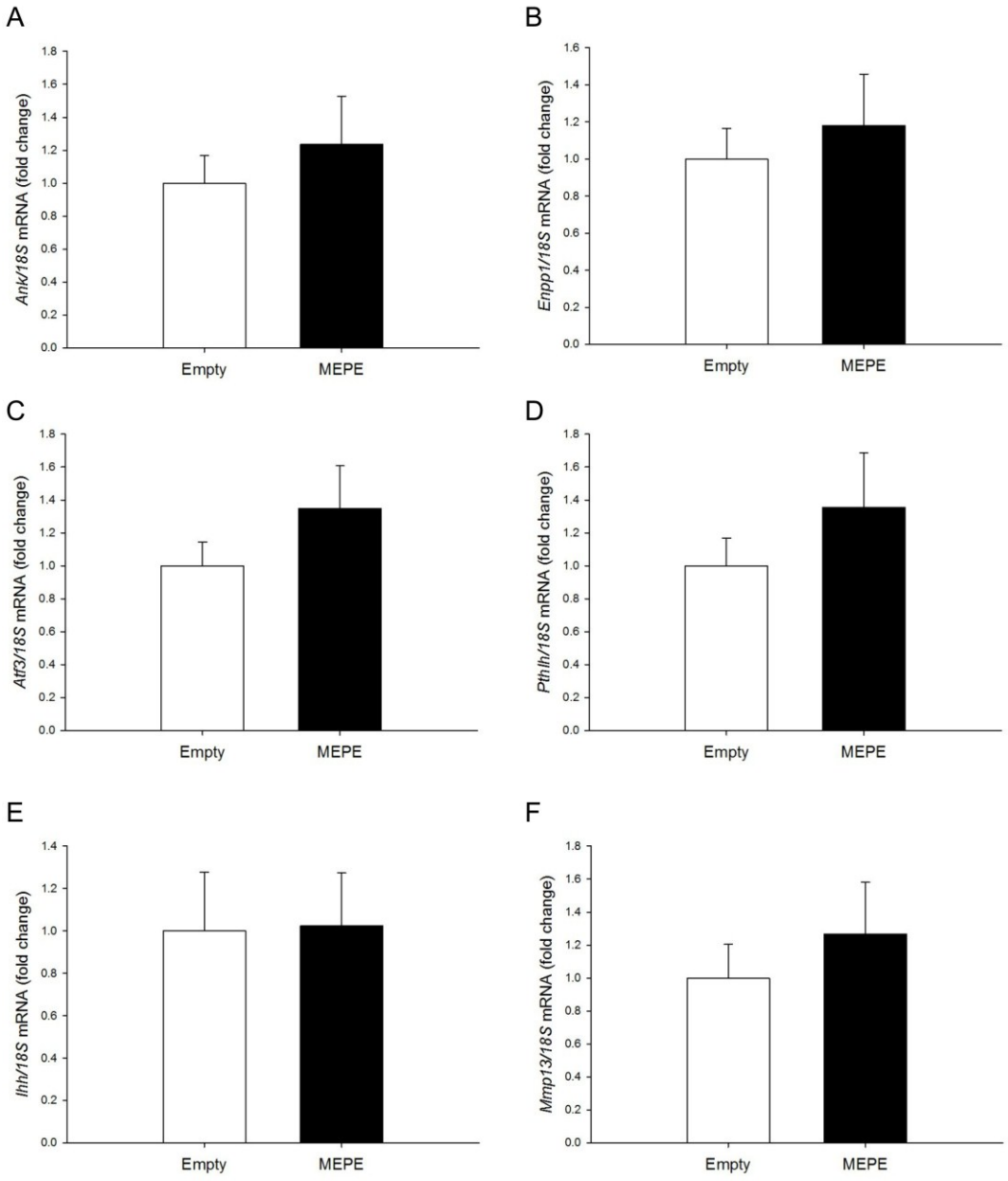

Figure 5.4 The lack of effect of MEPE overexpression on chondrocyte differentiation and mineralisation gene expression

Analysis of mRNA expression in MEPE-overexpressing and empty-vector control clones after 15 days of culture **(A)** *Ank* **(B)** *Enpp1* **(C)** *Atf3* **(D)** *PthIh* **(E)** *Ihh* **(F)** *Mmp13* Data are represented as mean of 3 clones ± SEM (n=3 replicates).

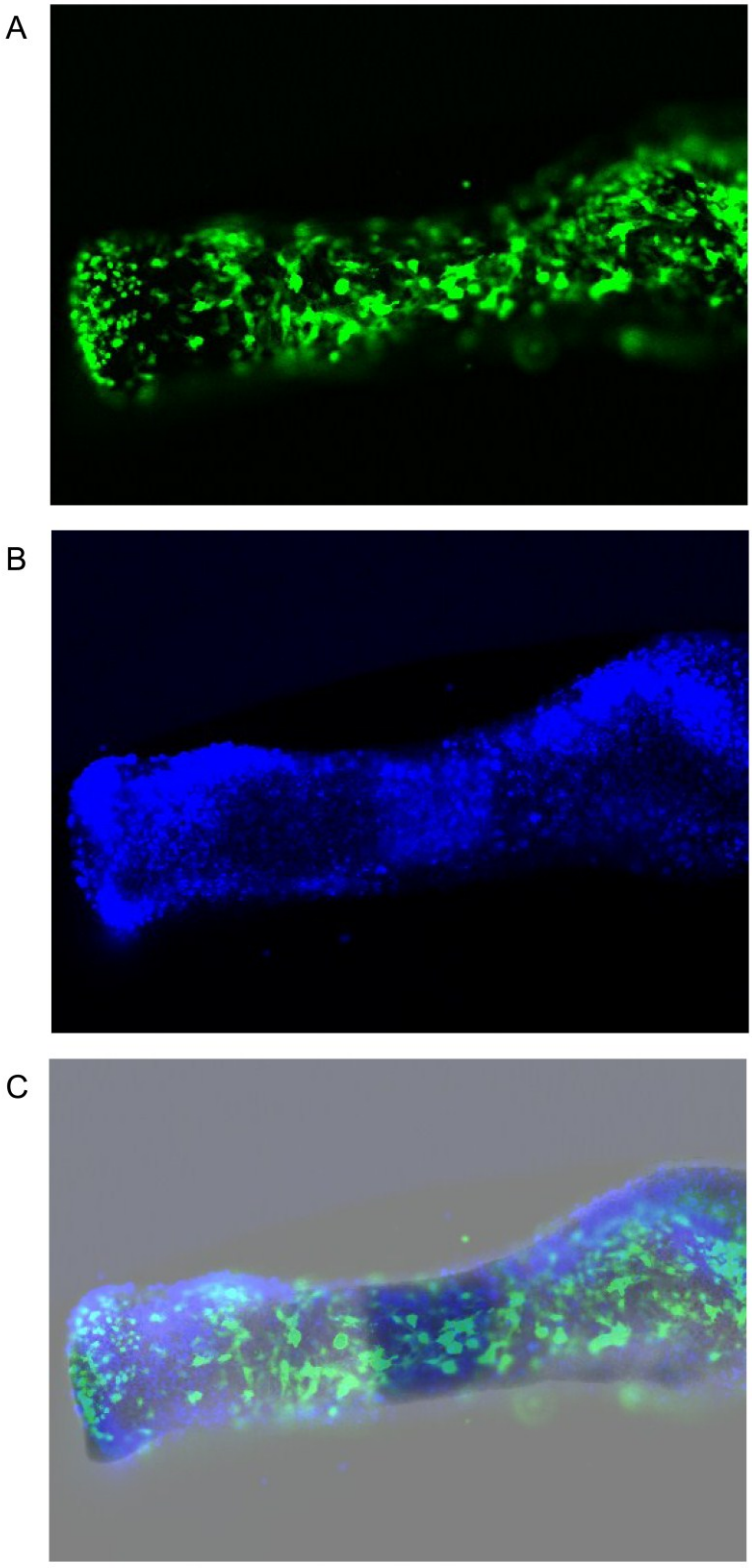

Figure 5.5 E15 metatarsals transfected with GFP virus particles

E15 metatarsal bones were transfected with GFP virus particles for proof of concept **(A)** and stained with DAPI stain for DNA visualisation using a confocal microscope **(B)**. Dual images indicated successful transfection of GFP virus throughout the metatarsal bone **(C)**.

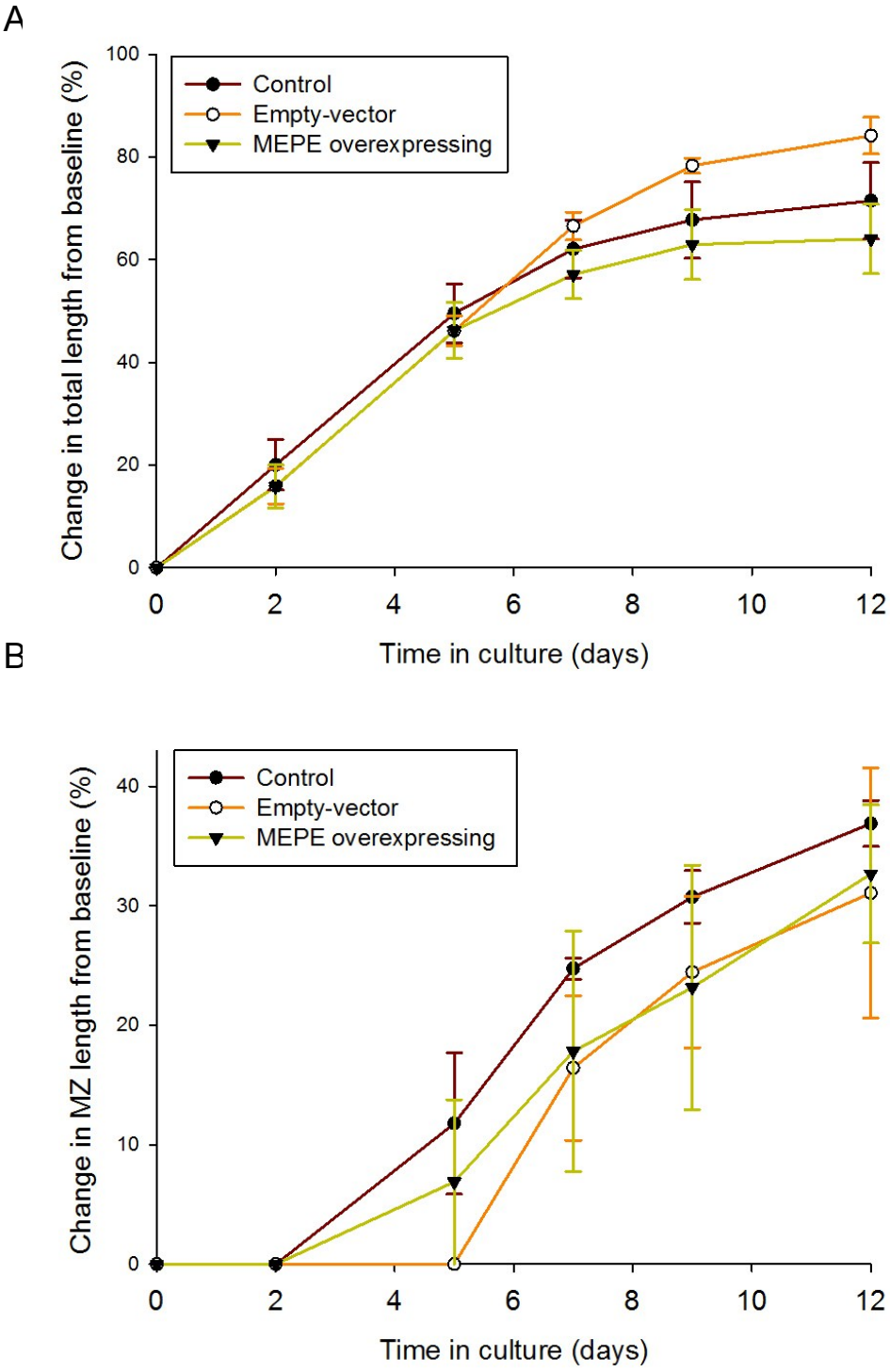

Figure 5.6 The lack of effect of MEPE overexpression on E15 metatarsal bones

(A) The growth rate of E15 metatarsal bones was not affected by the overexpression of MEPE when cultured for up to 12 days **(B)** The change in mineralisation zone as a percentage of the total length was also unchanged during the culture period. Data are represented as mean ± SEM of six bones.

5.5.4 Analysis of MEPE shRNA knockdown in ATDC5 cells

To further elucidate the role of MEPE in chondrocyte matrix mineralisation, ATDC5 cells were transfected with vectors containing a shRNA sequence targeted against MEPE. This technique is routinely used in various cells to knockdown various genes of interest. The efficiency of the MEPE knockdown was assessed after 48 and 72 hours at the mRNA and protein level by qPCR and western blotting respectively in comparison to empty shRNA and non-transfected control cells.

qPCR analysis indicated no differences in *Mepe* mRNA expression in ATDC5 cells subjected to shRNA MEPE knockdown after 48 hours (Fig. 5.7A). Neither was there any difference observed between knockdown and control cells at the protein level (Fig. 5.7C). After 72 hours, there were still no differences (Fig. 5.7B & C) thus suggesting that the knockdown was ineffective at both the mRNA and protein level. This experiment was repeated but effective knockdown could not be confirmed.

5.5.5 Dose- and phosphorylation-dependent effects of the ASARM peptide on ATDC5 cell matrix mineralisation

It is known that PHEX prevents the cleavage of MEPE to its ASARM peptide, a 2.2kDa peptide common to the SIBLING family of proteins. The decreased mRNA expression of *Phex* in ATDC5 cells overexpressing MEPE (Fig. 5.3) suggests that the ASARM peptide is the functional component of MEPE in this system. Therefore to determine the role of the ASARM peptide in chondrocyte matrix mineralisation, the mineralisation capability of ATDC5 cells in response to MEPE-ASARM peptides was examined.

The posttranslational modifications of the SIBLING proteins are important in determining their function (Staines *et al.* 2012b). As such, varying concentrations of the MEPE ASARM peptide in both its pASARM and npASARM form were added to ATDC5 cell cultures under mineralising conditions over a 15-day culture period.

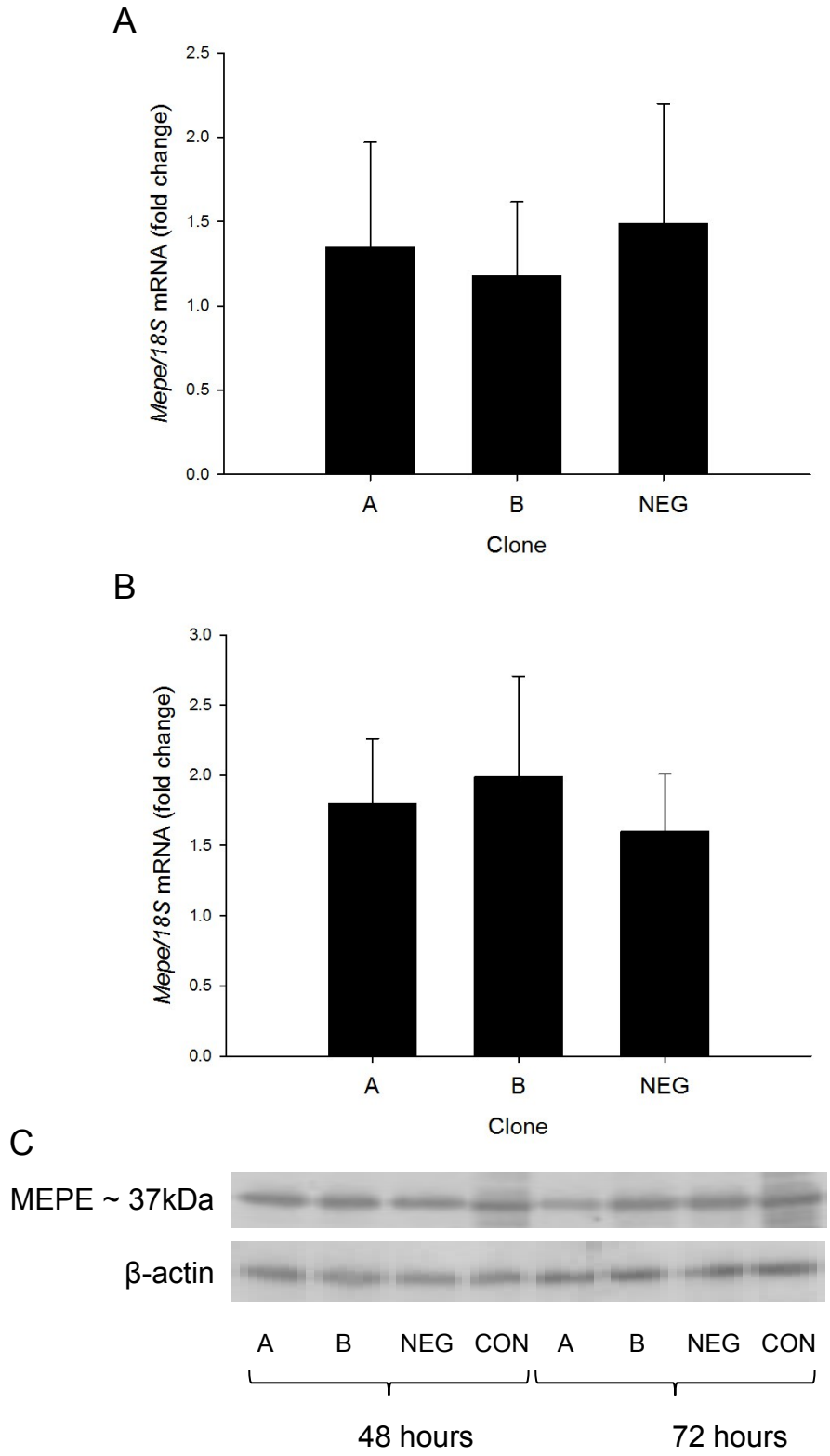

Figure 5.7 MEPE shRNA knockdown efficiency

Quantification of *Mepe* mRNA by RT-qPCR in ATDC5 cells transfected with 2 different MEPE shRNA vectors (A and B) and an empty shRNA vector after **(A)** 48 hours **(B)** 72 hours. mRNA levels are expressed as a fold change in comparison to the control, non-transfected cells. Data are normalised to *18S* mRNA and are represented as mean ± SEM (n= 3 separate transfections) **(C)** MEPE protein expression in MEPE shRNA and empty shRNA cells as well as control cells. β-actin was used as a loading control.

There was no apparent morphological difference between control and ASARM-treated cells. pASARM peptide inhibited mineralisation in a dose-dependent manner as visualised by alizarin red staining and quantified by spectrophotometry (at 20μM and 50μM in comparison to control; $P<0.01$) (Fig. 5.8A). Interestingly, it was found that npASARM peptide promoted mineralisation over the 15-day culture period (at 20μM and 50μM in comparison to control; $P<0.01$) (Fig. 5.8B). Due to the physiological relevance of 20μM in XLH patients and *Hyp* mice, this concentration was selected for use in future experiments (Addison *et al.* 2008).

5.5.6 Absence of an effect of MEPE-ASARM peptides on ATDC5 cell differentiation

To investigate whether the MEPE-ASARM peptides affect chondrocyte differentiation, the ability of the ATDC5 cells to produce a collagenous matrix when treated with the MEPE-ASARM peptides was examined. Collagen deposition (Fig. 5.9A) and glycosaminoglycan production (Fig. 5.9B), as visualised by sirius red and alcian blue stains respectively, were unaffected by addition of 20μM pASARM or npASARM peptide. Furthermore, cellular expression of *Alpl* mRNA and ALP activity were unchanged (Fig 5.10 B & C), as were concentrations of the mineralisation inhibitor PP_i (Fig. 5.10A).

5.5.7 pASARM peptide inhibit the mineralisation capability of E17 metatarsal bones

The data determined in ATDC5 cells are supportive of a direct role for MEPE-ASARM peptides in chondrocyte matrix mineralisation and thus to next examine these effects in a more physiologically relevant model, the metatarsal organ culture model was used. When dissected, E17 mice metatarsals display a central core of mineralised cartilage juxtaposed by a translucent area on both sides representing the hypertrophic chondrocytes (Mushtaq *et al.* 2004). These bones were cultured in the presence of varying concentrations of pASARM and npASARM peptides over a 10- day period to examine their effects on longitudinal bone growth and the growth of the central mineralisation zone. These data indicated that MEPE-ASARM

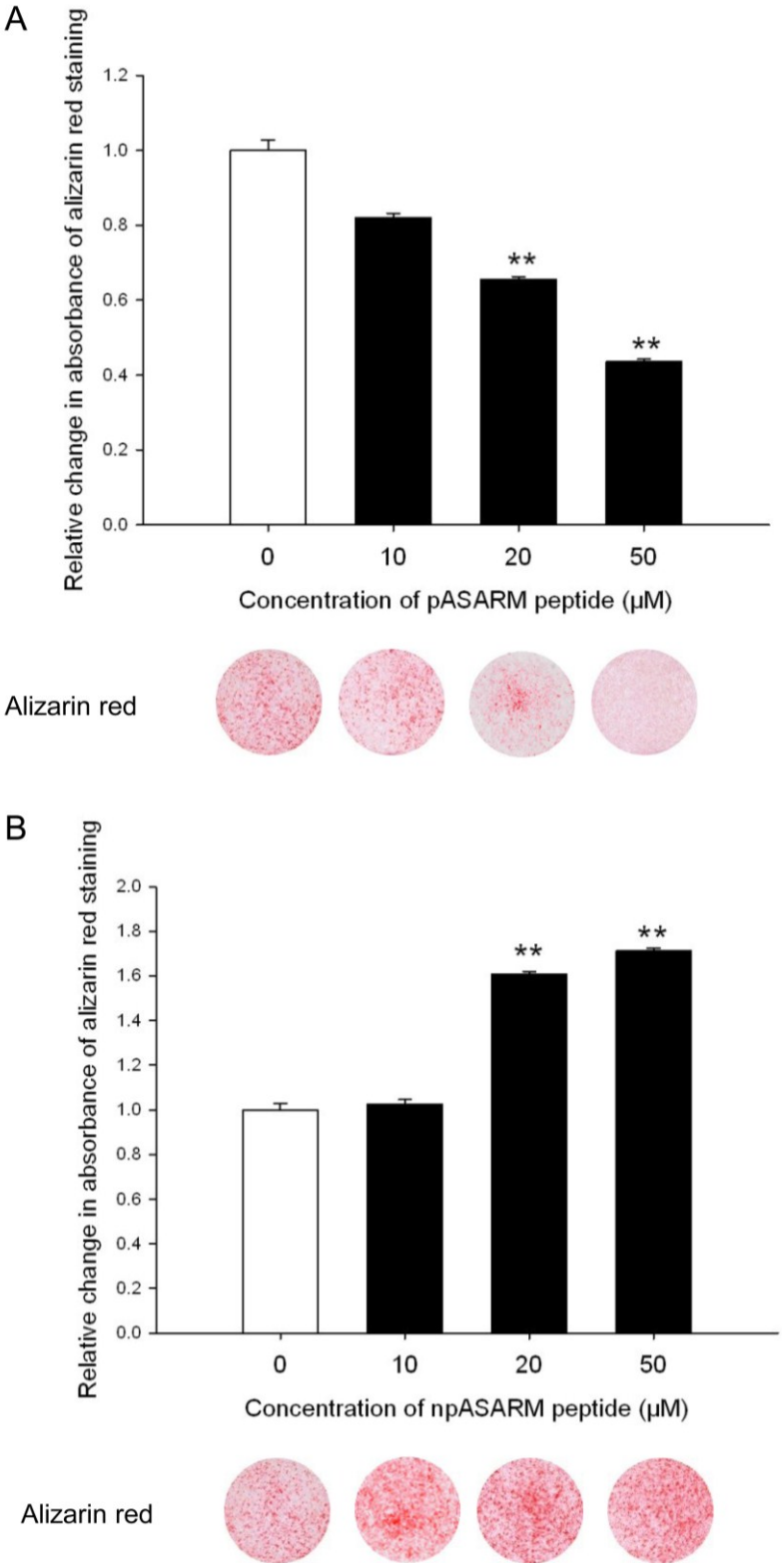

Figure 5.8 Dose- and phosphorylation-dependent effects of the ASARM peptide on ATDC5 matrix mineralisation

Mineralisation of ATDC5 matrix in the presence of varying concentrations (0-50μM) of **(A)** pASARM and **(B)** npASARM peptides was visualised by alizarin red staining (images) and quantified after 15 days of culture. Data are represented as mean ± SEM of three wells analysed in triplicate **P<0.01.

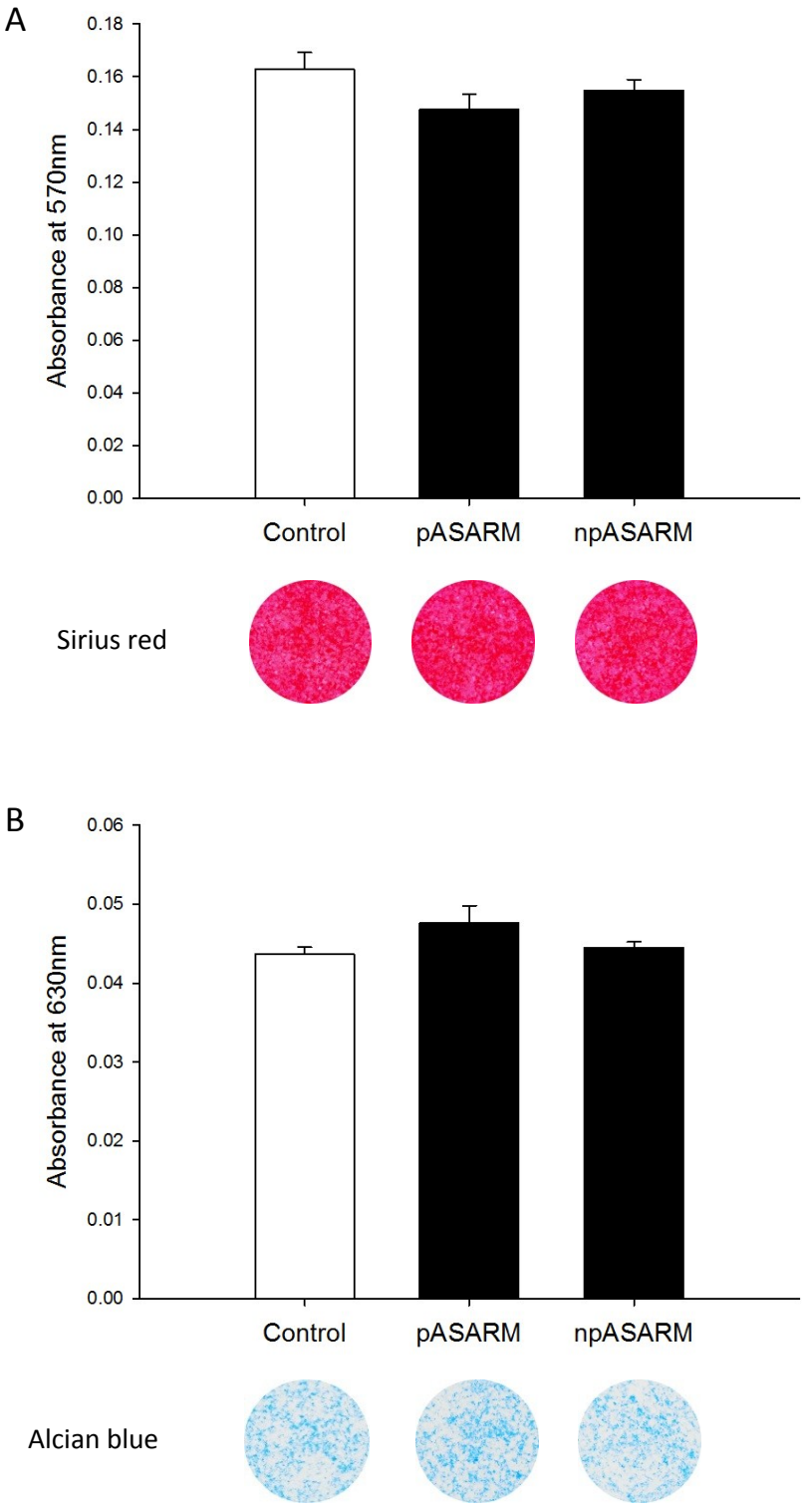

Figure 5.9 The lack of effect of MEPE-ASARM peptides on ATDC5 cell differentiation

Quantification of sirius red staining **(A)** and alcian blue staining **(B)** (images) of ATDC5 cells following 15 days of culture with 20μM pASARM and npASARM peptides. Data are represented as mean ± SEM of three wells analysed in triplicate.

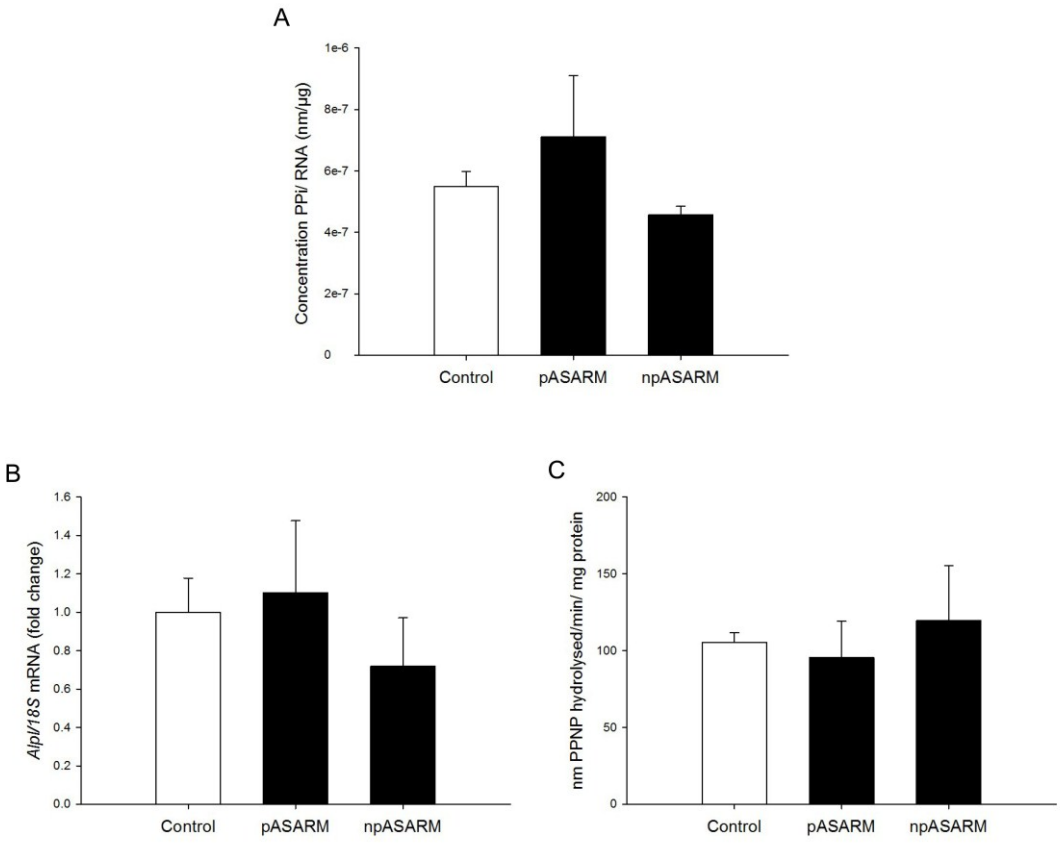

Figure 5.10 The lack of effect of MEPE-ASARM peptides on known regulators of mineralisation

(A) Concentration of PP_i was unchanged in ATDC5 cultures treated with 20µM pASARM and npASARM peptides in comparison to control cultures. **(B)** *Alpl* mRNA expression was also unchanged as was **(C)** ALP activity. Data are represented as mean ± SEM of three wells analysed in triplicate.

peptide inhibit mineralisation of metatarsal bones across a range of concentrations (Fig. 5.11B, $P<0.01$) despite no significant difference in the total longitudinal bone growth (Fig. 5.11A). In concordance with the ATDC5 cell data, 20μM MEPE-ASARM peptides were used in future experiments.

Metatarsal bones cultured in the presence of 20μM pASARM and npASARM peptides grew in length at the same rate as the control bones (up to 80%) after 7 days in culture (Figs. 5.12C - F). However, whereas in the control and npASARM treated metatarsals the central mineralisation zone increased in length throughout the culture period (increased approximately 5-6 fold from initial lengths, Fig. 5.12C, D & G), in the pASARM treated cultures no changes in mineralisation zone length were noted ($p<0.01$ at day 6, $p<0.001$ at days 8 and 10 in comparison to the control bones, Fig. 5.12C, E & G).

5.5.8 pASARM peptide inhibit the mineralisation capability of E15 metatarsal bones

To examine this apparent inhibitory effect further, the E15 metatarsal model characterised in Chapter 3 was utilised. As previously described, these bones consist of early proliferating chondrocytes (Fig. 5.13B) and no evidence of a mineralised core. After 7 days in culture, the chondrocytes in the centre of the bone become hypertrophic and mineralise their surrounding matrix as is previously documented and described in Chapter 3 (Haaijman *et al.* 1999) (Fig. 5.13C).

This central core of mineralised cartilage formed in control bones and bones treated with 20μM npASARM peptide (Figs. 5.13C & D), however it was minimal in metatarsal bones treated with 20μM pASARM peptide (Fig. 5.13E), as seen in the phase contrast images.

This was further confirmed by von kossa staining of histological sections for mineralisation (Fig. 5.14B & C) and by μCT scanning of the metatarsal bones to

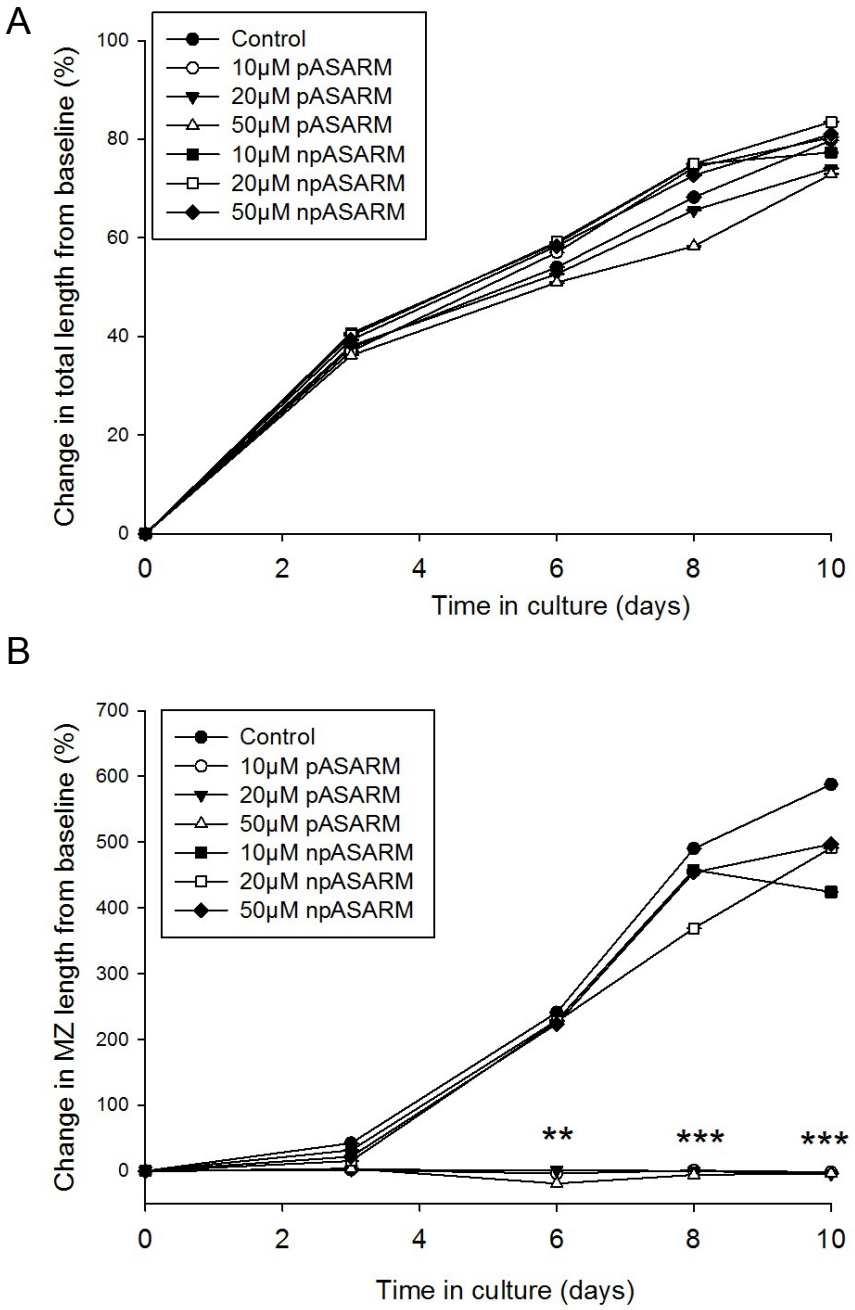

Figure 5.11 The inhibition of E17 metatarsal bone mineralisation by the pASARM peptide

(A) The growth rate of E17 metatarsal bones was not affected by treatment with 10, 20 or 50μM MEPE-ASARM peptides when cultured for up to 10 days **(B)** The percentage change in mineralisation zone increased in control and npASARM treated bones whereas the mineralisation zone in bones treated with pASARM peptides did not increase at all during the culture period. Data are represented as mean ± SEM of at least six bones **P<0.01, ***P<0.001 Error bars are too small to be visualised due to the size of the symbols.

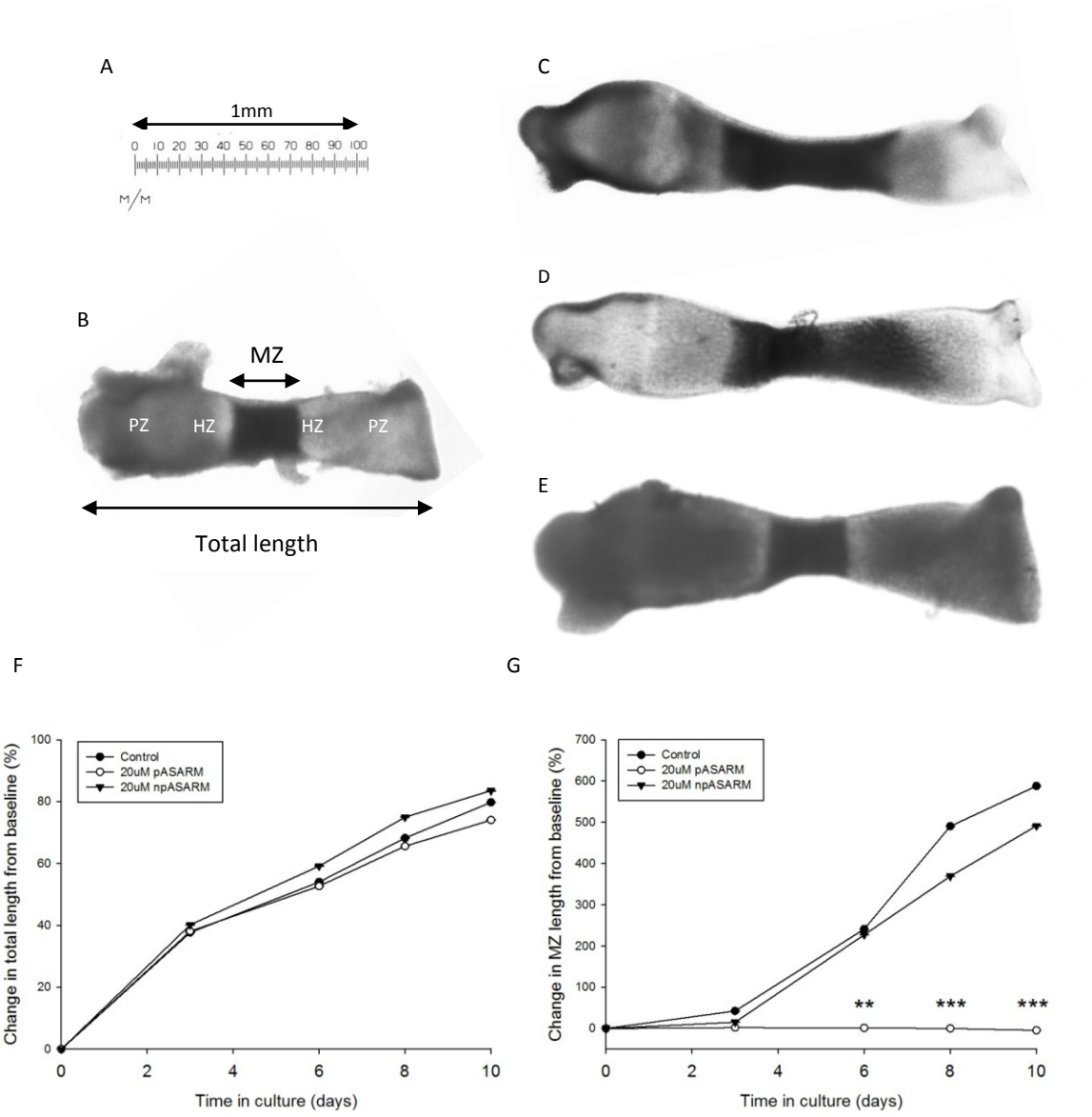

Figure 5.12 pASARM inhibition of E17 metatarsal mineralisation

Measurements of digital images of E17 mouse metatarsal bones in culture with clearly delineated mineralising zones **(B-E)** were taken using a calibrated ruler **(A)**. Images clearly show the harvesting length **(B)** with the locations of the proliferating (PZ), hypertrophic (HZ) and mineralising (MZ) zones, as well as the total length measurement. A control metatarsal bone is illustrated in **(C)** and bones treated with continuous 20μM npASARM **(D)** and pASARM peptides **(E)** after 10 days of culture. The growth rate of the embryonic metatarsal bones was not affected by treatment with 20μM MEPE-ASARM peptides **(F)** when cultured for up to 10 days. There was no significant difference in the percentage change in mineralisation length between control and npASARM treated bones, both of which increased over the culture period. However the mineralisation zone length in bones treated with pASARM peptides remained the same during the culture period **(G)**. Data are represented as mean ± SEM of at least six bones **P<0.01, ***P<0.001 in comparison to control bones at equivalent days of culture. Error bars are too small to be visualised.

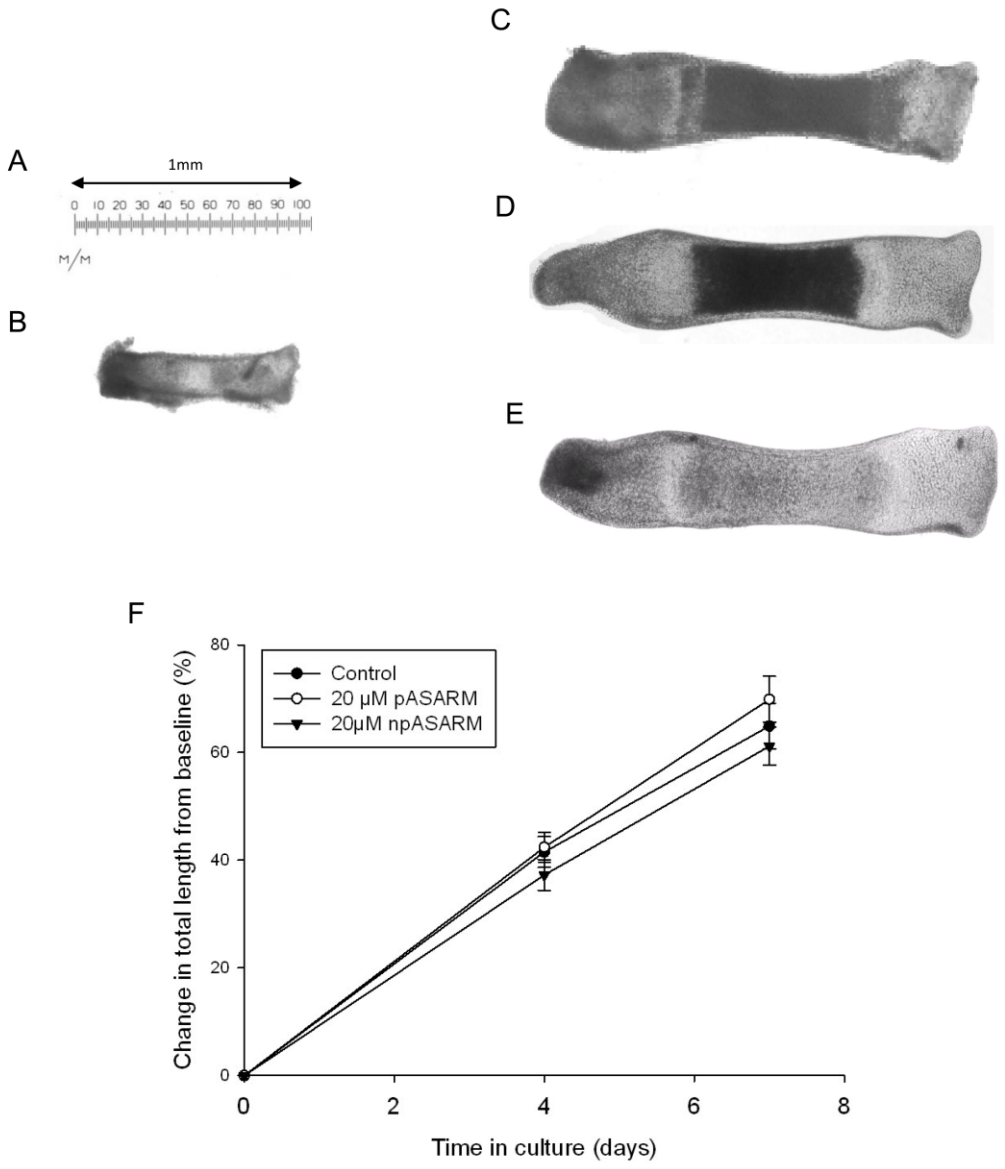

Figure 5.13 pASARM inhibition of E15 metatarsal mineralisation

Measurements of digital images of E15 mouse metatarsal bones in culture were taken using a calibrated ruler **(A)**. At time of harvesting, bones did not have a central mineralisation zone as indicated by the asterisk **(B)**. After 7 days in culture, control **(C)** and npASARM **(D)** treated bones formed a large mineralisation zone however this was inhibited in pASARM treated bones **(E)**. Despite this, all metatarsal bones grew at a similar rate **(F)**. Data are represented as mean ± SEM of at least six bones.

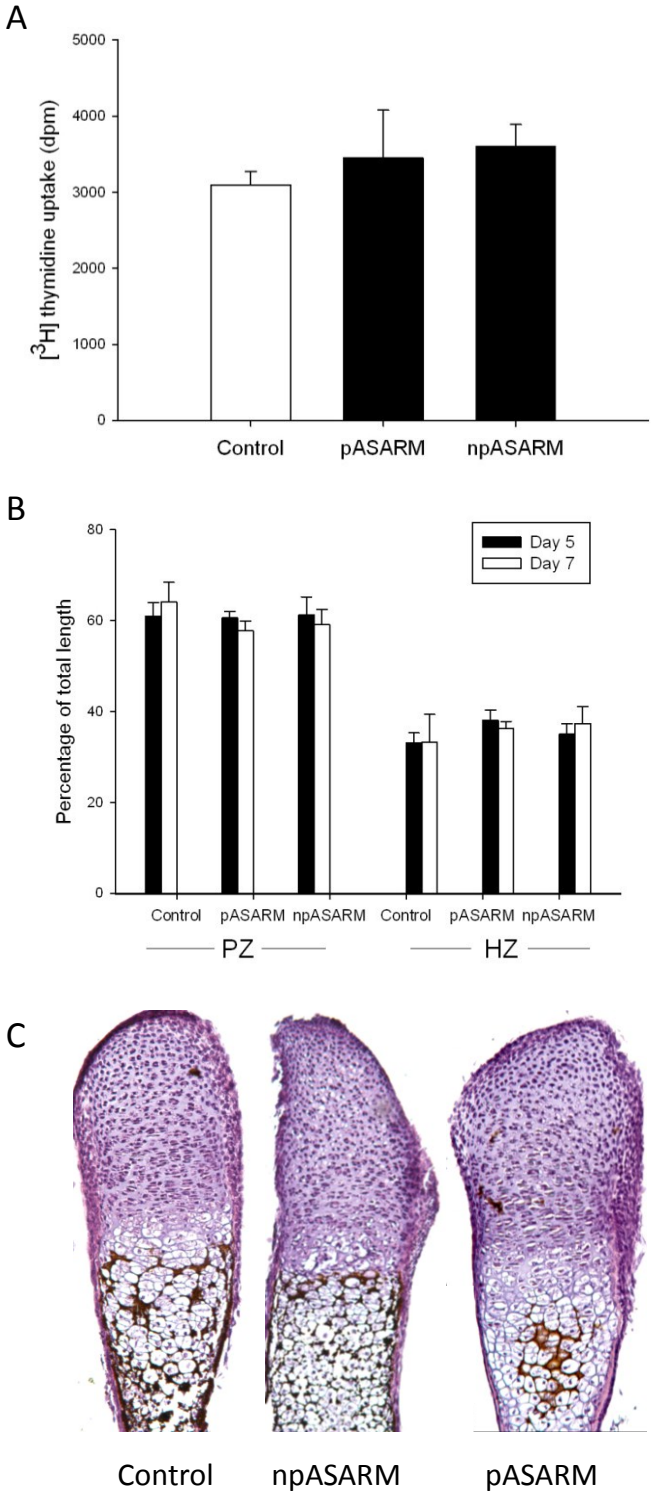

Figure 5.14 The lack of effect of the MEPE-ASARM peptides on metatarsal chondrocyte differentiation

There was no difference in the proliferation of the chondrocytes within the control and MEPE-ASARM treated bones **(A)**. Histological sections **(C)** showed control and npASARM treated bones to have abundant mineral as indicated by von kossa staining. This was not seen in pASARM treated metatarsals. There was no difference in the widths of the PZ and HZ of chondrocytes between the different groups of metatarsals at either day 5 or day 7 of culture **(B)**. Data are represented as mean ± SEM of six bones.

allow the visualisation of the bones in a 3D context (Fig. 5.15B). In comparison to the control and npASARM treated bones, metatarsal bones cultured in the presence of pASARM peptide had a significantly reduced BV/TV ($P<0.001$) (Fig. 5.15A), as is clearly visible in the μCT scan images (Fig. 5.15B). This unequivocally shows the inhibition of mineralisation in metatarsal bones by the pASARM peptide. Despite the increase in ATDC5 ECM mineralisation upon addition of npASARM peptide, here the mean density of the mineralised bone was unchanged between control and npASARM treated bones (control 163.4 ±12.1mg hydroxyapatite/ccm, npASARM 173.2 ±21.9mg hydroxyapatite/ccm, not significant) suggesting that the result seen in the ATDC5 cell cultures may be artifactual.

Apart from the inhibition of mineralisation by the pASARM peptide, there were no other obvious morphological differences in the development of these bones in comparison to the control bones. All bones grew at the same rate (increased approximately 65% from initial lengths) (Fig. 5.13B - F) and by incorporating [^{3}H]-thymidine into the bones at the end of the culture period, day 7, it was determined that the proliferation rate of the chondrocytes was unchanged (Fig. 5.14A). The lengths of the PZ and HZ zones of chondrocytes were also measured. The MEPE-ASARM peptides had no effect on the percentage sizes of the maturational zones of the metatarsal bones, or on the cell numbers within the bones (Control: 1139.13 ± 172.01, pASARM: 1594.97 ± 226.9, npASARM 1233.71 ± 126.08) (Fig. 5.14B & C).

This therefore suggests that the MEPE-ASARM peptides had no effect on the differentiation capability of the metatarsal chondrocytes. To examine this further, the mRNA expressions of chondrocyte differentiation markers were determined (*Col10a1*, *Col2a1*, *Atf3*, *PthIh* and *Ihh*). There were no significant differences between the control and pASARM treated bones at days 5 and 7 of culture (Fig. 5.16A - E, Fig. 5.17A - E), as is in concordance with the histological and proliferation data.

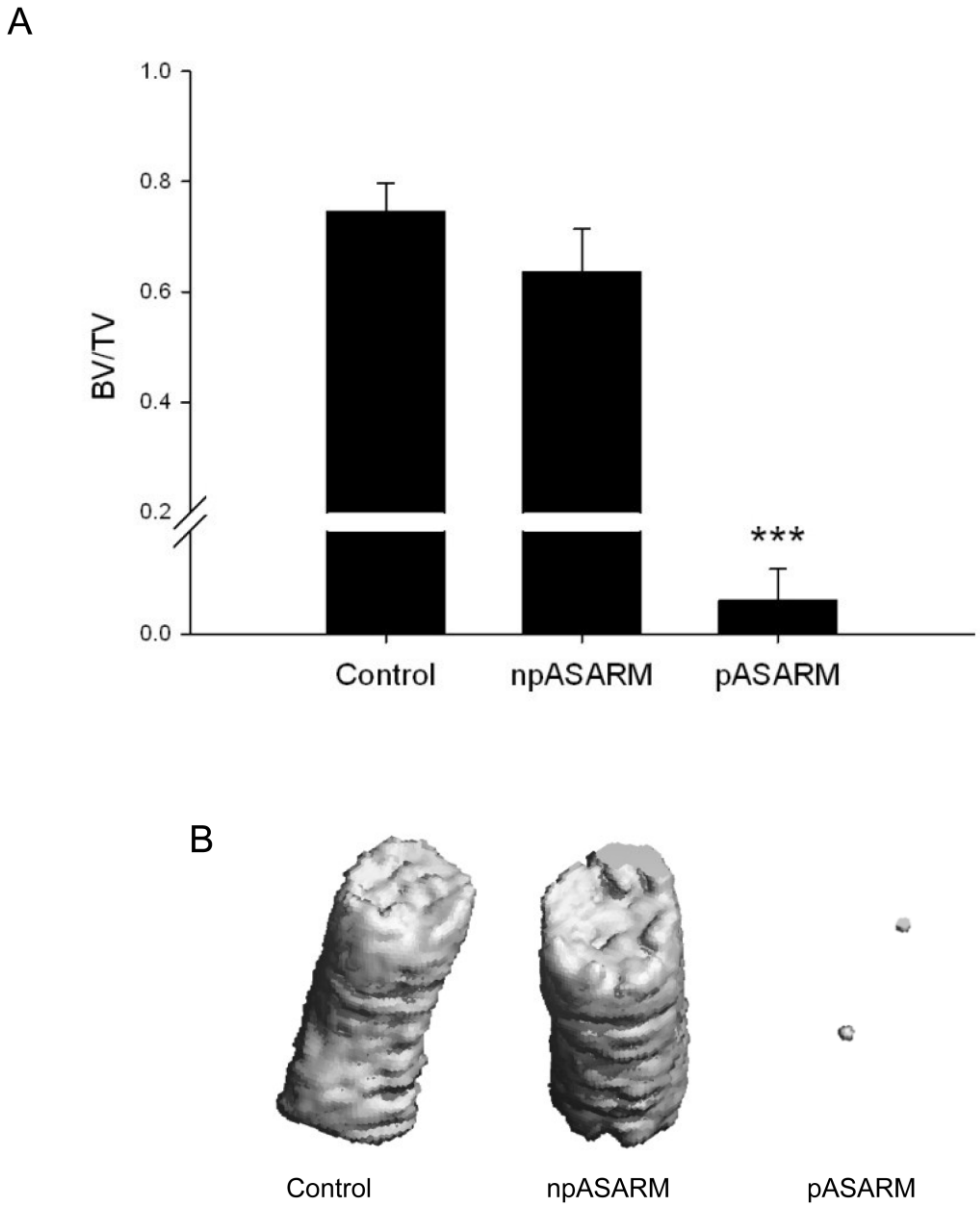

Figure 5.15 Inhibition of E15 metatarsal mineralisation by μCT analysis

μCT analysis of E15 metatarsal bones treated with npASARM and pASARM peptides and cultured for 7 days. Bones treated with pASARM had a significantly reduced BV/TV in comparison to the control and npASARM treated bones **(A)**. This was clearly visible in the μCT images **(B)**. Data are represented as mean ± SEM of three bones ***P<0.001.

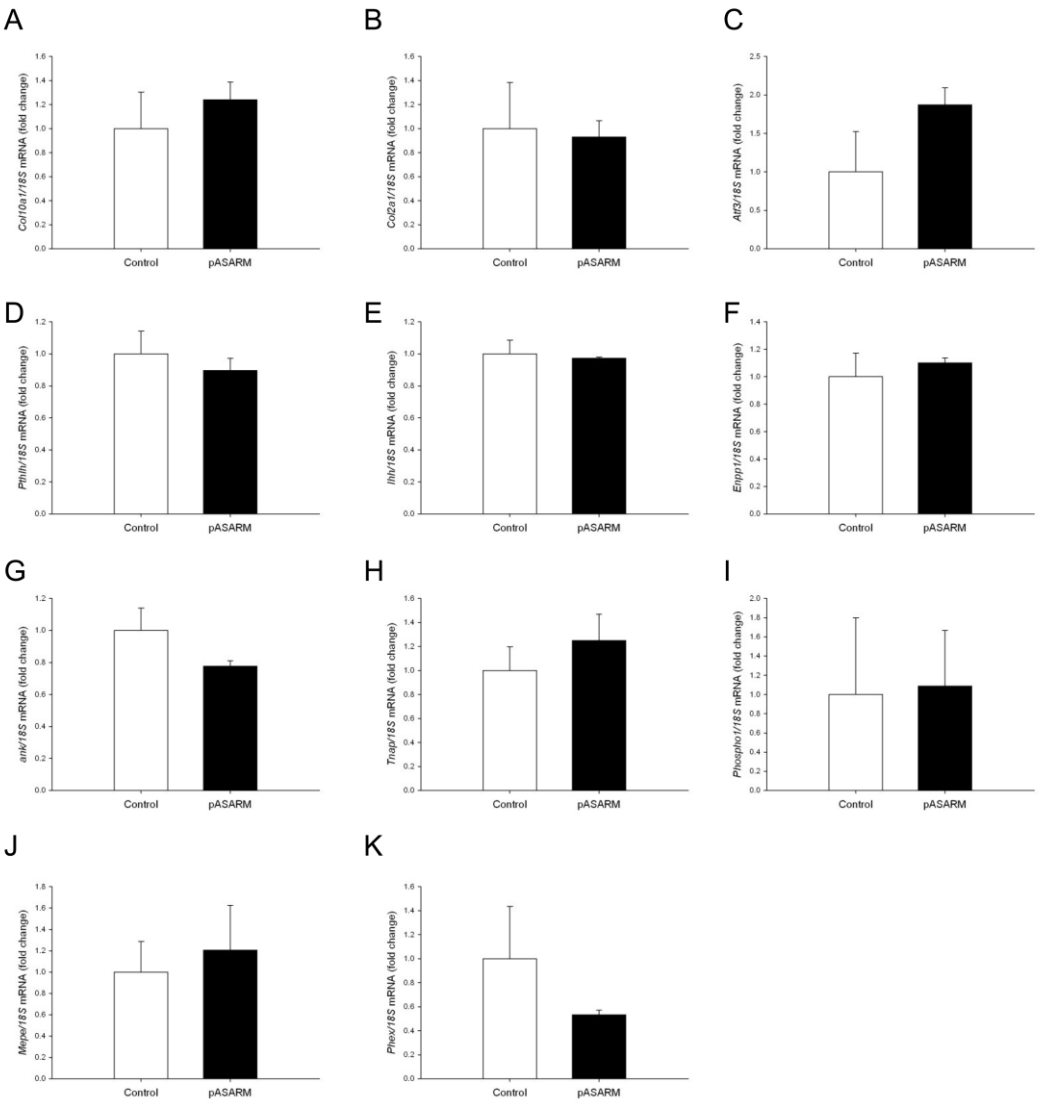

Figure 5.16 The lack of effects of the pASARM peptide on chondrogenic gene expression in E15 after 5 days of culture

Analysis of mRNA expression in E15 control and pASARM treated metatarsals at day 5 of culture **(A)** *Col10a1* **(B)** *Col2a1* **(C)** *Atf3* **(D)** *PthIh* **(E)** *Ihh* **(F)** *Enpp1* **(G)** *Ank* **(H)** *Alpl* **(I)** *Phospho1* **(J)** *Mepe* **(K)** *Phex* Data are represented as mean ± SEM of 3 groups of 4 pooled bones.

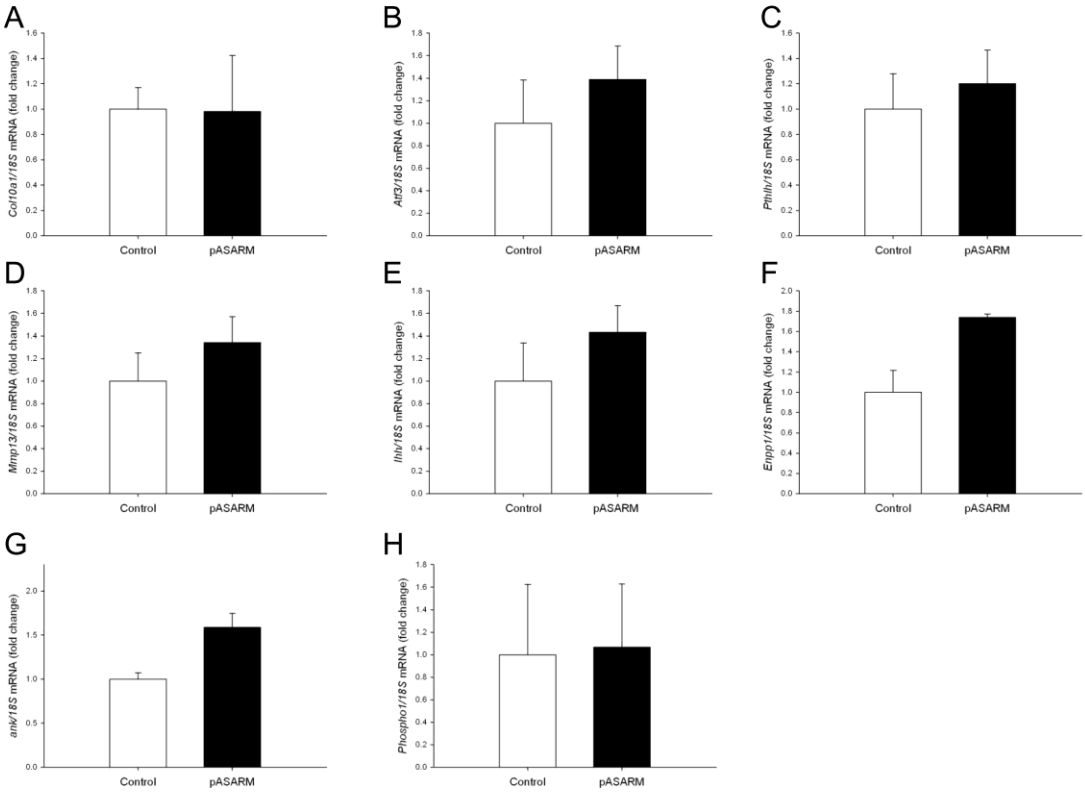

Figure 5.17 The lack of effect of the pASARM peptide on chondrogenic gene expression in E15 after 7 days of culture

Analysis of mRNA expression in E15 control and pASARM treated metatarsals at day 7 of culture **(A)** *Col10a1* **(B)** *Atf3* **(C)** *PthIh* **(D)** *Mmp13* **(E)** *Ihh* **(F)** *Enpp1* **(G)** *Ank* **(H)** *Phospho1.* Data are represented as mean ± SEM of 3 groups of 4 pooled bones.

To examine the mechanism of inhibition by the pASARM peptide, the expression and activity of key enzymes associated with cartilage mineralisation were determined. Interestingly after 7 days of culture, there was no significant difference in the activity of ALP (Fig. 5.18A), a well-recognised regulator of chondrocyte matrix mineralisation. This was further confirmed by mRNA expression analysis of *Alpl* by qPCR at days 5 and 7 of culture (Fig. 5.16H & 5.18B). Analysis of the mRNA expression of other mineralisation regulators, *Ank, Enpp* and *Phospho1,* also showed no difference between control and treated bones at days 5 and 7 of culture (Fig. 5.16F - I, Fig. 5.17F - I).

To assess the possible interactions of PHEX with MEPE, the mRNA expression of *Phex* was examined and like in the MEPE-overexpressing ATDC5 cultures (Fig. 5.3D), was found to be significantly decreased in the pASARM treated bones compared to the control bones at day 7 of culture ($P<0.05$, Fig. 5.18C). Furthermore, *Mepe* mRNA expression was significantly increased ($P<0.001$) (Fig. 5.18D). At day 5 of culture, there was no significant difference in the mRNA expression of *Mepe* or *Phex* (Fig. 5.16J & K).

The vascular invasion of the cartilage model via VEGF stimulated angiogenesis is critical for matrix mineralisation (Gerber *et al.* 1999). Thus, the effects of the expression levels of *Cd31*, *Cd34,* and *VEGFR2/Flk1* following 7 days of culture in the presence of 20μM pASARM compared to control bones ($P<0.05$, Figs. 5.19A - C). pASARM peptide on the mRNA expression of endothelial cell specific markers and VEGF was examined. qPCR indicated a significant decrease in the mRNA Furthermore, there was also a concomitant decrease in VEGF isoform expression specifically $VEGF_{164}$ and $VEGF_{120}$ (Figs. 5.19E - G). $VEGF_{188}$ was not detected in either control or treated metatarsals. MMP13, which has been implicated in VEGF-induced angiogenesis (Nagai & Aoki 2002; Zijlstra *et al.* 2004) also had a significantly decreased mRNA expression (in pASARM treated bones compared to control; $P<0.05$, Fig. 5.19D).

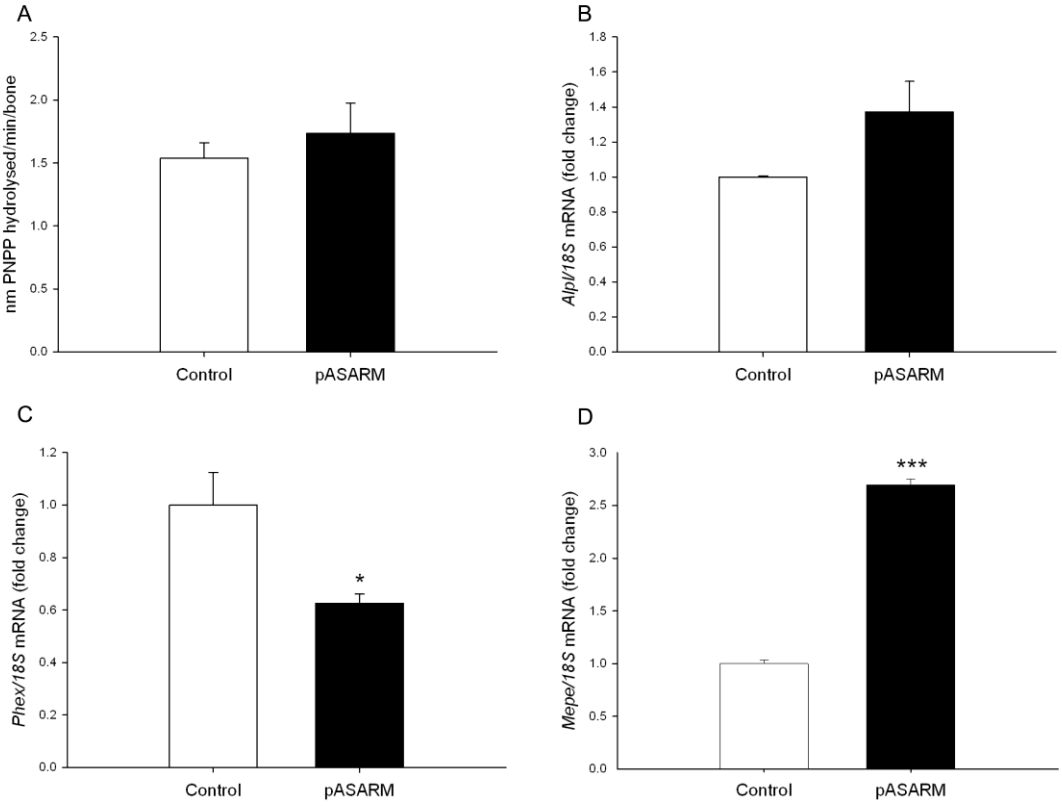

Figure 5.18 The effects of pASARM peptides on alkaline phosphatase and the PHEX-MEPE axis in E15 metatarsal bones

ALP activity was unchanged in metatarsal bones treated with 20μM pASARM peptides in comparison to control bones **(A)**. *Alpl* mRNA expression was also unchanged **(B)**. *Phex* mRNA expression was significantly decreased in pASARM treated bones **(C)** whilst *Mepe* mRNA expression was increased **(D)**. Data are represented as mean ± SEM *P<0.05 ***P<0.001 of 3 groups of 4 pooled bones at day 7 of culture.

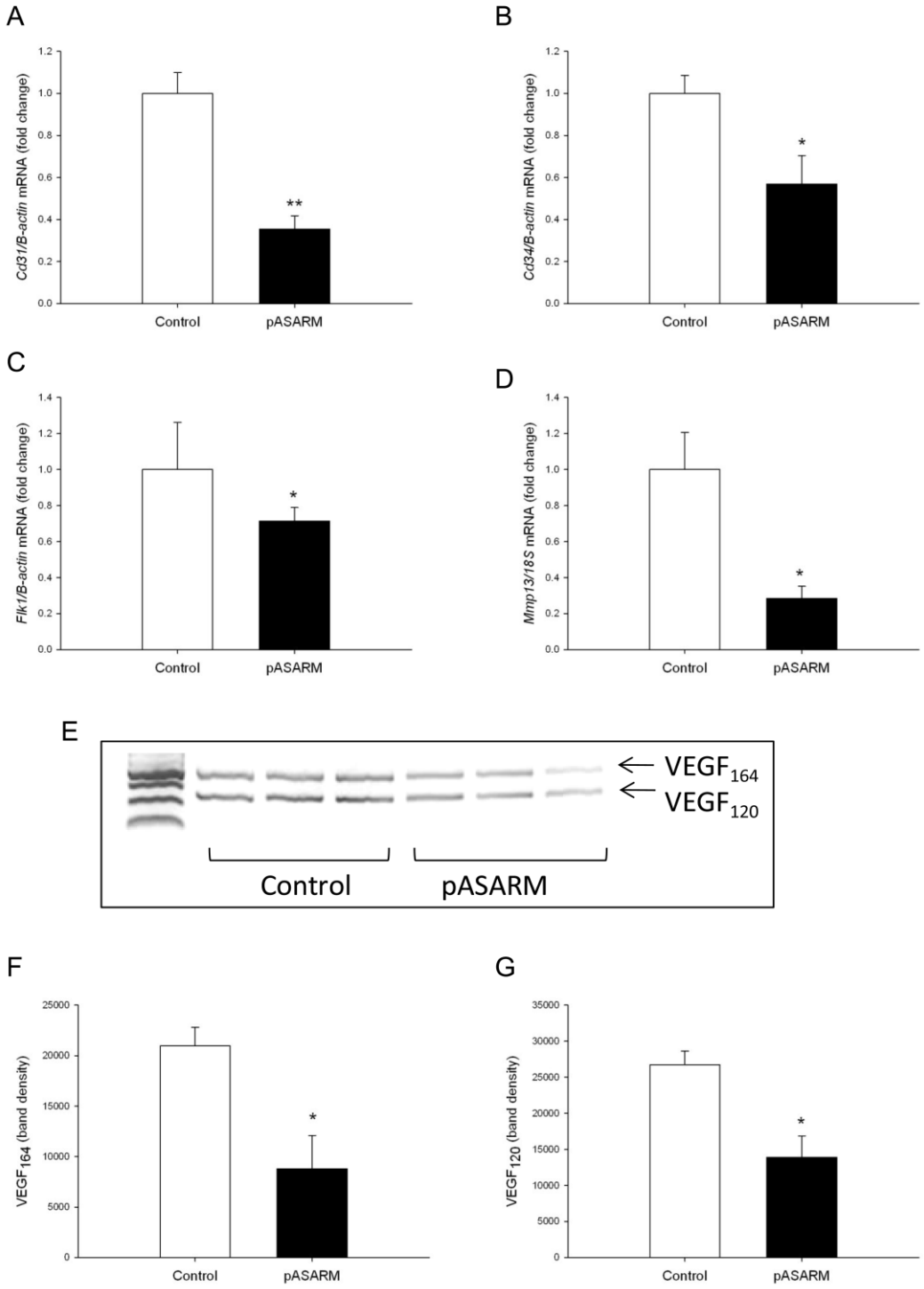

Figure 5.19 The inhibition of endothelial cell markers in E15 metatarsals treated with the pASARM peptide

mRNA expression of endothelial cell markers *Cd31* **(A)**, *Cd34* **(B)**, *VEGFR2*/*Flk1* **(C)** and *Mmp13* ***(D)*** in control and pASARM treated bones at day 7 of culture. PCR analysis of pro-angiogenic VEGF-A splice variants **(E)** and densitometry of the $VEGF_{164}$ isoform **(F)** and the $VEGF_{120}$ isoform **(G)**. Data are represented as mean ± SEM *P<0.05, **P<0.01 of 3 groups of 4 pooled bones. PCR analysis represents replicates of pooled bones at day 7 of culture.

5.6 Discussion

The hypertrophic chondrocytes of the epiphyseal growth plate mineralise their surrounding ECM and facilitate the deposition of hydroxyapatite, a process imperative for longitudinal bone growth. Determining the function of key proteins involved in this process is crucial in furthering our understanding. MEPE has been proposed as one such protein due to its emerging direct and indirect roles in biomineralisation, however its function as a regulator of chondrocyte matrix mineralisation has yet to be elucidated (Martin *et al.* 2008; Addison *et al.* 2008).

MEPE is a member of the SIBLING family of proteins which is degraded by cathepsin B to an acidic, negatively charged ASARM peptide. Patients with XLH have elevated serum levels of this ASARM peptide as does the mouse model of XLH, the *Hyp* mouse (Bresler *et al.* 2004). Further studies of the *Hyp* mouse show severe morphological disruption of the growth plate which can be corrected by the administration of cathepsin inhibitors (Rowe *et al.* 2006). Moreover, the MEPE transgenic mice displayed wider epiphyseal growth plates, expanded primary spongiosa and a significant decrease in the MAR therefore suggesting dysregulation of endochondral bone growth (David *et al.* 2009). In concordance with this, the studies described here show an inhibition of chondrocyte matrix mineralisation by MEPE.

The engineering of cells to over-express a gene of interest is a commonly used *in vitro* method to determine the effects of this gene. Here *Mepe* mRNA was increased in expression in mineralising ATDC5 cells however there was a lack of overexpression of the protein product therefore suggestive of a post-translational or post-transcriptional regulatory mechanism of MEPE expression (Fig. 5.1). Several mechanisms of such regulation exist including micro ribonucleic acid (miRNA) silencing, histone modification and protease degradation (Halbeisen *et al.* 2008). The activity of miRNAs in chondrocytes, and in ATDC5 cells, has been reported however it is more likely that the unreported overexpression of MEPE protein is

due to its rapid cleavage to its functional component, the ASARM peptide (Swingler *et al.* 2012; Dong *et al.* 2012). To fully elucidate the role of MEPE in chondrocyte matrix mineralisation, it would be beneficial to ablate MEPE and examine the matrix mineralisation observed. In order to do this, attempts were made to target *Mepe* using shRNA constructs. These attempts were unfortunately unsuccessful with no significant decreased expressions of MEPE protein or mRNA levels (Fig. 5.7). The reasons behind this are unclear but could be due to a lack of the specific complex cellular machinery required to process and guide shRNA to target mRNA in this immortalised cell line. Whilst a MEPE knockout mouse has been generated, there has not been a histomorphometric characterisation of its growth plate however this analysis would also be beneficial in fully understanding the precise role of MEPE in chondrocyte matrix mineralisation (Gowen *et al.* 2003).

Like the other SIBLING proteins, the activity of MEPE is dependent upon its state of cleavage and its phosphorylation with recent work identifying the 2.2kDa ASARM peptide of MEPE as its functional component. Previous studies have shown the ASARM peptide to inhibit matrix mineralisation in *in vitro* osteoblast cultures (Rowe *et al.* 2004; Addison *et al.* 2008; Atkins *et al.* 2011). This was unequivocally corroborated here in the ATDC5 cells and the metatarsal organ culture model, a well-established model of cartilage mineralisation and endochondral bone growth which occurs without the vascular supply (Figs. 5.8, 5.12 & 5.13). Although a widening of the hypertrophic zone of chondrocytes would be expected as seen in XLH and as is observed in the MEPE-overexpressing mouse, here no differences in the widths of the cartilage zones in the metatarsal bones were observed (Fig. 5.14) (David *et al.* 2009). However, this is not surprising as there was also no difference in the growth potential, chondrocyte proliferation or mRNA expression of chondrocyte differentiation markers, of the treated and untreated bones. This therefore suggests that the MEPE-ASARM peptide has no effect on chondrocyte function *per se*. Instead it affects chondrocyte matrix mineralisation directly, as is in

concordance with studies done on bone mineralisation (Addison *et al.* 2008; Martin *et al.* 2008).

It is well recognised that ALP activity is a key regulator of cartilage matrix mineralisation. ALP is located to the outer surface of the trilaminar membrane of MVs, which form from the hypertrophic chondrocytes (Anderson 2003). It is widely accepted that ALP generates P_i for hydroxyapatite formation and its lack of activity results in an excess of PP_i (Addison *et al.* 2007). The interaction between ALP, PP_i and other SIBLING proteins has previously been documented (Wang *et al.* 2006; Addison *et al.* 2007). It was therefore postulated that the effects of the pASARM peptide could act through a decrease in ALP activity/expression as has been shown in a previously and as is observed in the MEPE overexpressing mouse (Martin *et al.* 2008; David *et al.* 2009). However, no effect on ALP activity or expression by the ASARM peptide was observed (Fig. 5.18). This is in concordance with a previous study investigating the role of MEPE in osteoblast mineralisation (Addison *et al.* 2008).

Furthermore no differences were observed in the expression of NPP1 which cleaves extracellular nucleotides such as ATP to generate the mineralisation inhibitor PP_i (Fig. 5.16). These nucleotides have a dual inhibitory effect on matrix mineralisation through purinergic signalling (Orriss *et al.* 2007; Burnstock *et al.* 2010; Gartland *et al.* 2012). Although this was not examined here, there is currently nothing in the literature to suggest that the ASARM peptide increases ATP levels, and this is certainly corroborated by the unchanged PP_i levels observed here. The pASARM peptide had no effect on PHOSPHO1 expression, which together with ALP regulates bone and cartilage mineralisation suggesting that in the models utilised here, the mechanism of inhibition is not a result of decreased enzyme activity (Yadav *et al.* 2011; Huesa *et al.* 2011). Rather, it is likely that the pASARM peptide exerts its effects by a physio-chemical interaction through its direct binding to the hydroxyapatite as has previously been suggested (Addison *et al.* 2008).

It has recently been shown that a truncated form of MEPE which has the ASARM peptide removed, can promote bone mineralisation in culture and in mice (Sprowson *et al.* 2008). Furthermore, a mid-terminal fragment of MEPE has been shown to enhance cell binding and taken together these results highlight the importance of the post translational processing of MEPE in determining its functional role (Hayashibara *et al.* 2004). The data presented here have shown that the phosphorylation of the ASARM peptide is crucial in determining its functional role. Despite the observed promotion of mineralisation by the npASARM peptide in the ATDC5 cultures, this was not corroborated by the metatarsal data. Furthermore in other *in vitro* studies, it has been shown that the function of the MEPE-ASARM peptide is entirely dependent upon its phosphorylation (Martin *et al.* 2008; Addison *et al.* 2008; Boskey *et al.* 2009a). Indeed it is likely that the npASARM peptide does not physiologically exist and is in fact inactive. One can reasonably infer that since the pASARM serine-phosphorylated casein kinase sites are highly conserved across species (including whales, dolphins, primates, rodents, marsupials, elephants, dogs, and cats) and the phosphorylated form is active that there might be a physiological mechanism that plays a role in regulating the ASARM-phosphorylation status (Rowe 2012b).

PHEX protects MEPE from cathepsin B cleavage *in vitro* (Guo *et al.* 2002; Rowe *et al.* 2005) thus the inhibition of *Phex* mRNA expression in pASARM treated metatarsal bones and in ATDC5 cells overexpressing MEPE suggests a feedback mechanism by which ASARM peptides can prevent PHEX expression (Fig. 5.3 & 5.18). This, in correlation with an increase in *Mepe* expression seen, would allow the release of ASARM peptides therefore further increasing the inhibition of mineralisation. Furthermore, the reduction in *Phex* mRNA expression may be due to the ASARM peptide protecting itself from sequestration and hydrolysis by PHEX, as has previously been suggested (Liu *et al.* 2007a; Martin *et al.* 2008; Addison *et al.* 2008). A decrease in *Phex* mRNA has also been observed in osteoblast cell cultures treated with the pASARM peptide, concomitant with an increase in FGF23 expression

(Martin *et al.* 2008). In the MEPE-overexpressing mouse however, an increase in *Phex* mRNA is observed and this, coupled with the expected hydrolysis of the ASARM peptide, leads to altered MEPE processing and therefore the hyperphosphatemia observed in this mouse model (David *et al.* 2009). These data are also in agreement with previous reports showing increased MEPE expression by osteoblasts of *Hyp* mice and this positive regulation of MEPE expression by pASARM may exacerbate the condition (Rowe *et al.* 2000; Argiro *et al.* 2001; Rowe *et al.* 2004; Liu *et al.* 2007a). It is reasonable to speculate that physiologically there must be a regulatory mechanism to ensure that there is not an overproduction of ASARM peptides and as such a pathological state. The precise nature of the counter balancing mechanism is presently unknown but as the SIBLING proteins are closely related and it is possible that one of the other members of this family may be responsible.

Key to endochondral ossification is the vascularisation of the mineralised matrix (Gerber *et al.* 1999). MMPs proteolytically degrade the mineralised cartilage matrix, facilitating blood vessel penetration into the growth plate and allowing the recruitment of osteoclast precursors and osteoblast progenitors. Pro-angiogenic VEGF is produced by hypertrophic chondrocytes of the growth plate and $VEGF_{164/188}$ deletion from the cartilage of developing mice results in delayed recruitment of blood vessels to the perichondrium along with a delayed invasion of vessels into the primary ossification centre (Zelzer *et al.* 2002). Here a decrease in *Mmp13* mRNA expression following pASARM treatment was observed (Fig. 5.14). Of the collagenases, MMP13 has been considered to have an important role in skeletal biology in view of its exclusive presence in the skeleton during embryonic development in cartilaginous growth plates and primary centers of ossification. Deficiencies in MMP13 have been shown to cause a transient elongation in the hypertrophic zone in the growth plate during the early stages of growth and development (Nagai & Aoki 2002; Stickens *et al.* 2004; Behonick *et al.* 2007). Additionally, a lack of MMP13 can also lead to a significant delay in the fracture

healing process further endorsing a role for MMP13 in the regulation of the vasculature in bone (Kosaki *et al.* 2007).

Furthermore, the pASARM peptide reduced the levels of endothelial cells present during metatarsal organ culture due to the vessel invasion of the bones at approximately E14 - E15 (Fig. 5.14). This was associated with reduced $VEGF_{120/164}$ mRNA expression levels. It is entirely possible that the influence of the pASARM peptide on endothelial cell populations is indirect; by impacting hypertrophic chondrocyte VEGF expression. However, any direct effects of the pASARM peptide on endothelial cell function remain under investigated. The possible implications of MEPE on bone renal vascularisation has recently been described in the MEPE-overexpressing mouse, which in contrast to the results here exhibits defective mineralisation associated with increased blood vessels (David *et al.* 2009). It is likely that in the *Mepe*-overexpressing mice, unknown compensatory mechanisms could exist to allow for effective vascularisation of the skeleton. Like MEPE, DMP1, another SIBLING protein, has also been suggested as an inhibitor of VEGF receptor 2 mediated angiogenesis although the precise role of its ASARM peptide in this circumstance has yet to be elucidated (Pirotte *et al.* 2011).

To conclude, these studies detail MEPE as a key protein in regulating the pace of endochondral bone growth due the apparent inhibitory effects of its pASARM peptide on chondrocyte matrix mineralisation and the vascularisation of the mineralised matrix (Staines *et al.* 2012c).

Chapter 6

Osteocyte regulation of endochondral ossification: a MEPE-dependent mechanism?

6.1 Introduction

Endochondral bone growth is regulated by numerous autocrine, paracrine and endocrine factors (section 1.3) which work in synergy to allow effective matrix mineralisation. Whilst this thesis has defined the role of MEPE in this phenomenon, it has not yet examined the potential interaction of MEPE with other regulators of mineralisation. Of particular interest is sclerostin, an inhibitor of bone formation that has promising therapeutic potential.

sclerostin was only identified fairly recently as the product of the *SOST* gene, mutations of which cause high-bone mass diseases in humans such as Van Buchem disease and sclerosteosis (Balemans *et al.* 2001; Brunkow *et al.* 2001). This high bone mass is also seen in *SOST* null mice, and mice administrated with neutralising antibodies to sclerostin (Li *et al.* 2009; Li *et al.* 2010). sclerostin is a known antagonist of the Wnt signalling pathway through its specific binding to the Wnt coreceptor LRP5 and 6 (Winkler *et al.* 2003; Semenov *et al.* 2005; Li *et al.* 2005; van Bezooijen *et al.* 2007; Staines *et al.* 2012a). More recently, LRP4 has been implicated as a receptor for sclerostin (Choi *et al.* 2009). The binding of Wnt ligands to these coreceptors activates the Wnt signalling pathway which regulates osteoblast differentiation and bone formation (Ott 2005; Krishnan *et al.* 2006b). The Wnt signalling pathway has also been implicated as a critical regulator of cartilage homeostasis with expression throughout the development of the skeleton and with known roles in chondrocyte proliferation and hypertrophy (Witte *et al.* 2009; Staines *et al.* 2012a).

A comprehensive recent study has determined that sclerostin may function through mechanisms outwith the Wnt signalling pathway. It has been shown that sclerostin increases *Mepe* mRNA expression in human primary osteoblasts with a concomitant decrease in *Phex* mRNA. Most importantly, antibody-mediated neutralisation of MEPE-ASARM antagonised the effects of recombinant sclerostin on matrix mineralisation, as did the PHEX synthetic peptide SPR4 (Atkins *et al.* 2011). This

therefore suggests that sclerostin may act, at least in part, through the regulation of the MEPE-ASARM/PHEX axis in the process of osteoblast matrix mineralisation.

However, whether sclerostin has a functional role in chondrocyte matrix mineralisation has yet to be elucidated. There is some evidence of sclerostin expression in the mineralised hypertrophic chondrocytes of the growth plate and if this is confirmed, then this certainly is suggestive of a function for sclerostin (Winkler *et al.* 2003; van Bezooijen *et al.* 2009). However if there is not local production of sclerostin by the growth plate chondrocytes, then it is plausible to suggest that there is a paracrine mechanism by which osteocytes cross-talk with growth plate chondrocytes through sclerostin expression. Indeed osteocytes are suitable for this function since they form an extensive network with each other, lining cells, and osteoblasts through gap junction connections (Klein-Nulend *et al.* 2003; Bonewald 2006). More recently, it has been shown that osteocytes can communicate with osteoclast cells through RANKL expression (Xiong *et al.* 2011; Nakashima *et al.* 2011). Determination of the intercellular communications regulating growth plate matrix mineralisation will provide new insights into the molecular mechanisms surrounding endochondral ossification.

6.2 Hypothesis

Local chondrocyte sclerostin and/or osteocyte sclerostin inhibits chondrocyte matrix mineralisation through a MEPE dependent mechanism.

6.3 Aims

I. Examine the expression of sclerostin in growth plate chondrocytes

II. Analyse the effects of sclerostin on chondrocyte matrix mineralisation

III. Establish whether sclerostin acts through a MEPE-dependent mechanism

6.4 Materials and Methods

6.4.1 Immunohistochemical staining of the murine growth plate *in vivo*

4-week old C57BL/6 mice were sacrificed by cervical dislocation and the tibiae were dissected and fixed in 70% ethanol for 24 hours. The tibiae were decalcified in 10% EDTA and processed into wax as described in section 2.6.1. Immunohistochemical staining of 5μm-thick tibiae sections was performed using antibodies for sclerostin (1:100) and the Vectastain ABC kit, as outlined in section 2.9 and Appendix III. Immunohistochemical labelling was visualised using DAB chromagen. Appropriate IgG concentrations were used instead of the primary antibodies as negative controls.

6.4.2 Primary cell cultures

Primary chondrocytes were extracted from the rib cages of 1-3 day old mice as detailed in section 2.2.3. Cells were cultured for 2 days at 37°C in primary cell culture media before RNA was extracted and reverse transcribed (sections 2.12.1 and 2.12.3). For PCR analysis, cDNA was used at 25ng/μl and amplified as described in section 2.12.4. PCR products were analysed on a 1.5% agarose gel and visualised under UV light using a Gel Logic 200 Imaging System and software (Kodak). Primers used are detailed in Appendix II.

6.4.3 IDG-SW3 cell line

The IDG-SW3 cell line, isolated from 3-month-old *Immortomouse*$^{+/-}$/*Dmp1-GFP*$^{+/-}$ mice which carry an IFN-γ inducible promoter enabling immortalisation of cells, was a generous gift from Professor Lynda Bonewald (University of Missouri-Kansas City, Missouri, USA) and was cultured as detailed previously (section 2.2.4) (Woo *et al.* 2011). For mineralisation experiments, cells, at passage 12, were seeded at 8 x 10^4

cells/cm^2 in osteogenic conditions (37^{o}C with 50μg/ml ascorbic acid and 4mM βGP) in the absence of IFN-γ for up to 28 days.

6.4.4 ATDC5 cells

As outlined in section 2.2.1, ATDC5 cells were cultured at a density of 6 x 10^3 cells/cm^2 in a humidified atmosphere (37°C, 5% CO_2) for up to 30 days. When confluent, cells were supplemented with 10mM βGP and 50μg/ml ascorbic acid with the medium being changed every 2-3 days.

6.4.5 Metatarsal organ culture

The middle three metatarsals of E15 mice were isolated under a dissecting microscope, as described in section 2.5.2. Metatarsals were cultured in metatarsal media for up to 7 days. The total length of the bone through the centre of the mineralising zone was determined using image analysis software (DS Camera Control Unit DS-L1; Nikon) every second or third day. The length of the central mineralisation zone was also measured.

6.4.6 IDG-SW3 conditioned media

IDG-SW3 cells were cultured in T175 flasks as described in section 6.4.3. Media was changed every 3 days and on days 4 and 21 was removed from the cells, centrifuged to remove particulates and frozen at -20^{o}C until required. In ATDC5 and E15 metatarsal cultures, 20% conditioned media was added every other day. As a control, IDG-SW3 media (Appendix I) was used.

6.4.7 Co-culture of embryonic murine metatarsals and IDG-SW3 cells

For co-culture experiments, 12 Well Thincert, 0.4μm pore diameter, transparent co-culture plates were used (Grenier Bio-one Inc, Stonehouse, UK). IDG-SW3 cells were plated and maintained for up to 21 days as described in section 6.4.3. At this point, E15 metatarsal bones were dissected as detailed in section 2.5.2, and were placed upon the insert which was suspended above the IDG-SW3 cells to allow diffusion of the two cell mediums. Metatarsal bones were cultured for up to 7 days in a

humidified atmosphere. The total length of the bone through the centre of the mineralising zone, as well as the length of the central mineralisation zone, was determined using image analysis software (DS Camera Control Unit DS-L1; Nikon) every second or third day.

6.4.8 SPR4 peptides, CA074 and sclerostin neutralising antibodies

SPR4, a single PHEX peptide (4.2 kDa) was synthesised as TVNAFYSASTNYPRSLSYGAIGVIVGHEFTHGFDNNGRGENIADNG (Peptide Synthetics, Bishops Waltham, UK). This was added to co-cultures at a concentration of 20μM with controls treated with a DMSO carrier (0.1%). CA074, a specific cathepsin B inhibitor, was purchased (Merck, Darmstadt, Germany) and also added to co-cultures at a concentration of 20μM with controls treated with a DMSO carrier (0.1%). sclerostin neutralising antibodies were obtained from Eli Lilly (Indianapolis, USA) for use in this project under a material transfer agreement. Antibodies were added to co-cultures at varying concentrations (0-2nM) to examine their effects. Concentrations were determined as to section 6.5.5.

6.4.9 Histochemical analysis of IDG-SW3 cultures

IDG-SW3 cell cultures were stained for calcium deposition (alizarin red), collagen production (Sirius red), and glycosaminoglycan presence (alcian blue) as described in section 2.4. The optical densities of the resultant stains were analysed using a spectrophotometer (Thermo Scientific, Northumberland, UK) along with an appropriate blank control. Reactions were completed in triplicate at each time point.

6.4.10 RNA analysis of IDG-SW3 cells and metatarsals

RNA was extracted from IDG-SW3 cell cultures using an RNeasy mini kit according to the manufacturer's instructions (section 2.12.1). For metatarsal organ cultures, 4 bones from each control or experimental group were pooled in 100μl Trizol reagant at either day 5 or 7 of culture, and RNA was extracted according to the manufacturer's instructions (section 2.12.2). For each sample, total RNA content was assessed by absorbance at 260nm and purity by A260/A280 ratios, and then reverse-

transcribed as described in section 2.12.3. RT-qPCR was performed using the SYBR green detection method on a Stratagene Mx3000P real-time qPCR system as detailed in section 2.12.5. Primers were purchased from PrimerDesign Ltd, or designed in house and synthesised by MWG Eurofins (Appendix II). Reactions were run in triplicate and routinely normalised against *18S.*

6.4.11 ELISA analysis of sclerostin expression

A mouse Quantikine® ELISA kit for sclerostin was purchased (R&D systems, Minneapolis, USA). This was a sandwich ELISA where a monoclonal antibody specific for mouse/rat SOST was pre-coated onto the microplate. 50µl of assay diluent was added to each well of the provided microplate. Standards, controls, and samples were prepared according to the manufacturer's instructions and added at 50µl/well before being incubated at room temperature for 3 hours. Each well was then aspirated and washed with the provided wash buffer for a total of five washes. 100µl of mouse SOST conjugate was added to each well and incubated for 1 hour at room temperature. Wells were subsequently aspirated and washed for a total of five washes. 100µl of substrate solution was added to each well and was incubated for 30 minutes at room temperature, protected by light. Then, 100µl stop solution was added before the optical density was determined using a microplate reader (Thermo Scientific, Northumberland, UK) at 450nm. Concentration of sclerostin was calculated according to the manufacturer's instructions.

6.4.12 Recombinant sclerostin

Recombinant sclerostin was added to E15 murine metatarsal bones (section 6.4.5) at concentrations of 0 - 1000µM from day one of culture. Recombinant sclerostin was added to cultured metatarsal bones every second day for up to six days of culture. The total length of the bone and the length of central mineralisation zone was determined using image analysis software (DS Camera Control Unit DS-L1; Nikon).

6.5 Results

6.5.1 Expression of sclerostin by growth plate chondrocytes

There is currently conflicting evidence regarding the expression of sclerostin by growth plate chondrocytes thus its protein localisation in the growth plate was examined by immunohistochemistry. sclerostin was not expressed by the resting, proliferating or hypertrophic chondrocytes of 4-week old murine growth plates (Fig. 6.1A). Neither was sclerostin expression apparent in the osteoblasts. As a positive control, the osteocytes of these bones were found to stain positive for sclerostin immunolocalisation confirming the specificity of the sclerostin antibodies (Fig. 6.1B). Representative images of the appropriate negative control are shown (Fig. 6.1C & D). Interestingly, primary chondrocytes cultured for 2 days were positive for *Sost* mRNA expression as examined by PCR analysis possibly suggesting that sclerostin expression by growth plate chondrocytes is below the detection level of IHC (Fig. 6.1E).

6.5.2 Characterisation of IDG-SW3 osteocyte-like cells

Sclerostin protein is evidently not expressed by growth plate chondrocytes, but as it is a secreted protein of the mature osteocyte it is plausible that it could still act to regulate growth plate development and/or mineralisation. The cell line IDG-SW3 is a novel and exciting cell line that is capable of overcoming the current limitations that exist in current osteocyte cell lines. Existing osteocyte-like cell lines, for example MLO-Y4 and MLO-A5, are limited by their transformation, their lack of sclerostin or FGF-23 expression, and/or their absence of a mineralised matrix. Although a full characterisation of these cells has previously been published, it was deemed necessary to examine their differentiation and expression of sclerostin before the cells could be utilised here to examine the effects of sclerostin on the growth plate (Woo *et al.* 2011).

Visualisation of cells by phase contrast microscopy indicated IDG-SW3 cells to differentiate into an osteocyte phenotype by day 7 with clearly visible dendritic

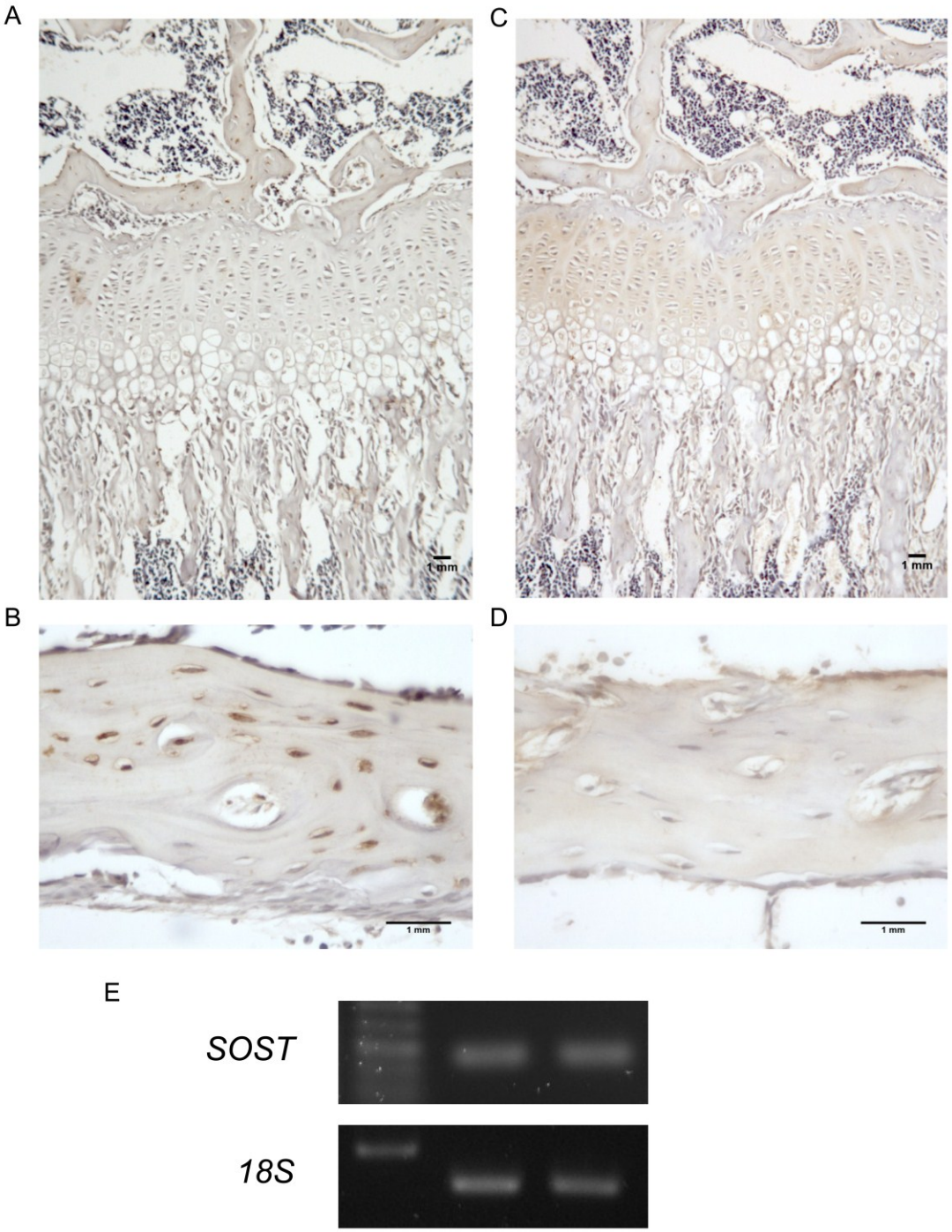

Figure 6.1 The lack of expression of sclerostin by growth plate chondrocytes

Immunohistochemical staining of a 4-week old murine tibia for sclerostin. No expression was observed in the growth plate **(A)**, however there was positive expression in the osteocytes of the cortical bone **(B)**. Representative images of the appropriate controls are shown **(C & D).** Brown stain indicates sclerostin expression. *Sost* mRNA was present in primary chondrocyte cells as indicated by PCR analysis. *18S* mRNA expression was used as a loading control (n=2 separate cell cultures, A & B). The molecular weight marker (*Sost* – 40kDa) is in the left hand lane **(E)**.

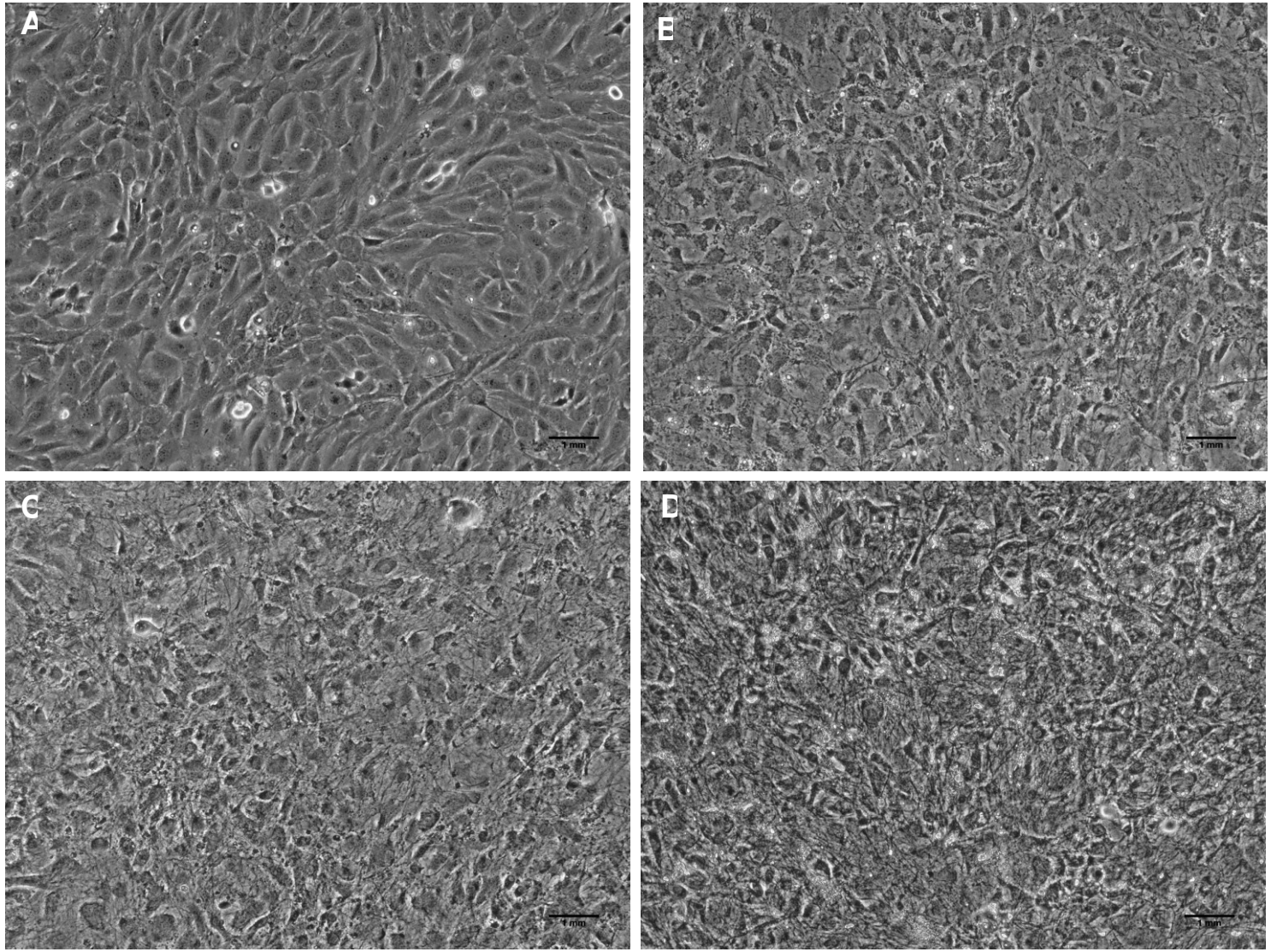

Figure 6.2 Phase contrast images of IDG-SW3 cells

Phase contrast images of IDG-SW3 cells cultured for up to 21 days in the presence of ascorbic acid and 4mM βGP (**A)** Cells reach confluency by day 2 of culture and by day 7 **(B)** display an osteocyte phenotype. This is associated with mineralisation of the matrix throughout the culture period **(C & D)**. Scale bars are 1mm.

processes (arrows, Fig. 6.2B). Associated with these cells was apparent focal nodular mineralisation which increased throughout the culture period to day 21 (Fig. 6.2C & D). Assessment of collagen deposition by Sirius red stain indicated increased matrix formation at day 21 of culture in comparison to day 4 of culture (Fig. 6.3A).

Concomitant with this was increased matrix mineralisation, as assessed by alizarin red staining (Fig. 6.3B). Examination of mRNA expression levels by qPCR at day 21 of culture in comparison to day 4 indicated increased expression of *Mepe* (Fig. 6.3C, $P<0.001$). There was no difference in *Phex* mRNA expression levels (Fig. 6.3D). Furthermore, ELISA analysis of sclerostin expression in these cells indicated that almost no detectable sclerostin protein was present in the conditioned medium of day 4 cultures but this was significantly higher (184pg/ml $P<0.05$, in comparison to day 4 cultures, Fig. 6.4B) in day 21 conditioned medium.

6.5.3 The effects of IDG-SW3 conditioned media on ATDC5 mineralisation

To examine the potential crosstalk between osteocytes and chondrocytes, mineralising ATDC5 cells were cultured with 20% conditioned media from day 4 (CM4) and day 21 (CM21) IDG-SW3 cells. Mineralisation of ATDC5 cells was assessed at days 15, 20, 25 and 30 of culture by alizarin red staining and this was quantified by spectrophotometry. Overall there was little consistent effect of conditioned medium on ATDC5 matrix mineralisation. However, at day 15, ATDC5 cells cultured in the presence of CM4 and CM21 displayed a significantly decreased matrix mineralisation (Fig. 6.5A & B, $P<0.05$). There were no effects observed at days 20 and 25 of culture, however a small decreased mineralisation was also observed at day 30 in CM21 cultured ATDC5 cells (Fig. 6.5A & B, $P<0.05$).

6.5.4 The effects of IDG-SW3 conditioned media on E15 metatarsal bones

Due to the somewhat inconsistent results observed in the ADTC5 cultures and to establish the effects of IDG-SW3 conditioned medium in a more physiologically relevant model, the E15 metatarsal organ culture model was adopted. Similar to the

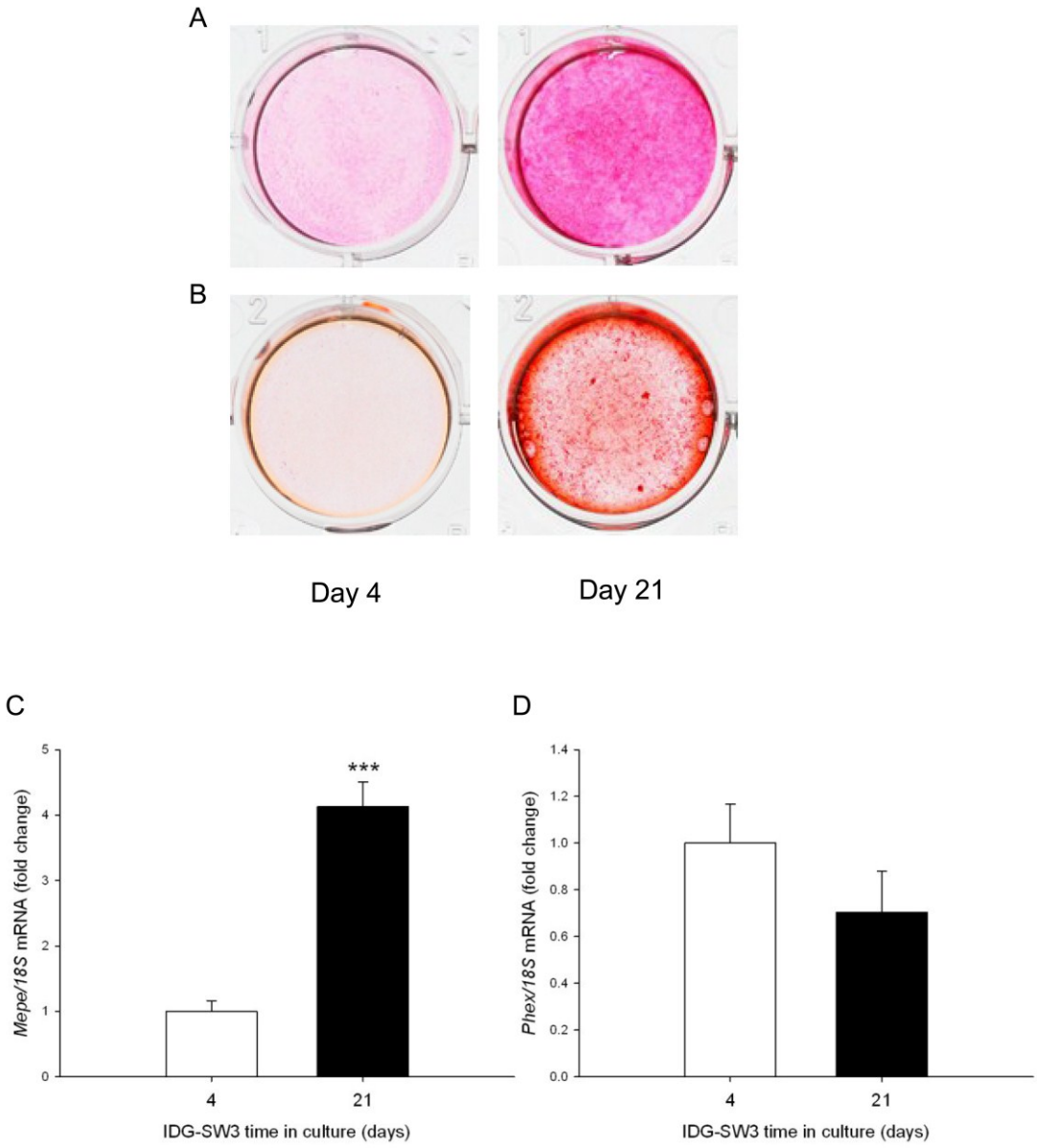

Figure 6.3 Characterisation of IDG-SW3 osteocyte-like cells

Sirius red stain for collagen deposition indicated increased matrix formation at day 21 of culture in comparison to day 4 of culture **(A)**. Alizarin red staining indicated increased matrix mineralisation at day 21 in comparison to day 4 of culture **(B)**. qPCR analysis indicated that *Mepe* mRNA was significantly increased at day 21 of culture in comparison to day 4 **(C)** whereas there was no difference in *Phex* mRNA expression levels **(D).** Data are represented as mean ± S.E.M (n=3 replicates), ***P<0.001.

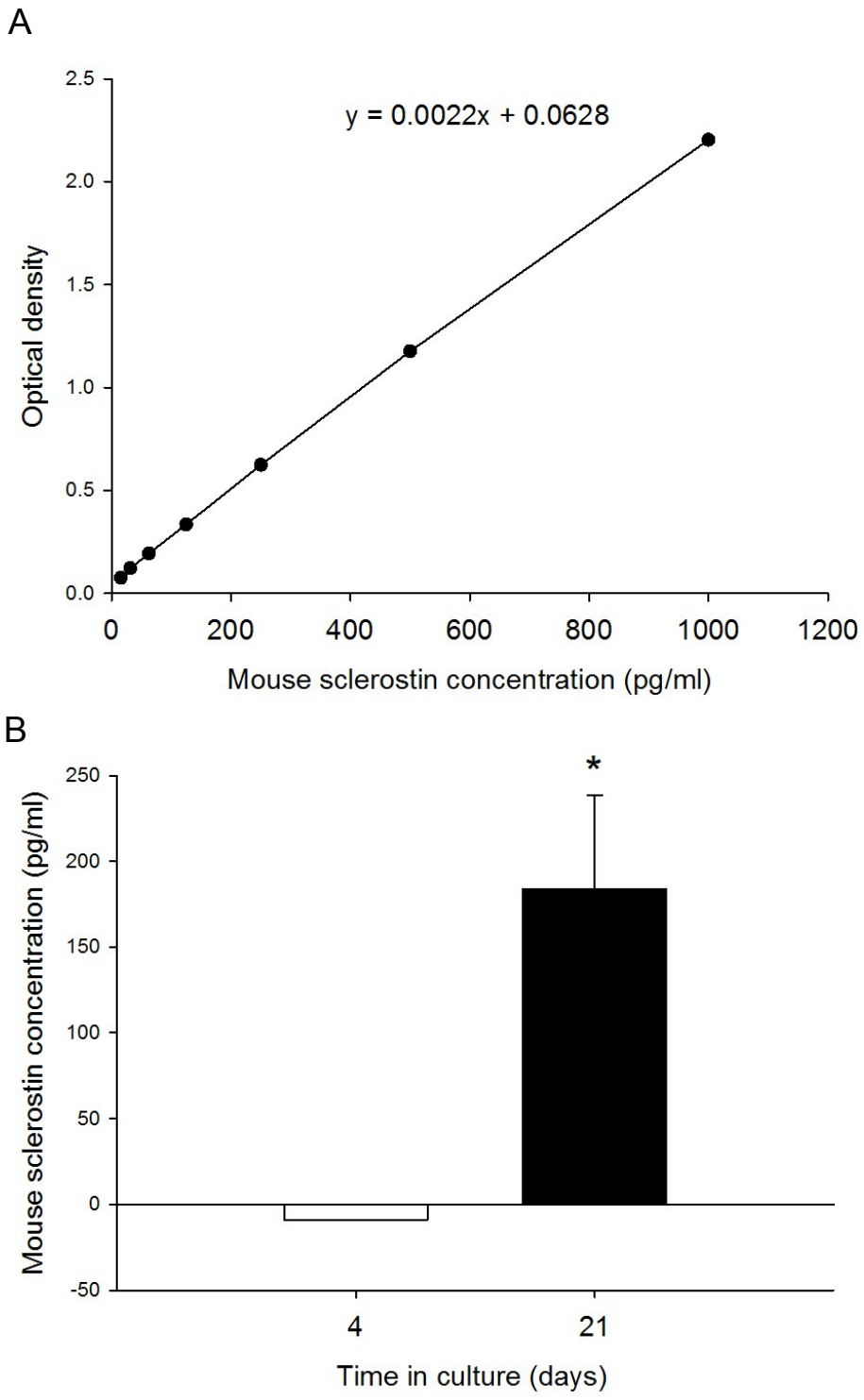

Figure 6.4 Sclerostin ELISA of IDG-SW3 cells

Mouse sclerostin ELISA standard graph line **(A)** and ELISA analysis of mouse sclerostin concentration in the conditioned media of 4-day old and 21-day old IDG-SW3 cells **(B)**. Data are represented as mean ± SEM of three separate cell cultures, * $P<0.05$.

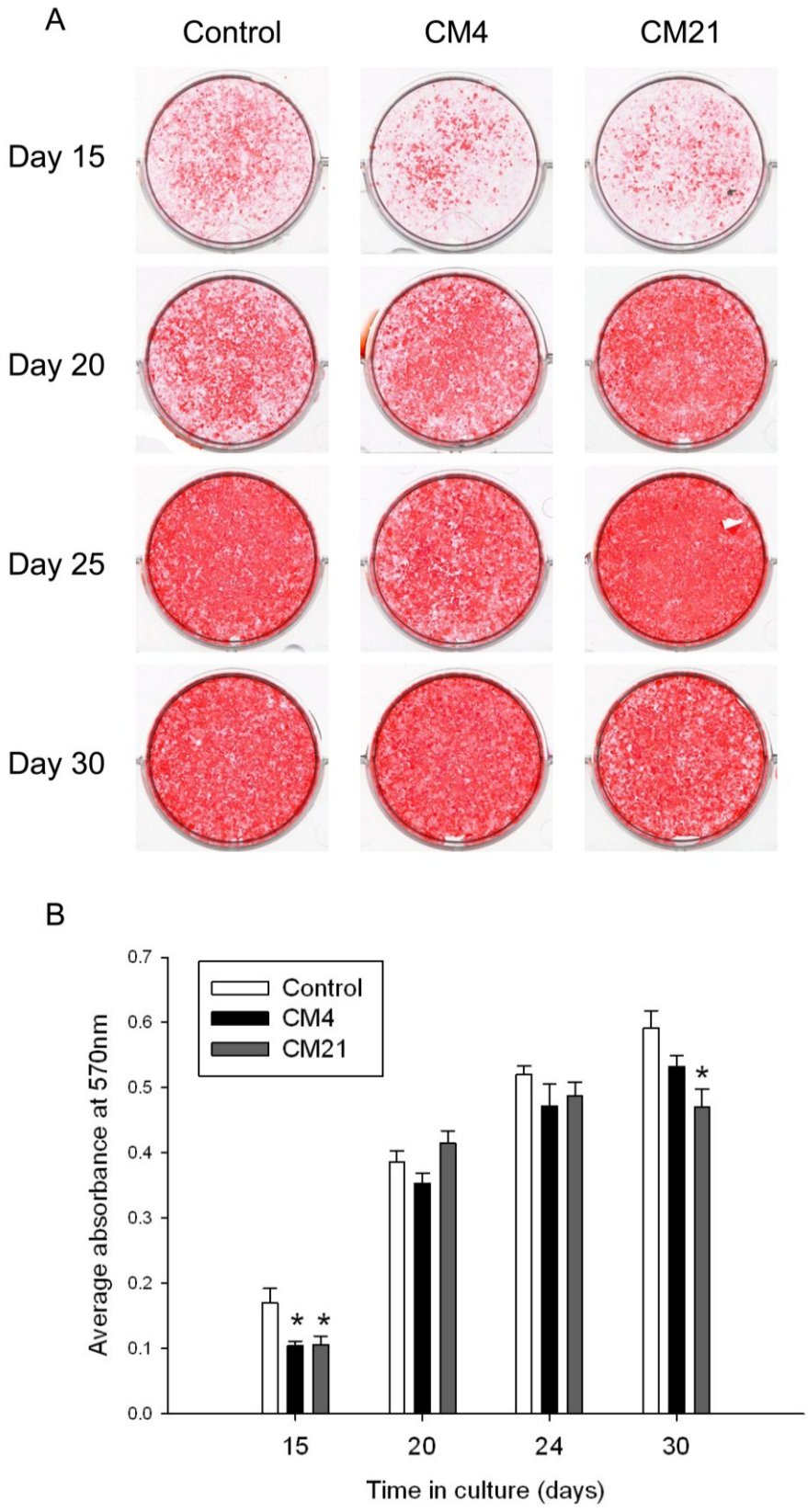

Figure 6.5 Effects of IDG-SW3 conditioned media on ATDC5 matrix mineralisation

20% conditioned media (CM) from day 4 and day 21 IDG-SW3 cells was added to mineralising ATDC5 cells for up to 30 days of culture. Alizarin red staining was conducted **(A)** and quantified **(B)** to evaluate matrix mineralisation at days 15, 20, 25 and 30 of culture. Data are represented as mean ± SEM (n=3 replicates) in comparison to control cultures *P<0.05.

ATDC5 cultures, these bones were cultured in the presence of 20% CM4 and CM21 for up to 7 days. In comparison to control bones and CM4 treated bones, bones cultured with CM21 had a significantly decreased percentage change in total length from baseline at days 5 and 7 (Fig. 6.6A-D, $P<0.001$). Furthermore, the formation of the central mineralisation zone of these bones was noticeably inhibited as visualised under the microscope (Fig. 6.6A - C). The length of the mineralisation zone as a proportion of the total bone length (MZ/TL) in the CM21-treated bones was significantly different from control and CM4-treated bones at days 5 and 7 of culture ($P<0.05$, Fig. 6.6E).

6.5.5 Co-culture of metatarsal bones and IDG-SW3 cells

Whilst the culture of metatarsal bones in 20% IDG-SW3 conditioned media provides an indication of the potential cross talk between osteocytes and chondrocytes, the co-culture of these bones with the IDG-SW3 cells would allow for better examination of this as it more closely replicates the *in vivo* situation. Therefore a co-culture system was conducted between IDG-SW3 cells and E15 metatarsal bones so that the two distinct cell populations could be cultured in close proximity in the same culture environment.

Mineralisation of metatarsal bones was inhibited by co-culture with 21-day old IDG-SW3 cells in comparison to control co-cultures and to IDG-SW3 cells at day 4 of culture ($P<0.001$ at days 3, 5, and 7 of culture, Fig. 6.7A, B, C, E). There were no differences in the total length of the bones except at day 3 at which point 21-day old IDG-SW3 co-cultures grew significantly more from baseline than the control counterparts ($P<0.05$, Fig. 6.7D). This therefore suggests that the IDG-SW3 cells are producing a mineralisation inhibitory factor at day 21 of culture that is not produced at day 4 of culture. The qPCR analysis of *Mepe* mRNA and the ELISA analysis of sclerostin in section 6.5.2 suggest that these could be the inhibitory factor, or as has been proposed in previous studies a combined effect of the two.

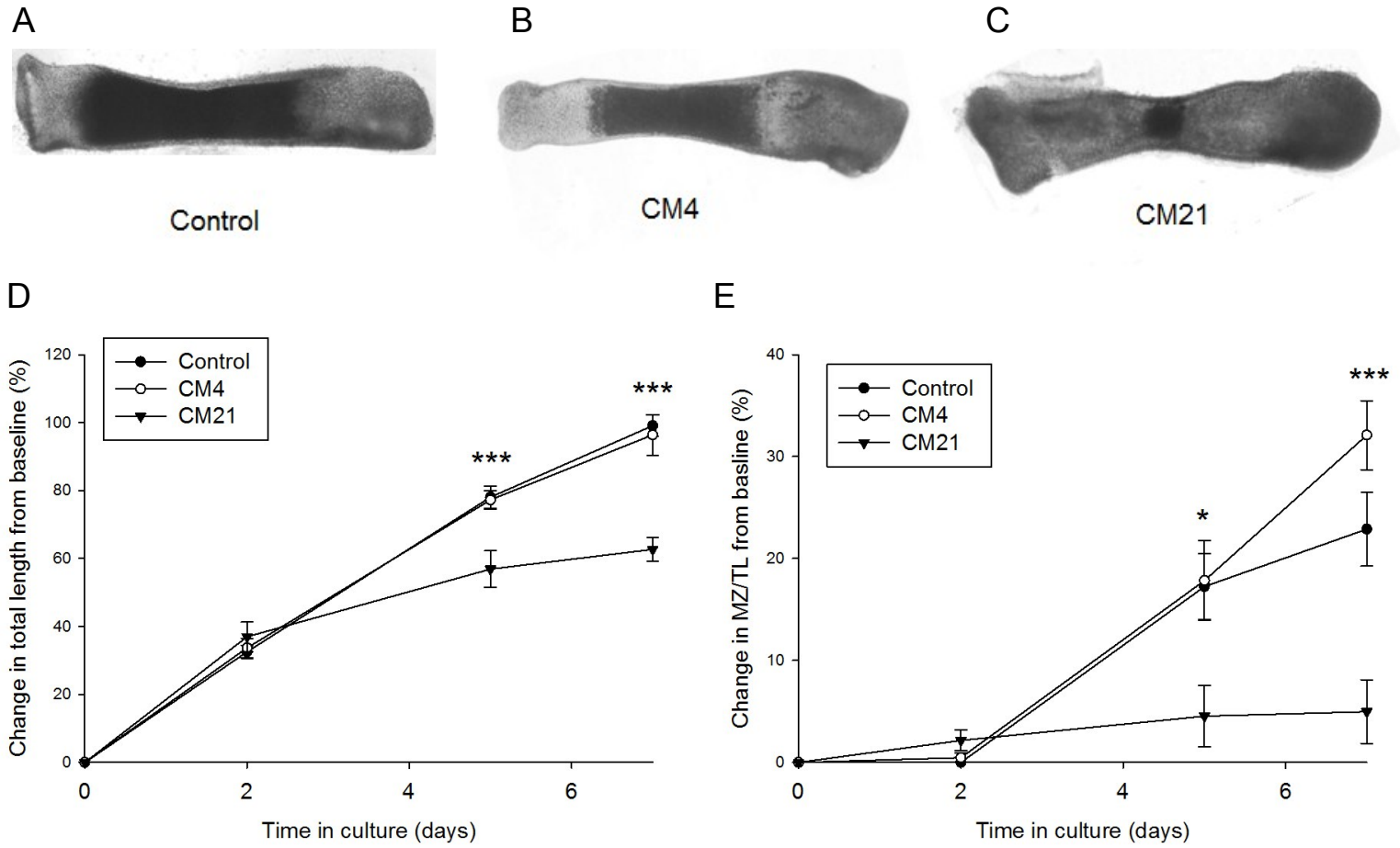

Figure 6.6 The inhibition of E15 metatarsal mineralisation by IDG-SW3 conditioned media

Conditioned media (CM) from day 4 and day 21 IDG-SW3 cells was added to E15 metatarsal bones and cultured for up to 7 days. A control metatarsal bone (with 20% IDG-SW3 day 0 medium) is illustrated in **(A)** and bones treated with continuous 20% CM4 **(B)** and CM21 **(C)** for 7 days of culture. The growth rate of the embryonic metatarsal bones treated with 20% CM21 was significantly inhibited at days 5 and 7 of culture **(D).** There was no significant difference in the mineralisation zone as a percentage of the total length (MZ/TL) between control and CM4 treated bones, both of which increased over the culture period **(A, B & E)**. However the mineralisation zone length in bones treated with 20% CM21 was minimal and significantly different from control and CM4 cultures at days 5 and 7 of culture **(C & E)**. Data are represented as mean ± SEM of at least six bones *P<0.05, ***P<0.001 in comparison to control bones at equivalent days of culture.

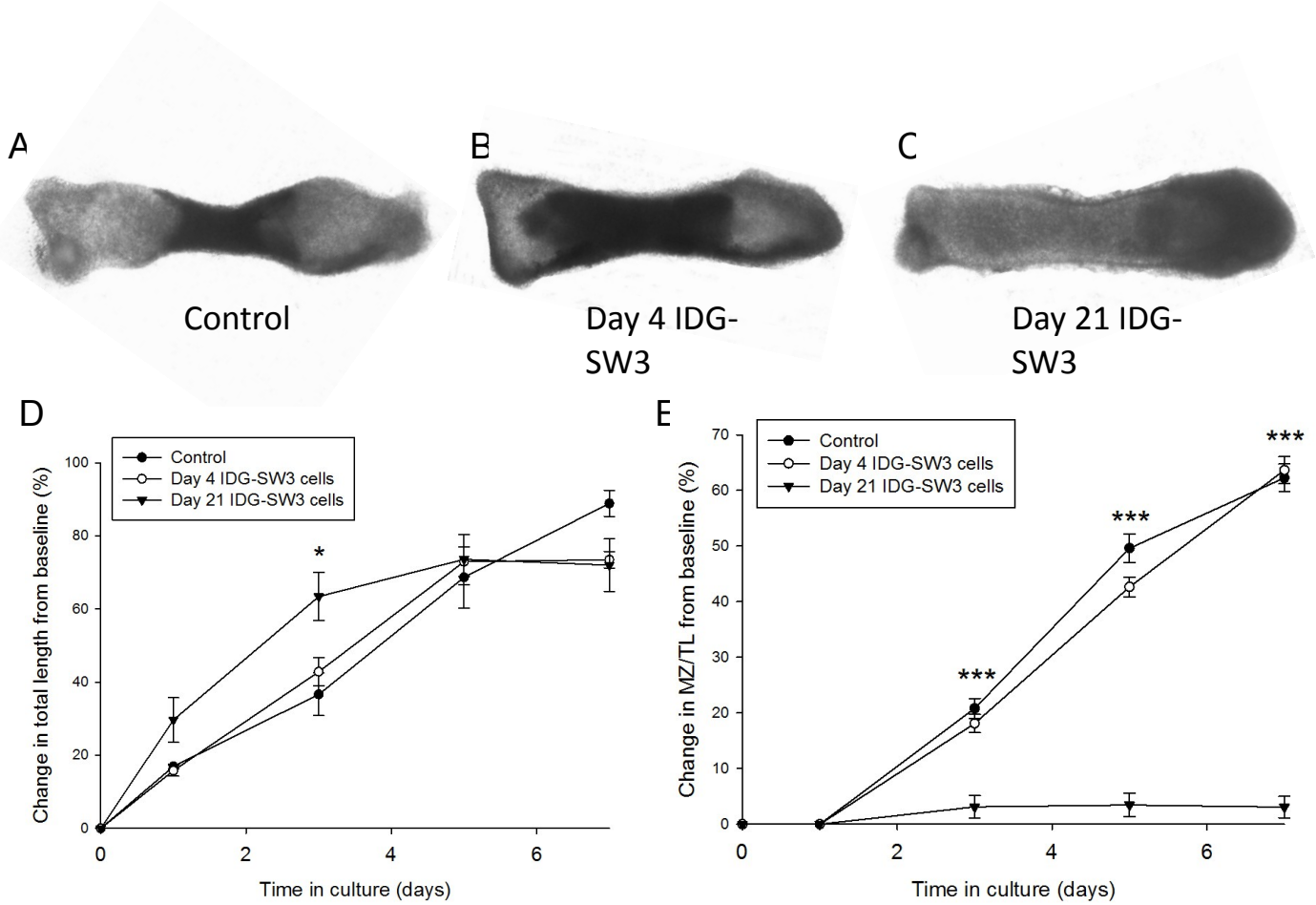

Figure 6.7 Inhibition of E15 metatarsal mineralisation upon co-culture with 21-day-old IDG-SW3 cells

E15 metatarsals were co-cultured with IDG-SW3 cells at days 4 and 21 of culture for 7 days. A control metatarsal bone (cultured in the presence of no IDG-SW3 cells) is illustrated in **(A)** and bones co-cultured with day 4 IDG-SW3 cells **(B)** and day 21 IDG-SW3 cells (**C)** after 7 days in culture. The growth rate of the embryonic metatarsal bones co-cultured with day 4 cells was unchanged in comparison to control cultures; bones co-cultured with day 21 cells had a significant promotion of total length growth at day 3 of culture **(D)**. There was no significant difference in the mineralisation zone as a percentage of the total length (MZ/TL) between control and day 4 IDG-SW3 cell co-cultures, both of which increased over the culture period. However the mineralisation zone length in bones co-cultured with day 21 IDG-SW3 cells was minimal and significantly different from control and day 4 cultures at days 3, 5 and 7 of culture **(E)**. Data are represented as mean ± SEM of at least six bones *P<0.05, ***P<0.001 in comparison to control bones at equivalent days of culture.

To examine whether this inhibition of mineralisation by day 21 IDG-SW3 cells is mediated by MEPE and its ASARM peptide, inhibitors of MEPE cleavage were added to the co-cultures. SPR4 is a PHEX peptide which binds to the ASARM peptide thus preventing its release (Martin *et al.* 2008). 20μM SPR4 was added to co-cultures to prevent the ASARM inhibition of mineralisation shown in Chapter 5. There were no differences in the MZ/TL of bones treated with SPR4 and those treated with a DMSO-carrier (Fig, 6.8A). As such, the metatarsal bones co-cultured with 21-day old IDG-SW3 cells still showed a significant inhibition of mineralisation, despite treatment with SPR4, in comparison to control and IDG-SW3 cells at day 4 of culture (Fig 6.8A, $P<0.01$). Furthermore CA074, a specific cathepsin B inhibitor, was added to co-cultures at a concentration of 20μM. Similar to SPR4, CA074 was unable to rescue the inhibition of mineralisation seen in the metatarsal bones co-cultured with IDG-SW3 cells at day 21 of culture (Fig. 6.8B, $P<0.001$). This inability of SPR4 and CA074 to rescue the mineralisation of the metatarsal bones co-cultured with 21-day old IDG-SW3 cells therefore suggests that the inhibition of mineralisation seen is not due to a MEPE-ASARM mediated effect.

Furthermore, and in support of a non MEPE mediated role, qPCR analysis of *Mepe* mRNA expression indicated no significant differences between metatarsals cultured as controls, with day 4 IDG-SW3 cell co-cultured bones and with day 21 IDG-SW3 cell co-cultured bones (Fig. 6.9A). Nor were there any differences in *Phex* mRNA expression (Fig. 6.9B). However, interestingly metatarsal bones co-cultured with day 21 IDG-SW3 cells showed a decreased mRNA expression of *Dmp1* ($P<0.01$, Fig. 6.9C).

This therefore suggests that the inhibitory effects of the day 21 IDG-SW3 cells on chondrocyte matrix mineralisation are not due to the increased MEPE levels and instead suggests the direct involvement of the increased sclerostin expression levels, independent of a MEPE mechanism.

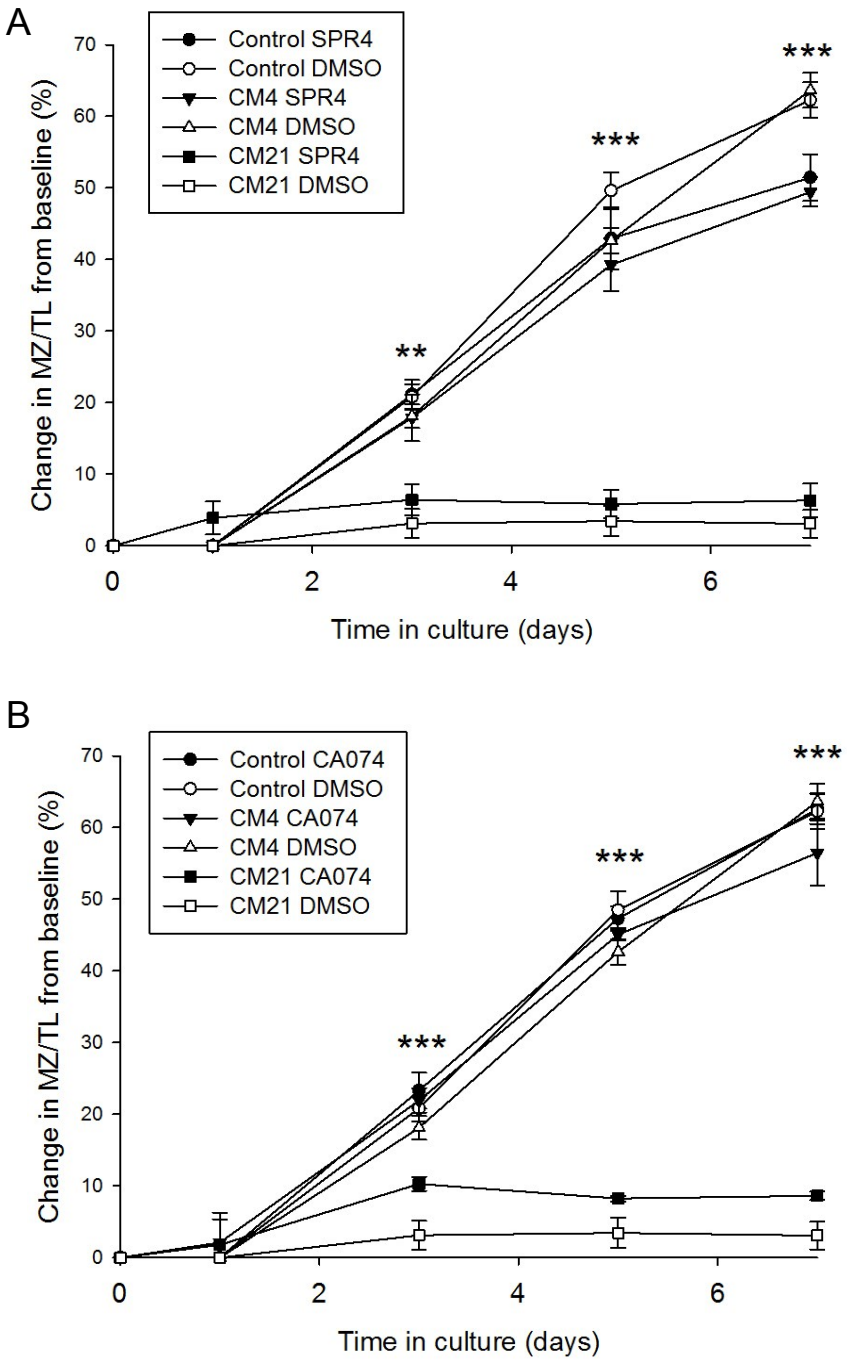

Figure 6.8 Addition of MEPE inhibitors to E15 metatarsal and IDG-SW3 co-cultures fails to rescue the inhibition of mineralisation seen

E15 metatarsals were co-cultured with IDG-SW3 cells at days 4 and 21 of culture for 7 days and measurements of the mineralisation zone as a percentage of the total length (MZ/TL) made. **(A)** 20μM SPR4 was added to co-cultures with a DMSO carrier as a control. There were no differences between SPR4 and DMSO treated bones and a significant inhibition of MZ/TL was observed in all bones co-cultured with day 21 IDG-SW3 cells. **(B)** 20μM CA074 was added to co-cultures with a DMSO carrier as a control. There were no differences between CA074 and DMSO treated bones and a significant inhibition of MZ/TL was observed in all bones co-cultured with day 21 IDG-SW3 cells. Data are represented as mean ± SEM of at least six bones **P<0.01, ***P<0.001 in comparison to control bones at equivalent days of culture.

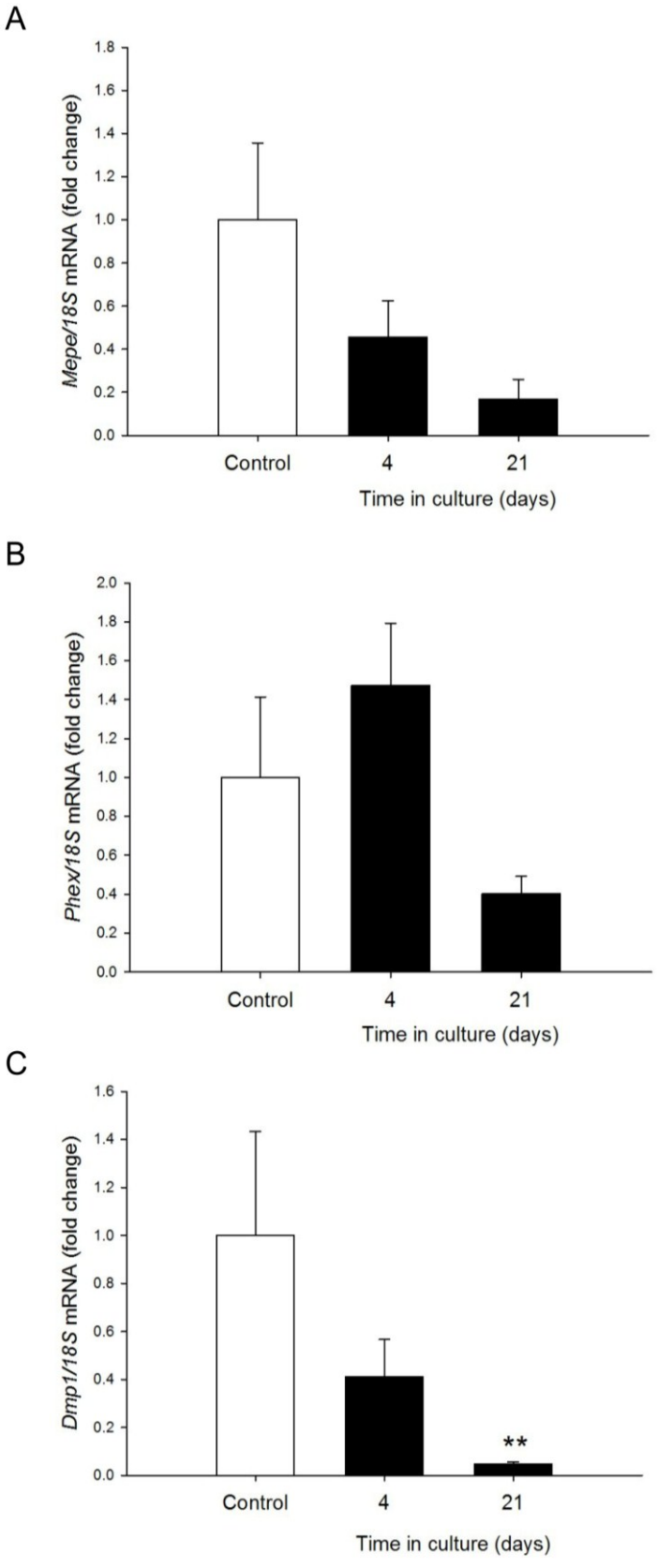

Figure 6.9 Gene expression in E15 metatarsal and IDG-SW3 co-cultures

Analysis of mRNA expression in E15 metatarsals following co-culture with day 4 and day 21 IDG-SW3 cells for 7 days **(A)** *Mepe* **(B)** *Phex* **(C)** *Dmp1* Data are represented as mean ± SEM of 3 groups of 4 pooled bones.

6.5.5 The effects of sclerostin on E15 metatarsal matrix mineralisation

To further investigate the potential role for sclerostin on the inhibition of mineralisation seen, sclerostin neutralising antibodies were obtained under a MTA from Eli-Lilly and were added to E15 metatarsal bones and IDG-SW3 cell co-cultures at varying concentrations to examine whether they could rescue the inhibition of metatarsal matrix mineralisation seen in the presence of the 21-day old cells.

The maximum concentration of sclerostin present in the cell cultures was calculated from the ELISA results (Fig. 6.4) and then this was used to calculate the concentrations of antibodies used. The antibody affinity for mouse sclerostin is very high (personal communication, Stuart Kuhstoss, Eli Lilly) and therefore it effectively neutralises sclerostin on a molar basis. Furthermore, because the antibody has 2 arms, one antibody molecule can block two sclerostin molecules. For these reasons, it was estimated that 0.02nM antibody would effectively neutralise the sclerostin in these co-cultures. However, whilst this concentration was based on a number of assumptions it has not been empirically derived and therefore to cover a range of sclerostin concentrations in conditioned medium and antibody binding affinities excess concentrations (0.2 and 2nM) were also used.

Measurements of total length showed a significant difference between control and IDG-SW3 co-cultured bones at day 7 of culture, similar to that seen in Fig. 6.7D ($P<005$, Fig. 6.10A). However, the sclerostin neutralising antibodies had no effect on the total length of the bones in the control, day 4 IDG-SW3 and day 21 IDG-SW3 co-cultures (Fig. 6.10B – D). Determination of the effects of the sclerostin antibodies on the mineralisation zone length of the metatarsal bones indicated no effects of the varying concentrations of antibodies on control and day 4 IDG-SW3 co-cultured metatarsal bones (Fig. 6.11A-C). The mineralisation zone length was significantly inhibited in all E15 metatarsal bones co-cultured with 21-day old IDG-SW3 cells as

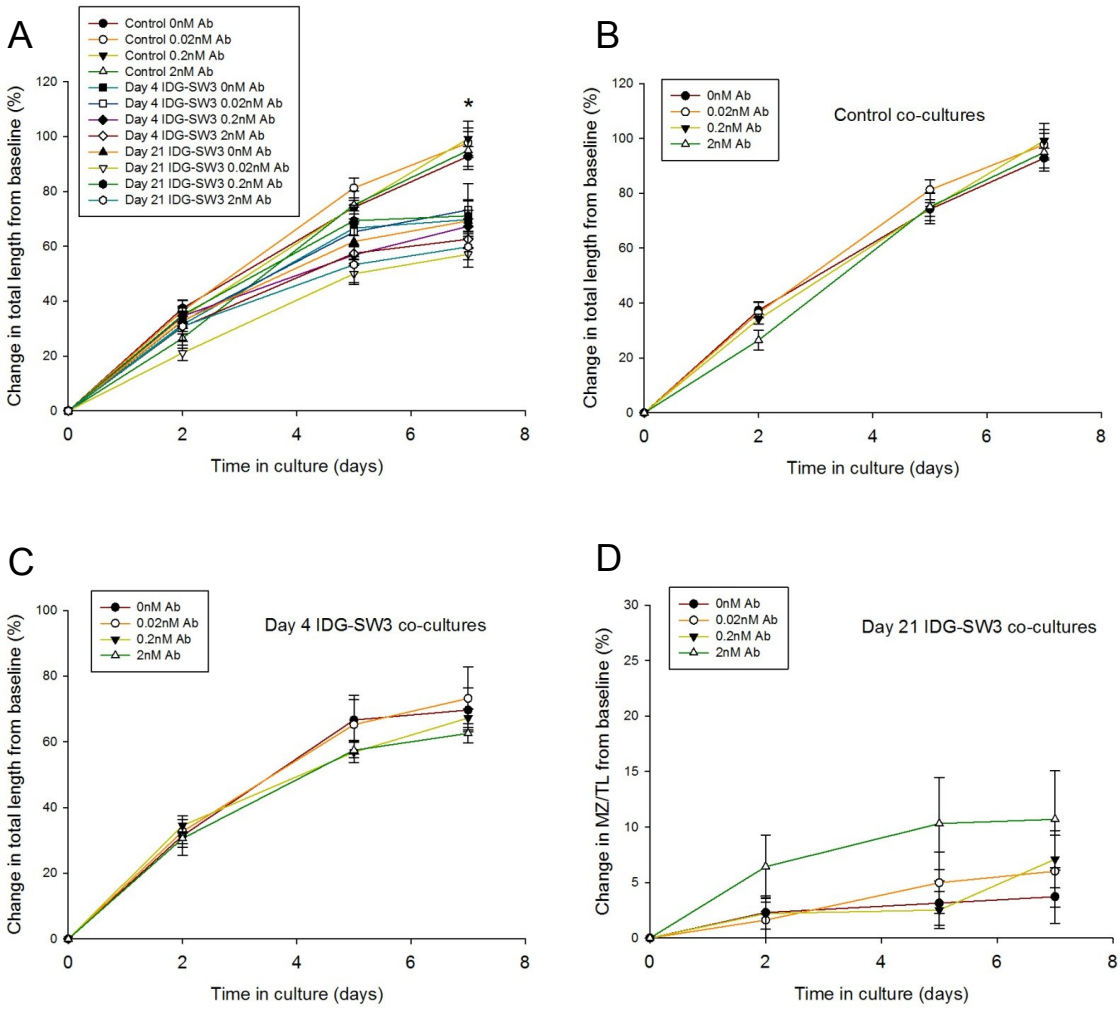

Figure 6.10 The lack of effect of 0-2nm sclerostin neutralising antibodies on the total length of E15 metatarsals co-cultured with IDG-SW3 cells

E15 metatarsals were co-cultured with IDG-SW3 cells at days 4 and 21 of culture for 7 days in the presence on varying concentrations of sclerostin neutralising antibodies (Ab) (0-2nM). As a control, metatarsal bones were cultured in IDG-SW3 media with no cells present. Measurements of the total length of the bones were made as a percentage of the baseline value **(A).** There was a significant difference in the total length of the control bones in comparison to the day 4 and day 21 IDG-SW3 cell co-cultured bones at day 7. When divided into separate graphs, there were no differences in the total lengths of the bones treated with the varying concentration of antibodies in control **(B)**, day 4 IDG-SW3 **(C)** and day 21 IDG-SW3 **(D)** co-cultures. Data are represented as mean ± SEM of six bones *P<0.05 in comparison to control bones at equivalent days of culture.

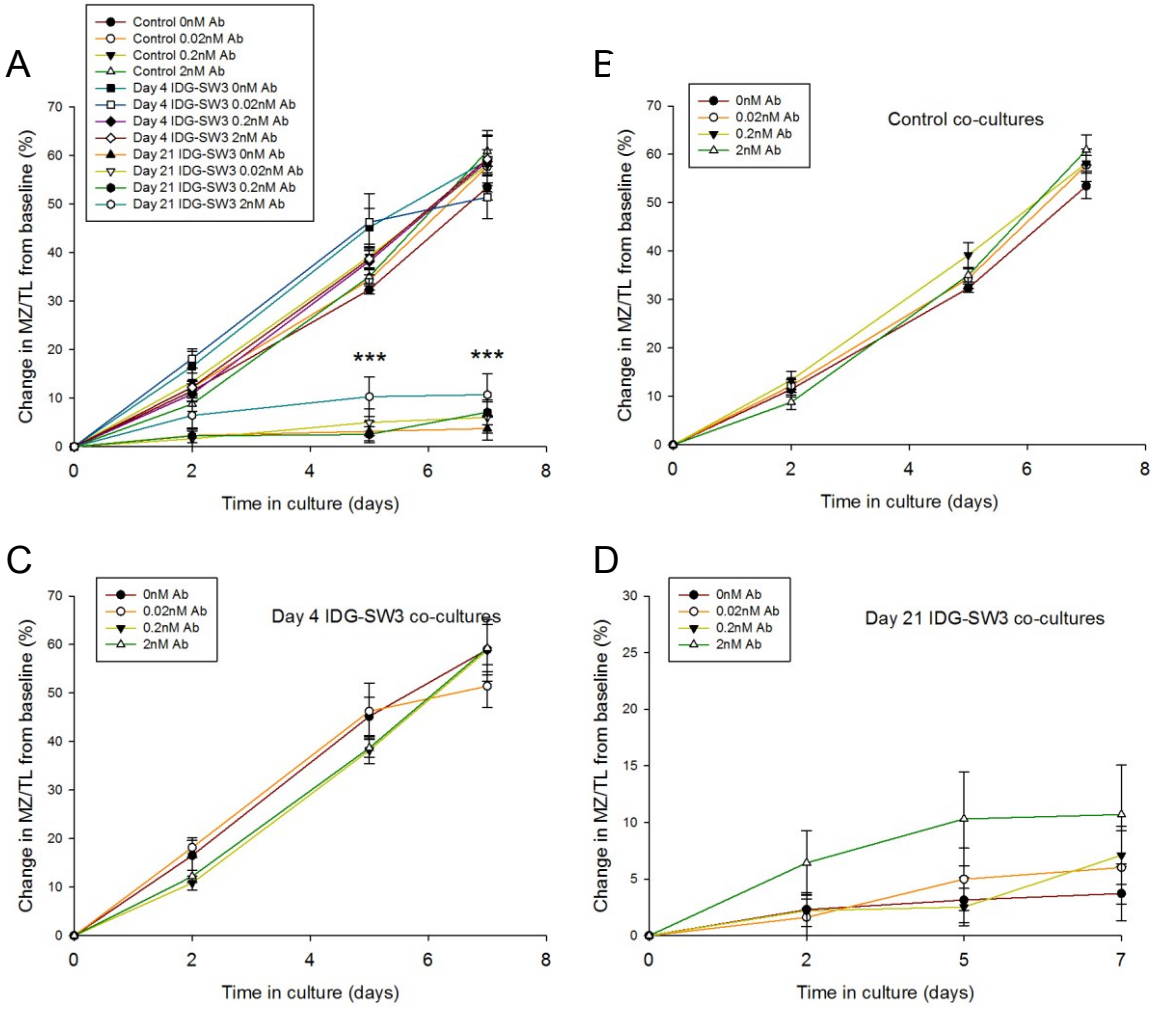

Figure 6.11 The lack of effect of 0-2nM sclerostin neutralising antibodies on the mineralisation capability of E15 metatarsals co-cultured with IDG-SW3 cells

E15 metatarsals were co-cultured with IDG-SW3 cells at days 4 and 21 of culture for 7 days in the presence on varying concentrations of sclerostin neutralising antibodies (Ab) (0-2nM). As a control, metatarsal bones were cultured in IDG-SW3 media with no cells present. Measurements of the mineralisation zone (MZ) as a percentage of the total length (TL) of the bones were made as a percentage of the baseline value **(A).** When divided into separate graphs, there were no differences in the MZ/TL treated with the varying concentration of antibodies in control **(B)**, day 4 IDG-SW3 **(C)** treated bones. However in the day 21 IDG-SW3 co-cultures there appeared to be increased MZ/TL in the 2nM antibody treated cultures, although this did not reach statistical significance (**D).** Data are represented as mean ± SEM of six bones.

is in concordance with the data presented in Fig. 6.7E (Fig. 6.11A & D, Fig. 6.12). Whilst there appeared to be a moderate increase in mineralisation, indicating possible rescue from sclerostin inhibitory effects, in the metatarsal co-cultures treated with 2nM sclerostin antibodies, this was not significantly different from those treated with the lesser concentrations and without any antibodies (Fig. 6.11& 6.12).

This is possibly due to an underestimation of the concentration of antibody required to neutralise the sclerostin present in the cultures. To this end, the sclerostin production by the E15 metatarsal bones was examined by ELISA analysis. This showed the metatarsal bones to produce large amounts of sclerostin (<109pg/ml) at days 2, 5 and 7 days of culture (Fig. 6.13). This therefore warrants the future investigation of the effects of higher concentrations of sclerostin antibodies on metatarsal matrix mineralisation.

Because of this slight trend towards a rescued inhibition of mineralisation in the sclerostin antibody treated bones, recombinant sclerostin was added to metatarsal cultures to further determine whether it is sclerostin which is mediating the inhibition seen. Interestingly the addition of varying concentrations of recombinant sclerostin (0-1000μM) to cultured metatarsals had no effect on the percentage change in the total length of the bone (Fig. 6.14C), or in the percentage change in the size of the mineralisation zone (Fig. 6.14A, B, D).

6.6 Discussion

Identification of the intercellular communications regulating endochondral ossification will provide new insights into potential therapeutic targets. Recent evidence suggests the osteocyte as playing a pivotal role in intercellular cross talk within the bone microenvironment (Klein-Nulend *et al.* 2003; Bonewald 2006; Xiong *et al.* 2011; Nakashima *et al.* 2011). Sclerostin is an osteocyte secretory product which accumulating evidence has implicated as a key regulator of bone formation,

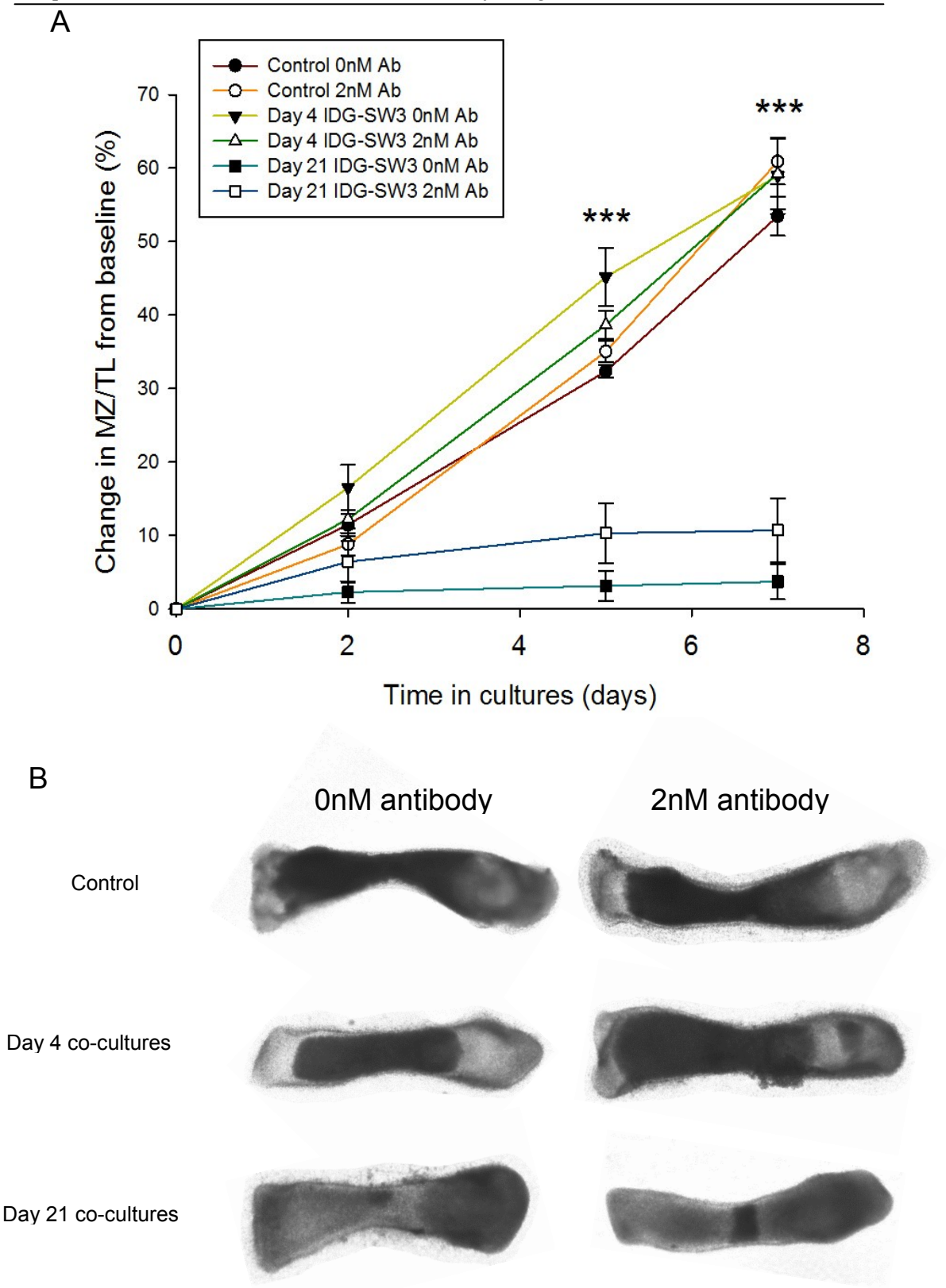

Figure 6.12 The effects of 2nM sclerostin antibodies on E15 metatarsal matrix mineralisation

The percentage change in the mineralisation zone (MZ) as a percentage of the total length (TL) of E15 metatarsal bones cultured in the presence and absence of 2nM sclerostin neutralising antibodies (Ab) **(A)**. Displayed are representative images of the metatarsal bones **(B).** Data are represented as mean ± SEM of six bones, *** P<0.001.

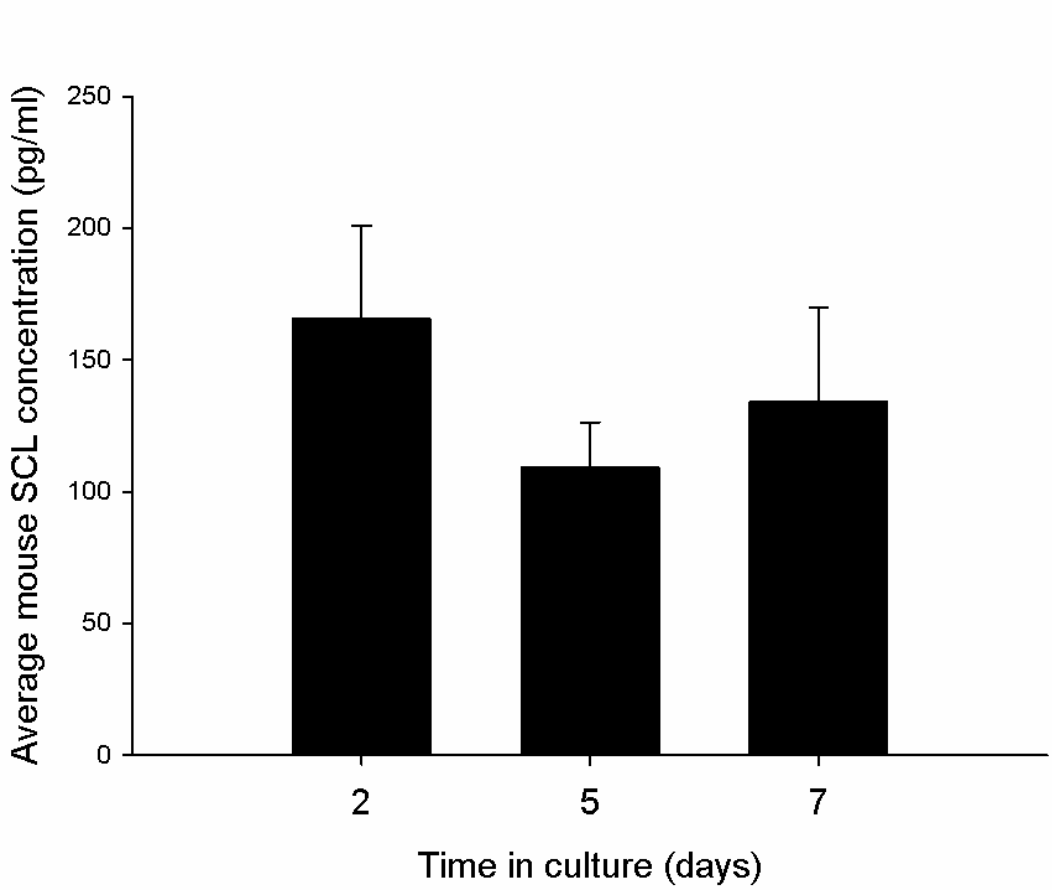

Figure 6.13 Expression of sclerostin by cultured E15 metatarsals by ELISA analysis

ELISA analysis of mouse sclerostin concentrations in the conditioned medium of E15 metatarsal bones cultured for up to 7 days. Data are represented as mean ± SEM of three bones.

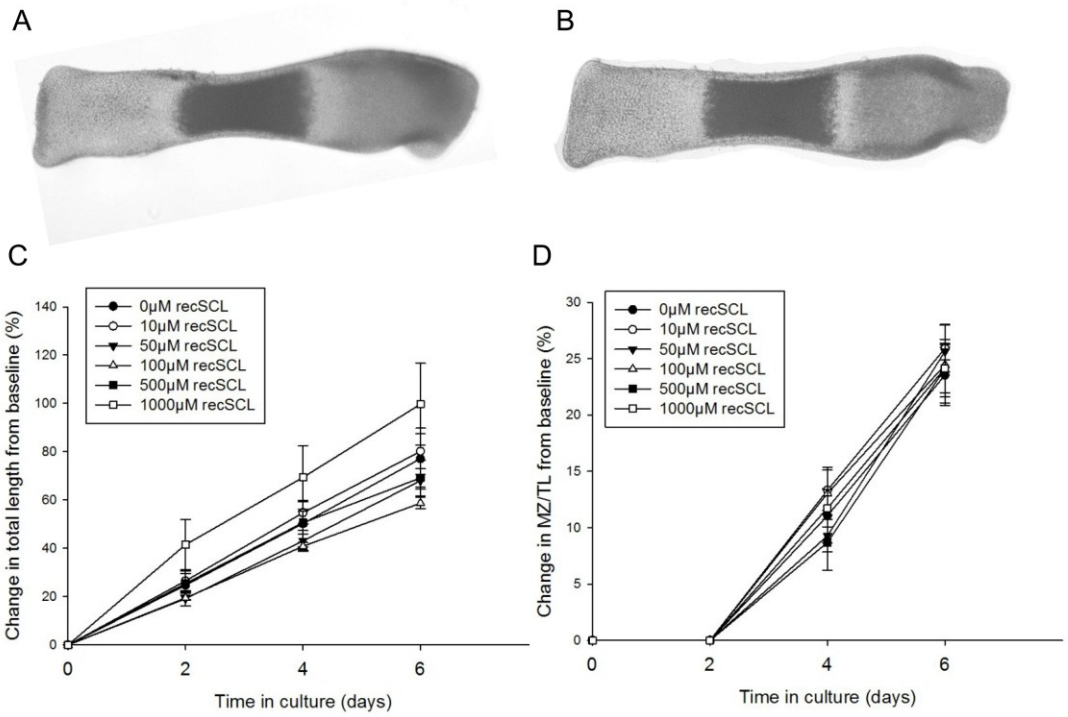

Figure 6.14 The lack of effect of 0-1mM recombinant sclerostin on E15 metatarsal mineralisation

E15 metatarsals were treated with varying concentrations of recSCL (0-1000μM) for 6 days. A control metatarsal bone is illustrated in **(A)** and a bone treated with 1000μM in **(B)** after 6 days in culture. The growth rate of all the embryonic metatarsal bones was unchanged **(C)**. Similarly there was no significant difference in the mineralisation zone as a percentage of the total length (MZ/TL) between control and recSCL treated bones **(D).** Data are represented as mean ± SEM of at least six bones in comparison to control bones at equivalent days of culture.

however little is known about its target cell type, mechanism of action and precise function. Recently it has been shown that sclerostin inhibits osteoblast matrix mineralisation through a MEPE-dependent mechanism (Atkins *et al.* 2011). It has yet to be established whether sclerostin could have a similar function in chondrocyte matrix mineralisation through either a local or paracrine mechanism.

Current data regarding the expression of sclerostin by chondrocytes is somewhat limited and conflicting. In the growth plate, sclerostin has been reported in the mineralising hypertrophic chondrocytes by immunohistochemistry (Winkler *et al.* 2003; van Bezooijen *et al.* 2009). However, analysis of *Sost* mRNA in the developing long bones showed no expression in the cartilaginous primordium except for in the perichondrium of the hypertrophic chondrocyte region. Sclerostin was also absent from the skull and rib cartilaginous tissue (Kusu *et al.* 2003). Similarly, here immunohistochemical staining failed to detect sclerostin protein in the growth plates of 4-week-old murine tibias. However, interestingly, PCR analysis did indicate *Sost* mRNA in costochondral primary chondrocytes cultures after 3 days (Fig. 6.1). This could likely be due to developmental differences, the differing populations of cells examined, or due to the sensitivity of the techniques used.

Despite this potential lack of local chondrocyte sclerostin expression the osteocytes of tibial cortical bone stained positive for sclerostin expression, as would be expected. The morphology of the osteocyte is suggestive of a role in mechanosensation and due to its reported crosstalk with other bone cell types including other osteocytes, osteoblasts and osteoclasts (Klein-Nulend *et al.* 2003; Bonewald 2006; Xiong *et al.* 2011; Nakashima *et al.* 2011). Here it was hypothesised that the osteocyte may have a functional role in the regulation of chondrocyte matrix mineralisation. The use of osteocytes for *in vitro* studies has been somewhat limited due to their location deep within the mineralised matrix and the resultant difficulty in isolating purified populations. The IDG-SW3 osteocyte-like cells, an immortomouse/Dmp1-GFP–derived bone cell line, have recently been characterised

and replicate the normal *in vivo* differentiation process, representing a late osteocyte cell phenotype after 21 days in culture (Woo *et al.* 2011). This is in comparison to the widely used MLO-Y4 and MLO-A5 cell lines both of which express early osteocyte markers such as E11/gp38 (Kato *et al.* 1997; Kato *et al.* 2001; Prideaux *et al.* 2012). Unlike these two well established cell lines, the IDG-SW3 cells express high levels of sclerostin, as has been shown here and as was originally characterised (Fig. 6.3) (Woo *et al.* 2011).

The role of sclerostin in osteoblast matrix mineralisation is well documented. An increase in sclerostin expression in mineralising cultures has been reported, and whilst PTH treatment and mechanical loading suppress this expression and promote bone formation, the pro-inflammatory cytokines tumour necrosis factor (TNF)-α and TNF-related weak inducer of apoptosis induce it (Sutherland *et al.* 2004; Ohyama *et al.* 2004; Poole *et al.* 2005; Silvestrini *et al.* 2007; Irie *et al.* 2008; Robling *et al.* 2008; Vincent *et al.* 2009; Atkins *et al.* 2009). This implicates sclerostin in diseases such as rheumatoid arthritis in which it is known that TNF-α plays a critical role (Franchimont *et al.* 1988). Indeed anti-TNF-α therapy has revolutionised treatment for rheumatoid arthritis (Tanaka 2012). It was hypothesised that the high IDG-SW3 osteocyte production of sclerostin has an inhibitory role in chondrocyte matrix mineralisation, and the results presented certainly suggest this with conditioned media and co-cultures of IDG-SW3 cells inhibiting the mineralisation capability of E15 murine metatarsals (Figs. 6.6 & 6.7).

The problems associated with using conditioned media should certainly be considered. As the media is taken from cells which have been cultured for long periods of time, it is likely that it contains large amounts of ATP which has previously been shown to be a potent inhibitor of osteoblast and chondrocyte matrix mineralisation directly and through the acidification of the culture medium (Hatori *et al.* 1995; Brandao-Burch *et al.* 2005; Orriss *et al.* 2007). However, the inhibition of mineralisation was not observed in cultures using 4-day old IDG-SW3 cells. Whilst

it is possible that there are differences in ATP production between the two time points, these are currently undocumented and likely to be minimal. Furthermore, it is entirely possible that the pH of the media is different and may be tending towards the lower end of the pH scale. This has previously been shown to inhibit osteoblast matrix mineralisation *in vitro* and as such, should be considered upon interpretation of the results presented here (Brandao-Burch *et al.* 2005).

Another potential explanation for the inhibition of matrix mineralisation seen upon co-culture with the day 21 IDG-SW3 cells is that these cells produce significantly more MEPE in comparison to day 4 IDG-SW3 cells. As has been shown in this thesis thus far, MEPE inhibits chondrocyte matrix mineralisation through its ASARM peptide (Chapter 5) (Staines *et al.* 2012c). CA074 is a cathepsin B inhibitor which can correct the mineralisation defect seen in *Hyp* mice due to its inhibition of MEPE cleavage by cathepsin B (Murata *et al.* 1991; Rowe *et al.* 2006). Similarly, SPR4 is a single PHEX peptide (4.2 kDa) that was found to bind to the pASARM peptide and inhibit the pASARM mediated inhibition of osteoblast matrix mineralisation (Martin *et al.* 2008). The addition of these specific inhibitors of MEPE function to the co-cultures was unable to rescue the inhibition of mineralisation seen (Fig. 6.8). This therefore suggests that the effects on chondrocyte matrix mineralisation seen are not due to MEPE expression. This is inconsistent with the recent publication detailing the interaction of sclerostin with MEPE in mineralising osteoblast cultures (Atkins *et al.* 2011). The reasons for this are unclear however it could be due to the differential regulation of sclerostin in differing cell types.

To confirm the role of sclerostin in the inhibition of mineralisation seen, antibodies which inhibit the biological activity of sclerostin were used (Eli-Lilly). These are currently an attractive therapeutic approach for stimulating bone formation; a strategy that has already been successful with Denosumab, an antibody against RANKL (Cummings *et al.* 2009). Sclerostin antibodies increase bone mineral density, bone volume and bone strength in ovariectomised rats and primates. They are also

effective in fracture healing (Li *et al.* 2009; Ominsky *et al.* 2010; Agholme *et al.* 2010). More recently, a study in post-menopausal women showed that a single injection of the sclerostin antibody significantly increased bone mineral density as well as markers of bone formation such as bone-specific ALP and osteocalcin expression (Padhi *et al.* 2011).

These antibodies were utilised here to examine the hypothesis that the inhibition of metatarsal matrix mineralisation seen is dependent upon sclerostin production. Administration of increasing concentrations of sclerostin antibodies failed to rescue the inhibition seen, however there did appear to be a marginal increase in matrix mineralisation by day 7 of culture which warrants their further investigation using higher concentrations of antibodies (Fig. 6.12). Moreover, the high production of sclerostin expression by E15 metatarsal bones presented here further suggests that higher concentrations of antibodies may be required to elicit a response (Fig. 6.13).

Whether the source of this sclerostin production is the chondrocytes of the metatarsal bones is unknown. It is entirely plausible that the perichondrium could be synthesising these high levels of sclerostin concentration, as has been shown in a previous study (Kusu *et al.* 2003). Certainly the perichondrium is known to produce essential factors that act to regulate endochondral bone growth and this could be the case here (Haaijman *et al.* 1999; Alvarez *et al.* 2001). Future investigations could examine the production of sclerostin in metatarsal bones cultured with the perichondrium removed. It is also interesting to note that the sclerostin production in these metatarsal bones remained fairly consistent throughout the culture period.

Interestingly, the inhibitory effects of sclerostin on metatarsal mineralisation were non-existent in metatarsal organ cultures treated with recombinant sclerostin (Fig. 6.14). This could be explained by a potential difference between the *in vivo* concentration of sclerostin produced by the osteocytes, and with those tested in this experiment. However the results presented here from the sclerostin ELISA placed

the concentrations of sclerostin from the IDG-SW3 cells in the pica-molar range whereas recombinant sclerostin was added in the micro-molar range, therefore suggesting that this is not the case. Instead it is entirely possible that the recombinant sclerostin could non-specifically bind to the cell surface through its heparan sulfate proteoglycan binding domain and therefore be inactive (Stuart Kuhstoss, Eli Lilly, personal communications). To examine this further, the use of such compounds as dextran sodium sulphate would allow release of recombinant sclerostin from the cell surface and would hopefully allow it to function as seen *in vivo.* Furthermore it is possible that there are differences in the biological activity of recombinant proteins depending upon their source. Therefore the lack of response to recombinant sclerostin, here purchased from R&D systems, could be due to dubious biological activity and the sclerostin produced by the IDG-SW3 cells is in fact more efficacious. Whilst there is currently no evidence to suggest such problems, this is certainly something that should be considered in the interpretation of these results.

The mechanism by which sclerostin functions to inhibit matrix mineralisation is unclear. It is well established that sclerostin specifically binds to the LRP5/6 Wnt coreceptors antagonising the Wnt pathway (Semenov *et al.* 2005). This has significant effects on both chondrogenesis and chondrocyte hypertrophy (Staines *et al.* 2012a). It would certainly be worth investigating whether sclerostin is inhibiting Wnt signalling in the metatarsal bones and whether this alters the histology of the chondrocytes within the bones.

Whilst the co-culture of E15 metatarsals and IDG-SW3 cells had no effect on *Mepe* or *Phex* mRNA expression, interestingly it significantly inhibited the expression of *Dmp1* mRNA (Fig. 6.9). This is in concordance with a previous study in which the addition of recombinant sclerostin decreased *Dmp1* mRNA expression in mineralising osteoblasts (Atkins *et al.* 2011). In bone, DMP1 is primarily expressed by osteocytes but also by osteoblasts and hypertrophic chondrocytes (Toyosawa *et*

al. 2001; Fen *et al.* 2002; Feng *et al.* 2003). Whilst, like the other SIBLING proteins, DMP1 has an ASARM motif which is thought to inhibit matrix mineralisation, it has also a well described role as a hydroxyapatite nucleator (Narayanan *et al.* 2001; Martin *et al.* 2008; Staines *et al.* 2012b). The DMP1 deficient mouse displays a highly widened growth plate suggesting an impairment of mineralisation at the chondro-osseous junction (Ye et al. 2005). It is therefore plausible that sclerostin may function through diminishing the activity of DMP1. Furthermore, although not investigated here, it is likely that sclerostin regulates the other members of the SIBLING family of proteins and this should be investigated in future studies.

In conclusion, these studies detail the potential for cross-talk between the osteocytes of the cortical bone and the adjacent growth plate chondrocytes through the expression of the Wnt signalling antagonist sclerostin. Contradictory to previous studies, it was found that the inhibitory effects of sclerostin on chondrocyte matrix mineralisation are independent of MEPE expression.

Chapter 7

Final discussion

7.1 General discussion

Biomineralisation of the growth plate is a key process allowing effective longitudinal bone growth. It is therefore imperative that we unravel the precise mechanisms controlling this complex process to prevent clinical disorders of bone development. Recent advances in this field have identified a group of NCPs and based upon the hypothesis that they are key regulators of matrix mineralisation the focus of these studies was on one such NCP, namely MEPE, and its functional role in maintaining the fine balance of mineral formation at the growth plate.

The absence of a practical and accessible *in vitro* chondrocyte mineralisation model has hindered a fuller appreciation of how cartilage mineralisation and endochondral ossification are disrupted by factors such as cytokines and drugs that are responsible for impaired linear bone growth in children. It is well recognised that primary chondrocyte cells undergo de-differentiation, as was reported here, and as such, a mineralising method for the chondrogenic ATDC5 cell line was characterised (Lefebvre *et al.* 1994; Hering *et al.* 1994). The work presented in Chapter 3 showed that under the conditions defined these ATDC5 cells undergo the expected stages of chondrogenic differentiation and produce a physiologic mineralised matrix after 15 days in culture. This method will enable future research into chondrocyte matrix mineralisation in the context of both endochondral bone growth, and in the *in vitro* examination of pathological chondrocyte hypertrophy and matrix mineralisation seen in such diseases as osteoarthritis (Kirsch *et al.* 2000; Johnson & Terkeltaub 2004). It will also help us understand better the underpinning molecular mechanisms responsible for poor linear bone growth which is observed in a number of chronic diseases such as cystic fibrosis, chronic kidney disease, rheumatological conditions and inflammatory bowel disease. Despite this it is well recognised that as with all *in vitro* systems, problems still remain. It is difficult to achieve precise replication of the cells normal environment and thus to this end, the metatarsal organ culture system was also adopted.

The embryonic metatarsal organ culture provides an idea model as it provides conditions closer to the *in vivo* situation as the chondrocytes within the bones exist in the three principal stages of chondrogenesis whilst retaining their direct interactions with each other and their matrix. This allows the metatarsal bones to be cultured devoid of serum, therefore removing a potential confounding variable. This *ex vivo* culture system is widely used within chondrocyte research and here was developed to allow assessment of matrix mineralisation, and the potential role that MEPE may play.

It was important before such role could be defined, to establish the spatial expression of MEPE in the growth plate. The localisation patterns presented in Chapter 4 serve to strengthen its potential role in this phenomenon. Specifically, MEPE was preferentially expressed by the hypertrophic chondrocytes as is in concordance with a previous microarray study and as is observed in the MEPE overexpressing mouse (David *et al.* 2009; Horvat-Gordon *et al.* 2010). Moreover, the data presented here localised a 2.2kDa cleavage product of MEPE, the ASARM peptide, to sites of ossification. This is similar to another SIBLING family member, DMP1, which is processed into two fragments, the COOH-terminal fragment of which contains the ASARM peptide and in the growth plate, is localised to the calcification front and ossification zone (Martin *et al.* 2008; Maciejewska *et al.* 2008). This suggests a co-localisation of the DMP1 and MEPE ASARM peptides, potentiating their effects.

Whilst these effects have been established in osteoblast matrix mineralisation, this thesis presents for the first time the precise role of the ASARM peptide in the growth plate. Specifically MEPE was shown to have an inhibitory role on chondrocyte matrix mineralisation dependent upon its cleavage and phosphorylation of the ASARM peptide. Despite this it was suggested that the MEPE-ASARM peptide has no effect on chondrocyte function *per se* and instead affects the process of mineralisation directly, as is in concordance with previous

studies examining osteoblast matrix mineralisation (Addison *et al.* 2008; Martin *et al.* 2008). The critical activity of the ASARM peptide is evidenced by the ASARM hypothesis proposed by Peter Rowe which describes the role of the SIBLING ASARM peptides, PHEX, and FGF23 in bone renal P_i homeostasis as well as in matrix mineralisation both at the osteoblast, and now at the chondrocyte level (Rowe 2004; David *et al.* 2010).

This inhibitory effect of the MEPE ASARM peptide has been shown here to be further potentiated by a positive feedback loop induced by ASARM peptides. The data presented here suggests that the pASARM peptide enhances MEPE expression, whilst negatively regulating the expression of PHEX, a known inhibitor of MEPE functional activity (Liu *et al.* 2007a; Addison *et al.* 2008; Martin *et al.* 2008). This observation is consistent a previous study in which osteoblast cell cultures treated with pASARM peptide displayed decreased PHEX expression (Martin *et al.* 2008). Because of this, it is reasonable to speculate that physiologically there must be a regulatory mechanism to ensure that there is not an overproduction of ASARM peptides and as such a pathological state. Although the precise nature of the counter balancing mechanism has yet to be elucidated, it is plausible to suggest that one of the other SIBLING family members is responsible due to their similar structural features and yet differing functions (Staines *et al.* 2012b). When this postulated regulatory mechanism does dysfunction, the resulting pathology would be characterised by increased MEPE expression and an abundance of ASARM peptides.

Certainly in patients with XLH and in the *Hyp* mouse model of this hereditary hypophosphatemic disease, an increased expression of ASARM peptides is observed (Rowe *et al.* 2000; Argiro *et al.* 2001; Rowe *et al.* 2004; Bresler *et al.* 2004; Liu *et al.* 2007a). Caused by an inactivating mutation in the *Phex* gene, patients with XLH display defective bone and tooth mineralisation, growth retardation, and defective renal re-absorption of P_i (Carpenter *et al.* 2011). Moreover, analysis of the

Hyp mouse growth plate indicates severe morphological disruption (Liu *et al.* 2006). The data presented in this thesis certainly indicates a critical role for MEPE and its ASARM peptide in this disorder. Furthermore, the MEPE positive feedback loop described acts to exacerbate the condition. It is plausible to suggest that the administration of a PHEX peptide or of cathepsin inhibitors may provide some therapeutic intervention in patients with XLH as these would inhibit the cleavage of MEPE to the ASARM peptide. Certainly this seems viable as their administration to the *Hyp* mouse has been shown to correct the mineralisation defect seen (Rowe *et al.* 2006).

It is evident that much remains to be learnt regarding the *in vivo* role of the SIBLING proteins and the ASARM peptide in bone diseases. This is not just in disorders related to P_i homeostasis, but to other bone diseases such as osteoporosis and osteoarthritis. Indeed there are close links between the SIBLING proteins and osteoarthritis with microarray data and gene analysis studies highlighting MEPE and DMP1 as being differentially expressed in osteoarthritic tissues (Hopwood *et al.* 2007; Sanchez *et al.* 2008). Furthermore serum BSP and OPN levels significantly correlate with osteoarthritic disease severity (Petersson *et al.* 1998; Hasegawa *et al.* 2011). There is increasing evidence for a role for developmental processes in the pathology of osteoarthritis and this highlights the importance of the work presented in this thesis (Pitsillides & Beier 2011).

Osteoporosis is a pervasive public health issue worldwide and recent genetic studies have highlighted MEPE as a gene of interest associated with risk of fracture (Estrada *et al.* 2012). The process of fracture healing is highly complex and involves a well-orchestrated series of biological events. The results here further implicate MEPE in endochondral fracture healing. Indeed MEPE expression has also been observed in both the early stages of non-stabilised tibia fracture repair and during fracture healing (Lu *et al.* 2004).

It is also interesting to note that recent seminal and exciting discoveries have described the skeleton as a dynamic endocrine organ that plays a critical role in the regulation of energy metabolism and fat mass (Confavreux *et al.* 2009). Concomitant with this, there is exciting new data that implicates the ASARM hypothesis as a key orchestrator in the evidenced cross talk between the skeleton and energy metabolism (David *et al.* 2009; David *et al.* 2010).

The Wnt signalling pathway is emerging as a potent regulator of cellular development and function in a variety of tissues (Macsai *et al.* 2008; Macsai *et al.* 2012). Post-natally, Wnt signalling is crucial for the regulation of skeletal bone mass throughout life and over the past two decades, studies have identified the Wnt signalling pathway as having a crucial role in growth plate biology, bone formation and skeletal remodelling (Krishnan *et al.* 2006b; Staines *et al.* 2012a). Of the Wnt signalling inhibitors identified, sclerostin is proving the most interesting from a therapeutic standpoint. Clinical trials are currently underway for an antibody which neutralises sclerostin activity, a potent Wnt signalling antagonist, in an attempt to stimulate bone formation in osteoporotic patients. This strategy has already proved successful in targeting osteoporosis with Denosumab, an antibody against RANKL (Cummings *et al.* 2009). The results certainly look promising with sclerostin antibodies increasing bone formation in ovariectomized rats and primates, and in post-menopausal women subjected to a single injection of the antibody (Li *et al.* 2009; Ominsky *et al.* 2010; Agholme *et al.* 2010; Padhi *et al.* 2011).

The recently described interaction between MEPE and sclerostin is an exciting development in the field of biomineralisation due to the known anabolic effects of the sclerostin-neutralising antibodies on osteoporosis (Li *et al.* 2009; Li *et al.* 2010; Atkins *et al.* 2011). This could therefore warrant investigation into the potential therapeutic use of MEPE in osteoporosis and potentially in osteoarthritis due to the ever emerging role of sclerostin in this debilitating disease (Power *et al.* 2010; Chan *et al.* 2011; gado-Calle *et al.* 2011).

Although unable to determine a local production of sclerostin by growth plate chondrocytes, the work presented in Chapter 6 details the potential for cross-talk between osteocytes and chondrocytes in the regulation of chondrocyte matrix mineralisation. This is in concordance with another study which utilised a computational model to detail the regulation of mineralised cartilage turnover by adjacent osteocytes (Cox *et al.* 2011). Indeed the osteocyte is certainly suited to this function as structurally it has extensive processes which, through gap junction connections, form an extensive syncytium with other osteocytes and osteoblasts (Klein-Nulend *et al.* 2003; Bonewald 2006). The recent discovery that osteocytes have a greater capacity to support osteoclastogenesis than osteoblasts due to their high expression of RANKL highlights their complex and crucial role in the bone microenvironment (Nakashima *et al.* 2011; Xiong *et al.* 2011). sclerostin, along with nitric oxide and prostaglandins, has been suggested as the mediator of the osteocyte mechano-response (van Bezooijen *et al.* 2004; Bonewald 2006). The data presented here, although it cannot confirm conclusively a role for sclerostin, it does suggest a potential function for it in the regulation of endochondral bone growth.

In conclusion, this thesis has identified a critical inhibitory role for MEPE and its ASARM peptide in regulating the fine balance of effective mineral formation at the growth plate (Table. 7.1). Moreover, mechanisms which may exist to exacerbate the expression of MEPE have been identified. Whilst the studies presented here complement previous findings of MEPE and its role in biomineralisation, it also highlights the multiple and complex functions of the SIBLING ASARM peptides in both P_i homeostasis and matrix mineralisation in disease and health. It is therefore vital that we endeavour to fully establish the interactions within this hypothesis to allow future therapeutic developments.

Cellular expression pattern	Mouse bone phenotype		Clinical condition of gene mutation	Cleavage product & post translational modification	Role of cleavage products in mineralisation	Role of cleavage products in mineral metabolism	References
	Knockout	Overexpression					
Osteoblasts & osteocytes	Increased bone mass, MAR, trabecular number & thickness	Decreased MAR, bone remodelling, bone mass and increased growth plate widths	Unknown	> ASARM peptide - 3 serine phosphorylation > AC100	Inhibition Promotion	ASARM peptide inhibits phosphate uptake in the kidney & increases FGF23	Gowen *et al.,* 2003 Hayashubara *et al*., 2004 Nampei *et al.*, 2004 Addison *et al*., 2008 Marks *et al.,* 2008 Martin *et al.,* 2008 David *et al*., 2009 Staines *et al*., 2012

Table 7.1 The functional role of MEPE in biomineralisation

The functional role of MEPE in biomineralisation as is dependent upon its cleavage and post translational modification. Detailed is (i) the cellular expression pattern (ii) the phenotype of the knockout mouse (iii) the phenotype of the transgenic mouse (iv) clinical conditions association with mutation in this gene (v) cleavage products and post translational modifications (vi) known role of each cleavage product in ECM mineralisation (vii) list of relevant references (adapted from (Staines *et al.* 2012b)).

7.2 Directions for future research

The results presented in this thesis have identified a critical role for MEPE in regulating chondrocyte matrix mineralisation. They have pinpointed this functional role to be dependent upon the phosphorylation and cleavage of the ASARM peptide, and have investigated the potential interaction of MEPE with the already known mineralisation inhibitor, sclerostin. However, further work is necessary to fully elucidate the mechanism by which MEPE exerts its function in endochondral ossification and its regulation in the physiological context.

Certainly the examination of the growth plates of the MEPE knockout and overexpressing mice would be of great benefit in furthering our understanding of the role of MEPE in endochondral ossification. Both these mice have been generated but were unattainable in this PhD. Whilst the growth plates of MEPE overexpressing mice display considerable widening, the precise histomorphometric phenotype of the growth plate has not been examined. This has also not been examined in the MEPE knockout mouse. Due to the known role of MEPE in regulating P_i homeostasis, what would be of greater benefit would be a cartilage specific deletion of MEPE using the Cre recombinase-*LoxP* system.

These mice could also be used to better examine the role of MEPE-ASARM peptides on angiogenesis. Here it was reported that the pASARM peptide inhibited endothelial cell specific markers, and therefore it would be interesting to examine the direct effects of the pASARM peptide on endothelial cell function. Access to the aforementioned mouse models would allow further examination of this. Concomitant with this, MMP mRNA profiling would be useful in identifying whether the MEPE-ASARM interacts with any other MMPs in addition to MMP13.

In this thesis, a feedback system was reported by which the ASARM peptide prevented PHEX expression allowing their further release and thereby increasing

the inhibition of matrix mineralisation. However it is likely that *in vivo* there is a physiological mechanism regulating this to ensure that there is not an increased expression of ASARM peptides. Similarly there must be a regulatory mechanism controlling ASARM-phosphorylation as its function is dependent upon this phosphorylation. It is plausible that the other SIBLING proteins may be acting to regulate this and it would be interesting to examine the interactions of MEPE with the other SIBLING proteins, and their place within the current ASARM hypothesis (section 1.7.3). This will allow the investigation into their potential therapeutic application to disorders of mineralisation including disorders of hypophosphatemia, osteoporosis and osteoarthritis.

Canonical Wnt signalling is a potent regulator of cartilage development and function and it has recently been suggested that it can enhance MEPE expression in osteoblasts through, somewhat confusingly, either the Wnt ligand Wnt3a or by the Wnt inhibitor, sclerostin (Cho *et al.* 2011; Atkins *et al.* 2011; Staines *et al.* 2012a). Attempts were made here to examine the potential interaction of MEPE and sclerostin in the growth plate and these were unfortunately proved as non-existent. However it would certainly be interesting to elucidate the precise regulation of MEPE expression by the Wnt signalling pathway in the growth plate, and establish this as a therapeutic approach to disorders of bone and cartilage mineralisation. The work in this thesis also identified the potential for cross-talk between chondrocytes and osteocytes. The proteins released by the osteocyte, including sclerostin, are therefore of great interest in determining the precise mechanisms and signalling pathways surrounding the apparent complex conversation between osteocytes and the growth plate.

Reference List

Abbott J & Holtzer H 1966 The loss of phenotypic traits by differentiated cells. 3. The reversible behavior of chondrocytes in primary cultures. *Journal of Cell Biology* **28** 473-487.

Adams CS & Shapiro IM 2002 The fate of the terminally differentiated chondrocyte: evidence for microenvironmental regulation of chondrocyte apoptosis. *Critical Reviews of Oral Biology & Medicine* **13** 465-473.

Addison WN, Azari F, Sorensen ES, Kaartinen MT & McKee MD 2007 Pyrophosphate inhibits mineralization of osteoblast cultures by binding to mineral, up-regulating osteopontin, and inhibiting alkaline phosphatase activity. *Journal of Biological Chemistry* **282** 15872-15883.

Addison WN, Masica DL, Gray JJ & McKee MD 2010 Phosphorylation-dependent inhibition of mineralization by osteopontin ASARM peptides is regulated by PHEX cleavage. *Journal of Bone and Mineral Research* **25** 695-705.

Addison WN, Nakano Y, Loisel T, Crine P & McKee MD 2008 MEPE-ASARM peptides control extracellular matrix mineralization by binding to hydroxyapatite: an inhibition regulated by PHEX cleavage of ASARM. *Journal of Bone and Mineral Research* **23** 1638-1649.

Agholme F, Li X, Isaksson H, Ke HZ & Aspenberg P 2010 Sclerostin antibody treatment enhances metaphyseal bone healing in rats. *Journal of Bone and Mineral Research* **25** 2412-2418.

Ahmed SF & Farquharson C 2010 The effect of GH and IGF1 on linear growth and skeletal development and their modulation by SOCS proteins. *Journal of Endocrinology* **206** 249-259.

Albrecht C, Helmreich M, Tichy B, Marlovits S, Plasenzotti R, Egerbacher M & Haeusler G 2009 Impact of 3D-culture on the expression of differentiation markers and hormone receptors in growth plate chondrocytes as compared to articular chondrocytes. *International Journal of Molecular Medicine* **23** 347-355.

Ali SY, Sajdera SW & Anderson HC 1970 Isolation and characterization of calcifying matrix vesicles from epiphyseal cartilage. *Proceedings of the National Academy of Sciences USA* **67** 1513-1520.

Altaf FM, Hering TM, Kazmi NH, Yoo JU & Johnstone B 2006 Ascorbate-enhanced chondrogenesis of ATDC5 cells. *European Cells & Materials* **12** 64-69.

Alvarez J, Horton J, Sohn P & Serra R 2001 The perichondrium plays an important role in mediating the effects of TGF-beta1 on endochondral bone formation. *Developmental Dynamics* **221** 311-321.

Amling M, Neff L, Tanaka S, Inoue D, Kuida K, Weir E, Philbrick WM, Broadus AE & Baron R 1997 Bcl-2 lies downstream of parathyroid hormone-related peptide in a signaling pathway that regulates chondrocyte maturation during skeletal development. *Journal of Cell Biology* **136** 205-213.

Anderson HC 1995 Molecular biology of matrix vesicles. *Clinical Orthopaedic Related Research* 266-280.

Anderson HC 2003 Matrix vesicles and calcification. *Current Rheumatology Reports* **5** 222-226.

Anderson HC, Sipe JB, Hessle L, Dhanyamraju R, Atti E, Camacho NP & Millan JL 2004 Impaired calcification around matrix vesicles of growth plate and bone in alkaline phosphatase-deficient mice. *American Journal of Pathology* **164** 841-847.

Andrade AC, Chrysis D, Audi L & Nilsson O 2011 Methods to study cartilage and bone development. *Endocrine Development* **21** 52-66.

Argiro L, Desbarats M, Glorieux FH & Ecarot B 2001 Mepe, the gene encoding a tumor-secreted protein in oncogenic hypophosphatemic osteomalacia, is expressed in bone. *Genomics* **74** 342-351.

Arnett T 2003 Regulation of bone cell function by acid-base balance. *Proceedings of the Nutrition Society* **62** 511-520.

Arnett TR 2010 Acidosis, hypoxia and bone. *Archives of Biochemistry and Biophysics* **503** 103-109.

Atkins GJ, Rowe PS, Lim HP, Welldon KJ, Ormsby R, Wijenayaka AR, Zelenchuk L, Evdokiou A & Findlay DM 2011 Sclerostin is a locally acting regulator of late-osteoblast/preosteocyte differentiation and regulates mineralization through a MEPE-ASARM-dependent mechanism. *Journal of Bone and Mineral Research* **26** 1425-1436.

Atkins GJ, Welldon KJ, Halbout P & Findlay DM 2009 Strontium ranelate treatment of human primary osteoblasts promotes an osteocyte-like phenotype while eliciting an osteoprotegerin response. *Osteoporosis International* **20** 653-664.

Atsumi T, Miwa Y, Kimata K & Ikawa Y 1990 A chondrogenic cell line derived from a differentiating culture of AT805 teratocarcinoma cells. *Cell Differentiation and Development* **30** 109-116.

Balemans W, Ebeling M, Patel N, Van HE, Olson P, Dioszegi M, Lacza C, Wuyts W, Van Den EJ, Willems P, Paes-Alves AF, Hill S, Bueno M, Ramos FJ, Tacconi P, Dikkers FG, Stratakis C, Lindpaintner K, Vickery B, Foernzler D & Van HW 2001 Increased bone density in sclerosteosis is due to the deficiency of a novel secreted protein (SOST). *Human Molecular Genetics* **10** 537-543.

Ballock RT & O'Keefe RJ 2003 The biology of the growth plate. *Journal of Bone and Joint Surgery* **85-A** 715-726.

Ballock RT & Reddi AH 1994 Thyroxine is the serum factor that regulates morphogenesis of columnar cartilage from isolated chondrocytes in chemically defined medium. *Journal of Cell Biology* **126** 1311-1318.

Behonick DJ, Xing Z, Lieu S, Buckley JM, Lotz JC, Marcucio RS, Werb Z, Miclau T & Colnot C 2007 Role of matrix metalloproteinase 13 in both endochondral and intramembranous ossification during skeletal regeneration. *PLoS.One.* **2** e1150.

Bellahcene A, Castronovo V, Ogbureke KU, Fisher LW & Fedarko NS 2008 Small integrin-binding ligand N-linked glycoproteins (SIBLINGs): multifunctional proteins in cancer. *Nature Reviews Cancer* **8** 212-226.

Bennett VD, Weiss IM & Adams SL 1989 Cartilage-specific 5' end of chick alpha 2(I) collagen mRNAs. *Journal of Biological Chemistry* **264** 8402-8409.

Bernier SM & Goltzman D 1993 Regulation of expression of the chondrocytic phenotype in a skeletal cell line (CFK2) in vitro. *Journal of Bone and Mineral Research* **8** 475-484.

Bodine PV, Zhao W, Kharode YP, Bex FJ, Lambert AJ, Goad MB, Gaur T, Stein GS, Lian JB & Komm BS 2004 The Wnt antagonist secreted frizzled-related protein-1 is a negative regulator of trabecular bone formation in adult mice. *Molecular Endocrinology* **18** 1222-1237.

Bonewald LF 2002 Osteocytes: a proposed multifunctional bone cell. *Journal of Musculoskeletal & Neuronal Interactions* **2** 239-241.

Bonewald LF 2006 Mechanosensation and Transduction in Osteocytes. *Bonekey Osteovision.* **3** 7-15.

Bonewald LF 2007 Osteocytes as dynamic multifunctional cells. *Annals of the New York Academy of Sciences* **1116** 281-290.

Bonewald LF 2010 The Amazing Osteocyte. *Journal of Bone and Mineral Research* **26** 229-238.

Bonewald LF, Harris SE, Rosser J, Dallas MR, Dallas SL, Camacho NP, Boyan B & Boskey A 2003 von Kossa staining alone is not sufficient to confirm that

mineralization in vitro represents bone formation. *Calcified Tissue International* **72** 537-547.

Bonewald LF & Johnson ML 2008 Osteocytes, mechanosensing and Wnt signaling. *Bone* **42** 606-615.

Borgers M 1973 The cytochemical application of new potent inhibitors of alkaline phosphatases. *Journal of Histochemistry and Cytochemistry* **21** 812-824.

Borjesson AE, Lagerquist MK, Liu C, Shao R, Windahl SH, Karlsson C, Sjogren K, Moverare-Skrtic S, Antal MC, Krust A, Mohan S, Chambon P, Savendahl L & Ohlsson C 2010 The role of estrogen receptor alpha in growth plate cartilage for longitudinal bone growth. *Journal of Bone & Mineral Research* **25** 2690-2700.

Borjesson AE, Windahl SH, Karimian E, Eriksson EE, Lagerquist MK, Engdahl C, Antal MC, Krust A, Chambon P, Savendahl L & Ohlsson C 2012 The role of estrogen receptor-alpha and its activation function-1 for growth plate closure in female mice. *American Journal of Physiology Endocrinology & Metabolism* **302** E1381-E1389.

Boskey AL, Chiang P, Fermanis A, Brown J, Taleb H, David V & Rowe PS 2009a MEPE's Diverse Effects on Mineralization. *Calcified Tissue International* **86** 42-46.

Boskey AL, Doty SB, Stiner D & Binderman I 1996 Viable cells are a requirement for in vitro cartilage calcification. *Calcified Tissue International* **58** 177-185.

Boskey AL, Gelb BD, Pourmand E, Kudrashov V, Doty SB, Spevak L & Schaffler MB 2009b Ablation of cathepsin k activity in the young mouse causes hypermineralization of long bone and growth plates. *Calcified Tissue International* **84** 229-239.

Boskey AL & Roy R 2008 Cell culture systems for studies of bone and tooth mineralization. *Chemical Reviews* **108** 4716-4733.

Boukpessi T, Gaucher C, Leger T, Salmon B, Le FJ, Willig C, Rowe PS, Garabedian M, Meilhac O & Chaussain C 2010 Abnormal presence of the matrix extracellular phosphoglycoprotein-derived acidic serine- and aspartate-rich motif peptide in human hypophosphatemic dentin. *American Journal of Pathology* **177** 803-812.

Bowe AE, Finnegan R, Jan de Beur SM, Cho J, Levine MA, Kumar R & Schiavi SC 2001 FGF-23 inhibits renal tubular phosphate transport and is a PHEX substrate. *Biochemical Biophysical Research Communications* **284** 977-981.

Brandao-Burch A, Utting JC, Orriss IR & Arnett TR 2005 Acidosis inhibits bone formation by osteoblasts in vitro by preventing mineralization. *Calcified Tissue International* **77** 167-174.

Bresler D, Bruder J, Mohnike K, Fraser WD & Rowe PS 2004 Serum MEPE-ASARM-peptides are elevated in X-linked rickets (HYP): implications for phosphaturia and rickets. *Journal of Endocrinology* **183** R1-R9.

Brunkow ME, Gardner JC, Van NJ, Paeper BW, Kovacevich BR, Proll S, Skonier JE, Zhao L, Sabo PJ, Fu Y, Alisch RS, Gillett L, Colbert T, Tacconi P, Galas D, Hamersma H, Beighton P & Mulligan J 2001 Bone dysplasia sclerosteosis results from loss of the SOST gene product, a novel cystine knot-containing protein. *American Journal of Human Genetics* **68** 577-589.

Buckwalter JA, Mower D, Ungar R, Schaeffer J & Ginsberg B 1986 Morphometric analysis of chondrocyte hypertrophy. *Journal of Bone and Joint Surgery* **68** 243-255.

Burger EH & Klein-Nulend J 1999 Mechanotransduction in bone--role of the lacuno-canalicular network. *FASEB Journal* **13 Suppl** S101-S112.

Burnstock G, Fredholm BB, North RA & Verkhratsky A 2010 The birth and postnatal development of purinergic signalling. *Acta Physiology (Oxf)* **199** 93-147.

Bush PG, Parisinos CA & Hall AC 2008 The osmotic sensitivity of rat growth plate chondrocytes in situ; clarifying the mechanisms of hypertrophy. *Journal of Cell Physiology* **214** 621-629.

Bush PG, Pritchard M, Loqman MY, Damron TA & Hall AC 2010 A key role for membrane transporter NKCC1 in mediating chondrocyte volume increase in the mammalian growth plate. *Journal of Bone & Mineral Research* **25** 1594-1603.

Cancedda R, Descalzi CF & Castagnola P 1995 Chondrocyte differentiation. *International Review of Cytology* **159** 265-358.

Carames B, Taniguchi N, Otsuki S, Blanco FJ & Lotz M 2010 Autophagy is a protective mechanism in normal cartilage, and its aging-related loss is linked with cell death and osteoarthritis. *Arthritis and Rheumatism* **62** 791-801.

Carpenter TO, Imel EA, Holm IA, Jan de Beur SM & Insogna KL 2011 A clinician's guide to X-linked hypophosphatemia. *Journal of Bone and Mineral Research* **26** 1381-1388.

Castagnola P, Dozin B, Moro G & Cancedda R 1988 Changes in the expression of collagen genes show two stages in chondrocyte differentiation in vitro. *Journal of Cell Biology* **106** 461-467.

Chan BY, Fuller ES, Russell AK, Smith SM, Smith MM, Jackson MT, Cake MA, Read RA, Bateman JF, Sambrook PN & Little CB 2011 Increased chondrocyte sclerostin may protect against cartilage degradation in osteoarthritis. *Osteoarthritis & Cartilage* **8** 874 - 85.

Cho YD, Kim WJ, Yoon WJ, Woo KM, Baek JH, Lee G, Kim GS & Ryoo HM 2011 Wnt3a stimulates Mepe, matrix extracellular phosphoglycoprotein, expression directly by the activation of the canonical Wnt signaling pathway and indirectly through the stimulation of autocrine Bmp-2 expression. *Journal of Cell Physiol*ogy **227** 2287-2296.

Choi HY, Dieckmann M, Herz J & Niemeier A 2009 Lrp4, a novel receptor for Dickkopf 1 and sclerostin, is expressed by osteoblasts and regulates bone growth and turnover in vivo. *PLoS.One.* **4** e7930.

Coe MR, Summers TA, Parsons SJ, Boskey AL & Balian G 1992 Matrix mineralization in hypertrophic chondrocyte cultures. Beta glycerophosphate increases type X collagen messenger RNA and the specific activity of pp60c-src kinase. *Bone and Mineral* **18** 91-106.

Confavreux CB, Levine RL & Karsenty G 2009 A paradigm of integrative physiology, the crosstalk between bone and energy metabolisms. *Molecular Cell Endocrinology* **310** 21-29.

Cox LG, van RB, van Donkelaar CC & Ito K 2011 The turnover of mineralized growth plate cartilage into bone may be regulated by osteocytes. *Journal of Biomechanics* **44** 1765-1770.

Coxam V, Miller MA, Bowman MB & Miller SC 1996 Ontogenesis of IGF regulation of longitudinal bone growth in rat metatarsal rudiments cultured in serum-free medium. *Archives Physiology Biochemistry* **104** 173-179.

Cummings SR, San MJ, McClung MR, Siris ES, Eastell R, Reid IR, Delmas P, Zoog HB, Austin M, Wang A, Kutilek S, Adami S, Zanchetta J, Libanati C, Siddhanti S & Christiansen C 2009 Denosumab for prevention of fractures in postmenopausal women with osteoporosis. *New England Journal of Medicine* **361** 756-765.

Dallas SL & Bonewald LF 2010 Dynamics of the transition from osteoblast to osteocyte. *Annals of the New York Academy of Sciences* **1192** 437-443.

David V, Martin A, Hedge AM & Rowe PS 2009 Matrix extracellular phosphoglycoprotein (MEPE) is a new bone renal hormone and vascularization modulator. *Endocrinology* **150** 4012-4023.

David V, Martin AC, Hedge AM, Drezner MK & Rowe PS 2010 ASARM peptides: PHEX-dependent & independent regulation of serum phosphate. *American Journal of Physiology & Renal Physiology* **300** F783-91.

Dean DD, Boyan BD, Schwart Z, Muniz OE, Carreno MR, Maeda S & Howell DS 2001 Effect of 1alpha,25-dihydroxyvitamin D3 and 24R,25-dihydroxyvitamin D3 on metalloproteinase activity and cell maturation in growth plate cartilage in vivo. *Endocrine.* **14** 311-323.

DeChiara TM, Robertson EJ & Efstratiadis A 1991 Parental imprinting of the mouse insulin-like growth factor II gene. *Cell* **64** 849-859.

DeLise AM, Fischer L & Tuan RS 2000 Cellular interactions and signaling in cartilage development. *Osteoarthritis & Cartilage.* **8** 309-334.

DeLise AM & Tuan RS 2002 Analysis of N-cadherin function in limb mesenchymal chondrogenesis in vitro. *Developmental Dynamics* **225** 195-204.

Dessau W, von der MH, von der MK & Fischer S 1980 Changes in the patterns of collagens and fibronectin during limb-bud chondrogenesis. *Journal of Embryology and Experimental Morphology* **57** 51-60.

Dobbie H, Unwin RJ, Faria NJ & Shirley DG 2008 Matrix extracellular phosphoglycoprotein causes phosphaturia in rats by inhibiting tubular phosphate reabsorption. *Nephrology & Dialysis Transplant.* **23** 730-733.

Dong S, Yang B, Guo H & Kang F 2012 MicroRNAs regulate osteogenesis and chondrogenesis. *Biochemical and Biophysical Research Communications* **418** 587-591.

Ducy P 2000 Cbfa1: a molecular switch in osteoblast biology. *Developmental Dynamics* **219** 461-471.

Dudley HR & Spiro D 1961 The fine structure of bone cells. *Journal of Biophysical & Biochemical Cytology* **11** 627-649.

Ecarot B & Desbarats M 1999 1,25-(OH)2D3 down-regulates expression of Phex, a marker of the mature osteoblast. *Endocrinology* **140** 1192-1199.

Ecarot B, Glorieux FH, Desbarats M, Travers R & Labelle L 1992 Effect of dietary phosphate deprivation and supplementation of recipient mice on bone formation by transplanted cells from normal and X-linked hypophosphatemic mice. *Journal of Bone and Mineral Research* **7** 523-530.

Emons J, Chagin AS, Hultenby K, Zhivotovsky B, Wit JM, Karperien M & Savendahl L 2009 Epiphyseal fusion in the human growth plate does not involve classical apoptosis. *Pediatric Research* **66** 654-659.

Engsig MT, Chen QJ, Vu TH, Pedersen AC, Therkidsen B, Lund LR, Henriksen K, Lenhard T, Foged NT, Werb Z & Delaisse JM 2000 Matrix metalloproteinase 9 and vascular endothelial growth factor are essential for osteoclast recruitment into developing long bones. *Journal of Cell Biology* **151** 879-889.

Estrada K, Styrkarsdottir U, Evangelou E, Hsu YH, Duncan EL, Ntzani EE, Oei L, Albagha OM, Amin N, Kemp JP, Koller DL, Li G, Liu CT, Minster RL, Moayyeri A, Vandenput L, Willner D, Xiao SM, Yerges-Armstrong LM, Zheng HF, Alonso N, Eriksson J, Kammerer CM, Kaptoge SK, Leo PJ, Thorleifsson G, Wilson SG, Wilson

JF, Aalto V, Alen M, Aragaki AK, Aspelund T, Center JR, Dailiana Z, Duggan DJ, Garcia M, Garcia-Giralt N, Giroux S, Hallmans G, Hocking LJ, Husted LB, Jameson KA, Khusainova R, Kim GS, Kooperberg C, Koromila T, Kruk M, Laaksonen M, Lacroix AZ, Lee SH, Leung PC, Lewis JR, Masi L, Mencej-Bedrac S, Nguyen TV, Nogues X, Patel MS, Prezelj J, Rose LM, Scollen S, Siggeirsdottir K, Smith AV, Svensson O, Trompet S, Trummer O, van Schoor NM, Woo J, Zhu K, Balcells S, Brandi ML, Buckley BM, Cheng S, Christiansen C, Cooper C, Dedoussis G, Ford I, Frost M, Goltzman D, Gonzalez-Macias J, Kahonen M, Karlsson M, Khusnutdinova E, Koh JM, Kollia P, Langdahl BL, Leslie WD, Lips P, Ljunggren O, Lorenc RS, Marc J, Mellstrom D, Obermayer-Pietsch B, Olmos JM, Pettersson-Kymmer U, Reid DM, Riancho JA, Ridker PM, Rousseau F, Slagboom PE, Tang NL, Urreizti R, Van HW, Viikari J, Zarrabeitia MT, Aulchenko YS, Castano-Betancourt M, Grundberg E, Herrera L, Ingvarsson T, Johannsdottir H, Kwan T, Li R, Luben R, Medina-Gomez C, Palsson ST, Reppe S, Rotter JI, Sigurdsson G, van Meurs JB, Verlaan D, Williams FM, Wood AR, Zhou Y, Gautvik KM, Pastinen T, Raychaudhuri S, Cauley JA, Chasman DI, Clark GR, Cummings SR, Danoy P, Dennison EM, Eastell R, Eisman JA, Gudnason V, Hofman A, Jackson RD, Jones G, Jukema JW, Khaw KT, Lehtimaki T, Liu Y, Lorentzon M, McCloskey E, Mitchell BD, Nandakumar K, Nicholson GC, Oostra BA, Peacock M, Pols HA, Prince RL, Raitakari O, Reid IR, Robbins J, Sambrook PN, Sham PC, Shuldiner AR, Tylavsky FA, van Duijn CM, Wareham NJ, Cupples LA, Econs MJ, Evans DM, Harris TB, Kung AW, Psaty BM, Reeve J, Spector TD, Streeten EA, Zillikens MC, Thorsteinsdottir U, Ohlsson C, Karasik D, Richards JB, Brown MA, Stefansson K, Uitterlinden AG, Ralston SH, Ioannidis JP, Kiel DP & Rivadeneira F 2012 Genome-wide meta-analysis identifies 56 bone mineral density loci and reveals 14 loci associated with risk of fracture. *Nature Genetics* **44** 491-501.

Farnum CE, Lee R, O'Hara K & Urban JP 2002 Volume increase in growth plate chondrocytes during hypertrophy: the contribution of organic osmolytes. *Bone* **30** 574-581.

Farquharson C, Berry JL, Mawer EB, Seawright E & Whitehead CC 1995 Regulators of chondrocyte differentiation in tibial dyschondroplasia: an in vivo and in vitro study. *Bone* **17** 279-286.

Fell HB & Mellanby E 1952 The effect of hypervitaminosis A on embryonic limb bones cultivated in vitro. *Journal of Physiology* **116** 320-349.

Fen JQ, Zhang J, Dallas SL, Lu Y, Chen S, Tan X, Owen M, Harris SE & MacDougall M 2002 Dentin matrix protein 1, a target molecule for Cbfa1 in bone, is a unique bone marker gene. *Journal of Bone and Mineral Research* **17** 1822-1831.

Feng JQ, Huang H, Lu Y, Ye L, Xie Y, Tsutsui TW, Kunieda T, Castranio T, Scott G, Bonewald LB & Mishina Y 2003 The Dentin matrix protein 1 (Dmp1) is specifically expressed in mineralized, but not soft, tissues during development. *Journal of Dental Research* **82** 776-780.

Feng JQ, Ward LM, Liu S, Lu Y, Xie Y, Yuan B, Yu X, Rauch F, Davis SI, Zhang S, Rios H, Drezner MK, Quarles LD, Bonewald LF & White KE 2006 Loss of DMP1 causes rickets and osteomalacia and identifies a role for osteocytes in mineral metabolism. *Nature Genetics* **38** 1310-1315.

Fisher LW & Fedarko NS 2003 Six genes expressed in bones and teeth encode the current members of the SIBLING family of proteins. *Connective Tissue Research* **44 Suppl 1** 33-40.

Fisher LW, Torchia DA, Fohr B, Young MF & Fedarko NS 2001 Flexible structures of SIBLING proteins, bone sialoprotein, and osteopontin. *Biochemical and Biophysical Research Communications* **280** 460-465.

Focht RJ & Adams SL 1984 Tissue specificity of type I collagen gene expression is determined at both transcriptional and post-transcriptional levels. *Molecular Cell Biology* **4** 1843-1852.

Franchimont P, Reuter A, Vrindts-Gevaert Y, Bastings M, Malaise M, Sondag C, Frere MC & Gysen P 1988 Production of tumour necrosis factor-alpha, interferon-gamma and interleukin-2 by peripheral blood mononuclear cells of subjects suffering from rheumatoid arthritis. *Scandinavian Journal of Rheumatology* **17** 203-212.

Frost HM 1990 Skeletal structural adaptations to mechanical usage (SATMU): 1. Redefining Wolff's law: the bone modeling problem. *Anatomical Records* **226** 403-413.

gado-Calle J, Arozamena J, Garcia-Renedo R, Garcia-Ibarbia C, Pascual-Carra MA, Gonzalez-Macias J & Riancho JA 2011 Osteocyte deficiency in hip fractures. *Calcified Tissue International* **89** 327-334.

Garimella R, Bi X, Camacho N, Sipe JB & Anderson HC 2004 Primary culture of rat growth plate chondrocytes: an in vitro model of growth plate histotype, matrix vesicle biogenesis and mineralization. *Bone* **34** 961-970.

Gartland A, Mason-Savas A, Yang M, MacKay CA, Birnbaum MJ & Odgren PR 2009 Septoclast deficiency accompanies postnatal growth plate chondrodysplasia in the toothless (tl) osteopetrotic, colony-stimulating factor-1 (CSF-1)-deficient rat and is partially responsive to CSF-1 injections. *American Journal of Pathology* **175** 2668-2675.

Gartland A, Mechler J, Mason-Savas A, MacKay CA, Mailhot G, Marks SC, Jr. & Odgren PR 2005 In vitro chondrocyte differentiation using costochondral chondrocytes as a source of primary rat chondrocyte cultures: an improved isolation and cryopreservation method. *Bone* **37** 530-544.

Gartland A, Orriss IR, Rumney RM, Bond AP, Arnett T & Gallagher JA 2012 Purinergic signalling in osteoblasts. *Front Biosciences* **17** 16-29.

Gentili C & Cancedda R 2009 Cartilage and bone extracellular matrix. *Current Pharmeutical Des*ign **15** 1334-1348.

Gerber HP, Vu TH, Ryan AM, Kowalski J, Werb Z & Ferrara N 1999 VEGF couples hypertrophic cartilage remodeling, ossification and angiogenesis during endochondral bone formation. *Nature Medicine* **5** 623-628.

Gilbert SF, 2006, Developmental Biology, 8th Edition, in: ISBN 0-87893-250-X

Goldring MB 2005 Human chondrocyte cultures as models of cartilage-specific gene regulation. *Methods Molecular Medicine* **107** 69-95.

Goldring MB, Tsuchimochi K & Ijiri K 2006 The control of chondrogenesis. *Journal of Cell Biochemistry* **97** 33-44.

Golub EE 2011 Biomineralization and matrix vesicles in biology and pathology. *Seminars in Immunopathology* **33** 409-417.

Gong MQ, Gu Y, Hu XB, Sun Y, Ma L, Li XL, Sun LX, Sun J, Qian J & Zhu CL 2005 Cloning and overexpression of CYP6F1, a cytochrome P450 gene, from deltamethrin-resistant Culex pipiens pallens. *Acta Biochemica & Biophysica Sinica(Shanghai)* **37** 317-326.

Gowen LC, Petersen DN, Mansolf AL, Qi H, Stock JL, Tkalcevic GT, Simmons HA, Crawford DT, Chidsey-Frink KL, Ke HZ, McNeish JD & Brown TA 2003 Targeted disruption of the osteoblast/osteocyte factor 45 gene (OF45) results in increased bone formation and bone mass. *Journal of Biological Chemistry* **278** 1998-2007.

Grigoriadis AE, Heersche JN & Aubin JE 1996 Analysis of chondroprogenitor frequency and cartilage differentiation in a novel family of clonal chondrogenic rat cell lines. *Differentiation* **60** 299-307.

Grimsrud CD, Romano PR, D'Souza M, Puzas JE, Schwarz EM, Reynolds PR, Roiser RN & O'Keefe RJ 2001 BMP signaling stimulates chondrocyte maturation and the expression of Indian hedgehog. *Journal of Orthopaedic Research* **19** 18-25.

Gronowicz G, Woodiel FN, McCarthy MB & Raisz LG 1989 In vitro mineralization of fetal rat parietal bones in defined serum-free medium: effect of beta-glycerol phosphate. *Journal of Bone and Mineral Research* **4** 313-324.

Guo J, Chung UI, Yang D, Karsenty G, Bringhurst FR & Kronenberg HM 2006 PTH/PTHrP receptor delays chondrocyte hypertrophy via both Runx2-dependent and -independent pathways. *Developmental Biology* **292** 116-128.

Guo R, Rowe PS, Liu S, Simpson LG, Xiao ZS & Quarles LD 2002 Inhibition of MEPE cleavage by Phex. *Biochemical and Biophysical Research Communications* **297** 38-45.

Haaijman A, Karperien M, Lanske B, Hendriks J, Lowik CW, Bronckers AL & Burger EH 1999 Inhibition of terminal chondrocyte differentiation by bone morphogenetic protein 7 (OP-1) in vitro depends on the periarticular region but is independent of parathyroid hormone-related peptide. *Bone* **25** 397-404.

Hakim FT, Cranley R, Brown KS, Eanes ED, Harne L & Oppenheim JJ 1984 Hereditary joint disorder in progressive ankylosis (ank/ank) mice. I. Association of calcium hydroxyapatite deposition with inflammatory arthropathy. *Arthritis and Rheumatism* **27** 1411-1420.

Halbeisen RE, Galgano A, Scherrer T & Gerber AP 2008 Post-transcriptional gene regulation: from genome-wide studies to principles. *Cell Molecular Life Sciences* **65** 798-813.

Hall BK & Miyake T 2000 All for one and one for all: condensations and the initiation of skeletal development. *Bioessays* **22** 138-147.

Hasegawa M, Segawa T, Maeda M, Yoshida T & Sudo A 2011 Thrombin-cleaved osteopontin levels in synovial fluid correlate with disease severity of knee osteoarthritis. *Journal of Rheumatology* **38** 129-134.

Hatori M, Teixeira CC, Debolt K, Pacifici M & Shapiro IM 1995 Adenine nucleotide metabolism by chondrocytes in vitro: role of ATP in chondrocyte maturation and matrix mineralization. *Journal of Cell Physiology* **165** 468-474.

Hayashibara T, Hiraga T, Sugita A, Wang L, Hata K, Ooshima T & Yoneda T 2007 Regulation of osteoclast differentiation and function by phosphate: potential role of osteoclasts in the skeletal abnormalities in hypophosphatemic conditions. *Journal of Bone and Mineral Research* **22** 1743-1751.

Hayashibara T, Hiraga T, Yi B, Nomizu M, Kumagai Y, Nishimura R & Yoneda T 2004 A synthetic peptide fragment of human MEPE stimulates new bone formation in vitro and in vivo. *Journal of Bone and Mineral Research* **19** 455-462.

Heinegard D 2009 Proteoglycans and more--from molecules to biology. *International Journal of Experimental Pathology* **90** 575-586.

Heinrichs C, Yanovski JA, Roth AH, Yu YM, Domene HM, Yano K, Cutler GB, Jr. & Baron J 1994 Dexamethasone increases growth hormone receptor messenger ribonucleic acid levels in liver and growth plate. *Endocrinology* **135** 1113-1118.

Henriksen K, Neutzsky-Wulff AV, Bonewald LF & Karsdal MA 2009 Local communication on and within bone controls bone remodeling. *Bone* **44** 1026-1033.

Hering TM, Kollar J, Huynh TD, Varelas JB & Sandell LJ 1994 Modulation of extracellular matrix gene expression in bovine high-density chondrocyte cultures by

ascorbic acid and enzymatic resuspension. *Archives of Biochemistry and Biophysics* **314** 90-98.

Hessle L, Johnson KA, Anderson HC, Narisawa S, Sali A, Goding JW, Terkeltaub R & Millan JL 2002 Tissue-nonspecific alkaline phosphatase and plasma cell membrane glycoprotein-1 are central antagonistic regulators of bone mineralization. *Proceedings of the National Academy of Sciences USA* **99** 9445-9449.

Hill PA 1998 Bone remodelling. *British Journal of Orthodontics* **25** 101-107.

Hirao M, Hashimoto J, Yamasaki N, Ando W, Tsuboi H, Myoui A & Yoshikawa H 2007 Oxygen tension is an important mediator of the transformation of osteoblasts to osteocytes. *Journal of Bone & Mineral Metabolism* **25** 266-276.

Ho AM, Johnson MD & Kingsley DM 2000 Role of the mouse ank gene in control of tissue calcification and arthritis. *Science* **289** 265-270.

Hochberg Z 2002 Clinical physiology and pathology of the growth plate. *Best Practice & Research in Clinical Endocrinology & Metabolism* **16** 399-419.

Holm IA, Huang X & Kunkel LM 1997 Mutational analysis of the PEX gene in patients with X-linked hypophosphatemic rickets. *American Journal of Human Genetics* **60** 790-797.

Hopwood B, Tsykin A, Findlay DM & Fazzalari NL 2007 Microarray gene expression profiling of osteoarthritic bone suggests altered bone remodelling, WNT and transforming growth factor-beta/bone morphogenic protein signalling. *Arthritis Research & Therapy.* **9** R100.

Horner A, Bishop NJ, Bord S, Beeton C, Kelsall AW, Coleman N & Compston JE 1999 Immunolocalisation of vascular endothelial growth factor (VEGF) in human neonatal growth plate cartilage. *Journal of Anatomy* **194 (Pt 4)** 519-524.

Horton WA & Degnin CR 2009 FGFs in endochondral skeletal development. *Trends in Endocrinology & Metabolism* **20** 341-348.

Horvat-Gordon M, Praul CA, Ramachandran R, Bartell PA & Leach RM, Jr. 2010 Use of microarray analysis to study gene expression in the avian epiphyseal growth plate. *Comparative Biochemistry & Physiology Part D.Genomics Proteomics* **5** 12-23.

Houston B, Paton IR, Burt DW & Farquharson C 2002 Chromosomal localization of the chicken and mammalian orthologues of the orphan phosphatase PHOSPHO1 gene. *Animal Genetics* **33** 451-454.

Huang W, Chung UI, Kronenberg HM & de CB 2001 The chondrogenic transcription factor Sox9 is a target of signaling by the parathyroid hormone-related

peptide in the growth plate of endochondral bones. *Proceedings of the National Academy of Sciences USA* **98** 160-165.

Huesa C, Yadav MC, Finnila MA, Goodyear SR, Robins SP, Tanner KE, Aspden RM, Millan JL & Farquharson C 2011 PHOSPHO1 is essential for mechanically competent mineralization and the avoidance of spontaneous fractures. *Bone* **48** 1066-1074.

Hunziker EB, Schenk RK & Cruz-Orive LM 1987 Quantitation of chondrocyte performance in growth-plate cartilage during longitudinal bone growth. *Journal of Bone and Joint Surgery* **69** 162-173.

Hunziker EB, Wagner J & Zapf J 1994 Differential effects of insulin-like growth factor I and growth hormone on developmental stages of rat growth plate chondrocytes in vivo. *Journal of Clinical Investigations* **93** 1078-1086.

Huq NL, Cross KJ, Ung M & Reynolds EC 2005 A review of protein structure and gene organisation for proteins associated with mineralised tissue and calcium phosphate stabilisation encoded on human chromosome 4. *Archives of Oral Biology* **50** 599-609.

Hutchison MR, Bassett MH & White PC 2007 Insulin-like growth factor-I and fibroblast growth factor, but not growth hormone, affect growth plate chondrocyte proliferation. *Endocrinology* **148** 3122-3130.

Idelevich A, Rais Y & Monsonego-Ornan E 2011 Bone Gla protein increases HIF-1alpha-dependent glucose metabolism and induces cartilage and vascular calcification. *Arteriosclerosis, Thrombosis, and Vascular Biology* **31** e55-e71.

Irie K, Ejiri S, Sakakura Y, Shibui T & Yajima T 2008 Matrix mineralization as a trigger for osteocyte maturation. *Journal of Histochemistry and Cytochemistry* **56** 561-567.

Isaksson OG, Jansson JO & Gause IA 1982 Growth hormone stimulates longitudinal bone growth directly. *Science* **216** 1237-1239.

Johnson K, Polewski M, van ED & Terkeltaub R 2005 Chondrogenesis mediated by PPi depletion promotes spontaneous aortic calcification in NPP1-/- mice. *Arteriosclerosis & Thrombosis Vascular Biology* **25** 686-691.

Johnson K & Terkeltaub R 2004 Upregulated ank expression in osteoarthritis can promote both chondrocyte MMP-13 expression and calcification via chondrocyte extracellular PPi excess. *Osteoarthritis & Cartilage.* **12** 321-335.

Juul A 2001 The effects of oestrogens on linear bone growth. *Human Reproductie Update.* **7** 303-313.

Kao J, Huey G, Kao R & Stern R 1990 Ascorbic acid stimulates production of glycosaminoglycans in cultured fibroblasts. *Experimental and Molecular Pathology* **53** 1-10.

Kato Y, Boskey A, Spevak L, Dallas M, Hori M & Bonewald LF 2001 Establishment of an osteoid preosteocyte-like cell MLO-A5 that spontaneously mineralizes in culture. *Journal of Bone and Mineral Research* **16** 1622-1633.

Kato Y, Windle JJ, Koop BA, Mundy GR & Bonewald LF 1997 Establishment of an osteocyte-like cell line, MLO-Y4. *Journal of Bone and Mineral Research* **12** 2014-2023.

Kawano Y & Kypta R 2003 Secreted antagonists of the Wnt signalling pathway. *Journal of Cell Science* **116** 2627-2634.

Kawasaki K 2011 The SCPP gene family and the complexity of hard tissues in vertebrates. *Cells Tissues Organs* **194** 108-112.

Kawasaki K, Buchanan AV & Weiss KM 2007 Gene duplication and the evolution of vertebrate skeletal mineralization. *Cells Tissues Organs* **186** 7-24.

Kawasaki K & Weiss KM 2006 Evolutionary genetics of vertebrate tissue mineralization: the origin and evolution of the secretory calcium-binding phosphoprotein family. *Journal of Experiemtnal Zoology B. Molecular Development Evolution.* **306** 295-316.

Khouja HI, Bevington A, Kemp GJ & Russell RG 1990 Calcium and orthophosphate deposits in vitro do not imply osteoblast-mediated mineralization: mineralization by betaglycerophosphate in the absence of osteoblasts. *Bone* **11** 385-391.

Kipp DE, McElvain M, Kimmel DB, Akhter MP, Robinson RG & Lukert BP 1996 Scurvy results in decreased collagen synthesis and bone density in the guinea pig animal model. *Bone* **18** 281-288.

Kirsch T, Swoboda B & Nah H 2000 Activation of annexin II and V expression, terminal differentiation, mineralization and apoptosis in human osteoarthritic cartilage. *Osteoarthritis & Cartilage.* **8** 294-302.

Klein-Nulend J, Nijweide PJ & Burger EH 2003 Osteocyte and bone structure. *Current Osteoporosis Reports* **1** 5-10.

Komori T, Yagi H, Nomura S, Yamaguchi A, Sasaki K, Deguchi K, Shimizu Y, Bronson RT, Gao YH, Inada M, Sato M, Okamoto R, Kitamura Y, Yoshiki S & Kishimoto T 1997 Targeted disruption of Cbfa1 results in a complete lack of bone formation owing to maturational arrest of osteoblasts. *Cell* **89** 755-764.

Kosaki N, Takaishi H, Kamekura S, Kimura T, Okada Y, Minqi L, Amizuka N, Chung UI, Nakamura K, Kawaguchi H, Toyama Y & D'Armiento J 2007 Impaired

bone fracture healing in matrix metalloproteinase-13 deficient mice. *Biochemical and Biophysical Research Communications* **354** 846-851.

Krakow D & Rimoin DL 2010 The skeletal dysplasias. *Genetics Medicine* **12** 327-341.

Kramer I, Halleux C, Keller H, Pegurri M, Gooi JH, Weber PB, Feng JQ, Bonewald LF & Kneissel M 2010 Osteocyte Wnt/beta-catenin signaling is required for normal bone homeostasis. *Molecular Cell Biology.* **30** 3071-3085.

Krishnan V, Bryant HU & MacDougald OA 2006a Regulation of bone mass by Wnt signaling. *Journal of Clinical Investigations* **116** 1202-1209.

Krishnan V, Bryant HU & MacDougald OA 2006b Regulation of bone mass by Wnt signaling. *Journal of Clinical Investigations* **116** 1202-1209.

Kronenberg HM 2003 Developmental regulation of the growth plate. *Nature* **423** 332-336.

Kusu N, Laurikkala J, Imanishi M, Usui H, Konishi M, Miyake A, Thesleff I & Itoh N 2003 Sclerostin is a novel secreted osteoclast-derived bone morphogenetic protein antagonist with unique ligand specificity. *Journal of Biological Chemistry* **278** 24113-24117.

Lazarus JE, Hegde A, Andrade AC, Nilsson O & Baron J 2007 Fibroblast growth factor expression in the postnatal growth plate. *Bone* **40** 577-586.

Leboy PS, Vaias L, Uschmann B, Golub E, Adams SL & Pacifici M 1989 Ascorbic acid induces alkaline phosphatase, type X collagen, and calcium deposition in cultured chick chondrocytes. *Journal of Biological Chemistry* **264** 17281-17286.

Lee ER, Lamplugh L, Shepard NL & Mort JS 1995 The septoclast, a cathepsin B-rich cell involved in the resorption of growth plate cartilage. *Journal of Histochemistry and Cytochemistry* **43** 525-536.

Lee NK & Karsenty G 2008 Reciprocal regulation of bone and energy metabolism. *Trends in Endocrinology Metabolism* **19** 161-166.

Lee NK, Sowa H, Hinoi E, Ferron M, Ahn JD, Confavreux C, Dacquin R, Mee PJ, McKee MD, Jung DY, Zhang Z, Kim JK, Mauvais-Jarvis F, Ducy P & Karsenty G 2007 Endocrine regulation of energy metabolism by the skeleton. *Cell* **130** 456-469.

Lefebvre V, Garofalo S, Zhou G, Metsaranta M, Vuorio E & de CB 1994 Characterization of primary cultures of chondrocytes from type II collagen/beta-galactosidase transgenic mice. *Matrix Biology* **14** 329-335.

Lefebvre V, Li P & de CB 1998 A new long form of Sox5 (L-Sox5), Sox6 and Sox9 are coexpressed in chondrogenesis and cooperatively activate the type II collagen gene. *EMBO Journal* **17** 5718-5733.

Lewis R, Feetham CH & Barrett-Jolley R 2011 Cell volume regulation in chondrocytes. *Cell Physiology Biochemistry* **28** 1111-1122.

Li S, Crenshaw EB, III, Rawson EJ, Simmons DM, Swanson LW & Rosenfeld MG 1990 Dwarf locus mutants lacking three pituitary cell types result from mutations in the POU-domain gene pit-1. *Nature* **347** 528-533.

Li X, Ominsky MS, Warmington KS, Morony S, Gong J, Cao J, Gao Y, Shalhoub V, Tipton B, Haldankar R, Chen Q, Winters A, Boone T, Geng Z, Niu QT, Ke HZ, Kostenuik PJ, Simonet WS, Lacey DL & Paszty C 2009 Sclerostin antibody treatment increases bone formation, bone mass, and bone strength in a rat model of postmenopausal osteoporosis. *Journal of Bone and Mineral Research* **24** 578-588.

Li X, Warmington KS, Niu QT, Asuncion FJ, Barrero M, Grisanti M, Dwyer D, Stouch B, Thway TM, Stolina M, Ominsky MS, Kostenuik PJ, Simonet WS, Paszty C & Ke HZ 2010 Inhibition of sclerostin by monoclonal antibody increases bone formation, bone mass, and bone strength in aged male rats. *Journal of Bone and Mineral Research* **25** 2647-2656.

Li X, Zhang Y, Kang H, Liu W, Liu P, Zhang J, Harris SE & Wu D 2005 Sclerostin binds to LRP5/6 and antagonizes canonical Wnt signaling. *Journal of Biological Chemistry* **280** 19883-19887.

Liu S, Rowe PS, Vierthaler L, Zhou J & Quarles LD 2007a Phosphorylated acidic serine-aspartate-rich MEPE-associated motif peptide from matrix extracellular phosphoglycoprotein inhibits phosphate regulating gene with homologies to endopeptidases on the X-chromosome enzyme activity. *Journal of Endocrinology* **192** 261-267.

Liu S, Tang W, Zhou J, Vierthaler L & Quarles LD 2007b Distinct roles for intrinsic osteocyte abnormalities and systemic factors in regulation of FGF23 and bone mineralization in Hyp mice. *American Journal of Physiology & Endocrinology Metabolism* **293** E1636-E1644.

Liu S, Zhou J, Tang W, Jiang X, Rowe DW & Quarles LD 2006 Pathogenic role of Fgf23 in Hyp mice. *American Journal of Physiology & Endocrinology Metabolism* **291** E38-E49.

Livak KJ & Schmittgen TD 2001 Analysis of relative gene expression data using real-time quantitative PCR and the 2(-Delta Delta C(T)) Method. *Methods* **25** 402-408.

Lorenz-Depiereux B, Bastepe M, et-Pages A, Amyere M, Wagenstaller J, Muller-Barth U, Badenhoop K, Kaiser SM, Rittmaster RS, Shlossberg AH, Olivares JL, Loris

C, Ramos FJ, Glorieux F, Vikkula M, Juppner H & Strom TM 2006 DMP1 mutations in autosomal recessive hypophosphatemia implicate a bone matrix protein in the regulation of phosphate homeostasis. *Nature Genetics* **38** 1248-1250.

Lu C, Huang S, Miclau T, Helms JA & Colnot C 2004 Mepe is expressed during skeletal development and regeneration. *Histochemistry and Cell Biology* **121** 493-499.

Lui JC & Baron J 2011 Effects of glucocorticoids on the growth plate. *Endocrine Development* **20** 187-193.

MacDougall M, Gu TT, Luan X, Simmons D & Chen J 1998 Identification of a novel isoform of mouse dentin matrix protein 1: spatial expression in mineralized tissues. *Journal of Bone and Mineral Research* **13** 422-431.

Maciejewska I, Cowan C, Svoboda K, Butler WT, D'Souza R & Qin C 2008 The NH2-terminal and COOH-terminal Fragments of Dentin Matrix Protein 1 (DMP1) Localize Differently in the Compartments of Dentin and Growth Plate of Bone. *Journal of Histochemistry and Cytochemistry* **57** 155-166.

Mackenzie NC, Zhu D, Milne EM, van 't HR, Martin A, Quarles DL, Millan JL, Farquharson C & MacRae VE 2012 Altered bone development and an increase in FGF-23 expression in Enpp1(-/-) mice. *PLoS.One.* **7** e32177.

Mackie EJ, Ahmed YA, Tatarczuch L, Chen KS & Mirams M 2008 Endochondral ossification: how cartilage is converted into bone in the developing skeleton. *International Journal of Biochemistry and Cell Biology* **40** 46-62.

Mackie EJ, Tatarczuch L & Mirams M 2011 The growth plate chondrocyte and endochondral ossification. *Journal of Endocrinology*. **211** 109-121.

MacRae VE, Ahmed SF, Mushtaq T & Farquharson C 2007 IGF-I signalling in bone growth: inhibitory actions of dexamethasone and IL-1beta. *Growth Hormone & IGF Research* **17** 435-439.

MacRae VE, Horvat S, Pells SC, Dale H, Collinson RS, Pitsillides AA, Ahmed SF & Farquharson C 2009 Increased bone mass, altered trabecular architecture and modified growth plate organization in the growing skeleton of SOCS2 deficient mice. *Journal of Cell Physiology* **218** 276-284.

Macsai CE, Foster BK & Xian CJ 2008 Roles of Wnt signalling in bone growth, remodelling, skeletal disorders and fracture repair. *Journal of Cell Physiology* **215** 578-587.

Macsai CE, Georgiou KR, Foster BK, Zannettino AC & Xian CJ 2012 Microarray expression analysis of genes and pathways involved in growth plate cartilage injury responses and bony repair. *Bone* **50** 1081-1091.

Magne D, Bluteau G, Faucheux C, Palmer G, Vignes-Colombeix C, Pilet P, Rouillon T, Caverzasio J, Weiss P, Daculsi G & Guicheux J 2003 Phosphate is a specific signal for ATDC5 chondrocyte maturation and apoptosis-associated mineralization: possible implication of apoptosis in the regulation of endochondral ossification. *Journal of Bone and Mineral Research* **18** 1430-1442.

Majeska RJ & Wuthier RE 1975 Studies on matrix vesicles isolated from chick epiphyseal cartilage. Association of pyrophosphatase and ATPase activities with alkaline phosphatase. *Biochimica et Biophysica Acta* **391** 51-60.

Manolagas SC 2000 Birth and death of bone cells: basic regulatory mechanisms and implications for the pathogenesis and treatment of osteoporosis. *Endocrine Reviews* **21** 115-137.

Marks J, Churchill LJ, Debnam ES & Unwin RJ 2008 Matrix extracellular phosphoglycoprotein inhibits phosphate transport. *Journal American Society Nephrology* **19** 2313-2320.

Martin A, David V, Laurence JS, Schwarz PM, Lafer EM, Hedge AM & Rowe PS 2008 Degradation of MEPE, DMP1, and release of SIBLING ASARM-peptides (minhibins): ASARM-peptide(s) are directly responsible for defective mineralization in HYP. *Endocrinology* **149** 1757-1772.

Martin A, Liu S, David V, Li H, Karydis A, Feng JQ & Quarles LD 2011 Bone proteins PHEX and DMP1 regulate fibroblastic growth factor Fgf23 expression in osteocytes through a common pathway involving FGF receptor (FGFR) signaling. *FASEB Journal* **25** 2551-2562.

Mellis DJ, Itzstein C, Helfrich MH & Crockett JC 2011 The skeleton: a multi-functional complex organ: the role of key signalling pathways in osteoclast differentiation and in bone resorption. *Journal of Endocrinology* **211** 131-143.

Melmed S 1999 Insulin-like growth factor I--a prototypic peripheral-paracrine hormone? *Endocrinology* **140** 3879-3880.

Melrose J, Smith SM, Smith MM & Little CB 2008 The use of Histochoice for histological examination of articular and growth plate cartilages, intervertebral disc and meniscus. *Biotechnic and Histochemistry* **83** 47-53.

Meyer JL 1984 Can biological calcification occur in the presence of pyrophosphate? *Archives of Biochemistry and Biophysics* **231** 1-8.

Miao D, Bai X, Panda DK, Karaplis AC, Goltzman D & McKee MD 2004 Cartilage abnormalities are associated with abnormal Phex expression and with altered matrix protein and MMP-9 localization in Hyp mice. *Bone* **34** 638-647.

Minina E, Kreschel C, Naski MC, Ornitz DM & Vortkamp A 2002 Interaction of FGF, Ihh/Pthlh, and BMP signaling integrates chondrocyte proliferation and hypertrophic differentiation. *Development Cell* **3** 439-449.

Minina E, Wenzel HM, Kreschel C, Karp S, Gaffield W, McMahon AP & Vortkamp A 2001 BMP and Ihh/PTHrP signaling interact to coordinate chondrocyte proliferation and differentiation. *Development* **128** 4523-4534.

Morishima A, Grumbach MM, Simpson ER, Fisher C & Qin K 1995 Aromatase deficiency in male and female siblings caused by a novel mutation and the physiological role of estrogens. *Journal of Clinical Endocrinology Metabolism* **80** 3689-3698.

Moss DW, Eaton RH, Smith JK & Whitby LG 1967 Association of inorganic-pyrophosphatase activity with human alkaline-phosphatase preparations. *Biochemical Journal* **102** 53-57.

Murata M, Miyashita S, Yokoo C, Tamai M, Hanada K, Hatayama K, Towatari T, Nikawa T & Katunuma N 1991 Novel epoxysuccinyl peptides. Selective inhibitors of cathepsin B, in vitro. *FEBS Letters* **280** 307-310.

Mushtaq T, Bijman P, Ahmed SF & Farquharson C 2004 Insulin-like growth factor-I augments chondrocyte hypertrophy and reverses glucocorticoid-mediated growth retardation in fetal mice metatarsal cultures. *Endocrinology* **145** 2478-2486.

Nagai H & Aoki M 2002 Inhibition of growth plate angiogenesis and endochondral ossification with diminished expression of MMP-13 in hypertrophic chondrocytes in FGF-2-treated rats. *Journal of Bone & Mineral Metabolism* **20** 142-147.

Nakashima T, Hayashi M, Fukunaga T, Kurata K, Oh-Hora M, Feng JQ, Bonewald LF, Kodama T, Wutz A, Wagner EF, Penninger JM & Takayanagi H 2011 Evidence for osteocyte regulation of bone homeostasis through RANKL expression. *Nature Medicine* **17** 1231-1234.

Nampei A, Hashimoto J, Hayashida K, Tsuboi H, Shi K, Tsuji I, Miyashita H, Yamada T, Matsukawa N, Matsumoto M, Morimoto S, Ogihara T, Ochi T & Yoshikawa H 2004 Matrix extracellular phosphoglycoprotein (MEPE) is highly expressed in osteocytes in human bone. *Journal of Bone & Mineral Metabolism* **22** 176-184.

Narayanan K, Srinivas R, Ramachandran A, Hao J, Quinn B & George A 2001 Differentiation of embryonic mesenchymal cells to odontoblast-like cells by overexpression of dentin matrix protein 1. *Proceedings of the National Academy of Sciences USA* **98** 4516-4521.

Nilsson A, Isgaard J, Lindahl A, Dahlstrom A, Skottner A & Isaksson OG 1986 Regulation by growth hormone of number of chondrocytes containing IGF-I in rat growth plate. *Science* **233** 571-574.

Nilsson O, Marino R, De LF, Phillip M & Baron J 2005 Endocrine regulation of the growth plate. *Hormone Research* **64** 157-165.

Nilsson O, Parker EA, Hegde A, Chau M, Barnes KM & Baron J 2007 Gradients in bone morphogenetic protein-related gene expression across the growth plate. *Journal of Endocrinology* **193** 75-84.

Nurnberg P, Thiele H, Chandler D, Hohne W, Cunningham ML, Ritter H, Leschik G, Uhlmann K, Mischung C, Harrop K, Goldblatt J, Borochowitz ZU, Kotzot D, Westermann F, Mundlos S, Braun HS, Laing N & Tinschert S 2001 Heterozygous mutations in ANKH, the human ortholog of the mouse progressive ankylosis gene, result in craniometaphyseal dysplasia. *Nature Genetics* **28** 37-41.

O'Shea PJ, Harvey CB, Suzuki H, Kaneshige M, Kaneshige K, Cheng SY & Williams GR 2003 A thyrotoxic skeletal phenotype of advanced bone formation in mice with resistance to thyroid hormone. *Molecular Endocrinology* **17** 1410-1424.

Ogbureke KU & Fisher LW 2004 Expression of SIBLINGs and their partner MMPs in salivary glands. *Journal of Dental Research* **83** 664-670.

Ogbureke KU & Fisher LW 2005 Renal expression of SIBLING proteins and their partner matrix metalloproteinases (MMPs). *Kidney International* **68** 155-166.

Ohyama Y, Nifuji A, Maeda Y, Amagasa T & Noda M 2004 Spaciotemporal association and bone morphogenetic protein regulation of sclerostin and osterix expression during embryonic osteogenesis. *Endocrinology* **145** 4685-4692.

Ominsky MS, Vlasseros F, Jolette J, Smith SY, Stouch B, Doellgast G, Gong J, Gao Y, Cao J, Graham K, Tipton B, Cai J, Deshpande R, Zhou L, Hale MD, Lightwood DJ, Henry AJ, Popplewell AG, Moore AR, Robinson MK, Lacey DL, Simonet WS & Paszty C 2010 Two doses of sclerostin antibody in cynomolgus monkeys increases bone formation, bone mineral density, and bone strength. *Journal of Bone and Mineral Research* **25** 948-959.

Orriss IR, Utting JC, Brandao-Burch A, Colston K, Grubb BR, Burnstock G & Arnett TR 2007 Extracellular nucleotides block bone mineralization in vitro: evidence for dual inhibitory mechanisms involving both P2Y2 receptors and pyrophosphate. *Endocrinology* **148** 4208-4216.

Ott SM 2005 Sclerostin and Wnt signaling--the pathway to bone strength. *Journal of Clinical Endocrinology Metabolism* **90** 6741-6743.

Owen HC, Ahmed SF & Farquharson C 2009 Chondrocyte p21(WAF1/CIP1) expression is increased by dexamethasone but does not contribute to dexamethasone-induced growth retardation in vivo. *Calcified Tissue International* **85** 326-334.

Oz OK, Millsaps R, Welch R, Birch J & Zerwekh JE 2001 Expression of aromatase in the human growth plate. *Journal of Molecular Endocrinology* **27** 249-253.

Padhi D, Jang G, Stouch B, Fang L & Posvar E 2011 Single-dose, placebo-controlled, randomized study of AMG 785, a sclerostin monoclonal antibody. *Journal of Bone and Mineral Research* **26** 19-26.

Parker EA, Hegde A, Buckley M, Barnes KM, Baron J & Nilsson O 2007 Spatial and temporal regulation of GH-IGF-related gene expression in growth plate cartilage. *Journal of Endocrinology* **194** 31-40.

Paschalis EP, Jacenko O, Olsen B, deCrombrugghe B & Boskey AL 1996 The role of type X collagen in endochondral ossification as deduced by Fourier transform infrared microscopy analysis. *Connective Tissue Research* **35** 371-377.

Pass C, MacRae VE, Ahmed SF & Farquharson C 2009 Inflammatory cytokines and the GH/IGF-I axis: novel actions on bone growth. *Cell Biochemistry and Function* **27** 119-127.

Petersen DN, Tkalcevic GT, Mansolf AL, Rivera-Gonzalez R & Brown TA 2000 Identification of osteoblast/osteocyte factor 45 (OF45), a bone-specific cDNA encoding an RGD-containing protein that is highly expressed in osteoblasts and osteocytes. *Journal of Biological Chemistry* **275** 36172-36180.

Petersson IF, Boegard T, Svensson B, Heinegard D & Saxne T 1998 Changes in cartilage and bone metabolism identified by serum markers in early osteoarthritis of the knee joint. *British Journal of Rheumatology* **37** 46-50.

Pirotte S, Lamour V, Lambert V, varez Gonzalez ML, Ormenese S, Noel A, Mottet D, Castronovo V & Bellahcene A 2011 Dentin matrix protein 1 induces membrane expression of VE-cadherin on endothelial cells and inhibits VEGF-induced angiogenesis by blocking VEGFR-2 phosphorylation. *Blood* **117** 2515-2526.

Pitsillides AA & Beier F 2011 Cartilage biology in osteoarthritis--lessons from developmental biology. *Nature Reviews Rheumatology* **7** 654-663.

Poole KE, van Bezooijen RL, Loveridge N, Hamersma H, Papapoulos SE, Lowik CW & Reeve J 2005 Sclerostin is a delayed secreted product of osteocytes that inhibits bone formation. *FASEB Journal* **19** 1842-1844.

Power J, Poole KE, van BR, Doube M, Caballero-Alias AM, Lowik C, Papapoulos S, Reeve J & Loveridge N 2010 Sclerostin and the regulation of bone formation: Effects

in hip osteoarthritis and femoral neck fracture. *Journal of Bone & Mineral Research* **25** 1867-1876.

Prideaux M, Loveridge N, Pitsillides AA & Farquharson C 2012 Extracellular Matrix Mineralization Promotes E11/gp38 Glycoprotein Expression and Drives Osteocytic Differentiation. *PLoS One* **7** e36786.

Puchtler H, Meloan SN & Terry MS 1969 On the history and mechanism of alizarin and alizarin red S stains for calcium. *Journal of Histochemistry and Cytochemistry* **17** 110-124.

Qin C, Baba O & Butler WT 2004 Post-translational modifications of sibling proteins and their roles in osteogenesis and dentinogenesis. *Critical Reviews Oral Biology Medicine* **15** 126-136.

Quarles LD 2003 FGF23, PHEX, and MEPE regulation of phosphate homeostasis and skeletal mineralization. *American Journal of Physiology Endocrinology Metabolism* **285** E1-E9.

Roach HI 1997 New aspects of endochondral ossification in the chick: chondrocyte apoptosis, bone formation by former chondrocytes, and acid phosphatase activity in the endochondral bone matrix. *Journal of Bone and Mineral Research* **12** 795-805.

Roach HI & Clarke NM 2000 Physiological cell death of chondrocytes in vivo is not confined to apoptosis. New observations on the mammalian growth plate. *Journal of Bone and Joint Surgery.British Volume* **82** 601-613.

Roberts SJ, Stewart AJ, Sadler PJ & Farquharson C 2004 Human PHOSPHO1 exhibits high specific phosphoethanolamine and phosphocholine phosphatase activities. *Biochemical Journal* **382** 59-65.

Robling AG, Niziolek PJ, Baldridge LA, Condon KW, Allen MR, Alam I, Mantila SM, Gluhak-Heinrich J, Bellido TM, Harris SE & Turner CH 2008 Mechanical stimulation of bone in vivo reduces osteocyte expression of Sost/sclerostin. *Journal of Biological Chemistry* **283** 5866-5875.

Rodriguez L, Cheng Z, Chen TH, Tu C & Chang W 2005 Extracellular calcium and parathyroid hormone-related peptide signaling modulate the pace of growth plate chondrocyte differentiation. *Endocrinology* **146** 4597-4608.

Rohde M & Mayer H 2007 Exocytotic process as a novel model for mineralization by osteoblasts in vitro and in vivo determined by electron microscopic analysis. *Calcified Tissue International* **80** 323-336.

Ronziere MC, Farjanel J, Freyria AM, Hartmann DJ & Herbage D 1997 Analysis of types I, II, III, IX and XI collagens synthesized by fetal bovine chondrocytes in high-density culture. *Osteoarthritis.Cartilage.* **5** 205-214.

Rowe PS 2004 The wrickkened pathways of FGF23, MEPE and PHEX. *Critical Reviews Oral Biology Medicine* **15** 264-281.

Rowe PS 2012a The chicken or the egg: PHEX, FGF23 and SIBLINGs unscrambled. *Cell Biochemistry & Function* **30** 355-375.

Rowe PS, de Zoysa PA, Dong R, Wang HR, White KE, Econs MJ & Oudet CL 2000 MEPE, a new gene expressed in bone marrow and tumors causing osteomalacia. *Genomics* **67** 54-68.

Rowe PS, Garrett IR, Schwarz PM, Carnes DL, Lafer EM, Mundy GR & Gutierrez GE 2005 Surface plasmon resonance (SPR) confirms that MEPE binds to PHEX via the MEPE-ASARM motif: a model for impaired mineralization in X-linked rickets (HYP). *Bone* **36** 33-46.

Rowe PS, Kumagai Y, Gutierrez G, Garrett IR, Blacher R, Rosen D, Cundy J, Navvab S, Chen D, Drezner MK, Quarles LD & Mundy GR 2004 MEPE has the properties of an osteoblastic phosphatonin and minhibin. *Bone* **34** 303-319.

Rowe PS, Matsumoto N, Jo OD, Shih RN, Oconnor J, Roudier MP, Bain S, Liu S, Harrison J & Yanagawa N 2006 Correction of the mineralization defect in hyp mice treated with protease inhibitors CA074 and pepstatin. *Bone* **39** 773-786.

Rubin CT & Lanyon LE 1984 Regulation of bone formation by applied dynamic loads. *Journal of Bone and Joint Surgery* **66** 397-402.

Salmon WD, Jr. & Daughaday WH 1957 A hormonally controlled serum factor which stimulates sulfate incorporation by cartilage in vitro. *Journal of Laboratory Clinical Medicine* **49** 825-836.

Sambrook P, Kelly P & Eisman J 1993 Bone mass and ageing. *Baillieres Clinical Rheumatology* **7** 445-457.

Sanchez C, Deberg MA, Bellahcene A, Castronovo V, Msika P, Delcour JP, Crielaard JM & Henrotin YE 2008 Phenotypic characterization of osteoblasts from the sclerotic zones of osteoarthritic subchondral bone. *Arthritis Rheumatism* **58** 442-455.

Sandell LJ 1994 In situ expression of collagen and proteoglycan genes in notochord and during skeletal development and growth. *Microscopy Research and Technique* **28** 470-482.

Scheven BA & Hamilton NJ 1991 Longitudinal bone growth in vitro: effects of insulin-like growth factor I and growth hormone. *Acta Endocrinology (Copenhagen)* **124** 602-607.

Schwarz RI, Mandell RB & Bissell MJ 1981 Ascorbate induction of collagen synthesis as a means for elucidating a mechanism of quantitative control of tissue-specific function. *Molecular Cell Biology* **1** 843-853.

Semenov M, Tamai K & He X 2005 SOST is a ligand for LRP5/LRP6 and a Wnt signaling inhibitor. *Journal of Biological Chemistry* **280** 26770-26775.

Shao YY, Wang L & Ballock RT 2006 Thyroid hormone and the growth plate. *Reviews Endocrinology Metabolism Disorders* **7** 265-271.

Shapiro IM, Adams CS, Freeman T & Srinivas V 2005 Fate of the hypertrophic chondrocyte: microenvironmental perspectives on apoptosis and survival in the epiphyseal growth plate. *Birth Defects Research C Embryo Today* **75** 330-339.

Shen G 2005 The role of type X collagen in facilitating and regulating endochondral ossification of articular cartilage. *Orthodontic & Craniofacial Research* **8** 11-17.

Shiang R, Thompson LM, Zhu YZ, Church DM, Fielder TJ, Bocian M, Winokur ST & Wasmuth JJ 1994 Mutations in the transmembrane domain of FGFR3 cause the most common genetic form of dwarfism, achondroplasia. *Cell* **78** 335-342.

Shirley DG, Faria NJ, Unwin RJ & Dobbie H 2010 Direct micropuncture evidence that matrix extracellular phosphoglycoprotein inhibits proximal tubular phosphate reabsorption. *Nephrology Dialysis Transplant* **25** 3191-3195.

Shukunami C, Ishizeki K, Atsumi T, Ohta Y, Suzuki F & Hiraki Y 1997 Cellular hypertrophy and calcification of embryonal carcinoma-derived chondrogenic cell line ATDC5 in vitro. *Journal of Bone and Mineral Research* **12** 1174-1188.

Shukunami C, Shigeno C, Atsumi T, Ishizeki K, Suzuki F & Hiraki Y 1996 Chondrogenic differentiation of clonal mouse embryonic cell line ATDC5 in vitro: differentiation-dependent gene expression of parathyroid hormone (PTH)/PTH-related peptide receptor. *Journal of Cell Biology* **133** 457-468.

Siggelkow H, Schmidt E, Hennies B & Hufner M 2004 Evidence of downregulation of matrix extracellular phosphoglycoprotein during terminal differentiation in human osteoblasts. *Bone* **35** 570-576.

Silvestrini G, Ballanti P, Leopizzi M, Sebastiani M, Berni S, Di VM & Bonucci E 2007 Effects of intermittent parathyroid hormone (PTH) administration on SOST mRNA and protein in rat bone. *Journal of Molecular Histology* **38** 261-269.

Sims NA, Clement-Lacroix P, Da PF, Bouali Y, Binart N, Moriggl R, Goffin V, Coschigano K, Gaillard-Kelly M, Kopchick J, Baron R & Kelly PA 2000 Bone homeostasis in growth hormone receptor-null mice is restored by IGF-I but independent of Stat5. *Journal of Clincal Investigations* **106** 1095-1103.

Sinha YN, Salocks CB & Vanderlaan WP 1975 Pituitary and serum concentrations of prolactin and GH in Snell dwarf mice. *Proceedings of the Society for Experimental Biology and Medicine* **150** 207-210.

Sitara D, Razzaque MS, Hesse M, Yoganathan S, Taguchi T, Erben RG, Juppner H & Lanske B 2004 Homozygous ablation of fibroblast growth factor-23 results in hyperphosphatemia and impaired skeletogenesis, and reverses hypophosphatemia in Phex-deficient mice. *Matrix Biology* **23** 421-432.

Skerry TM, Bitensky L, Chayen J & Lanyon LE 1989 Early strain-related changes in enzyme activity in osteocytes following bone loading in vivo. *Journal of Bone and Mineral Research* **4** 783-788.

Smith EP, Boyd J, Frank GR, Takahashi H, Cohen RM, Specker B, Williams TC, Lubahn DB & Korach KS 1994 Estrogen resistance caused by a mutation in the estrogen-receptor gene in a man. *New England Journal of Medicine* **331** 1056-1061.

Sommer B, Bickel M, Hofstetter W & Wetterwald A 1996 Expression of matrix proteins during the development of mineralized tissues. *Bone* **19** 371-380.

Sommerfeldt DW & Rubin CT 2001 Biology of bone and how it orchestrates the form and function of the skeleton. *European Spine Journal* **10 Suppl 2** S86-S95.

Sornson MW, Wu W, Dasen JS, Flynn SE, Norman DJ, O'Connell SM, Gukovsky I, Carriere C, Ryan AK, Miller AP, Zuo L, Gleiberman AS, Andersen B, Beamer WG & Rosenfeld MG 1996 Pituitary lineage determination by the Prophet of Pit-1 homeodomain factor defective in Ames dwarfism. *Nature* **384** 327-333.

Sprowson AP, McCaskie AW & Birch MA 2008 ASARM-truncated MEPE and AC-100 enhance osteogenesis by promoting osteoprogenitor adhesion. *Journal of Orthopaedic Research* **26** 1256-1262.

St-Jacques B, Hammerschmidt M & McMahon AP 1999 Indian hedgehog signaling regulates proliferation and differentiation of chondrocytes and is essential for bone formation. *Genes and Development* **13** 2072-2086.

Staines K, Macrae V & Farquharson C 2012a Cartilage development and degeneration: a Wnt Wnt situation. *Cell Biochemistry and Function* doi: 10.1002/cbf2852.

Staines K, Macrae V & Farquharson C 2012b The importance of the SIBLING family of proteins on skeletal mineralisation and bone remodelling. *Journal of Endocrinology* **214** 241-255.

Staines KA, Mackenzie NC, Clarkin CE, Zelenchuk L, Rowe PS, MacRae VE & Farquharson C 2012c MEPE is a novel regulator of growth plate cartilage mineralization. *Bone* **51** 418-430.

Stevens DA, Hasserjian RP, Robson H, Siebler T, Shalet SM & Williams GR 2000 Thyroid hormones regulate hypertrophic chondrocyte differentiation and expression of parathyroid hormone-related peptide and its receptor during endochondral bone formation. *Journal of Bone and Mineral Research* **15** 2431-2442.

Stewart AJ, Roberts SJ, Seawright E, Davey MG, Fleming RH & Farquharson C 2006 The presence of PHOSPHO1 in matrix vesicles and its developmental expression prior to skeletal mineralization. *Bone* **39** 1000-1007.

Stickens D, Behonick DJ, Ortega N, Heyer B, Hartenstein B, Yu Y, Fosang AJ, Schorpp-Kistner M, Angel P & Werb Z 2004 Altered endochondral bone development in matrix metalloproteinase 13-deficient mice. *Development* **131** 5883-5895.

Sutherland MK, Geoghegan JC, Yu C, Winkler DG & Latham JA 2004 Unique regulation of SOST, the sclerosteosis gene, by BMPs and steroid hormones in human osteoblasts. *Bone* **35** 448-454.

Swingler TE, Wheeler G, Carmont V, Elliott HR, Barter MJ, Abu-Elmagd M, Donell ST, Boot-Handford RP, Hajihosseini MK, Munsterberg A, Dalmay T, Young DA & Clark IM 2012 The expression and function of microRNAs in chondrogenesis and osteoarthritis. *Arthritis and Rheumatism* **64** 1909-1919.

Takigawa M, Tajima K, Pan HO, Enomoto M, Kinoshita A, Suzuki F, Takano Y & Mori Y 1989 Establishment of a clonal human chondrosarcoma cell line with cartilage phenotypes. *Cancer Research* **49** 3996-4002.

Tanaka Y 2012 Intensive treatment and treatment holiday of TNF-inhibitors in rheumatoid arthritis. *Current Opinion in Rheumatology* **24** 319-326.

Temu TM, Wu KY, Gruppuso PA & Phornphutkul C 2010 The mechanism of ascorbic acid-induced differentiation of ATDC5 chondrogenic cells. *American Journal of Physiology & Endocrinology Metabolism* **299** E325-E334.

Terkeltaub R, Rosenbach M, Fong F & Goding J 1994 Causal link between nucleotide pyrophosphohydrolase overactivity and increased intracellular inorganic pyrophosphate generation demonstrated by transfection of cultured fibroblasts and osteoblasts with plasma cell membrane glycoprotein-1. Relevance to calcium pyrophosphate dihydrate deposition disease. *Arthritis and Rheumatism* **37** 934-941.

Toyosawa S, Shintani S, Fujiwara T, Ooshima T, Sato A, Ijuhin N & Komori T 2001 Dentin matrix protein 1 is predominantly expressed in chicken and rat osteocytes but not in osteoblasts. *Journal of Bone and Mineral Research* **16** 2017-2026.

van Bezooijen RL, Bronckers AL, Gortzak RA, Hogendoorn PC, van dW-P, Balemans W, Oostenbroek HJ, Van HW, Hamersma H, Dikkers FG, Hamdy NA,

Papapoulos SE & Lowik CW 2009 Sclerostin in mineralized matrices and van Buchem disease. *Journal of Dental Research* **88** 569-574.

van Bezooijen RL, Roelen BA, Visser A, Wee-Pals L, de WE, Karperien M, Hamersma H, Papapoulos SE, ten DP & Lowik CW 2004 Sclerostin is an osteocyte-expressed negative regulator of bone formation, but not a classical BMP antagonist. *Journal of Experimental Medicine* **199** 805-814.

van Bezooijen RL, Svensson JP, Eefting D, Visser A, van der HG, Karperien M, Quax PH, Vrieling H, Papapoulos SE, ten DP & Lowik CW 2007 Wnt but not BMP signaling is involved in the inhibitory action of sclerostin on BMP-stimulated bone formation. *Journal of Bone and Mineral Research* **22** 19-28.

van der Eerden BC, Karperien M & Wit JM 2003 Systemic and local regulation of the growth plate. *Endocrine Reviews* **24** 782-801.

Van BH 1976 Alkaline phosphatase. I. Kinetics and inhibition by levamisole of purified isoenzymes from humans. *Clinical Chemistry* **22** 972-976.

Vincent C, Findlay DM, Welldon KJ, Wijenayaka AR, Zheng TS, Haynes DR, Fazzalari NL, Evdokiou A & Atkins GJ 2009 Pro-inflammatory cytokines TNF-related weak inducer of apoptosis (TWEAK) and TNFalpha induce the mitogen-activated protein kinase (MAPK)-dependent expression of sclerostin in human osteoblasts. *Journal of Bone and Mineral Research* **24** 1434-1449.

Vortkamp A, Lee K, Lanske B, Segre GV, Kronenberg HM & Tabin CJ 1996 Regulation of rate of cartilage differentiation by Indian hedgehog and PTH-related protein. *Science* **273** 613-622.

Wang H, Kawashima N, Iwata T, Xu J, Takahashi S, Sugiyama T & Suda H 2010a Differentiation of Odontoblasts Is Negatively Regulated by MEPE via Its C-Terminal Fragment. *Biochemical and Biophysical Research Communications*. **398** 406-412.

Wang J, Zhou HY, Salih E, Xu L, Wunderlich L, Gu X, Hofstaetter JG, Torres M & Glimcher MJ 2006 Site-specific in vivo calcification and osteogenesis stimulated by bone sialoprotein. *Calcified Tissue International* **79** 179-189.

Wang L, Shao YY & Ballock RT 2007 Thyroid hormone interacts with the Wnt/beta-catenin signaling pathway in the terminal differentiation of growth plate chondrocytes. *Journal of Bone and Mineral Research* **22** 1988-1995.

Wang L, Shao YY & Ballock RT 2010b Thyroid hormone-mediated growth and differentiation of growth plate chondrocytes involves IGF-1 modulation of beta-catenin signaling. *Journal of Bone and Mineral Research* **25** 1138-1146.

Wang Y, Cheng Z, Elalieh HZ, Nakamura E, Nguyen MT, Mackem S, Clemens TL, Bikle DD & Chang W 2011 IGF-1R signaling in chondrocytes modulates growth

plate development by interacting with the PTHrP/Ihh pathway. *Journal of Bone and Mineral Research* **26** 1437-1446.

Whyte MP 1994 Hypophosphatasia and the role of alkaline phosphatase in skeletal mineralization. *Endocrine Reviews* **15** 439-461.

Wilsman NJ, Farnum CE, Leiferman EM, Fry M & Barreto C 1996 Differential growth by growth plates as a function of multiple parameters of chondrocytic kinetics. *Journal of Orthopaedic Research* **14** 927-936.

Winkler DG, Sutherland MK, Geoghegan JC, Yu C, Hayes T, Skonier JE, Shpektor D, Jonas M, Kovacevich BR, Staehling-Hampton K, Appleby M, Brunkow ME & Latham JA 2003 Osteocyte control of bone formation via sclerostin, a novel BMP antagonist. *EMBO Journal* **22** 6267-6276.

Witte F, Dokas J, Neuendorf F, Mundlos S & Stricker S 2009 Comprehensive expression analysis of all Wnt genes and their major secreted antagonists during mouse limb development and cartilage differentiation. *Gene Expression Patterns* **9** 215-223.

Woo SM, Rosser J, Dusevich V, Kalajzic I & Bonewald LF 2011 Cell line IDG-SW3 replicates osteoblast-to-late-osteocyte differentiation in vitro and accelerates bone formation in vivo. *Journal of Bone and Mineral Research* **26** 2634-2646.

Wu LN, Genge BR, Kang MW, Arsenault AL & Wuthier RE 2002 Changes in phospholipid extractability and composition accompany mineralization of chicken growth plate cartilage matrix vesicles. *Journal of Biological Chemistry* **277** 5126-5133.

Wu LN, Sauer GR, Genge BR & Wuthier RE 1989 Induction of mineral deposition by primary cultures of chicken growth plate chondrocytes in ascorbate-containing media. Evidence of an association between matrix vesicles and collagen. *Journal of Biological Chemistry* **264** 21346-21355.

Xiao ZS, Crenshaw M, Guo R, Nesbitt T, Drezner MK & Quarles LD 1998 Intrinsic mineralization defect in Hyp mouse osteoblasts. *American Journal of Physiology* **275** E700-E708.

Xiong J, Onal M, Jilka RL, Weinstein RS, Manolagas SC & O'Brien CA 2011 Matrix-embedded cells control osteoclast formation. *Nature Medicine* **17** 1235-1241.

Yadav MC, Simao AM, Narisawa S, Huesa C, McKee MD, Farquharson C & Millan JL 2011 Loss of skeletal mineralization by the simultaneous ablation of PHOSPHO1 and alkaline phosphatase function: a unified model of the mechanisms of initiation of skeletal calcification. *Journal of Bone and Mineral Research* **26** 286-297.

Yakar S, Canalis E, Sun H, Mejia W, Kawashima Y, Nasser P, Courtland HW, Williams V, Bouxsein M, Rosen C & Jepsen KJ 2009 Serum IGF-1 determines skeletal

strength by regulating subperiosteal expansion and trait interactions. *Journal of Bone and Mineral Research* **24** 1481-1492.

Yamaguchi A, Komori T & Suda T 2000 Regulation of osteoblast differentiation mediated by bone morphogenetic proteins, hedgehogs, and Cbfa1. *Endocrine Reviews* **21** 393-411.

Yoon BS, Pogue R, Ovchinnikov DA, Yoshii I, Mishina Y, Behringer RR & Lyons KM 2006 BMPs regulate multiple aspects of growth-plate chondrogenesis through opposing actions on FGF pathways. *Development* **133** 4667-4678.

Zelzer E, McLean W, Ng YS, Fukai N, Reginato AM, Lovejoy S, D'Amore PA & Olsen BR 2002 Skeletal defects in VEGF(120/120) mice reveal multiple roles for VEGF in skeletogenesis. *Development* **129** 1893-1904.

Zhang GX, Mizuno M, Tsuji K & Tamura M 2004 Regulation of mRNA expression of matrix extracellular phosphoglycoprotein (MEPE)/ osteoblast/osteocyte factor 45 (OF45) by fibroblast growth factor 2 in cultures of rat bone marrow-derived osteoblastic cells. *Endocrine* **24** 15-24.

Zijlstra A, Aimes RT, Zhu D, Regazzoni K, Kupriyanova T, Seandel M, Deryugina EI & Quigley JP 2004 Collagenolysis-dependent angiogenesis mediated by matrix metalloproteinase-13 (collagenase-3). *Journal of Biological Chemistry* **279** 27633-27645.

Appendix

Appendix I

Cell culture buffers

ATDC5 Maintenance medium

DMEM/F-12 (1:1) with GlutaMAX I, supplemented with 5% foetal bovine serum (FBS), $3x10^{-8}$M sodium selenite, 10µg/ml human transferring, 1mM sodium pyruvate, and 0.05mg/ml gentamicin

ATDC5 Differentiation medium

DMEM/F-12 (1:1) with GlutaMAX I containing 5% FBS, 1X insulin transferrin selenium (ITS), 1mM sodium pyruvate and 0.05mg/ml gentamicin

Freezing mix

60% DMEM/F-12; 20% FBS; 20% DMSO

Primary chondrocyte medium

DMEM; 4.5g/L glucose and L-Glutamine containing 5% FBS and 0.05% gentamicin

IWG-SW3 cell medium

α-MEM with 0.1% gentamicin and 10% FBS

HEK293T medium

DMEM-glutamax with 10% FCS and 1X Non-essential amino acids

In vivo studies

Metatarsal preparation medium

0.8ml αMEM medium (without ribonucleosides), 10.45ml sterile PBS, 22.5mg BSA (Fraction V)

Metatarsal medium

αMEM medium (without ribonucleosides) supplemented with 0.2% BSA (Fraction V); 5μg/ml L-ascorbic acid phosphate; 1mM βGP; 0.05mg/ml gentamicin; 1.25μg/ml fungizone

In situ hybridisation

TE buffer

10mM Tris-Cl; and 1mMS EDTA, pH 7–8

TNE buffer

0.5M NaCl, 0.1M Tris/Cl, pH 7.4 0.2M EDTA

LB media

1% bacto-tryptone, 0.5% bacto-yeast extract, 150mM NaCl, adjusted to pH 7.5

LB agar

LB supplemented with 1.5% bactoagar

TAE

40mM Tris, 1mM EDTA, 0.1 % acetic acid

Qiagen kit buffer compositions

Maxiprep re-suspension buffer P1

50 mM Tris-HCl, pH 8.0; 10 mM EDTA; 100 μg/ml RNase A

Maxiprep bacterial lysis buffer P2

200 mM NaOH, 1% SDS

Maxiprep elution buffer EB

10 mM Tris-HCl, pH 8.5

Maxiprep neutralisation buffer P3

3M potassium acetate, pH 5.5

Maxiprep equilibration buffer QBT

750 mM NaCl; 50 mM 3-[N-morpholino] propanesulfonic acid (MOPS), pH 7.0; 15% isopropanol (v/v); 0.15% Triton X-100 (v/v)

Maxiprep column wash buffer QC

1M NaCl, 50mM MOPS pH7.0, 15% isopropanol (v/v) and 0.15% Triton X-100 (v/v)

Maxiprep elution buffer QN

1.6 M NaCl, 50 mM MOPS, pH 7.0, 15 % isopropanol (v/v)

DNA re-suspension buffer TE

10 mM Tris HCl, pH 8.0, 1 mM EDTA

Immunohistochemistry

10mM Citric acid buffer

1.92g citric acid / L dH_2O at pH 3.0

Viral Transductions

Cell Culture medium

DMEM-Glutamax, 10% Foetal calf serum (FCS), 1X NEAA

TSSM

To make up 1L add 4.84g Trizma base, 11.8g NaCl, 20g sucrose and 20g D-mannitol to 1L sterile H_20, pH to 7.4 and filter

Western Blotting

RIPA buffer

20mM Tris-HCl (pH8), 135mM NaCl, 10% Glycerol, 1% IGEPAL, 0.1% SDS, 0.5% Na Deoxycholate, 2mM EDTA

LDS Sample reducing agent

40% glycerol, 4% LDS, 4% Ficoll*-400, 0.8 M triethanolamine-Cl pH 7.6, 0.025% phenol red, 0.025% coomassie G250, 2mM EDTA disodium

1X Transfer buffer

100ml 10X transfer buffer, 200ml 98% Ethanol, 700ml dH_2O.

10X Transfer buffer

29.3mg/ml glycine, 58mg/ml Tris Base (trismethylamine), 18.8µl/ml 20% SDS in dH_2O

TBS/T

Tris-buffered saline/Tween-20 consisting of 50mM Tris-HCl, 300mM NaCl, 0.1% Tween-20

MOPS running buffer

50 mM MOPS pH 7.7, 50 mM Tris, 0.1% SDS, 1mM EDTA

Appendix II

Gene	Source		Sequence (5'-3')
Mepe	Primer Design	F	AGAAATATCACGCAGCCTGTAA
		R	GGAGACTTTAGCATCATTGACATC
Phex	Primer Design	F	CTAACCACCCACTCCCACTT
		R	CCAATAGACTCCAAACCTGAAGA
Alpl	Primer Design	F	GGGACGAATCTCAGGGTACA
		R	AGTAACTGGGGTCTCTCTCTTT
Phospho1	Primer Design	F	TTCTCATTTCGGATGCCAACA
		R	TGAGGATGCGGCGGAATAA
Ank	Primer Design	F	GATGCCACTAGAGCGAGAAG
		R	TCAGAAGTTACGAGACAAGACC
Enpp1	Primer Design	F	GCTAATCATCAGGAGGTCAAG
		R	GCTAATCATCAGGAGGTCAAG
Mmp13	Primer Design	F	CCAACCCTAAGCATCCCAAA
		R	TCCTCGGAGACTGGTAATGG
Ihh	Primer Design	F	TTCTTCACACGCATTCCATCT
		R	GCCAACAGTAAAGTCACAATCC
PthIh	Primer Design	F	CGGTTTGGGTCAGACGATG
		R	GCTTGCCTTTCTTCTTCTTC
Atf3	Primer Design	F	ACTGGTATTTGAGGATTTTGCTAAC
		R	TGTTGTTGACGGTAACTGACTC
Dmp1	Primer Design	F	ATACCACAATACTGAATCTGAAAGC
		R	CACTATTTGCCTGTCCCTCTG
Cd31	Dr Claire Clarkin	F	GAGCCCAATCACGTTTCAGTT
		R	TCCTTCCTGCTTCTTGCTAGC
Cd34	Dr Claire Clarkin	F	GTTACCTCTGGGATCCCTTCA
		R	GAATAACGTAACCAGTGGAGA
Flk-1	Dr Claire Clarkin	F	TCTGTGGTTCTGCGTGGAGA
		R	GTATCATTTCCAACCAACCCT
VEGF	Dr Claire Clarkin	F	GAAGTCCCATGAAGTGATCCAG
		R	TCACCGCCTTGGCTTGTCA
β-actin	Dr Claire Clarkin	F	ATGAAGTGTGACGTTGACATCCGT
		R	CCTAGAAGCATTTGCGGTGCACGATG

Gene	Source		Sequence (5'-3')
Sost	Applied Biosystems	F	Not available
		R	Not available
Col2a1	MWG Eurofins	F	GTAACCCGTTGAACCCCATT
		R	CCATCCAATCGGTAGTAGCG
Col10a1	MWG Eurofins	F	CATAAAGGGCCCACTTGCTA
		R	CAGGAATGCCTTGTTCTCCT
18S	MWG Eurofins	F	CGGTCCTACGGTGTCAGG
		R	GCAGAGGACATTCCCAGTGT

Appendix III

Primary antibodies

Antibody	Species	Source	Use	Dilution
MEPE-ASARM	Rabbit	Prof. Peter Rowe	Immunohistochemistry	1:200
MEPE mid terminal	Rabbit	Prof. Peter Rowe	Immunohistochemistry	1:200
MEPE	Sheep	R&D	Western Blotting	1:200
Cathepsin B	Goat	R&D	Immunohistochemistry	1:50
Sclerostin	Goat	R&D	Immunohistochemistry	1:100
β-actin (HRP-linked)	Mouse	Sigma	Western Blotting	1:50000

Secondary antibodies

Antibody	Source	Use	Dilution
Rabbit anti-goat	Dako	Western Blotting	1 in 5000
Goat anti-rabbit	Dako	Western Blotting	1 in 5000
Donkey anti-sheep	Abcam	Western Blotting	1 in 5000

Appendix IV

MEPE-overexpressing vector map

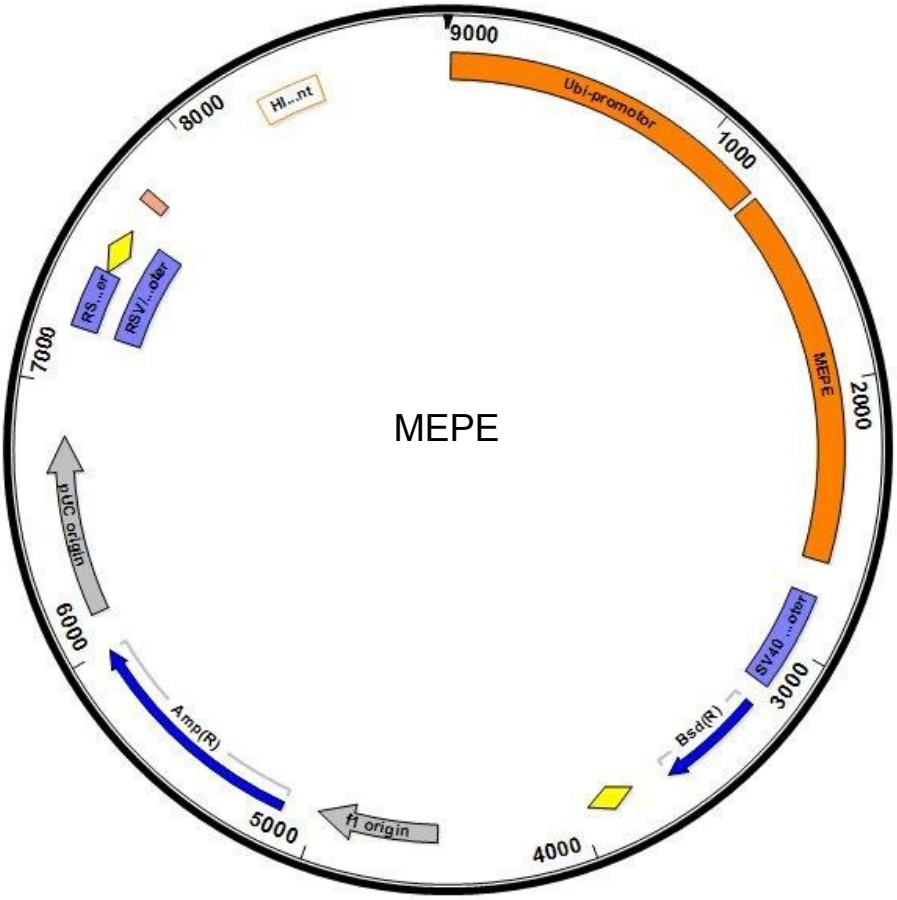

MEPE-shRNA vector map

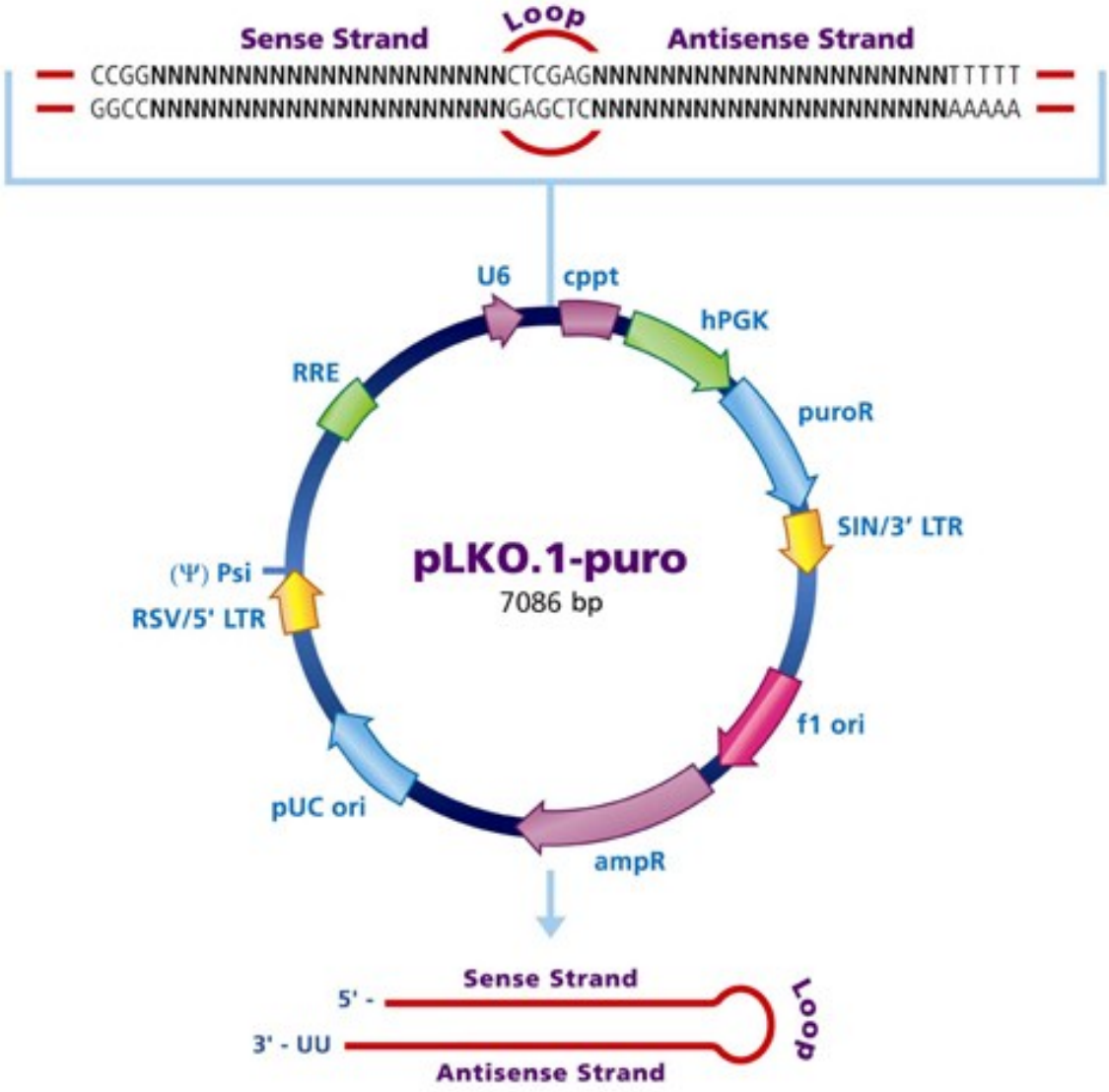

Chondrogenic ATDC5 cells: An optimised model for rapid and physiological matrix mineralisation

P.T. NEWTON[1,2*], K.A. STAINES[1*], L. SPEVAK[3], A.L. BOSKEY[3], C.C. TEIXEIRA[4], V.E. MACRAE[1], A.E. CANFIELD[2] and C. FARQUHARSON[1]

[1]The Roslin Institute and R(D)SVS, University of Edinburgh, Easter Bush, Midlothian EH25 9RG; [2]Wellcome Trust Centre for Cell-Matrix Research and Cardiovascular Research Group, Manchester M13 9PT, UK; [3]Musculoskeletal Integrity Program, Hospital for Special Surgery, New York, NY; [4]Basic Science and Craniofacial Biology, New York University, College of Dentistry, New York, NY, USA

Received July 3, 2012; Accepted August 1, 2012

DOI: 10.3892/ijmm.2012.1114

Abstract. The development of chondrogenic cell lines has led to major advances in the understanding of how chondrocyte differentiation is regulated, and has uncovered many signalling pathways and gene regulatory mechanisms required to maintain normal function. ATDC5 cells are a well established *in vitro* model of endochondral ossification; however, current methods are limited for mineralisation studies. In this study we demonstrate that culturing cells in the presence of ascorbic acid and 10 mM β-glycerophosphate (βGP) significantly increases the rate of extracellular matrix (ECM) synthesis and reduces the time required for mineral deposition to occur to 15 days of culture. Furthermore, the specific expression patterns of *Col2a1* and *Col10a1* are indicative of ATDC5 chondrogenic differentiation. Fourier transform-infrared spectroscopy analysis and transmission electron microscopy (TEM) showed that the mineral formed by ATDC5 cultures is similar to physiological hydroxyapatite. Additionally, we demonstrated that in cultures with βGP, the presence of alkaline phosphatase (ALP) is required for this mineralisation to occur, further indicating that chondrogenic differentiation is required for ECM mineralisation. Together, these results demonstrate that when cultured in the presence of ascorbic acid and 10 mM βGP, ATDC5 cells undergo chondrogenic differentiation and produce a physiological mineralised ECM from Day 15 of culture onwards. The rapid and novel method for ATDC5 culture described in this study is a major improvement compared with currently published methods and this will prove vital in the pursuit of underpinning the molecular mechanisms responsible for poor linear bone growth observed in a number of chronic diseases such as cystic fibrosis, chronic kidney disease, rheumatological conditions and inflammatory bowel disease.

Correspondence to: Katherine Ann Staines, The Roslin Institute and R(D)SVS, University of Edinburgh, Easter Bush, Midlothian EH25 9RG, UK
E-mail: katherine.staines@roslin.ed.ac.uk

*Contributed equally

Key words: ATDC5, chondrocyte, mineralisation, β-glycerophosphate, endochondral ossification, growth plate

Introduction

The growth plate and its primary cell type, the chondrocyte, are integral to endochondral ossification and thus the linear growth of the long bones (1). The continuing development of *in vitro* chondrocyte cell lines has furthered our understanding of the underlying mechanisms of endochondral ossification.

The ATDC5 cell line, which was first isolated from the differentiating teratocarcinoma stem cell line AT805, is commonly used as a model for *in vitro* chondrocyte research (2). To date, the ATDC5 cell line has been utilised in approximately 300 studies. Previous studies have detailed a well-characterised method of ATDC5 differentiation and mineralisation, initially by Shukunami *et al* (3). This method has provided a reliable model of *in vitro* chondrocyte mineralisation for a number of years and has been widely used in the field since its publication; however it does contain some drawbacks. For example, mineralisation studies require a culture time of at least 34 days and a change of culture conditions. Both the cell culture medium and the CO_2 concentration have to be altered after 21 days of culture to facilitate extracellular matrix (ECM) mineralisation 13 days later. Since its publication, a number of groups have attempted to simplify the culture method. For example, the addition of inorganic phosphate to ATDC5 cultures has been shown to increase differentiation and the rate of ECM mineralisation (4,5). Another study has detailed that the addition of ascorbic acid shortened the proliferation phase of the ATDC5 cells from 21 to 7 days (6); while the temporal expression of markers of chondrogenic differentiation was examined, the ECM mineralisation capability of the ATDC5 cells under these culture conditions was not.

Therefore, our aim was to develop a culture model for ATDC5 cells which produced both consistent chondrogenesis

and physiological ECM mineralisation in a reduced time period for *in vitro* experimentation. In this study, β-glycerophosphate (βGP) was added throughout the culture period. βGP is cleaved by alkaline phosphatase (ALP) and other phosphohydrolases produced by the chondrocytes once they have reached hypertrophy to release inorganic phosphate, thus mimicking the phosphate availability *in vivo* (3,7,8). It was hypothesised that this strategy would facilitate an incremental increase in mineral deposition once an appropriate ECM had been deposited. This would thereby increase the rate of mineralisation compared with previous methods while retaining the expected stages of chondrogenic differentiation as well as crucially, the formation of physiological mineral.

Materials and methods

Cell culture. Chondrogenic ATDC5 cells (Riken Cell Bank, Ibaraki, Japan) (3) were cultured in a differentiation medium [DMEM/F-12 (1:1) with GlutaMAX I containing 5% FBS, 1% insulin transferrin and selenium, 1% sodium pyruvate and 0.5% gentamicin (Invitrogen, Paisley, UK)] at a density of 6,000 cells/cm^2 in multi-well plates (Iwaki Cell Biology; Sterilin, Feltham, UK) (9,10). Cells were left for 6 days to reach confluency at which point the medium was supplemented with 10 mM βGP and 50 μg/ml L-ascorbate-2-phosphate (ascorbic acid). Cells were incubated in a humidified atmosphere (37˚C, 5% CO_2) for up to 41 days and the medium was changed every second or third day. For levamisole experiments, ATDC5 cells were cultured in varying concentrations of levamisole (Sigma, Gillingham, UK) (0-1,000 μM) for up to 15 days.

Histochemical staining. Calcium deposition in ATDC5 cells was evaluated by Alizarin red staining as described previously (11). Briefly, cells were fixed in 4% paraformaldehyde and then 2% Alizarin red (Sigma, pH 4.2) was added to the cell layers for 5 min at room temperature. Cells were washed with distilled water (dH_20) and images were captured. Alizarin red-stained cultures were extracted with 10% cetylpyridinium chloride for 10 min and the optical density (OD) of the digests was measured at 570 nm by spectrophotometry (Multiskan Ascent; Thermo Electron Corporation, Vantaa, Finland). Proteoglycan synthesis was evaluated by staining the cell layers with Alcian blue (Sigma). Cells were fixed in 95% methanol for 20 min and stained with 1% Alcian blue 8GX in 0.1 M HCl overnight. Cells were washed in dH_20 and images were captured. Alcian blue-stained cultures were extracted with 6 M guanidine-HCl for 6 h at room temperature and the OD was determined at 630 nm by spectrophotometry (11).

Real-time quantitative PCR (qRT-PCR). RNA was extracted using the RNeasy Mini kit (Qiagen Ltd., Crawley, West Sussex, UK), according to the manufacturer's instructions. For each sample, total RNA content was assessed by absorbance at 260 nm and purity by A260/A280 ratios, and then reverse-transcribed. cDNA was diluted to 10 ng/μl in nuclease-free water (Sigma), and stored at -20˚C. qRT-PCR reactions were conducted with a MX3000P qPCR machine (Stratagene, Stockport, UK) using a SYBR-Green detection method. Primers were designed in-house and synthesised by MWG Eurofins, London, UK. Reactions were run in triplicate and routinely normalised against GAPDH. Primer sequences: *Col2a1*, forward, 5'-CGGTCCTACGGTGTCAGG-3' and reverse, 5'-GCAGAGGACATTCCCAGTGT-3'; *Col10a1*, forward, 5'-CATAAAGGGCCCACTTGCTA-3' and reverse,5'-CAGGAATGCCTTGTTCTCCT-3'; GAPDH forward, 5'-TGAGGCCGGTGCTGAGTATGTCG-3' and reverse, 5'-CCACAGTCTTCTGGGTGGCAGTG-3'. qRT-PCR products were sequenced by the GenePool, University of Edinburgh.

Transmission electron microscopy (TEM). ATDC5 cells were cultured at 6,000 cells/cm^2 on nitrocellulose discs (Nunc, Roskilde, Denmark) in mineralising conditions for 15 days. Cells were fixed in 2.5% glutaraldehyde in 0.1 M sodium cacodylate buffer at 37˚C for 1 h. During processing, the cell monolayers were washed in 0.1 M sodium cacodylate, post-fixed in 1% osmium tetroxide and dehydrated through graded alcohols (35, 70, 95 and 100%). The monolayers were then processed to Epon in a vacuum oven at 60˚C. Monolayers were viewed using a Phillips CMIRO TEM (FEI Vic Ltd., Cambridge, UK) and images were captured on Gatan Orius ICD camera (Gatan, Oxford, UK).

Fourier transform-infrared spectroscopy (FTIR). ATDC5 cells were cultured for 41 days in mineralising conditions as previously described. Cell monolayers were fixed in 95% methanol and embedded in LR White. Spectral images of 2 μm-thick culture sections were collected using a Spectrum Spotlight 100 system (Perkin-Elmer, Waltham, MA, USA) with a spectral resolution of 4 μm and 6.25 μm pixel size in transmission mode. The collected spectra were truncated, base-lined and the contribution of LR White was spectrally subtracted using ISYS software (Spectral Dimensions, Olney, MD, USA) and then analysed using ISys Chemical Imaging software. Spectra extracted from these images were analysed using Grams/32 software (Thermo Electron Corporation, Waltham, MA, USA). The parameters measured included mineral/matrix ratio, carbonate/phosphate ratio, crystallinity and collagen maturity (12).

Statistics. Data were analysed by one-way analysis of variance (ANOVA), with Tukey simultaneous tests used to identify differences between individual time-points, using SigmaPlot 11.0 software (Systat Software UK Ltd., London, UK). Cell culture experiments were repeated at least twice and $P<0.05$ was considered statistically significant.

Results

ATDC5 cells undergo the expected stages of chondrocyte differentiation. Images collected by light microscopy over a 34-day time-course indicated comparable differentiation to previously characterised ATDC5 cultures (3,4). ATDC5 cell cultures reached confluency 6 days after seeding with no extensive ECM formation (Fig. 1A). At this point, ATDC5 cells were then cultured in the presence of 10 mM βGP and 50 μg/ml ascorbic acid. This facilitates cell differentiation and the secretion of an extensive ECM which assembles around the cells as visualised at Day 13 of culture by the

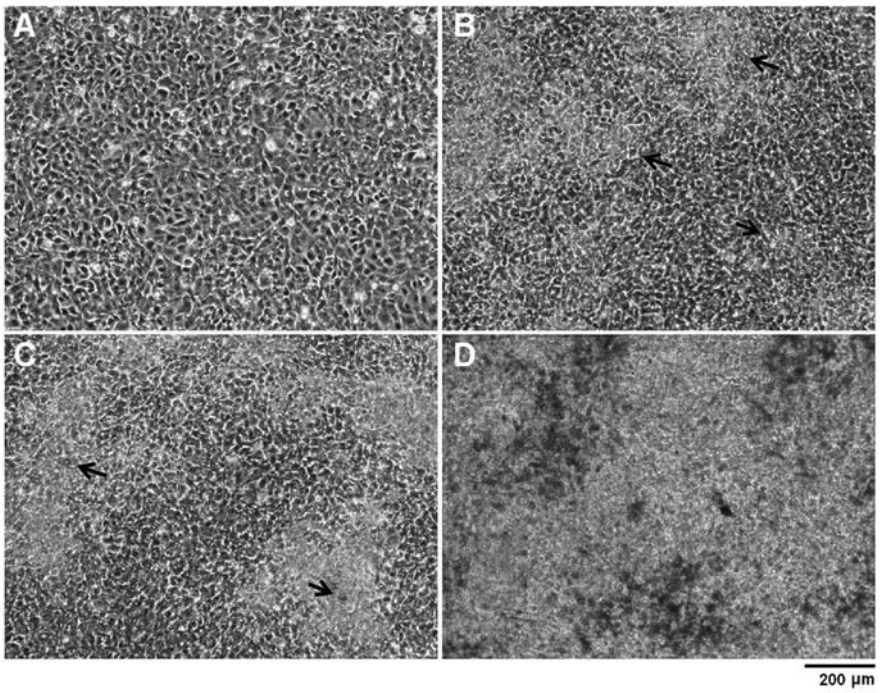

Figure 1. Chondrogenic differentiation of ATDC5 cells. ATDC5 cells were grown over a period of 34 days and light microscopy images were collected during this time period. (A) Image captured at confluence, Day 6 of culture. (B) Arrows indicate translucent ECM which begins to form in discrete locations at Day 13 of culture. (C) The arrows denote opaque regions which represent the onset of mineralisation within the ECM at Day 14. (D) The nodules of ECM conjoin over the ECM and mineralisation increases.

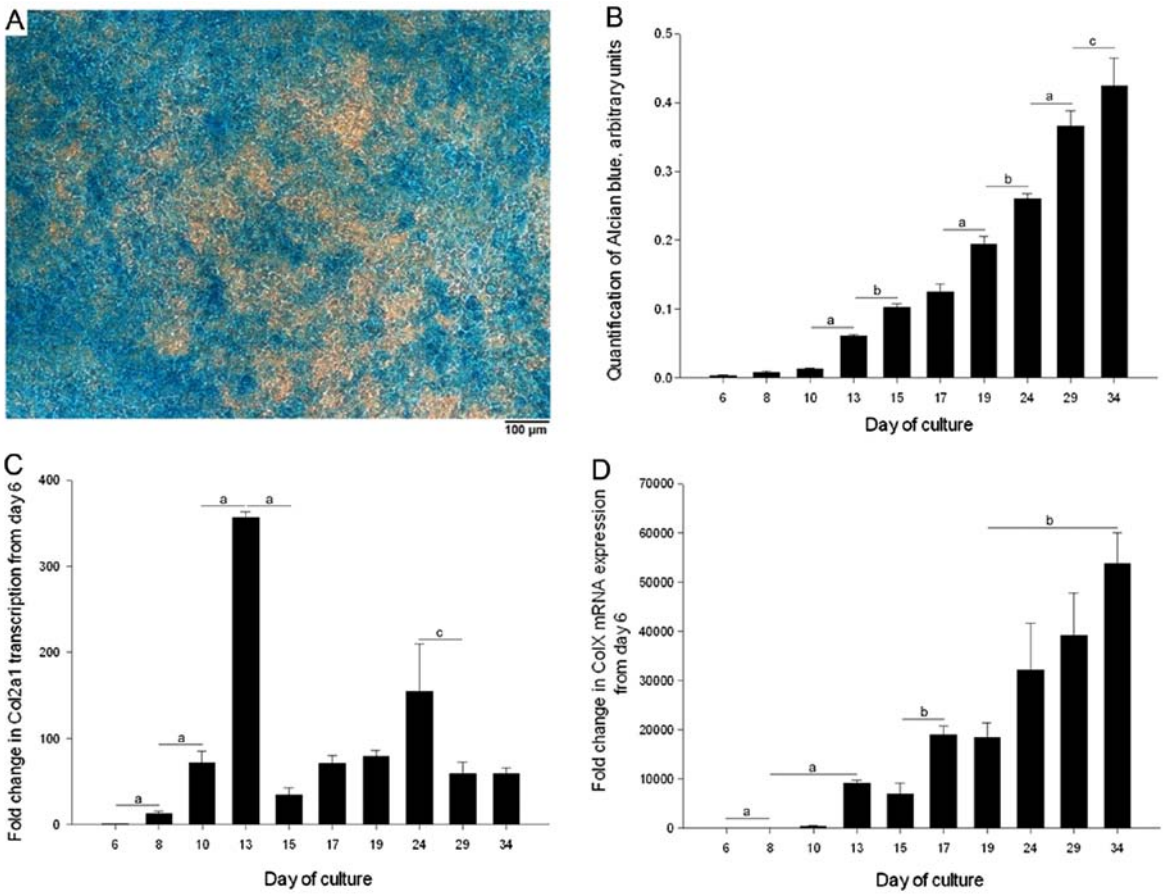

Figure 2. Chondrocyte marker analysis during ATDC5 cell differentiation. (A) The monolayer was fixed following 34 days of culture and stained for GAG using Alcian blue. (B) Quantification of Alcian blue staining was conducted over 10 time-points. (C) qRT-PCR analysis of *Col2a1* and (D) qRT-PCR analysis of *Col10a1* transcription, normalised to GAPDH, over 10 time-points in the ATDC5 monolayers. Mean (n=3) ± SEM, with the exception of *Col10a1* at Day 10 where n=2; [a]P<0.05; [b]P<0.01; [c]P<0.001, where all significant differences between consecutive time-points are shown.

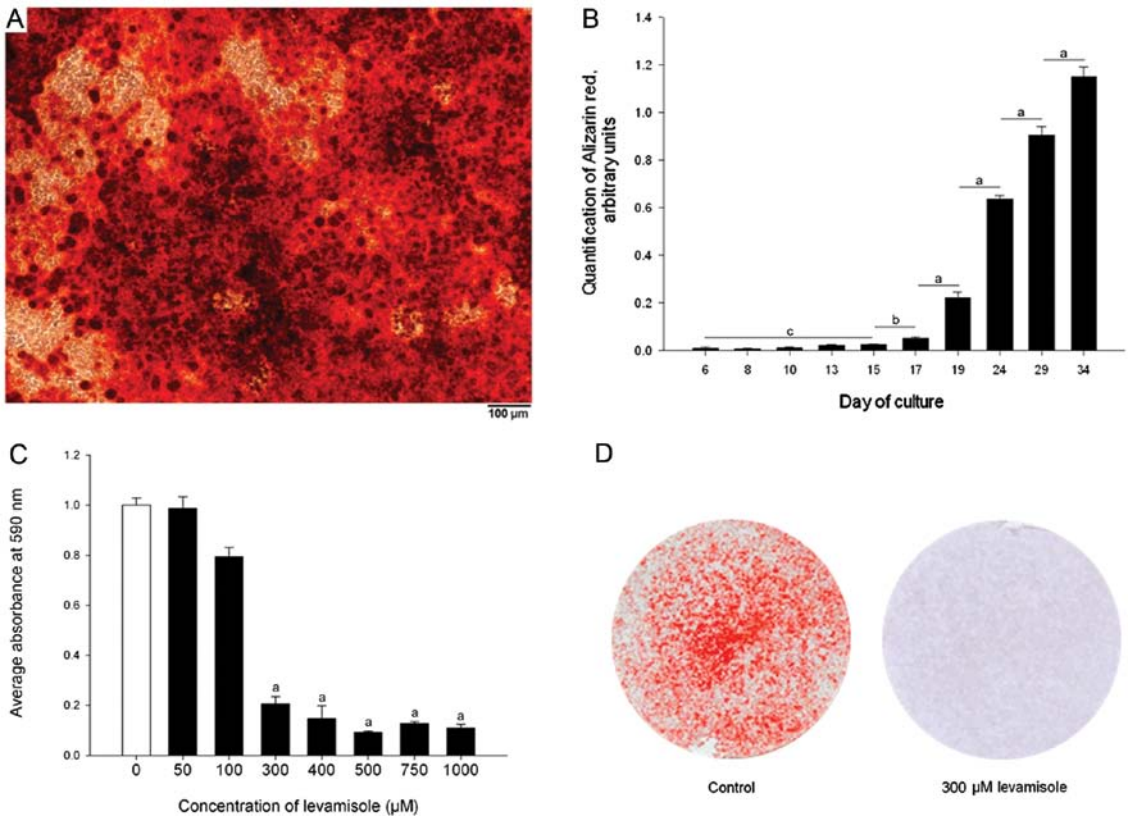

Figure 3. ATDC5 cell ECM mineralisation. (A) Mineralisation was examined by Alizarin red staining of monolayers fixed at Day 34 of culture. (B) Quantification of Alizarin red staining was conducted over 10 time-points. Mean (n=3) ± SEM; [a]P<0.05; [b]P<0.01; [c]P<0.001, where all significant differences between consecutive time-points are shown. (C) Levamisole, an inhibitor of ALP enzyme activity, was added to ATDC5 cell cultures from when they reached confluency. Levamisole dose-dependently inhibited ATDC5 ECM mineralisation as indicated by quantification of Alizarin red staining. (D) Alizarin red stained images of the control cells and cells treated with 300 μM levamisole at Day 15 of culture. Data are represented as the means ± SEM (n=3 replicates) in comparison to 0 μM levamisole [c]P<0.001.

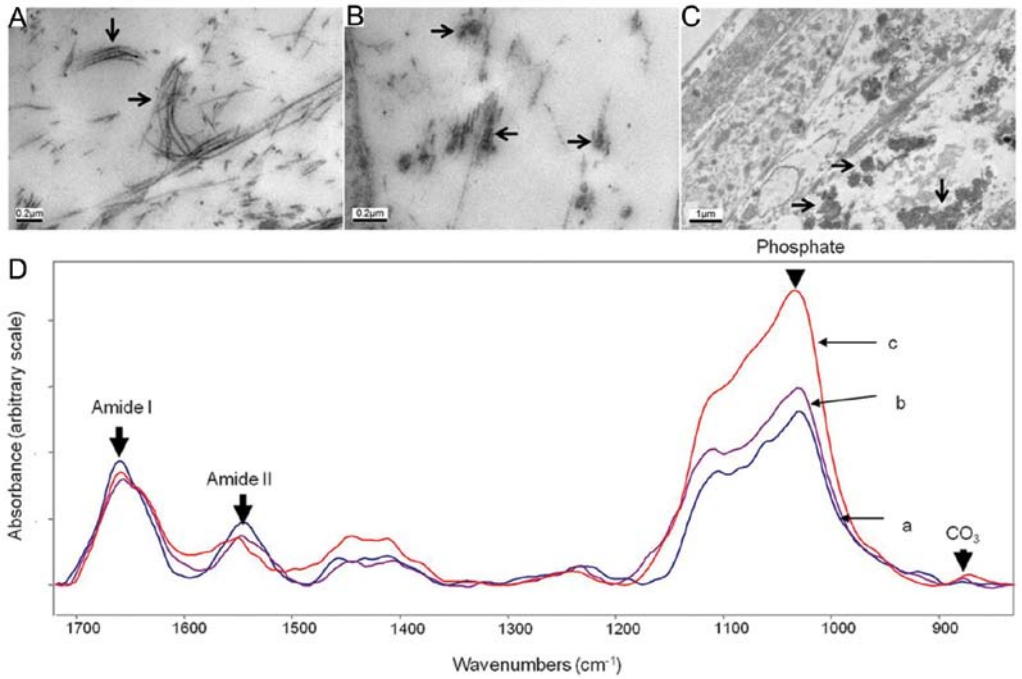

Figure 4. Analysis of ATDC5 mineral deposition. TEM images of ATDC5 cultures at Day 16 of culture. (A) Collagen fibers are present in the ECM; arrows denote collagen fibers. (B) Mineral deposition is noted along collagen fibers; arrows indicate an electron-dense material, likely to be mineralisation spreading along the collagen fibers within the ECM. (C) Mineral deposition within the ECM; arrows indicate electron-dense mineralised regions of the ECM. (D) FTIR analysis of (a) ATDC5 monolayer at 41 days of culture; (b) mineralised embryonic mouse bone at E14; (c) cortical bone from the tibia of a 4-month-old mouse. Absorbances of the phosphate peaks (900-1200 cm^{-1}), which represents mineralisation and the amide-I peak (1585-1725 cm^{-1}), which indicates protein, were used to estimate the mineral-to-matrix ratio of the mineralised ECM. Absorbance values for each plot are arbitrary and not to scale.

Table I. Mineralisation parameters from FTIR samples.

Sample	Mineral-to-matrix ratio	Carbonate-to-mineral ratio	Crystallinity
A	3.000±0.917	0.008±0.005	1.128±0.009
B	2.200±2.500	0.005±0.002	1.072±0.062
C	6.500±0.900	0.006±0.001	1.130±0.030

Using peak areas from FTIR spectra, the mineral-to-matrix ratio (900-1,200 cm^{-1}/1,585-1,725 cm^{-1}), carbonate-to-mineral ratio (850-950 cm^{-1}/900-1,200 cm^{-1}) and crystallinity (1,030 cm^{-1}/1,020 cm^{-1}) were calculated for mineralised regions of (A) ATDC5 monolayer grown to 41 days of culture, (B) mineralised E14 mouse bone and (C) ortical bone from the tibia of a 4-month-old mouse.

phase contrast images (Fig. 1B) and by Alcian blue staining (data not shown). As differentiation continues, these nodules increased in area and began to conjoin (Fig. 1C). A large proportion of each ATDC5 monolayer was Alcian blue-positive by Day 34 of culture, indicating that ATDC5 cells produced a glycosaminoglycan (GAG)-rich ECM and underwent chondrogenesis (Fig. 2A). The temporal increase in GAG-deposition over a 34-day time-course was established by quantifying Alcian blue staining (Fig. 2B). GAG-deposition progressively increased from Day 6, such that there were significant increases in Alcian blue staining between various time-points within the culture period.

To examine the process of chondrogenesis and hypertrophic differentiation of the ATDC5 cells during monolayer culture, *Col2a1* and *Col10a1* gene transcription at specific time-points was analysed by qRT-PCR. *Col2a1* transcription increased significantly between each time-point from Day 6 to 13; transcription then decreased but even at Day 34, transcription was greater compared to Day 6 (by >58-fold, $P<0.001$) (Fig. 2C). *Col10a1* transcription also increased significantly over the first 4 time-points up to Day 13 over a 10,000-fold range, which by Day 34 progressed to a greater than 50,000-fold increase in transcription compared to that of Day 6 (Fig. 2D).

ATDC5 cells mineralise their surrounding ECM, producing physiological mineral. Phase contrast images indicated mineralisation of the ATDC5 ECM from Day 14 onwards and this was confirmed by Alizarin red staining over a 34-day time-course (Fig. 1C and D, Fig. 3A and B). Quantification of this staining indicated that after an initial delay, presumably while early differentiation stages were occurring, calcium accumulation increased rapidly from Day 17 to 34 (Fig. 3B) ($P<0.001$).

Levamisole, a well established inhibitor of ALP, inhibited ATDC5 ECM mineralisation at Day 15 of culture at concentrations in excess of 300 μM ($P<0.001$) (Fig. 3C) with no apparent alterations in the morphology of the ATDC5 cells (Fig. 3D) (13). This indicated that the enzyme ALP is required, and therefore that chondrogenic differentiation of the ATDC5 cells is necessary for effective mineralisation.

FTIR and TEM were adopted as two well recognised methods to determine whether the properties of the mineral formed in culture is similar to that which is formed by mineralised cartilage *in vivo* (14). ATDC5 cells were shown to produce a collagenous ECM by TEM in which banded fibers, synonymous with collagen fibers, were present in the ECM (Fig. 4A) (15). Along some of the collagen fibers, electron-dense regions were present, indicative of the onset of mineralisation (Fig. 4B). In some discrete regions of the ECM, electron-dense spheres of ~200-500 nm were present which were also associated with the collagenous fibers (Fig. 4C); these are possibly mineralised matrix vesicles (MVs) (1,8,9). These results suggest that ATDC5 cells produce a collagenous ECM and that the mineral formed is in alignment with the collagen fibrils, as is observed in endochondral ossification. ATDC5 cells were cultured for 41 days for FTIR analysis (Fig. 4D-a). The FTIR spectra were compared with those of E14 embryonic mouse bone (Fig. 4D-b) and 4-month-old cortical mouse bone (Fig. 4D-c), and were used to generate numerical parameters which may be compared with *in vivo* samples (Table I). The resulting data strongly suggest that the mineralisation of the ATDC5 monolayers resembles that of embryonic mouse bone.

Discussion

Attempts to unravel the underlying mechanisms of endochondral ossification have been limited by current models. The data presented in this manuscript characterise a novel, rapid culture method for studying physiological chondrocyte ECM mineralisation using ATDC5 cells that we observed to be highly reproducible. A mineralisation method for ATDC5 cell culture was first described by Shukunami *et al* (3), however its drawbacks have been identified by several other groups and thus the method has been gradually developed with time. In this study, we cultured ATDC5 cells in the presence of ascorbic acid and 10 mM βGP.

ATDC5 cells have previously been cultured with ascorbic acid, which facilitates collagen synthesis. This reduces the proliferation phase of the cells and promotes their differentiation (6,16). Ascorbic acid has also been shown to promote the hypertrophic differentiation of cultured primary chick chondrocytes (17). In the present study, cells were cultured in the presence of 50 μg/ml ascorbic acid from when they reached confluency and in concurrence with previous studies, this promoted ECM formation. The increased mRNA expression of the chondrogenic marker *Col2a1* correlated with the onset of Alcian blue-stained cartilaginous nodules and the increased mRNA expression of *Col10a1* with the differentiation of the cells to a hypertrophic phenotype. The delayed onset of *Col10a1* transcription at Day 10 is consistent with the 2 stages of differentiation that must occur from Day 6 for the cells to become hypertrophic. The observation that *Col10a1*

expression preceded the first observations of mineral formation provides further evidence that the model is able to mimic the *in vivo* endochondral ossification. During differentiation the histology of the cultures was similar to that described by Shukunami *et al* (3).

In addition to ascorbic acid, an exogenous phosphate source is routinely added to cell cultures to induce and stimulate mineralisation of the ECM. βGP is a preferential exogenous organic phosphate source as it is a substrate for ALP and therefore the cells directly dictate when it is cleaved to release inorganic phosphate with their differentiation to a hypertrophic phenotype. In this study we cultured ATDC5 cells in the presence of 10 mM βGP and observed mineral formation from Day 15 of culture upon collagen fibrils and within MVs. However, in a number of osteoblast and chondrocyte cultures, the growth of cells in the presence of βGP has been shown to lead to the formation of sporadic mineral formation on the cell surface and in the culture medium and not upon collagen fibrils which is regarded to be dystrophic mineralisation and not physiological hydroxyapatite (18,19).

In the present study we showed that the presence of ALP is necessary for βGP-induced ATDC5 mineralisation. This is consistent with previous studies in which the activity of ALP has been investigated in ATDC5 cells (3). Furthermore, the addition of levamisole, a potent inhibitor of ALP, to ATDC5 cultures inhibited their ECM mineralisation. Mineralisation was also inhibited in cells cultured in the presence of βGP and in the absence of insulin, which is required for their differentiation (data not shown) (20). This result, therefore, suggests that mineral formation is dependent upon both chondrogenic differentiation and the subsequent presence of ALP. Additionally, the inhibition of ECM mineralisation when ATDC5 cells were cultured without insulin further emphasises that the mineral formed is not dystrophic and is dependent on their differentiation status.

Although routinely used as indicators of mineralisation, Alizarin red and von Kossa staining are not sufficient to conclude that mineralisation is physiological since the presence of calcium and/or phosphate does not indicate HA formation *per se* (21). For this reason, we adopted FTIR and TEM to examine whether or not the mineral formed in culture is physiological (14).

Shukunami *et al* (3) have previously used TEM for ATDC5 analysis and reported the presence of extremely dark calcium-containing spherites which they identified as mineralised MVs in discrete regions between the cells, associated with collagenous fibers. In the present study, structures were noted in our TEM analysis which were indistinguishable in shape and size from those reported by Shukunami *et al* (3). The MVs derived from ATDC5 cells are of a similar size and appearance to MVs derived from *in vivo* tissues including chicken growth plate chondrocytes and rat epiphyseal hypertrophic chondrocytes (22). These results indicate that the ultrastructure of the collagenous fibrils appears as expected and that mineralisation of ATDC5 cultures appears to form in a physiological manner.

Furthermore, in this study we showed that the spectra of the ATDC5 monolayer more closely resembled that of the developing embryonic bone compared to the fully developed cortical bone. The mineral-to-matrix ratio of the ATDC5 cultures, a key determinant of mineral composition is similar to the values for mineralised embryonic bone, E14, which is the earliest point at which mineralisation occurs in the mouse (23). The mineral-matrix ratios in other publications provide additional comparisons: in 10-day-old and 10-week-old wild-type mouse calcified growth plate cartilage the ratios have been calculated as 2.7 and 5.48, respectively (24,25). There is a considerable variation in these parameters, but the mineral-matrix ratio within the ATDC5 monolayer is within the expected region. The ATDC5 monolayer model characterised by Shukunami *et al* (3) was analysed by FTIR and spectra were compared with those of cultured primary rabbit chondrocytes, resulting in spectra which were almost super-imposable. These spectra show that the absorbance is greater in the amide-range compared to the phosphate-range, thus although the mineral-to matrix ratio is not provided, it is certainly less than those reported in the present study. Therefore, ECM mineralisation is greater in this ATDC5 model compared to the method generated by Shukunami *et al* (3). If mineralisation in the cultures is ectopic and mineral is accumulated simply due to ALP cleavage of βGP, the ratio of mineral-to-matrix would be expected to be extremely high, which is not the case. A study by Huitema *et al* (26), demonstrated this; inorganic phosphate was added to medium conditioned by ATDC5 cells which generated flat, mineralised structures, with extremely small amide-I peaks, relative to phosphate peaks.

The mineralised product of the ATDC5 monolayer produced a phosphate peak with a clear shoulder at approximately 1,130 cm^{-1}. This is characteristic of the hydroxyapatite containing acid phosphate which is gradually lost as the crystal matures; thus both the ATDC5 monolayer and the embryonic bone contain this peak, which is absent in the mature hydroxyapatite sample (27,28). The values obtained from the carbonate substitution and crystallinity are within the range of biologically relevant *in vivo* samples, which also indicates that this ATDC5 model generates physiologically relevant mineral (24,29).

The development and characterisation of a rapidly mineralising chondrocyte model has the potential to assist us in better understanding the underpinning molecular mechanisms responsible for poor linear bone growth which is observed in a number of chronic diseases such as cystic fibrosis, chronic kidney disease, rheumatological conditions and inflammatory bowel disease. Chondrocyte models, including the ATDC5 cell line, have proved invaluable for determining the effects of pro-inflammatory cytokines and glucocorticoids on chondrocyte proliferation, differentiation and gene expression (9,10). However, the absence of a practical and accessible *in vitro* chondrocyte mineralisation model has hindered a fuller appreciation of how cartilage mineralisation and endochondral ossification are disrupted by factors e.g. cytokines and drugs, that are responsible for impaired linear bone growth in children.

In conclusion, in this study we developed and characterised an improved and rapid method of ATDC5 differentiation which develops a physiologic mineralised ECM 15 days after seeding. To our knowledge, this is the earliest report of mineralisation in which physiological attributes of the mineral have been characterised.

Acknowledgements

The authors thank Steve Mitchell, University of Edinburgh, for assisting with the TEM technique. This project was funded by the Biotechnology and Biological Sciences Research Council (BBSRC), a scholarship award from the UK (P.N. and K.S.), the Institute Strategic Programme Grant Funding (C.F. and V.M.) and the Institute Career Path Fellowship Funding (V.M.). A.B. and L.S. received funding from NIH grant AR046121.

References

1. Kronenberg HM: Developmental regulation of the growth plate. Nature 423: 332-336, 2003.
2. Atsumi T, Miwa Y, Kimata K and Ikawa Y: A chondrogenic cell line derived from a differentiating culture of AT805 teratocarcinoma cells. Cell Differ Dev 30: 109-116, 1990.
3. Shukunami C, Ishizeki K, Atsumi T, Ohta Y, Suzuki F and Hiraki Y: Cellular hypertrophy and calcification of embryonal carcinoma-derived chondrogenic cell line ATDC5 in vitro. J Bone Miner Res 12: 1174-1188, 1997.
4. Magne D, Bluteau G, Faucheux C, Palmer G, Vignes-Colombeix C, Pilet P, Rouillon T, Caverzasio J, Weiss P, Daculsi G and Guicheux J: Phosphate is a specific signal for ATDC5 chondrocyte maturation and apoptosis-associated mineralization: possible implication of apoptosis in the regulation of endochondral ossification. J Bone Miner Res 18: 1430-1442, 2003.
5. Fujita T, Meguro T, Izumo N, Yasutomi C, Fukuyama R, Nakamuta H and Koida M: Phosphate stimulates differentiation and mineralization of the chondroprogenitor clone ATDC5. Jpn J Pharmacol 85: 278-281, 2001.
6. Altaf FM, Hering TM, Kazmi NH, Yoo JU and Johnstone B: Ascorbate-enhanced chondrogenesis of ATDC5 cells. Eur Cell Mater 12: 64-70, 2006.
7. Coe MR, Summers TA, Parsons SJ, Boskey AL and Balian G: Matrix mineralization in hypertrophic chondrocyte cultures. Beta glycerophosphate increases type X collagen messenger RNA and the specific activity of pp60c-src kinase. Bone Miner 18: 91-106, 1992.
8. Matsuzawa T and Anderson HC: Phosphatases of epiphyseal cartilage studied by electron microscopic cytochemical methods. J Histochem Cytochem 19: 801-808, 1971.
9. MacRae VE, Farquharson C and Ahmed SF: The restricted potential for recovery of growth plate chondrogenesis and longitudinal bone growth following exposure to pro-inflammatory cytokines. J Endocrinol 189: 319-328, 2006.
10. Owen HC, Miner JN, Ahmed SF and Farquharson C: The growth plate sparing effects of the selective glucocorticoid receptor modulator, AL-438. Mol Cell Endocrinol 264: 164-170, 2007.
11. MacRae VE, Davey MG, McTeir L, Narisawa S, Yadav MC, Millan JL and Farquharson C: Inhibition of PHOSPHO1 activity results in impaired skeletal mineralization during limb development of the chick. Bone 46: 1146-1155, 2010.
12. Gourion-Arsiquaud S, West PA and Boskey AL: Fourier transform-infrared microspectroscopy and microscopic imaging. Methods Mol Biol 455: 293-303, 2008.
13. Van BH: Alkaline phosphatase. I. Kinetics and inhibition by levamisole of purified isoenzymes from humans. Clin Chem 22: 972-976, 1976.
14. Boskey AL and Roy R: Cell culture systems for studies of bone and tooth mineralization. Chem Rev 108: 4716-4733, 2008.
15. Hughes LC, Archer CW and ap Gwynn I The ultrastructure of mouse articular cartilage: collagen orientation and implications for tissue functionality. A polarised light and scanning electron microscope study and review. Eur Cell Mater 9: 68-84, 2005.
16. Temu TM, Wu KY, Gruppuso PA and Phornphutkul C: The mechanism of ascorbic acid-induced differentiation of ATDC5 chondrogenic cells. Am J Physiol Endocrinol Metab 299: E325-E334, 2010.
17. Leboy PS, Vaias L, Uschmann B, Golub E, Adams SL and Pacifici M: Ascorbic acid induces alkaline phosphatase, type X collagen, and calcium deposition in cultured chick chondrocytes. J Biol Chem 264: 17281-17286, 1989.
18. Rohde M and Mayer H: Exocytotic process as a novel model for mineralization by osteoblasts in vitro and in vivo determined by electron microscopic analysis. Calcif Tissue Int 80: 323-336, 2007.
19. Gronowicz G, Woodiel FN, McCarthy MB and Raisz LG: In vitro mineralization of fetal rat parietal bones in defined serum-free medium: effect of beta-glycerol phosphate. J Bone Miner Res 4: 313-324, 1989.
20. Borgers M: The cytochemical application of new potent inhibitors of alkaline phosphatases. J Histochem Cytochem 21: 812-824, 1973.
21. Bonewald LF, Harris SE, Rosser J, Dallas MR, Dallas SL, Camacho NP, Boyan B and Boskey A: von Kossa staining alone is not sufficient to confirm that mineralization in vitro represents bone formation. Calcif Tissue Int 72: 537-547, 2003.
22. Wu LN, Genge BR, Dunkelberger DG, LeGeros RZ, Concannon B and Wuthier RE: Physicochemical characterization of the nucleational core of matrix vesicles. J Biol Chem 272: 4404-4411, 1997.
23. Caplan AI: Bone development. Ciba Found Symp 136: 3-21, 1988.
24. Boskey AL, Doty SB, Stiner D and Binderman I: Viable cells are a requirement for in vitro cartilage calcification. Calcif Tissue Int 58: 177-185, 1996.
25. Anderson HC, Sipe JB, Hessle L, Dhanyamraju R, Atti E, Camacho NP and Millan JL: Impaired calcification around matrix vesicles of growth plate and bone in alkaline phosphatase-deficient mice. Am J Pathol 164: 841-847, 2004.
26. Huitema LF, van Weeren PR, van Balkom BW, Visser T, van de Lest CH, Barneveld A, Helms JB and Vaandrager AB: Soluble factors released by ATDC5 cells affect the formation of calcium phosphate crystals. Biochim Biophys Acta 1774: 1108-1117, 2007.
27. Sauer GR and Wuthier RE: Fourier transform infrared characterization of mineral phases formed during induction of mineralization by collagenase-released matrix vesicles in vitro. J Biol Chem 263: 13718-13724, 1988.
28. LeGeros RZ: Preparation of octacalcium phosphate (OCP): a direct fast method. Calcif Tissue Int 37: 194-197, 1985.
29. Paschalis EP, Jacenko O, Olsen B, deCrombrugghe B and Boskey AL: The role of type X collagen in endochondral ossification as deduced by Fourier transform infrared microscopy analysis. Connect Tissue Res 35: 371-377, 1996.

Bone 51 (2012) 418–430

Contents lists available at SciVerse ScienceDirect

Bone

journal homepage: www.elsevier.com/locate/bone

Original Full Length Article

MEPE is a novel regulator of growth plate cartilage mineralization

K.A. Staines [a,*], N.C.W. Mackenzie [a], C.E. Clarkin [b], L. Zelenchuk [c], P.S. Rowe [c], V.E. MacRae [a], C. Farquharson [a]

[a] The Roslin Institute and Royal (Dick) School of Veterinary Studies, The University of Edinburgh, Easter Bush, Midlothian EH25 9RG, UK
[b] Centre for Biological Sciences, University of Southampton, Southampton General Hospital, Southampton SO16 6YD, UK
[c] Department of Internal Medicine, The Kidney Institute and Division of Nephrology, University of Kansas Medical Center, Kansas City, KS, USA

ARTICLE INFO

Article history:
Received 10 April 2012
Revised 21 June 2012
Accepted 23 June 2012
Available online 7 July 2012

Edited by: J. Aubin

Keywords:
MEPE
ASARM
Growth plate
Mineralization
Chondrocyte

ABSTRACT

Matrix extracellular phosphoglycoprotein (MEPE) belongs to the SIBLING protein family which play key roles in biomineralization. Although the growth plates of MEPE-overexpressing mice display severe morphological disruption, the expression and function of MEPE in growth plate matrix mineralization remains largely undefined. Here we show MEPE and its cleavage product, the acidic serine aspartate-rich MEPE-associated motif (ASARM) peptide, to be localised to the hypertrophic zone of the growth plate. We also demonstrate that the phosphorylated (p)ASARM peptide inhibits ATDC5 chondrocyte matrix mineralization. Stable MEPE-overexpressing ATDC5 cells also had significantly reduced matrix mineralization in comparison to the control cells. Interestingly, we show that the addition of the non-phosphorylated (np)ASARM peptide promoted mineralization in the ATDC5 cells. The peptides and the overexpression of MEPE did not affect the differentiation of the ATDC5 cells. For a more physiologically relevant model, we utilized the metatarsal organ culture model. We show the pASARM peptide to inhibit mineralization at two stages of development, as shown by histological and μCT analysis. Like in the ATDC5 cells, the peptides did not affect the differentiation of the metatarsals indicating that the effects seen on mineralization are direct, as is additionally confirmed by no change in alkaline phosphatase activity or mRNA expression. In the metatarsal organ cultures, the pASARM peptide also reduced endothelial cell markers and vascular endothelial growth factor mRNA expression. Taken together these results show MEPE to be an important regulator of growth plate chondrocyte matrix mineralization through its cleavage to an ASARM peptide.

Introduction

Linear bone growth involves the replacement of a cartilaginous template by mineralized bone through endochondral ossification. This growth process is orchestrated by various actions at the growth plate, a developmental region consisting of chondrocytes in distinct cellular zones. The proliferation, hypertrophy and apoptosis of these growth plate chondrocytes are regulated by a tight array of factors ensuring effective cartilage mineralization and thus longitudinal growth [1].

Hydroxyapatite (HA) crystals form associated with the trilaminar membrane bound matrix vesicles (MV) which in the growth plate are localised to the mineralized longitudinal septae and form from the plasma membrane of the terminal hypertrophic chondrocytes [2]. Mineralization is a biphasic process which is under tight control so as to ensure levels of calcium (Ca^{2+}) and inorganic phosphate (P_i) are permissive for effective HA formation [2]. Three molecules have been identified as imperative in controlling levels of the mineralization inhibitors inorganic pyrophosphate (PP_i), and osteopontin [2,3]. These are alkaline phosphatase (ALP), a nucleotide pyrophosphatase/phosphodiesterase isozyme (NPP1), and the Ankylosis protein (ANK). However, mechanisms beyond the supply and hydrolysis of PP_i likely exist to control chondrocyte matrix mineralization.

Once such mechanism could involve matrix extracellular phosphoglycoprotein (MEPE, OF45). This was originally isolated and cloned from tumors of oncogenic hypophosphatemic osteomalacia (OHO) as a candidate substrate for phosphate-regulating gene with homologies to endopeptidases on the X chromosome (PHEX) [4]. MEPE is a 56–58 kDa SIBLING (small integrin-binding ligand N-linked glycosylated) protein along with dentin matrix protein 1 (DMP1), osteopontin (OPN), dentin sialophosphoprotein (DSPP) and bone sialoprotein (BSP) [5]. SIBLING proteins are expressed in bone and dentin, and have roles in extracellular matrix (ECM) formation and mineralization [6]. Their structures are similar; all display an Arg-Gly-Asp (RGD) motif which facilitates cell attachment, and all are commonly located on the human chromosome 4q21-23 [4,7,8].

In bone, MEPE is primarily expressed by osteocytes, but *Mepe* mRNA expression has also been observed in osteoblasts [9]. The expression of MEPE is increased during osteoblast matrix mineralization suggesting a function for MEPE in bone mineralization [10,11]. This has been further fuelled by analysis of the MEPE null mouse in which the ablation of MEPE leads to an increased bone mass due to increased numbers and activity of osteoblasts [12]. Furthermore, the

* Corresponding author.
E-mail address: katherine.staines@roslin.ed.ac.uk (K.A. Staines).

8756-3282/$ – see front matter © 2012 Elsevier Inc. All rights reserved.
doi:10.1016/j.bone.2012.06.022

overexpression of MEPE in mice, under the control of the Col1a1 promoter, leads to defective mineralization coupled with an increased level of MEPE-ASARM peptides in bone [13]. The MEPE-overexpressing mice displayed wider epiphyseal growth plates, with associated expanded primary spongiosa and a significant decrease in mineral apposition rate [13]. Further studies in vitro have confirmed the inhibitory effect of MEPE on mineralization and have identified that MEPE is cleaved to a 2.2 kDa ASARM peptide which causes this effect [14,15]. The ASARM motif is located immediately downstream of a cathepsin B cleavage site, and it is responsible for the mineralization defect observed in X-linked hypophosphatemic rickets, the most common form of inherited rickets [4,14,15]. This defect can be reversed by administration of cathepsin inhibitors CAO74 or pepstatin [16]. PHEX plays a central role in the protection of MEPE from proteolytic cleavage by cathepsin B; it can bind to MEPE and prevent the release of the ASARM peptide [17]. The *Hyp* mouse, a spontaneous *Phex* knockout model, has an increased expression of cathepsin D, an upstream activator of cathepsin B [16]. Therefore PHEX may also assist in decreasing the activation of cathepsin B.

Previous studies have shown that the post translational modification of the MEPE-ASARM peptide is key to its functional role. MEPE has a number of potential casein kinase II phosphorylation motifs, and it is here that the ASARM peptide is phosphorylated at 3 serine residues [4]. This has been shown to inhibit mineralization in murine calvarial osteoblasts and in bone marrow stromal cells by the direct binding of the MEPE-ASARM peptide to HA crystals [14,18].

To elucidate the interactions of MEPE in the growth plate, this study was undertaken to examine the presence and function of MEPE and its ASARM peptide in growth plate matrix mineralization during the endochondral ossification process. The data indicated that MEPE is expressed by growth plate chondrocytes, in particular in the hypertrophic zone of chondrocytes consistent with a potential role in matrix mineralization. MEPE has a functional role in the inhibition of chondrocyte ECM mineralization, involving its cleavage, and subsequent phosphorylation, to the ASARM peptide.

Materials and methods

Animals

Proximal tibiae from 3- and 4-week-old C57/BL6 mice were dissected and excess tissue was removed before preparation of the tissues for in situ hybridization, immunohistochemistry and microdissection of the growth plate. For metatarsal organ culture, the middle three metatarsals were aseptically dissected from E17 and E15 C57/BL6 mice. All experimental protocols were approved by Roslin Institute's Animal Users Committee and the animals were maintained in accordance with UK Home Office guidelines for the care and use of laboratory animals.

In situ hybridization

Bone tissue was fixed in 10% neutral buffered formalin (Sigma, Gillingham, UK) for 48 h at 4 °C, before being decalcified in 10% ethylenediaminetetraacetic acid (EDTA) (Sigma) pH 7.4 at 4 °C for approximately 4 weeks with regular changes. Tissues were dehydrated and embedded in paraffin wax using standard procedures, before being sectioned at 5 μm. A full length murine MEPE cDNA IMAGE clone (ID: 8733911) was purchased (Source BioScience UK Ltd, Nottingham). Anti-sense and sense constructs were linearised, using *Nco1*, and digoxigenin-labeled cRNA probes were synthesised using T3 and T7 RNA polymerases respectively (Roche, Burgess Hill, UK). Hybridizations were completed following an optimised in situ hybridization protocol as previously detailed [19].

Growth plate microdissection

Bone tissue samples were coated in 5% polyvinyl acetate and then immersed in a cooled hexane bath for 30 s after which they were stored at −80 °C until use. Using optimal cutting temperature (OCT) embedding medium (Brights, Huntingdon, UK) 30 μm sections were cut at −30 °C (Brights, OT model cryostat), and then stored at −80 °C. Slides were briefly thawed and then microdissection was performed as previously detailed [20]. For each zone, tissue was dissected from both proximal tibias of three animals (14–22 sections) and RNA isolation was performed as previously described [21].

Immunohistochemistry

After dissection, tissue was fixed in 70% ethanol for 24 h at 4 °C before being decalcified in 10% EDTA (pH 7.4) for approximately 4 weeks at 4 °C with regular changes. Tissues were finally dehydrated and embedded in paraffin wax, using standard procedures, after which they were sectioned at 5 μm. For immunohistochemical analysis, sections were dewaxed in xylene and rehydrated. Sections were incubated at 37 °C for 30 min in 0.1% trypsin (Sigma) for antigen demasking. Endogenous peroxidases were blocked by treatment with 0.03% H_2O_2 in methanol (Sigma). From this point onwards, the Vectastain ABC (Goat) kit (Vector Laboratories, Peterborough) was used according to the manufacturer's instructions. ASARM and MEPE primary antibodies were used at a dilution of 1/200 with rabbit IgG used as a control [13]. Cathepsin B primary antibodies (R&D Systems, Abingdon, UK) were used at a dilution of 2 μg/ml with goat IgG used as an appropriate control. The sections were dehydrated, counterstained with haematoxylin and mounted in DePeX.

MEPE-ASARM peptides

MEPE-ASARM peptides were synthesised (Peptide Synthetics, UK) as phosphorylated ASARM (pASARM) with the sequence RDDSSESSD SG(Sp)S(Sp)SSE(Sp)SDGD, and non-phosphorylated ASARM (npASARM) with the sequence RDDSSESSDSGSSSESDGD. pASARM and npASARM peptides were added to ATDC5 cells and metatarsal organ cultures at concentrations of 10, 20 and 50 μM, with controls treated with a DMSO (Sigma) carrier only. In further studies, peptides were added at a final concentration of 20 μM with experiments being performed at least 3 times.

Metatarsal organ culture

Embryonic metatarsal organ cultures provide a well-established model of endochondral bone growth [22–24]. Metatarsal bones were cultured in a humidified atmosphere (37 °C, 5% CO_2) in 24-well plates for up to 10 days. Each culture well contained 300 μl α-minimum essential medium (MEM) supplemented with 0.2% BSA Fraction V; 1 mmol/l β-glycerophosphate (βGP); 0.05 mg/ml L-ascorbic acid phosphate; 0.05 mg/ml gentamicin and 1.25 μg/ml fungizone (Invitrogen, Paisley, UK) as previously described [22]. For the E17 bones, the medium was changed every second or third day and for the E15 bones, the medium was not changed throughout the culture period [25]. Concentrations of peptide and DMSO carrier were however added every second day.

Morphometric analysis of metatarsals

The total length of the bone through the centre of the mineralizing zone was determined using image analysis software (DS Camera Control Unit DS-L1; Nikon) every second or third day. The length of the central mineralization zone was also measured. All results are expressed as a percentage change from harvesting length which was regarded as baseline.

3D-Microtomography of metatarsals

Metatarsals were fixed in 70% ethanol, stained with eosin dye (for visualisation) and then embedded in paraffin blocks. Samples were then were scanned with a high-resolution μCT (μCT40; Scanco Medical, Southeastern, PA) as previously described [13,16]. Data were acquired at 55 KeV with 6 μm cubic voxels. Three-dimensional reconstructions for bone samples were generated with the following parameters: Gauss Sigma = 4.0; Support = 2, Lower Threshold = 90 and Upper Threshold = 1000. Tissue mineral density was derived from the linear attenuation coefficient of threshold bone through precalibration of the apparatus for the acquisition voltage chosen. The bone volume (BV/TV) was measured using sections encompassing the entire metatarsal on a set of 85 sections that was geometrically aligned for each sample.

Metatarsal [^{3}H]-thymidine proliferation assay

On day 7 of culture, 3 μCi/ml [^{3}H]-thymidine (Amersham Biosciences, Little Chalfont, UK) was added to each metatarsal for the last 6 h of culture [22]. After washing in PBS, the unbound thymidine was extracted using 5% trichloroacetic acid (Sigma). Metatarsals were then washed in PBS before being solubilised (NCS-II tissue solubiliser, 0.5 N, Amersham) at 60 °C for 1 h. [^{3}H]-thymidine incorporated into DNA was determined using a scintillation counter.

Cell culture

Chondrogenic ATDC5 cells (RIKEN cell bank, Ibaraki, Japan) were utilized as a well-established model of chondrocyte matrix mineralization with previous studies detailing their chondrogenic differentiation and subsequent mineralization [26]. Cells were cultured in differentiation medium (DMEM/F-12 (1:1) with GlutaMAX I containing 5% FBS, 1% insulin transferrin and selenium, 1% sodium pyruvate and 0.5% gentamicin (Invitrogen)) at a density of 6000 cells/cm^2. 10 mM beta-glycerophosphate (βGP) and 50 μg/ml ascorbic acid were added once the cells had reached confluency. Cells were incubated in a humidified atmosphere (37 °C, 5% CO_2) for up to 15 days with medium changed every second or third day.

Plasmid construction

The full length murine MEPE cDNA (IMAGE clone ID: 8733911) was supplied within a pCR4.TOPO vector (Source BioScience UK Ltd, Nottingham). The cDNA sequence was excised by digestion with *EcoRI* and sub-cloned into the pEN.Tmcs (MBA-251; LGC Standards, Middlesex, UK) using T4 DNA ligase (Roche). The expression vector pLZ2-Ub-GFP (kind gift from D. Zhao, Roslin Institute) was digested with *BamHI* and *XbaI* to remove the GFP cDNA. The MEPE cDNA was excised from the pEN.T-MEPE sub-cloning vector using *BamHI* and *XbaI* and ligated into pLZ2-Ub backbone to create a Ubiquitin driven MEPE expression construct, pLZ2-Ub.MEPE. To create the empty vector control (pLZ2-Ub.EMPTY) the pLZ2-Ub backbone was blunted using T4 polymerase (New England Bioscience, Hitchin, UK) and re-ligated.

Establishment of stable MEPE-overexpressing ATDC5 cells

ATDC5 cells were maintained in differentiation medium as previously described and seeded at 150,000 cells/cm^2. Cells were transfected with pLZ2-Ub.MEPE and pLZ2-Ub.EMPTY constructs at a ratio of 7:2 FuGENE HD (Roche) to DNA, according to the manufacturer's instructions. Blasticidin resistant colonies were picked using cloning cylinders (Sigma), expanded, frozen and maintained at −150 °C until further use. Three MEPE-overexpressing and three empty vector clones were picked for analysis.

Real-time quantitative PCR (RT-qPCR)

RNA was extracted from ATDC5 cell cultures using an RNeasy mini kit (Invitrogen) according to the manufacturer's instructions. For metatarsal organ cultures, 4 bones from each control or experimental group were pooled in 100 μl Trizol reagent (Invitrogen) at days 5 and 7 of culture, and RNA was extracted according to the manufacturer's instructions. For each sample, total RNA content was assessed by absorbance at 260 nm and purity by A260/A280 ratios, and then reverse-transcribed. RT-qPCR was performed using the SYBR green detection method on a Stratagene Mx3000P real-time qPCR system (Stratagene, CA, USA), or a LC480 instrument (Roche). Primers were purchased (PrimerDesign Ltd, Southampton, UK) or designed in house and synthesised by MWG Eurofins, London, UK, or Sigma. Sequences are detailed in Supplemental Table S1. Reactions were run in triplicate and routinely normalized against *18S* or *β-actin*.

Endpoint PCR analysis

Expression of specific pro-angiogenic vascular endothelial growth factor (VEGF)-A isoforms namely $VEGF_{120,164}$ and $_{188}$ was analysed as previously detailed [27]. The VEGF isoform primer sequences were: forward GAAGTCCCATGAAGTGATCCAG and reverse TCACCGCCTTGG CTTGTCA. Located on exon 3 (forward) and exon 8 (reverse), these amplify all the isoforms of murine VEGF. Different isoform mRNA expression profiles were identified in a 2.5% agarose (Sigma) gel according to the molecular weight of PCR products using cDNA synthesised from equal amounts of RNA. Product band densities were analysed using Image J software (U. S. National Institutes of Health, Maryland, USA).

Histological procedures

After 15 days of culture, calcium and collagen deposition in ATDC5 cells were evaluated by alizarin red stain (Sigma) and sirius red stain (Biocolor Ltd., Newtownabbey, UK) respectively [28]. Cells were fixed in 4% paraformaldehyde following washes with PBS. 2% alizarin red (pH 4.2) was added to the cell layers for 5 min at room temperature and then rinsed off with distilled water. Alizarin red-stained cultures were extracted with 10% cetylpyridinium chloride for 10 min [28–30]. Sirius red was added to cell cultures for 1 h at room temperature before being rinsed with distilled water. 0.001 M hydrochloric acid was then used to remove unbound dye. To quantify staining, 0.1 M sodium hydroxide was used for 30 min. The optical density (OD) of the alizarin red and sirius red digests was measured at 570 nm by spectrophotometry (Multiskan Ascent, Thermo Electron Corporation, Vantaa, Finland). Proteoglycan synthesis content was evaluated by staining the cell layers with alcian blue (Sigma). Cells were fixed in 95% methanol for 20 min and stained with 1% alcian blue 8GX in 0.1 M HCl overnight. Alcian blue-stained cultures were extracted with 1 ml of 6 M guanidine–HCl for 6 h at room temperature and the OD was determined at 630 nm by spectrophotometry [28].

Alkaline phosphatase enzyme activity

At the end of the culture period, alkaline phosphatase (ALP) activity within the metatarsal bones was determined using an assay for ALP (Thermo Fisher Scientific, Epsom, UK) according to the manufacturer's instructions. Briefly, each metatarsal was permeabilized in 100 μl of 10 mmol/l glycine (pH 10.5) containing 0.1 mmol/l $MgCl_2$, 0.01 mmol/l $ZnCl_2$, and 0.1% Triton X-100 by freeze-thawing three times [22]. Each extract was assayed for ALP activity by measuring the rate of cleavage of 10 mM *p*-nitrophenyl phosphate. Total ALP activity was expressed as nanomoles *p*-nitrophenyl phosphate hydrolysed per minute per bone.

Lactate dehydrogenase activity

Lactate dehydrogenase (LDH) activity was determined in the culture medium of 15-day-old 0 mM and 10 mM βGP treated ATDC5 cells using a kit from Roche Diagnostics (Lewes, East Sussex, UK). LDH activity was related to the total LDH activity of the cultures.

Statistical analysis

Data were analysed by one-way analysis of variance (ANOVA), the Student's *t*-test, or a suitable non-parametric test using Sigma Plot 11 (Germany). All data are expressed as the mean ± SEM.

Results

The expression of MEPE in the murine growth plate

To assess the expression of MEPE by growth plate chondrocytes we examined *Mepe* mRNA localization in the murine growth plate of 3-week-old mice by in situ hybridization. *Mepe* was expressed abundantly by growth plate chondrocytes and by osteoblasts within the metaphysis (Fig. 1A). In the growth plate, high levels of *Mepe* mRNA were observed, especially in the hypertrophic chondrocytes (Fig. 1B and C). This spatial expression pattern was further examined and quantified by microdissection of growth plates. To validate the microdissection technique, RT-qPCR of collagen type X mRNA expression was conducted to ensure that the hypertrophic zone could be considered as an enriched pool of hypertrophic chondrocytes (Fig. 1D). There was approximately a 10-fold increase in collagen type X mRNA expression in the hypertrophic zone in comparison to the proliferative zone ($P<0.001$). This is in concordance with previous studies done using a similar technique [31]. *Mepe* mRNA had a significantly higher expression ($P<0.05$) in the hypertrophic zone in comparison to the proliferative zone of the growth plate (Fig. 1E). Immunolocalization of MEPE and the MEPE-ASARM peptide in 4-week-old growth plates verified the in situ hybridization and microdissection data as demonstrated by its localization to the hypertrophic zone of chondrocytes (Fig. 1F and H). This ASARM peptide is cleaved from MEPE by cathepsin B; thus, we examined the immunolocalization of cathepsin B in the growth plate (Fig. 1J). Here we show it to be expressed at the chondro-osseous junction as is in concordance with previous studies [32,33]. Representative images of the appropriate negative controls are shown (Fig. 1G, I and K). Together these data indicate that MEPE-ASARM peptide is preferentially expressed by hypertrophic chondrocytes of the growth plate and this localization is consistent with a role for this peptide in regulating cartilage mineralization.

The functional role of MEPE in ATDC5 cells

It is known that the C-terminal fragment is the active form of MEPE. This fragment contains the ASARM peptide; thus, we next determined the role of the ASARM peptide in chondrocyte matrix mineralization by examining the mineralization capability of ATDC5 cells in response to MEPE-ASARM peptides. The ATDC5 cell line is a teratocarcinoma derived cell line which has been shown to display the multistep chondrogenic differentiation process, from mesenchymal condensation to matrix mineralization [26,34], at approximately day 15 of culture. The culture method used here did not result in metabolic stress leading to cell death as indicated by assessment of released LDH activity as a percentage of total LDH release (0 mM βGP 33.5% ± 2.5, 10 mM βGP 35.2% ± 0.9, NS). Here we added pASARM and npASARM peptides to ATDC5 cell cultures under calcifying conditions over a 15-day culture period. There was no apparent morphological difference between control and ASARM-treated cells. pASARM peptides inhibited mineralization in a dose-dependent manner as visualised by alizarin red staining and quantified by spectrophotometry (at 20 μM and 50 μM in comparison to control; $P<0.01$) (Fig. 2A). Interestingly, it was found that npASARM promoted mineralization over the 15-day culture period (at 20 μM and 50 μM in comparison to control; $P<0.01$) (Fig. 2B). Given that MEPE has been postulated to have direct effects on osteoblast mineralization and not via altered matrix production [14,18], we investigated whether this was the case with ATDC5 cells by examining their ability to produce their collagenous matrix when treated with the MEPE-ASARM peptides. Collagen deposition (Fig. 2C) and glycosaminoglycan production (Fig. 2D), as visualised by sirius red and alcian blue stains, respectively, were unaffected by addition of 20 μM pASARM or npASARM peptide. These data are therefore supportive of a direct role for MEPE-ASARM peptides in chondrocyte matrix mineralization.

We next overexpressed MEPE in ATDC5 cells to examine this functional role further. When cultured under calcifying conditions, MEPE-overexpressing cells showed an inhibition of matrix mineralization throughout the culture period as visualised by alizarin red staining and quantified by spectrophotometry (at day 8 in comparison to empty vector control $P<0.01$, at days 12 and 15 in comparison to empty vector control $P<0.001$) (Fig. 3A). RT-qPCR amplifications showed that stable individual MEPE-overexpressing ATDC5 cell clones expressed significantly higher *Mepe* mRNA levels than individual empty vector clones ($P<0.001$) (Fig. 3B). *Phex* mRNA levels were significantly decreased in the MEPE-overexpressing clones in comparison to the empty vector controls ($P<0.05$) (Fig. 3C). Chondrocyte marker genes of differentiation and mineralization were examined for mRNA expression and no differences were found between the MEPE-overexpressing and the empty vector controls (Fig. 3D and E, Supplemental Fig. S1).

Phosphorylated MEPE-ASARM peptides inhibit the mineralization capability of E17 metatarsal bones

We next wanted to examine the effects of the MEPE-ASARM peptides on a more physiologically relevant model. Primary chondrocytes provide difficulties when culturing as they tend to dedifferentiate to a fibroblastic-like phenotype during long-term culture [35–38]; thus, we utilized the metatarsal organ culture model. When dissected, E17 mice metatarsals display a central core of mineralized cartilage juxtaposed by a translucent area on both sides representing the hypertrophic chondrocytes [22] (Fig. 4B). These bones were cultured in the presence of varying concentrations of pASARM and npASARM peptides over a 10-day period to examine their effects on longitudinal bone growth and the growth of the central mineralization zone. This preliminary data indicated that MEPE-ASARM peptides inhibit mineralization of metatarsal bones across a range of concentrations (Supplemental Fig. S2). Due to the physiological relevance of 20 μM in XLH patients and *Hyp* mice, this concentration was used throughout

Fig. 1. In situ hybridization of *Mepe* in 3-week-old mouse tibia. *Mepe* was found to be abundantly expressed by growth plate chondrocytes and osteoblasts of the metaphysis (A). Expression was present in both the proliferating zone (PZ) and the hypertrophic zone (HZ) of the growth plate, as indicated by the arrows (B), with an apparent increase in expression in the hypertrophic zone of chondrocytes (C). Microdissection of the growth plate was adopted to assess *Mepe* mRNA expression. The accuracy of the microdissection technique was determined by the relative change in *col10a1* mRNA expression throughout the zones of the growth plate and the trabecular bone (D). This was then used to examine the relative change in *Mepe* mRNA expression in these zones (E). Immunohistochemistry shows MEPE (F and G) and the MEPE-ASARM peptide (I and J) to be expressed in the tibia of 4-week-old growth plates. Its expression in the growth plate is limited to the hypertrophic zone (HZ) of chondrocytes, as indicated by the arrows. Cathepsin B immunolocalization (L and M) was exclusive to the chondro-osseous junction, as highlighted by the arrows. Representative images of appropriate negative control are shown (H, K, and N). Values generated by RT-qPCR and normalized to *18S*. Data are represented as mean ± SEM, in comparison to the PZ, $^{*}P<0.05$ $^{**}P<0.005$. Scale bars are (A, B, F, H, I, K, L, N) 0.5 mm, (C) 0.1 mm, and (G, J, M) 0.01 mm.

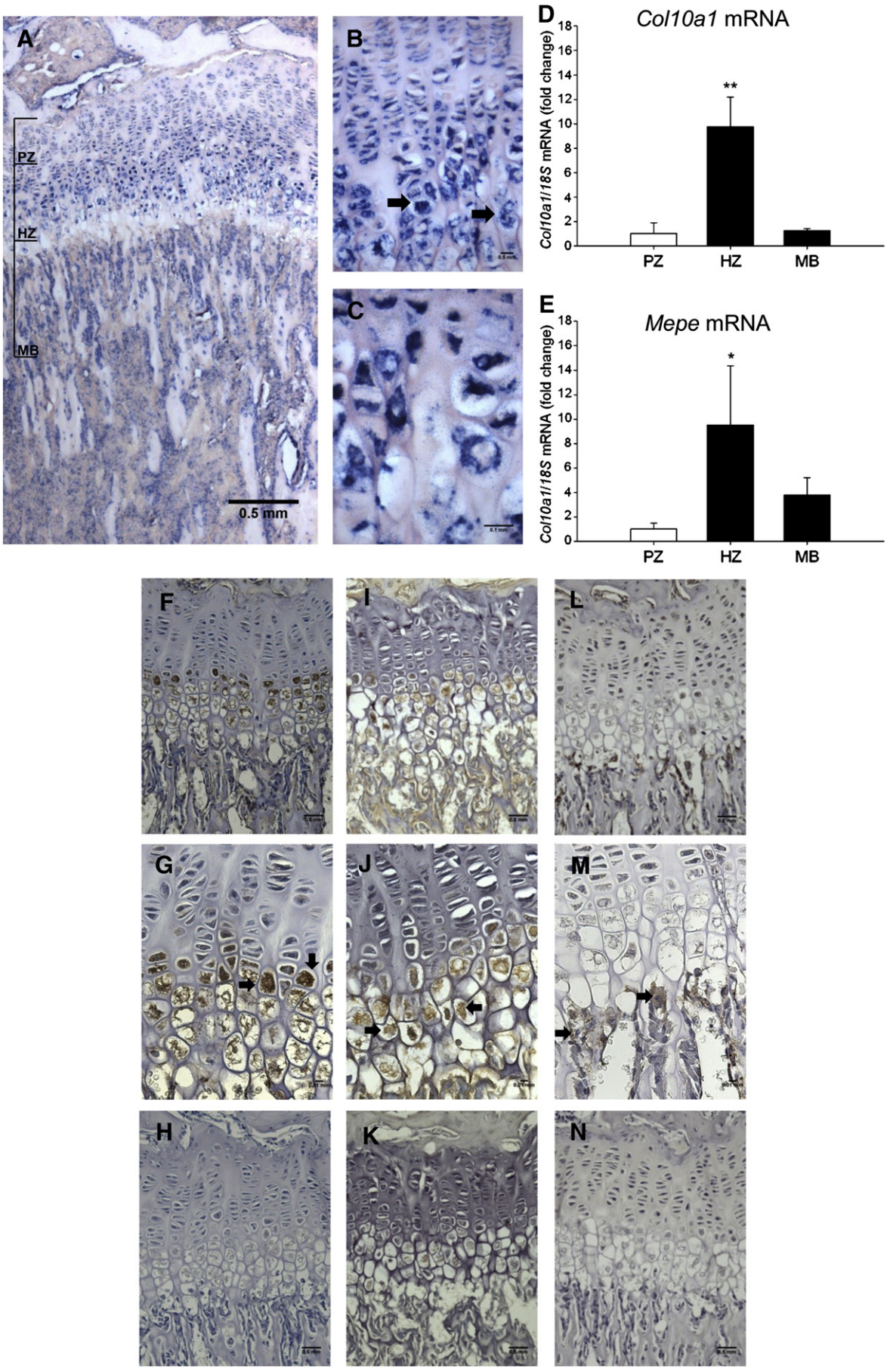
A
PZ
HZ
MB
0.5 mm
B
C
D
Col10a1 mRNA
Col10a1/18S mRNA (fold change)
**
PZ
HZ
MB
E
Mepe mRNA
Col10a1/18S mRNA (fold change)
*
PZ
HZ
MB
F
I
L
G
J
M
H
K
N

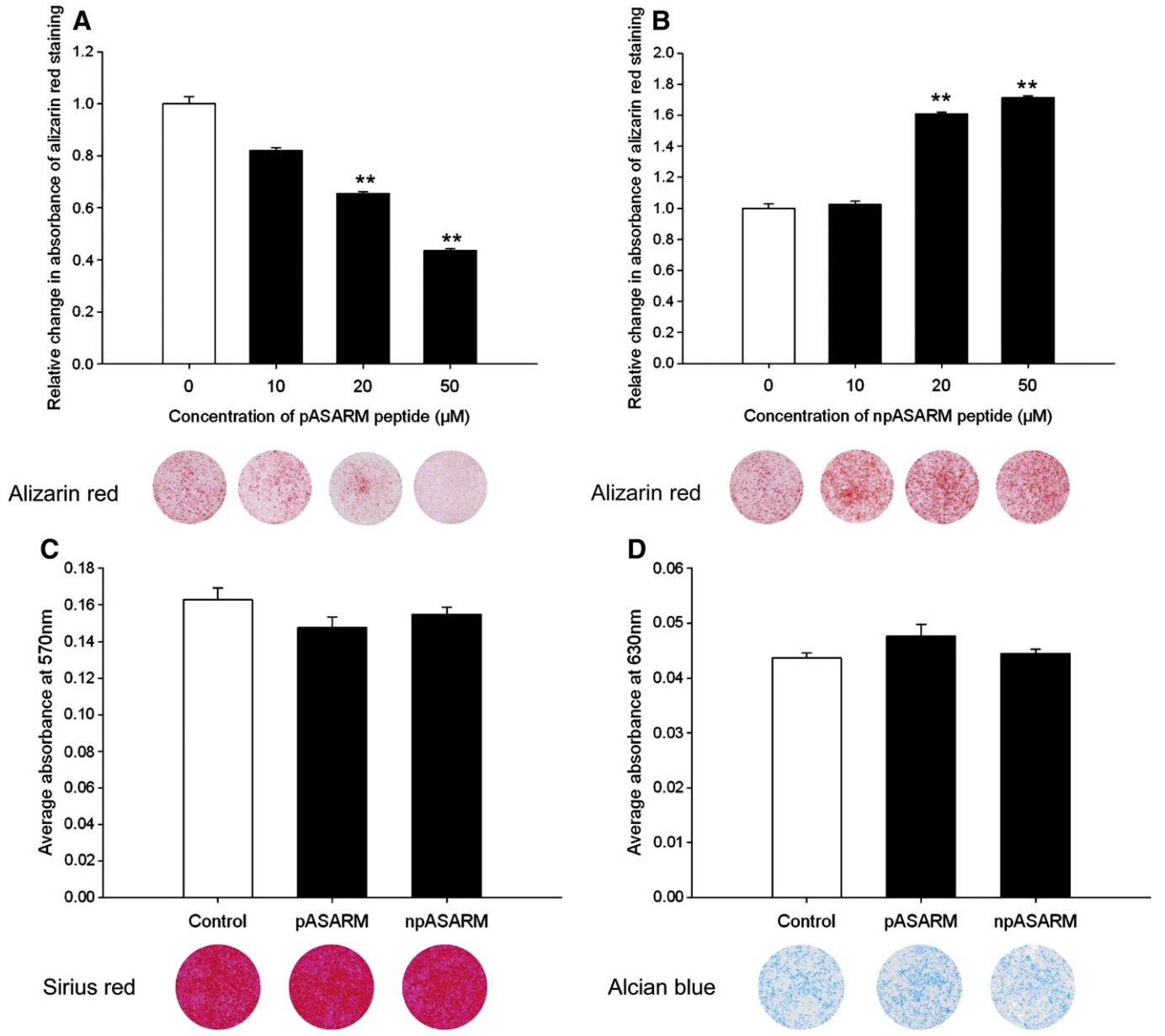

Fig. 2. Mineralization of ATDC5 matrix in the presence of (A) pASARM and (B) npASARM peptides was visualised by alizarin red staining (images) and quantified after 15 days of culture. Quantification of sirius red staining (C) and alcian blue staining (D) (images) of ATDC5 cells following 15 days of culture with 20 μM pASARM and npASARM peptides. Data are represented as mean ± SEM of three wells analysed in triplicate. $^{**}P<0.01$.

these experiments [18]. Bones treated with 20 μM MEPE-ASARM peptides grew in length at the same rate as the control bones (up to 80%) after 7 days in culture (Fig. 4C–F). However, whereas in the control and npASARM treated metatarsals the central mineralization zone increased in length throughout the culture period (increased approximately 5–6 fold from initial lengths, Fig. 4D and E), in the pASARM treated cultures no changes in length were noted ($P<0.01$ at day 6, $P<0.001$ at days 8 and 10 in comparison to the control) (Fig. 4C, E and G).

The effects of the MEPE-ASARM peptides on E15 metatarsal bones

To examine this apparent inhibitory effect further, we next determined the effects of the pASARM and npASARM peptides on E15 metatarsal bones. These bones consist of early proliferating chondrocytes (Fig. 5A) and no evidence of a mineralized core. After 7 days in culture, the chondrocytes in the centre of the bone become hypertrophic and mineralize their surrounding matrix as is previously documented [25] (Fig. 5B). This central core of mineralized cartilage formed in control bones and bones treated with 20 μM npASARM peptides (Fig. 5B and C); however, it was minimal in metatarsal bones treated with 20 μM pASARM peptides (Fig. 5D), as seen in the phase contrast images. This was further confirmed by von kossa staining of histological sections for mineralization (Fig. 5H) and by μCT scanning of the metatarsal bones to allow the visualisation of the bones in a 3D context. In comparison to the control and npASARM treated bones, metatarsal bones cultured in the presence of pASARM peptides had a significantly reduced BV/TV ($P<0.001$) (Fig. 5I), as is clearly visible in the μCT scan images (Fig. 5J). This unequivocally shows the inhibition of mineralization in metatarsal bones by the pASARM peptide. Despite the increase in ATDC5 ECM mineralization upon addition of npASARM peptides, here the mean density of the mineralised bone was unchanged between control and npASARM treated bones (control 163.4 ± 12.1 mg HA/ccm, npASARM 173.2 ± 21.9 mg HA/ccm, not significant).

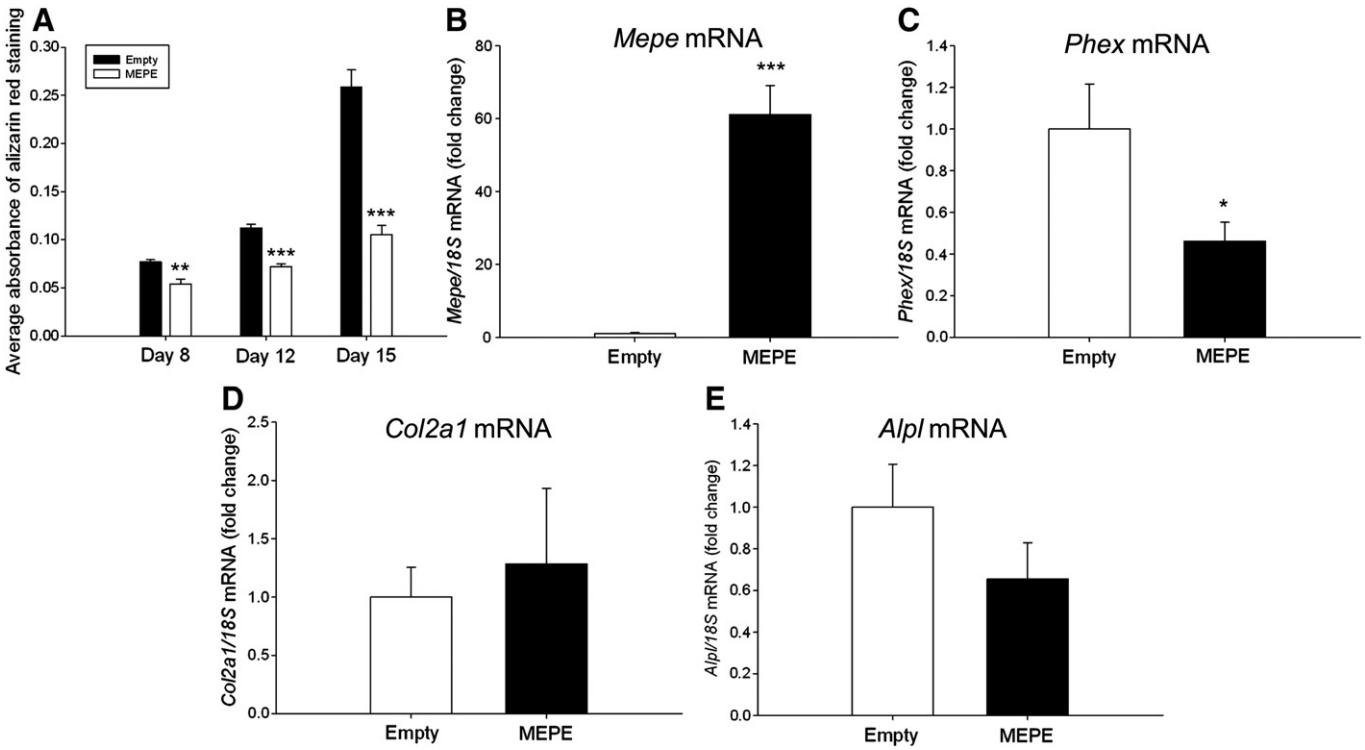

Fig. 3. MEPE-overexpressing ATDC5 cells showed inhibited mineralization in comparison to empty vector cells at days 8, 12 and 15 of culture as visualised by alizarin red staining and quantified by spectrophotometry (A). *Mepe* mRNA expression was significantly increased in MEPE-overexpressing ATDC5 clones (B), whilst *Phex* mRNA expression was significantly decreased in comparison to empty vector controls (C). There was no difference in mRNA expression levels of (D) *Col2a1* or (E) *Alpl*. Data are represented as mean of 3 clones ± SEM. $^{*}P<0.05$, $^{**}P<0.01$, $^{***}P<0.001$.

Apart from the inhibition of mineralization by the pASARM peptide, there were no other obvious morphological differences in the development of these bones in comparison to the control bones. All bones grew at the same rate (increased approximately 65% from initial lengths) (Fig. 5E) and by incorporating [^{3}H]-thymidine into the bones at the end of the culture period, day 7, it was determined that the proliferation rate of the chondrocytes was unchanged (Fig. 5F). The lengths of the proliferating (PZ) and hypertrophic (HZ) zones of chondrocytes were also measured. The MEPE-ASARM peptides had no effect on the percentage sizes of the maturational zones of the metatarsal bones, or on the cell numbers within the bones (Control: 1139.13 ± 172.01, pASARM: 1594.97 ± 226.9, npASARM 1233.71 ± 126.08). This therefore suggests that the MEPE-ASARM peptides had no effect on the differentiation capability of the metatarsal chondrocytes (Fig. 5G). To examine this further, we looked at mRNA expressions of chondrocyte differentiation markers for which there were no significant differences between the control and pASARM treated bones at days 5 and 7 of culture (Supplemental Fig. S3, Supplemental Fig. S4) as is in concordance with our histological and proliferation data.

We also examined the expression and activity of key enzymes associated with cartilage mineralization to establish whether these are involved in the mechanism of inhibition by the pASARM peptides. Interestingly there was no significant difference in the activity of ALP (Fig. 6A), a well recognised regulator of chondrocyte matrix mineralization. This was further confirmed by mRNA expression analysis of *Alpl* by RT-qPCR (Fig. 6B). Analysis of the mRNA expression of other mineralization regulators, *Ank*, *Enpp* and *Phospho1*, also showed no difference between control and treated bones at days 5 and 7 of culture (Supplemental Figs. S3 and S4).

To assess the possible interactions of PHEX with MEPE, we examined mRNA expression of *Phex* and found it to be significantly decreased in the pASARM treated bones compared to the control bones at day 7 of culture ($P<0.05$) (Fig. 6C). Furthermore, *Mepe* mRNA expression was significantly increased ($P<0.001$) (Fig. 6D). At day 5 of culture, there was no significant difference in the mRNA expression of *Mepe* or *Phex* (Supplemental Fig. S3).

The vascular invasion of the cartilage model via VEGF stimulated angiogenesis is critical for matrix mineralization [39]. Thus, we examined the effects of the pASARM peptide on the mRNA expression of endothelial cell specific markers and VEGF. We found a significant decrease in the expression levels of *Cd31*, *Cd34*, and *VEGFR2/Flk1* following 7 days of culture in the presence of 20 μM pASARM compared to controls ($P<0.01$, $P<0.05$) (Fig. 7A–C). Furthermore, we also found a concomitant decrease in VEGF isoform expression specifically $VEGF_{164}$ and $_{120}$ (Fig. 7D–F). $VEGF_{188}$ was not detected in either control or treated metatarsals. Matrix metalloproteinase 13 (MMP13), which has been implicated in VEGF-induced angiogenesis [40,41], also had a significantly decreased mRNA expression following 5 days of culture (in pASARM treated bones compared to control; $P<0.05$) (Fig. 7G). Despite this there was histologically no apparent inhibition of vascularization in the metatarsal bones.

Discussion

The hypertrophic chondrocytes of the epiphyseal growth plate mineralize their surrounding ECM and facilitate the deposition of HA, a process imperative for longitudinal bone growth. It is widely accepted that ALP, NPP1 and ANK are all central regulators of levels of PP_i, a mineralization inhibitor, and thus the deposition of HA [42–46]. Recently it has come to light that mechanisms beyond the supply and hydrolysis of PP_i also exist to control matrix mineralization. Studies into rare genetic disorders, such as X-linked hypophosphatemic rickets (XLH), have identified a family of proteins, FGF23, PHEX, and MEPE which act through a bone-kidney axis to modulate phosphate homeostasis and thus bone mineralization indirectly [4,47–49]. However, these proteins have been shown to have direct effects on mineralization, independent

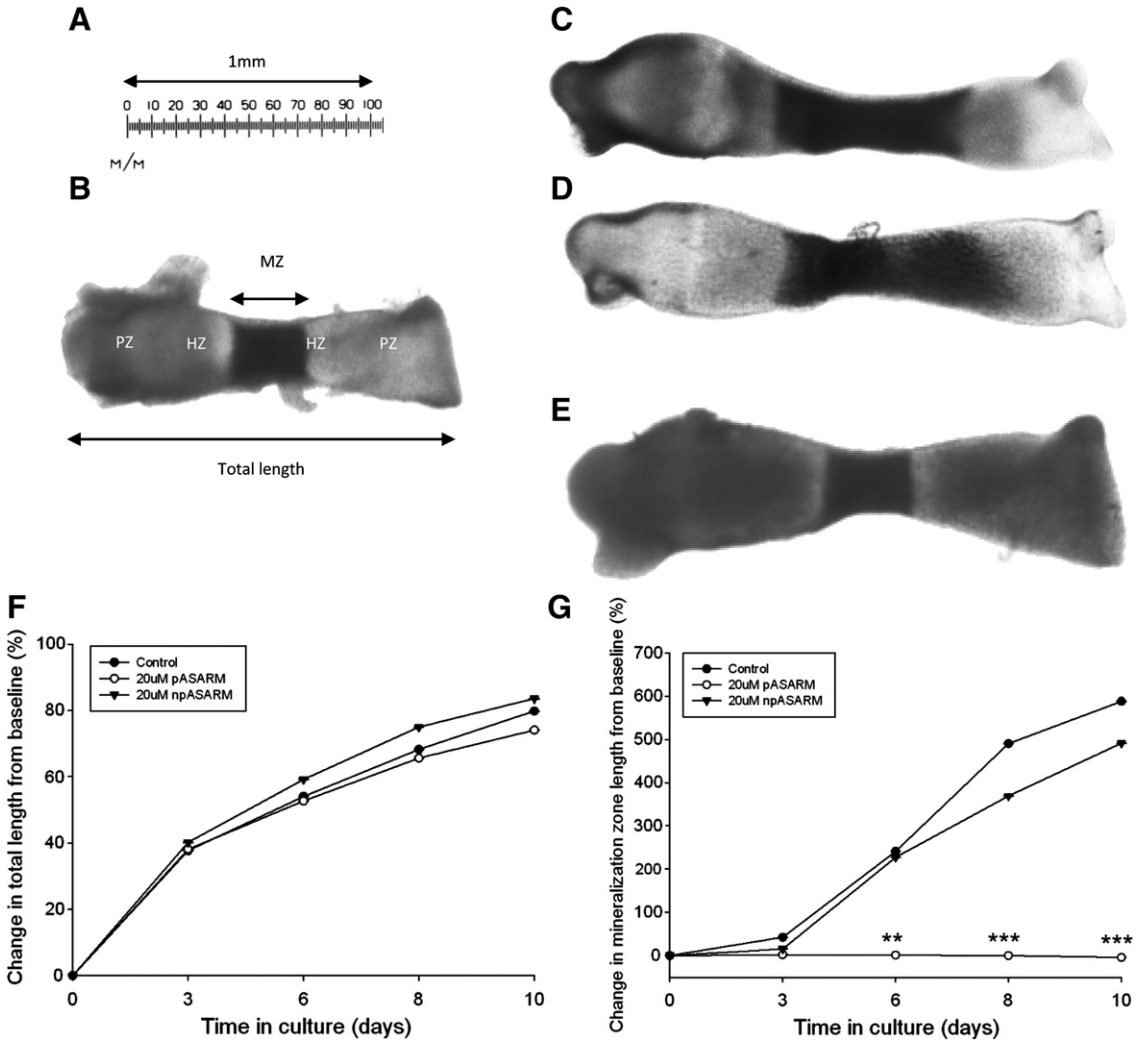

Fig. 4. Measurements of digital images of E17 mouse metatarsal bones in culture with clearly delineated mineralizing zones (B–D) were taken using a calibrated ruler (A). Images clearly show the harvesting length (B) with the locations of the proliferating (PZ), hypertrophic (HZ) and mineralizing (MZ) zones, as well as the total length measurement. A control metatarsal bone is illustrated in (C) and bones treated with continuous 20 μM npASARM (D) and pASARM peptides (E) after 10 days of culture. The growth rate of the embryonic metatarsal bones was not affected by treatment with 20 μM MEPE-ASARM peptides (F) when cultured for up to 10 days. There was no significant difference in the percentage change in mineralization length between control and npASARM treated bones, both of which increased over the culture period. However the mineralization zone length in bones treated with pASARM peptides remained the same during the culture period (G). Data are represented as mean ± SEM of six bones. $^{**}P<0.01$, $^{***}P<0.001$ in comparison to control bones at equivalent days of culture. Error bars are too small to be visualised.

of the bone-kidney axis [50,51]. Here we provide evidence for MEPE as a novel regulator of growth plate cartilage mineralization.

MEPE is a member of the SIBLING family of proteins and is expressed by mature osteoblasts, osteocytes, odontoblasts and the proximal convoluted tubules of the kidney [12,16,52,53]. It is degraded by cathepsin B to an acidic, negatively charged ASARM peptide which inhibits osteoblast matrix mineralization by directly binding to HA [14,15,18]. Patients with XLH have elevated serum levels of this ASARM peptide as does the mouse model of XLH, the *Hyp* mouse [54]. Further studies of the *Hyp* mouse show severe morphological disruption of the growth plate which can be corrected by the administration of cathepsin inhibitors [16]. This growth plate disruption is also observed in mice overexpressing MEPE [13]. Here we provide evidence of the spatial localization pattern of MEPE and its mRNA in the growth plate; more specifically we have shown it to be predominantly expressed by the terminally differentiated hypertrophic chondrocytes. It is recognised that due to the binding nature of MEPE to HA, EDTA decalcification may in fact provide an underestimation of the total MEPE/ASARM protein produced however the results seen here are consistent with those observed in the MEPE-overexpressing mouse and with a presumed role for MEPE in regulating the fine balance of mineral formation at the growth plate. The localization of cathepsin B at the chondro-osseous junction is in concordance with previous studies detailing the cathepsin B rich septoclast [32,33]. These cells, thought to be of macrophage or osteoclast origin, are postulated to play a key role in the degradation of unmineralized cartilage

Fig. 5. Measurements of digital images of E15 mouse metatarsal bones in culture. At time of harvesting, bones did not have a central mineralization zone as indicated by the asterisk (A). After 7 days in culture, control (B) and npASARM (C) treated bones formed a large mineralization zone; however, this was inhibited in pASARM treated bones (D). All metatarsal bones grew at a similar rate (E) and there was no difference in the proliferation of the chondrocytes within (F). Histological sections (H) showed control and npASARM treated bones to have abundant mineral as indicated by von kossa staining. This was not seen in pASARM treated metatarsals. There was no difference in the widths of the proliferating zone (PZ) and hypertrophic zone (HZ) of chondrocytes between the different groups of metatarsals at either day 5 or day 7 of culture (G). Data are represented as mean ± SEM of six bones. μCT analysis of metatarsal bones treated with npASARM and pASARM peptides. Bones treated with pASARM had a significantly reduced BV/TV in comparison to the control and npASARM treated bones (I). This was clearly visible in the μCT images (J). Data are represented as mean ± SEM of three bones. $^{***}P<0.001$.

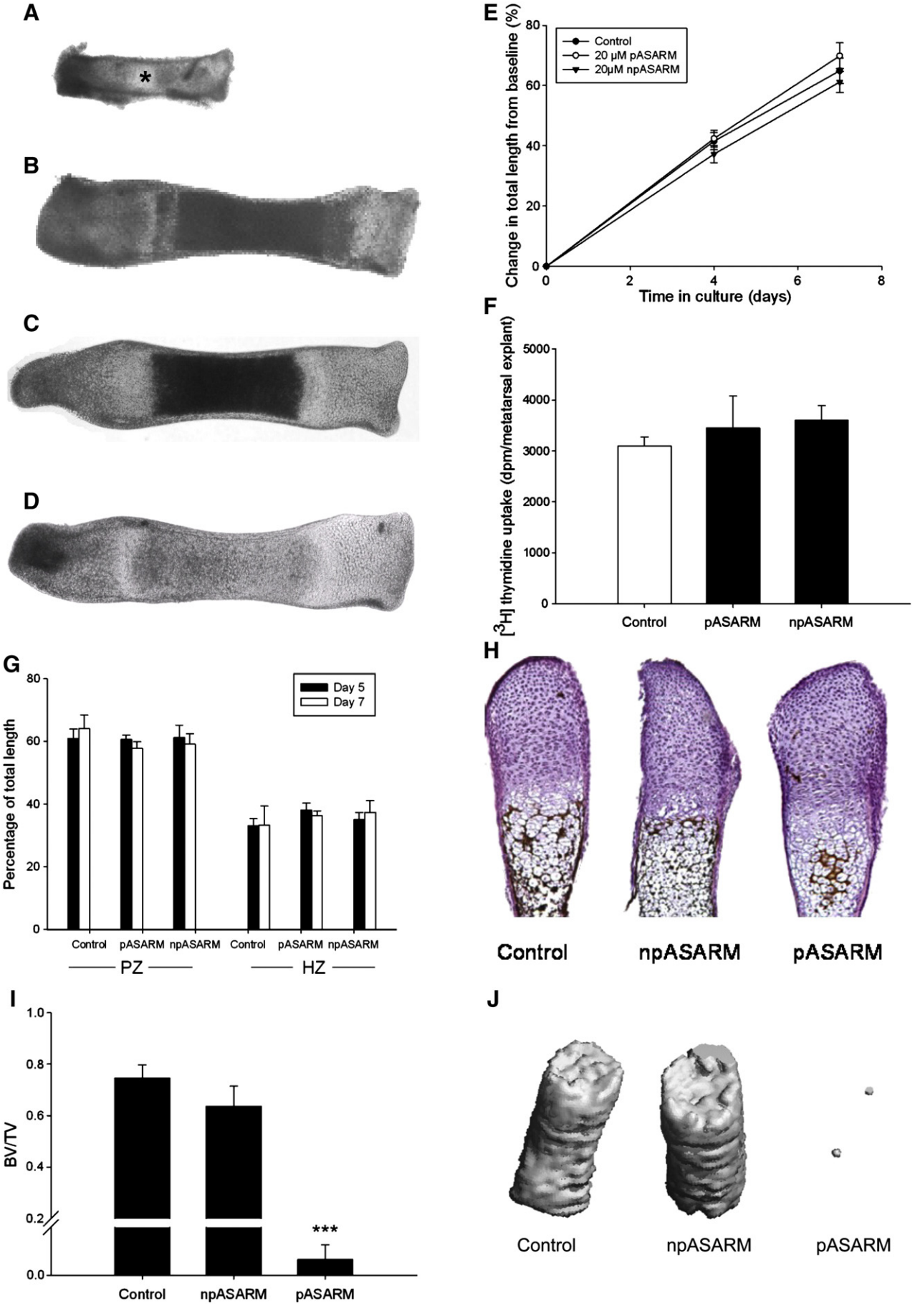
A
B
C
D
E
Control
20 μM pASARM
20μM npASARM
Change in total length from baseline (%)
Time in culture (days)
F
[3H] thymidine uptake (dpm/metatarsal explant)
Control
pASARM
npASARM
G
Day 5
Day 7
Percentage of total length
Control pASARM npASARM Control pASARM npASARM
PZ
HZ
H
Control
npASARM
pASARM
I
BV/TV
***
Control
npASARM
pASARM
J
Control
npASARM
pASARM

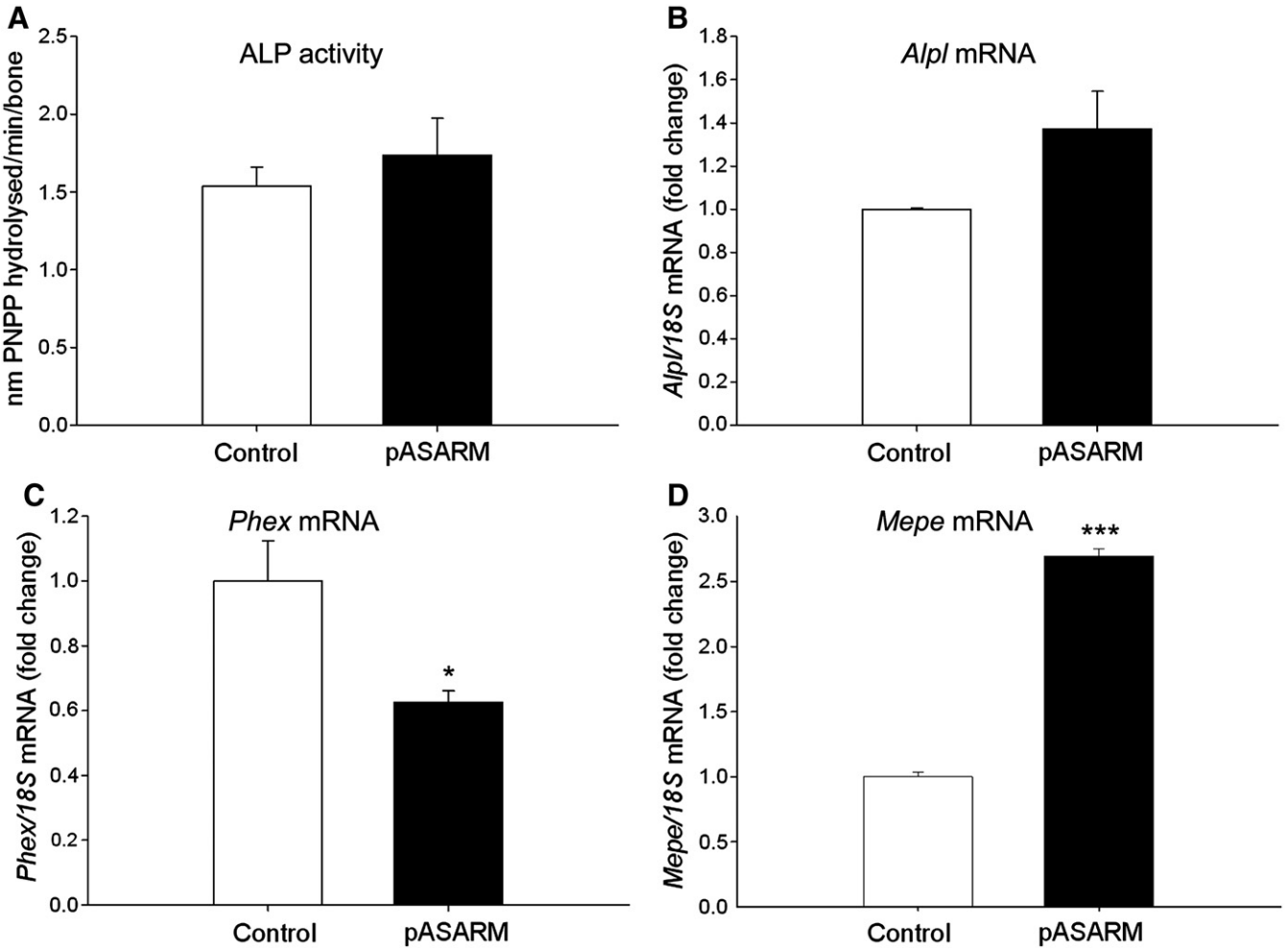

Fig. 6. Alkaline phosphatase (ALP) activity was unchanged in metatarsal bones treated with 20 μM pASARM peptides in comparison to control bones (A). *Alpl* mRNA expression was also unchanged (B). *Phex* mRNA expression was significantly decreased in pASARM treated bones (C) whilst *Mepe* mRNA expression was increased (D). Data are represented as mean ± SEM. $^{*}P<0.05$ $^{***}P<0.001$ of 3 groups of 4 pooled bones at day 7 of culture.

[33]. It is likely that the cathepsin B provided at the chondro-osseous junction cleaves MEPE at its distal COOH-region to the ASARM peptide which we have shown here to be localised exclusively to the hypertrophic chondrocyte region.

Previous studies have shown the ASARM peptide to inhibit matrix mineralization in in vitro osteoblast cultures [15,18,55]. It is well recognised that the post translational phosphorylation of the MEPE-ASARM peptide is essential for its inhibitory role. Here we utilized the metatarsal organ culture model, a well-established model of cartilage mineralization and endochondral bone growth. Developmentally in mice by E15, the point at which we use metatarsal bones in these studies, despite a considerable degree of periosteal ossification occurring in the long bones, the metatarsal bones exist as a cartilage model. Here our results unequivocally show that the phosphorylated ASARM peptide (pASARM) has a significant inhibitory role on chondrocyte matrix mineralization. Here we report no difference in the widths of the cartilage zones in the metatarsal bones. A widening of the hypertrophic zone would be expected as seen in hypophosphatemic rickets, and as is observed in the MEPE-overexpressing mouse [13]. This is not surprising though as there was also no difference in the growth potential, chondrocyte proliferation or mRNA expression of chondrocyte differentiation markers, of the treated and untreated bones. This therefore suggests that the MEPE-ASARM peptide has no effect on chondrocyte function per se. Instead it affects chondrocyte matrix mineralization directly, as is in concordance with studies done on bone mineralization [14,18].

It is well recognised that ALP activity is a key regulator of cartilage matrix mineralization. ALP is located to the outer surface of the trilaminar membrane of MVs, which form from the hypertrophic chondrocytes [56]. It is widely accepted that ALP generates P_i for HA formation and its lack of activity results in an excess of PP_i [57]. The interaction between ALP, PP_i and other SIBLING proteins has previously been documented [57,58]. It was therefore postulated that the effects of the pASARM peptide could act through a decrease in ALP activity/expression as has been shown in a previous study of bone mineralization and as is observed in the MEPE-overexpressing mouse [13,14]. However here we show no effect on ALP activity or expression by the ASARM peptide and as is in concordance with a previous study investigating the role of MEPE in osteoblast mineralization [18]. No effect was also seen on PHOSPHO1 expression, which together with ALP regulates bone and cartilage mineralization suggesting that in the models utilized here, the mechanism of inhibition is not a result of decreased enzyme activity [59,60]. Rather, it is likely that the pASARM peptide exerts its effects through its direct binding to the HA as has previously been suggested.

It has recently been shown that a truncated form of MEPE, which has the ASARM peptide removed, can promote bone mineralization in culture and in mice [61]. Furthermore, a mid-terminal fragment of MEPE has been shown to enhance cell binding and taken together these results highlight the importance of the post translational processing of MEPE in determining its functional role [62]. Here we have shown that the phosphorylation of the ASARM peptide is crucial

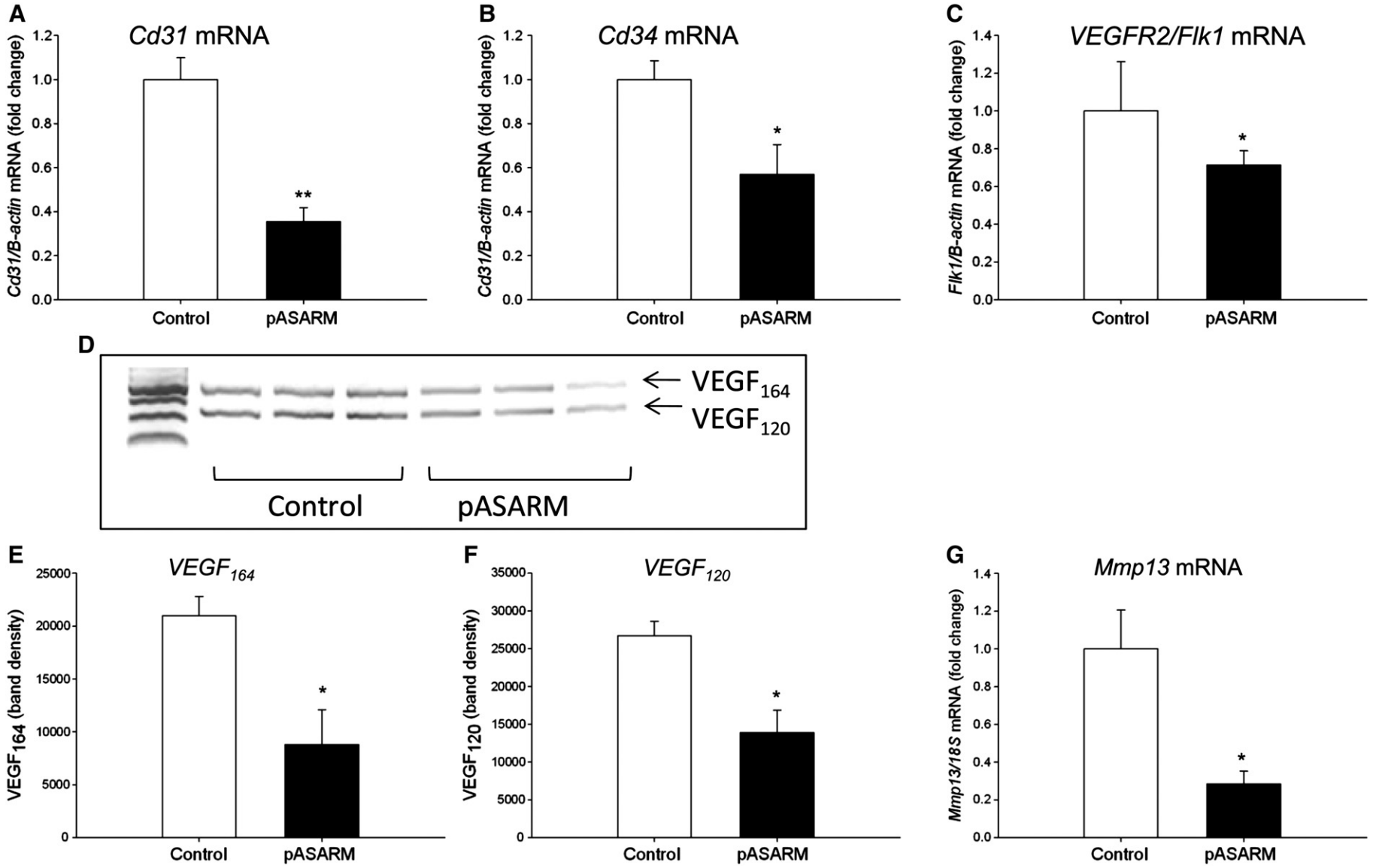

Fig. 7. mRNA expression of endothelial cell markers *Cd31* (A), *Cd34* (B), and *VEGFR2/Flk1* (C) in control and pASARM treated bones at day 7 of culture. PCR analysis of pro-angiogenic VEGF-A splice variants (D) and densitometry of the $VEGF_{164}$ isoform (E) and the $VEGF_{120}$ isoform (F). mRNA expression of *Mmp13* in control and pASARM treated bones at day 5 of culture (G). Data are represented as mean ± SEM. $^{*}P<0.05$, $^{**}P<0.01$ of 3 groups of 4 pooled bones. PCR analysis represents replicates of pooled bones at day 7 of culture.

in determining its functional role. Despite the observed promotion of mineralization by the npASARM peptide in the ATDC5 cultures, this was not corroborated by our metatarsal data. Furthermore in other in vitro studies, it has been shown that the function of the MEPE-ASARM peptide is entirely dependent upon its phosphorylation [14,18,63]. Indeed it is likely that the npASARM peptide does not physiologically exist and is in fact inactive. One can reasonably infer that since the pASARM serine-phosphorylated casein kinase sites are highly conserved across species (including whales, dolphins, primates, rodents, marsupials, elephants, dogs, and cats) and the phosphorylated form is active that there might be a physiological mechanism that plays a role in regulating the ASARM-phosphorylation status [64].

PHEX protects MEPE from cathepsin B cleavage in vitro [17,65]; thus, the inhibition of *Phex* mRNA expression in pASARM treated metatarsal bones and in ATDC5 cells overexpressing MEPE suggests a feedback mechanism by which ASARM peptides can prevent PHEX expression. This, in correlation with an increase in *Mepe* expression seen, would allow the release of ASARM peptides therefore further increasing the inhibition of mineralization. Furthermore, the reduction in *Phex* mRNA expression may be due to the ASARM peptide protecting itself from sequestration and hydrolysis by PHEX, as has previously been suggested [14,18,66]. A decrease in *Phex* mRNA has also been observed in osteoblast cell cultures treated with the pASARM peptide, concomitant with an increase in FGF23 expression [14]. In the MEPE-overexpressing mouse, however, an increase in *Phex* mRNA is observed and this, coupled with the expected hydrolysis of the ASARM peptide, leads to altered MEPE processing and therefore the hyperphosphatemia observed in this mouse model [13]. These data are also in agreement with previous reports showing increased MEPE expression by osteoblasts of HYP mice and this positive regulation of MEPE expression by pASARM may exacerbate the condition [4,10,15,66]. It is reasonable to speculate that physiologically there must be a regulatory mechanism to ensure that there is not an overproduction of ASARM peptides and as such a pathological state. The precise nature of the counter balancing mechanism is presently unknown but as the SIBLING proteins are closely related and it is possible that one of the other members of this family may be responsible.

Key to endochondral ossification is the vascularization of the mineralized matrix [39]. Matrix metalloproteinases (MMPs) proteolytically degrade the mineralized cartilage matrix, facilitating blood vessel penetration into the growth plate and allowing the recruitment of osteoclast precursors and osteoblast progenitors. Pro-angiogenic VEGF is produced by hypertrophic chondrocytes of the growth plate and $VEGF_{164/188}$ deletion from the cartilage of developing mice results in delayed recruitment of blood vessels to the perichondrium along with a delayed invasion of vessels into the primary ossification centre [67]. Here we have shown that the pASARM peptide reduces the levels of endothelial cells present during metatarsal organ culture due to the vessel invasion of the bones at approximately E14– E15. This was associated with reduced $VEGF_{120/164}$ mRNA expression levels. It is entirely possible that the influence of the pASARM peptide on endothelial cell populations is indirect, by impacting hypertrophic chondrocyte VEGF expression. However, any direct effects of the pASARM peptide on endothelial cell function remain uninvestigated. The possible implications of MEPE on bone renal vascularization have recently been described in the MEPE-overexpressing mouse, which in contrast to our studies exhibits defective mineralization associated with increased blood vessels [13]. Similarly, we also found a decrease in *Mmp13* mRNA expression following pASARM treatment which has been implicated in angiogenesis despite there being a lack of impairment of vascularization in the *Mmp13* knockout mouse [40,41,68]. It is likely that in the *Mmp13* knockout and the *Mepe*-overexpressing mice, unknown compensatory mechanisms could exist to allow for effective vascularization of the skeleton. Like MEPE, DMP1, another SIBLING protein, has also been suggested as an inhibitor of VEGF receptor 2 mediated angiogenesis although the precise role of its ASARM peptide in this circumstance has yet to be elucidated [69].

To conclude, our studies detail for the first time the functional role that MEPE and its ASARM peptide have in chondrocyte matrix mineralization. We have shown MEPE to be expressed by growth plate chondrocytes, in particular in the hypertrophic zone of chondrocytes consistent with a role in matrix mineralization. We have shown this role to be dependent upon the extent of the cleavage and subsequent phosphorylation of MEPE, and that mechanisms may exist which positively regulate the further expression of MEPE. Our studies complement previous findings of MEPE and its role in biomineralization; however, much remains to be learnt regarding the in vivo role of MEPE and the ASARM peptide in bone disease.

Supplementary data related to this article can be found online at http://dx.doi.org/10.1016/j.bone.2012.06.022.

Acknowledgments

The authors thank Graham Williams and Marta Archanco (Imperial College London, UK) for assistance with the in situ hybridization technique, and Ola Nilsson and Anenisia Andrade (The Karolinska Institutet, Sweden) for their assistance with the microdissection technique. We thank Debiao Zhao (Roslin Institute, UK) for the pLZ2.Ub-GFP vectors and Elaine Seawright (Roslin Institute, UK) for technical assistance during the completion of these studies. The authors also would like to recognise the European Calcified Tissue Society for providing a lab exchange grant. We also acknowledge the support of an NIH grant to PR (R01AR051598-06A2), Diabetes UK for funding to CC, and the BBSRC for funding to KS, VM, and CF.

References

[1] Kronenberg HM. Developmental regulation of the growth plate. Nature 2003;423:332–6.
[2] Anderson HC. Molecular biology of matrix vesicles. Clin Orthop Relat Res 1995:266–80.
[3] Meyer JL. Can biological calcification occur in the presence of pyrophosphate? Arch Biochem Biophys 1984;231:1–8.
[4] Rowe PS, de Zoysa PA, Dong R, Wang HR, White KE, Econs MJ, et al. MEPE, a new gene expressed in bone marrow and tumors causing osteomalacia. Genomics 2000;67:54–68.
[5] Fisher LW, Fedarko NS. Six genes expressed in bones and teeth encode the current members of the SIBLING family of proteins. Connect Tissue Res 2003;44(Suppl. 1):33–40.
[6] Qin C, Brunn JC, Jones J, George A, Ramachandran A, Gorski JP, et al. A comparative study of sialic acid-rich proteins in rat bone and dentin. Eur J Oral Sci 2001;109:133–41.
[7] Aplin HM, Hirst KL, Crosby AH, Dixon MJ. Mapping of the human dentin matrix acidic phosphoprotein gene (DMP1) to the dentinogenesis imperfecta type II critical region at chromosome 4q21. Genomics 1995;30:347–9.
[8] Crosby AH, Lyu MS, Lin K, McBride OW, Kerr JM, Aplin HM, et al. Mapping of the human and mouse bone sialoprotein and osteopontin loci. Mamm Genome 1996;7:149–51.
[9] Nampei A, Hashimoto J, Hayashida K, Tsuboi H, Shi K, Tsuji I, et al. Matrix extracellular phosphoglycoprotein (MEPE) is highly expressed in osteocytes in human bone. J Bone Miner Metab 2004;22:176–84.
[10] Argiro L, Desbarats M, Glorieux FH, Ecarot B. Mepe, the gene encoding a tumor-secreted protein in oncogenic hypophosphatemic osteomalacia, is expressed in bone. Genomics 2001;74:342–51.
[11] Petersen DN, Tkalcevic GT, Mansolf AL, Rivera-Gonzalez R, Brown TA. Identification of osteoblast/osteocyte factor 45 (OF45), a bone-specific cDNA encoding an RGD-containing protein that is highly expressed in osteoblasts and osteocytes. J Biol Chem 2000;275:36172–80.
[12] Gowen LC, Petersen DN, Mansolf AL, Qi H, Stock JL, Tkalcevic GT, et al. Targeted disruption of the osteoblast/osteocyte factor 45 gene (OF45) results in increased bone formation and bone mass. J Biol Chem 2003;278:1998–2007.
[13] David V, Martin A, Hedge AM, Rowe PS. Matrix extracellular phosphoglycoprotein (MEPE) is a new bone renal hormone and vascularization modulator. Endocrinology 2009;150:4012–23.
[14] Martin A, David V, Laurence JS, Schwarz PM, Lafer EM, Hedge AM, et al. Degradation of MEPE, DMP1, and release of SIBLING ASARM-peptides (minhibins): ASARM-peptide(s) are directly responsible for defective mineralization in HYP. Endocrinology 2008;149:1757–72.
[15] Rowe PS, Kumagai Y, Gutierrez G, Garrett IR, Blacher R, Rosen D, et al. MEPE has the properties of an osteoblastic phosphatonin and minhibin. Bone 2004;34:303–19.

[16] Rowe PS, Matsumoto N, Jo OD, Shih RN, Oconnor J, Roudier MP, et al. Correction of the mineralization defect in hyp mice treated with protease inhibitors CA074 and pepstatin. Bone 2006;39:773–86.
[17] Guo R, Rowe PS, Liu S, Simpson LG, Xiao ZS, Quarles LD. Inhibition of MEPE cleavage by Phex. Biochem Biophys Res Commun 2002;297:38–45.
[18] Addison WN, Nakano Y, Loisel T, Crine P, McKee MD. MEPE-ASARM peptides control extracellular matrix mineralization by binding to hydroxyapatite: an inhibition regulated by PHEX cleavage of ASARM. J Bone Miner Res 2008;23:1638–49.
[19] Stevens DA, Hasserjian RP, Robson H, Siebler T, Shalet SM, Williams GR. Thyroid hormones regulate hypertrophic chondrocyte differentiation and expression of parathyroid hormone-related peptide and its receptor during endochondral bone formation. J Bone Miner Res 2000;15:2431–42.
[20] Nilsson O, Parker EA, Hegde A, Chau M, Barnes KM, Baron J. Gradients in bone morphogenetic protein-related gene expression across the growth plate. J Endocrinol 2007;193:75–84.
[21] Heinrichs C, Yanovski JA, Roth AH, Yu YM, Domene HM, Yano K, et al. Dexamethasone increases growth hormone receptor messenger ribonucleic acid levels in liver and growth plate. Endocrinology 1994;135:1113–8.
[22] Mushtaq T, Bijman P, Ahmed SF, Farquharson C. Insulin-like growth factor-I augments chondrocyte hypertrophy and reverses glucocorticoid-mediated growth retardation in fetal mice metatarsal cultures. Endocrinology 2004;145:2478–86.
[23] Owen HC, Miner JN, Ahmed SF, Farquharson C. The growth plate sparing effects of the selective glucocorticoid receptor modulator, AL-438. Mol Cell Endocrinol 2007;264:164–70.
[24] MacRae VE, Farquharson C, Ahmed SF. The restricted potential for recovery of growth plate chondrogenesis and longitudinal bone growth following exposure to pro-inflammatory cytokines. J Endocrinol 2006;189:319–28.
[25] Haaijman A, Karperien M, Lanske B, Hendriks J, Lowik CW, Bronckers AL, et al. Inhibition of terminal chondrocyte differentiation by bone morphogenetic protein 7 (OP-1) in vitro depends on the periarticular region but is independent of parathyroid hormone-related peptide. Bone 1999;25:397–404.
[26] Shukunami C, Ishizeki K, Atsumi T, Ohta Y, Suzuki F, Hiraki Y. Cellular hypertrophy and calcification of embryonal carcinoma-derived chondrogenic cell line ATDC5 in vitro. J Bone Miner Res 1997;12:1174–88.
[27] Zhang L, Conejo-Garcia JR, Yang N, Huang W, Mohamed-Hadley A, Yao W, et al. Different effects of glucose starvation on expression and stability of VEGF mRNA isoforms in murine ovarian cancer cells. Biochem Biophys Res Commun 2002;292:860–8.
[28] MacRae VE, Davey MG, McTeir L, Narisawa S, Yadav MC, Millan JL, et al. Inhibition of PHOSPHO1 activity results in impaired skeletal mineralization during limb development of the chick. Bone 2010;46:1146–55.
[29] Prideaux M, Loveridge N, Pitsillides AA, Farquharson C. Extracellular matrix mineralization promotes E11/gp38 glycoprotein expression and drives osteocytic differentiation. PLoS One 2012;7:e36786.
[30] Saito A, Hino S, Murakami T, Kanemoto S, Kondo S, Saitoh M, et al. Regulation of endoplasmic reticulum stress response by a BBF2H7-mediated Sec23a pathway is essential for chondrogenesis. Nat Cell Biol 2009;11:1197–204.
[31] Hutchison MR, Bassett MH, White PC. Insulin-like growth factor-I and fibroblast growth factor, but not growth hormone, affect growth plate chondrocyte proliferation. Endocrinology 2007;148:3122–30.
[32] Gartland A, Mason-Savas A, Yang M, MacKay CA, Birnbaum MJ, Odgren PR. Septoclast deficiency accompanies postnatal growth plate chondrodysplasia in the toothless (tl) osteopetrotic, colony-stimulating factor-1 (CSF-1)-deficient rat and is partially responsive to CSF-1 injections. Am J Pathol 2009;175:2668–75.
[33] Lee ER, Lamplugh L, Shepard NL, Mort JS. The septoclast, a cathepsin B-rich cell involved in the resorption of growth plate cartilage. J Histochem Cytochem 1995;43:525–36.
[34] Altaf FM, Hering TM, Kazmi NH, Yoo JU, Johnstone B. Ascorbate-enhanced chondrogenesis of ATDC5 cells. Eur Cell Mater 2006;12:64–9.
[35] Anderson HC, Chacko S, Abbott J, Holtzer H. The loss of phenotypic traits by differentiated cells in vitro. VII. Effects of 5-bromodeoxyuridine and prolonged culturing on fine structure of chondrocytes. Am J Pathol 1970;60:289–312.
[36] Chacko S, Abbott J, Holtzer S, Holtzer H. The loss of phenotypic traits by differentiated cells. VI. Behavior of the progeny of a single chondrocyte. J Exp Med 1969;130:417–42.
[37] Nameroff M, Holtzer H. The loss of phenotypic traits by differentiated cells. IV. Changes in polysaccharides produced by dividing chondrocytes. Dev Biol 1967;16:250–81.
[38] Abbott J, Holtzer H. The loss of phenotypic traits by differentiated cells. 3. The reversible behavior of chondrocytes in primary cultures. J Cell Biol 1966;28:473–87.
[39] Gerber HP, Vu TH, Ryan AM, Kowalski J, Werb Z, Ferrara N. VEGF couples hypertrophic cartilage remodeling, ossification and angiogenesis during endochondral bone formation. Nat Med 1999;5:623–8.
[40] Zijlstra A, Aimes RT, Zhu D, Regazzoni K, Kupriyanova T, Seandel M, et al. Collagenolysis-dependent angiogenesis mediated by matrix metalloproteinase-13 (collagenase-3). J Biol Chem 2004;279:27633–45.
[41] Nagai H, Aoki M. Inhibition of growth plate angiogenesis and endochondral ossification with diminished expression of MMP-13 in hypertrophic chondrocytes in FGF-2-treated rats. J Bone Miner Metab 2002;20:142–7.
[42] Anderson HC, Sipe JB, Hessle L, Dhanyamraju R, Atti E, Camacho NP, et al. Impaired calcification around matrix vesicles of growth plate and bone in alkaline phosphatase-deficient mice. Am J Pathol 2004;164:841–7.
[43] Hessle L, Johnson KA, Anderson HC, Narisawa S, Sali A, Goding JW, et al. Tissue-nonspecific alkaline phosphatase and plasma cell membrane glycoprotein-1 are central antagonistic regulators of bone mineralization. Proc Natl Acad Sci U S A 2002;99:9445–9.
[44] Johnson K, Polewski M, van ED, Terkeltaub R. Chondrogenesis mediated by PPi depletion promotes spontaneous aortic calcification in NPP1−/− mice. Arterioscler Thromb Vasc Biol 2005;25:686–91.
[45] Nurnberg P, Thiele H, Chandler D, Hohne W, Cunningham ML, Ritter H, et al. Heterozygous mutations in ANKH, the human ortholog of the mouse progressive ankylosis gene, result in craniometaphyseal dysplasia. Nat Genet 2001;28:37–41.
[46] Sohn P, Crowley M, Slattery E, Serra R. Developmental and TGF-beta-mediated regulation of Ank mRNA expression in cartilage and bone. Osteoarthritis Cartilage 2002;10:482–90.
[47] Rowe PS. The wrickkened pathways of FGF23, MEPE and PHEX. Crit Rev Oral Biol Med 2004;15:264–81.
[48] Autosomal dominant hypophosphataemic rickets is associated with mutations in FGF23. Nat Genet 2000;26:345–8.
[49] Sitara D, Razzaque MS, Hesse M, Yoganathan S, Taguchi T, Erben RG, et al. Homozygous ablation of fibroblast growth factor-23 results in hyperphosphatemia and impaired skeletogenesis, and reverses hypophosphatemia in Phex-deficient mice. Matrix Biol 2004;23:421–32.
[50] Sitara D, Kim S, Razzaque MS, Bergwitz C, Taguchi T, Schuler C, et al. Genetic evidence of serum phosphate-independent functions of FGF-23 on bone. PLoS Genet 2008;4:e1000154.
[51] Yu X, White KE. FGF23 and disorders of phosphate homeostasis. Cytokine Growth Factor Rev 2005;16:221–32.
[52] Ogbureke KU, Fisher LW. Expression of SIBLINGs and their partner MMPs in salivary glands. J Dent Res 2004;83:664–70.
[53] Boukpessi T, Gaucher C, Leger T, Salmon B, Le FJ, Willig C, et al. Abnormal presence of the matrix extracellular phosphoglycoprotein-derived acidic serine- and aspartate-rich motif peptide in human hypophosphatemic dentin. Am J Pathol 2010;177:803–12.
[54] Bresler D, Bruder J, Mohnike K, Fraser WD, Rowe PS. Serum MEPE-ASARM-peptides are elevated in X-linked rickets (HYP): implications for phosphaturia and rickets. J Endocrinol 2004;183:R1–9.
[55] Atkins GJ, Rowe PS, Lim HP, Welldon KJ, Ormsby R, Wijenayaka AR, et al. Sclerostin is a locally acting regulator of late-osteoblast/preosteocyte differentiation and regulates mineralization through a MEPE-ASARM-dependent mechanism. J Bone Miner Res 2011;26:1425–36.
[56] Anderson HC. Matrix vesicles and calcification. Curr Rheumatol Rep 2003;5:222–6.
[57] Addison WN, Azari F, Sorensen ES, Kaartinen MT, McKee MD. Pyrophosphate inhibits mineralization of osteoblast cultures by binding to mineral, up-regulating osteopontin, and inhibiting alkaline phosphatase activity. J Biol Chem 2007;282:15872–83.
[58] Wang J, Zhou HY, Salih E, Xu L, Wunderlich L, Gu X, et al. Site-specific in vivo calcification and osteogenesis stimulated by bone sialoprotein. Calcif Tissue Int 2006;79:179–89.
[59] Yadav MC, Simao AM, Narisawa S, Huesa C, McKee MD, Farquharson C, et al. Loss of skeletal mineralization by the simultaneous ablation of PHOSPHO1 and alkaline phosphatase function: a unified model of the mechanisms of initiation of skeletal calcification. J Bone Miner Res 2011;26:286–97.
[60] Huesa C, Yadav MC, Finnila MA, Goodyear SR, Robins SP, Tanner KE, et al. PHOSPHO1 is essential for mechanically competent mineralization and the avoidance of spontaneous fractures. Bone 2011;48:1066–74.
[61] Sprowson AP, McCaskie AW, Birch MA. ASARM-truncated MEPE and AC-100 enhance osteogenesis by promoting osteoprogenitor adhesion. J Orthop Res 2008;26:1256–62.
[62] Hayashibara T, Hiraga T, Yi B, Nomizu M, Kumagai Y, Nishimura R, et al. A synthetic peptide fragment of human MEPE stimulates new bone formation in vitro and in vivo. J Bone Miner Res 2004;19:455–62.
[63] Boskey AL, Chiang P, Fermanis A, Brown J, Taleb H, David V, et al. MEPE's diverse effects on mineralization. Calcif Tissue Int 2009;86(1):42–6.
[64] Rowe PS. The chicken or the egg: PHEX, FGF23 and SIBLINGs unscrambled. Cell Biochem Funct 2012;30(5):355–75.
[65] Rowe PS, Garrett IR, Schwarz PM, Carnes DL, Lafer EM, Mundy GR, et al. Surface plasmon resonance (SPR) confirms that MEPE binds to PHEX via the MEPE-ASARM motif: a model for impaired mineralization in X-linked rickets (HYP). Bone 2005;36:33–46.
[66] Liu S, Rowe PS, Vierthaler L, Zhou J, Quarles LD. Phosphorylated acidic serine-aspartate-rich MEPE-associated motif peptide from matrix extracellular phosphoglycoprotein inhibits phosphate regulating gene with homologies to endopeptidases on the X-chromosome enzyme activity. J Endocrinol 2007;192:261–7.
[67] Zelzer E, McLean W, Ng YS, Fukai N, Reginato AM, Lovejoy S, et al. Skeletal defects in VEGF(120/120) mice reveal multiple roles for VEGF in skeletogenesis. Development 2002;129:1893–904.
[68] Stickens D, Behonick DJ, Ortega N, Heyer B, Hartenstein B, Yu Y, et al. Altered endochondral bone development in matrix metalloproteinase 13-deficient mice. Development 2004;131:5883–95.
[69] Pirotte S, Lamour V, Lambert V, varez Gonzalez ML, Ormenese S, Noel A, et al. Dentin matrix protein 1 induces membrane expression of VE-cadherin on endothelial cells and inhibits VEGF-induced angiogenesis by blocking VEGFR-2 phosphorylation. Blood 2011;117:2515–26.

REVIEW

The importance of the SIBLING family of proteins on skeletal mineralisation and bone remodelling

Katherine A Staines, Vicky E MacRae and **Colin Farquharson**

The Roslin Institute and Royal (Dick) School of Veterinary Studies, The University of Edinburgh, Easter Bush, Edinburgh, Midlothian EH25 9RG, UK
(Correspondence should be addressed to K A Staines; Email: katherine.staines@roslin.ed.ac.uk)

Abstract

The small integrin-binding ligand N-linked glycoprotein (SIBLING) family consists of osteopontin, bone sialoprotein, dentin matrix protein 1, dentin sialophosphoprotein and matrix extracellular phosphoglycoprotein. These proteins share many structural characteristics and are primarily located in bone and dentin. Accumulating evidence has implicated the SIBLING proteins in matrix mineralisation. Therefore, in this review, we discuss the individual role that each of the SIBLING proteins has in this highly orchestrated process. In particular, we emphasise how the nature and extent of their proteolytic processing and post-translational modification affect their functional role. Finally, we describe the likely roles of the SIBLING proteins in clinical disorders of hypophosphataemia and their potential therapeutic use.

Journal of Endocrinology (2012) **214,** 241–255

Introduction

The skeleton is a highly intricate and complex organ that has a range of functions spanning from locomotion to ion homoeostasis. It is structurally adapted to suit its function: strong and stiff to withstand loading and yet light for movement and flexible to prevent fracture. The organic component of bone, termed the osteoid, comprises an extracellular matrix (ECM) primarily composed of collagen type I together with several non-collagenous proteins (NCPs).

One such family of NCPs is the small integrin-binding ligand N-linked glycoprotein (SIBLING) family. This consists of osteopontin (OPN), bone sialoprotein (BSP (IBSP)), dentin matrix protein 1 (DMP1), dentin sialophosphoprotein (DSPP) and matrix extracellular phosphoglycoprotein (MEPE). It is likely that this protein family arose from the secretory calcium-binding phosphoprotein family by gene duplication due to their apparent common evolutionary heritage, as is elegantly reviewed by Kawasaki & Weiss (2006), Kawasaki *et al.* (2007), Kawasaki (2011) and Rowe (2012). It is therefore somewhat surprising that the SIBLING proteins have little intrinsic sequence homology and yet they share the following characteristics: i) all are located to a 375 kb region on the human chromosome 4q21 and mouse chromosome 5q, ii) display similar exon structures, iii) display an Arg-Gly-Asp (RGD) motif that mediates cell attachment/signalling and iv) are principally expressed in bone and dentin and are secreted into the ECM during osteoid formation and subsequent mineralisation. These similarities in SIBLING gene and protein structure have been well illustrated in other reviews (Rowe *et al.* 2000, Fisher *et al.* 2001, Fisher & Fedarko 2003, Qin *et al.* 2004, Rowe 2004, 2012, Huq *et al.* 2005, Bellahcene *et al.* 2008).

All SIBLING proteins undergo similar post-translational modifications such as phosphorylation and glycosylation, the extent of which is crucial in determining their function (Boskey *et al.* 2009). It has long been known that the SIBLING proteins have an RGD sequence that facilitates cell attachment and cell signalling by binding to cell surface integrins (Fisher *et al.* 2001). More recently, work by Rowe *et al.* (2000, 2004), primarily focused on MEPE, has identified a new functional domain termed the acidic serine- and aspirate-rich motif (ASARM) peptide, which is highly conserved across species. This peptide is proving critical in the functional activity of the SIBLING proteins, as is evidenced by the ASARM hypothesis proposed by Peter Rowe (Rowe 2004, David *et al.* 2010). This hypothesis describes the role of the SIBLING ASARM peptides, the cell membrane-associated glycoprotein phosphate-regulating endopeptidase homologue, X-linked (PHEX) and fibroblast growth factor 23 (FGF23) in bone renal phosphate (P_i) homoeostasis and mineralisation. This hypothesis can be used to explain numerous disorders of mineralisation including tumour-induced osteomalacia, autosomal-dominant

DOI: 10.1530/JOE-12-0143
0022–0795/12/0214–241
Online version via http://www.endocrinology-journals.org

hypophosphataemic rickets (ADHR) and X-linked hypophosphataemic rickets (XLH) and will be discussed in more detail in this review.

The SIBLING proteins have been extensively reviewed individually; however, in the present review, we focus on the role that each of the SIBLING proteins has on skeletal matrix mineralisation and bone remodelling, as well as their clinical relevance in disorders of bone matrix mineralisation and bone remodelling (Denhardt & Guo 1993, Ganss *et al.* 1999, Sodek *et al.* 2000, Fisher *et al.* 2001, Prasad *et al.* 2010).

Matrix mineralisation and bone remodelling

Endochondral ossification is a carefully orchestrated process responsible for the formation and postnatal linear growth of the long bones. It involves the replacement of a cartilage scaffold by mineralised bone. Integral to this process is the epiphyseal growth plate, a highly specialised cartilaginous structure derived from a mesenchyme precursor that is located between the head and the shaft of the bone. The growth plate consists of chondrocytes arranged in columns that parallel the axis of the bone surrounded by their ECM that is rich in collagens, proteoglycans and numerous other NCPs (Ballock & O'Keefe 2003, Mackie *et al.* 2008, 2011, Gentili & Cancedda 2009, Heinegard 2009). The chondrocytes of the growth plate sit in distinct cellular zones of maturation and proceed through various stages of differentiation while maintaining their spatially fixed locations (Hunziker *et al.* 1987). It is the terminally differentiated hypertrophic chondrocyte that mineralises its surrounding ECM, localised to the longitudinal septa of the growth plate (Castagnola *et al.* 1988).

Chondrocyte, as well as osteoblast, mineralisation of the ECM is widely accepted to involve membrane-limited matrix vesicles (MVs) within which calcium (Ca^{2+}) and inorganic P_i accumulate to initiate the biphasic process of mineralisation (Anderson 2003). When sufficient concentrations of both exist, Ca^{2+} and P_i begins to precipitate to form hydroxyapatite (HA) crystals. This initial stage of mineralisation is followed by the penetration of HA crystals through the MV trilaminar membrane and the modulation of ECM composition, promoting the propagation of HA outside of the MVs (Anderson 1995, 2003, Wu *et al.* 2002, Golub 2011).

Mineralisation of the ECM is a tightly regulated process such that concentrations of Ca^{2+} and P_i are permissive for effective mineralisation and that the levels of mineralisation inhibitors such as inorganic pyrophosphate (PP_i) and matrix gla protein are balanced. Extracellular PP_i is a well-recognised and potent inhibitor of mineralisation that is regulated by ALP (Meyer 1984). In bone, ALP is an ectoenzyme located on the cell membrane's outer surface of osteoblasts and chondrocytes as well as on the membrane of their MVs (Anderson 1995). Classically, ALP was thought to generate the P_i required for HA formation; however, it has since been shown to also hydrolyse PP_i, thus achieving a ratio of P_i/PP_i permissive for HA crystal formation and growth (Moss *et al.* 1967, Majeska & Wuthier 1975, Hessle *et al.* 2002, Anderson 2003). PP_i inhibits the enzymatic activity of ALP, offering a feedback loop by which mineralisation is regulated (Addison *et al.* 2007).

Other regulators of ECM biomineralisation include nucleotide pyrophosphatase phosphodiesterase 1 (NPP1) and the ankylosis protein (ANK) that work in synergy to increase extracellular PP_i levels. While NPP1 ectoplasmically generates PP_i from nucleoside triphosphates, ANK mediates its intracellular to extracellular channelling (Hakim *et al.* 1984, Terkeltaub *et al.* 1994, Ho *et al.* 2000). Analysis of mutant mice deficient in ALP function ($Akp2^{-/-}$ ($Alpl^{-/-}$)), which were surprisingly found to exhibit normal levels of bone mineralisation at birth, led us to search for other phosphatases that might also contribute to bone mineralisation, and this led to our description of PHOSPHO1 (Houston *et al.* 2002). As its discovery and characterisation, PHOSPHO1 has been proposed to play a crucial role in the accumulation of P_i within the MV and bone mineralisation (Houston *et al.* 2002, Stewart *et al.* 2006, Roberts *et al.* 2007, 2008, MacRae *et al.* 2010, Huesa *et al.* 2011). PHOSPHO1 has a non-redundant functional role during bone mineralisation, and the ablation of both PHOSPHO1 and ALP results in the complete lack of bone mineralisation throughout the whole skeleton (Yadav *et al.* 2011).

Mineralisation of the ECM not only facilitates the deposition of HA but also enables vascular invasion, a significant phase in endochondral ossification and the development of the skeleton. Hypertrophic chondrocytes express factors such as vascular endothelial growth factor (VEGF) that induce vascular invasion, allowing the infiltration of osteoclasts and differentiating osteoblasts that resorb the cartilaginous mineralised matrix and replace it with trabecular bone respectively (Zelzer *et al.* 2002). This process of bone remodelling continues throughout life and is responsible for the annual replacement of ~10% of the adult skeleton (Frost 1990). Tight regulation of this process maintains an equilibrium such that disorders of bone mass, such as osteoporosis or osteopetrosis, do not occur (Manolagas 2000). During bone resorption, osteoclasts adhere to the bone surface forming a tight connection and allowing efficient resorption through extracellular acidification (Palokangas *et al.* 1997, Mellis *et al.* 2011). Like bone formation, this is under tight control by a variety of autocrine, paracrine, and endocrine factors and is thought to be primarily regulated by the terminally differentiated osteoblast, the osteocyte (Hill 1998, Manolagas 2000, Henriksen *et al.* 2009).

The SIBLING family of proteins

The SIBLING family of proteins consists of OPN, BSP, DMP1, DSPP and MEPE, all of which share common characteristics. Despite this, they display differential tissue distributions and functions that are highly dependent on their

post-translational modifications. The key role that each of the SIBLING proteins plays in biomineralisation is described in detail below (Fig. 1).

Matrix extracellular phosphoglycoprotein

MEPE, originally identified as a substrate for PHEX, is primarily expressed by osteocytes as well as by osteoblasts (Nampei *et al*. 2004). In the mouse skeleton, *Mepe* is detected as early as 2 days *post partum*, and several regulators of this expression have been documented in the literature (Lu *et al*. 2004). The addition of FGF2 to osteoblasts downregulates *Mepe* levels in a dose-dependent manner. The mechanism of action is part through the MAPK pathway (Zhang *et al*. 2004). Furthermore, osteoblasts stimulated by bone morphogenetic protein 2 (BMP2) also display a decreased *Mepe* expression level (Siggelkow *et al*. 2004). Recently, it has been shown that Wnt3a, a canonical Wnt signalling stimulator, induces this BMP2 signal and also as has its own direct stimulatory effects on *Mepe* expression through β-catenin and LEF1 (Cho *et al*. 2011).

The first evidence for a direct role of MEPE in bone mineralisation came from the increased mRNA expression levels of *Mepe* seen during osteoblast matrix mineralisation (Petersen *et al*. 2000, Argiro *et al*. 2001). The development of a *Mepe* null mouse further fuelled the proposed role of MEPE in mineralisation. This mouse model had increased bone mass with associated increased numbers and thickness of trabeculae. The mineral apposition rate (MAR) was dramatically increased as was the activity of *Mepe* null osteoblasts in culture (Gowen *et al*. 2003). Conversely, the overexpression of MEPE in mice, under the control of the col1a1 promoter, leads to a growth and mineralisation defect due to a decrease in bone remodelling. *Mepe* transgenic mice displayed wider epiphyseal growth plates and expanded primary spongiosa and a significant decrease in the MAR (David *et al*. 2009).

Like the other SIBLING proteins, the activity of MEPE is dependent on its state of cleavage and its phosphorylation. Recent work has identified the 2·2 kDa ASARM peptide of MEPE as the functional component of MEPE. This ASARM peptide is highly conserved across the SIBLING proteins, and in MEPE it is located immediately downstream of a

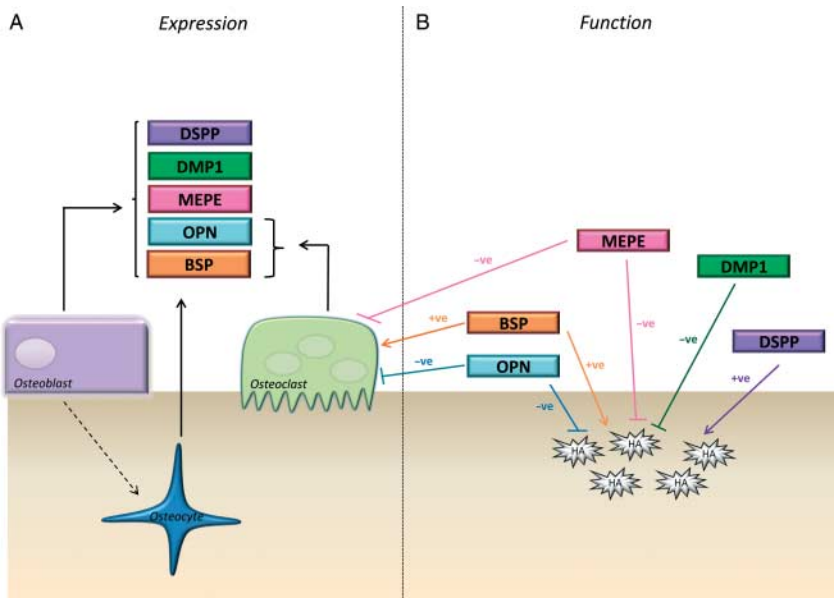

Figure 1 A schematic figure detailing the (A) expression and (B) function of the SIBLING family of proteins: dentin sialophosphoprotein (DSPP), dentin matrix protein 1 (DMP1), bone sialoprotein (BSP), matrix extracellular phosphoglycoprotein (MEPE) and osteopontin (OPN). MEPE is expressed by osteoblasts and the terminally differentiated osteoblast (indicated by the dashed arrow), the osteocyte. MEPE directly inhibits hydroxyapatite (HA) formation in bone through its cleavage product, a small acidic serine- and aspirate-rich motif (ASARM) that undergoes post-translational phosphorylation. MEPE also inhibits the numbers and activities of osteoclasts. OPN has similar functional effects to MEPE in bone mineralisation; however, along with BSP, it is also expressed by osteoclasts. BSP is well established as a HA nucleator and is proving pivotal in diseases of increased bone formation as it increases osteoclastogenesis. DMP1 and DSPP are both expressed by bone and both are processed into numerous fragments. While DSPP promotes biomineralisation in both bones and teeth, DMP1 inhibits it. The full details of the cleavage products of the SIBLING proteins and their roles in biomineralisation are detailed in Table 1.

Table 1 The functional role of each of the SIBLING proteins: dentin sialophosphoprotein (DSPP), dentin matrix protein 1 (DMP1), bone sialoprotein (BSP), matrix extracellular phosphoglycoprotein (MEPE) and osteopontin (OPN), in biomineralisation and phosphate homoeostasis, as is dependent on their cleavage and post-translational modification. Detailed are i) the cellular expression pattern, ii) the phenotype of the knockout mouse, iii) the phenotype of transgenic mice, iv) clinical conditions associated with mutation in this gene, v) cleavage product and post-translational modification, vi) known role of each cleavage product in ECM mineralisation, vii) role of cleavage product mineral metabolism, and viii) list of relevant references

		Mouse bone phenotype						
	Cellular expression pattern	Knockout	Overexpression	**Clinical condition of gene mutation**	**Cleavage product and post-translational modification**	**Role of cleavage products in mineralisation**	**Role of cleavage products in mineral metabolism**	**References**
Protein								
MEPE	Osteoblasts and osteocytes	Increased bone mass, MAR, trabecular number and thickness	Decreased MAR, bone remodelling, bone mass and increased growth plate widths	Unknown	> ASARM peptide-3 serine phosphorylation > AC100	Inhibition Promotion	ASARM peptide inhibits phosphate uptake in the kidney and increases FGF23	Gowen *et al.* (2003), Hayashibara *et al.* (2004), Nampei *et al.* (2004), Addison *et al.* (2008), Marks *et al.* (2008), Martin *et al.* (2008) and David *et al.* (2009)
DMP1	Osteoblasts, osteoclasts, osteocytes, hypertrophic chondrocytes and dentin	Lower mineral content, defective cartilage formation resembling dwarfism with chondrodysplasia. Hypophosphataemia and increased FGF23	Narrow growth plate with accelerated mineralisation and increased bone turnover	Autosomal recessive hypophosphataemic rickets	Full-length, unphosphorylated DMP1 Full-length, phosphorylated DMP1 N-terminal fragment C-terminal fragment ASARM peptide	Promotion Inhibition Promotion Promotion Inhibition	Interacts with PHEX to orchestrate P_i homoeostasis through decreasing FGF23 levels	Toyosawa *et al.* (2001), Fen *et al.* (2002), Feng *et al.* (2003), Qin *et al.* (2003), Tartaix *et al.* (2004), Ye *et al.* (2005), Feng *et al.* (2006) and Martin *et al.* (2008)
OPN	Osteoblasts, osteoclasts, osteocytes and hypertrophic chondrocytes	Increased mineral content and size Increased osteoclast production	Bone phenotype not defined	Unknown	> ASARM peptide-3 serine phosphorylation > N-terminal fragment > C-terminal fragment > Central fragment	Inhibition Promotion Promotion Inhibition	*Opn* knockout mice have no differences in serum P_i or Ca^{2+}; however, known interactions with PTH suggest an indirect role	Dodds *et al.* (1995), Sodek *et al.* (1995), Boskey *et al.* (2002, 2012), Landis *et al.* (2003) and Addison *et al.* (2007)
BSP	Osteoblasts, osteoclasts, osteocytes, chondrocytes and dentin	Short hypomineralised bones with high trabecular bone mass and low bone turnover	Multi-dwarfism decreased BMD and decreased trabecular bone volume	Unknown	Unknown	Promoter	*Bsp* transgenic mice have increased Ca^{2+} levels but no difference in P_i levels compared with WT mice	Chen *et al.* (1992), Gordon *et al.* (2007), Malaval *et al.* (2008) and Valverde *et al.* (2008)

(continued)

Table 1 *Continued*

	Cellular expression pattern	Mouse bone phenotype		Clinical condition of gene mutation	Cleavage product and post-translational modification	Role of cleavage products in mineralisation	Role of cleavage products in mineral metabolism	References
		Knockout	Overexpression					
DSPP	Dentin, bone and cementum	Defect in dentin mineralisation. Bones display accelerated mineralisation and changes in structural properties	DSP-accelerated mineralisation in teeth yet DPP-deleterious effects on enamel	Dentinogenesis imperfecta type II/III and dentine dysplasia	DPP, phosphorylated DPP, unphosphorylated DSP DGP	Promoter No effect Promoter Unknown	DPP fragment (ASARM containing) may competitively displace the DMP1–PHEX complex)	Sreenath *et al.* (2003), Kim *et al.* (2005), Yamakoshi *et al.* (2005), Verdelis *et al.* (2008) and Prasad *et al.* (2010)

cathepsin B cleavage site (Rowe *et al.* 2000). The administration of the MEPE–ASARM peptide *in vitro* and *in vivo* can inhibit the uptake of P_i. This is likely through a decreased expression of the type II sodium-dependent P_i cotransporter NPT2a, or through the promotion of FGF23 expression, a potent inhibitor of P_i (Liu *et al.* 2007, Dobbie *et al.* 2008, Marks *et al.* 2008, Martin *et al.* 2008, David *et al.* 2010, Shirley *et al.* 2010). It has, however, been suggested that MEPE may have a direct effect on matrix mineralisation outwith the supply and demand of P_i. The ASARM peptide of MEPE inhibits mineralisation by osteoblasts by directly binding to HA crystals (Addison *et al.* 2008, Martin *et al.* 2008). Integral to this inhibitory effect is the post-translational phosphorylation of the ASARM peptide at three serine residues. In osteoblasts, it appears that without this phosphorylation, the ASARM peptide has no effect on mineralisation (Addison *et al.* 2008, Martin *et al.* 2008). This is not the only evidence for a role for MEPE in the promotion of mineralisation. Recently, it has been shown that a truncated form of MEPE, which has the ASARM peptide removed, can promote bone mineralisation in culture and in mice (Sprowson *et al.* 2008). Furthermore, a mid-terminal fragment of MEPE (termed 'AC100') has been shown to enhance cell binding, through the stimulation of focal adhesion kinase and ERK (Hayashibara *et al.* 2004). Taken together, these results highlight the importance of post-translational processing in determining the functional role of MEPE.

The interaction between MEPE and PHEX is well documented in the literature. PHEX plays a central role in the protection of MEPE from proteolytic cleavage by cathepsin B; it can bind to MEPE and prevent the release of the ASARM peptide (Guo *et al.* 2002). The *Hyp* mouse, a spontaneous *Phex* knockout model, has an increased expression of cathepsin D, an upstream activator of cathepsin B (Rowe *et al.* 2006). This therefore suggests that PHEX can alter the activation of cathepsin B and therefore the cleavage of MEPE to the ASARM peptide. Furthermore, PHEX can bind to free ASARM peptides, therefore neutralising their activity by sequestration and hydrolysis (Liu *et al.* 2007, Addison *et al.* 2008, Martin *et al.* 2008). Recently, it has been shown that sclerostin (SCL), a potent inhibitor of the canonical Wnt signalling pathway, may act through the MEPE–PHEX axis, highlighting its significance in biomineralisation (Atkins *et al.* 2011).

Mepe transgenic mice display a decrease in ALP enzyme activity in both the growth plate and the primary spongiosa (David *et al.* 2009). *In vivo*, the addition of the phosphorylated ASARM peptide also reduced the number of ALP-positive cells in an osteoblast cell culture model (Martin *et al.* 2008). However, this remains controversial as normal ALP activity has been reported in osteoblasts treated with phosphorylated ASARM peptide (Addison *et al.* 2008). In the MEPE-overexpressing mouse, vascularisation is increased, as is VEGF expression, highlighting a role for MEPE in angiogenesis, an important stage in endochondral ossification (David *et al.* 2009). Consonant with angiogenesis is the

infiltration of osteoclasts for bone resorption. Interestingly, mice administered with recombinant MEPE or transgenic for MEPE had a significant decrease in the numbers and activity of osteoclasts (Hayashibara *et al.* 2007, David *et al.* 2009). This therefore suggests that MEPE is highly relevant to both bone mineralisation and P_i homoeostasis. Future studies should focus on the interactions between MEPE and the Wnt signalling pathway due to its known implications in bone and cartilage mechanobiology.

Osteopontin

OPN, also known as secreted phosphoprotein 1 (SPP1), is a 34 kDa protein, originally identified as the bridge between the cells and HA in the ECM of bone (Sodek *et al.* 2000). The protein and gene structures, as well as the localisation, of OPN are well described in several excellent reviews (Denhardt & Guo 1993, Sodek *et al.* 2000, Fisher *et al.* 2001). In bone, OPN is produced by osteoblasts and osteocytes, as well as osteoclasts (Dodds *et al.* 1995, Sodek *et al.* 1995, Zohar *et al.* 1997). It has also been localised to hypertrophic cartilage of the growth plate (Landis *et al.* 2003).

Several studies have documented the inhibitory role of OPN in HA formation and growth (Boskey *et al.* 1993, 2012, Hunter *et al.* 1994). It has also been shown to inhibit mineralisation in vascular smooth muscle cells (Wada *et al.* 1999, Jono *et al.* 2000). This inhibitory role of OPN is confirmed further by analysis of the *Opn* knockout mouse that has increased mineral content and size, as shown by Fourier transform infrared spectroscopy analysis in two different lines of $Opn^{-/-}$ mice at two different ages (Boskey *et al.* 2002). More specifically, it has recently been shown that the ASARM peptide of OPN inhibits ECM matrix mineralisation by binding to HA crystals (Addison *et al.* 2010, Boskey *et al.* 2012). Furthermore, a recent study by Boskey *et al.* showed the C- and N-terminal fragments of OPN, in this study, derived from milk OPN to promote *de novo* HA formation. Conversely, a central fragment inhibited it as is similar to bone OPN (Boskey *et al.* 2012). This highlights the importance of the post-translational fragmentation of OPN in determining its function. The study by Addison *et al.* (2010) also showed that, like MEPE, the ability of the OPN-ASARM to inhibit mineralisation is dependent on its phosphorylation at specific serine residues.

The importance of post-translational phosphorylation is further confirmed when examining the interaction between OPN, ALP and PP_i. Several studies have shown that ALP dephosphorylates OPN, thus preventing much of its inhibitory activity on HA formation and growth (Boskey *et al.* 1993, Hunter *et al.* 1994, Jono *et al.* 2000). Furthermore, PP_i directly upregulates *Opn* expression in osteoblasts, and therefore the hydrolysis of PP_i by ALP will have a significant effect on the expression levels of OPN (Addison *et al.* 2007). This is in concordance with the *Enpp1*-deficient mouse in which PP_i deficiency brings about a deficiency in OPN (Johnson *et al.* 2003). The *Akp2*-deficient mouse displays a similar decreased PP_i and OPN with an associated hypomineralisation. This hypomineralisation can be partially rescued by the double knockout: the $Akp2^{-/-}/Opn^{-/-}$ mouse (Harmey *et al.* 2006). Although previous studies have implicated a P_i-dependent mechanism (Beck *et al.* 2000, Beck & Knecht 2003), work by Addison *et al.* has implicated the MAPK signalling pathways responsible for the regulation of OPN by PP_i.

Analysis of the $Opn^{-/-}$ mouse has also indicated a role for OPN in the function and activity of osteoclasts. In these mice, there is an increase in osteoclast production, which could be a compensatory mechanism for the observed disabled motility and resorption activity of the osteoclast cells (Rittling *et al.* 1998, Chellaiah *et al.* 2003). Further studies have attempted to elucidate the precise role of OPN in bone resorption and have implicated CD44, a major cell surface receptor for hyaluronate (Aruffo *et al.* 1990) and a receptor for OPN (Suzuki *et al.* 2002, Chellaiah *et al.* 2003).

The loading of the skeleton in daily function results in the continuous modelling and remodelling of the skeleton (Frost 1990). This loading upregulates *OPN* expression in bone *in vivo*, and more recently it has been shown that the cyclical loading of rabbit joints has shown increased cellular *OPN* expression in the cartilage as well (Terai *et al.* 1999, Morinobu *et al.* 2003, Gross *et al.* 2005, King *et al.* 2005, Fujihara *et al.* 2006). This upregulation in response to loading has also been shown in *in vitro* cell cultures, and it is thought that MAPKs are involved in the transduction of the stimulus for *OPN* expression (Klein-Nulend *et al.* 1997, Owan *et al.* 1997, You *et al.* 2001). These intriguing results provide some clues into the molecular mechanisms underpinning adaptive bone remodelling.

Bone sialoprotein

BSP is a 70–80 kDa protein for which its gene and protein structures have been extensively reviewed (Ganss *et al.* 1999). The localisation of BSP is unique to the SIBLING family of proteins as it is exclusively located to the mineralised tissues such as bone, dentin and mineralising cartilage (Bianco *et al.* 1991, Chen *et al.* 1991). In bone, it is expressed in abundance by osteoblasts, as well as by osteoclasts, osteocytes and chondrocytes (Fisher & Fedarko 2003, Gordon *et al.* 2007).

During embryogenesis, BSP is first expressed at the onset of bone formation, thus suggesting it to be a strong candidate for a role in HA nucleation (Chen *et al.* 1992). This certainly seems convincing as numerous studies have documented BSP, which is localised to MVs, to be involved in the initial formation of HA (Harris *et al.* 2000, Fisher *et al.* 2001, Tye *et al.* 2003, Wang *et al.* 2006, Nahar *et al.* 2008). Indeed, the *Bsp* null mouse displays shorter, hypomineralised bones with associated higher trabecular bone mass with low bone turnover (Malaval *et al.* 2008). Moreover, it has been shown that as little as 9 nM BSP is required to nucleate HA, and recently the overexpression of BSP in osteoblasts has been shown to enhance mineralisation (Hunter *et al.* 1996,

Gordon *et al.* 2007). Similarly, osteoblast cultures grown in the presence of an anti-BSP antibody exhibit reduced mineralisation (Cooper *et al.* 1998, Mizuno *et al.* 2000). This nucleation potency is increased on BSP binding to collagen, suggesting a cooperative relationship (Baht *et al.* 2008).

The role of BSP as a HA nucleator is thought to involve the membrane-bound enzyme, ALP. Indeed, in the presence of BSP, high levels of ALP activity can promote the initiation of mineral deposition (Wang *et al.* 2006). This is further confirmed in BSP-overexpressing cell cultures that have a higher ALP activity (Valverde *et al.* 2008). It is likely that, like the other SIBLING proteins, the function of BSP is highly dependent on its post-translational modification (Stubbs *et al.* 1997).

BSP increases osteoclastogenesis and therefore bone resorption, making it crucial in the homoeostasis of bone remodelling (Ross *et al.* 1993, Raynal *et al.* 1996, Malaval *et al.* 2008, Valverde *et al.* 2008). This has been further examined in BSP transgenic mice in which an uncoupling of bone formation and resorption resulted in an osteopenia-like phenotype (Valverde *et al.* 2008). Furthermore, serum *BSP* expression in bone diseases characterised by excessive bone resorption, e.g. Paget's disease, is abnormally high (Valverde *et al.* 2008). This highlights the need to investigate whether antibodies to BSP could decrease the pathological bone loss observed in the *Bsp* transgenic mouse and as such be an important therapeutic target for patients with bone diseases characterised by high BSP.

Dentin sialophosphoprotein

The role of DSPP in biomineralisation has recently been reviewed (Prasad *et al.* 2010). Although originally thought to be exclusively expressed by dentin, DSPP is also expressed in bone, cementum and in non-mineralising tissues including the lung and kidney (Qin *et al.* 2002, Baba *et al.* 2004, Alvares *et al.* 2006, Ogbureke & Fisher 2007, Verdelis *et al.* 2008).

Analysis of the *Dspp* knockout mouse reveals defects in dentin mineralisation (Sreenath *et al.* 2003), as well as bone hypomineralisation (Verdelis *et al.* 2008). In humans, a mutation in the *DSPP* gene results in dentinogenesis imperfecta, characterised by dentin hypomineralisation and significant tooth decay (Kim *et al.* 2005). Of particular interest are the variations in the mineralisation properties observed at different ages in the $Dspp^{-/-}$ mouse. At 5 weeks of age, these mice displayed accelerated mineralisation, while at 9 months of age significant changes in bone structural properties were observed. This therefore suggests that DSPP has roles not only in the initial mineralisation of bone but also in the remodelling of the skeleton and therefore on bone turnover (Verdelis *et al.* 2008).

DSPP is proteolytically processed to two fragments: dentin phosphoprotein and dentin sialoprotein (DSP), both of which have important functions in mineralisation. Interestingly, a third fragment called dentin glycoprotein (DGP) has been identified as being cleaved from the C-terminal end of DSP by matrix metalloproteinase 2 (MMP2) and MMP20 (Yamakoshi *et al.* 2005). It has been suggested that the proteolytic processing of DSPP to DPP, DSP and DGP is the activating stage in the mechanism of DSPP function (Zhang *et al.* 2001, Qin *et al.* 2004, Prasad *et al.* 2010). The cleavage of DPP from DSPP is catalysed by a group of zinc metallopeptidases that includes BMP1, and it is this fragment of DSPP that contains the ASARM peptide (Tsuchiya *et al.* 2011). Various studies have shown DPP to be important in the formation and growth of HA as it has a strong affinity to Ca^{2+} when bound to collagen fibrils (Boskey *et al.* 1990, Saito *et al.* 1997, He *et al.* 2005). The phosphorylation of DPP is believed to be crucial to its function as removal of the phosphate groups results in a loss of its role in HA promotion (Saito *et al.* 1997). On the other hand, although DSP has been shown to be involved in the initiation of mineralisation, it appears not to have a functional role in the maturation of the tissue (Suzuki *et al.* 2009). The mechanism by which DSPP regulates HA formation is thought to involve the canonical BMP2 signalling pathway as BMP2 has been shown to increase *Dspp* expression via BMPR Smads, Runx2 and DIx5 (Iohara *et al.* 2004, Chen *et al.* 2008, Cho *et al.* 2010).

The vast information obtained about the DPP and DSP fragments over the past few decades serves to strengthen knowledge on the role of DSPP in biomineralisation. Future studies should focus on the recently identified DGP fragment and its specific functional role, as well as further detailing the mechanisms of DSP and DPP functions.

Dentin matrix protein 1

DMP1 was first cloned from dentin and has since been identified in dentin, bone and cementum as well as in other non-mineralised tissues (George *et al.* 1993, MacDougall *et al.* 1998, Sun *et al.* 2011). In bone, DMP1 is primarily expressed not only by osteocytes but also by osteoblasts and hypertrophic chondrocytes (Toyosawa *et al.* 2001, Fen *et al.* 2002, Feng *et al.* 2003).

The first evidence of a role for DMP1 in biomineralisation was its promotion of ECM mineralisation in MC3T3 cells overexpressing DMP1 (Narayanan *et al.* 2001). The generation of a *Dmp1*-null mouse has further fuelled the potential role of DMP1 in bone mineralisation. The knockout mice have significantly lower mineral content when compared with their control counterparts (Ling *et al.* 2005). Interestingly, the re-expression of DMP1 in these *Dmp1* null mice rescues the skeletal defects seen (Lu *et al.* 2011).

Additionally, the *Dmp1*-deficient mice displayed a severe defect in cartilage formation as is similar to the human hereditary hypophosphatemic disease autosomal recessive hypophosphatemic rickets (ARHR) that is caused by mutations in *Dmp1* (Feng *et al.* 2006, Farrow *et al.* 2009). These mice display a highly widened growth plate, suggesting an impairment of mineralisation at the chondro-osseous junction. Indeed, this cartilage defect results in a phenotype resembling dwarfism with chondrodysplasia (Ye *et al.* 2005).

It has since been shown that the distorted growth plates seen in the *Dmp1* null mouse are in fact due to disorganisation as opposed to growth plate enlargement (Sun *et al.* 2010). Interestingly, the *Dmp1* null mouse displays increased serum FGF23 levels and associated hypophosphataemia (Feng *et al.* 2006). Correction of this hypophosphataemia, by a high P_i diet, restored the *Dmp1* null mouse growth plate defect (Feng *et al.* 2006). Furthermore, the $DMP1^{-/-}$ and $FGF23^{-/-}$ double knockout mice display growth plate widths similar to that seen in the single *Fgf23* null mouse (Liu *et al.* 2008). This therefore suggests that the defective cartilage mineralisation observed in the *Dmp1* null mouse is not simply a direct consequence of the lack of DMP1. More recently, a transgenic mouse has been developed the expresses a mutant form of *Dmp1*. The substitution of Asp213 with Ala213 blocks the processing of mouse *Dmp1*. Crossing this transgenic mouse with the *Dmp1* null mouse recovered the growth plate disorganisation seen in the null mouse alone (Sun *et al.* 2011).

Like other SIBLING proteins, the proteolytic processing of DMP1 appears essential to its function and localisation. In bone and dentin, DMP1 is processed to two fragments: one 37 kDa fragment originating from the NH_2-terminal and one 57 kDa fragment originating from the COOH-terminal (Qin *et al.* 2003). In DMP1, it is the COOH-terminal fragment that contains the ASARM peptide (Martin *et al.* 2008). The full-length DMP1 is expressed at much lower levels than its fragments, which themselves have different localisation patterns in bone (Huang *et al.* 2008, Maciejewska *et al.* 2008). In the growth plate, while the NH_2-terminal fragment is localised to the resting, proliferation and pre-hypertrophic zones, the COOH-terminal fragment is found in the calcification front and ossification zone (Maciejewska *et al.* 2008).

The localisation of the COOH-terminal fragment is consistent with areas that are targets for the vascular invasion of the cartilage, a significant phase in matrix mineralisation. DMP1 has been postulated to play a role in angiogenesis as treatment with DMP1-induced vascular endothelial cadherin (VE-cadherin) and inhibited the VEGFR2 activity, therefore suggesting DMP1 to be an inhibitor of VEGF-induced angiogenesis (Pirotte *et al.* 2011). The direct role of DMP1 on HA formation is highly dependent on its processing and its post-translational modification. When phosphorylated, full-length DMP1 has been shown to inhibit the formation and growth of HA; however, its dephosphorylated form and its two fragments are well-established nucleators of HA formation (He *et al.* 2003, Tartaix *et al.* 2004, Gericke *et al.* 2010). Thus, native DMP1 inhibits mineralisation unless it becomes cleaved or dephosphorylated, in which case it initiates mineralisation (Tartaix *et al.* 2004).

In addition to the ASARM peptide, signalling pathways are involved in DMP1 function and have recently been investigated in osteoblasts. Wu *et al.* (2011) showed that DMP1, through the activation of the αvβ3 integrin, activated the downstream effectors of the MAPK pathway, ERK and JNK (Wu *et al.* 2011). Concomitant to this is the stimulation of phosphorylated JNK translocation coupled with an upregulation of phosphorylated c-jun activation (Wu *et al.* 2011). Furthermore, it has been shown that the internalisation of DMP1 not only results in a release of stored Ca^{2+} but also activates p38 MAP kinase (Eapen *et al.* 2011). *Dmp1* null mice have distinct abnormalities in the morphology and maturation of their osteocytes (Feng *et al.* 2006). The two DMP1 fragments also display differing localisation patterns in osteocytes (Maciejewska *et al.* 2009), suggesting that osteocytes may play a critical role in ECM mineralisation that involves DMP1. This is further supported by the stimulation of *DMP1* expression in response to mechanical loading (Gluhak-Heinrich *et al.* 2007). Furthermore, the deletion of DMP1 leads to a dramatic increase in *Fgf23* expression in the osteocytes, likely due to the defects seen in osteoblast–osteocyte transition (Feng *et al.* 2006, Qin *et al.* 2007). FGF23, a hormone produced by osteoblasts and osteocytes, has allowed the definition of bone as an endocrine organ as it targets the kidney to regulate P_i homoeostasis. This therefore suggests that DMP1 can control P_i levels, as is consistent with the hypophosphataemia observed in the *Dmp1* null mouse (Ye *et al.* 2005, Feng *et al.* 2006). This important discovery has allowed the further development of the ASARM hypothesis and has implicated DMP1 as central to biomineralisation and P_i homoeostasis.

The ASARM hypothesis and bone diseases

Accumulating evidence has implicated the members of the SIBLING family of proteins in bone and mineralisation diseases. Their varying involvements in the process of matrix mineralisation make them potentially attractive candidates for therapeutic targets and therapies.

XLH is the most common form of inherited rickets, characterised by defective bone and tooth mineralisation, growth retardation and defective renal reabsorption of P_i (Carpenter *et al.* 2011). Mutations in PHEX have been associated with XLH in humans and have led to the development of the *Hyp* mouse (Holm *et al.* 1997). Hypophosphataemia alone is insufficient to explain the bone defect seen in the *Hyp* mouse as correction of the hypophosphataemia failed to correct the mineralisation defect observed (Ecarot *et al.* 1992, Rowe *et al.* 2006). Furthermore, when osteoblast cells from the *Hyp* mouse are grown in culture, they have defective ECM production and thus reduced mineralisation (Xiao *et al.* 1998). This therefore suggests that PHEX has multiple substrates that are involved in regulating mineralisation directly and this has allowed the creation of the ASARM hypothesis, as previously mentioned and as has recently been elegantly reviewed (Rowe 2004, 2012, David *et al.* 2010). The ASARM hypothesis is based on the concept of a minhibin, an unknown secreted factor that is a substrate for PHEX and therefore would accumulate in the *Hyp* mouse and in patients with XLH.

MEPE was first identified as a potential substrate for PHEX; however, *in vitro* studies have failed to demonstrate

PHEX-dependent hydrolysis of MEPE (Guo *et al.* 2002). It has also been suggested that PHEX is likely responsible for the cleavage of DMP1 and DSPP, as it has a strong preference for cleaving bonds at the N-terminal of these two SIBLING proteins (Qin *et al.* 2004). However, analysis of the *Hyp* mouse indicated no differences in *Dmp1* and *Dspp* expression in comparison with their WT controls, suggesting that DMP1 and DSPP are in fact properly processed in the *Phex*-deficient mouse (Zhang *et al.* 2010). In addition to this, there is an accumulation of SIBLING ASARM peptides in the *Hyp* mouse and patients, thus challenging the hypothesis that the SIBLING proteins are substrates for PHEX. Instead, it appears that it is the ASARM peptide that PHEX digests (Addison *et al.* 2008, 2010), and the rise in SIBLING ASARM peptides in the *Hyp* mouse and XLH therefore further implicates them as substrates for PHEX (Bresler *et al.* 2004, Martin *et al.* 2008, Boukpessi *et al.* 2010).

It also appears that PHEX regulates *Fgf23* expression as increased *Fgf23* expression is observed in the *Hyp* mouse and patients with XLH (Liu *et al.* 2006). Accordingly, *Fgf23* knockout reversed the hypophosphataemia observed in *Hyp* mice (Sitara *et al.* 2004). Although initial studies appeared to confirm FGF23 as a substrate for PHEX, this has not been shown since (Bowe *et al.* 2001). Interestingly, a similar increase in *FGF23* expression is observed in models of loss of DMP1, along with associated ARHR (Feng *et al.* 2006, Lorenz-Depiereux *et al.* 2006). This has led to the suggestion that a PHEX–DMP1 interaction is responsible for orchestrating mineralisation through decreasing *FGF23* expression. Furthermore, current paradigm suggests that ASARM peptides can competitively displace this PHEX complex and this would therefore increase FGF23 activity, as is seen in the *Hyp* mouse and in patients with XLH (David *et al.* 2010, Martin *et al.* 2011, Rowe 2012).

Additionally, the accumulation of ASARM peptides can directly inhibit Na^+-dependent P_i uptake in the kidney, as has been shown both *in vivo* and *in vitro*, thus exacerbating the upregulation of *FGF23* expression, the downregulation of $1,25(OH)_2D_3$ and the inhibition of hypophosphataemia observed in XLH, ARHR and ADHR (Rowe *et al.* 2004, Dobbie *et al.* 2008, Marks *et al.* 2008, David *et al.* 2010, Shirley *et al.* 2010). The decrease in $1,25(OH)_2D_3$ provides a feedback loop for increased *PHEX* expression through the increased expression of a 100 kDa transcription factor, a requirement for this *PHEX* expression (Ecarot & Desbarats 1999).

This regulatory loop of *ASARM*, *PHEX* and *FGF23* expression and function highlights the multiple and complex functions of the SIBLING ASARM peptides in both P_i homoeostasis and matrix mineralisation in disease and health. It is therefore vital that we endeavour to fully establish the interactions within this hypothesis to allow future therapeutic developments.

Certainly, much remains to be learnt regarding the *in vivo* role of the SIBLING proteins and the ASARM peptide in bone diseases. This is not just in disorders related to P_i homoeostasis but also to other bone diseases such as osteoporosis and osteoarthritis (OA). Indeed, there are close links between the SIBLING proteins and OA, with serum BSP and OPN levels significantly correlating with OA disease severity (Petersson *et al.* 1998, Hasegawa *et al.* 2011). Furthermore, microarray data and gene analysis studies have highlighted MEPE and DMP1 as being differentially expressed in OA tissues (Hopwood *et al.* 2007, Sanchez *et al.* 2008). The interaction between MEPE and SCL, as described previously, is an exciting development due to the known anabolic effects of the SCL-neutralising antibodies on osteoporosis (Li *et al.* 2009, 2010, Atkins *et al.* 2011). This could therefore warrant investigation into the potential therapeutic use of MEPE in osteoporosis and potentially in OA due to the ever emerging role of SCL in this debilitating disease (Power *et al.* 2010, Chan *et al.* 2011, Delgado-Calle *et al.* 2011).

Conclusions

The aim of this review is to present an overview of the role of each member of the SIBLING family of proteins in matrix mineralisation. The SIBLING proteins are principally found in bone and dentin and are secreted into the ECM during its formation and subsequent mineralisation. It is apparent that the functional role of the SIBLING proteins is highly dependent on their state of cleavage and their post-translational modification (Table 1). Furthermore, the identification of the ASARM peptide, which is present across the SIBLING proteins, is proving critical in the functional activity of the SIBLING proteins. Future investigations should focus on determining the underpinning interactions between the SIBLING proteins and their place within the current ASARM hypothesis. This will allow the investigation into their potential therapeutic application to disorders of mineralisation including disorders of hypophosphataemia, osteoporosis and OA.

Declaration of interest

The authors declare that there is no conflict of interest that could be perceived as prejudicing the impartiality of the research reported.

Funding

The authors acknowledge the Institute Strategic Programme Grant Funding from the Biotechnology and Biological Sciences Research Council (BBSRC) UK (C F, V M) and BBSRC studentship funding (K S) for support.

Author contribution statement

K S drafted the manuscript. K S, V M and C F revised the manuscript content. K S, V M and C F approved the final manuscript.

References

Addison WN, Azari F, Sorensen ES, Kaartinen MT & McKee MD 2007 Pyrophosphate inhibits mineralization of osteoblast cultures by binding to mineral, up-regulating osteopontin, and inhibiting alkaline phosphatase activity. *Journal of Biological Chemistry* **282** 15872–15883. (doi:10.1074/jbc.M701116200)

Addison WN, Nakano Y, Loisel T, Crine P & McKee MD 2008 MEPE–ASARM peptides control extracellular matrix mineralization by binding to hydroxyapatite: an inhibition regulated by PHEX cleavage of ASARM. *Journal of Bone and Mineral Research* **23** 1638–1649. (doi:10.1359/jbmr.080601)

Addison WN, Masica DL, Gray JJ & McKee MD 2010 Phosphorylation-dependent inhibition of mineralization by osteopontin ASARM peptides is regulated by PHEX cleavage. *Journal of Bone and Mineral Research* **25** 695–705. (doi:10.1002/jbmr.110)

Alvares K, Kanwar YS & Veis A 2006 Expression and potential role of dentin phosphophoryn (DPP) in mouse embryonic tissues involved in epithelial–mesenchymal interactions and branching morphogenesis. *Developmental Dynamics* **235** 2980–2990. (doi:10.1002/dvdy.20935)

Anderson HC 1995 Molecular biology of matrix vesicles. *Clinical Orthopaedics and Related Research* **314** 266–280.

Anderson HC 2003 Matrix vesicles and calcification. *Current Rheumatology Reports* **5** 222–226. (doi:10.1007/s11926-003-0071-z)

Argiro L, Desbarats M, Glorieux FH & Ecarot B 2001 Mepe, the gene encoding a tumor-secreted protein in oncogenic hypophosphatemic osteomalacia, is expressed in bone. *Genomics* **74** 342–351. (doi:10.1006/geno.2001.6553)

Aruffo A, Stamenkovic I, Melnick M, Underhill CB & Seed B 1990 CD44 is the principal cell surface receptor for hyaluronate. *Cell* **61** 1303–1313. (doi:10.1016/0092-8674(90)90694-A)

Atkins GJ, Rowe PS, Lim HP, Welldon KJ, Ormsby R, Wijenayaka AR, Zelenchuk L, Evdokiou A & Findlay DM 2011 Sclerostin is a locally acting regulator of late-osteoblast/preosteocyte differentiation and regulates mineralization through a MEPE–ASARM-dependent mechanism. *Journal of Bone and Mineral Research* **26** 1425–1436. (doi:10.1002/jbmr.345)

Baba O, Qin C, Brunn JC, Wygant JN, McIntyre BW & Butler WT 2004 Colocalization of dentin matrix protein 1 and dentin sialoprotein at late stages of rat molar development. *Matrix Biology* **23** 371–379. (doi:10.1016/j.matbio.2004.07.008)

Baht GS, Hunter GK & Goldberg HA 2008 Bone sialoprotein–collagen interaction promotes hydroxyapatite nucleation. *Matrix Biology* **27** 600–608. (doi:10.1016/j.matbio.2008.06.004)

Ballock RT & O'Keefe RJ 2003 The biology of the growth plate. *Journal of Bone and Joint Surgery* **85-A** 715–726.

Beck GR Jr & Knecht N 2003 Osteopontin regulation by inorganic phosphate is ERK1/2-, protein kinase C-, and proteasome-dependent. *Journal of Biological Chemistry* **278** 41921–41929. (doi:10.1074/jbc.M304470200)

Beck GR Jr, Zerler B & Moran E 2000 Phosphate is a specific signal for induction of osteopontin gene expression. *PNAS* **97** 8352–8357. (doi:10.1073/pnas.140021997)

Bellahcene A, Castronovo V, Ogbureke KU, Fisher LW & Fedarko NS 2008 Small integrin-binding ligand N-linked glycoproteins (SIBLINGs): multifunctional proteins in cancer. *Nature Reviews. Cancer* **8** 212–226. (doi:10.1038/nrc2345)

Bianco P, Fisher LW, Young MF, Termine JD & Robey PG 1991 Expression of bone sialoprotein (BSP) in developing human tissues. *Calcified Tissue International* **49** 421–426. (doi:10.1007/BF02555854)

Boskey AL, Maresca M, Doty S, Sabsay B & Veis A 1990 Concentration-dependent effects of dentin phosphophoryn in the regulation of *in vitro* hydroxyapatite formation and growth. *Bone and Mineral* **11** 55–65. (doi:10.1016/0169-6009(90)90015-8)

Boskey AL, Maresca M, Ullrich W, Doty SB, Butler WT & Prince CW 1993 Osteopontin–hydroxyapatite interactions *in vitro*: inhibition of hydroxyapatite formation and growth in a gelatin-gel. *Bone and Mineral* **22** 147–159. (doi:10.1016/S0169-6009(08)80225-5)

Boskey AL, Spevak L, Paschalis E, Doty SB & McKee MD 2002 Osteopontin deficiency increases mineral content and mineral crystallinity in mouse bone. *Calcified Tissue International* **71** 145–154. (doi:10.1007/s00223-001-1121-z)

Boskey AL, Chiang P, Fermanis A, Brown J, Taleb H, David V & Rowe PS 2009 MEPE's diverse effects on mineralization. *Calcified Tissue International* **86** 42–46. (doi:10.1007/s00223-009-9313-z)

Boskey AL, Christensen B, Taleb H & Sorensen ES 2012 Post-translational modification of osteopontin: effects on *in vitro* hydroxyapatite formation and growth. *Biochemical and Biophysical Research Communications* **419** 333–338. (doi:10.1016/j.bbrc.2012.02.024)

Boukpessi T, Gaucher C, Leger T, Salmon B, Le FJ, Willig C, Rowe PS, Garabedian M, Meilhac O & Chaussain C 2010 Abnormal presence of the matrix extracellular phosphoglycoprotein-derived acidic serine- and aspartate-rich motif peptide in human hypophosphatemic dentin. *American Journal of Pathology* **177** 803–812. (doi:10.2353/ajpath.2010.091231)

Bowe AE, Finnegan R, Jan de Beur SM, Cho J, Levine MA, Kumar R & Schiavi SC 2001 FGF-23 inhibits renal tubular phosphate transport and is a PHEX substrate. *Biochemical and Biophysical Research Communications* **284** 977–981. (doi:10.1006/bbrc.2001.5084)

Bresler D, Bruder J, Mohnike K, Fraser WD & Rowe PS 2004 Serum MEPE–ASARM-peptides are elevated in X-linked rickets (HYP): implications for phosphaturia and rickets. *Journal of Endocrinology* **183** R1–R9. (doi:10.1677/joe.1.05989)

Carpenter TO, Imel EA, Holm IA, Jan de Beur SM & Insogna KL 2011 A clinician's guide to X-linked hypophosphatemia. *Journal of Bone and Mineral Research* **26** 1381–1388. (doi:10.1002/jbmr.340)

Castagnola P, Dozin B, Moro G & Cancedda R 1988 Changes in the expression of collagen genes show two stages in chondrocyte differentiation *in vitro*. *Journal of Cell Biology* **106** 461–467. (doi:10.1083/jcb.106.2.461)

Chan BY, Fuller ES, Russell AK, Smith SM, Smith MM, Jackson MT, Cake MA, Read RA, Bateman JF, Sambrook PN *et al.* 2011 Increased chondrocyte sclerostin may protect against cartilage degradation in osteoarthritis. *Osteoarthritis and Cartilage* **19** 874–885. (doi:10.1016/j.joca.2011.04.014)

Chellaiah MA, Kizer N, Biswas R, Alvarez U, Strauss-Schoenberger J, Rifas L, Rittling SR, Denhardt DT & Hruska KA 2003 Osteopontin deficiency produces osteoclast dysfunction due to reduced CD44 surface expression. *Molecular Biology of the Cell* **14** 173–189. (doi:10.1091/mbc.E02-06-0354)

Chen JK, Shapiro HS, Wrana JL, Reimers S, Heersche JN & Sodek J 1991 Localization of bone sialoprotein (BSP) expression to sites of mineralized tissue formation in fetal rat tissues by *in situ* hybridization. *Matrix* **11** 133–143. (doi:10.1016/S0934-8832(11)80217-9)

Chen J, Shapiro HS & Sodek J 1992 Development expression of bone sialoprotein mRNA in rat mineralized connective tissues. *Journal of Bone and Mineral Research* **7** 987–997. (doi:10.1002/jbmr.5650070816)

Chen S, Gluhak-Heinrich J, Martinez M, Li T, Wu Y, Chuang HH, Chen L, Dong J, Gay I & MacDougall M 2008 Bone morphogenetic protein 2 mediates dentin sialophosphoprotein expression and odontoblast differentiation via NF-Y signaling. *Journal of Biological Chemistry* **283** 19359–19370. (doi:10.1074/jbc.M709492200)

Cho YD, Yoon WJ, Woo KM, Baek JH, Park JC & Ryoo HM 2010 The canonical BMP signaling pathway plays a crucial part in stimulation of dentin sialophosphoprotein expression by BMP-2. *Journal of Biological Chemistry* **285** 36369–36376. (doi:10.1074/jbc.M110.103093)

Cho YD, Kim WJ, Yoon WJ, Woo KM, Baek JH, Lee G, Kim GS & Ryoo HM 2011 Wnt3a stimulates Mepe, matrix extracellular phosphoglycoprotein, expression directly by the activation of the canonical Wnt signaling pathway and indirectly through the stimulation of autocrine Bmp-2 expression. *Journal of Cellular Physiology* **227** 2287–2296. (doi:10.1002/jcp.24038)

Cooper LF, Yliheikkila PK, Felton DA & Whitson SW 1998 Spatiotemporal assessment of fetal bovine osteoblast culture differentiation indicates a role for BSP in promoting differentiation. *Journal of Bone and Mineral Research* **13** 620–632. (doi:10.1359/jbmr.1998.13.4.620)

David V, Martin A, Hedge AM & Rowe PS 2009 Matrix extracellular phosphoglycoprotein (MEPE) is a new bone renal hormone and vascularization modulator. *Endocrinology* **150** 4012–4023. (doi:10.1210/en.2009-0216)

David V, Martin AC, Hedge AM, Drezner MK & Rowe PS 2010 ASARM peptides: PHEX-dependent, independent regulation of serum phosphate. *American Journal of Physiology - Renal Physiology* **300** F783–F791. (doi:10.1152/ajprenal.00304.2010)

Delgado-Calle J, Arozamena J, Garcia-Renedo R, Garcia-Ibarbia C, Pascual-Carra MA, Gonzalez-Macias J & Riancho JA 2011 Osteocyte deficiency in hip fractures. *Calcified Tissue International* **89** 327–334. (doi:10.1007/s00223-011-9522-0)

Denhardt DT & Guo X 1993 Osteopontin: a protein with diverse functions. *FASEB Journal* **7** 1475–1482.

Dobbie H, Unwin RJ, Faria NJ & Shirley DG 2008 Matrix extracellular phosphoglycoprotein causes phosphaturia in rats by inhibiting tubular phosphate reabsorption. *Nephrology, Dialysis, Transplantation* **23** 730–733. (doi:10.1093/ndt/gfm535)

Dodds RA, Connor JR, James IE, Rykaczewski EL, Appelbaum E, Dul E & Gowen M 1995 Human osteoclasts, not osteoblasts, deposit osteopontin onto resorption surfaces: an *in vitro* and *ex vivo* study of remodeling bone. *Journal of Bone and Mineral Research* **10** 1666–1680. (doi:10.1002/jbmr.5650101109)

Eapen A, Ramachandran A, Pratap J & George A 2011 Activation of the ERK1/2 mitogen-activated protein kinase cascade by dentin matrix protein 1 promotes osteoblast differentiation. *Cells, Tissues, Organs* **194** 255–260. (doi:10.1159/000324258)

Ecarot B & Desbarats M 1999 1,25-$(OH)_2D_3$ down-regulates expression of Phex, a marker of the mature osteoblast. *Endocrinology* **140** 1192–1199. (doi:10.1210/en.140.3.1192)

Ecarot B, Glorieux FH, Desbarats M, Travers R & Labelle L 1992 Effect of dietary phosphate deprivation and supplementation of recipient mice on bone formation by transplanted cells from normal and X-linked hypophosphatemic mice. *Journal of Bone and Mineral Research* **7** 523–530. (doi:10.1002/jbmr.5650070508)

Farrow EG, Davis SI, Ward LM, Summers LJ, Bubbear JS, Keen R, Stamp TC, Baker LR, Bonewald LF & White KE 2009 Molecular analysis of DMP1 mutants causing autosomal recessive hypophosphatemic rickets. *Bone* **44** 287–294. (doi:10.1016/j.bone.2008.10.040)

Fen JQ, Zhang J, Dallas SL, Lu Y, Chen S, Tan X, Owen M, Harris SE & MacDougall M 2002 Dentin matrix protein 1, a target molecule for Cbfa1 in bone, is a unique bone marker gene. *Journal of Bone and Mineral Research* **17** 1822–1831. (doi:10.1359/jbmr.2002.17.10.1822)

Feng JQ, Huang H, Lu Y, Ye L, Xie Y, Tsutsui TW, Kunieda T, Castranio T, Scott G, Bonewald LB *et al.* 2003 The dentin matrix protein 1 (Dmp1) is specifically expressed in mineralized, but not soft, tissues during development. *Journal of Dental Research* **82** 776–780. (doi:10.1177/154405910308201003)

Feng JQ, Ward LM, Liu S, Lu Y, Xie Y, Yuan B, Yu X, Rauch F, Davis SI, Zhang S *et al.* 2006 Loss of DMP1 causes rickets and osteomalacia and identifies a role for osteocytes in mineral metabolism. *Nature Genetics* **38** 1310–1315. (doi:10.1038/ng1905)

Fisher LW & Fedarko NS 2003 Six genes expressed in bones and teeth encode the current members of the SIBLING family of proteins. *Connective Tissue Research* **44** (Suppl 1) 33–40. (doi:10.1080/713713644)

Fisher LW, Torchia DA, Fohr B, Young MF & Fedarko NS 2001 Flexible structures of SIBLING proteins, bone sialoprotein, and osteopontin. *Biochemical and Biophysical Research Communications* **280** 460–465. (doi:10.1006/bbrc.2000.4146)

Frost HM 1990 Skeletal structural adaptations to mechanical usage (SATMU): 1. Redefining Wolff's law: the bone modeling problem. *Anatomical Record* **226** 403–413. (doi:10.1002/ar.1092260402)

Fujihara S, Yokozeki M, Oba Y, Higashibata Y, Nomura S & Moriyama K 2006 Function and regulation of osteopontin in response to mechanical stress. *Journal of Bone and Mineral Research* **21** 956–964. (doi:10.1359/jbmr.060315)

Ganss B, Kim RH & Sodek J 1999 Bone sialoprotein. *Critical Reviews in Oral Biology and Medicine* **10** 79–98. (doi:10.1177/10454411990100010401)

Gentili C & Cancedda R 2009 Cartilage and bone extracellular matrix. *Current Pharmaceutical Design* **15** 1334–1348. (doi:10.2174/138161209787846739)

George A, Sabsay B, Simonian PA & Veis A 1993 Characterization of a novel dentin matrix acidic phosphoprotein, Implications for induction of biomineralization. *Journal of Biological Chemistry* **268** 12624–12630.

Gericke A, Qin C, Sun Y, Redfern R, Redfern D, Fujimoto Y, Taleb H, Butler WT & Boskey AL 2010 Different forms of DMP1 play distinct roles in mineralization. *Journal of Dental Research* **89** 355–359. (doi:10.1177/0022034510363250)

Gluhak-Heinrich J, Pavlin D, Yang W, MacDougall M & Harris SE 2007 MEPE expression in osteocytes during orthodontic tooth movement. *Archives of Oral Biology* **52** 684–690. (doi:10.1016/j.archoralbio.2006.12.010)

Golub EE 2011 Biomineralization and matrix vesicles in biology and pathology. *Seminars in Immunopathology* **33** 409–417. (doi:10.1007/s00281-010-0230-z)

Gordon JA, Tye CE, Sampaio AV, Underhill TM, Hunter GK & Goldberg HA 2007 Bone sialoprotein expression enhances osteoblast differentiation and matrix mineralization *in vitro*. *Bone* **41** 462–473. (doi:10.1016/j.bone.2007.04.191)

Gowen LC, Petersen DN, Mansolf AL, Qi H, Stock JL, Tkalcevic GT, Simmons HA, Crawford DT, Chidsey-Frink KL, Ke HZ *et al.* 2003 Targeted disruption of the osteoblast/osteocyte factor 45 gene (OF45) results in increased bone formation and bone mass. *Journal of Biological Chemistry* **278** 1998–2007. (doi:10.1074/jbc.M203250200)

Gross TS, King KA, Rabaia NA, Pathare P & Srinivasan S 2005 Upregulation of osteopontin by osteocytes deprived of mechanical loading or oxygen. *Journal of Bone and Mineral Research* **20** 250–256. (doi:10.1359/JBMR.041004)

Guo R, Rowe PS, Liu S, Simpson LG, Xiao ZS & Quarles LD 2002 Inhibition of MEPE cleavage by Phex. *Biochemical and Biophysical Research Communications* **297** 38–45. (doi:10.1016/S0006-291X(02)02125-3)

Hakim FT, Cranley R, Brown KS, Eanes ED, Harne L & Oppenheim JJ 1984 Hereditary joint disorder in progressive ankylosis (ank/ank) mice. I. Association of calcium hydroxyapatite deposition with inflammatory arthropathy. *Arthritis and Rheumatism* **27** 1411–1420. (doi:10.1002/art.1780271212)

Harmey D, Johnson KA, Zelken J, Camacho NP, Hoylaerts MF, Noda M, Terkeltaub R & Millan JL 2006 Elevated skeletal osteopontin levels contribute to the hypophosphatasia phenotype in Akp2(−/−) mice. *Journal of Bone and Mineral Research* **21** 1377–1386. (doi:10.1359/jbmr.060619)

Harris NL, Rattray KR, Tye CE, Underhill TM, Somerman MJ, D'Errico JA, Chambers AF, Hunter GK & Goldberg HA 2000 Functional analysis of bone sialoprotein: identification of the hydroxyapatite-nucleating and cell-binding domains by recombinant peptide expression and site-directed mutagenesis. *Bone* **27** 795–802. (doi:10.1016/S8756-3282(00)00392-6)

Hasegawa M, Segawa T, Maeda M, Yoshida T & Sudo A 2011 Thrombin-cleaved osteopontin levels in synovial fluid correlate with disease severity of knee osteoarthritis. *Journal of Rheumatology* **38** 129–134. (doi:10.3899/jrheum.100637)

Hayashibara T, Hiraga T, Yi B, Nomizu M, Kumagai Y, Nishimura R & Yoneda T 2004 A synthetic peptide fragment of human MEPE stimulates new bone formation *in vitro* and *in vivo*. *Journal of Bone and Mineral Research* **19** 455–462. (doi:10.1359/JBMR.0301263)

Hayashibara T, Hiraga T, Sugita A, Wang L, Hata K, Ooshima T & Yoneda T 2007 Regulation of osteoclast differentiation and function by phosphate: potential role of osteoclasts in the skeletal abnormalities in hypophosphatemic conditions. *Journal of Bone and Mineral Research* **22** 1743–1751. (doi:10.1359/jbmr.070709)

He G, Dahl T, Veis A & George A 2003 Dentin matrix protein 1 initiates hydroxyapatite formation *in vitro*. *Connective Tissue Research* **44** (Suppl 1) 240–245.

He G, Ramachandran A, Dahl T, George S, Schultz D, Cookson D, Veis A & George A 2005 Phosphorylation of phosphophoryn is crucial for its function as a mediator of biomineralization. *Journal of Biological Chemistry* **280** 33109–33114. (doi:10.1074/jbc.M500159200)

Heinegard D 2009 Proteoglycans and more – from molecules to biology. *International Journal of Experimental Pathology* **90** 575–586. (doi:10.1111/j.1365-2613.2009.00695.x)

Henriksen K, Neutzsky-Wulff AV, Bonewald LF & Karsdal MA 2009 Local communication on and within bone controls bone remodeling. *Bone* **44** 1026–1033. (doi:10.1016/j.bone.2009.03.671)

Hessle L, Johnson KA, Anderson HC, Narisawa S, Sali A, Goding JW, Terkeltaub R & Millan JL 2002 Tissue-nonspecific alkaline phosphatase and plasma cell membrane glycoprotein-1 are central antagonistic regulators of bone mineralization. *PNAS* **99** 9445–9449. (doi:10.1073/pnas.142063399)

Hill PA 1998 Bone remodelling. *British Journal of Orthodontics* **25** 101–107. (doi:10.1093/ortho/25.2.101)

Ho AM, Johnson MD & Kingsley DM 2000 Role of the mouse ank gene in control of tissue calcification and arthritis. *Science* **289** 265–270. (doi:10.1126/science.289.5477.265)

Holm IA, Huang X & Kunkel LM 1997 Mutational analysis of the PEX gene in patients with X-linked hypophosphatemic rickets. *American Journal of Human Genetics* **60** 790–797.

Hopwood B, Tsykin A, Findlay DM & Fazzalari NL 2007 Microarray gene expression profiling of osteoarthritic bone suggests altered bone remodelling, WNT and transforming growth factor-beta/bone morphogenic protein signalling. *Arthritis Research and Therapy* **9** R100. (doi:10.1186/ar2301)

Houston B, Paton IR, Burt DW & Farquharson C 2002 Chromosomal localization of the chicken and mammalian orthologues of the orphan phosphatase PHOSPHO1 gene. *Animal Genetics* **33** 451–454. (doi:10.1046/j.1365-2052.2002.00900.x)

Huang B, Maciejewska I, Sun Y, Peng T, Qin D, Lu Y, Bonewald L, Butler WT, Feng J & Qin C 2008 Identification of full-length dentin matrix protein 1 in dentin and bone. *Calcified Tissue International* **82** 401–410. (doi:10.1007/s00223-008-9140-7)

Huesa C, Yadav MC, Finnila MA, Goodyear SR, Robins SP, Tanner KE, Aspden RM, Millan JL & Farquharson C 2011 PHOSPHO1 is essential for mechanically competent mineralization and the avoidance of spontaneous fractures. *Bone* **48** 1066–1074. (doi:10.1016/j.bone.2011.01.010)

Hunter GK, Kyle CL & Goldberg HA 1994 Modulation of crystal formation by bone phosphoproteins: structural specificity of the osteopontin-mediated inhibition of hydroxyapatite formation. *Biochemical Journal* **300** (pt 3) 723–728.

Hunter GK, Hauschka PV, Poole AR, Rosenberg LC & Goldberg HA 1996 Nucleation and inhibition of hydroxyapatite formation by mineralized tissue proteins. *Biochemical Journal* **317** 59–64.

Hunziker EB, Schenk RK & Cruz-Orive LM 1987 Quantitation of chondrocyte performance in growth-plate cartilage during longitudinal bone growth. *Journal of Bone and Joint Surgery* **69** 162–173. (doi:10.1097/01241398-198707000-00027)

Huq NL, Cross KJ, Ung M & Reynolds EC 2005 A review of protein structure and gene organisation for proteins associated with mineralised tissue and calcium phosphate stabilisation encoded on human chromosome 4. *Archives of Oral Biology* **50** 599–609. (doi:10.1016/j.archoralbio.2004.12.009)

Iohara K, Nakashima M, Ito M, Ishikawa M, Nakasima A & Akamine A 2004 Dentin regeneration by dental pulp stem cell therapy with recombinant human bone morphogenetic protein 2. *Journal of Dental Research* **83** 590–595. (doi:10.1177/154405910408300802)

Johnson K, Goding J, van Etten D, Sali A, Hu SI, Farley D, Krug H, Hessle L, Millan JL & Terkeltaub R 2003 Linked deficiencies in extracellular PP(i) and osteopontin mediate pathologic calcification associated with defective PC-1 and ANK expression. *Journal of Bone and Mineral Research* **18** 994–1004. (doi:10.1359/jbmr.2003.18.6.994)

Jono S, Peinado C & Giachelli CM 2000 Phosphorylation of osteopontin is required for inhibition of vascular smooth muscle cell calcification. *Journal of Biological Chemistry* **275** 20197–20203. (doi:10.1074/jbc.M909174199)

Kawasaki K 2011 The SCPP gene family and the complexity of hard tissues in vertebrates. *Cells, Tissues, Organs* **194** 108–112. (doi:10.1159/000324225)

Kawasaki K & Weiss KM 2006 Evolutionary genetics of vertebrate tissue mineralization: the origin and evolution of the secretory calcium-binding phosphoprotein family. *Journal of Experimental Zoology. Part B, Molecular Development and Evolution* **306** 295–316. (doi:10.1002/jez.b.21088)

Kawasaki K, Buchanan AV & Weiss KM 2007 Gene duplication and the evolution of vertebrate skeletal mineralization. *Cells, Tissues, Organs* **186** 7–24. (doi:10.1159/000102678)

Kim JW, Hu JC, Lee JI, Moon SK, Kim YJ, Jang KT, Lee SH, Kim CC, Hahn SH & Simmer JP 2005 Mutational hot spot in the DSPP gene causing dentinogenesis imperfecta type II. *Human Genetics* **116** 186–191. (doi:10.1007/s00439-004-1223-6)

King KB, Opel CF & Rempel DM 2005 Cyclical articular joint loading leads to cartilage thinning and osteopontin production in a novel *in vivo* rabbit model of repetitive finger flexion. *Osteoarthritis and Cartilage* **13** 971–978. (doi:10.1016/j.joca.2005.06.015)

Klein-Nulend J, Roelofsen J, Semeins CM, Bronckers AL & Burger EH 1997 Mechanical stimulation of osteopontin mRNA expression and synthesis in bone cell cultures. *Journal of Cellular Physiology* **170** 174–181. (doi:10.1002/(SICI)1097-4652(199702)170:2<174::AID-JCP9>3.0.CO;2-L)

Landis WJ, Jacquet R, Hillyer J & Zhang J 2003 Analysis of osteopontin in mouse growth plate cartilage by application of laser capture microdissection and RT-PCR. *Connective Tissue Research* **44** (Suppl 1) 28–32.

Li X, Ominsky MS, Warmington KS, Morony S, Gong J, Cao J, Gao Y, Shalhoub V, Tipton B, Haldankar R *et al.* 2009 Sclerostin antibody treatment increases bone formation, bone mass, and bone strength in a rat model of postmenopausal osteoporosis. *Journal of Bone and Mineral Research* **24** 578–588. (doi:10.1359/jbmr.081206)

Li X, Warmington KS, Niu QT, Asuncion FJ, Barrero M, Grisanti M, Dwyer D, Stouch B, Thway TM, Stolina M *et al.* 2010 Inhibition of sclerostin by monoclonal antibody increases bone formation, bone mass, and bone strength in aged male rats. *Journal of Bone and Mineral Research* **25** 2647–2656. (doi:10.1002/jbmr.182)

Ling Y, Rios HF, Myers ER, Lu Y, Feng JQ & Boskey AL 2005 DMP1 depletion decreases bone mineralization *in vivo*: an FTIR imaging analysis. *Journal of Bone and Mineral Research* **20** 2169–2177. (doi:10.1359/JBMR.050815)

Liu S, Zhou J, Tang W, Jiang X, Rowe DW & Quarles LD 2006 Pathogenic role of Fgf23 in Hyp mice. *American Journal of Physiology. Endocrinology and Metabolism* **291** E38–E49. (doi:10.1152/ajpendo.00008.2006)

Liu S, Rowe PS, Vierthaler L, Zhou J & Quarles LD 2007 Phosphorylated acidic serine-aspartate-rich MEPE-associated motif peptide from matrix extracellular phosphoglycoprotein inhibits phosphate regulating gene with homologies to endopeptidases on the X-chromosome enzyme activity. *Journal of Endocrinology* **192** 261–267. (doi:10.1677/joe.1.07059)

Liu S, Zhou J, Tang W, Menard R, Feng JQ & Quarles LD 2008 Pathogenic role of Fgf23 in Dmp1-null mice. *American Journal of Physiology. Endocrinology and Metabolism* **295** E254–E261. (doi:10.1152/ajpendo.90201.2008)

Lorenz-Depiereux B, Bastepe M, Benet-Pages A, Amyere M, Wagenstaller J, Muller-Barth U, Badenhoop K, Kaiser SM, Rittmaster RS, Shlossberg AH *et al.* 2006 DMP1 mutations in autosomal recessive hypophosphatemia implicate a bone matrix protein in the regulation of phosphate homeostasis. *Nature Genetics* **38** 1248–1250. (doi:10.1038/ng1868)

Lu C, Huang S, Miclau T, Helms JA & Colnot C 2004 Mepe is expressed during skeletal development and regeneration. *Histochemistry and Cell Biology* **121** 493–499. (doi:10.1007/s00418-004-0653-5)

Lu Y, Yuan B, Qin C, Cao Z, Xie Y, Dallas SL, McKee MD, Drezner MK, Bonewald LF & Feng JQ 2011 The biological function of DMP-1 in osteocyte maturation is mediated by its 57-kDa C-terminal fragment. *Journal of Bone and Mineral Research* **26** 331–340. (doi:10.1002/jbmr.226)

MacDougall M, Gu TT, Luan X, Simmons D & Chen J 1998 Identification of a novel isoform of mouse dentin matrix protein 1: spatial expression in mineralized tissues. *Journal of Bone and Mineral Research* **13** 422–431. (doi:10.1359/jbmr.1998.13.3.422)

Maciejewska I, Cowan C, Svoboda K, Butler WT, D'Souza R & Qin C 2008 The NH_2-terminal and COOH-terminal fragments of dentin matrix

protein 1 (DMP1) localize differently in the compartments of dentin and growth plate of bone. *Journal of Histochemistry and Cytochemistry* **57** 155–156. (doi:10.1369/jhc.2008.952630)

Maciejewska I, Qin D, Huang B, Sun Y, Mues G, Svoboda K, Bonewald L, Butler WT, Feng JQ & Qin C 2009 Distinct compartmentalization of dentin matrix protein 1 fragments in mineralized tissues and cells. *Cells, Tissues, Organs* **189** 186–191. (doi:10.1159/000151372)

Mackie EJ, Ahmed YA, Tatarczuch L, Chen KS & Mirams M 2008 Endochondral ossification: how cartilage is converted into bone in the developing skeleton. *International Journal of Biochemistry and Cell Biology* **40** 46–62. (doi:10.1016/j.biocel.2007.06.009)

Mackie EJ, Tatarczuch L & Mirams M 2011 The growth plate chondrocyte and endochondral ossification. *Journal of Endocrinology* **211** 109–121. (doi:10.1530/JOE-11-0048)

MacRae VE, Davey MG, McTeir L, Narisawa S, Yadav MC, Millan JL & Farquharson C 2010 Inhibition of PHOSPHO1 activity results in impaired skeletal mineralization during limb development of the chick. *Bone* **46** 1146–1155. (doi:10.1016/j.bone.2009.12.018)

Majeska RJ & Wuthier RE 1975 Studies on matrix vesicles isolated from chick epiphyseal cartilage. Association of pyrophosphatase and ATPase activities with alkaline phosphatase. *Biochimica et Biophysica Acta* **391** 51–60.

Malaval L, Wade-Gueye NM, Boudiffa M, Fei J, Zirngibl R, Chen F, Laroche N, Roux JP, Burt-Pichat B, Duboeuf F *et al.* 2008 Bone sialoprotein plays a functional role in bone formation and osteoclastogenesis. *Journal of Experimental Medicine* **205** 1145–1153. (doi:10.1084/jem.20071294)

Manolagas SC 2000 Birth and death of bone cells: basic regulatory mechanisms and implications for the pathogenesis and treatment of osteoporosis. *Endocrine Reviews* **21** 115–137. (doi:10.1210/er.21.2.115)

Marks J, Churchill LJ, Debnam ES & Unwin RJ 2008 Matrix extracellular phosphoglycoprotein inhibits phosphate transport. *Journal of the American Society of Nephrology* **19** 2313–2320. (doi:10.1681/ASN.2008030315)

Martin A, David V, Laurence JS, Schwarz PM, Lafer EM, Hedge AM & Rowe PS 2008 Degradation of MEPE, DMP1, and release of SIBLING ASARM-peptides (minhibins): ASARM-peptide(s) are directly responsible for defective mineralization in HYP. *Endocrinology* **149** 1757–1772. (doi:10.1210/en.2007-1205)

Martin A, Liu S, David V, Li H, Karydis A, Feng JQ & Quarles LD 2011 Bone proteins PHEX and DMP1 regulate fibroblastic growth factor Fgf23 expression in osteocytes through a common pathway involving FGF receptor (FGFR) signaling. *FASEB Journal* **25** 2551–2562. (doi:10.1096/fj.10-177816)

Mellis DJ, Itzstein C, Helfrich MH & Crockett JC 2011 The skeleton: a multifunctional complex organ: the role of key signalling pathways in osteoclast differentiation and in bone resorption. *Journal of Endocrinology* **211** 131–143. (doi:10.1530/JOE-11-0212)

Meyer JL 1984 Can biological calcification occur in the presence of pyrophosphate? *Archives of Biochemistry and Biophysics* **231** 1–8. (doi:10.1016/0003-9861(84)90356-4)

Mizuno M, Imai T, Fujisawa R, Tani H & Kuboki Y 2000 Bone sialoprotein (BSP) is a crucial factor for the expression of osteoblastic phenotypes of bone marrow cells cultured on type I collagen matrix. *Calcified Tissue International* **66** 388–396. (doi:10.1007/s002230010078)

Morinobu M, Ishijima M, Rittling SR, Tsuji K, Yamamoto H, Nifuji A, Denhardt DT & Noda M 2003 Osteopontin expression in osteoblasts and osteocytes during bone formation under mechanical stress in the calvarial suture *in vivo*. *Journal of Bone and Mineral Research* **18** 1706–1715. (doi:10.1359/jbmr.2003.18.9.1706)

Moss DW, Eaton RH, Smith JK & Whitby LG 1967 Association of inorganic-pyrophosphatase activity with human alkaline-phosphatase preparations. *Biochemical Journal* **102** 53–57.

Nahar NN, Missana LR, Garimella R, Tague SE & Anderson HC 2008 Matrix vesicles are carriers of bone morphogenetic proteins (BMPs), vascular endothelial growth factor (VEGF), and noncollagenous matrix proteins. *Journal of Bone and Mineral Metabolism* **26** 514–519. (doi:10.1007/s00774-008-0859-z)

Nampei A, Hashimoto J, Hayashida K, Tsuboi H, Shi K, Tsuji I, Miyashita H, Yamada T, Matsukawa N, Matsumoto M *et al.* 2004 Matrix extracellular phosphoglycoprotein (MEPE) is highly expressed in osteocytes in human bone. *Journal of Bone Mineral and Metabolism* **22** 176–184. (doi:10.1007/s00774-003-0468-9)

Narayanan K, Srinivas R, Ramachandran A, Hao J, Quinn B & George A 2001 Differentiation of embryonic mesenchymal cells to odontoblast-like cells by overexpression of dentin matrix protein 1. *PNAS* **98** 4516–4521. (doi:10.1073/pnas.081075198)

Ogbureke KU & Fisher LW 2007 SIBLING expression patterns in duct epithelia reflect the degree of metabolic activity. *Journal of Histochemistry and Cytochemistry* **55** 403–409. (doi:10.1369/jhc.6A7075.2007)

Owan I, Burr DB, Turner CH, Qiu J, Tu Y, Onyia JE & Duncan RL 1997 Mechanotransduction in bone: osteoblasts are more responsive to fluid forces than mechanical strain. *American Journal of Physiology* **273** C810–C815.

Palokangas H, Mulari M & Vaananen HK 1997 Endocytic pathway from the basal plasma membrane to the ruffled border membrane in bone-resorbing osteoclasts. *Journal of Cell Science* **110** 1767–1780.

Petersen DN, Tkalcevic GT, Mansolf AL, Rivera-Gonzalez R & Brown TA 2000 Identification of osteoblast/osteocyte factor 45 (OF45), a bone-specific cDNA encoding an RGD-containing protein that is highly expressed in osteoblasts and osteocytes. *Journal of Biological Chemistry* **275** 36172–36180. (doi:10.1074/jbc.M003622200)

Petersson IF, Boegard T, Svensson B, Heinegard D & Saxne T 1998 Changes in cartilage and bone metabolism identified by serum markers in early osteoarthritis of the knee joint. *British Journal of Rheumatology* **37** 46–50. (doi:10.1093/rheumatology/37.1.46)

Pirotte S, Lamour V, Lambert V, Alvarez Gonzalez ML, Ormenese S, Noel A, Mottet D, Castronovo V & Bellahcene A 2011 Dentin matrix protein 1 induces membrane expression of VE-cadherin on endothelial cells and inhibits VEGF-induced angiogenesis by blocking VEGFR-2 phosphorylation. *Blood* **117** 2515–2526. (doi:10.1182/blood-2010-08-298810)

Power J, Poole KE, van Bezooijen R, Doube M, Caballero-Alias AM, Lowik C, Papapoulos S, Reeve J & Loveridge N 2010 Sclerostin and the regulation of bone formation: effects in hip osteoarthritis and femoral neck fracture. *Journal of Bone Mineral Research* **25** 1867–1876. (doi:10.1002/jbmr.70)

Prasad M, Butler WT & Qin C 2010 Dentin sialophosphoprotein in biomineralization. *Connective Tissue Research* **51** 404–417. (doi:10.3109/03008200903329789)

Qin C, Brunn JC, Cadena E, Ridall A, Tsujigiwa H, Nagatsuka H, Nagai N & Butler WT 2002 The expression of dentin sialophosphoprotein gene in bone. *Journal of Dental Research* **81** 392–394. (doi:10.1177/154405910208100607)

Qin C, Brunn JC, Cook RG, Orkiszewski RS, Malone JP, Veis A & Butler WT 2003 Identification and characterization of processed fragments and cleavage sites. *Journal of Biological Chemistry* **278** 34700–34708. (doi:10.1074/jbc.M305315200)

Qin C, Baba O & Butler WT 2004 Post-translational modifications of sibling proteins and their roles in osteogenesis and dentinogenesis. *Critical Reviews in Oral Biology and Medicine* **15** 126–136. (doi:10.1177/154411130401500302)

Qin C, D'Souza R & Feng JQ 2007 Dentin matrix protein 1 (DMP1): new and important roles for biomineralization and phosphate homeostasis. *Journal of Dental Research* **86** 1134–1141. (doi:10.1177/154405910708601202)

Raynal C, Delmas PD & Chenu C 1996 Bone sialoprotein stimulates *in vitro* bone resorption. *Endocrinology* **137** 2347–2354. (doi:10.1210/en.137.6.2347)

Rittling SR, Matsumoto HN, McKee MD, Nanci A, An XR, Novick KE, Kowalski AJ, Noda M & Denhardt DT 1998 Mice lacking osteopontin show normal development and bone structure but display altered osteoclast formation *in vitro*. *Journal of Bone and Mineral Research* **13** 1101–1111. (doi:10.1359/jbmr.1998.13.7.1101)

Roberts S, Narisawa S, Harmey D, Millan JL & Farquharson C 2007 Functional involvement of PHOSPHO1 in matrix vesicle-mediated skeletal mineralization. *Journal of Bone and Mineral Research* **22** 617–627. (doi:10.1359/jbmr.070108)

Roberts SJ, Owen HC & Farquharson C 2008 Identification of a novel splice variant of the haloacid dehalogenase: PHOSPHO1. *Biochemical and Biophysical Research Communications* **371** 872–876. (doi:10.1016/j.bbrc.2008.04.163)

Ross FP, Chappel J, Alvarez JI, Sander D, Butler WT, Farach-Carson MC, Mintz KA, Robey PG, Teitelbaum SL & Cheresh DA 1993 Interactions between the bone matrix proteins osteopontin and bone sialoprotein and the osteoclast integrin alpha v beta 3 potentiate bone resorption. *Journal of Biological Chemistry* **268** 9901–9907.

Rowe PS 2004 The wrickkened pathways of FGF23, MEPE and PHEX. *Critical Reviews in Oral Biology and Medicine* **15** 264–281. (doi:10.1177/154411130401500503)

Rowe PS 2012 The chicken or the egg: PHEX, FGF23 and SIBLINGs unscrambled. *Cell Biochemistry and Function* (doi: 10.1002/cbf.2841).

Rowe PS, de Zoysa PA, Dong R, Wang HR, White KE, Econs MJ & Oudet CL 2000 MEPE, a new gene expressed in bone marrow and tumors causing osteomalacia. *Genomics* **67** 54–68. (doi:10.1006/geno.2000.6235)

Rowe PS, Kumagai Y, Gutierrez G, Garrett IR, Blacher R, Rosen D, Cundy J, Navvab S, Chen D, Drezner MK *et al*. 2004 MEPE has the properties of an osteoblastic phosphatonin and minhibin. *Bone* **34** 303–319. (doi:10.1016/j.bone.2003.10.005)

Rowe PS, Matsumoto N, Jo OD, Shih RN, Oconnor J, Roudier MP, Bain S, Liu S, Harrison J & Yanagawa N 2006 Correction of the mineralization defect in hyp mice treated with protease inhibitors CA074 and pepstatin. *Bone* **39** 773–786. (doi:10.1016/j.bone.2006.04.012)

Saito T, Arsenault AL, Yamauchi M, Kuboki Y & Crenshaw MA 1997 Mineral induction by immobilized phosphoproteins. *Bone* **21** 305–311. (doi:10.1016/S8756-3282(97)00149-X)

Sanchez C, Deberg MA, Bellahcene A, Castronovo V, Msika P, Delcour JP, Crielaard JM & Henrotin YE 2008 Phenotypic characterization of osteoblasts from the sclerotic zones of osteoarthritic subchondral bone. *Arthritis and Rheumatism* **58** 442–455. (doi:10.1002/art.23159)

Shirley DG, Faria NJ, Unwin RJ & Dobbie H 2010 Direct micropuncture evidence that matrix extracellular phosphoglycoprotein inhibits proximal tubular phosphate reabsorption. *Nephrology, Dialysis, Transplantation* **25** 3191–3195. (doi:10.1093/ndt/gfq263)

Siggelkow H, Schmidt E, Hennies B & Hufner M 2004 Evidence of downregulation of matrix extracellular phosphoglycoprotein during terminal differentiation in human osteoblasts. *Bone* **35** 570–576. (doi:10.1016/j.bone.2004.03.033)

Sitara D, Razzaque MS, Hesse M, Yoganathan S, Taguchi T, Erben RG, Juppner H & Lanske B 2004 Homozygous ablation of fibroblast growth factor-23 results in hyperphosphatemia and impaired skeletogenesis, and reverses hypophosphatemia in Phex-deficient mice. *Matrix Biology* **23** 421–432. (doi:10.1016/j.matbio.2004.09.007)

Sodek J, Chen J, Nagata T, Kasugai S, Todescan R Jr, Li IW & Kim RH 1995 Regulation of osteopontin expression in osteoblasts. *Annals of the New York Academy of Sciences* **760** 223–241. (doi:10.1111/j.1749-6632.1995.tb44633.x)

Sodek J, Ganss B & McKee MD 2000 Osteopontin. *Critical Reviews in Oral Biology and Medicine* **11** 279–303. (doi:10.1177/10454411000110030101)

Sprowson AP, McCaskie AW & Birch MA 2008 ASARM-truncated MEPE and AC-100 enhance osteogenesis by promoting osteoprogenitor adhesion. *Journal of Orthopaedic Research* **26** 1256–1262. (doi:10.1002/jor.20606)

Sreenath T, Thyagarajan T, Hall B, Longenecker G, D'Souza R, Hong S, Wright JT, MacDougall M, Sauk J & Kulkarni AB 2003 Dentin sialophosphoprotein knockout mouse teeth display widened predentin zone and develop defective dentin mineralization similar to human dentinogenesis imperfecta type III. *Journal of Biological Chemistry* **278** 24874–24880. (doi:10.1074/jbc.M303908200)

Stewart AJ, Roberts SJ, Seawright E, Davey MG, Fleming RH & Farquharson C 2006 The presence of PHOSPHO1 in matrix vesicles and its developmental expression prior to skeletal mineralization. *Bone* **39** 1000–1007. (doi:10.1016/j.bone.2006.05.014)

Stubbs JT III, Mintz KP, Eanes ED, Torchia DA & Fisher LW 1997 Characterization of native and recombinant bone sialoprotein: delineation of the mineral-binding and cell adhesion domains and structural analysis of the RGD domain. *Journal of Bone and Mineral Research* **12** 1210–1222. (doi:10.1359/jbmr.1997.12.8.1210)

Sun Y, Prasad M, Gao T, Wang X, Zhu Q, D'Souza R, Feng JQ & Qin C 2010 Failure to process dentin matrix protein 1 (DMP1) into fragments leads to its loss of function in osteogenesis. *Journal of Biological Chemistry* **285** 31713–31722. (doi:10.1074/jbc.M110.137059)

Sun Y, Chen L, Ma S, Zhou J, Zhang H, Feng JQ & Qin C 2011 Roles of DMP1 processing in osteogenesis, dentinogenesis and chondrogenesis. *Cells, Tissues, Organs* **194** 199–204. (doi:10.1159/000324672)

Suzuki K, Zhu B, Rittling SR, Denhardt DT, Goldberg HA, McCulloch CA & Sodek J 2002 Colocalization of intracellular osteopontin with CD44 is associated with migration, cell fusion, and resorption in osteoclasts. *Journal of Bone and Mineral Research* **17** 1486–1497. (doi:10.1359/jbmr.2002.17.8.1486)

Suzuki S, Sreenath T, Haruyama N, Honeycutt C, Terse A, Cho A, Kohler T, Muller R, Goldberg M & Kulkarni AB 2009 Dentin sialoprotein and dentin phosphoprotein have distinct roles in dentin mineralization. *Matrix Biology* **28** 221–229. (doi:10.1016/j.matbio.2009.03.006)

Tartaix PH, Doulaverakis M, George A, Fisher LW, Butler WT, Qin C, Salih E, Tan M, Fujimoto Y, Spevak L *et al*. 2004 *In vitro* effects of dentin matrix protein-1 on hydroxyapatite formation provide insights into *in vivo* functions. *Journal of Biological Chemistry* **279** 18115–18120. (doi:10.1074/jbc.M314114200)

Terai K, Takano-Yamamoto T, Ohba Y, Hiura K, Sugimoto M, Sato M, Kawahata H, Inaguma N, Kitamura Y & Nomura S 1999 Role of osteopontin in bone remodeling caused by mechanical stress. *Journal of Bone and Mineral Research* **14** 839–849. (doi:10.1359/jbmr.1999.14.6.839)

Terkeltaub R, Rosenbach M, Fong F & Goding J 1994 Causal link between nucleotide pyrophosphohydrolase overactivity and increased intracellular inorganic pyrophosphate generation demonstrated by transfection of cultured fibroblasts and osteoblasts with plasma cell membrane glycoprotein-1. Relevance to calcium pyrophosphate dihydrate deposition disease. *Arthritis and Rheumatism* **37** 934–941. (doi:10.1002/art.1780370624)

Toyosawa S, Shintani S, Fujiwara T, Ooshima T, Sato A, Ijuhin N & Komori T 2001 Dentin matrix protein 1 is predominantly expressed in chicken and rat osteocytes but not in osteoblasts. *Journal of Bone and Mineral Research* **16** 2017–2026. (doi:10.1359/jbmr.2001.16.11.2017)

Tsuchiya S, Simmer JP, Hu JC, Richardson AS, Yamakoshi F & Yamakoshi Y 2011 Astacin proteases cleave dentin sialophosphoprotein (Dspp) to generate dentin phosphoprotein (Dpp). *Journal of Bone and Mineral Research* **26** 220–228. (doi:10.1002/jbmr.202)

Tye CE, Rattray KR, Warner KJ, Gordon JA, Sodek J, Hunter GK & Goldberg HA 2003 Delineation of the hydroxyapatite-nucleating domains of bone sialoprotein. *Journal of Biological Chemistry* **278** 7949–7955. (doi:10.1074/jbc.M211915200)

Valverde P, Zhang J, Fix A, Zhu J, Ma W, Tu Q & Chen J 2008 Overexpression of bone sialoprotein leads to an uncoupling of bone formation and bone resorption in mice. *Journal of Bone and Mineral Research* **23** 1775–1788. (doi:10.1359/jbmr.080605)

Verdelis K, Ling Y, Sreenath T, Haruyama N, MacDougall M, van der Meulen MC, Lukashova L, Spevak L, Kulkarni AB & Boskey AL 2008 DSPP effects on *in vivo* bone mineralization. *Bone* **43** 983–990. (doi:10.1016/j.bone.2008.08.110)

Wada T, McKee MD, Steitz S & Giachelli CM 1999 Calcification of vascular smooth muscle cell cultures: inhibition by osteopontin. *Circulation Research* **84** 166–178. (doi:10.1161/01.RES.84.2.166)

Wang J, Zhou HY, Salih E, Xu L, Wunderlich L, Gu X, Hofstaetter JG, Torres M & Glimcher MJ 2006 Site-specific *in vivo* calcification and osteogenesis stimulated by bone sialoprotein. *Calcified Tissue International* **79** 179–189. (doi:10.1007/s00223-006-0018-2)

Wu LN, Genge BR, Kang MW, Arsenault AL & Wuthier RE 2002 Changes in phospholipid extractability and composition accompany mineralization of chicken growth plate cartilage matrix vesicles. *Journal of Biological Chemistry* **277** 5126–5133. (doi:10.1074/jbc.M107899200)

Wu H, Teng PN, Jayaraman T, Onishi S, Li J, Bannon L, Huang H, Close J & Sfeir C 2011 Dentin matrix protein 1 (DMP1) signals via cell surface integrin. *Journal of Biological Chemistry* **286** 29462–29469. (doi:10.1074/jbc.M110.194746)

Xiao ZS, Crenshaw M, Guo R, Nesbitt T, Drezner MK & Quarles LD 1998 Intrinsic mineralization defect in Hyp mouse osteoblasts. *American Journal of Physiology* **275** E700–E708.

Yadav MC, Simao AM, Narisawa S, Huesa C, McKee MD, Farquharson C & Millan JL 2011 Loss of skeletal mineralization by the simultaneous ablation of PHOSPHO1 and alkaline phosphatase function: a unified model of the mechanisms of initiation of skeletal calcification. *Journal of Bone and Mineral Research* **26** 286–297. (doi:10.1002/jbmr.195)

Yamakoshi Y, Hu JC, Fukae M, Zhang H & Simmer JP 2005 Dentin glycoprotein: the protein in the middle of the dentin sialophosphoprotein chimera. *Journal of Biological Chemistry* **280** 17472–17479. (doi:10.1074/jbc.M413220200)

Ye L, Mishina Y, Chen D, Huang H, Dallas SL, Dallas MR, Sivakumar P, Kunieda T, Tsutsui TW, Boskey A *et al.* 2005 Dmp1-deficient mice display severe defects in cartilage formation responsible for a chondrodysplasia-like phenotype. *Journal of Biological Chemistry* **280** 6197–6203. (doi:10.1074/jbc.M412911200)

You J, Reilly GC, Zhen X, Yellowley CE, Chen Q, Donahue HJ & Jacobs CR 2001 Osteopontin gene regulation by oscillatory fluid flow via intracellular calcium mobilization and activation of mitogen-activated protein kinase in MC3T3-E1 osteoblasts. *Journal of Biological Chemistry* **276** 13365–13371. (doi:10.1074/jbc.M009846200)

Zelzer E, McLean W, Ng YS, Fukai N, Reginato AM, Lovejoy S, D'Amore PA & Olsen BR 2002 Skeletal defects in VEGF(120/120) mice reveal multiple roles for VEGF in skeletogenesis. *Development* **129** 1893–1904.

Zhang X, Zhao J, Li C, Gao S, Qiu C, Liu P, Wu G, Qiang B, Lo WH & Shen Y 2001 DSPP mutation in dentinogenesis imperfecta Shields type II. *Nature Genetics* **27** 151–152. (doi:10.1038/84765)

Zhang GX, Mizuno M, Tsuji K & Tamura M 2004 Regulation of mRNA expression of matrix extracellular phosphoglycoprotein (MEPE)/osteoblast/osteocyte factor 45 (OF45) by fibroblast growth factor 2 in cultures of rat bone marrow-derived osteoblastic cells. *Endocrine* **24** 15–24. (doi:10.1385/ENDO:24:1:015)

Zhang B, Sun Y, Chen L, Guan C, Guo L & Qin C 2010 Expression and distribution of SIBLING proteins in the predentin/dentin and mandible of hyp mice. *Oral Diseases* **16** 453–464. (doi:10.1111/j.1601-0825.2010.01656.x)

Zohar R, Lee W, Arora P, Cheifetz S, McCulloch C & Sodek J 1997 Single cell analysis of intracellular osteopontin in osteogenic cultures of fetal rat calvarial cells. *Journal of Cellular Physiology* **170** 88–100. (doi:10.1002/(SICI)1097-4652(199701)170:1<88::AID-JCP10>3.0.CO;2-K)

Received in final form 28 May 2012
Accepted 13 June 2012
Made available online as an Accepted Preprint
13 June 2012

CELL BIOCHEMISTRY & FUNCTION

CELL BIOCHEMISTRY AND FUNCTION
Cell Biochem Funct (2012)
Published online in Wiley Online Library
(wileyonlinelibrary.com) **DOI**: 10.1002/cbf.2852

Cartilage development and degeneration: a Wnt Wnt situation

Katherine Ann Staines*, Vicky Elizabeth MacRae and Colin Farquharson

The Roslin Institute and Royal (Dick) School of Veterinary Studies, The University of Edinburgh, Easter Bush, Midlothian, Scotland

The Wnt signaling pathway plays a crucial role in the development and homeostasis of a variety of adult tissues and, as such, is emerging as an important therapeutic target for numerous diseases. Factors involved in the Wnt pathway are expressed throughout limb development and chondrogenesis and have been shown to be critical in joint homeostasis and endochondral ossification. Therefore, in this review, we discuss Wnt regulation of chondrogenic differentiation, hypertrophy and cartilage function. Moreover, we detail the role of the Wnt signaling pathway in cartilage degeneration and its potential to act as a target for therapy in osteoarthritis. Copyright © 2012 John Wiley & Sons, Ltd.

KEY WORDS—cartilage; bone; osteoarthritis; Wnt signaling; sclerostin

INTRODUCTION

The Wnt signaling pathway is emerging as a potent regulator of cellular development and function in a variety of tissues and as such has been the focus of numerous studies and review articles. More specifically, Wnt signaling is required for many embryonic developmental processes including sex determination and organ development.[1,2] Post-natally, Wnt signaling is crucial for the regulation of skeletal bone mass throughout life, and over the past 2 decades, the role of Wnt in cartilage development and function has been established.[3]

Cartilage is a tough, flexible and elastic connective tissue, which has numerous functions. It is mainly composed of an abundant collagen and proteoglycan-rich extracellular matrix (ECM) in which the primary cell type of cartilage, the chondrocyte, resides. This composition gives rise to a highly hydrated tissue, which allows effective completion of its primary functions; to disperse forces on the joints during movement and to act as a template for bone formation and longitudinal bone growth. Abnormalities in the ECM cause a multitude of skeletal malformation syndromes, as well as degenerative diseases, such as osteoarthritis (OA) and rheumatoid arthritis (RA), which will be discussed within this review.

The expression of Wnt factors in the embryonic skeleton have been well detailed in comprehensive studies by Summerhurst *et al*. and Witte *et al*.[4,5] The vast array of Wnt factors expressed throughout the development of the embryonic skeleton suggests an important role for Wnt signaling pathway in this process. This review summarizes the current knowledge on the role of the Wnt signaling components in cartilage development and function and highlights their potential therapeutic use. Despite numerous reviews about Wnt signaling, one which explores all these themes has not been published in recent years.

Wnt signaling

Wnts constitute a family of secreted signaling proteins that bind with their respective receptors and activate such signaling pathways as the Wnt/β-catenin pathway, the Wnt/Ca^{2+} pathway, the Wnt/planar cell polarity (Wnt/PCP) pathway and the Wnt/protein kinase A (Wnt/PKA) pathway.[6–8] The repertoire of Wnt ligands, Wnt receptors and Wnt agonists and antagonists is large and complex, with various interactions occurring that are important in embryogenesis, postnatal development and tissue homeostasis throughout life. For this reason, the Wnt signaling pathway, in particular the Wnt/β-catenin pathway, is one of the most intensively studied signaling pathways in mammalian cells.

The Wnt/β-catenin pathway. The Wnt/β-catenin pathway, often referred to as the canonical Wnt pathway, is activated upon binding of Wnt to Frizzled (Fz) receptors and low-density lipoprotein receptor-related protein (LRP) 5/6 co-receptors at the cell surface.[9–11] Currently, there are at least 7 of the 19 known Wnt proteins that activate this pathway. In the absence of appropriate Wnt ligands, β-catenin is phosphorylated using glycogen synthase kinase 3 (GSK3) and, subsequently, is targeted for ubiquitination and degradation via the proteasome (Figure 1).[12] However, in the presence of a Wnt ligand, its binding to the receptor complex initiates the activation of an intracellular protein termed Dishevelled (Dvl) which in turn inhibits GSK3 activity.[13] Therefore, β-catenin is not targeted for degradation and instead it accumulates and translocates to the nucleus. Here

*Correspondence to: Katherine Ann Staines, The Roslin Institute and R(D)SVS, The University of Edinburgh, Easter Bush, Midlothian, EH25 9RG, Scotland.
E-mail: katherine.staines@roslin.ed.ac.uk

Received 2 April 2012
Revised 25 April 2012
Accepted 20 May 2012

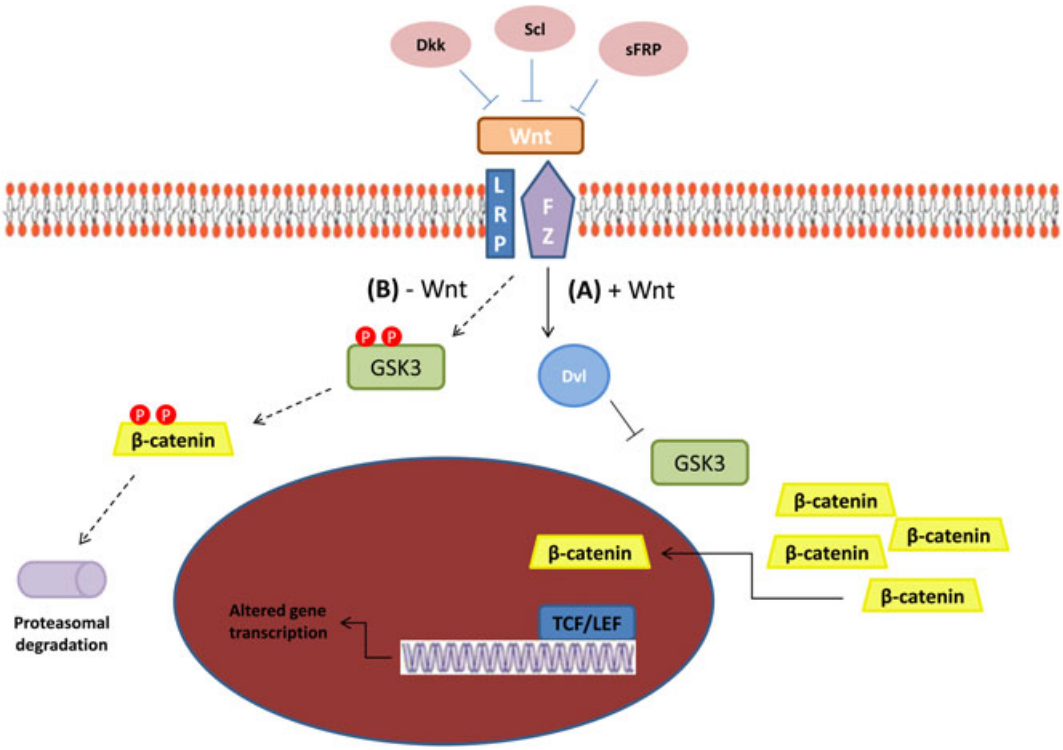

Figure 1. **The canonical Wnt signaling pathway**. Wnt ligands bind to Fz receptors and LRP5/6 coreceptors to initiate the canonical Wnt pathway. **(A)** Upon binding, Dishevelled is activated, which in turn, inhibits GSK3 activity. This allows translocation of β-catenin to the nucleus where it activates the transcription of Wnt-associated genes. **(B)** In the absence of appropriate Wnt ligand binding, because of inhibitors such as sFRP, Dkk1 and SCL, GSK3 becomes phosphorylated, which in turn, phosphorylates β-catenin. Phosphorylated β-catenin is subsequently targeted for ubiquitination and proteasomal degradation

it activates the transcription of a wide range of Wnt associated genes such as c-myc and cyclin D1 (Figure 1).[14] There are several known activators of the Wnt/β-catenin pathway including norrin and R-spondin.[15] The R-spondin family of proteins have recently been described, and although they are structurally unrelated to the classic Wnt ligands, they also are able to activate the Wnt/β-catenin signaling pathway through interacting with the LRP5/6 co-receptor complex. Furthermore, the R-spondins, of which, there are four described, are able to prevent the interaction of the LRP5/6 complex with the Wnt antagonists later described.[16–18] Although knockout models of all R-spondins have been described, it is only the R-spondin2 null mouse, which exhibits a skeletal phenotype.[19–21]

The non-canonical Wnt signaling pathway. In animal cells, the three non-canonical Wnt pathways described in the literature remain poorly understood. These pathways function independently of β-catenin, and thus, Wnt binds solely to Fz receptors and to co-receptors such as ROR2 and RYK but not to LRP5/6 co-receptors.[22] Wnt binding activates the Wnt/Ca^{2+} pathway, the Wnt/PCP pathway or the Wnt/PKA pathway. The Wnt/PCP pathway influences the planner organization of cells by inducing modifications to the actin cytoskeleton through activation of the small GTPase RhoA and c-Jun amino (N)-terminal kinase (JNK).[23] The Wnt/PKA pathway plays a role in myogenic gene expression through the activation of cyclic AMP.[24] The Wnt/Ca^{2+} pathway increases intracellular calcium levels through Fz-activated phospholipase C and phosphodiesterase. This subsequently regulates cell adhesion and motility.[25] The Wnt/Ca^{2+} pathway also inhibits the canonical Wnt pathway by promoting GSK3-independent β-catenin degradation.[26]

Wnt signaling antagonists. There are several reported antagonists of Wnt signaling, reflecting its complexity and importance in cellular function. These known inhibitors include Dickkopfs (Dkks), secreted Fz-related proteins (sFRPs) and sclerostin (SCL). sFRPs antagonize the Wnt pathway by binding directly to Wnt proteins or by preventing their binding to the Fz receptors, therefore blocking both Wnt pathways.[27] Interestingly, the sFRPs compete with each other to facilitate their actions.[28] The Dkk family of proteins consist of four members (Dkk1-Dkk4), which are known to antagonize Wnt signaling by binding to the LRP5/6 Wnt co-receptors, thus blocking the canonical pathway.[27] Additionally, Dkks also bind to another cell surface protein, Kremen.[29] In a similar fashion to Dkk, SCL, a secretory product of the mature osteocyte, also specifically binds to the LRP5/6 Wnt coreceptors antagonizing the Wnt pathway.[30] More recently, LRP4 has been implicated as a receptor for SCL.[31] Other known antagonists of the Wnt signaling pathway include Wnt-1-induced secreted protein (WISE), Wnt-inhibitory factor 1 (Wif-1) and Chibby.[1]

The role of Wnt in chondrogenesis

Chondrogenesis, the differentiation of mesenchymal precursor cells into chondrocytes, is critical for cartilage development. These mesenchymal precursors arise from three sources: cells derived from the neural crest, which give rise to the craniofacial bones, the somites, which give rise to the axial skeleton, and the somatopleure of the lateral plate mesoderm, which gives rise to the appendicular skeleton.[32] The mesenchymal cells have the ability to differentiate into either cartilage, fat, muscle or bone cells; however, for chondrocyte differentiation, there are four recognized steps involved. Initially, the mesenchyme precursors are recruited to the future sites of skeletal development where they produce an ECM which is rich in hyaluronan and collagen type I.[33] Following this, cellular aggregation and then condensation occur. Concomitant with cellular condensation is an increase in hyaluronidase activity, the expression of adhesion molecules such as neural cadherin (N-cadherin) and neural cell adhesion molecule (N-CAM) and the expression of the nuclear transcription factor Sox9. Despite not being expressed in early mesenchymal condensations, Sox5 and Sox6 are co-expressed with Sox9 during chondrocyte differentiation.[34] Finally, the mesenchymal cells undergo differentiation to the chondrogenic lineage with simultaneous expression of chondrocyte-specific molecules such as collagen type II and aggrecan.[35,36]

It is well established that chondrogenesis is highly dependent upon cell–ECM and cell–cell adhesion interactions. Several studies have demonstrated that Wnt signaling can influence chondrogenesis by acting upon these interactions (Figure 2). Wnt3a has been shown to be upregulated in response to bone morphogenic protein (BMP) 2. Wnt3a also induces cytoskeleton reorganization, a crucial step in mesenchymal chondrogenesis.[37–39] It has also been shown that Wnt3a enhances BMP2-mediated chondrogenesis.[40] This stands in contrast to further experiments in which Wnt3a was shown to inhibit chondrogenesis through a β-catenin dependent mechanism. More specifically, Wnt3a was shown to stabilize cell–cell adhesion through promoting sustained expression of N-cadherin and of β-catenin.[41] Recently, Wif-1, an inhibitor of Wnt signaling, has been localized to areas of chondrocyte condensation in the developing chick limb.[4] Importantly, Wif-1 is able to neutralize Wnt3a-mediated inhibition of chondrogenesis.[42] Furthermore, Sox9 has been suggested as a target for Wnt3a-mediated inhibition of chondrogenesis.[43] This transcription factor has also been implicated in the inhibitory role of Wnt6 in chondrogenesis. This inhibition is at an early stage of chondrogenesis, upstream of Sox9 and, therefore, prior to chondrogenic differentiation.[44] The effects of Wnt3a on chondrogenesis mimic those seen in studies investigating the role of other Wnt factors. Retroviral-mediated misexpression of Wnt7a, Wnt4, Wnt9a (formerly known as Wnt14) and Wnt1 inhibits cell condensation and thus chondrogenesis.[45–48] Similarly, the conditional overexpression of Wnt4 in mice leads to dwarfism with associated craniofacial abnormalities.[49] Like Wnt3a, the effects of Wnt7a have been attributed to the prolonged stabilization of N-cadherin.[47,50] It has also been shown that Wnt7a signaling can be inhibited by the increased activation of BMP2-mediated p38 mitogen-activated protein kinase (MAPK) signaling.[51] It is not only the Wnt factors, which have an inhibitory role in chondrogenesis: the forced expression of the Wnt receptor Fz7 inhibits mesenchymal condensation at the precartilage aggregate formation event through suppressed expression of N-cadherin.[52]

Despite the compelling evidence for the Wnt components having an inhibitory effect on mesenchymal chondrogenesis, some Wnt family members do promote chondrogenesis. For example, studies have shown that Wnt5a and Wnt5b can promote early chondrogenesis as indicated by an increase in the number of cartilaginous nodules formed *in vitro*.[45] Similarly, experimental Wnt5a knockout limbs display

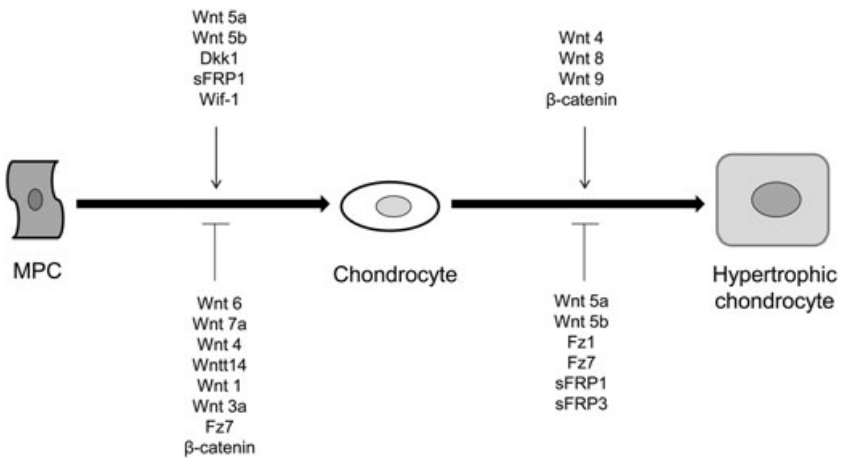

Figure 2. **Wnt regulation of chondrocyte differentiation**. Schematic representation of the role of Wnt in chondrogenic differentiation and hypertrophy. Mesenchymal precursor cells differentiate into chondrocytes, which then undergo hypertrophy under the regulation of various Wnt factors and inhibitors. However, not all chondrocytes mature into a hypertrophic phenotype as some retain their chondrogenic phenotype, and these cells constitute the articular cartilage

terminal adactyly and the otic capsule, a cartilaginous structure that surrounds the inner ear, is compromised in its ability to differentiate into cartilage when extracted from the Wnt5a null mouse.[53,54] However, unlike Wnt7a and Wnt3a, Wnt5a does not have an obvious effect on cell adhesion as the expression of N-cadherin is normal.[47] It has been suggested that Wnt5a may act through the activation of the phosphatidyl-inositol/Ca^{2+} or protein kinase C (PKC) pathways.[45,55] Furthermore, LEF-1, one of the nuclear transcription factors with which β-catenin forms a complex and also promotes chondrogenic differentiation.[56]

The role of the Wnt antagonists in chondrogenesis has recently been investigated. One such study has shown that Dkk1 and sFRP1 can promote early chondrogenesis in human mesenchymal stem cells.[57,58] However, this is in contrast with the examination of the sFRP1 knockout mouse, which exhibited increased chondrogenesis.[59] In light of this contradictory evidence, there is a timely need for further investigation into the therapeutic potential of the Wnt antagonists.

The role of Wnt in chondrocyte hypertrophic maturation

Differentiated chondrocytes either maintain their chondrogenic phenotype to form articular cartilage, or they undergo hypertrophic maturation in the process of endochondral ossification. The formation and longitudinal growth of the long bones is attributable to the process of endochondral ossification, which involves the replacement of a hyaline cartilage template by mineralized bone.[60] This cartilage anlagen is the growth plate, a developmental region located between the head and shaft of the long bones. The cells of the growth plate sit in distinct cellular zones of maturation and proceed through various stages of differentiation while maintaining their spatially fixed locations.[61] Following the cessation of chondrocyte proliferation, cells undergo hypertrophic maturation and display major phenotypic changes. These cells have an increase in cellular volume of approximately ten times larger than that of the proliferative chondrocytes, and a height increase of approximately fivefold between the proliferative and hypertrophic zones.[61–63] This voluminous increase is due to an increase in organelles such as mitochondria and the endoplasmic reticulum.[61,63,64] Associated with this differentiation is the increased expression of collagen type X, chondrocalcin, osteonectin and osteopontin, as well as the increased membrane activity of alkaline phosphatase.[65,66] It is also associated with the decreased expression of collagen type II, and other early chondrocyte marker genes, indicative of the final maturation phase. During this terminal differentiation, the hypertrophic chondrocytes mineralize their surrounding matrix, localized to the longitudinal septa of the growth plate.[67] This mineralization facilitates the deposition of hydroxyapatite and allows vascular invasion, a significant phase in the development of the skeleton, which allows osteoclasts and differentiating osteoblasts to remodel the new cartilage into bone tissue. It is well accepted that the terminally differentiated chondrocyte needs to be removed so as to maintain the steady-state thickness of the growth plate, and it is likely that this is by apoptosis.[68,69] Numerous factors have been identified as regulators of chondrocyte hypertrophy including Indian hedgehog (Ihh), Runx2 and PTHrP.

More recently, the role of Wnt signaling in the hypertrophic maturation of chondrocytes has been investigated (Figure 2). The activation of β-catenin in mature chondrocytes increases cell hypertrophy, as does the overexpression of β-catenin in chick sternal chondrocytes.[70–72] Additionally, β-catenin knockout mice display delayed chondrocyte maturation.[73] It has been suggested that the positive effects of β-catenin may be through the activation of RUNX2 or Ihh signaling, which, in turn, may induce collagen type X expression.[71,74] It may also act through inhibiting PTHrP signaling or through IGF-1 signaling.[75,76] It is not just β-catenin/LRP5/6 signaling that is involved in chondrocyte maturation. It has been shown that this is particularly dependent upon the Wnt/PKC signaling, initiated by the LRP1 receptor.[77] Several Wnt factors have been identified as promoters of chondrocyte hypertrophy including Wnt4 and Wnt8.[45,78] In contrast, Wnt5a and 5b have both been shown to inhibit the hypertrophic maturation of chondrocytes.[79,80] Moreover, the inhibitory effect of Wnt5a is associated with an increase in NF-κB activation and inhibition of RUNX2.[79] Fz1 and Fz7 have also been shown to delay chondrocyte maturation as has the misexpression of the Wnt inhibitor sFRP3.[50,78,81] Similarly, sFRP1 knockout mice show increased chondrocyte maturation with associated reduced growth plate widths and increased hypertrophic mineralization, suggesting accelerated endochondral ossification. This promotion of chondrocyte hypertrophic maturation is also observed in *in vitro* studies.[59]

The Wnt signaling pathway has great potential as a therapeutic target for cartilage degradation. β-catenin accelerates chondrocyte hypertrophy, and this may lead to a loss in cartilage integrity.[70–73] Therefore, blocking β-catenin, through the use of inhibitors of β-catenin such as TCF-4 (ICAT) or XAV939, could potentially be a therapeutic strategy.[82,83] However, this must come with caution as it has also been shown that the inhibition of β-catenin causes chondrocyte apoptosis.[84] It is therefore imperative that levels of β-catenin remain normal for effective cartilage function and that any new Wnt-related drug will need to be carefully targeted, as any off-target effects are likely to be accompanied by significant risk.

The role of Wnt in joint formation and homeostasis

As previously discussed, as opposed to maturing into a hypertrophic phenotype, some chondrocytes retain their chondrocyte phenotype and form articular cartilage. The articular cartilage is a key component of the complex joint, and it works in synergy with various other tissues within the joint to ensure fluid movement of the bones and mechanical stability. More specifically, articular cartilage functions to reduce friction and to withstand the mechanical stress placed upon the ends of the long bones during joint movement. For this reason, articular cartilage is structurally

adapted to fit this need. Like in the growth plate, articular cartilage is organized in a strict hierarchy, the organization, and thus, the mechanical efficiency of which increases with maturity. Articular cartilage is hypocellular, avascular, aneural and alymphatic. Chondrocytes constitute less than 5% of articular cartilage with their vast ECM comprising the rest and as such, their viability is critical. The homeostatic equilibrium of ECM synthesis and degradation is also crucial in maintaining healthy and fully functioning articular cartilage.

The Wnt pathway in joint cavitation. The formation of synovial joints in the appendicular skeleton is dependent upon the induction of genes involved in prechondrogenic condensations and the formation of the joint interzone. With regard to Wnt signaling, Wnt9a was first identified as a major player in the induction of joint interzone formation in chick limb studies.[46] It has since been shown that targeted inactivation of Wnt9a in mice results in ectopic cartilage nodule formation in some synovial joints, known as synovial chondroid metaplasia in humans.[81] Wnt4 has also been localized to the cells of future joint formation; however the Wnt4:Wnt9a double mutant mouse displays limited joint disruption.[46,85,86] This therefore suggests that the third Wnt factor expressed in the joint interzone area, Wnt16, is compensating for the absence of Wnts 4 and 9a.[85] The expression of these Wnt factors in the presumptive joint results in a decrease in Sox9 and collagen type II expression, whereas it upregulates β-catenin protein levels.[85] Moreover, it has been found that the ectopic expression of active β-catenin in chondrocytes leads to severely compromised cartilage and joint formation.[73,85,87] This therefore suggests that joint induction is regulated by Wnt4, 9a and 16 controlled β-catenin signaling. Furthermore, a role for Ihh has been proposed in joint formation as upregulation of its signaling in mice results in mild joint fusion.[88,89]

Wnt signaling appears critical for not only the formation of the joint but also its maintenance as indicated by the numerous transgenic mouse models which invariably display postnatal phenoytpes.[90] Any dysregulation in the integrity of the articular cartilage can lead to its degradation, as is commonly seen in OA and RA. In these prevalent and debilitating diseases, the integrity of the cartilage ECM is compromised with proteoglycan loss and disruption to the collagen fibrils, making it brittle and susceptible to fibrillation, fissuring and subsequent fragmentation with associated chondrocyte cell apoptosis. This subsequently causes the sufferer pain and disability.

The Wnt pathway in RA. RA is an autoimmune disease, which is pathologically characterized by bone and cartilage degradation as well as inflammation of the synovium. The most prominent change seen is the production of a pannus. For this, the synovial cells and the underlying connective tissue form a mesh of proliferating tissue, which produces large concentrations of enzymes, aiding its growth and destroying the articular cartilage. Activators of this pannus formation include the inflammatory cytokines tumour necrosis factor (TNF)-α and interleukin (IL)-1; however, despite RA sufferers undergoing anti-inflammatory therapy, this pannus can still be activated. Recently, components of the Wnt pathway have been implemented in the pathophysiology of RA (Table 1).

Analysis of RA synovial tissue has identified the increased expression of Wnts 1, 5a, 7b, 10b, 11 and 13 and Fzs 2, 5 and 7. In particular, increases in the expressions of Wnt5a and Fz5 in RA synovial tissue have been observed.[91] Wnt5a and Fz5 have been shown to activate the formation of the pannus, potentially through the PKC signaling cascade and NF-κB activation. Furthermore, Wnt5a and Fz5 signaling has been shown to increase the production of the pro-inflammatory cytokines IL-6, IL-15 and receptor activator for NF-κB ligand (RANKL) causing further joint destruction.[92–94] Similarly, synovial cells transfected with Wnt7b display increased expression of TNF-α, IL-1 and IL-6, all of which shift cartilage homeostasis towards catabolism in RA.[95,96]

Wnt1 is known to promote cell adhesion, cell growth and survival. In RA patients, Wnt1 is overexpressed. The *in vitro* transfection of synovial cells with Wnt1 has shown that this results in an increased expression of fibronectin and pro-matrix metalloproteinase (MMP) 3. These proteins are known to promote survival and invasiveness.[97] The Wnt1-inducible secreted protein, WISP3, although not directly induced by Wnt1, is also proving to be important in the molecular regulation of RA with a WISP3 gene polymorphism being associated with juvenile idiopathic arthritis.[98,99] WISP3 mRNA is increased in RA synovium compared with control counterparts, and this is increased even more so by pro-inflammatory cytokines *in vitro*.[100] It is known that WISP3 acts to maintain cartilage integrity by regulating the expression of type II collagen and aggrecan, and by repressing such catabolic molecules as ADAMTS5 and MMP10.[101,102] Another Wnt1-inducible secreted protein, WISP2, has also been reported in RA.[103]

The role of the Wnt antagonists in RA has also been investigated with sFRP1–being observed in the synovial cells of patients with RA.[96,104,105] Dkk1 is also present in RA tissue, and its expression can be upregulated by the pro-inflammatory cytokine TNF-α, thus suggesting that inflammation is an inducer of Dkk1 expression.[106] This recent and comprehensive study showed that treatment with an anti-Dkk1 antibody induced osteophyte formation in RA joints and protected them from bone erosions through decreased osteoclast formation and increased OPG expression.[106] This may form the basis of some future therapeutic strategy for RA. Moreover, another interesting approach may be to target molecules downstream of β-catenin signaling that are known to be upregulated in RA, such as WISP2 and WISP3, or to target Wnt factors known to be involved in the major pathologies of RA. Both Wnt5a and Fz5 are known to activate pannus formation, as well as to increase proinflammatory cytokine expression, making them attractive therapeutic targets, which may provide further insights into the specific roles of Wnt in RA and cartilage homeostasis.

The Wnt pathway in OA. OA is a degenerative disease primarily characterized by the progressive destruction of the articular cartilage. Associated with this are subchondral bone thickening, osteophyte formation and inflammation of the synovial membrane causing pain. It is thought that biochemical changes in MMP and aggrecanase production mediate the cartilage destruction, with the pro-inflammatory cytokines also being implicated. Recently, it has been suggested that abnormal Wnt signaling may contribute to OA pathogenesis. This stems from multiple studies, which have sought to examine the genetic component of OA: it is known that primary OA has an estimated heritability of 40% for the knee, 60% for the hip and 65% for the hand.[107] Several Wnt-related factors have been identified to be associated with OA through these genetic studies, and their functional role is slowly being established Table 1.

Genetic analysis of polymorphisms associated with OA has identified a single nucleotide polymorphism in sFRP3 as a target for OA susceptibility.[108–111] Generation of the sFRP3 null mouse showed no developmental changes; however, upon induction of OA via either inflammatory, surgical or enzymatic methods, cartilage degradation in the sFRP3 null mice was greater than their control counterparts. This was associated with increased Wnt/β-catenin signaling and with the inhibition of MMP3.[112] Other Wnt antagonists have been identified as having a role in the pathogenesis of OA. sFRP1, sFRP2 and sFRP4 expression have all been reported in OA synovium, and like in RA, Dkk1 expression has been observed.[96,113] This Dkk1 expression has been shown to impair chondrocyte growth while promoting chondrocyte apoptosis. Furthermore, Dkk1 expression can be induced by IL-1β.[113,114] Dkk2 expression is higher in OA osteoblasts compared with control counterparts.[115] Correction of the Dkk2 expression by siRNA gene silencing enhanced Wnt signaling and corrected the abnormal phenotype, as well as increased osteoblast mineralization. The increased expression of Dkk2 was shown to be induced by transforming growth factor β (TGF-β) expression.[115] SCL is a well-established inhibitor of Wnt signaling and, therefore, bone formation. Its role in OA is slowly emerging; despite no changes in SCL serum levels, there is a decreased number of SCL positive osteocytes in human OA patients.[116,117] This has been further examined using mouse and sheep OA models. Interestingly, there was an increase in SCL expression in the articular chondrocytes of post-meniscectomy sheep specimens in comparison to sham-operated animals. This was further confirmed in a mouse DMM model and in human samples. The increased expression of SCL in these chondrocytes was further increased in response to IL-α but not to TNF-α. SCL expression appeared to inhibit Wnt signaling and the expression of catabolic MMPs. Contradictory to this, incubation of chondrocytes with recombinant SCL decreased the expression of aggrecan, collagen type II and TIMPs.[118]

Polymorphisms in LRP5 and LRP6 have also been associated with OA, with their expression being greater in OA tissues.[110] Furthermore, the blocking of LRP5 expression results in a significant decrease in MMP13 mRNA and protein levels.[119] GSK3β promotes the degradation of β-catenin, and the inhibition of its activity has been shown to induce OA features in murine metatarsal bones, highlighting the importance of GSK3β in maintaining the chondrocyte phenotype.[120]

Numerous Wnt factors have been identified as being unregulated in OA tissue including Wnts 2b, 3a, 4, 6, 7a, 7b, 9b, 10a and 16.[95,121–124] Moreover, the Fz2, Fz5 and Fz7 have been identified.[91] The role of Wnt3a in OA has been well investigated as its activity is reduced in OA. Articular chondrocytes cultured with Wnt3a exhibited rapid matrix loss and protease expression. Similar results were seen with overexpression of β-catenin.[125] Furthermore, Wnt3a stimulated chondrocytes exhibit an upregulation of MMP3 and ADAMTS-4.[126] Wnt3a-dependent activity is reduced in OA, and this can be corrected by the addition of recombinant R-spondin2. Moreover, in OA osteoblasts, R-spondin2 expression is decreased, thought to be because of the elevated levels of TGF-β in these cells.[127] Like in RA, WISP3 is expressed by OA tissue, and this can be increased by the pro-inflammatory cytokines TNF-α and IL-1.[100] A polymorphism in the WISP1 gene has been linked to spinal OA, and similarly, its increased expression in OA tissue has been observed.[122,128,129] Furthermore, it has been shown that the *in vivo* and *in vitro* stimulation of articular chondrocytes with WISP1 increased cartilage degeneration through the induction of MMPs and aggrecanase.[122]

Molecular mechanisms involved in the expression of proteins relevant to the pathological changes of cartilage degeneration, subchondral bone thickening and osteophyte formation in OA may form potential therapeutic strategies. β-catenin accelerates chondrocyte hypertrophy, a key aspect of OA. However, targeting this comes with significant risk, as previously discussed, and therefore, it seems the development of drugs, which selectively inhibit the Wnt pathway, may prove useful as therapeutic targets. In OA, the blockade of Dkk1 by a neutralizing antibody led to attenuation

Table 1. **Aberrant Wnt expression in joint disease**. Detailed is the aberrant expression of Wnt and Wnt associated factors in both RA (rheumatoid arthritis) and OA (osteoarthritis). Literature detailing the role of the individual factors is cited

	Wnt	Frizzled	Antagonists	Other
RA	Wnt1,[97] Wnt5a,[92–94] Wnt7,[95,96] and Wnt10b, Wnt11, Wnt13[96]	Fz2,[91] Fz5,[91–94] Fz7[91]	sFRP1-5,[104,105] Dkk1[106]	WISP2,[103] WISP3[101,102]
OA	Wnt3a,[95,121–126] and Wnt2b, Wnt4, Wnt6, Wnt7a, Wnt7b, Wnt9b, Wnt10a, Wnt16[95,121–124]	Fz2, Fz5, Fz7[91]	sFRP1-4,[108–111] Dkk1,[113,114] Dkk2,[115] SCL[118]	WISP1,[122] WISP3,[100] R-spondin2,[127] LRP5/6,[110,119] GSK3β[120]

of chondrocyte apoptosis, whereas recombinant Dkk1 promoted apoptosis, a key component of OA pathogenesis.[114] However, before any finite conclusions can be made, a more detailed analysis of the role of Dkk1 in OA is required. Like Dkk1, SCL inhibits Wnt signaling by specifically binding to the LRP5/6 receptors. Antibodies to SCL have great therapeutic use in the osteoanabolic therapy of osteoporosis and inflammatory bone loss, as is currently emerging.[130–133] As highlighted by Chan and colleagues, it is imperative that the effects of blocking SCL activity on OA progression are fully investigated.[118]

Conversely, (hetero)arylpyrimidines have been identified as agonists of Wnt, and this warrants their investigation, along with other Wnt agonists such as R-spondin2, as therapeutic targets.[134] R-spondin2 and Dkk2 display decreased and increased expression respectively in response to the increased TGF-β observed in OA. Both these molecules contribute to the pathological changes observed in OA cartilage and, as such, warrant the future investigation of neutralizing TGF-β activity in OA. Certainly the injection of TGF-β into mouse knees produces OA-like features; however, any therapeutic strategy involving TGF-β may prove complex because its varying reported effects on the joint as are extensively reviewed by Blaney-Davidson *et al*.[135–139] In view of the complexity of the molecular mechanisms surrounding OA, it is important that future studies focus upon the specific and precise roles that Wnt signaling plays in the individual components and pathologies of the joint.

CONCLUSION

The evidence presented in this review highlights the critical role of the Wnt signaling pathway in chondrogenesis and cartilage development and homeostasis. The precise individual roles that the Wnt factors play are complex as they can trigger multiple Wnt pathways. Future directions should focus upon better understanding the individual roles of the Wnt factors in cartilage homeostasis, their downstream targets and the interactions that they may have with other pathways (Table 1).

CONFLICT OF INTEREST

The authors have declared that there is no conflict of interest.

ACKNOWLEDGEMENTS

The authors acknowledge the Institute Strategic Programme Grant Funding from the Biotechnology and Biological Sciences Research Council (BBSRC) UK (CF, VM) and BBSRC studentship funding (KS) for support.

REFERENCES

1. Macsai CE, Foster BK, Xian CJ. Roles of Wnt signalling in bone growth, remodelling, skeletal disorders and fracture repair. *J Cell Physiol* 2008; **215**: 578–587.
2. Macsai CE, Georgiou KR, Foster BK, Zannettino AC, Xian CJ. Microarray expression analysis of genes and pathways involved in growth plate cartilage injury responses and bony repair. *Bone* 2012; **50**: 1081–1091.
3. Krishnan V, Bryant HU, MacDougald OA. Regulation of bone mass by Wnt signaling. *J Clin Invest* 2006; **116**: 1202–1209.
4. Witte F, Dokas J, Neuendorf F, Mundlos S, Stricker S. Comprehensive expression analysis of all Wnt genes and their major secreted antagonists during mouse limb development and cartilage differentiation. *Gene Expr Patterns* 2009; **9**: 215–223.
5. Summerhurst K, Stark M, Sharpe J, Davidson D, Murphy P. 3D representation of Wnt and Frizzled gene expression patterns in the mouse embryo at embryonic day 11.5 (Ts19). *Gene Expr Patterns* 2008; **8**: 331–348.
6. Nelson WJ, Nusse R. Convergence of Wnt, beta-catenin, and cadherin pathways. *Science* 2004; **303**: 1483–1487.
7. Moon RT. Wnt/beta-catenin pathway. *Sci STKE* 2005; **271**: cm1.
8. Moon RT, Kohn AD, De Ferrari GV, Kaykas A. WNT and beta-catenin signalling: diseases and therapies. *Nat Rev Genet* 2004; **5**: 691–701.
9. Bhanot P, Brink M, Samos CH, *et al*. A new member of the frizzled family from Drosophila functions as a Wingless receptor. *Nature* 1996; **382**: 225–230.
10. Dann CE, Hsieh JC, Rattner A, Sharma D, Nathans J, Leahy DJ. Insights into Wnt binding and signalling from the structures of two Frizzled cysteine-rich domains. *Nature* 2001; **412**: 86–90.
11. Hsieh JC, Rattner A, Smallwood PM, Nathans J. Biochemical characterization of Wnt-frizzled interactions using a soluble, biologically active vertebrate Wnt protein. *Proc Natl Acad Sci U S A* 1999; **96**: 3546–3551.
12. Aberle H, Bauer A, Stappert J, Kispert A, Kemler R. Beta-catenin is a target for the ubiquitin-proteasome pathway. *EMBO J* 1997; **16**: 3797–3804.
13. Nusse R. Wnt signaling in disease and in development. *Cell Res* 2005; **15**: 28–32.
14. Ott SM. Sclerostin and Wnt signaling--the pathway to bone strength. *J Clin Endocrinol Metab* 2005; **90**: 6741–6743.
15. Xu Q, Wang Y, Dabdoub A, *et al*. Vascular development in the retina and inner ear: control by Norrin and Frizzled-4, a high-affinity ligand-receptor pair. *Cell* 2004; **116**: 883–895.
16. Kim KA, Zhao J, Andarmani S, *et al*. R-Spondin proteins: a novel link to beta-catenin activation. *Cell Cycle* 2006; **5**: 23–26.
17. Nam JS, Turcotte TJ, Smith PF, Choi S, Yoon JK. Mouse cristin/R-spondin family proteins are novel ligands for the Frizzled 8 and LRP6 receptors and activate beta-catenin-dependent gene expression. *J Biol Chem* 2006; **281**: 13247–13257.
18. Kim KA, Wagle M, Tran K, *et al*. R-Spondin family members regulate the Wnt pathway by a common mechanism. *Mol Biol Cell* 2008; **19**: 2588–2596.
19. Nam JS, Park E, Turcotte TJ, *et al*. Mouse R-spondin2 is required for apical ectodermal ridge maintenance in the hindlimb. *Dev Biol* 2007; **311**: 124–135.
20. Aoki M, Kiyonari H, Nakamura H, Okamoto H. R-spondin2 expression in the apical ectodermal ridge is essential for outgrowth and patterning in mouse limb development. *Dev Growth Differ* 2008; **50**: 85–95.
21. Yamada W, Nagao K, Horikoshi K, *et al*. Craniofacial malformation in R-spondin2 knockout mice. *Biochem Biophys Res Commun* 2009; **381**: 453–458.
22. Chen Y, Alman BA. Wnt pathway, an essential role in bone regeneration. *J Cell Biochem* 2009; **106**: 353–362.
23. Fanto M, McNeill H. Planar polarity from flies to vertebrates. *J Cell Sci* 2004; **117**: 527–533.
24. Chen AE, Ginty DD, Fan CM. Protein kinase A signalling via CREB controls myogenesis induced by Wnt proteins. *Nature* 2005; **433**: 317–322.
25. Wang HY, Malbon CC. Wnt signaling, Ca2+, and cyclic GMP: visualizing Frizzled functions. *Science* 2003; **300**: 1529–1530.
26. Topol L, Jiang X, Choi H, Garrett-Beal L, Carolan PJ, Yang Y. Wnt-5a inhibits the canonical Wnt pathway by promoting GSK-3-independent beta-catenin degradation. *J Cell Biol* 2003; **162**: 899–908.

27. Kawano Y, Kypta R. Secreted antagonists of the Wnt signalling pathway. *J Cell Sci* 2003; **116**: 2627–2634.
28. Yoshino K, Rubin JS, Higinbotham KG, *et al*. Secreted Frizzled-related proteins can regulate metanephric development. *Mech Dev* 2001; **102**: 45–55.
29. Mao B, Wu W, Davidson G, *et al*. Kremen proteins are Dickkopf receptors that regulate Wnt/beta-catenin signalling. *Nature* 2002; **417**: 664–667.
30. Semenov M, Tamai K, He X. SOST is a ligand for LRP5/LRP6 and a Wnt signaling inhibitor. *J Biol Chem* 2005; **280**: 26770–26775.
31. Choi HY, Dieckmann M, Herz J, Niemeier A. Lrp4, a novel receptor for Dickkopf 1 and sclerostin, is expressed by osteoblasts and regulates bone growth and turnover in vivo. *PLoS One* 2009; **4**: e7930.
32. Olsen BR, Reginato AM, Wang W. Bone development. *Annu Rev Cell Dev Biol* 2000; **16**: 191–220.
33. Sandell LJ. In situ expression of collagen and proteoglycan genes in notochord and during skeletal development and growth. *Microsc Res Tech* 1994; **28**: 470–482.
34. Lefebvre V, Li P, de Crombrugghe B. A new long form of Sox5 (L-Sox5), Sox6 and Sox9 are coexpressed in chondrogenesis and cooperatively activate the type II collagen gene. *EMBO J* 1998; **17**: 5718–5733.
35. Hall BK, Miyake T. All for one and one for all: condensations and the initiation of skeletal development. *Bioessays* 2000; **22**: 138–147.
36. Goldring MB, Tsuchimochi K, Ijiri K. The control of chondrogenesis. *J Cell Biochem* 2006; **97**: 33–44.
37. Shibamoto S, Higano K, Takada R, Ito F, Takeichi M, Takada S. Cytoskeletal reorganization by soluble Wnt-3a protein signalling. *Genes Cells* 1998; **3**: 659–670.
38. Kengaku M, Capdevila J, Rodriguez-Esteban C, *et al*. Distinct WNT pathways regulating AER formation and dorsoventral polarity in the chick limb bud. *Science* 1998; **280**: 1274–1277.
39. Fischer L, Boland G, Tuan RS. Wnt signaling during BMP-2 stimulation of mesenchymal chondrogenesis. *J Cell Biochem* 2002; **84**: 816–831.
40. Fischer L, Boland G, Tuan RS. Wnt-3A enhances bone morphogenetic protein-2-mediated chondrogenesis of murine C3H10T1/2 mesenchymal cells. *J Biol Chem* 2002; **277**: 30870–30878.
41. Hwang SG, Yu SS, Lee SW, Chun JS. Wnt-3a regulates chondrocyte differentiation via c-Jun/AP-1 pathway. *FEBS Lett* 2005; **579**: 4837–4842.
42. Surmann-Schmitt C, Widmann N, Dietz U, *et al*. Wif-1 is expressed at cartilage-mesenchyme interfaces and impedes Wnt3a-mediated inhibition of chondrogenesis. *J Cell Sci* 2009; **122**: 3627–3637.
43. ten Berge D, Brugmann SA, Helms JA, Nusse R. Wnt and FGF signals interact to coordinate growth with cell fate specification during limb development. *Development* 2008; **135**: 3247–3257.
44. Geetha-Loganathan P, Nimmagadda S, Christ B, Huang R, Scaal M. Ectodermal Wnt6 is an early negative regulator of limb chondrogenesis in the chicken embryo. *BMC Dev Biol* 2010; **10**: 32.
45. Church V, Nohno T, Linker C, Marcelle C, Francis-West P. Wnt regulation of chondrocyte differentiation. *J Cell Sci* 2002; **115**: 4809–4818.
46. Hartmann C, Tabin CJ. Wnt-14 plays a pivotal role in inducing synovial joint formation in the developing appendicular skeleton. *Cell* 2001; **104**: 341–351.
47. Tufan AC, Tuan RS. Wnt regulation of limb mesenchymal chondrogenesis is accompanied by altered N-cadherin-related functions. *FASEB J* 2001; **15**: 1436–1438.
48. Rudnicki JA, Brown AM. Inhibition of chondrogenesis by Wnt gene expression in vivo and in vitro. *Dev Biol* 1997; **185**: 104–118.
49. Lee HH, Behringer RR. Conditional expression of Wnt4 during chondrogenesis leads to dwarfism in mice. *PLoS One* 2007; **2**: e450.
50. Daumer KM, Tufan AC, Tuan RS. Long-term in vitro analysis of limb cartilage development: involvement of Wnt signaling. *J Cell Biochem* 2004; **93**: 526–541.
51. Jin EJ, Lee SY, Choi YA, Jung JC, Bang OS, Kang SS. BMP-2-enhanced chondrogenesis involves p38 MAPK-mediated down-regulation of Wnt-7a pathway. *Mol Cells* 2006; **22**: 353–359.
52. Tufan AC, Daumer KM, Tuan RS. Frizzled-7 and limb mesenchymal chondrogenesis: effect of misexpression and involvement of N-cadherin. *Dev Dyn* 2002; **223**: 241–253.
53. Al-Qattan MM. WNT pathways and upper limb anomalies. *J Hand Surg Eur Vol* 2011; **36**: 9–22.
54. Liu W, Li L, Li G, Garritano F, Shanske A, Frenz DA. Coordinated molecular control of otic capsule differentiation: functional role of Wnt5a signaling and opposition by sfrp3 activity. *Growth Factors* 2008; **26**: 343–354.
55. Slusarski DC, Yang-Snyder J, Busa WB, Moon RT. Modulation of embryonic intracellular Ca2+ signaling by Wnt-5A. *Dev Biol* 1997; **182**: 114–120.
56. Yano F, Kugimiya F, Ohba S, *et al*. The canonical Wnt signaling pathway promotes chondrocyte differentiation in a Sox9-dependent manner. *Biochem Biophys Res Commun* 2005; **333**: 1300–1308.
57. Im GI, Lee JM, Kim HJ. Wnt inhibitors enhance chondrogenesis of human mesenchymal stem cells in a long-term pellet culture. *Biotechnol Lett* 2011; **33**: 1061–1068.
58. Im GI, Quan Z. The effects of Wnt inhibitors on the chondrogenesis of human mesenchymal stem cells. *Tissue Eng Part A* 2010; **16**: 2405–2413.
59. Gaur T, Rich L, Lengner CJ, *et al*. Secreted frizzled related protein 1 regulates Wnt signaling for BMP2 induced chondrocyte differentiation. *J Cell Physiol* 2006; **208**: 87–96.
60. Kronenberg HM. Developmental regulation of the growth plate. *Nature* 2003; **423**: 332–336.
61. Hunziker EB, Schenk RK, Cruz-Orive LM. Quantitation of chondrocyte performance in growth-plate cartilage during longitudinal bone growth. *J Bone Joint Surg Am* 1987; **69**: 162–173.
62. Farnum CE, Lee R, O'Hara K, Urban JP. Volume increase in growth plate chondrocytes during hypertrophy: the contribution of organic osmolytes. *Bone* 2002; **30**: 574–581.
63. Buckwalter JA, Mower D, Ungar R, Schaeffer J, Ginsberg B. Morphometric analysis of chondrocyte hypertrophy. *J Bone Joint Surg Am* 1986; **68**: 243–255.
64. DeLise AM, Fischer L, Tuan RS. Cellular interactions and signaling in cartilage development. *Osteoarthritis Cartilage* 2000; **8**: 309–334.
65. Shen G. The role of type X collagen in facilitating and regulating endochondral ossification of articular cartilage. *Orthod Craniofac Res* 2005; **8**: 11–17.
66. Sommer B, Bickel M, Hofstetter W, Wetterwald A. Expression of matrix proteins during the development of mineralized tissues. *Bone* 1996; **19**: 371–380.
67. Castagnola P, Dozin B, Moro G, Cancedda R. Changes in the expression of collagen genes show two stages in chondrocyte differentiation in vitro. *J Cell Biol* 1988; **106**: 461–467.
68. Shapiro IM, Adams CS, Freeman T, Srinivas V. Fate of the hypertrophic chondrocyte: microenvironmental perspectives on apoptosis and survival in the epiphyseal growth plate. *Birth Defects Res C Embryo Today* 2005; **75**: 330–339.
69. Magne D, Bluteau G, Faucheux C, *et al*. Phosphate is a specific signal for ATDC5 chondrocyte maturation and apoptosis-associated mineralization: possible implication of apoptosis in the regulation of endochondral ossification. *J Bone Miner Res* 2003; **18**: 1430–1442.
70. Tamamura Y, Otani T, Kanatani N, *et al*. Developmental regulation of Wnt/beta-catenin signals is required for growth plate assembly, cartilage integrity, and endochondral ossification. *J Biol Chem* 2005; **280**: 19185–19195.
71. Dong YF, Soung dY, Schwarz EM, O'Keefe RJ, Drissi H. Wnt induction of chondrocyte hypertrophy through the Runx2 transcription factor. *J Cell Physiol* 2006; **208**: 77–86.
72. Kitagaki J, Iwamoto M, Liu JG, Tamamura Y, Pacifci M, Enomoto-Iwamoto M. Activation of beta-catenin-LEF/TCF signal pathway in chondrocytes stimulates ectopic endochondral ossification. *Osteoarthritis Cartilage* 2003; **11**: 36–43.
73. Akiyama H, Lyons JP, Mori-Akiyama Y, *et al*. Interactions between Sox9 and beta-catenin control chondrocyte differentiation. *Genes Dev* 2004; **18**: 1072–1087.
74. Mak KK, Kronenberg HM, Chuang PT, Mackem S, Yang Y. Indian hedgehog signals independently of PTHrP to promote chondrocyte hypertrophy. *Development* 2008; **135**: 1947–1956.

75. Wang L, Shao YY, Ballock RT. Thyroid hormone-mediated growth and differentiation of growth plate chondrocytes involves IGF-1 modulation of beta-catenin signaling. *J Bone Miner Res* 2010; **25**: 1138–1146.
76. Guo X, Mak KK, Taketo MM, Yang Y. The Wnt/beta-catenin pathway interacts differentially with PTHrP signaling to control chondrocyte hypertrophy and final maturation. *PLoS One* 2009; **4**: e6067.
77. Kawata K, Kubota S, Eguchi T, *et al*. Role of the low-density lipoprotein receptor-related protein-1 in regulation of chondrocyte differentiation. *J Cell Physiol* 2010; **222**: 138–148.
78. Enomoto-Iwamoto M, Kitagaki J, Koyama E, *et al*. The Wnt antagonist Frzb-1 regulates chondrocyte maturation and long bone development during limb skeletogenesis. *Dev Biol* 2002; **251**: 142–156.
79. Bradley EW, Drissi MH. WNT5A regulates chondrocyte differentiation through differential use of the CaN/NFAT and IKK/NF-kappaB pathways. *Mol Endocrinol* 2010; **24**: 1581–1593.
80. Bradley EW, Drissi MH. Wnt5b regulates mesenchymal cell aggregation and chondrocyte differentiation through the planar cell polarity pathway. *J Cell Physiol* 2011; **226**: 1683–1693.
81. Hartmann C, Tabin CJ. Dual roles of Wnt signaling during chondrogenesis in the chicken limb. *Development* 2000; **127**: 3141–3159.
82. Gottardi CJ, Gumbiner BM. Role for ICAT in beta-catenin-dependent nuclear signaling and cadherin functions. *Am J Physiol Cell Physiol* 2004; **286**: C747–C756.
83. Huang SM, Mishina YM, Liu S, *et al*. Tankyrase inhibition stabilizes axin and antagonizes Wnt signalling. *Nature* 2009; **461**: 614–620.
84. Zhu M, Chen M, Zuscik M, *et al*. Inhibition of beta-catenin signaling in articular chondrocytes results in articular cartilage destruction. *Arthritis Rheum* 2008; **58**: 2053–2064.
85. Guo X, Day TF, Jiang X, Garrett-Beal L, Topol L, Yang Y. Wnt/beta-catenin signaling is sufficient and necessary for synovial joint formation. *Genes Dev* 2004; **18**: 2404–2417.
86. Spater D, Hill TP, Gruber M, Hartmann C. Role of canonical Wnt-signalling in joint formation. *Eur Cell Mater* 2006; **12**: 71–80.
87. Day TF, Guo X, Garrett-Beal L, Yang Y. Wnt/beta-catenin signaling in mesenchymal progenitors controls osteoblast and chondrocyte differentiation during vertebrate skeletogenesis. *Dev Cell* 2005; **8**: 739–750.
88. Spater D, Hill TP, O'sullivan RJ, Gruber M, Conner DA, Hartmann C. Wnt9a signaling is required for joint integrity and regulation of Ihh during chondrogenesis. *Development* 2006; **133**: 3039–3049.
89. Mak KK, Chen MH, Day TF, Chuang PT, Yang Y. Wnt/beta-catenin signaling interacts differentially with Ihh signaling in controlling endochondral bone and synovial joint formation. *Development* 2006; **133**: 3695–3707.
90. Luyten FP, Tylzanowski P, Lories RJ. Wnt signaling and osteoarthritis. *Bone* 2009; **44**: 522–527.
91. Sen M, Lauterbach K, El-Gabalawy H, Firestein GS, Corr M, Carson DA. Expression and function of wingless and frizzled homologs in rheumatoid arthritis. *Proc Natl Acad Sci U S A* 2000; **97**: 2791–2796.
92. Sen M, Chamorro M, Reifert J, Corr M, Carson DA. Blockade of Wnt-5A/frizzled 5 signaling inhibits rheumatoid synoviocyte activation. *Arthritis Rheum* 2001; **44**: 772–781.
93. Wilson L, Szabo C, Salzman AL. Protein kinase C-dependent activation of NF-kappaB in enterocytes is independent of IkappaB degradation. *Gastroenterology* 1999; **117**: 106–114.
94. Kim J, Kim J, Kim DW, *et al*. Wnt5a induces endothelial inflammation via beta-catenin-independent signaling. *J Immunol* 2010; **185**: 1274–1282.
95. Nakamura Y, Nawata M, Wakitani S. Expression profiles and functional analyses of Wnt-related genes in human joint disorders. *Am J Pathol* 2005; **167**: 97–105.
96. Imai K, Morikawa M, D'Armiento J, Matsumoto H, Komiya K, Okada Y. Differential expression of WNTs and FRPs in the synovium of rheumatoid arthritis and osteoarthritis. *Biochem Biophys Res Commun* 2006; **345**: 1615–1620.
97. Sen M, Reifert J, Lauterbach K, *et al*. Regulation of fibronectin and metalloproteinase expression by Wnt signaling in rheumatoid arthritis synoviocytes. *Arthritis Rheum* 2002; **46**: 2867–2877.
98. Pennica D, Swanson TA, Welsh JW, *et al*. WISP genes are members of the connective tissue growth factor family that are up-regulated in wnt-1-transformed cells and aberrantly expressed in human colon tumors. *Proc Natl Acad Sci U S A* 1998; **95**: 14717–14722.
99. Lamb R, Thomson W, Ogilvie E, Donn R. Wnt-1-inducible signaling pathway protein 3 and susceptibility to juvenile idiopathic arthritis. *Arthritis Rheum* 2005; **52**: 3548–3553.
100. Cheon H, Boyle DL, Firestein GS. Wnt1 inducible signaling pathway protein-3 regulation and microsatellite structure in arthritis. *J Rheumatol* 2004; **31**: 2106–2114.
101. Sen M, Cheng YH, Goldring MB, Lotz MK, Carson DA. WISP3-dependent regulation of type II collagen and aggrecan production in chondrocytes. *Arthritis Rheum* 2004; **50**: 488–497.
102. Baker N, Sharpe P, Culley K, *et al*. Dual regulation of metalloproteinase expression in chondrocytes by WISP3/CCN6. *Arthritis Rheum* 2012; **50**: 3925–3933.
103. Tanaka I, Morikawa M, Okuse T, Shirakawa M, Imai K. Expression and regulation of WISP2 in rheumatoid arthritic synovium. *Biochem Biophys Res Commun* 2005; **334**: 973–978.
104. Ijiri K, Nagayoshi R, Matsushita N, *et al*. Differential expression patterns of secreted frizzled related protein genes in synovial cells from patients with arthritis. *J Rheumatol* 2002; **29**: 2266–2270.
105. Corallini F, Secchiero P, Castellino G, Montecucco M, Trotta F, Zauli G. Circulating levels of frizzled-related protein (FRZB) are increased in patients with early rheumatoid arthritis and decrease in response to disease-modifying antirheumatic drugs. *Ann Rheum Dis* 2010; **69**: 1733–1734.
106. Diarra D, Stolina M, Polzer K, *et al*. Dickkopf-1 is a master regulator of joint remodeling. *Nat Med* 2007; **13**: 156–163.
107. Valdes AM, Spector TD. The contribution of genes to osteoarthritis. *Med Clin North Am* 2009; **93**: 45–66, x.
108. Loughlin J, Dowling B, Chapman K, *et al*. Functional variants within the secreted frizzled-related protein 3 gene are associated with hip osteoarthritis in females. *Proc Natl Acad Sci U S A* 2004; **101**: 9757–9762.
109. Min JL, Meulenbelt I, Riyazi N, *et al*. Association of the Frizzled-related protein gene with symptomatic osteoarthritis at multiple sites. *Arthritis Rheum* 2005; **52**: 1077–1080.
110. Kerkhof JM, Uitterlinden AG, Valdes AM, *et al*. Radiographic osteoarthritis at three joint sites and FRZB, LRP5, and LRP6 polymorphisms in two population-based cohorts. *Osteoarthritis Cartilage* 2008; **16**: 1141–1149.
111. Evangelou E, Chapman K, Meulenbelt I, *et al*. Large-scale analysis of association between GDF5 and FRZB variants and osteoarthritis of the hip, knee, and hand. *Arthritis Rheum* 2009; **60**: 1710–1721.
112. Lories RJ, Peeters J, Bakker A, *et al*. Articular cartilage and biomechanical properties of the long bones in Frzb-knockout mice. *Arthritis Rheum* 2007; **56**: 4095–4103.
113. Weng LH, Wang CJ, Ko JY, Sun YC, Su YS, Wang FS. Inflammation induction of Dickkopf-1 mediates chondrocyte apoptosis in osteoarthritic joint. *Osteoarthritis Cartilage* 2009; **17**: 933–943.
114. Weng LH, Wang CJ, Ko JY, Sun YC, Wang FS. Control of Dkk-1 ameliorates chondrocyte apoptosis, cartilage destruction, and subchondral bone deterioration in osteoarthritic knees. *Arthritis Rheum* 2010; **62**: 1393–1402.
115. Chan TF, Couchourel D, Abed E, Delalandre A, Duval N, Lajeunesse D. Elevated Dickkopf-2 levels contribute to the abnormal phenotype of human osteoarthritic osteoblasts. *J Bone Miner Res* 2011; **26**: 1399–1410.
116. gado-Calle J, Arozamena J, Garcia-Renedo R, *et al*. Osteocyte deficiency in hip fractures. *Calcif Tissue Int* 2011; **89**: 327–334.
117. Power J, Poole KE, van Bezooijen R, *et al*. Sclerostin and the regulation of bone formation: Effects in hip osteoarthritis and femoral neck fracture. *J Bone Miner Res* 2010; **25**: 1867–1876.
118. Chan BY, Fuller ES, Russell AK, *et al*. Increased chondrocyte sclerostin may protect against cartilage degradation in osteoarthritis. *Osteoarthritis Cartilage* 2011; **19**: 874–885.
119. Papathanasiou I, Malizos KN, Tsezou A. Low-density lipoprotein receptor-related protein 5 (LRP5) expression in human osteoarthritic chondrocytes. *J Orthop Res* 2010; **28**: 348–353.
120. Miclea RL, Siebelt M, Finos L, *et al*. Inhibition of Gsk3beta in cartilage induces osteoarthritic features through activation of the canonical Wnt signaling pathway. *Osteoarthritis Cartilage* 2011; **19**: 1363–1372.

121. Velasquillo C, Garciadiego-Cazares D, Almonte M, *et al*. Expression of MIG-6, WNT-9A, and WNT-7B during osteoarthritis. *Ann N Y Acad Sci* 2007; **1117**: 175–180.
122. Blom AB, Brockbank SM, van Lent PL, *et al*. Involvement of the Wnt signaling pathway in experimental and human osteoarthritis: prominent role of Wnt-induced signaling protein 1. *Arthritis Rheum* 2009; **60**: 501–512.
123. Hopwood B, Tsykin A, Findlay DM, Fazzalari NL. Microarray gene expression profiling of osteoarthritic bone suggests altered bone remodelling, WNT and transforming growth factor-beta/bone morphogenic protein signalling. *Arthritis Res Ther* 2007; **9**: R100.
124. Velasco J, Zarrabeitia MT, Prieto JR, *et al*. Wnt pathway genes in osteoporosis and osteoarthritis: differential expression and genetic association study. *Osteoporos Int* 2010; **21**: 109–118.
125. Yuasa T, Otani T, Koike T, Iwamoto M, Enomoto-Iwamoto M. Wnt/beta-catenin signaling stimulates matrix catabolic genes and activity in articular chondrocytes: its possible role in joint degeneration. *Lab Invest* 2008; **88**: 264–274.
126. Thomas RS, Clarke AR, Duance VC, Blain EJ. Effects of Wnt3A and mechanical load on cartilage chondrocyte homeostasis. *Arthritis Res Ther* 2011; **13**: R203.
127. Abed E, Chan TF, Delalandre A, Martel-Pelletier J, Pelletier JP, Lajeunesse D. R-spondins are newly recognized players in osteoarthritis that regulate Wnt signaling in osteoblasts. *Arthritis Rheum* 2011; **63**: 3865–3875.
128. Urano T, Narusawa K, Shiraki M, *et al*. Association of a single nucleotide polymorphism in the WISP1 gene with spinal osteoarthritis in postmenopausal Japanese women. *J Bone Miner Metab* 2007; **25**: 253–258.
129. Geyer M, Grassel S, Straub RH, *et al*. Differential transcriptome analysis of intraarticular lesional vs intact cartilage reveals new candidate genes in osteoarthritis pathophysiology. *Osteoarthritis Cartilage* 2009; **17**: 328–335.
130. Li X, Ominsky MS, Warmington KS, *et al*. Sclerostin antibody treatment increases bone formation, bone mass, and bone strength in a rat model of postmenopausal osteoporosis. *J Bone Miner Res* 2009; **24**: 578–588.
131. Li X, Warmington KS, Niu QT, *et al*. Inhibition of sclerostin by monoclonal antibody increases bone formation, bone mass, and bone strength in aged male rats. *J Bone Miner Res* 2010; **25**: 2647–2656.
132. Eddleston A, Marenzana M, Moore AR, *et al*. A short treatment with an antibody to sclerostin can inhibit bone loss in an ongoing model of colitis. *J Bone Miner Res* 2009; **24**: 1662–1671.
133. Marenzana M, Greenslade K, Eddleston A, *et al*. Sclerostin antibody treatment enhances bone strength but does not prevent growth retardation in young mice treated with dexamethasone. *Arthritis Rheum* 2011; **63**: 2385–2395.
134. Gilbert AM, Bursavich MG, Alon N, *et al*. Hit to lead studies on (hetero)arylpyrimidines--agonists of the canonical Wnt-beta-catenin cellular messaging system. *Bioorg Med Chem Lett* 2010; **20**: 366–370.
135. van Beuningen HM, Glansbeek HL, van der Kraan PM, van den Berg WB. Osteoarthritis-like changes in the murine knee joint resulting from intra-articular transforming growth factor-beta injections. *Osteoarthritis Cartilage* 2000; **8**: 25–33.
136. Blaney Davidson EN, Vitters EL, van der Kraan PM, van den Berg WB. Expression of transforming growth factor-beta (TGFbeta) and the TGFbeta signalling molecule SMAD-2P in spontaneous and instability-induced osteoarthritis: role in cartilage degradation, chondrogenesis and osteophyte formation. *Ann Rheum Dis* 2006; **65**: 1414–1421.
137. Blaney Davidson EN, Vitters EL, van den Berg WB, van der Kraan PM. TGF beta-induced cartilage repair is maintained but fibrosis is blocked in the presence of Smad7. *Arthritis Res Ther* 2006; **8**: R65.
138. Tang QO, Shakib K, Heliotis M, *et al*. TGF-beta3: A potential biological therapy for enhancing chondrogenesis. *Expert Opin Biol Ther* 2009; **9**: 689–701.
139. Blaney Davidson EN, van der Kraan PM, van den Berg WB. TGF-beta and osteoarthritis. *Osteoarthritis Cartilage* 2007; **15**: 597–604.

EDITORIAL

The skeleton: no bones about it

Colin Farquharson and **Katherine Staines**

Bone Biology Group, The Roslin Institute, Royal (Dick) School of Veterinary Studies, University of Edinburgh, Edinburgh EH25 9RG, UK
(Correspondence should be addressed to C Farquharson; Email: colin.farquharson@roslin.ed.ac.uk)

The skeleton is composed of bone and cartilage. These tissues are made of an exquisite assembly of functionally distinct cell populations and are required to support the structural, biochemical and mechanical integrity of the skeleton. The functions of the skeleton, which include its role in growth, locomotion, ion homeostasis and the protection of vital organs, are fundamental to the healthy organism. Development, growth and maintenance of the skeleton is under complex endocrine and genetic control and depends on a tight integration of cellular events within the skeleton and within the systems that deliver and accumulate mineral for hydroxyapatite formation (Karsenty 2003).

With few exceptions, bone formation is dependent on the development of the cartilage anlagen from mesenchymal precursors. These cartilage models of the future bones are replaced by bone through endochondral ossification, a process also responsible for linear bone growth at the epiphyseal plate during pre- and post-natal life (Kronenberg 2003). In essence, the laying down of a cartilage matrix by the chondrocyte, the primary cell type of cartilage, is a pre-requisite for future bone modelling and remodelling by the osteoblast and osteoclast. To fully appreciate the contribution of both cartilage and bone elements to skeletal physiology (and pathology), it is essential that we more thoroughly understand the molecular events responsible for the integration of the various signals and cues that impinge on, and direct, the activities of cartilage and bone cells.

To this goal, considerable advances have been made in our understanding of the regulatory mechanisms responsible for the formation and maintenance of the skeleton. This has been achieved through various classical *in vitro* and *in vivo* approaches including the analysis of specific knockout animals, transgenic mice and animals which bear spontaneous mutations. This progress in our understanding has been captured in these three thematic reviews, where the authors, in addition to providing a general review of endochondral ossification and bone formation and resorption, have focussed on some of the recent advances in chondrocyte, osteoblast and osteoclast biology.

In the first thematic review, Mackie *et al.* (2011) summarise the current concepts of growth plate chondrocyte activity and growth plate function. Chondrocyte proliferation is essential for bone growth, and the authors highlight recent advances in the control of chondrocyte proliferation by Indian hedgehog and bone morphogenetic proteins (BMPs). Of particular interest is the recently recognised cooperation between Schnurri proteins -2 and -3 and receptor-Smads in the regulation of BMP signalling (Jones *et al.* 2010). In addition, a role for the transcriptional repressor, TRPS1, which interacts with the activator form of Gli3, in chondrocyte cycle progression has been proposed (Wuelling *et al.* 2009). It is also worthy of mention that TRPS1 appears to be able to regulate chondrocyte hypertrophy by directly inhibiting PTHrP expression and RUNX2 function. This suggests that TRPS1 has an important function in the fine-tuning of cell-cycle exit and in the transition between the proliferative and the hypertrophic chondrocyte states (Napierala *et al.* 2008).

Mineralisation of the hypertrophic chondrocyte matrix is followed by vascular invasion of the growth plate, and the subsequent deposition of the bone matrix by osteoblasts on the vertical cartilage remnants remaining after osteoclastic matrix resorption. The regulation of invading cells is now considered to be an active process in which the chondrocytes produce factors that promote and attract the invasion of endothelial cells, osteoblasts and osteoclasts. In the second thematic review, new insights into osteoblast biology are summarised with a particular focus on the role of phosphatidylinositol 3-kinase (PI3K) signalling and its downstream effector, AKT (Guntur & Rosen 2011). Of topical interest is the ability of insulin/IGF1 signalling to up-regulate PI3K activity and, via the Forkhead group of transcription factors (FOXOs), influence osteoblast function and energy metabolism through altered osteocalcin and OST-PTP expression (Rached *et al.* 2010, Kousteni 2011). This is in addition to the previously recognised effects of PI3K signalling on the osteoblast-specific transcription factors, RUNX2, Osterix and ATF4. Interestingly, recent data suggest that conditional loss of *Pten*, a phosphatase that inactivates PI3K signalling, in osteoprogenitors results in increased proliferation of osteoblast progenitors and stimulation of fibroblast growth factor signalling (Guntur *et al.* 2011).

DOI: 10.1530/JOE-11-0274
0022–0795/11/0211–107 *Printed in Great Britain*
Online version via http://www.endocrinology-journals.org

The last thematic review concentrates on the bone resorbing osteoclast whose function is synchronised to that of the osteoblast during bone remodelling to ensure bone mass homeostasis (Mellis *et al.* 2011). The focus of this thematic review is the key signalling pathways involved in osteoclast formation and function. The coupling of osteoblast and osteoclast function is accepted to involve the receptor activator of nuclear factor kappa-β (RANK)/osteoprotegrin (OPG)/RANK ligand (RANKL) system, and this review summarises in detail the downstream signalling events that occur after RANK receptor activation, which result in osteoclast formation and bone resorption. Other pathways are also involved in osteoclast formation and one of these involves the ratio of the two isoforms – liver-enriched inhibitory protein (LIP) and liver-enriched activator protein (LAP) – of the transcription factor CCAAT enhancer-binding protein β. The ratio of LIP and LAP, which is modulated by the mechanistic target of rapamycin signalling pathway, regulates osteoclastogenesis through MafB (Smink *et al.* 2009). Once formed, osteoclast attachment to the bone matrix is essential for resorption and this is mediated by various signalling pathways such as those initiated by SRC kinase. SRC phosphorylation of cortactin and gelsolin is important for actin polymerisation and podosome turnover whereas phosphorylation of spleen tyrosine kinase, SYK, promotes the activation of small GTPases and cytoskeletal reorganisation (Itzstein *et al.* 2011).

The aim of these thematic reviews is to bring together in one collection an appreciation of our current understanding of the key factors, e.g. endocrine, genetic and signalling molecules, that regulate skeletal function via interactions with cells of both cartilage and bone. Each individual cell type (including the osteocyte, the terminally differentiated osteoblast) does not live in isolation or in a vacuum and there is much crosstalk and communication between them and also with their collagenous-rich extracellular matrix. Together, these cellular activities and matrix interactions result in the formation of a complex organ that is indispensable for life.

Declaration of interest

The authors declare that there is no conflict of interest that could be perceived as prejudicing the impartiality of the research reported.

Funding

The authors acknowledge the Institute Strategic Programme Grant Funding from the BBSRC (C F) and BBSRC studentship funding (K S) for support.

References

Guntur AR & Rosen CJ 2011 The skeleton: a multi-functional complex organ. New insights into osteoblasts and their role in bone formation: the central role of PI3kinase. *Journal of Endocrinology* **211** 123–130. (doi:10.1530/JOE-11-0175)

Guntur AR, Reinhold MI, Cuellar J & Naski MC 2011 Conditional ablation of Pten in osteoprogenitors stimulates FGF signaling. *Development* **138** 1433–1444. (doi:10.1242/dev.058016)

Itzstein C, Coxon FP & Rogers MJ 2011 The regulation of osteoclast function and bone resorption by small GTPases. *Small GTPases* **2** 117–130. (doi:10.4161/sgtp.2.3.16453)

Jones DC, Schweitzer MN, Wein M, Sigrist K, Takagi T, Ishii S & Glimcher LH 2010 Uncoupling of growth plate maturation and bone formation in mice lacking both Schnurri-2 and Schnurri-3. *PNAS* **107** 8254–8258. (doi:10.1073/pnas.1003727107)

Karsenty G 2003 The complexities of skeletal biology. *Nature* **423** 316–318. (doi:10.1038/nature01654)

Kousteni S 2011 FoxO1: a molecule for all seasons. *Journal of Bone and Mineral Research* **26** 912–917. (doi:10.1002/jbmr.306)

Kronenberg HM 2003 Developmental regulation of the growth plate. *Nature* **423** 332–336. (doi:10.1038/nature01657)

Mackie EJ, Tatarczuch L & Mirams M 2011 The skeleton: a multi-functional complex organ. The growth plate chondrocyte and endochondral ossification. *Journal of Endocrinology* **211** 109–121. (doi:10.1530/JOE-11-0048)

Mellis DJ, Itzstein C, Helfrich MH & Crockett JC 2011 The skeleton: a multi-functional complex organ. The role of key signalling pathways in osteoclast differentiation and in bone resorption. *Journal of Endocrinology* **211** 131–143. (doi:10.1530/JOE-11-0212)

Napierala DK, Sam K, Morello R, Zheng Q, Munivez E, Shivdasani RA & Lee B 2008 Uncoupling of chondrocyte differentiation and perichondrial mineralization underlies the skeletal dysplasia in tricho-rhino-phalangeal syndrome. *Human Molecular Genetics* **17** 2244–2254. (doi:10.1093/hmg/ddn125)

Rached M-T, Kode A, Silva BC, Jung DY, Gray S, Ong H, Paik J-H, dePinho RA, Kim JK, Karsenty G *et al.* 2010 FoxO1 expression in osteoblasts regulates glucose homeostasis through regulation of osteocalcin in mice. *Journal of Clinical Investigation* **120** 357–368. (doi:10.1172/JCI39901)

Smink JJ, Begay V, Schoenmaker T, Sterneck E, de Vries TJ & Leutz A 2009 Transcription factor C/EBP beta isoform ratio regulates osteoclastogenesis through MafB. *EMBO Journal* **28** 1769–1781. (doi:10.1038/emboj.2009.127)

Wuelling M, Kaiser FJ, Buelens LA, Braunholz D, Shivdasani RA, Depping R & Vortkamp A 2009 Trps1, a regulator of chondrocyte proliferation and differentiation, interacts with the activator form of Gli3. *Developmental Biology* **328** 40–53. (doi:10.1016/j.ydbio.2009.01.012)

Received in final form 11 July 2011
Accepted 21 July 2011